

**THE MEDICINAL CHEMISTRY OF THE
ISOMERS OF THE CYCLIC DIPEPTIDE:
CYCLO(TRP-PRO)**

HAJIERAH JAMIE

**THE MEDICINAL CHEMISTRY OF THE
ISOMERS OF THE CYCLIC DIPEPTIDE:
CYCLO(TRP-PRO)**

by

HAJIERAH JAMIE

Submitted in fulfilment of the requirements for the degree of

PHILOSOPHIAE DOCTOR

in the Faculty of Health Sciences, at the
University of Port Elizabeth

January 2002

Promoter : Prof. P. J. Milne

TABLE OF CONTENTS

TABLE OF CONTENTS	b
SUMMARY	i
ACKNOWLEDGEMENTS	iii
LIST OF ABBREVIATIONS	iv
LIST OF FIGURES	viii
LIST OF TABLES	xviii
CHAPTER 1	1
LITERATURE REVIEW	1
1.1 INTRODUCTION	1
1.1.1 The diketopiperazines	1
1.1.2 Cyclo(His-Pro), an endogenous DKP	3
1.1.3 Conformational features of DKPs.....	4
1.1.4 Factors affecting the conformation of the DKP ring	5
1.1.5 Simple diketopiperazines	6
1.1.6 Isomerization of amino acids	10
1.1.7 Tryptophan	12
1.1.7.1 Pathways of metabolism	12
1.1.7.2 Conversion of Trp to aminocarboxymuconate semialdehyde (ACS)	13
1.1.7.3 Conversion of ACS to acetoacetyl-CoA	13
1.1.7.4 Conversion of ACS to NAD ⁺	13
1.1.8 Proline	15
1.1.8.1 Biosynthesis of Pro	17
1.1.8.2 Pro catabolism.....	18
1.1.9 Why Cyclo(Trp-Pro)?	18
1.2 Objectives of the study	20
CHAPTER 2	21
SYNTHESIS AND STRUCTURAL ELUCIDATION	21
2.1 INTRODUCTION	21
2.1.1 Synthesis of the isomers of cyclo(Trp-Pro)	22
2.1.1.1 Background	22
2.1.1.2 Synthesis of the protected linear dipeptides.....	22
2.1.1.3 Removal of the protective Boc groups.....	24
2.1.1.4 Cyclization	24
2.1.2 Mass Spectrometry.....	26
2.1.3 Infrared Spectroscopy	31
2.1.4 Differential Scanning Calorimetry.....	37
2.1.5 X-ray crystallography	38
2.1.6 NMR Spectroscopy (Nuclear Magnetic Resonance)	47
2.2 CONCLUSIONS	62

CHAPTER 3.....	63
SCREEN FOR ANTIMICROBIAL ACTIVITY.....	63
3.1 INTRODUCTION.....	63
3.1.1 Antibacterial agents	63
3.1.2 Antifungal agents	67
3.1.3 Peptide antibiotics.....	69
3.1.3.1 Cycloserine	69
3.1.3.2 Tryptophan antimetabolites	70
3.1.3.3 Bacitracin	70
3.1.3.4 Tyrocidins and the Gramicidins.....	72
3.1.3.5 Polymyxin and Octapeptins	74
3.1.3.6 Valinomycin and Enniatin	76
3.1.4 Determining the level of antimicrobial activity	79
3.1.4.1 Colorimetric assays using tetrazolium salts.....	80
3.1.4.1.1 3-[4,5-Dimethylthiazol-2-yl]-2,5-diphenyltetrazolium bromide (MTT)	81
3.1.4.1.2 2,3,5-triphenyltetrazolium chloride (TTC)	83
3.1.4.1.3 2,3-bis[2-methoxy-4-nitro-5-sulphophenyl]-2H-tetrazolium-5-carboxanilide (XTT)	84
3.2 OBJECTIVES OF THE CHAPTER.....	86
3.2.1 Objectives of the present chapter	86
3.3 MATERIALS AND METHODS.....	87
3.3 MATERIALS AND METHODS	87
3.3.1 Microorganisms used in the screen for antimicrobial activity	87
3.3.1.1 Culturing the microorganisms.....	88
3.3.2 Solutions tested in the screen for antimicrobial activity	88
3.3.3 Colorimetric assays using tetrazolium dyes.....	89
3.3.3.1 MTT assay	89
3.3.3.2 TTC assay	90
3.3.3.3 XTT assay	90
3.3.4 Statistical analysis.....	91
3.4 RESULTS AND DISCUSSION.....	92
3.5 CONCLUSIONS	105
CHAPTER 4.....	106
ANTICANCER STUDIES.....	106
4.1 INTRODUCTION.....	106
4.1.1 The cell cycle	107
4.1.1.1 Cellular differentiation.....	108
4.1.2 Molecular and biochemical basis of neoplasia	109
4.1.2.1 Genetic changes in neoplasia	109
4.1.2.2 Oncogenes and tumour suppressor genes in normal physiology and neoplasia	110

4.1.2.3	Hormones, growth factors and growth inhibitors	110
4.1.2.4	Cellular changes in neoplasia.....	110
4.1.3	Pathophysiology of neoplasia	110
4.1.3.1	Colon carcinoma	111
4.1.3.2	Breast carcinoma.....	112
4.1.3.2	Cervical carcinoma	113
4.1.4	Anticancer drug development.....	113
4.1.4.1	Resistance to cytotoxic drugs.....	114
4.1.5	Antitumour therapy	115
4.1.5.1	Surgery.....	115
4.1.5.2	Radiation therapy	115
4.1.5.3	Chemotherapy	115
4.1.5.3.1	Chemotherapeutic drugs	116
4.1.5.3.1.1	Fluorouracil.....	116
4.1.5.3.1.2	Mitomycin.....	116
4.1.5.3.1.3	Estrogen and androgen inhibitors	116
4.1.5.4	Immunotherapy.....	117
4.1.5.5	Combination therapy.....	117
4.2	OBJECTIVES OF THE CHAPTER.....	118
4.2.1	Objectives of the present chapter	118
4.3	MATERIALS AND METHODS.....	119
4.3.1.1	The HT-29 cell line	120
4.3.1.2	The HeLa cell line.....	121
4.3.1.3	The MCF-7 cell line.....	121
4.3.2	Routine cell culture	121
4.3.3	The 3-[4,5-Dimethylthiazol-2-yl]-2,5-diphenyltetrazolium bromide (MTT) assay	122
4.3.3.1	Linearity for MTT assay	123
4.3.3.2	Growth curves.....	123
4.3.3.3	Effects of the isomers on cell viability	123
4.3.4	Alkaline phosphatase (AP) activity	124
4.3.4.1	Alkaline phosphatase assay.....	124
4.3.5	Statistical analysis.....	125
4.4	RESULTS AND DISCUSSION	126
4.5	CONCLUSIONS	146
CHAPTER 5.....	147	
HEPATOTOXICITY.....	147	
5.1 INTRODUCTION.....	147	
5.1.1	The liver	147
5.1.1.1	General metabolic functions	148
5.1.2	Liver injury-hepatotoxicity	151
5.1.3	Drug-induced hepatic injury	154
5.1.3.1	Idiosyncratic and intrinsic toxicity.....	154
5.1.3.2	Cell toxicity as a consequence of drug bioactivation.....	154

5.1.4	Drug-induced cell death: necrosis and apoptosis.....	155
5.1.5	Molecular mechanisms of toxicity.....	155
5.1.5.1	Impairment of cellular metabolism.....	155
5.1.6	Drug-induced lipid peroxidation.....	156
5.1.6.1	Drug-derived radicals and active oxygen species.....	157
5.1.7	Drug-induced oxidative stress.....	157
5.1.7.1	Drug redox cycling as a cause of oxidative stress	158
5.1.7.2	Glutathione and oxidative stress	158
5.1.8	Calcium- and drug-induced cell injury	160
5.1.9	Covalent binding.....	162
5.1.9.1	Mechanisms of drug-protein adduct formation.....	162
5.1.9.2	Covalent binding and hepatotoxicity	162
5.1.10	Immunological mechanisms of drug hepatotoxicity.....	163
5.1.11	Screening for potential hepatotoxicity for new drugs.....	163
5.2.	OBJECTIVES OF THE CHAPTER.....	165
5.2.1	Objectives of the present chapter	165
5.3	MATERIALS AND METHODS	166
5.3.1	<i>In vitro</i> examination of hepatotoxicity.....	166
5.3.1.1	Albumin-binding assay (Modified method of Taki <i>et al.</i> , 1998).....	167
5.3.1.1.1	HPLC of compounds.....	168
5.3.1.2	Blood absorption of the drugs.....	168
5.3.1.2.1	Determination of blood absorption of cyclo(L-Trp-L-Pro) and cyclo(L-Trp-D-Pro).....	169
5.3.1.3	Isolation of hepatocytes	170
5.3.1.3.1	Isolation procedure.....	171
5.3.1.3.2	Cell yield and viability.....	173
5.3.1.3.2.1	MTT assay for cells in suspension.....	173
5.3.1.3.3	Culture medium and conditions	173
5.3.2	<i>In vivo</i> examination of hepatotoxicity.....	174
5.3.2.1	Treatment of animals	174
5.3.2.2	Determination of serum LDH levels.....	175
5.3.2.2.1	LDH Assay.....	176
5.3.2.3	Determination of alkaline phosphatase levels.....	176
5.3.2.3.1	Alkaline phosphatase assay.....	177
5.3.2.4	Serum transaminases.....	177
5.3.2.4.1	Determination of serum AST and ALT content	178
5.3.2.5	Lipid peroxidation determination	179
5.3.2.6	Assessment of the state of energy metabolism	180
5.3.2.6.1	ATP concentration assay.....	180
5.3.2.7	Serum calcium determination	181
5.3.2.7.1	Ca ²⁺ -concentration assay.....	182
5.3.2.8	Assessment of protective mechanisms.....	182
5.3.2.8.1	Reduced glutathione assay.....	182
5.3.2.9	Assessment of ureogenesis	183
5.3.2.9.1	Urea nitrogen assay.....	183
5.3.2.10	Assessment of protein synthesis	184

5.3.2.10.1 Albumin assay.....	184
5.3.2.11 Determination of bilirubin content in serum.....	184
5.3.2.11.1 Bilirubin assay	185
5.3.3 Statistical analysis.....	185
5.4 RESULTS AND DISCUSSION	186
5.4.1 In vitro examination of hepatotoxicity.....	186
5.4.2 In vivo examination of hepatotoxicity	193
5.5 CONCLUSIONS	210
CHAPTER 6.....	212
HAEMATOLOGICAL STUDIES	212
6.1 INTRODUCTION.....	212
6.1.1 Platelets	212
6.1.1.1 Counting of platelets	213
6.1.2 Haemostasis	213
6.1.3 Disorders of haemostasis	220
6.1.4 Thrombosis and cancer	223
6.2 OBJECTIVES OF THE CHAPTER.....	224
6.2.1 Objectives of the present chapter	224
6.3 MATERIALS AND METHODS	225
6.3.1 Platelet count	225
6.3.2 Platelet aggregation	226
6.3.2.1 Thrombin-induced platelet aggregation.....	226
6.3.2.2 ADP-induced platelet aggregation.....	227
6.3.3 Thrombin assay	228
6.3.4 Platelet adhesion.....	229
6.3.4.1 Adhesion in the presence of ADP	229
6.3.4.1.1 Adhesion, stimulated by ADP, in the presence of the isomers	230
6.3.4.2 Adhesion in the presence of thrombin	230
6.3.4.2.1 Adhesion, stimulated by thrombin, in the presence of the isomers	230
6.3.5 Statistical analysis	230
6.4 RESULTS AND DISCUSSION	231
6.5 CONCLUSIONS	253
CHAPTER 7.....	254
EFFECT OF THE ISOMERS ON HEART	254
AND ION CHANNEL ACTIVITY.....	254
7.1 INTRODUCTION.....	254

7.1.1 Electrophysiology of the heart	255
7.1.2 Cardiac performance.....	255
7.1.3 Movement of ions during an action potential.....	256
7.1.4 Voltage-dependent calcium channels	259
7.1.5 Potassium channels	261
7.1.6 The electrocardiogram	262
7.1.6.1 ECG analysis.....	263
7.1.7 The need for new antiarrhythmic agents.....	264
7.1.8 The use of the rat model	264
7.1.9 Patch-clamp techniques-A brief overview	265
7.2 OBJECTIVES OF THE CHAPTER.....	268
7.2.1 Objectives of the present chapter	268
7.3 MATERIALS AND METHODS	269
7.3.1 Whole-cell patch-clamp method	269
7.3.1.1 Ca ²⁺ -channel activity.....	269
7.3.1.2 Potassium channel activity.....	270
7.3.2 Isolated heart perfusion.....	270
7.3.2.1 Measurement of ventricular tachycardia and arrhythmia, time to sinus rhythm and QRS interval	273
7.3.3 Statistical analysis	273
7.4 RESULTS AND DISCUSSION	274
7.5 CONCLUSIONS	296
<i>CONCLUSIONS</i>	<i>298</i>
<i>FURTHER RECOMMENDATIONS</i>	<i>299</i>
<i>RESEARCH OUTPUT</i>	<i>300</i>
<i>REFERENCE LIST.....</i>	<i>301</i>
<i>APPENDIX A.....</i>	<i>315</i>
<i>AMINO ACID TABLE</i>	<i>315</i>
<i>APPENDIX B.....</i>	<i>316</i>
<i>SPECTRA, GRAPHS, ETC.</i>	<i>316</i>
<i>APPENDIX C.....</i>	<i>338</i>
<i>SOLUTION LIST.....</i>	<i>338</i>
<i>APPENDIX D</i>	<i>354</i>
<i>HUMAN ETHICS LETTER OF APPROVAL.....</i>	<i>354</i>

APPENDIX E..... 356
ARTICLES THAT HAVE BEEB SUBMITTED FOR PUBLICATION 356
 Article 1..... 357
 Article 2..... 376

SUMMARY

The isomers of cyclo(Trp-Pro) (cyclo(L-Trp-L-Pro), cyclo(L-Trp-D-Pro), cyclo(D-Trp-L-Pro) and cyclo(D-Trp-D-Pro)) have been successfully synthesized and screened for biological activity. High percentage yields were obtained by using the three phase synthesis system, which involves the synthesis of the intermediate protected linear dipeptides, followed by the removal of the protecting Boc groups. This step is followed by cyclization and crystallization of the isomers.

The diketopiperazines rings of cyclo(L-Trp-L-Pro) and cyclo(D-Trp-D-Pro) contain *cis*-amide bonds, while cyclo(L-Trp-D-Pro) and cyclo(D-Trp-L-Pro) contain *trans*-amide bonds. These bonds govern the conformation of the diketopiperazines ring. The isomers have shown different degrees of biological activity, possibly as a result of the orientation of the side chain of tryptophan and this difference in conformation, leading to varying interactions between isomer and a range of receptors.

Under experimental conditions, 10^{-3} M cyclo(L-Trp-D-Pro) and cyclo(D-Trp-L-Pro) showed effective anticancer activity against the cervical cancer cell line, HeLa, resulting in a <50% reduction in cell viability. Cytotoxicity screening with cyclo(D-Trp-L-Pro) indicated that it was hepatocyte-specific in its toxicity, whilst the other isomers were cytotoxic against the other cell types tested. At 1mg/ml, cyclo(L-Trp-L-Pro) proved to be an effective antimicrobial agent against Gram positive bacteria, while cyclo(L-Trp-D-Pro) effectively inhibited the growth of the Gram negative bacteria, *Esherichia coli*. Cyclo(D-Trp-L-Pro) proved to be effective against *Streptococcus*, while cyclo(D-Trp-D-Pro) effectively reduced viability of the yeast, *Candida albicans*. Cyclo(D-Trp-L-Pro) was the only isomer to show Ca^{2+} -channel antagonism, whilst the other isomers resulted in opening of the Ca^{2+} -channel. No effects were observed on K^{+} -channel activity for all the isomers tested. The isomers also proved to be valuable antiarrhythmic agents by effectively reducing the time spent in ventricular tachycardia and arrhythmia, as well as decreasing the time for the heart rate to return to a normal sinus rhythm. Furthermore, cyclo(L-Trp-D-Pro) showed positive chronotropic activity, while cyclo(D-Trp-L-Pro)

showed negative chronotropic activity. In addition, cyclo(L-Trp-D-Pro) and cyclo(D-Trp-L-Pro) also increased the coronary flow rate. 0.125 –1 mM Cyclo(L-Trp-D-Pro) decreased aggregation in washed platelets induced by thrombin. All isomers increased adhesion to an artificial surface when the platelets were stimulated by ADP, yet caused reduced adhesion when the platelets were stimulated by thrombin.

These results prove the potential of these compounds as novel agents in a range of biological fields, indicating that a combination of L- and D- amino acids may prove more effective than an agent consisting solely of L-amino acids.

Keywords: cyclic dipeptides, isomers, structural elucidation, antimicrobial, haematological effects, anticancer, ion channel studies, hepatotoxicity.

ACKNOWLEDGEMENTS

I would like to extend my thanks and sincere appreciation to all who helped make the present study possible:

The Almighty for divine guidance and strength.

Prof. P. J. Milne for his invaluable guidance throughout the year.

The National Research Foundation for financial support.

Mr Gareth Kilian, for his unbelievable effort and valuable time.

Dr C. Frost, for her invaluable input and time.

Dr K. Dyason, University of Potchefstroom, for help with the channel studies.

The members of the Cyclic Peptide Research Unit for motivation and support.

All staff and post-graduate students in the Department of Biochemistry and Microbiology and Department of Pharmacy, University of Port Elizabeth, for their never-ending support and encouragement.

My mother for her everlasting faith in me.

My soulmate, Fahdiel, for all his time, patience and motivation.

LIST OF ABBREVIATIONS

α : alpha	CaCl ₂ : calcium chloride
β : beta	<i>C. albicans</i> : <i>Candida albicans</i>
γ : gamma	cAMP : cyclic adenosine 3',5'
δ : delta	monophosphate
λ : lambda	CF : coronary flow
ϵ : molar extinction coefficient	CFU : colony forming units
% : percentage	Chlor : chloramphenicol
°C : degree Celsius	CPU-23 : (1-{1-[(6-methoxy)-naphth-2-yl]}-propyl-2-(1-piperidine)-acetyl-6,7-dimethoxy-1,2,3,4-tetrahydroisoquinoline
μ l : microlitre	CoA : coenzyme A
μ M : micro molar	CO ₂ : carbon dioxide
2n : diploid	CS-747 : 2-acetoxy-5(α -cyclopropylcarbonyl-2-fluorobenzyl)-4,5,6,7-tetrahydrothieno[3,2-c]pyridine
4n : tetraploid	CsCl ₂ : cesium chloride
Å : Angstrom	D : dextrorotatory
Abs : absorbance	Da : Daltons
ACS : 2-amino-3-carboxymuconate-6-semialdehyde	DAB : α,β -diaminobutyric acid
ADP : adenosine-5'-diphosphate	DEPC : diethylphosphoryl cyanide
AEA : arachidonylethanolamide	dH ₂ O : deionised water
ALT : alanine transaminase	D-HOV : D- α -hydroxyisovaleric acid
AMP: adenosine-5'-monophosphate	DKP : diketopiperazine
AP: Alkaline Phosphatase	DMEM : Dulbecco's modification of Eagle's essential minimal medium
Ar : argon / aromatic	DMSO : dimethyl sulfoxide
AST : aspartate transaminase	DMSO-d ₆ : deuterated dimethyl sulfoxide
ATP : adenosine-5'-triphosphate	
ATPase : adenosine-5'-triphosphatase	
t-Boc : t-butyloxycarbonyl	
BSA : bovine serum albumin	
C : carbon / cytosine	
Ca ²⁺ : calcium ions	

DNA : deoxyribonucleic acid
 DNPH : 2,4-dinitrophenylhydrazine
 DOP : dioxipiperazine
 DSC : differential scanning calorimetry
 ECG : electrocardiogram
E. coli : *Escherichia coli*
 EDTA : Ethylenediaminetetraacetic Acid
 EGF : epidermal growth factor
 EGTA : ethylene glycol-bis(β -aminoethyl ether)-N,N,N',N'-tetraacetic acid
 ER : estrogen receptor
 FAB : fast atom bombardment
 FCS : foetal calf serum
 FdUMP : 5'-fluoro-2'-deoxyuridine 5'-phosphate
 Fp : flavoprotein
 5-FU : fluorouracil
 G : guanine
 GR 127935 : N-[4-methoxy-3-(4-methyl-1-piperazinyl)phenyl]-2'-methyl-4'-(5-methyl-1,2,4-oxadiazol-3-yl)[1,1-biphenyl]-4-carboxamide
 GTN : nitroglycerine
 GSH : glutathione (reduced)
 GSSG : oxidized GSH
 H₃PO₄ : phosphoric acid
 HEPES : N-[2-hydroxyethyl]piperazine-N'-[2-ethanesulfonic acid]
 HBSS : Hanks balanced salt solution
 HCl : hydrochloric acid
 HIV : human immunodeficiency virus
 HOD : deuterated H₂O
 HPLC : high-performance liquid chromatography
 HPV : human papilloma virus
 hr : hours
 HR : heart rate
 HSV : Herpes Simplex Virus
 5-HT : 5- hydroxytryptamine
 H₂O : water
 Hz : Herz
 IC₅₀: inhibitory concentration (50%)
 ICa : inward Ca²⁺-current flow
 ICI 170,809 : 2-2-[dimethylamino-2-methylpropylthio]-3-phenylquinoline hydrochloride
 ICI 192,605 : 4(Z)-6-(2,4,5 *cis*)[2-chlorophenyl)-4-(2-hydroxyphenyl)1,3-dioxan-5-yl] hexenoic acid
 ID₅₀ : inhibitory dose (50%)
 IK1 : inward rectifier K⁺-current
 IR : infrared
 IU : international units
 K⁺ : potassium ions
 KBr : potassium bromide
 kcal : kilocalories
 KCl : potassium chloride
 KHBB : Krebs-Henseleit bicarbonate buffer
 K_i : inhibition constant

L : levorotatory
 LDH : lactate dehydrogenase
 LPS : lipopolysaccharide
 MAC : *Mycobacterium avium-M. intracellulare* complex
 MDL 28050 : N^α-succinyl-Tyr-Glu-Pro-Ile-Pro-Glu-Glu-Ala-Cha-D-Glu-OH
 m/e : mass/charge ratio
 Mg²⁺ : magnesium ions
 MgATP : ATP magnesium salt
 MgSO₄.7H₂O : magnesium sulfate
 MIC : minimal inhibitory concentration
 MIC₅₀ : MIC resulting in 50% inhibition
 min : minutes
 mM : milli molar
 Mn²⁺ : manganese ions
 MQH₂O : MilliQ H₂O
 M_r : relative molecular mass
 mRNA : messenger RNA
 MTT : 3-[4,5-dimethylthiazol-2-yl]-2,5-diphenyltetrazolium bromide
 mU : milliunits
 MV : millivolts
 N : nitrogen
 Na⁺ : sodium ions
 Na₂ATP : ATP disodium salt
 NaCl : sodium chloride
 NAD⁺ : nicotinamide adenine dinucleotide
 NADH : nicotinamide adenine dinucleotide, reduced form
 NADP⁺ : nicotinamide adenine dinucleotide phosphate
 NADPH : nicotinamide adenine dinucleotide phosphate, reduced form
 NaHCO₃ : sodium bicarbonate
 NaOH : sodium hydroxide
 Na₂SO₄ : sodium sulfate
 NB : nutrient broth
 NCCLS : National Committee for Clinical Laboratory Standards
 NCS : newborn calf serum
 NECA : 5'-N-ethylcarboxamidoadenosine
 NH-terminal: amino-terminal
 NIDDM : non-insulin dependent diabetes mellitus
 nm : nanometers
 NMR : nuclear magnetic resonance
 NSAIDs : non-steroidal anti-inflammatory drugs
 OH : hydroxyl
 OSu : N-hydroxysuccinimide
 P : phosphate
 p : statistical significance value
P. aeruginosa : *Pseudomonas aeruginosa*
 PBS : phosphate-buffered saline
 PDGF : platelet-derived growth factor
 Pg. : page
 P_i : pyrophosphate
 pI : isoelectric point

pK_1 : dissociation constant of the carboxyl group
 pK_2 : dissociation constant of the amino group
 $pNPP$: *p*-nitrophenyl phosphate
 Pp. : pages
 PPP : platelet-poor plasma
 PRP : platelet-rich plasma
 ps : picoseconds
 RES : reticuloendothelial system
 RNA : ribonucleic acid
 RSD 1019 : ((±)-*trans*-[2-(4-morpholinyl)cyclohexyl](4-bromophenyl) acetate monohydrochloride)
 s : seconds
 SAB : sabouraud
S. aureus : *Staphylococcus aureus*
 s.d. : standard deviation
 SH : thiol group
 SR : sinus rhythm
 TBA : thiobarbituric acid
 TCA : tricarboxylic acid
 TCDD : 2,3,7,8-tetrachlorodibenzo-*p*-dioxan
 TF : tissue factor
 TLC : thin layer chromatography
 TRI : triethylamine
 TTC : 2,3,5-triphenyltetrazolium chloride
 U-46619 : 9,11 dideoxy-11 α ,9 α -epoxymethano-prostaglandin F_{2 α}
 UK 66,914 : N-(4-{1-hydroxy-2-[4-(4-pyridinyl)-1-piperazinyl]ethyl} phenyl)methanesulphonamide
 ULN : upper limit of normal
 VA : ventricular arrhythmia
 VF : ventricular fibrillation
 VOCCs : voltage-operated Ca²⁺-channels
 VT : ventricular tachycardia
 XTT : 2,3-bis[2-methoxy-4-nitro-5-sulfophenyl]-2H-tetrazolium-5-carboxanilide
 Zn²⁺ : zinc ions

LIST OF FIGURES

Figure 1. 1: General structure of a diketopiperazine, where R1 and R2 represent the substituting amino acid residues (Anteunis, 1978).....	2
Figure 1. 2: Major conformations of the DKP ring in cyclic dipeptides. R represents the substituting amino acid residues (Adapted from Jankowska and Ciarkowski, 1987).	5
Figure 1. 3: Structure of compound 593 A (Sammes, 1975).	7
Figure 1. 4: Structure of rhodotorulic acid (Sammes, 1975).	7
Figure 1. 5: Structure of echinulin (Sammes, 1975).....	8
Figure 1. 6: Structure of aspergillic acid (Sammes, 1975).....	8
Figure 1. 7: Structure of gliotoxin (Sammes, 1975).	9
Figure 1. 8: Structure of verticillin A (Sammes, 1975).....	10
Figure 1. 9: The metabolism of tryptophan (Roskoski, 1996. Pg. 234).....	14
Figure 1. 10: Serotonin metabolism (Roskoski, 1996. Pg. 410).....	15
Figure 1. 11: Synthesis of proline from glutamate (Roskoski, 1996. Pg. 240).....	17
Figure 1. 12: Proline metabolism. Fp=flavoprotein (Roskoski, 1996. Pg. 224).....	18
Figure 2. 1: General structure of cyclo(Trp-Pro). Red atom = oxygen; blue atoms = nitrogen.....	26
Figure 2. 2: Mass spectrum of cyclo(L-Trp-L-Pro).....	29
Figure 2. 3: Mass spectrum of cyclo(L-Trp-D-Pro).....	29
Figure 2. 4: Mass spectrum of cyclo(D-Trp-L-Pro).....	30
Figure 2. 5: Mass spectrum of cyclo(D-Trp-D-Pro).	30
Figure 2. 6: IR spectra overlay of cyclo(L-Trp-L-Pro) and cyclo(D-Trp-D-Pro).....	34
Figure 2. 7: IR spectra overlay of cyclo(L-Trp-D-Pro) and cyclo(D-Trp-L-Pro).....	34
Figure 2. 8: IR spectra overlay of cyclo(D-Trp-D-Pro) and cyclo(D-Trp-L-Pro).	35
Figure 2. 9: IR spectra overlay of cyclo(L-Trp-L-Pro) and cyclo(D-Trp-L-Pro).	35
Figure 2. 10: IR spectra overlay of cyclo(D-Trp-D-Pro), cyclo(L-Trp-L-Pro) and cyclo(D-Trp-L-Pro).....	36
Figure 2. 11: IR spectra overlay of cyclo(L-Trp-D-Pro), cyclo(L-Trp-L-Pro) and cyclo(D-Trp-L-Pro).....	36
Figure 2. 12: ORTEP view of cyclo(D-Trp-L-Pro) (A - Conformer 1; B – Conformer 2).	39
Figure 2. 13: ¹³ C NMR spectrum of cyclo(L-Trp-L-Pro) in DMSO-d ₆	50
Figure 2. 14: ¹ H NMR spectrum of cyclo(L-Trp-L-Pro) in DMSO-d ₆	51
Figure 2. 15: ¹³ C NMR spectrum of cyclo(L-Trp-D-Pro) in DMSO-d ₆	52
Figure 2. 16: ¹ H NMR spectrum of cyclo(L-Trp-D-Pro) in DMSO-d ₆	53
Figure 2. 17: ¹³ C NMR spectrum of cyclo(D-Trp-L-Pro) in DMSO-d ₆	54
Figure 2. 18: ¹ H NMR spectrum of cyclo(D-Trp-L-Pro) in DMSO-d ₆	55
Figure 2. 19: ¹³ C NMR spectrum of cyclo(D-Trp-D-Pro) in DMSO-d ₆	56
Figure 2. 20: ¹ H NMR spectrum of cyclo(D-Trp-D-Pro) in DMSO-d ₆	57
Figure 3. 1: Structure of D-cycloserine (Anand, 1995. Pg. 716).	69
Figure 3. 2: Structures of 5-fluorotryptophan, 7-azatryptophan and indolylacrylic acid. (Lemke, 1995. Pg. 716).....	70

Figure 3. 3: Structure of bacitracin. The intramolecular hexapeptide ring is shown in bold-type. L-His*- the amino acid most likely involved in the binding of bacitracin to the pyrophosphate carrier. (Edwards, 1980. Pg. 130).	71
Figure 3.4: Structure of gramicidin A. Abbreviations: Val=valine; Gly=glycine; Ala=alanine; Leu=leucine; Trp=tryptophan. (Edwards, 1980. Pg. 145).	72
Figure 3. 5: Structure of the polymyxins. 6-MO=6-methyloctanoic acid; 6-MH=6-methylheptanoic acid; DAB=diaminobutyric acid; Thr=threonine; Leu=leucine; Phe=phenylalanine; Ser=serine; Ile=isoleucine (Edwards, 1980. Pg. 142).	74
Figure 3. 6: Structures of valinomycin and enniatin. Val=valine; HOV= α -hydroxyisovaleric acid, Lac=lactate; MV=N-methylvaline. (Edwards, 1980. Pg. 146).	77
Figure 3. 7: Structure of ramoplanin A ₂ . R ₁ =7-methyl-2,4-octadienoyl; R ₂ = α -D-mannosyl- α -D-mannosyl (Kirst, 1995. Pg. 501).	78
Figure 3. 8: Structure of daptomycin. (Kirst, 1995. Pg. 503).	78
Figure 3. 9: Structure of MTT (Sigma catalogue, 2000-2001. Pg. 686).	82
Figure 3. 10: Structure of XTT (Sigma catalogue, 2000-2001. Pg. 1017).	84
Figure 3. 11: Structure of chloramphenicol (Sigma catalogue, 2000-2001. Pg. 234).	89
Figure 3. 12: Structure of amphotericin B (Sigma catalogue, 2000-2001. Pg. 113).	89
Figure 3. 13: Resultant % viability of 0.5×10^6 cells/ml E. coli after exposure to the isomers at various concentrations for 24 hrs, as determined by the MTT assay. The final concentration of Chlor (chloramphenicol) in the eppendorfs was 0.05 mg/ml. The final isomer concentrations (mg/ml) are indicated on the graph. Values indicated are the mean \pm s.d. of quadruplicates.	92
Figure 3. 14: Resultant % viability of 0.5×10^6 cells/ml E. coli after exposure to the isomers at various concentrations for 24 hrs, as determined by the TTC assay. The final concentration of Chlor (chloramphenicol) in the eppendorfs was 0.05 mg/ml. The final isomer concentrations (mg/ml) are indicated on the graph. Values indicated are the mean \pm s.d. of quadruplicates.	93
Figure 3. 15: Resultant % viability of 0.5×10^6 cells/ml P. aeruginosa after exposure to the isomers at various concentrations for 24 hrs, as determined by the MTT assay. The final concentration of Chlor (chloramphenicol) in the eppendorfs was 0.05 mg/ml. The final isomer concentrations (mg/ml) are indicated on the graph. Values indicated are the mean \pm s.d. of quadruplicates.	94
Figure 3. 16: Resultant % viability of 0.5×10^6 cells/ml P. aeruginosa after exposure to the isomers at various concentrations for 24 hrs, as determined by the TTC assay. The final concentration of Chlor (chloramphenicol) in the eppendorfs was 0.05 mg/ml. The final isomer concentrations (mg/ml) are indicated on the graph. Values indicated are the mean \pm s.d. of quadruplicates.	95
Figure 3. 17: Resultant % viability of 0.5×10^6 cells/ml S. aureus after exposure to the isomers at various concentrations for 24 hrs, as determined by the MTT assay. The final concentration of Chlor (chloramphenicol) in the eppendorfs was 0.05 mg/ml. The final isomer concentrations (mg/ml) are indicated on the graph. Values indicated are the mean \pm s.d. of quadruplicates.	97
Figure 3. 18: Resultant % viability of 0.5×10^6 cells/ml Streptococcus after exposure to the isomers at various concentrations for 24 hrs, as determined by the MTT assay. The final concentration of Chlor (chloramphenicol) in the eppendorfs was 0.05 mg/ml. The final isomer concentrations (mg/ml) are indicated on the graph. Values indicated are the mean \pm s.d. of quadruplicates.	98

Figure 3. 19: Resultant % viability of 1×10^6 cells/ml *C. albicans* after exposure to the isomers at various concentrations for 24 hrs, as determined by the MTT assay. The final concentration of Ampho (Amphotericin B) in the eppendorfs was 0.125 mg/ml. Flucon (Fluconazole) was tested at final concentrations of 0.5 mg/ml (green bar) and 5 mg/ml (blue bar). The final isomer concentrations (mg/ml) are indicated on the graph. Values indicated are the mean \pm s.d. of quadruplicates. 100

Figure 3. 20: Resultant % viability of 1×10^6 cells/ml *C. albicans* after exposure to the isomers at various concentrations for 24 hrs, as determined by the XTT assay. The final concentration of Ampho (Amphotericin B) in the eppendorfs was 0.125 mg/ml. Flucon (Fluconazole) was tested at final concentrations of 0.5 mg/ml (green bar) and 5 mg/ml (blue bar). The final isomer concentrations (mg/ml) are indicated on the graph. Values indicated are the mean \pm s.d. of quadruplicates. 101

Figure 4. 1: Growth of a neoplasia. Tumour growth overtakes that of normal tissue as a result of a loss in regulation mechanisms that control cell growth. A neoplastic mass is formed (Nowak and Handford, 1999. Pg. 121). 106

Figure 4. 2: The eucaryotic cell cycle. The phases through which the cell must pass from one division to the next is shown (Karp, 1996. Pg. 602). 107

Figure 4. 3: Typical tumour structure. (a) A benign tumour (b) A malignant tumour (Nowak and Handford, 1999. Pg. 126). 111

Figure 4. 4: Structure of melphalan (Salmon and Sartorelli, 1989. Pg. 686). 124

Figure 4. 5: Correlation between HT-29 cell number and MTT formazan crystal production. $R^2=0.9994$. Values indicated are the mean \pm s.d. of quadruplicates. 126

Figure 4. 6: Correlation between MCF-7 cell number and MTT formazan crystal production. $R^2=0.9954$. Values indicated are the mean \pm s.d. of quadruplicates. 127

Figure 4. 7: Correlation between HeLa cell number and MTT formazan crystal production. $R^2=0.9935$. Values indicated are the mean \pm s.d. of quadruplicates. 127

Figure 4. 8: Growth curve of HT-29 cells in a microtiter plate over a 7 day period. Values indicated are the mean \pm s.d. of quadruplicates. 129

Figure 4. 9: Growth curve of MCF-7 cells in a microtiter plate over a 7 day period. Values indicated are the mean \pm s.d. of quadruplicates. 129

Figure 4. 10: Growth curve of HeLa cells in a microtiter plate over a 7 day period. Values indicated are the mean \pm s.d. of quadruplicates. 130

Figure 4. 11: The effect of cyclo(L-Trp-L-Pro) on HT-29, MCF-7 and HeLa growth after a 24 hr exposure period. Final concentrations of cyclo(L-Trp-L-Pro) are indicated. Values indicated are the mean \pm s.d. of quadruplicates. 131

Figure 4. 12: The effect of cyclo(L-Trp-L-Pro) on HT-29, MCF-7 and HeLa growth after a 72 hr exposure period. Final concentrations of cyclo(L-Trp-L-Pro) are indicated. Values indicated are the mean \pm s.d. of quadruplicates. 132

Figure 4. 13: The effect of cyclo(L-Trp-D-Pro) on HT-29, MCF-7 and HeLa growth after a 24 hr exposure period. Final concentrations of cyclo(L-Trp-D-Pro) are indicated. Values indicated are the mean \pm s.d. of quadruplicates. 132

Figure 4. 14: The effect of cyclo(L-Trp-D-Pro) on HT-29, MCF-7 and HeLa growth after a 72 hr exposure period. Final concentrations of cyclo(L-Trp-D-Pro) are indicated. Values indicated are the mean \pm s.d. of quadruplicates. 133

Figure 4. 15: The effect of cyclo(D-Trp-L-Pro) on HT-29, MCF-7 and HeLa growth after a 24 hr exposure period. Final concentrations of cyclo(D-Trp-L-Pro) are indicated. Values indicated are the mean \pm s.d. of quadruplicates.	134
Figure 4. 16: The effect of cyclo(D-Trp-L-Pro) on HT-29, MCF-7 and HeLa growth after a 72 hr exposure period. Final concentrations of cyclo(D-Trp-L-Pro) are indicated. Values indicated are the mean \pm s.d. of quadruplicates.	135
Figure 4. 17: The effect of cyclo(D-Trp-D-Pro) on HT-29, MCF-7 and HeLa growth after a 24 hr exposure period. Final concentrations of cyclo(D-Trp-D-Pro) are indicated. Values indicated are the mean \pm s.d. of quadruplicates.	136
Figure 4. 18: The effect of cyclo(D-Trp-D-Pro) on HT-29, MCF-7 and HeLa growth after a 72 hr exposure period. Final concentrations of cyclo(D-Trp-D-Pro) are indicated. Values indicated are the mean \pm s.d. of quadruplicates.	137
Figure 4. 19: The effect of melphalan on HT-29, MCF-7 and HeLa growth after a 24 hr exposure period. Final concentrations of melphalan are indicated. Values indicated are the mean \pm s.d. of quadruplicates.	138
Figure 4. 20: The effect of melphalan on HT-29, MCF-7 and HeLa growth after a 72 hr exposure period. Final concentrations of melphalan are indicated. Values indicated are the mean \pm s.d. of quadruplicates.	139
Figure 4. 21: Alkaline phosphatase activity in HT-29 cells, as a result of exposure to the isomers or melphalan at 10^{-3} M. Values indicated are the mean \pm s.d. of quadruplicates.	143
Figure 4. 22: Alkaline phosphatase activity in MCF-7 cells, as a result of exposure to the isomers or melphalan at 10^{-3} M. Values indicated are the mean \pm s.d. of quadruplicates.	144
Figure 4. 23: Alkaline phosphatase activity in HeLa cells, as a result of exposure to the isomers or melphalan at 10^{-3} M. Values indicated are the mean \pm s.d. of quadruplicates.	145
Figure 5. 1: The anterior surface of the liver, showing the right and left lobes, as well as the falciform ligament (Martini, 1995. Pg. 910).....	147
Figure 5. 2: Diagrammatic view of lobular organization (Martini, 1995. Pg. 911).	148
Figure 5. 3: Mechanisms involved in Ca^{2+} -mediated cell killing (Adapted from Orrenius et al., 1989). TCDD = 2,3,7,8-tetrachlorodibenzo-p-dioxin.....	161
Figure 5. 4: An illustration of the perfusion apparatus. (1) perfusion pump; (2) heating unit; (3) cannula unit; (4) liver support dish (in this instance, a sterilized wire mesh covered with sterile gauze was used); (5) perfusate reservoir (in the set-up used, the perfusate reservoir consisted of a perspex block that allowed drainage of perfusate for recirculation) (Adapted from Seglen, 1994. Pg. 97).....	172
Figure 5. 5: Rates of blood absorption of cyclo(L-Trp-L-Pro) and cyclo(L-Trp-D-Pro) in the rat. Values indicated are the mean \pm s.d. of triplicates.	188
Figure 5. 6: Liver cells in suspension (stained with trypan blue) prepared by the two-step collagenase perfusion method (The photograph was taken at a magnification of 272x, using a phase contrast filter 2 and $\frac{1}{8}$ s shutter speed).....	189
Figure 5. 7: Effects of the compounds on the viability of isolated rat hepatocytes. LL = cyclo(L-Trp-L-Pro); LD = cyclo(L-Trp-D-Pro); DL = cyclo(D-Trp-L-Pro); DD = cyclo(D-Trp-D-Pro). Values indicated are the mean \pm s.d. of 6 experiments per day per treatment.	190

Figure 5. 8: Effects of the compounds on the viability of Chang liver cells. LL = cyclo(L-Trp-L-Pro); LD = cyclo(L-Trp-D-Pro); DL = cyclo(D-Trp-L-Pro); DD = cyclo(D-Trp-D-Pro). Values indicated are the mean \pm s.d. of 6 experiments per day per treatment. 191

Figure 5. 9: Effects of the compounds on the viability of N-2-alpha cells. LL = cyclo(L-Trp-L-Pro); LD = cyclo(L-Trp-D-Pro); DL = cyclo(D-Trp-L-Pro); DD = cyclo(D-Trp-D-Pro). Values indicated are the mean \pm s.d. of 6 experiments per day per treatment. 192

Figure 5. 10: Effects of the compounds on wet liver weight, represented as a % of the total body weight. LL = cyclo(L-Trp-L-Pro); LD = cyclo(L-Trp-D-Pro); DL = cyclo(D-Trp-L-Pro); DD = cyclo(D-Trp-D-Pro). Values indicated are the mean \pm s.d. of 6 experiments per day per treatment. 194

Figure 5. 11: Effects of the compounds on lactate dehydrogenase activity in the blood stream. LL = cyclo(L-Trp-L-Pro); LD = cyclo(L-Trp-D-Pro); DL = cyclo(D-Trp-L-Pro); DD = cyclo(D-Trp-D-Pro). Values indicated are the mean \pm s.d. of 6 experiments per day per treatment. 196

Figure 5. 12: Effects of the compounds on the levels of alkaline phosphatase in the serum. LL = cyclo(L-Trp-L-Pro); LD = cyclo(L-Trp-D-Pro); DL = cyclo(D-Trp-L-Pro); DD = cyclo(D-Trp-D-Pro). Values indicated are the mean \pm s.d. of 6 experiments per day per treatment. 198

Figure 5. 13: Effects of the compounds on the concentration of aspartate transaminase in the blood stream. LL = cyclo(L-Trp-L-Pro); LD = cyclo(L-Trp-D-Pro); DL = cyclo(D-Trp-L-Pro); DD = cyclo(D-Trp-D-Pro). Values indicated are the mean \pm s.d. of 6 experiments per day per treatment. 199

Figure 5. 14: Effects of the compounds on alanine transaminase levels in the blood stream. LL = cyclo(L-Trp-L-Pro); LD = cyclo(L-Trp-D-Pro); DL = cyclo(D-Trp-L-Pro); DD = cyclo(D-Trp-D-Pro). Values indicated are the mean \pm s.d. of 6 experiments per day per treatment. 200

Figure 5. 15: Effects of the compounds on lipid peroxidation, as measured in terms of malondialdehyde concentrations in the serum of the rats. LL = cyclo(L-Trp-L-Pro); LD = cyclo(L-Trp-D-Pro); DL = cyclo(D-Trp-L-Pro); DD = cyclo(D-Trp-D-Pro). Values indicated are the mean \pm s.d. of 6 experiments per day per treatment. 201

Figure 5. 16: Effects of the compounds on energy metabolism in rat hepatocytes, measured in terms of ATP concentrations in the blood stream. LL = cyclo(L-Trp-L-Pro); LD = cyclo(L-Trp-D-Pro); DL = cyclo(D-Trp-L-Pro); DD = cyclo(D-Trp-D-Pro). Values indicated are the mean \pm s.d. of 6 experiments per day per treatment. 203

Figure 5. 17: Effects of the compounds on Ca^{2+} -levels in the blood stream. LL = cyclo(L-Trp-L-Pro); LD = cyclo(L-Trp-D-Pro); DL = cyclo(D-Trp-L-Pro); DD = cyclo(D-Trp-D-Pro). Values indicated are the mean \pm s.d. of 6 experiments per day per treatment. 204

Figure 5. 18: Effects of the compounds hepato-protective mechanisms, as measured by the levels of reduced glutathione present in the blood stream. LL = cyclo(L-Trp-L-Pro); LD = cyclo(L-Trp-D-Pro); DL = cyclo(D-Trp-L-Pro); DD = cyclo(D-Trp-D-Pro). Values indicated are the mean \pm s.d. of 6 experiments per day per treatment. 205

Figure 5. 19: Effects of the compounds on ureogenesis, as measured by urea nitrogen levels in the blood stream. LL = cyclo(L-Trp-L-Pro); LD = cyclo(L-Trp-D-Pro); DL = cyclo(D-Trp-L-Pro); DD = cyclo(D-Trp-D-Pro). Values indicated are the mean \pm s.d. of 6 experiments per day per treatment. 206

Figure 5. 20: Effects of the compounds on protein synthesis, as measured by albumin concentrations in the blood stream. LL = cyclo(L-Trp-L-Pro); LD = cyclo(L-Trp-D-Pro);

<i>DL = cyclo(D-Trp-L-Pro); DD = cyclo(D-Trp-D-Pro). Values indicated are the mean ± s.d. of 6 experiments per day per treatment.</i>	208
<i>Figure 5. 21: Effects of the compounds on the total bilirubin content in the blood stream.</i>	
<i>LL = cyclo(L-Trp-L-Pro); LD = cyclo(L-Trp-D-Pro); DL = cyclo(D-Trp-L-Pro); DD = cyclo(D-Trp-D-Pro). Values indicated are the mean ± s.d. of 6 experiments per day per treatment.</i>	209
<i>Figure 6. 1: The vascular and platelet phases of haemostasis (Martini, 1995. Pg. 671).</i>	
.....	214
<i>Figure 6. 2: The blood coagulation cascade, showing the extrinsic, intrinsic and common pathways. The green arrows indicate the positive feedback effects of thrombin (Tortora and Grabowski, 2000. Pg. 625).</i>	219
<i>Figure 6. 3: Linear relationship between platelet number and optical density. $R^2 = 0.9912$;</i>	231
<i>Figure 6. 4: Aggregation curves of washed platelets stimulated with varying concentrations of thrombin. Final concentrations of thrombin in the wells are indicated on the graph. Values indicated are the mean ± s.d. of quadruplicates.</i>	232
<i>Figure 6. 5: Aggregation curves obtained when washed platelets, stimulated by thrombin at a final concentration of 1.25 U/ml, were exposed to each isomer at a final concentration of 1 mM. Values indicated are the mean ± s.d. of quadruplicates.</i>	233
<i>Figure 6. 6: The effect of differing concentration of cyclo(L-Trp-D-Pro) on aggregation stimulated by thrombin at a final concentration of 1.25 U/ml. Concentrations of cyclo(L-Trp-D-Pro) indicated are the final concentrations in the wells. Values indicated are the mean ± s.d. of quadruplicates.</i>	234
<i>Figure 6. 7: Aggregation curves of PRP stimulated with varying concentrations of ADP. Final concentrations of ADP in the wells are indicated on the graph. Values indicated are the mean ± s.d. of quadruplicates.</i>	235
<i>Figure 6. 8: Aggregation curves of ADP-stimulated platelets in plasma with varying concentrations of cyclo(L-Trp-L-Pro). The respective final concentrations in the wells are indicated on the graph. Values indicated are the mean ± s.d. of quadruplicates.</i> ...	236
<i>Figure 6. 9: Aggregation curves of ADP-stimulated platelets in plasma with varying concentrations of cyclo(L-Trp-D-Pro). The respective final concentrations in the wells are indicated on the graph. Values indicated are the mean ± s.d. of quadruplicates.</i> ...	237
<i>Figure 6. 10: Aggregation curves of ADP-stimulated platelets in plasma with varying concentrations of cyclo(D-Trp-L-Pro). The respective final concentrations in the wells are indicated on the graph. Values indicated are the mean ± s.d. of quadruplicates.</i> ...	237
<i>Figure 6. 11: Aggregation curves of ADP-stimulated platelets in plasma with varying concentrations of cyclo(D-Trp-D-Pro). The respective final concentrations in the wells are indicated on the graph. Values indicated are the mean ± s.d. of quadruplicates.</i> ...	238
<i>Figure 6. 12: Progress curves obtained in the presence of varying concentrations of thrombin. Final concentrations of thrombin in the wells are indicated on the graph. Values indicated are the mean ± s.d. of quadruplicates.</i>	240
<i>Figure 6. 13: Correlation between thrombin concentration and change in absorbance over the linear portion of the progress curves. $R^2=0.9905$. Final concentrations of thrombin in the wells are indicated. Values indicated are the mean ± s.d. of quadruplicates.</i>	241

Figure 6. 14: Progress curves in the presence of cyclo(L-Trp-L-Pro). Final concentrations of the respective compounds are indicated on the graph. Values indicated are the mean \pm s.d. of quadruplicates. 242

Figure 6. 15: Progress curves in the presence of cyclo(L-Trp-D-Pro). Final concentrations of the respective compounds are indicated on the graph. Values indicated are the mean \pm s.d. of quadruplicates. 243

Figure 6. 16: Progress curves in the presence of cyclo(D-Trp-L-Pro). Final concentrations of the respective compounds are indicated on the graph. Values indicated are the mean \pm s.d. of quadruplicates. 243

Figure 6. 17: Progress curves in the presence of cyclo(D-Trp-D-Pro). Final concentrations of the respective compounds are indicated on the graph. Values indicated are the mean \pm s.d. of quadruplicates. 244

Figure 6. 18: Linear relationship between acid phosphatase activity and platelet number. Values indicated are mean \pm s.d. of quadruplicates. $R^2=0.9906$ 247

Figure 6. 19: The effects of various concentrations of ADP on platelet adhesion to a plasma-coated surface. Final concentrations of ADP in the wells are indicated on the graph. Values indicated are mean \pm s.d. of quadruplicates. 248

Figure 6. 20: The effects of various concentrations of thrombin on platelet adhesion to a plasma-coated surface. Final concentrations of thrombin in the wells are indicated on the graph. Values indicated are mean \pm s.d. of quadruplicates. 248

Figure 6. 21: Percentage adhesion of platelets, stimulated with 3.125 μ M ADP, in the presence of cyclo(Trp-Pro) isomers at final concentrations as indicated on the graph. Values indicated are mean \pm s.d. of quadruplicates. 249

Figure 6. 22: % Adhesion of platelets, stimulated with 0.1563 U/ml thrombin, in the presence of cyclo(Trp-Pro) isomers at final concentrations as indicated on the graph. Values indicated are mean \pm s.d. of quadruplicates. 250

Figure 7. 1: The anterior view of the heart, showing major anatomical features (Martini, 1995. Pg. 685). 254

Figure 7. 2: The three stages of an action potential in cardiac muscle (Martini, 1995. Pg. 696). 257

Figure 7. 3: Ion distribution across the cell membrane. At the resting potential, 3 Na^+ enter the cell for every 2 K^+ that leave the cell. These movements are countered by the Na^+ - K^+ exchange pump (Martini, 1995. Pg. 83). 258

Figure 7. 4: Voltage-operated Ca^{2+} -channel (Barritt, 1999). 259

Figure 7. 5: An electrocardiogram, indicating the major components and the measurements most often taken during clinical analysis (Martini, 1995. Pg. 701). 263

Figure 7. 6: Patch-clamp configurations (Cahalan and Neher, 1992). 267

Figure 7. 7: The Langendorff perfusion apparatus. Two perfusate reservoirs are shown with a single bubble-trap situated above the aortic cannula. In this set-up, the atria are left intact (Lubbe et al., 1978). 271

Figure 7. 8: The experimental protocol for the isolated rat heart perfusion. T= time in minutes, HR= heart rate, CF= coronary flow. 273

Figure 7. 9: The current-voltage relationship of inward currents recorded with the addition of 100 μ M cyclo (L-Trp-L-Pro). (■) = Control after 10 min (to ensure stable current). (●) = 100 μ M cyclo(L-Trp-L-Pro) for 1 min. (▲) = 100 μ M cyclo(L-Trp-L-Pro)

for 5 min. (▼) = Washout period of 1 min. (◆) = Washout period of 7 min. I_{Ca} = inward current flow. Values indicated are the mean \pm s.d of duplicates..... 274

Figure 7. 10: The current-voltage relationship of inward currents recorded with the addition of 100 μ M cyclo(L-Trp-L-Pro). (-) = Control after 10 min (to ensure stable current). (-) = 100 μ M cyclo(L-Trp-L-Pro) for 1 min. (-) = 100 μ M cyclo(L-Trp-L-Pro) for 5 min. (-) = Washout period of 1 min. 275

Figure 7. 11: The current-voltage relationship of inward currents recorded with the addition of 100 μ M cyclo(L-Trp-L-Pro). (■) = Control after 10 min (to ensure stable current). (●) = Second control current. (▲) = 100 μ M cyclo(L-Trp-L-Pro) for 1 min. (▼) = 100 μ M cyclo(L-Trp-L-Pro) for 3 min. (◆) = Washout period of 3 min. IK_1 = inward rectifier K^+ -current. Values indicated are the mean \pm s.d of duplicates. 276

Figure 7. 12: The current-voltage relationship of inward currents recorded with the addition of 100 μ M cyclo(L-Trp-D-Pro). (■) = Control after 10 min (to ensure stable current). (●) = 100 μ M cyclo(L-Trp-D-Pro) for 1 min. (▲) = 100 μ M cyclo(L-Trp-D-Pro) for 5 min. (◆) = Washout period of 4 min. I_{Ca} = inward current flow. (n=2) 276

Figure 7. 13: The current-voltage relationship of inward currents recorded with the addition of 100 μ M cyclo(L-Trp-D-Pro). (-) = Control after 10 min (to ensure stable current). (-) = 100 μ M cyclo(L-Trp-D-Pro) for 1 min. (-) = 100 μ M cyclo(L-Trp-D-Pro) for 5 min. (-) = Washout period of 7 min. I_{Ca} = inward current flow. (n=2) 277

Figure 7. 14: The current-voltage relationship of inward currents recorded with the addition of 100 μ M cyclo(L-Trp-D-Pro). (●) = Control after 10 min (to ensure stable current). (▲) = 100 μ M cyclo(L-Trp-D-Pro) for 1 min. (◆) = 100 μ M cyclo(L-Trp-D-Pro) for 3 min. (-+-) = Washout period of 3 min. IK_1 = inward rectifier K^+ -current. Values indicated are the mean \pm s.d of duplicates..... 278

Figure 7. 15: The current-voltage relationship of inward currents recorded with the addition of 100 μ M cyclo(D-Trp-L-Pro). (■) = Control 1 current after 10 min (to ensure stable current). (●) = Control 2 current. (▲) = 100 μ M cyclo(D-Trp-L-Pro) for 1 min. (▼) = 100 μ M cyclo(D-Trp-L-Pro) of 5 min. (◆) = Washout period of 1 min. (-+-) = Washout period for 5 min. I_{Ca} = inward current flow. Values indicated are the mean \pm s.d of duplicates. 278

Figure 7. 16: The current-voltage relationship of inward currents recorded with the addition of 100 μ M cyclo(D-Trp-L-Pro). (-) = Control after 10 min (to ensure stable current). (-) = 100 μ M cyclo(D-Trp-L-Pro) for 1 min. (-) = 100 μ M cyclo(D-Trp-L-Pro) for 5 min. (-) = Washout period of 1 min. (-) = Washout period of 5 min. I_{Ca} = inward current flow..... 279

Figure 7. 17: The current-voltage relationship of inward currents recorded with the addition of 100 μ M cyclo(D-Trp-L-Pro). (■) = Control after 10 min (to ensure stable current). (●) = 100 μ M cyclo(D-Trp-L-Pro) for 1 min. (▲) = 100 μ M cyclo(D-Trp-L-Pro) for 3 min. (▼) = Washout period of 3 min. IK_1 = inward rectifier K^+ -current. Values indicated are the mean \pm s.d of duplicates..... 279

Figure 7. 18: The current-voltage relationship of inward currents recorded with the addition of 100 μ M cyclo(D-Trp-D-Pro). (■) = Control after 10 min (to ensure stable current). (●) = 100 μ M cyclo(D-Trp-D-Pro) for 1 min. (▲) = Washout period of 5 min. I_{Ca} = inward current flow. Values indicated are the mean \pm s.d of duplicates. 280

Figure 7. 19: The current-voltage relationship of inward currents recorded with the addition of 100 μ M cyclo(D-Trp-D-Pro). (-) = Control after 10 min (to ensure stable

current). (-) = 100 μ M cyclo(D-Trp-D-Pro) for 1 min. (-) = 100 μ M cyclo(D-Trp-D-Pro) for 5 min. (-) = Washout period of 5 min. I _{Ca} = inward current flow.....	280
Figure 7. 20: The current-voltage relationship of inward currents recorded with the addition of 100 μ M cyclo(D-Trp-D-Pro). (■) = Control after 10 min (to ensure stable current). (●) = 100 μ M cyclo(D-Trp-D-Pro) for 1 min. (▲) = 100 μ M cyclo(D-Trp-D-Pro) for 3 min. (▼) = Washout period of 3 min. I _{K1} = inward rectifier K ⁺ -current. Values indicated are the mean \pm s.d of duplicates.....	281
Figure 7. 21: Effect of the isomers on the heart rate in isolated, rat heart. Values indicated are the mean \pm s.d of 6 experiments.....	284
Figure 7. 22: The effects of the isomers on coronary flow rate as determined in the isolated rat heart. Values indicated are the mean \pm s.d of 6 experiments.....	287
Figure 7. 23 A-F: Segments of ECGs showing (A) normal sinus rhythm (SR); (B) ventricular tachycardia (VT); (C) arrhythmias; (D) SR changing to VT; (E) VT changing to VA; and (F) VT changing to sinus rhythm, as recorded in the rat isolated heart.	290
Figure 7. 24: The time to stop VT (ventricular tachycardia), VA (ventricular arrhythmias) and time to return to SR (normal sinus rhythm) in the presence of 200 μ M LL (cyclo(L-Trp-L-Pro)), LD (cyclo(L-Trp-D-Pro)), DL (cyclo(D-Trp-L-Pro)) and DD (cyclo(D-Trp-D-Pro)). Values indicated are the mean \pm s.d of 6 experiments.	291
Figure 7. 25: QRS intervals as measured with perfusion of the isomers, from 15 min to 30 min. Values indicated are the mean \pm s.d of 6 experiments.....	294

Figure B1. 1: IR spectrum of cyclo(L-Trp-L-Pro).....	317
Figure B1. 2: IR spectrum of cyclo(L-Trp-D-Pro).....	318
Figure B1. 3: IR spectrum of cyclo(D-Trp-L-Pro).....	319
Figure B1. 4: IR spectrum of cyclo(D-Trp-D-Pro).....	320
Figure B1. 5: DSC thermogram for cyclo(L-Trp-L-Pro).....	321
Figure B1. 6: DSC thermogram for cyclo(L-Trp-D-Pro).....	322
Figure B1. 7: DSC thermogram for cyclo(D-Trp-L-Pro).....	323
Figure B1. 8: DSC thermogram for cyclo(D-Trp-D-Pro).....	324
Figure B1. 9: COSY spectrum of cyclo(D-Trp-D-Pro) in DMSO-d ₆	325
Figure B1. 10: Hetcor spectrum of cyclo(D-Trp-D-Pro) in DMSO-d ₆	326

Figure B2. 1: Correlation between turbidity of E. coli (540 nm) and MTT formazan production, measured at 540 nm. R ² =0.9936. Values indicated are the mean \pm s.d. of triplicates.	328
Figure B2. 2: Correlation between turbidity of E. coli (540 nm) and TTC formazan production, measured at 492 nm. R ² =0.9975. Values indicated are the mean \pm s.d. of triplicates.	329
Figure B2. 3: Correlation between turbidity of P. aeruginosa (540 nm) and MTT formazan production, measured at 540 nm. R ² =0.9958. Values indicated are the mean \pm s.d. of triplicates.....	329
Figure B2. 4: Correlation between turbidity of P. aeruginosa (540 nm) and TTC formazan production, measured at 492 nm. R ² =0.9967. Values indicated are the mean \pm s.d. of triplicates.	330

<i>Figure B2. 5: Correlation between turbidity of S. aureus (540 nm) and MTT formazan production, measured at 540 nm. R²=0.9945. Values indicated are the mean ± s.d. of triplicates.</i>	330
<i>Figure B2. 6: Correlation between turbidity of Streptococcus (540 nm) and MTT formazan production, measured at 540 nm. R²=0.9973. Values indicated are the mean ± s.d. of triplicates.</i>	331
<i>Figure B2. 7: Correlation between turbidity of C. albicans (600 nm) and MTT formazan production, measured at 540 nm. R²=0.9943. Values indicated are the mean ± s.d. of triplicates.</i>	331
<i>Figure B2. 8: Correlation between turbidity of C. albicans (600 nm) and XTT formazan production, measured at 492 nm. R²=0.9790. Values indicated are the mean ± s.d. of triplicates.</i>	332
<i>Figure B3. 1: Alkaline phosphatase standard curve (anticancer study). R²=0.9989.....</i>	332
<i>Figure B4. 1: Standard curve of cyclo(L-Trp-L-Pro) vs area (HPLC). R²=0.9988.....</i>	333
<i>Figure B4. 2: Standard curve of cyclo(L-Trp-D-Pro) vs area (HPLC). R²=0.9996.....</i>	333
<i>Figure B4. 3: Standard curve of cyclo(D-Trp-L-Pro) vs area (HPLC). R²=0.9983.....</i>	333
<i>Figure B4. 4: Standard curve of cyclo(D-Trp-D-Pro) vs area (HPLC). R²=0.9985.....</i>	334
<i>Figure B4. 5: Standard curve of isolated hepatocyte cell number vs MTT absorbance. R²=0.9985.....</i>	334
<i>Figure B4. 6: Standard curve of Chang liver cell number vs MTT absorbance. R²=0.9993.....</i>	334
<i>Figure B4. 7: Standard curve of N-2-alpha cell number vs MTT absorbance. R²=0.9985.....</i>	335
<i>Figure B4. 8: Alkaline phosphatase standard curve (hepatotoxicity study). R²=0.9970.....</i>	335
<i>Figure B4. 9: Aspartate transaminase standard curve. R²=0.9968.....</i>	336
<i>Figure B4. 10: Alanine transaminase standard curve. R²=0.9994.....</i>	336
<i>Figure B4. 11: Glutathione standard curve. R²=0.9988.....</i>	336
<i>Figure B4. 12: Bilirubin standard curve. R²=0.9983.....</i>	337

LIST OF TABLES

<i>Table 1. 1: Characteristics of tryptophan (Lehninger et al., 2000. Pg. 118).</i>	12
<i>Table 1. 2: Characteristics of proline (Lehninger et al., 2000. Pg 118).</i>	16
<i>Table 2. 1: Materials used in the synthesis of the isomers.</i>	23
<i>Table 3. 1: Mechanisms of antibacterial actions (Adapted from Volk et al., 1996. Pp. 253-285, 474-495).</i>	65
<i>Table 3. 2: Factors influencing formazan production in the cell.</i>	81
<i>Table 3. 3: MIC values of selected cyclic dipeptides against bacteria using the Kirby Bauer disc-diffusion method (Milne et al., 1998).</i>	104
<i>Table 4. 1: Concentrations of isomers producing similar effects as melphalan after a 72 hr exposure period.</i>	140
<i>Table 4. 2: IC₅₀ values of a number of commonly used drugs (Adapted from Jover et al., 1992).</i>	141
<i>Table 4. 3: IC₅₀ values of 3 chemotherapeutic agents against selected mouse cells (Adapted from Arnould et al., 1990).</i>	142
<i>Table 5. 1: Disease states associated with various protein compositions (Baron, 1982, Pp. 116-7).</i>	149
<i>Table 5. 2: Reaction mixtures for ALT and AST calibration curves.</i>	178
<i>Table 5. 3: Percentage binding of albumin to the isomers as determined by equilibrium dialysis. Values indicated are the mean ± s.d. of 6 experiments.</i>	186
<i>Table 5. 4: Average number of isomer bound per mole of albumin.</i>	187
<i>Table 5. 5: Concentrations of drugs resulting in a 50% reduction in cell viability (MTT₅₀) in three different cell types.</i>	193
<i>Table 5. 6 : A summary of the effects of the isomers and isoniazid on liver metabolism. Significant changes indicated show alterations that would adversely affect liver metabolism.</i>	211
<i>Table 6. 1: Procoagulation factors (Tortora and Grabowski, 2000. Pg. 626).</i>	216
<i>Table 7. 1: Advantages and disadvantages of the use of the rat model in myocardial infarction studies (Curtis et al., 1987).</i>	265
<i>Table 7. 2: Effects of the isomers on L-type Ca²⁺-channel activity.</i>	281
<i>Table 7. 3: Correlation data of the effects of the isomers on heart rate in the isolated, perfused rat heart.</i>	285
<i>Table 7. 4: Correlation data of the effects of the isomers on coronary flow in the isolated, perfused rat heart.</i>	287

<i>Table A. 1: Abbreviations and symbols of the amino acids as used in the text (Lehninger et al., 2000. Pg. 118).</i>	315
<i>Table B. 1: Dilutions of the different microbial cultures.</i>	328

CHAPTER 1

LITERATURE REVIEW

1.1 INTRODUCTION

Of the somewhat 30 000 known human diseases, only a disappointing one third of these diseases are treatable, while numerous others including central nervous system disorders and cancer are incurable (Hider, 1998). There is thus increased pressure in discovering new drugs that are more active and selective, produce little or no side effects and will not negatively influence the already disrupted environment. The emergence of multi-drug resistant microorganisms have added to the urgency in discovering novel drugs, a process that can take up to 20 years before a product reaches the market place. Thus, any advancement in technology that will reduce this time period to 1-2 years will, no doubt, become the major focus of the pharmaceutical scientist (Myers, 1997).

1.1.1 The diketopiperazines

As early as 1888, the parent compound, commonly referred to as cyclo(Gly-Gly)¹ was synthesized by Curtis and Gloebel (Prasad, 1995). In contrast to ordinary peptides, diketopiperazines (DKPs) or dioxipiperazines (DOPs) (Figure 1.1) are only slightly soluble in water and the simpler members occur as neutral compounds. In chemical reactions, no test is given with ninhydrin and, on reaction with picric acid, a reddish brown colour results. A white precipitate is produced when a DKP with unsubstituted nitrogen atoms of the piperazine ring is reacted with potassium mercuric iodide. DKPs containing aromatic side chains are useful as models for the determination of the optical behaviour of aromatic and peptide chromophores in proteins. In addition, they are also used to study the influence of solvents on the intramolecular interactions existing during chromophore excitation (Edelhoc *et al.*, 1968).

¹ Amino acid abbreviations are listed in Table A.1, Appendix A.

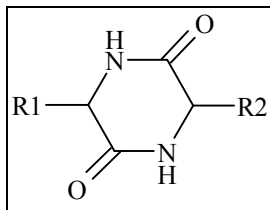


Figure 1. 1: General structure of a diketopiperazine, where R1 and R2 represent the substituting amino acid residues (Anteunis, 1978).

DKPs possess a number of biological properties in tissues and body fluids (Capasso *et al.*, 1998). DKPs are present in proteins and polypeptide hydrolysates (cyclo(Leu-Trp)) (Szafranek *et al.*, 1976), fermentation broths and cultures of yeasts, lichens and fungi (Prasad, 1995).

Some derivatives of DKPs show antiviral activities (gliotoxin, sporidesmins), potential as antibiotics (bicyclomycins, actinomycin), whilst others are phytotoxic (cyclo(Pro-Tyr)) (Prasad, 1995). They are formed spontaneously from higher linear peptides containing proline residues and serve as excellent models for theoretical studies as a result of their relative simplicity. In addition, they are useful tools in the study of peptide conformation (Szafranek *et al.*, 1976) and have been exploited for preparative purposes as a result of their sensitivity to oxidation. Furthermore, the DKP structures have also been used as intermediates during preparative strategies. The destruction of the secondary globular structure of a protein may be initiated by some DKPs (Anteunis, 1978). The N-terminal deprotonated amino group's nitrogen atom attacks the carbon of the carboxyl group of a second amino acid residue. The resultant formation of the DKP ring breaks the chain, thereby destroying the globular structure of the protein (Capasso *et al.*, 1998). Some N-acylated DKPs are useful in the preparation of cyclic depsipeptides. Cyclo(Leu-Trp), a bitter compound isolated from the fermentation of milk casein by *Bacillus subtilis*, opened up the field to flavour and fragrance properties. It was further noted that dipeptides became more bitter when blockage of both the amino and carboxyl groups occurred or the dipeptide was converted to a DKP. This phenomenon opened the field to the biological mechanism of taste exhibition (Shiba and Nunami, 1974). Cyclo(His-D-Leu) acts as a hydrolytic catalyst (Anteunis, 1978).

Cyclo(His-Pro) has been found at elevated levels in nutritional supplements originating from casein. At elevated temperatures, extremes in pH and/or moisture, the dipeptide sweetener aspartame is converted to cyclo(Asp-Phe). Simple DKPs are also synthesized by energy-dependent reactions by protists and plant kingdom members. Cyclo(Pro-Leu) and cyclo(Pro-Phe) are synthesized by *Rosellinia necatrix*, cyclo(Pro-Trp) by *Penicillium brevicompactum* and cyclo(Pro-Phe) by *Alternaria alternata* (Prasad, 1995).

To date, four naturally occurring DKPs that exhibit biological activity have been identified. These are cyclo(Leu-Gly), cyclo(Tyr-Arg) cyclo(Asp-Pro) and cyclo(His-Pro). Only cyclo(His-Pro) has been found to be endogenous in mammals (Prasad, 1995).

Cyclo(Leu-Gly) is structurally related to oxytocin and melanocyte-stimulating hormone release inhibiting factor. When this dipeptide occupies the carboxyl terminus of oxytocin, the molecule blocks puromycin-induced amnesia. It also acts to attenuate or block the development of physical dependence on morphine, tolerance to the pharmacological effects of β -endorphin, tolerance to haloperidol-induced catalepsy and hypothermia, and dopaminergic supersensitivity after chronic morphine administration (Prasad, 1995).

Cyclo(Tyr-Arg) exhibits high antinociceptive activity, while cyclo(Asp-Pro) decreases caloric intake in rats (Prasad, 1995).

1.1.2 Cyclo(His-Pro), an endogenous DKP

Cyclo(His-Pro) is an endogenous DKP that is found throughout the central nervous system and gastrointestinal tract (hypothalamus, stomach and esophagus), as well as a number of body fluids including cerebrospinal fluid, blood, urine, amniotic fluid, milk and semen (Prasad, 1995).

Cyclo(His-Pro) has been shown to attenuate the sedative effects of ethanol. When pain is induced by physical, mechanical, thermal and chemical stimuli, a role in the perception thereof is played by cyclo(His-Pro). It may also play a part in endogenous opioid-dependent antinociception. The analgesic effects of δ -9-tetrahydrocannabinol are attenuated by cyclo(His-Pro). In proestrus rats and GH3 cells in culture, cyclo(His-Pro)

has been shown to inhibit prolactin secretion. The excitory response to acetylcholine or quisqualic acid was enhanced by cyclo(His-Pro) in the cerebral cortex (Prasad, 1995).

1.1.3 Conformational features of DKPs

Cyclic dipeptides are useful for studying the influence that molecular forces impose on conformation. They provide excellent models in the conformation studies of various peptides (Szafranek *et al.*, 1976). For example, when no steric hindrance occurs, the side chain folds over the DKP ring, allowing the study of intramolecular stacking interactions that may play a role in various complex biomolecules (Ramani *et al.*, 1977).

The DKP ring (Figure 1.1) contains the atypical *cis*-amide bonds (Cotrait *et al.*, 1976). In the simplest case, the DKP ring structure is flanked by 2 hydrogen (H) atoms (Crescenzi *et al.*, 1973). The two *cis*-amide groups of the ring may form H bonds with the solvent or form hydrophobic interactions, depending on the substituents of the side chain groups (Crescenzi *et al.*, 1973). Derivatives of DKPs containing an aromatic side chain eg. phenylalanine or tryptophan (egs. include cyclo(Gly-Phe) and cyclo(Gly-Trp)), exhibits a shielding of the *cis*-disposed glyceryl H atom. This is explained by the side chain's aromatic ring that assumes a folded conformation over the DKP ring (Yamazaki *et al.*, 1991).

X-ray studies have shown that the six-membered DKP ring exists as either flat or slightly puckered forms, which are slightly flexible. Three conformations of the DKP ring have been identified in the solid state i.e. chairs, boat and twists (Figure 1.2) (Jankowska and Ciarkowski, 1987).

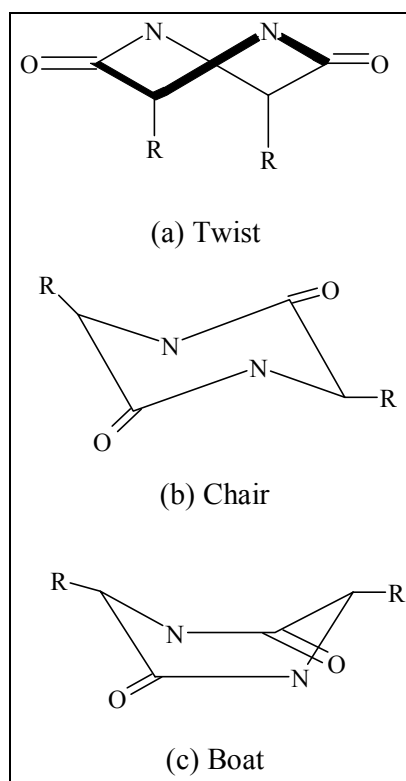


Figure 1. 2: Major conformations of the DKP ring in cyclic dipeptides. R represents the substituting amino acid residues (Adapted from Jankowska and Ciarkowski, 1987).

Due to the 2 *cis*-peptide bonds in the DKP rings that make it nearly planar, the occurrence of the twist-boat forms or chairs are less probable. When the constituting subunits are N-substituted and have opposite configuration, the chair conformation will result (Anteunis, 1978).

1.1.4 Factors affecting the conformation of the DKP ring

- Near planarity of two *cis*-peptide units – the ring will thus be flat or in a boat conformation, but not a chair conformation;
- Chirality; and
- Substitutions at the α -carbon atoms – if the substitutions differ and are of the same chirality, the DKP ring is buckled to a boat conformation, which is significant when the side chain contains proline (Ramani *et al.*, 1977).

The various forces resulting in a folded conformation of the DKP ring include dipole-induced dipole interactions, van der Waals forces, and interaction between aromatic π electrons and the polarised π system of the two amide groups (Ramani *et al.*, 1977).

When a cyclic dipeptide contains aromatic side chains, maximal overlap will occur between the DKP ring and aromatic ring, such as cyclo(Gly-X), where X is an aromatic amino acid (Deslauriers *et al.*, 1975).

When one considers a molecule such as cyclo(L-Y-L-X), an unfolded, buckled ring will result if Y is bulky. In this context, X refers to aromatic residues, while Y refers to non-aromatic residues. X will still interact with the DKP ring without interference between Y and X. If, however, both X and Y are non-aromatic, steric hinderance between X and Y will occur. This will result in the DKP ring taking on a boat conformation (Deslauriers *et al.*, 1975).

When the DKP ring-containing molecule has a centre of symmetry, eg. cyclo(L-Ala-D-Ala), the DKP ring exists in a planar conformation. However, when the ring is substituted in an unsymmetrical manner such as L-Pro-X derivatives (where X refers to any amino acid with the exception of Pro), the ring occurs in a buckled conformation (Edelhoch *et al.*, 1968).

1.1.5 Simple diketopiperazines

DKPs are widespread in nature as indicated by the various extracts and culture broths from which they were isolated. Several examples are listed below.

The antitumour compound, compound 593 A (Figure 1.3) is an unusual member of the simple DKPs. Alternatively referred to as 3,6-bis(5-chloro-2-piperidyl)-2,5-dioxopiperazine, the DKP-containing compound was isolated from *Streptomyces griseoluteus*. A unique feature is that it contains the β -chloramine function characteristic of the nitrogen (N) mustards. Derivatives of N mustards have been included in the synthetic cancer chemotherapeutic drugs (Sammes, 1975).

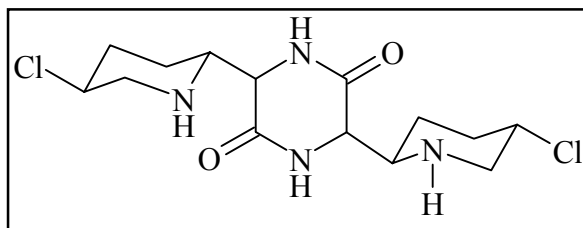


Figure 1. 3: Structure of compound 593 A (Sammes, 1975).

DKPs are useful in holding small peptide links together eg. in rhodotorulic acid (the dimer of δ -N-acetyl-L- δ -N-hydroxyornithine) (Figure 1.4). Isolated from cultures of *Rhodotorula pilimanae* that are iron-deficient, rhodotorulic acid is required by the microorganism for its iron-binding characteristics (Sammes, 1975).

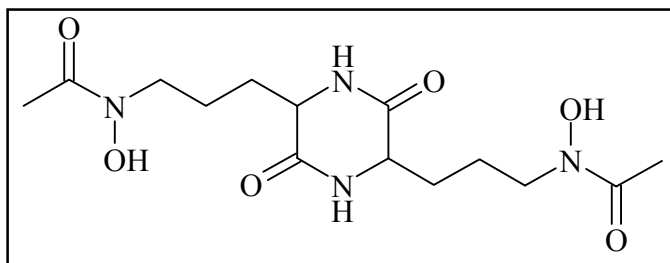


Figure 1. 4: Structure of rhodotorulic acid (Sammes, 1975).

Echinulin (Figure 1.5), a neutral, stable compound, was isolated from *Aspergillus echinulatus*. It contains an isoprenylated tryptophan unit. A unique feature of this compound is the unusual orientation of the isopentenyl unit at position 2. The most likely explanation of this is an initial alkylation at the N atoms (Sammes, 1975).

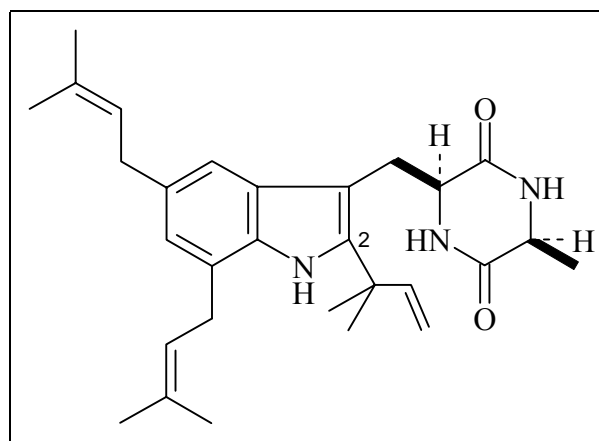


Figure 1.5: Structure of echinulin (Sammes, 1975).

Ten isoprenylated cyclo(L-Pro-L-Tyr) derivatives have been isolated by the parallel studies on *Penicillium brevicompactum* and *Aspergillus ustus*. Fumitremorgen B, isolated from *Aspergillus fumigatus*, induced strong tremors in mice and rabbits (Sammes, 1975).

Aspergillic acid (Figure 1.6), isolated from cultures of *Aspergillus flavus*, was the first substance detected after the discovery of penicillin. When mixed with iron salts, aspergillic acid gives characteristic deep red colours. It is a powerful antibiotic. When the culture fluids of *A. flavus* were further examined, a number of pyrazine derivatives ranging from flavacol to mutaaspergillic acid were detected. The former compound does not show any antibiotic properties, while the latter one shows antibiotic properties, in which the hydroxamic acid was shown to be essential for antimicrobial properties (Sammes, 1975).

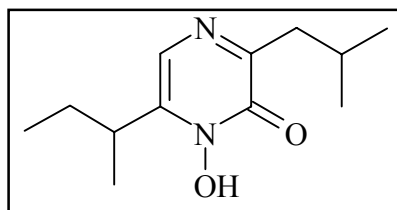


Figure 1.6: Structure of aspergillic acid (Sammes, 1975).

Methoxy-pyrazines, which are widespread in nature, are related to the above compounds. These have very powerful flavouring properties.

The active fragment of biologically active substances such as gliotoxin, sporidesmin and chaetocin are made up of DKP ring systems that are bridged via disulfide bonds (Varughese *et al.*, 1981). Two groups exist: (i) those related to gliotoxin and (ii) those related to sporidesmin.

First isolated in 1936, gliotoxin (Figure 1.7) is produced by *Trichoderma viride*. It is also produced by *Aspergillus fumigatus*, *Gliocladium fimbriatum* and *Penicillium terlikowskii*. This toxic substance is a highly selective antifungal agent. In addition, it is bacteriostatic and shows antiviral properties. Its unusual chemical structure contains a highly strained disulfide bridge with a 12° dihedral angle about the C-S-S-C system, as opposed to the 90-100° angle occurring in acyclic disulfides. This bridge is needed for antibacterial and antiviral activities as related compounds lacking the bridge are inactive (Sammes, 1975).

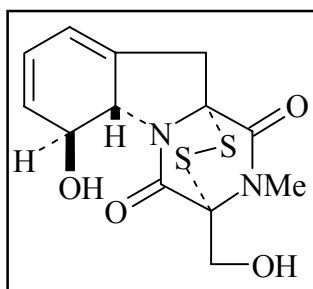


Figure 1. 7: Structure of gliotoxin (Sammes, 1975).

LL-S88 α and LL-S88 β , two antibiotics isolated from *Aspergillus terreus*, are identical to acetylaranotin and the thiomethyl derivative, respectively (Sammes, 1975).

Based on cyclo(Tyr-Ala), the sporidesmins are structurally related to the gliotoxin type. Sporidesmin, isolated from the fungus *Pithomyces chartarum*, causes facial eczema in sheep. Sporidesmin C, the most unique sporidesmin, contains a sulfur chain attached to only one end of the DKP system.

Verticillin A (Figure 1.8), a sporidesmin-related compound, shows antimicrobial activity against Gram positive bacteria, but is ineffective against Gram negative bacteria and fungi (Sammes, 1975).

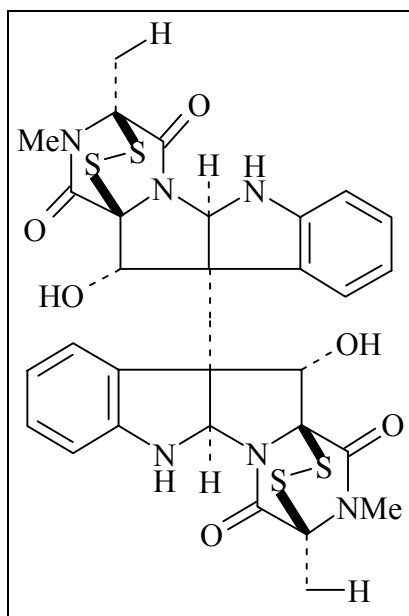


Figure 1.8: Structure of verticillin A (Sammes, 1975).

Bicyclomycin, an antibiotic, was isolated from *Streptomyces sapporonensis*. It is useful against Gram negative bacteria. An added advantage is that it does not result in cross-resistance to normal antibiotics (Sammes, 1975).

1.1.6 Isomerization of amino acids

Compounds that differ in their ability to rotate the plane of polarised light have been defined as optical isomers. Dextrorotatory (D) isomers rotate light in a clockwise fashion, while levorotatory (L) isomers rotate light in an anticlockwise manner (Mathison *et al.*, 1996. Pg. 25).

The chirality of the protein substrate determines the underlying chirality of drug-receptor interactions. It is thus expected that proteins containing solely the D-amino acids would exhibit the same folding characteristics but opposite chirality as the naturally occurring (L-amino acids) counterparts. This is noted for human immunodeficiency virus-1 (HIV-1) protease, where reciprocal chiral specificity with their substrate is exhibited by the D and L forms of the enzyme (Triggle, 1996. Pg. 550).

Biological activities of different isomers may differ in many ways:

- (i) All isomers may be as active as the next one, without exhibiting any stereochemistry of interaction.
- (ii) The isomers may differ both quantitatively and qualitatively in their biological activities - one isomer may not show any biological activities, or isomers may show unique biological activities (Triggle, 1996. Pg. 550).

As early as 1858, Louis Pasteur showed that the isomers of ammonium tartrate exhibited different biological activities. One isomer was capable of inhibiting the growth of *Penicillium glaucum*, while the other isomer showed no effect on its growth. The fact that different isomers may exhibit different biological activities is thus not a recent discovery (Mathison *et al.*, 1996. Pg. 31).

In nature, various peptides containing D-amino acids are found. D-amino acids form part of the bacterial cell walls (peptidoglycan) and antibiotics (such as penicillin and gramicidin). In vertebrate species, peptides containing D-amino acids are also found. *Phyllomedusa sauvagei*, an amphibian, secretes opioid peptides such as dermorphin (Tyr-D-Ala-Phe-Gly-Tyr-Pro-Ser-amide) from its skin. Dermorphin is used as an analgesic, and it is one thousand times more potent than morphine (Triggle, 1996. Pg. 550). If one were to substitute the L-amino acids with their D-amino acid configurational analogue, a conformational change will result that confers resistance to enzymatic cleavage of peptide bonds. This ultimately results in a longer duration of action, thus providing us with a novel approach in producing long-acting peptide drugs (Mathison *et al.*, 1996. Pg. 31). On the other hand, such a substitution may result in a compound that shows no biological activity. If one were to substitute the L-tyrosine at position 1 of dermorphin with D-tyrosine, the molecule loses its activity as an analgesic. Substitutions of other L-amino acids within this compound (dermorphin) with the D-amino acids resulted in a drastic reduction in potency. When active L-peptides such as oxytocin are synthesized as an all-D-analogue, inactive compounds are produced. This implied that the backbone of the peptide chain is of ultimate importance in the biological activity of the compounds (Mathison *et al.*, 1996. Pg. 32).

DKPs are synthesized biologically from proteinogenic L- α -amino acids and are usually in the *cis*-configuration. Some other *cis*- and *trans*-functional DKPs are derived from non-proteinogenic D- α -amino acids. Naturally occurring DKPs containing D- α -amino acids other than proline are not common, but do occur. Cyclo(D-Val-L-Trp) has been isolated from *Aspergillus chevalieri*, and cyclo(*N*'-carboxy-D-Trp-D-Ile) has been isolated from the marine sponge *Rhaphisa pallida* (Bull *et al.*, 1998).

1.1.7 Tryptophan

Tryptophan (Trp) contains an aromatic side chain consisting of an indole ring that is attached to a methylene group (Stryer, 1988. Pg. 17). It is an essential amino acid that must be supplied in the diet. Trp absorbs ultraviolet light maximally near a wavelength of 280 nm (Lehninger *et al.*, 2000. Pg. 120). It is both a ketogenic (gives rise to ketone bodies) and a glucogenic (catabolised to pyruvate) amino acid (Stryer, 1988. Pg. 503). Some characteristics of tryptophan are shown in Table 1.1.

Table 1. 1: Characteristics of tryptophan (Lehninger *et al.*, 2000. Pg. 118).

Abbreviated Names	Trp / W
Molecular weight (M_r)	204.22
Dissociation constant of the carboxyl group (pK_1)	2.38
Dissociation constant of the amino group (pK_2)	9.39
Isoelectric point (pI)	5.89
Hydropathy index	-0.9
Occurrence in proteins (%)	1.4

1.1.7.1 Pathways of metabolism

Only a small amount of Trp is metabolised daily (2 kcal) (Roskoski, 1996. Pg. 232). Trp metabolism includes its conversion to alanine (glucogenic) and glutaryl-CoA (ketogenic). About 2% of Trp is converted to the vitamin nicotinate. Trp metabolism is summarised in Figure 1.9.

1.1.7.2 Conversion of Trp to aminocarboxymuconate semialdehyde (ACS)

Trp is metabolised to alanine, 3-hydroxyanthranilate, α -ketoacidipate and acetoacetyl-CoA (Figure 1.9). In the first step, Trp is converted by dioxygenase to *N*-formylkynurenine (Figure 1.9-1). *N*-formylkynurenine is then converted to kynurenine by formamidase (Figure 1.9-2). The aromatic ring of kynurenine is hydroxylated via a monooxygenase reaction (Figure 1.9-3). Alanine and 3-hydroxyanthranilate are produced by hydrolytic cleavage of the side chain at the ketone group (Figure 1.9-4). 3-Hydroxyanthranilate then undergoes a dioxygenase reaction, which opens up the ring structure to form 2-amino-3-carboxymuconate-6-semialdehyde (ACS) (Figure 1.9-5) (Roskoski, 1996. Pg. 233).

1.1.7.3 Conversion of ACS to acetoacetyl-CoA

Ninety-eight percent of ACS is converted to α -ketoacidipate while the remaining 2% is converted to the vitamin derivative nicotinamide adenine dinucleotide (NAD^+) (Figure 1.9-6). In the major pathway, 3-carboxylate is removed via a decarboxylation reaction on ACS (Figure 1.9-7). 2-Aminomuconate-semialdehyde thus formed produces a second carboxylate, 2-aminomuconate, as a result of a dehydrogenase reaction (Figure 1.9-8). Reduction of the 4-*cis* double bond and hydrolytic deamination of 2-aminomuconate by the reduced form of nicotinamide adenine dinucleotide (phosphate) (NAD(P)H) produces α -ketoacidipate (Figure 1.9-9). Acetoacetyl-CoA is then produced from α -ketoacidipate (Roskoski, 1996. Pg. 233).

1.1.7.4 Conversion of ACS to NAD^+

Two percent of ACS spontaneously forms quinolinate by ring closure (Figure 1.9-6). Quinolinate ribonucleotide is produced via a reaction involving 5-phosphoribosyl-1-pyrophosphate. Quinolinate ribonucleotide then undergoes decarboxylation, followed by an adenylyl group donation by ATP (transferase reaction), forming desamido- NAD^+ . NAD^+ is then produced when glutamine donates its amido group to desamido- NAD^+ (Roskoski, 1996. Pg. 233).

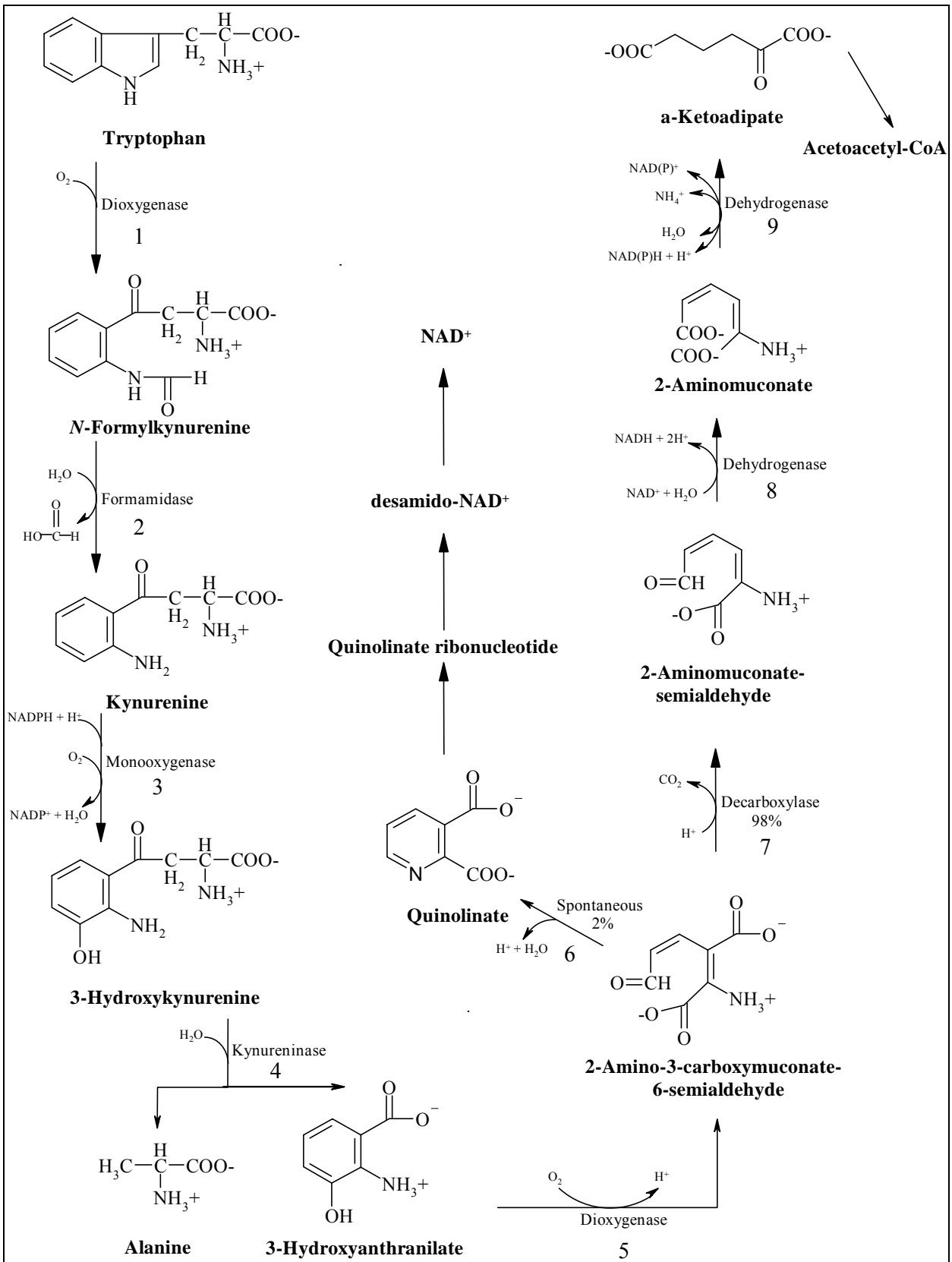


Figure 1. 9: The metabolism of tryptophan (Roskoski, 1996. Pg. 234).

Trp is also a precursor of the animal growth hormone serotonin (Figure 1.10), which is found in mast cells, platelets and enterochromaffin cells of the gut. In a reaction catalysed by Trp hydroxylase (Figure 1.10-1), Trp reacts with tetrahydrobiopterin and O_2 to produce water, dihydrobiopterin and 5-hydroxytryptophan. 5-Hydroxytryptophan undergoes decarboxylation (Figure 1.10-2) to serotonin (5-hydroxytryptamine), a reaction catalysed by aromatic amino acid decarboxylase (Roskoski, 1996. Pg. 409).

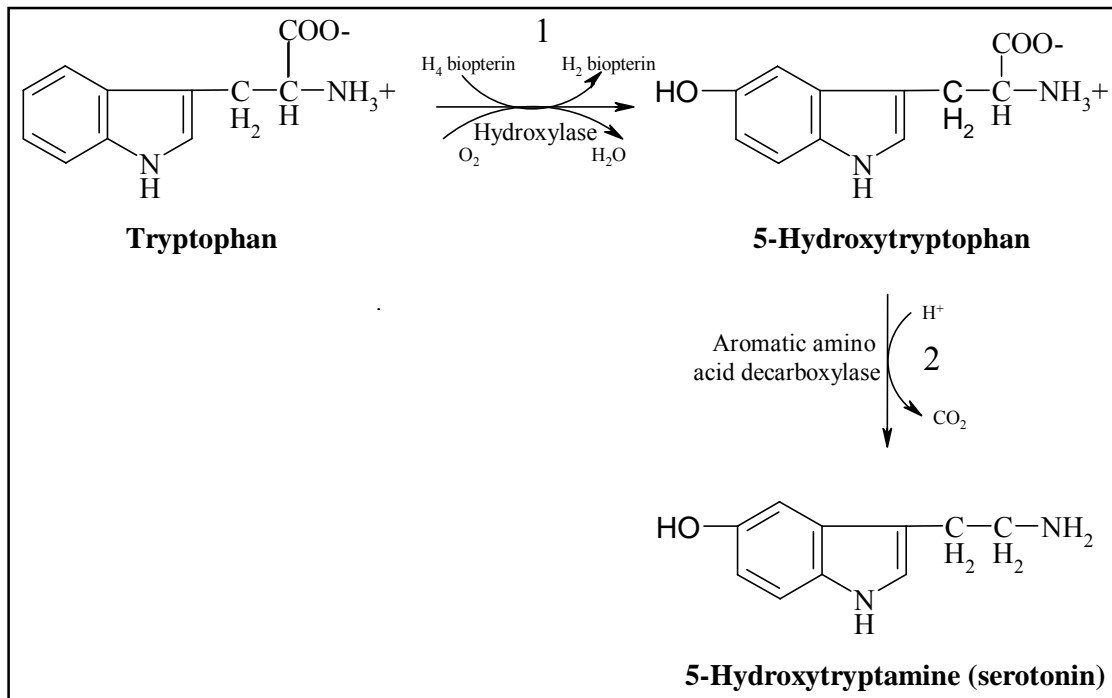


Figure 1. 10: Serotonin metabolism (Roskoski, 1996. Pg. 410).

1.1.8 Proline

Proline (Pro) occurs in a number of naturally occurring biologically active molecules including angiotensin, bradykinin, oxytocin, vasopressin, thyroid releasing factor, antamanide, actinomycin and gramicidin S, to name but a few (Deber *et al.*, 1976). Some characteristics of Pro (Lehninger *et al.*, 2000. Pg. 118) are shown in Table 1.2.

Table 1. 2: Characteristics of proline (Lehninger *et al.*, 2000. Pg 118).

Abbreviated names	Pro; P
M_r	115.13
pK₁	1.99
pK₂	10.96
pI	6.48
Hydropathy index	1.6
Occurrence in proteins (%)	5.2

Pro contains an aliphatic side chain and is unique in the sense that the side chain forms a cyclic structure because it is bonded to both the N- and C_α-atoms. Since Pro contains a secondary amino group, it is referred to as an *imino* acid (Stryer, 1988. Pg. 18). Pro is often found in bends of folded protein chains and is thus the conformational determinant in protein structure. In an α helix, the side chains of the amino acids protrude outward from the helical backbone, thus not interfering with it. The N atom of Pro is not capable of participating in H bonding because of the cyclic structure that the side chain forms and the bulky methylene group linked to the *imino* N atom (Ashida and Kakudo, 1974). Also, no rotation about the N-C_α bond is possible, reducing the number of conformational states of a peptide chain by limiting rotation of neighbouring groups. Studying compounds containing Pro allows the determination of factors that affect equilibrium between *cis*- and *trans*-peptide bonds. Although the normal molecular arrangement of peptide bonds is *trans*, *cis*-peptide bonds occur in proteins and in antamanide (Deber *et al.*, 1976).

In the first turn of an α helix, Pro is suitably fitted, but produces significant bends elsewhere in the helix. Whilst it can be assumed that Pro causes a bend in an α helix, the inverse is not always the case (Branden and Tooze, 1991. Pg. 14).

Pro is often found in β turns because peptide bonds that involve the N atom of Pro readily assume the *cis*-configuration that is highly suited to a tight turn (Lehninger *et al.*, 2000. Pg. 169).

In the ninhydrin reaction that is used to detect and quantify minute amounts of amino acids, all amino acids containing a free α -amino group form a purple product. Pro, in which the α -amino group forms an *imino* group, yields a yellow product (Lehninger *et al.*, 1993. Pg. 124).

Pro metabolism includes its conversion to α -ketoglutarate via glutamate, making it a glucogenic amino acid. It is a non-essential amino acid that can be produced from endogenous metabolites (Bender, 1995. Pg. 523).

1.1.8.1 Biosynthesis of Pro

Glutamate is the precursor of Pro (Figure 1.11). First, γ -glutamylphosphate is produced when the γ -carboxyl group of glutamate reacts with ATP (Figure 1.11-1).

In a reaction involving NADPH, this mixed anhydride is reduced to an aldehyde, glutamate semialdehyde (Figure 1.11-2). This aldehyde undergoes a dehydration reaction (Figure 1.11-3), resulting in the nonenzymatic formation of a 5-membered ring structure, producing 1-pyrroline 5-carboxylate. This intermediate is then reduced by NADPH to form Pro (Stryer, 1988. Pg. 579).

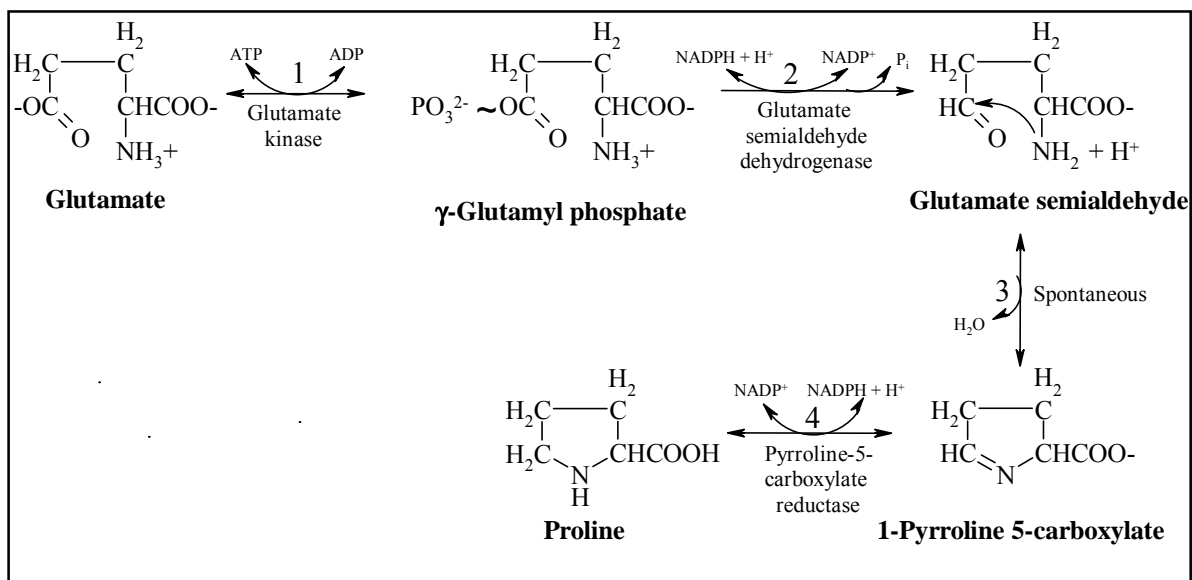


Figure 1. 11: Synthesis of proline from glutamate (Roskoski, 1996. Pg. 240).

1.1.8.2 Pro catabolism

Pro can enter the citric acid cycle via its conversion to α -ketoglutarate (Figure 1.12). It is converted to 1-pyrroline 5-carboxylate via a flavoprotein-dependent oxidation (Figure 1.12-1). Prior to the nonenzymatic opening of the ring structure, water is added to 1-pyrroline 5-carboxylate (Figure 1.12-2), resulting in the formation of glutamate γ -semialdehyde. Glutamate is produced via an NAD^+ -dependent oxidation reaction (Figure 1.12-3) (Roskoski, 1996. Pg. 225). The amino group of glutamate is oxidatively deaminated to form α -ketoglutarate, a reaction that is catalysed by glutamate dehydrogenase (Stryer, 1988. Pg. 505).

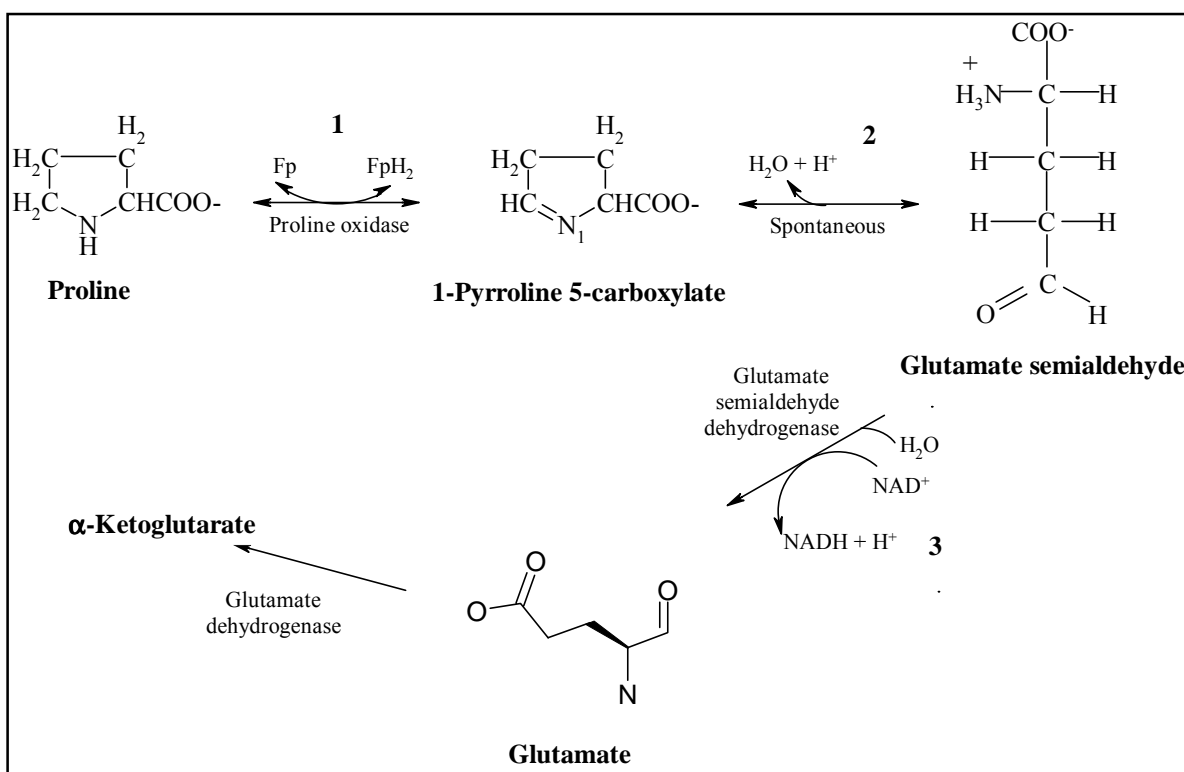


Figure 1. 12: Proline metabolism. Fp=flavoprotein (Roskoski, 1996. Pg. 224).

1.1.9 Why Cyclo(Trp-Pro)?

The *cis-trans* isomerisation of the N-alkylamide bond (amino group of Pro) is thought to play a major role in the biological activity of peptides eg. a major part in the transduction of transmembrane proteins. Biologically important compounds such as cyclosporin and didemnin contain the N-methyl amino acid. (Grant *et al.*, 1999).

Natural products based on Pro-containing DKPs are found throughout nature. The structural complexity and associated biological activity is quite impressive. Examples include cyclo(L-Phe-D-Pro), cyclo(L-Tyr-D-Pro) and cyclo(L-Val-D-Pro), all of which are isolated from *Aspergillus flavipes* (Bull *et al.*, 1998).

Trp is found in many pharmacologically active compounds including hallucinogens, and other drugs that have mental and emotional effects as a result of the intake of these drugs, such as lysergic acid diethylamide, *N,N*-dimethyltryptamine, harmaline and strychnine (Milne *et al.*, 1998). Many therapeutic uses have been assigned to the indole ring, from anti-emetics and anti-inflammatory effects to treatment for hypertension, migraines and Parkinsons disease (eg. bromocriptine, ergotamine and indomethacin) (Grant *et al.*, 1999).

Research in our laboratories have shown the potential of the cyclic dipeptide cyclo(Trp-Pro) as an antimicrobial substance, as well as potential usage in the treatment of cardiovascular dysfunction (Milne *et al.*, 1998). Investigation of the activities of the isomers may result in the formulation of a drug entity with greater activity and/or specificity than the L-form, or as the case may be, the isomers may show reduced or no activity at all. Nevertheless, all possibilities need to be investigated.

1.2 Objectives of the study

In the pursuit of the design and biological evaluation of new drug entities, this study aims to:

- Synthesize the isomers of the cyclic dipeptide cyclo(Trp-Pro);
- Elucidate the structures of the different isomers;
- Investigate the biological activities of the different isomers as an antibacterial and/or antifungal agent;
- Evaluate the potential of these peptides as anticancer agents;
- Investigate the hepatotoxicity of the different isomers using both *in vivo* and *in vitro* techniques;
- Determine the coagulant or anticoagulant activity of the isomers;
- Determine the effects of the isomers on potassium and calcium ion channel activities;
- Examine effects on heart rate and anti-arrhythmia activity; and
- Collate data collected in this study to assess the isomer/s that show the greatest potential to be used as a basis for a new drug entity.

These objectives, and how they were met, are described in the chapters that follow.

CHAPTER 2

SYNTHESIS AND STRUCTURAL ELUCIDATION

2.1 INTRODUCTION

Cyclic peptides exhibit greater stability *in vivo* than their linear counterparts, thereby increasing their potential as drug candidates (Lambert *et al.*, 2001). A common route, the Fischer method (Fischer, 1906), employed in synthesizing cyclic dipeptides is by the cyclization of free dipeptide esters. These are obtained by freeing the esters from the amine salts using ammonia. Disadvantages of this strategy include extensive racemisation (5-40%) and in some cases, cyclization only occurs after the reagents are exposed over prolonged periods (Sammes, 1975).

Under basic conditions, DKPs readily form from unprotected linear dipeptides. This is the case if head-to-tail folding is not limited by steric constraints (Anteunis, 1978). DKPs are also formed from dipeptide esters in a base-catalysed or aminolysis reaction. Disadvantages of this method include racemisation, poor yield and prolonged reaction times (Suzuki *et al.*, 1981).

Symmetrically substituted DKPs are synthesized by heating the amino acids in refluxing ethylene glycol, resulting in quite high yields. Racemisation is avoided by using the t-butyloxycarbonyl (t-Boc)-protected dipeptide methyl ester. The t-Boc protects the amine group of an amino acid, and is resistant to catalytic hydrogenation and sodium in liquid ammonia (Anderson and McGregor, 1957). These protected amino acids are generally crystalline in nature. The protecting group is removed with formic acid. Cyclization results from heating the unprotected linear dipeptide formate salt in a neutral medium (Nitecki *et al.*, 1968).

An alternate method in the synthesis of DKPs is the hydrogenolysis of benzyloxycarbonyl dipeptide methyl esters in methanol. This is achieved over a palladium or charcoal catalyst (Sammes, 1975).

An important aspect to consider in DKP synthesis is that the dipeptide precursors have to assume a folded conformation as opposed to the more stable, extended forms. An advantage of peptides containing proline is the inherent tendency to assume a folded conformation, making these more prone to form the DKP derivative on cyclization. Once the DKP has formed, it acts as a relatively stable dipeptide (Indelicato *et al.*, 1972).

Slight differences in chemical and physical properties amongst diastereoisomeric isomers of substituted derivatives exist. The LL-isomer of cyclo(Leu-Leu) hydrolyses 3.5 times faster than the DL isomer in the presence of 0.5 N HCl. This difference was explained by both steric shielding and steric strain (Sammes, 1975).

2.1.1 Synthesis of the isomers of cyclo(Trp-Pro)

2.1.1.1 Background

In the synthesis of cyclo(Trp-Pro), it is important to bear the following in mind during synthesis: 1) Tryptophan contains an indole ring that undergoes oxidation under acidic conditions (Yajima *et al.*, 1977); and 2) when the protective t-Boc group is removed, t-butyl cations may form if no carbonium ion scavengers are present to prevent butylation. This is achieved by the addition of anisole or methionine (Bodanzsky *et al.*, 1976).

Three major steps are involved in the synthesis of the isomers of cyclo(Trp-Pro). Firstly, the protected linear dipeptides are synthesized, which is followed by the removal of the protective t-Boc group. The final step involves the cyclization of the unprotected linear dipeptide. The methods used to synthesize these isomers were determined by comparing various methods per step, in order to achieve the highest yield and purity of the dipeptides (Haywood, 2000).

2.1.1.2 Synthesis of the protected linear dipeptides

The corresponding protected linear dipeptides were synthesized with diethylphosphoryl cyanide (DEPC) as the coupling agent and triethylamine (TRI) as base (Milne *et al.*, 1992). This was used in preference to activated N-hydroxysuccinimide (OSu) esters together with N-methyl morpholine, as the former method produced the best average

yield (Haywood, 2000). In addition, DEPC is more stable at room temperature than OSu esters, a consideration that is more suited to the method.

The materials used in the synthesis of the isomers are tabulated in Table 2.1.

Table 2. 1: Materials used in the synthesis of the isomers.

Synthesis of Cyclo-	Starting materials	Manufacturer	M _r (g/mol)	Starting mass (g)	DEPC/TRI (ml)
L-Trp-L-Pro	Boc-L-Trp	Fluka	304.35	3	1.64/2.87
	L-Pro-NH ₂	Fluka	114.2	1.12	
L-Trp-D-Pro	Boc-L-Trp	Fluka	304.35	3	1.64/2.87
	D-Pro-NH ₂	Bachem	114.2	1.12	
D-Trp-L-Pro	Boc-D-Trp	Bachem	304.35	2	1.09/1.91
	L-Pro-NH ₂	Fluka	114.2	0.75	
D-Trp-D-Pro	Boc-D-Trp	Bachem	304.35	2	1.09/1.91
	D-Pro-NH ₂	Bachem	114.2	0.75	

The t-Boc protected tryptophan and respective prolinamides were dissolved in 50 ml 1,2 dimethoxyethane (Fluka Chemika) at 0°C. The respective amounts of DEPC and triethylamine (Table 2.1) were added in a dropwise fashion. The entire reaction was carried out in a positive inert atmosphere. The reaction was stirred at 0°C for 1 hr, after which the reaction mixture was allowed to reach room temperature. The reaction mixture was then left at room temperature overnight to allow the reaction to run to completion (Table 2.2). The reaction mixture was then diluted with 100 ml chloroform and isolated by successive washing with 5% HCl (50 ml), 5% NaHCO₃ (50 ml) and saturated NaCl (50 ml). The organic phase was dried with Na₂SO₄ and protected from light.

Table 2. 1: Schematic outline of the DEPC/TRI method used to synthesize the intermediate protected linear dipeptides.

Boc-L-Trp + L-Pro-NH ₂ _____➔	Protected dipeptide Boc-L-Trp-L-Pro-OH*
Boc-L-Trp + D-Pro-NH ₂ _____➔	Protected dipeptide Boc-L-Trp-D-Pro-OH*
Boc-D-Trp + L-Pro-NH ₂ _____➔	Protected dipeptide Boc-D-Trp-L-Pro-OH*
Boc-D-Trp + D-Pro-NH ₂ _____➔	Protected dipeptide Boc-D-Trp-D-Pro-OH*

* Milne *et al.* (1992) proved the hydrolysis of NH₂ to OH

2.1.1.3 Removal of the protective Boc groups

Prior to the cyclization step, the protective groups had to be removed from the derived linear dipeptides (Table 2.2). Two methods, one involving formic acid and the other, toluene sulphonic acid in dioxane were available for this step. The choice of method was based on the quality of the product obtained by Haywood (2000). Removal of the Boc groups was achieved by the addition of 95% formic acid and 2% anisole. Formic acid is a weaker acid than the preferred HCl and trifluoroacetic acid for this step, thereby preventing oxidation of tryptophan (Yajima *et al.*, 1977).

0.2 ml Anisole and 10 ml formic acid were added to every 0.2 g of the respective protected linear dipeptides. The solution was stirred at room temperature for 4 hr, after which the reaction mixture was dried *in vacuo*.

2.1.1.4 Cyclization

In the cyclization of the unprotected linear dipeptides, various solutions were tested for overall yield and product quality. Methods involving the use of saturated NaHCO₃, butanol:toluene (4:1), methanol and a combination of butanol, acetic acid and N-methyl morpholine were tested. Of the methods tested, the greatest yield was obtained for the method using the saturated NaHCO₃ solution (Haywood, 2000).

50 ml saturated NaHCO₃ was added to the respective crude dipeptide formate salts. The reaction mixture was stirred at 5°C for a period of 5 days. Each isomer (see Figure 2.1 for general structure) was extracted with chloroform (4 x 50 ml) and white powder-like crystals were grown from chloroform:n-hexane (10:2). An exception was the cyclo(L-Trp-D-Pro) isomer. A yellow oil was obtained after the addition of the chloroform:n-

hexane solution. The oil was dissolved in chloroform. Activated charcoal was then added and the mixture was stirred overnight. After filtration, crystals were grown from chloroform:n-hexane (10:2).

Only the crystals of cyclo(L-Trp-L-Pro) and cyclo(D-Trp-L-Pro) were of diffraction quality. Crystals of cyclo(D-Trp-L-Pro) were sent for X-ray crystallography to compare the results to that of cyclo(L-Trp-L-Pro) (Haywood, 2000).

The purity of the compounds obtained was ascertained with thin layer chromatography (TLC) on silica gel plates (Silica gel 60 F₂₅₄, Merck, Germany), using two different solvent systems. The TLC plates were developed with the following visualizing reagents: ninhydrin, ultraviolet light at 254 nm and iodine. The R_f values obtained are shown in Table 2.3.

Table 2. 2: R_f values of the isomers in two different solvent systems.

Solvent system	Cyclo(L-Trp-L-Pro)	Cyclo(L-Trp-D-Pro)	Cyclo(D-Trp-L-Pro)	Cyclo(D-Trp-D-Pro)
Chloroform:methanol:acetic acid (14:2:1)	0.803	0.790	0.788	0.802
Chloroform:methanol (12:1)		0.457		0.446
Chloroform:methanol (7:3)	0.902		0.901	

The % yield of the respective isomers are shown in Table 2.4.

Table 2. 3: Percentage yield of the cyclic isomers.

Isomer	Yield (%)
Cyclo(L-Trp-L-Pro)	80
Cyclo(L-Trp-D-Pro)	70
Cyclo(D-Trp-L-Pro)	70.5
Cyclo(D-Trp-D-Pro)	81

Qualitative validation of the cyclic isomers included mass spectrometry, infrared spectroscopy, differential scanning calorimetry, X-ray crystallography (cyclo(D-Trp-L-Pro)) and nuclear magnetic resonance.

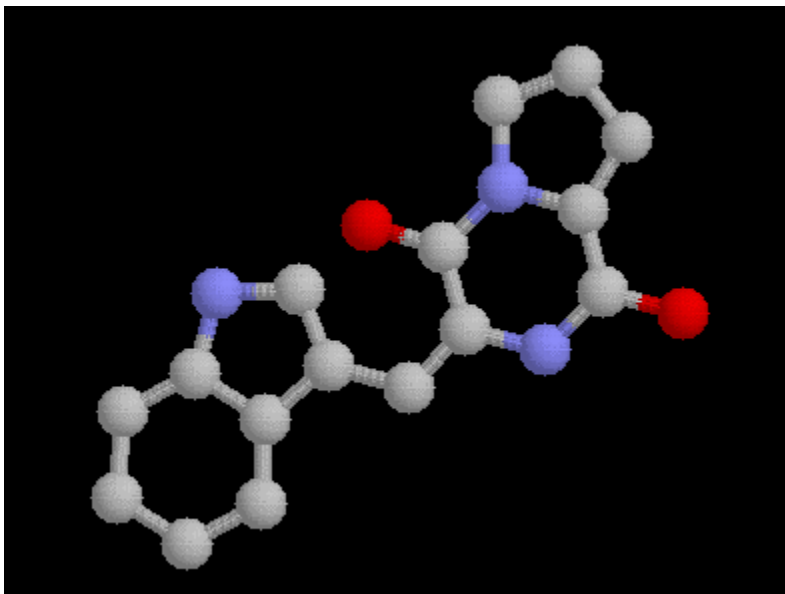


Figure 2. 1: General structure of cyclo(Trp-Pro). Red atom = oxygen; blue atoms = nitrogen.

2.1.2 Mass Spectrometry

Mass spectrometry is an important analytical tool that provides both qualitative and quantitative information pertaining to the molecular and atomic composition of organic and inorganic compounds (Willard *et al.*, 1988. Pg. 465).

The charged particles of the parent ion and ionic fragments of the original molecule are produced by the mass spectrometer. These ions are then categorized in relation to their mass/charge ratio (m/e). The mass spectrum obtained gives an indication as to the relative mass number of different kinds of ions. In comparison to other analytical techniques such as nuclear magnetic resonance and infrared spectroscopy, mass spectrometry has increased sensitivity and increased specificity (Willard *et al.*, 1988, Pg. 465).

The fast atom bombardment (FAB) mass spectrometry mode is used for non-volatile compounds (Silverman, 1992. Pg. 286), especially peptides and other high molecular weight organic compounds. It uses a high pressure of argon (Ar) gas that is placed

between the sample and the ionizer. The ionized Ar gas is directed initially at an atom beam (Ar^+) that bombards the sample. This high kinetic energy Ar^+ beam exchanges charge with the solvent used to dissolve the sample. The solvent is thereby ionized. Subsequently, protons are either transferred from the sample to the solvent, the sample undergoes hydride transfer or ion-pair reactions with the ion, thus producing pseudomolecular ions. These pseudomolecular ions are then extracted via a slit lens system and directed at the mass analyzer (Willard *et al.*, 1988. Pg. 473).

FAB mass spectra of the isomers were obtained on a VG-7070E spectrometer. The isomers were dissolved in deuterated dimethyl sulfoxide (DMSO-d_6) and 3-nitrobenzyl alcohol was used as the matrix.

In analysing mass spectra of simple DKPs, certain fragmentation patterns are evident. The parent ion dominates the following fragmentations:

- a) loss of CO or CHO;
- b) amine fragmentation ($\text{R}_2\text{CH}=\text{NH}_2^+$); and
- c) elimination of cyanuric acid (HNCO).

(Sammes, 1975).

When proline is present in some DKPs, there is a 2 mass unit shift to the left of some characteristic peaks (Svec and Junk, 1964). The following ions usually indicate the existence of a DKP ring: m/e 114; m/e 113; and m/e 85 (Szafranek *et al.*, 1976).

The peaks corresponding to the cleavage of the tryptophan side chain ($\text{C}_\alpha\text{-C}_\beta$ bond) is quite intense (m/e 130). This is explained by the fact that the β carbon atom of this side chain accommodates the positive charge exceptionally well (Ramachandran and Mitra, 1976).

The mass spectra of the isomers show a parent peak at m/e 284, the expected dipeptide form (Table 2.5).

Table 2. 4: Accurate mass observed as determined by mass spectrometry.

Isomer	Accurate Mass Observed
L-Trp-L-Pro	284.139867
L-Trp-D-Pro	284.139883
D-Trp-L-Pro	284.139859
D-Trp-D-Pro	284.139862

With reference to the molecular mass of the isomers, the following m/e ratios corresponding to the positive ion of the following fragmentations were of importance:

- a) the positive ion, relating to the cleavage of the tryptophan side chain – m/e 130
- b) DKP-pyrrolidine fragment – m/e 154
- c) Loss of the CHO group – m/e 255
- d) Amine fragmentation – m/e 159
- e) Elimination of HNCO – m/e 241.

As can be noted from the mass spectra of the isomers (Figures 2.2-2.5), the parent ion, the DKP-pyrrolidine and amine fragmentations are prominent in all the spectra. Loss of CO is noted for D-Trp-L-Pro (m/e 256) (Figure 2.4) and the elimination of cyanuric acid is evident at m/e 241 for cyclo(L-Trp-L-Pro), cyclo(D-Trp-L-Pro) and cyclo(D-Trp-D-Pro) (Figures 2.2, 2.4 and 2.5, respectively).

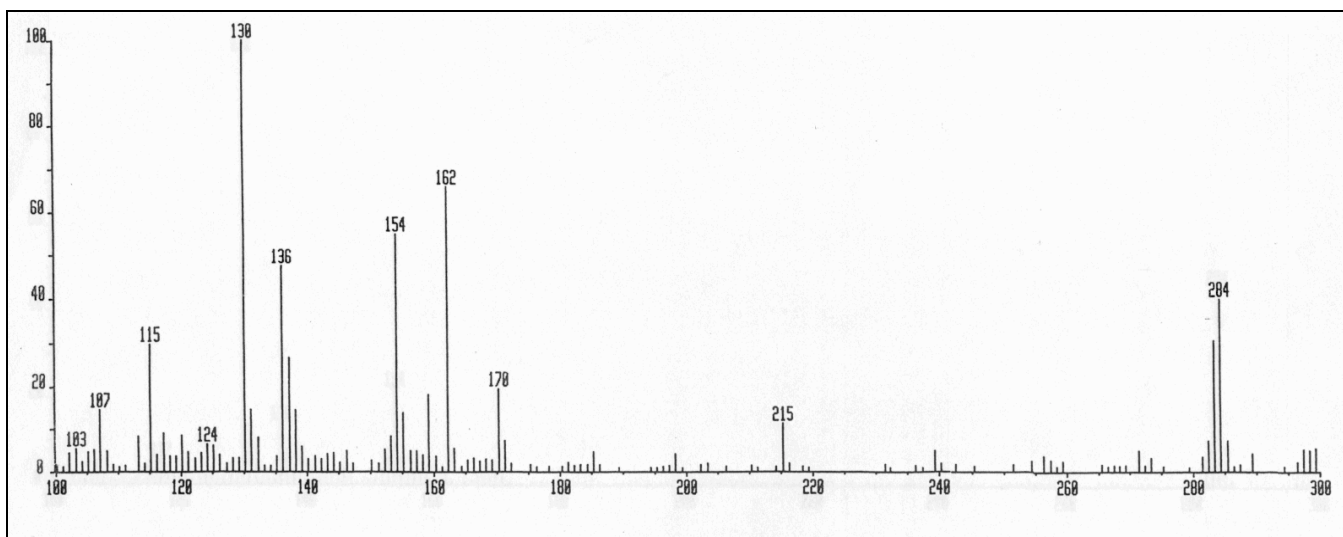


Figure 2. 2: Mass spectrum of cyclo(L-Trp-L-Pro).

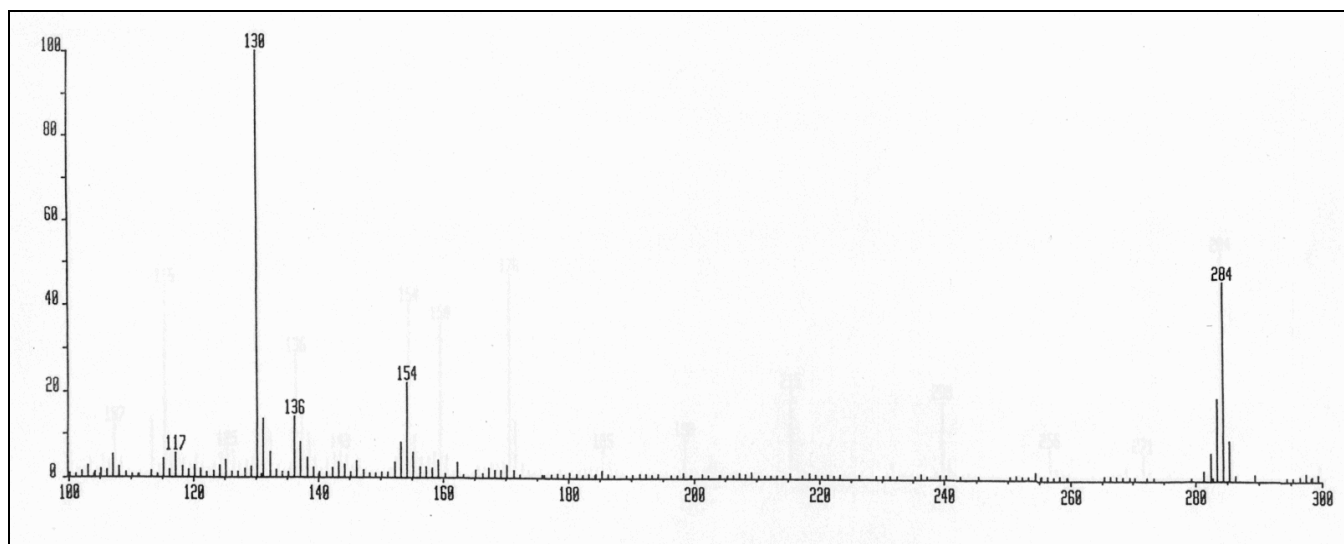


Figure 2. 3: Mass spectrum of cyclo(L-Trp-D-Pro)

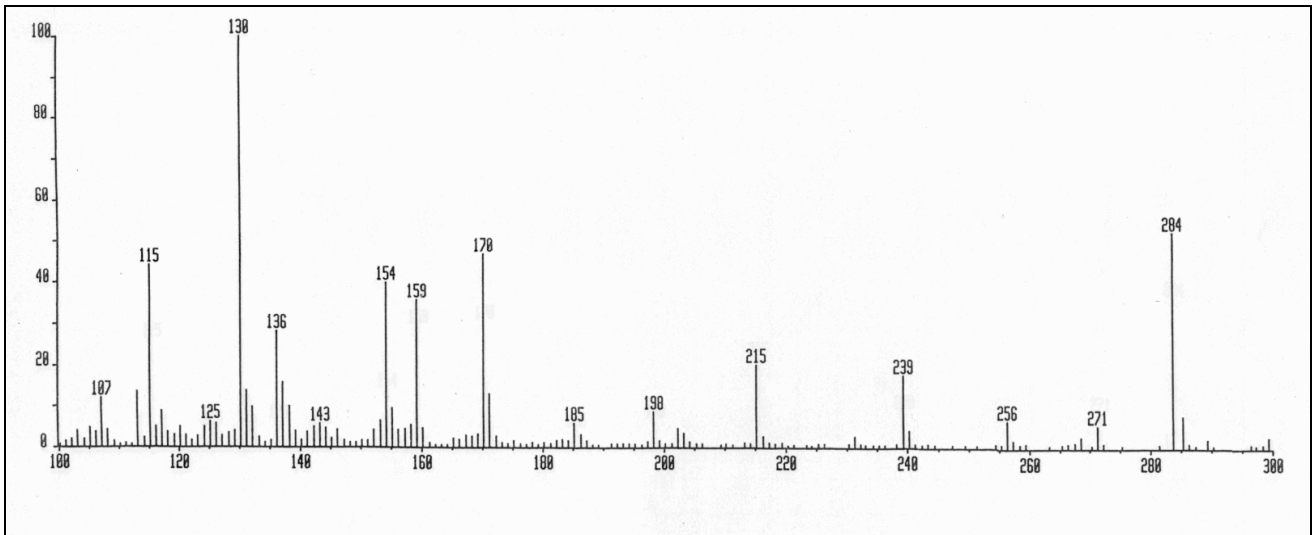


Figure 2. 4: Mass spectrum of cyclo(D-Trp-L-Pro).

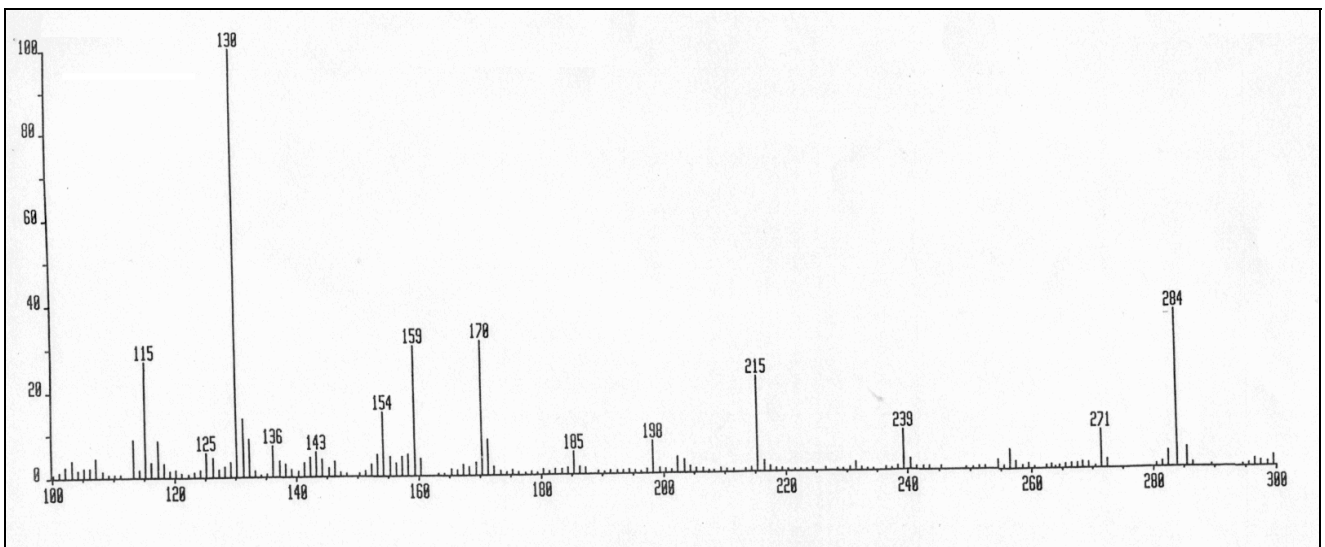


Figure 2. 5: Mass spectrum of cyclo(D-Trp-D-Pro).

2.1.3 Infrared Spectroscopy

Infrared (IR) spectroscopy is characterised by radiation at wavelengths between 0.7 and 500 μm ($14\ 000$ to $20\ \text{cm}^{-1}$), which extends from the visible spectrum's red end to the microwave region. It is used to examine the bending, twisting, rotating and vibrational motions of atoms present in a molecule. Absorption at specific wavelengths of portions of the incident radiation occurs once there is interaction with the IR radiation. A multitude of vibrations occur concurrently, producing a complex absorption spectrum. The spectrum is characterised by the functional groups that the molecule is composed of, as well as the overall configuration of the molecule (Willard *et al.*, 1988. Pg. 287).

In qualitative analysis, the presence or absence of absorption in specific frequency regions is characteristic of specific stretching and bending motions of a molecule (Willard *et al.*, 1988. Pg. 288). The absence of absorption between 2400 to $2700\ \text{cm}^{-1}$ and $1220\ \text{cm}^{-1}$, as well as the absence of a sharp absorption peak resultant of free NH_2 stretching at 3200 to $3400\ \text{cm}^{-1}$, indicates that no free carboxyl groups, amino groups or ester linkages are present (Minamiura *et al.*, 1972).

IR spectra of the isomers were recorded using a Perkin Elmer 1600 FTIR spectrophotometer using the potassium bromide (KBr)-disc method.

IR spectroscopy allows for the discrimination between *cis*- and *trans*-amide bonds (Ovchinnikov and Ivanov, 1975). The following absorption bands (Table 2.6) are characteristic of the *cis*- and *trans*-amide bonds found in DKPs (Sammes, 1975).

Table 2. 5: Characteristic absorption bands of DKPs (Sammes, 1975).

Description of band	<i>Cis</i> -amide absorption bands (cm ⁻¹)	<i>Trans</i> -amide absorption bands (cm ⁻¹)
Amide I band (CO stretch)	1670-1690	1650
Amide II band (NH-in plane vibration)	1440-1450	1550*
Amide III (<i>cis</i> CONH)	1300-1350	Not present
NH bending	1450	1450
CN stretching	1350	1350

* Existence of a band at 1550 cm⁻¹ is regarded as characteristic of the presence of a *trans*-amide bond (Bellamy, 1957).

The following absorption bands (Table 2.7) were noted for cyclo(L-Trp-L-Pro) (Appendix B, Figure B 1.1), cyclo(L-Trp-D-Pro) (Appendix B, Figure B 1.2), cyclo(D-Trp-L-Pro) (Appendix B, Figure B 1.3) and cyclo(D-Trp-D-Pro) (Appendix B, Figure B 1.4).

Table 2. 6: Absorption bands observed for the isomers.

Description of band	Cyclo(L-Trp-L-Pro)	Cyclo(L-Trp-D-Pro)	Cyclo(D-Trp-L-Pro)	Cyclo(D-Trp-D-Pro)
Amide I band (CO stretch)	1675.0	1639.4	1640.5	1662.3
Amide II band (NH-in plane vibration)	1424.9	1546.4	1547.2	1425.3
Amide III (<i>cis</i> CONH)	1300.1	Not present	Not present	1300.5
NH bending	1449.2	1468.9	1460.0	1457.3
CN stretching	1352.1	1341.2	1340.6	1351.1
<i>Cis</i> - or <i>Trans</i> - amide bond	<i>cis</i>	<i>trans</i>	<i>trans</i>	<i>cis</i>

The absorption bands obtained for the different isomers groups for cyclo(L-Trp-L-Pro) and cyclo(D-Trp-D-Pro) are *cis*, while the cyclo(L-Trp-D-Pro) and cyclo(D-Trp-L-Pro) fall into the *trans*-amide bond group (Table 2.7). The absence of the 1300-1350 cm^{-1} band for cyclo(L-Trp-D-Pro) and cyclo(D-Trp-L-Pro) (Appendix B, Figures B 1.2 and 1.3) give a strong indication that these isomers are in the *trans*-conformation. In addition, these two isomers exhibit the 1550 cm^{-1} frequency, indicating the presence of a *trans*-amide bond (Bellamy, 1957). The absence thereof in the cyclo(L-Trp-L-Pro) and cyclo(D-Trp-D-Pro) (Appendix B, Figures B 1.1 and 1.4) strongly suggests a *cis*-conformation for those two isomers.

The cyclo(L-Trp-L-Pro) and cyclo(D-Trp-D-Pro) (Figure 2.6) overlay show a very strong correlation, as also noted for the cyclo(L-Trp-D-Pro) and cyclo(D-Trp-L-Pro) overlays (Figure 2.7). The cyclo(D-Trp-D-Pro) and cyclo(D-Trp-L-Pro) overlay (Figure 2.8) show a peak at 1460 cm^{-1} for cyclo(D-Trp-L-Pro) that is not present for cyclo(D-Trp-D-Pro). This is also seen in the cyclo(L-Trp-L-Pro) and cyclo(D-Trp-L-Pro) overlay, where a peak at 1460.0 cm^{-1} is present in the spectrum of cyclo(D-Trp-L-Pro) (Figure 2.9).

An overlay of cyclo(D-Trp-D-Pro), cyclo(L-Trp-L-Pro) and cyclo(D-Trp-L-Pro) (Figure 2.10) show the 1460 cm^{-1} peak that is present in cyclo(D-Trp-L-Pro), but not in cyclo(D-Trp-D-Pro) and cyclo(L-Trp-L-Pro). Similarly, the overlay of cyclo(L-Trp-D-Pro), cyclo(L-Trp-L-Pro) and cyclo(D-Trp-L-Pro) (Figure 2.11) show the 1468.9 and 1460 cm^{-1} peaks present in the cyclo(L-Trp-D-Pro) and cyclo(D-Trp-L-Pro) respectively, but absent in cyclo(L-Trp-L-Pro).

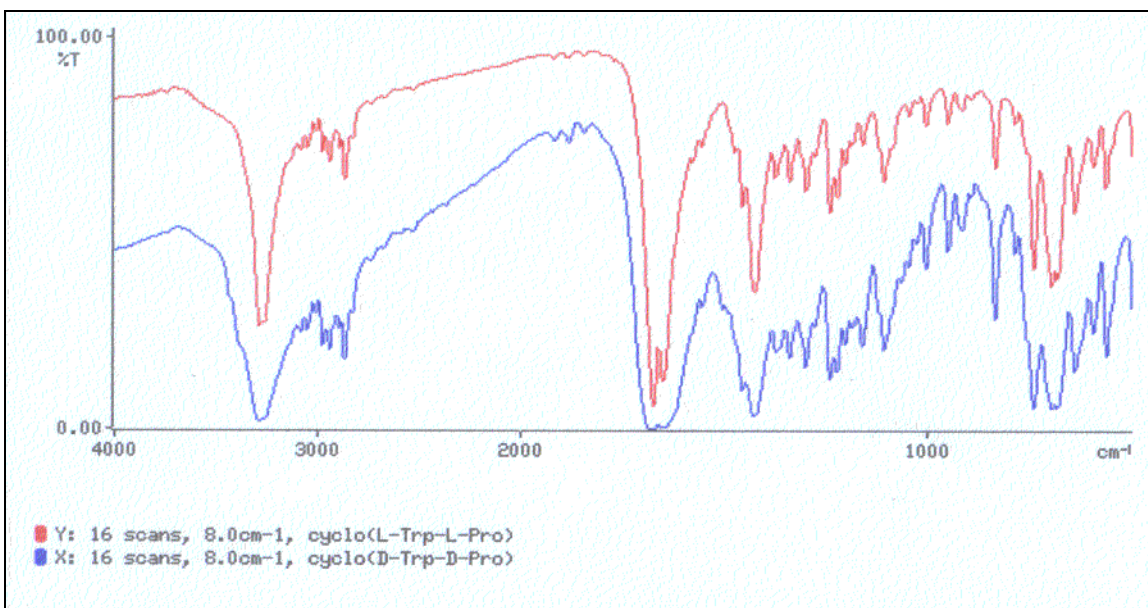


Figure 2. 6: IR spectra overlay of cyclo(L-Trp-L-Pro) and cyclo(D-Trp-D-Pro).

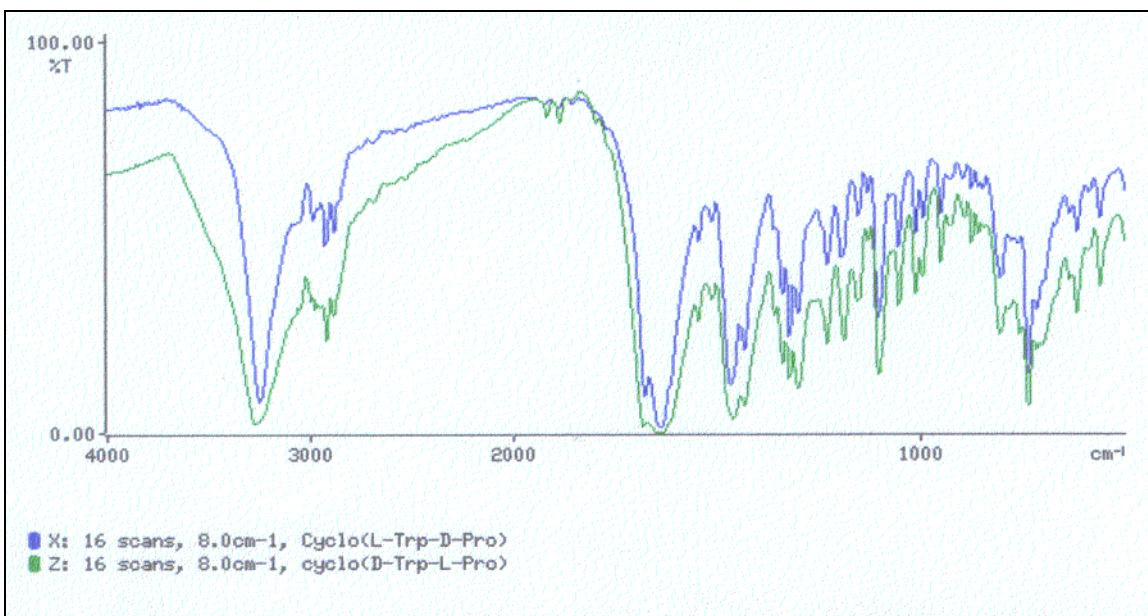


Figure 2. 7: IR spectra overlay of cyclo(L-Trp-D-Pro) and cyclo(D-Trp-L-Pro).

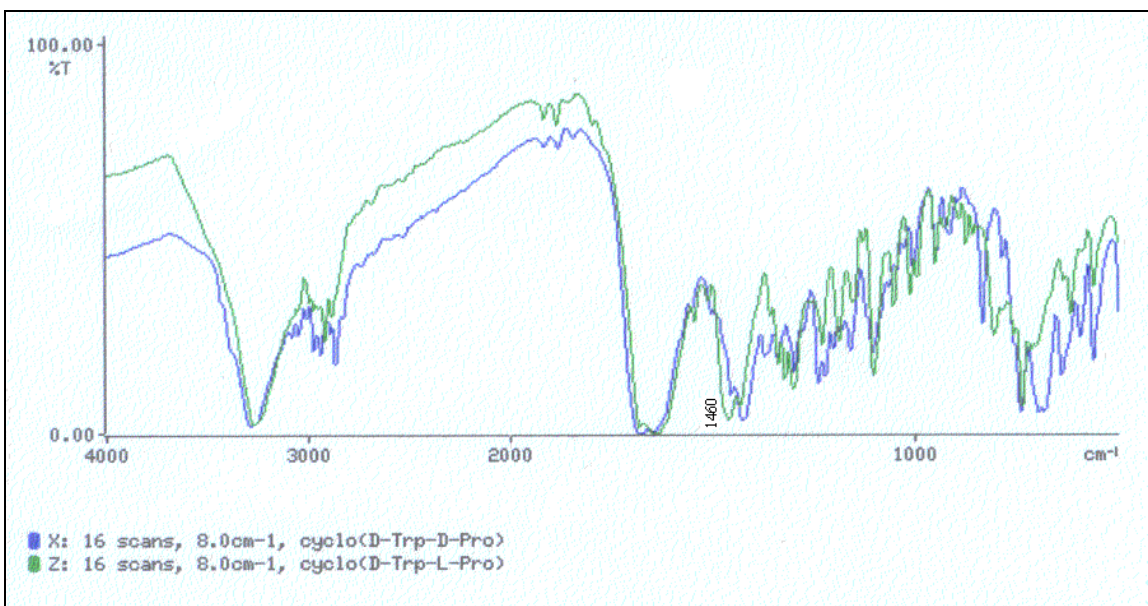


Figure 2. 8: IR spectra overlay of cyclo(D-Trp-D-Pro) and cyclo(D-Trp-L-Pro).

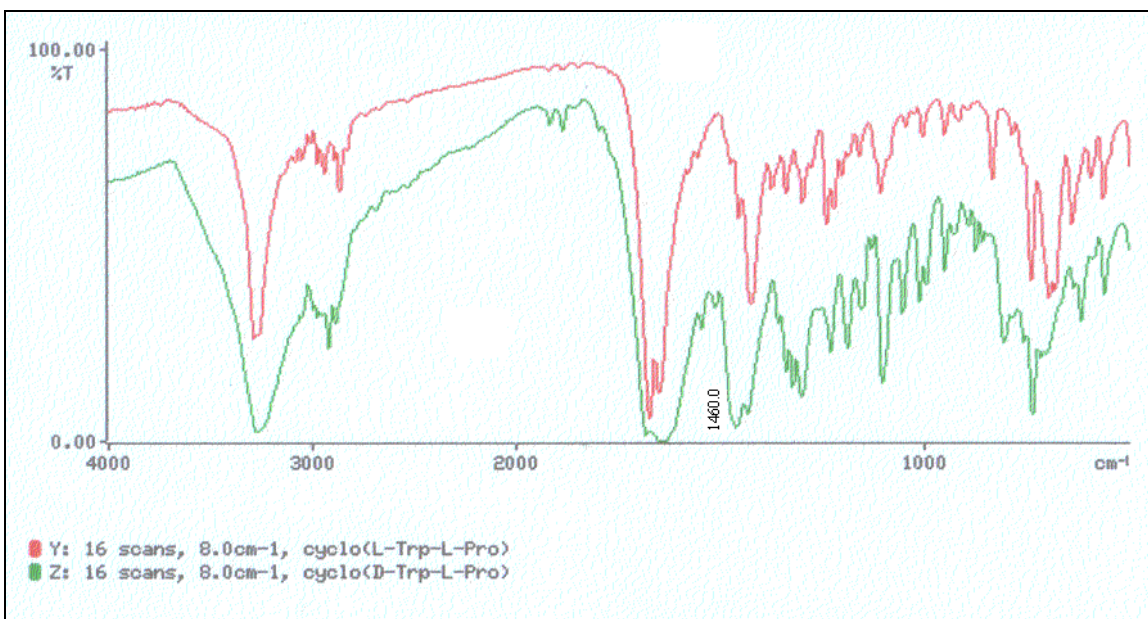


Figure 2. 9: IR spectra overlay of cyclo(L-Trp-L-Pro) and cyclo(D-Trp-L-Pro).

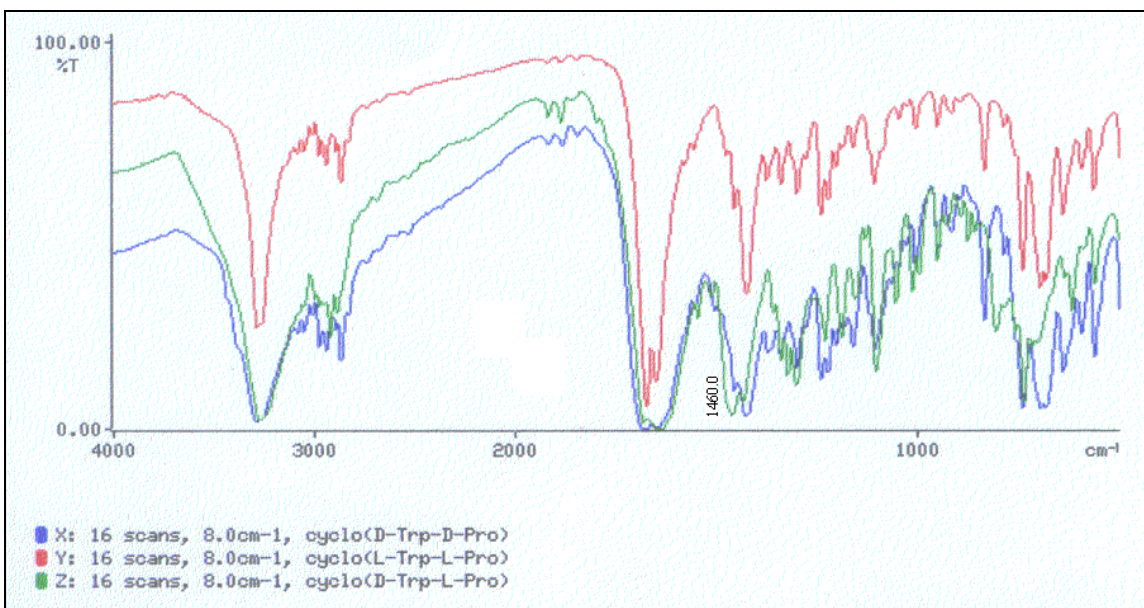


Figure 2. 10: IR spectra overlay of cyclo(D-Trp-D-Pro), cyclo(L-Trp-L-Pro) and cyclo(D-Trp-L-Pro).

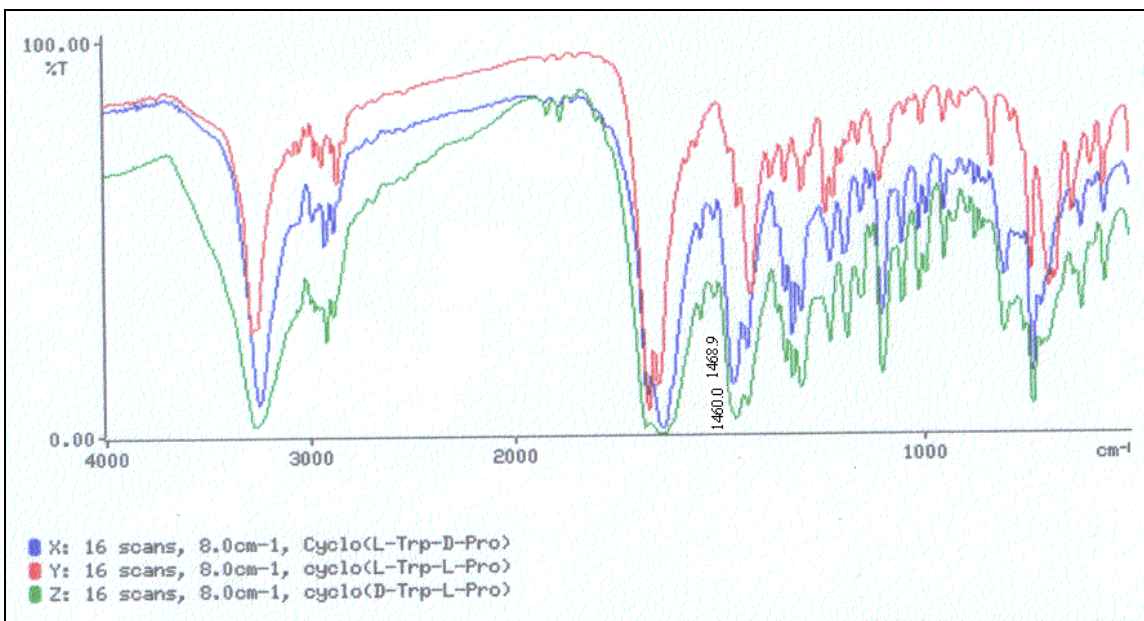


Figure 2. 11: IR spectra overlay of cyclo(L-Trp-D-Pro), cyclo(L-Trp-L-Pro) and cyclo(D-Trp-L-Pro).

2.1.4 Differential Scanning Calorimetry

Differential scanning calorimetry (DSC), a widely used thermal analysis technique, measures the heats and temperature of transition and reactions. It is applicable to, among others, reaction kinetics, purity analysis and polymer cures. Both sample and reference materials are subjected to an exact temperature change. Temperature in both the reference and sample materials are maintained at the same temperature by adding thermal energy to either material once a thermal transition occurs in the sample material. This additional energy is directly proportional to the energy absorbed or emitted from the sample during the transition, producing a means of determining a calorimetric measure of the transition energy (Willard *et al.*, 1988. Pg. 762).

DSCs were performed on a TA Instruments 10 DSC. 3.0 –5.0 mg of each isomer was weighed into an aluminium crimp cell. DSC curves were obtained at a heating rate of 10°C per min, under a nitrogen flow rate of 20 ml per min.

The thermal characteristics of the endothermic peaks are listed in Table 2.8.

Table 2. 7: Endothermic peaks of the isomers as determined by DSC.

Isomer	Peak Temperature (°C)
Cyclo(L-Trp-L-Pro)	175.09
Cyclo(L-Trp-D-Pro)	196.06
Cyclo(D-Trp-L-Pro)	196.42
Cyclo(D-Trp-D-Pro)	171.52

Analysis of the DSC thermograms indicated no significant desolvation endotherms or recrystallization exotherms for any of the isomers. The only significant endotherm observed for all the isomers correspond to the respective melting points for each isomer (Table 2.8). The *trans*-compounds showed a higher endothermic peak than the *cis* compounds. The DSC scans are shown in Appendix B, Figures B 1.5-1.8.

2.1.5 X-ray crystallography

Diffraction quality crystals of cyclo(D-Trp-L-Pro) were crystallized from chloroform:n-hexane (10:2) in the space group $P2_1$. Reflection indices collected were $h -14, +13$; $k -8, +8$ and $l -25, +26$. Data was collected on an Enraf Nonius CAD4 diffractometer with $MoK\alpha$ radiation (graphite monochromator, $\lambda = 0.7107 \text{ \AA}$). Least square methods from the position of 25 centered reflections for each crystal were used to obtain accurate unit cell parameters. No significant crystal decay occurred during data collection. Intensities were corrected for absorption, Lorentz and polarization effects. Absorption correction was achieved by applying an empirical method. In addition, standard intensity checks as well as orientation control were performed (North *et al.*, 1968). All structures were determined by direct methods (Sheldrick, 1986). The non-H atoms were defined anisotropically, while all H atoms were placed in calculated positions, and included in the refinement with common isotropic thermal parameters. Atomic scattering values were obtained from literature (Cromer and Liberman, 1974).

The ORTEP view, fractional coordinates and equivalent thermal factors and relevant torsion angles of the two conformers of cyclo(D-Trp-L-Pro) is shown in Figure 2.12 and Tables 2.9, 2.10 and 2.11, respectively.

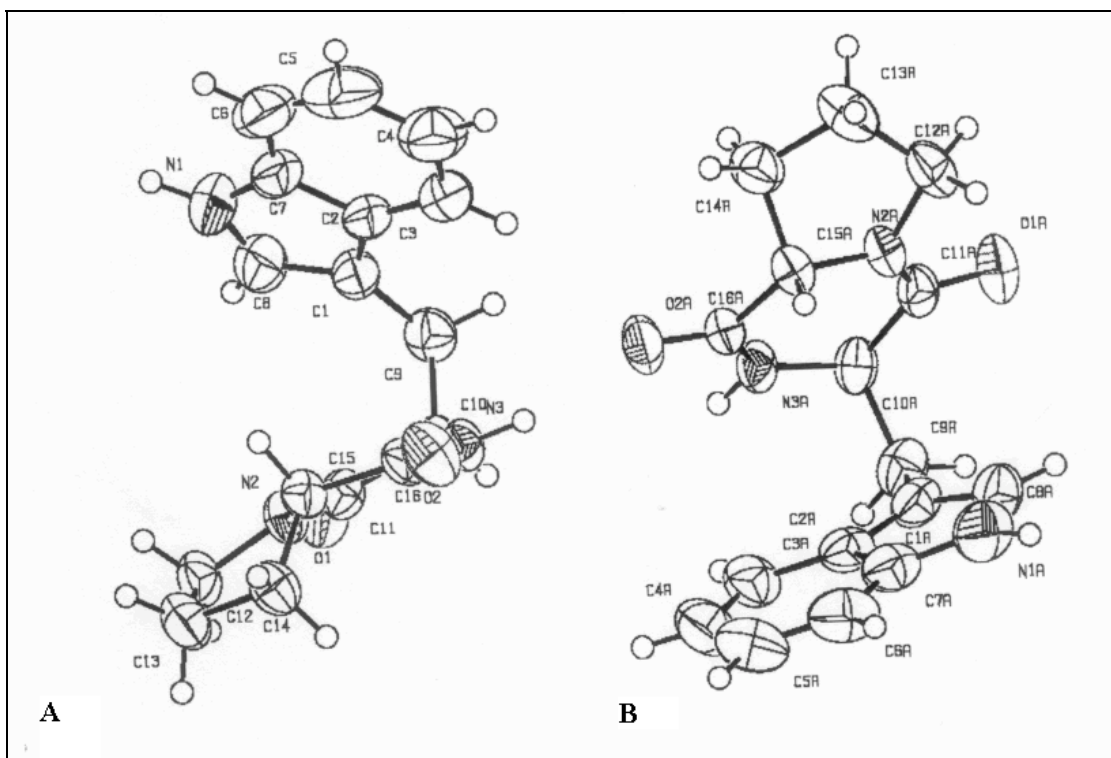


Figure 2. 12: ORTEP view of cyclo(D-Trp-L-Pro) (A - Conformer 1; B – Conformer 2).

Table 2. 8: Fractional atomic coordinates ($\times 10^4$) and equivalent thermal factors ($\text{\AA}^2 \times 10^3$) for conformer 1 of cyclo(D-Trp-L-Pro).

Atom	x/a	y/b	z/c	U_{eq}^a
N(1)	4022(2)	3839(5)	8978(1)	82(1)
C(1)	5248(2)	1578(4)	8592(1)	52(1)
C(2)	4942(2)	3152(4)	8095(1)	53(1)
O(1)	7406(2)	-644(3)	9982(1)	61(1)
N(2)	7832(2)	2629(3)	9779(1)	44(1)
C(3)	5220(2)	3488(4)	7452(1)	64(1)
C(4)	4741(2)	5156(5)	7090(2)	83(1)
C(5)	3977(3)	6514(6)	7355(2)	93(1)
C(6)	3689(3)	6223(5)	7980(2)	83(1)
C(7)	4170(2)	4536(4)	8351(1)	64(1)
O(2)	8406(2)	5086(3)	8255(1)	65(1)
C(8)	4656(2)	2069(5)	9115(1)	70(1)
C(9)	6058(2)	-197(4)	8555(1)	54(1)
C(10)	7398(2)	260(3)	8835(1)	44(1)
N(3)	7893(2)	1836(3)	8446(1)	44(1)
C(11)	7545(2)	734(3)	9580(1)	44(1)
C(12)	8153(2)	3229(4)	10492(1)	54(1)
C(13)	8916(2)	5147(4)	10472(1)	60(1)
C(14)	9099(2)	5379(4)	9733(1)	53(1)
C(15)	7988(2)	4345(3)	9341(1)	42(1)
C(16)	8101(2)	3765(3)	8631(1)	45(1)

$$^a U_{eq} = 1/3 \sum_i \sum_j U_{ij} \mathbf{a}_i \cdot \mathbf{a}_j^* (\mathbf{a}_i \cdot \mathbf{a}_j)$$

Table 2. 9: Fractional atomic coordinates ($\times 10^4$) and equivalent thermal factors ($\text{\AA}^2 \times 10^3$) for conformer 2 of cyclo(D-Trp-L-Pro).

Atom	x/a	y/b	z/c	U_{eq}^a
N(1A)	11262(2)	8125(4)	5803(1)	72(1)
C(1A)	10178(2)	6207(4)	6407(1)	52(1)
C(2A)	10637(2)	7939(4)	6805(1)	51(1)
O(1A)	7577(2)	4113(3)	5316(1)	63(1)
N(2A)	7327(2)	7433(3)	5548(1)	45(1)
C(3A)	10565(2)	8625(4)	7458(1)	62(1)
C(4A)	11151(3)	10380(5)	7690(1)	76(1)
C(5A)	11834(3)	11489(5)	7296(2)	79(1)
C(6A)	11919(2)	10870(5)	6659(1)	72(1)
C(7A)	11320(2)	9107(4)	6414(1)	58(1)
O(2A)	7455(2)	10038(3)	7143(1)	61(1)
C(8A)	10581(2)	6389(5)	5806(1)	65(1)
C(9A)	9389(2)	4546(4)	6600(1)	57(1)
C(10A)	8040(2)	5082(3)	6472(1)	46(1)
N(3A)	7770(2)	6734(3)	6912(1)	45(1)
C(11A)	7623(2)	5528(3)	5729(1)	45(1)
C(12A)	6765(2)	8028(4)	4861(1)	59(1)
C(13A)	5962(2)	9835(4)	4971(1)	68(1)
C(14A)	6104(2)	10120(4)	5738(1)	58(1)
C(15A)	7327(2)	9173(3)	5994(1)	43(1)
C(16A)	7534(2)	8660(3)	6737(1)	43(1)

$$^a U_{eq} = 1/3 \sum_i \sum_j U_{ij} a_i^* a_j^* (\mathbf{a}_i \cdot \mathbf{a}_j)$$

Table 2. 10: Relevant torsional angles of the two conformers of cyclo(D-Trp-L-Pro).

Conformer 1	Conformer 2			Conformer 1	Conformer 2
C16-N3-C10-C11	C16A-N3A-C10A-C11A	ϕ_1	DKP ring	-21.2 (3)	-19.9 (3)
C11-N2-C15-C16	C11A-N2A-C15A-C16A	ϕ_2		-14.3 (3)	-8.2 (3)
N3-C10-C11-N2	N3A-C10A-C11A-N2A	ψ_1		14.9 (3)	14.7 (3)
N2-C15-C16-N3	N2A-C15A-C16A-N3A	ψ_2		8.6 (3)	4.1 (3)
C10-C11-N2-C15	C10A-C11A-N2A-C15A	ω_1		1.9 (3)	-1.9 (3)
C10-N3-C16-C15	C10A-N3A-C16A-C15A	ω_2		9.2 (3)	10.4 (3)
N3-C10-C9-C1	N3A-C10A-C9A-C1A	χ_1^{1A}		-62.9 (2)	-66.6 (2)
C10-C9-C1-C2	C10A-C9A-C1A-C2A	χ_1^{2A}		88.2 (3)	83.9 (3)
C9-C1-C8-N1	C9A-C1A-C8A-N1A			178.2 (2)	178.7 (2)
C2-C1-C8-N1	C2A-C1A-C8A-N1A			-0.7 (3)	0.0 (3)
C9-C1-C2-C7	C9A-C1A-C2A-C7A			-178.7 (2)	-179.0 (2)
C1-C8-N1-C7	C1A-C8A-N1A-C7A			1.0 (3)	0.4 (3)
N1-C7-C2-C1	N1A-C7A-C2A-C1A			0.4 (3)	0.6 (2)
C8-C1-C2-C7	C8A-C1A-C2A-C7A			0.2 (3)	-0.4 (2)
C8-N1-C7-C2	C8A-N1A-C7A-C2A			-0.9 (3)	-0.6 (3)
C6-C7-C2-C3	C6A-C7A-C2A-C3A			-0.4 (3)	0.7 (3)
C4-C3-C2-C7	C4A-C3A-C2A-C7A			0.4 (4)	0.1 (3)
C2-C7-C6-C5	C2A-C7A-C6A-C5A			0.3 (4)	-0.5 (4)
C5-C4-C3-C2	C5A-C4A-C3A-C2A			-0.3 (4)	-1.0 (4)
C7-C6-C5-C4	C7A-C6A-C5A-C4A			-0.2 (5)	-0.5 (4)
C6-C5-C4-C3	C6A-C5A-C4A-C3A			0.2 (5)	1.2 (5)
C13-C14-C15-N2	C13A-C14A-C15A-N2A	χ_2^1	Proline ring	-37.9 (2)	-37.9 (2)
C12-C13-C14-C15	C12A-C13A-C14A-C15A	χ_2^2		27.5(2)	24.2 (2)
N2-C12-C13-C14	N2A-C12A-C13A-C14A	χ_2^3		-6.3 (2)	-1.4 (3)
C15-N2-C12-C13	C15A-N2A-C12A-C13A	χ_2^4		-18.8 (2)	-23.8 (2)
C12-N2-C15-C14	C12A-N2A-C15A-C14A	θ		36.2(2)	39.3 (2)
C11-C10-C9-C1	C11A-C10A-C9A-C1A			64.0 (2)	59.7 (3)
C10-C9-C1-C8	C10A-C9A-C1A-C8A			-90.4 (3)	-94.6 (3)

The crystal data (Table 2.12) shows the crystallization of two conformations of cyclo(D-Trp-L-Pro) in the $P2_1$ space group with the following cell dimensions:

$$\begin{aligned}
 A &= 11.226 \text{ \AA} & \alpha &= 90^\circ \\
 B &= 6.5501 \text{ \AA} & \beta &= 99.627^\circ \\
 C &= 20.049 \text{ \AA} & \gamma &= 90^\circ
 \end{aligned}$$

Table 2. 11: Crystal data of cyclo(D-Trp-L-Pro).

Compound	$C_{16}H_{17}N_3O_2$
Formula weight	284
Space group	$P2_1$
Temperature	293(2)K
Cell constants	
a, \AA	11.226(19)
b, \AA	6.5501(11)
c, \AA	20.049(3)
β , deg	99.627(3)
Cell volume, \AA ³	1453.4(4)
Formula units/unit cell	Z=4
D_{calc}	1.295 Mg/m ³
μ_{calc}	0.088 mm ⁻¹
Max. crystal dimension	0.48x0.20x0.12 mm ³
Reflections measured	10327
Range of h, k, l	h -14, +13; k -8, +8; l -25, +26
No. of parameters varied	394

Both conformers were similar with regard to the conformational orientation of the backbone around the torsional angles found within the DKP ring:

Conformer 1: $\phi_1 = -21.2^\circ$; $\phi_2 = -14.3^\circ$; $\psi_1 = 14.9^\circ$; and $\psi_2 = 8.6^\circ$

Conformer 2: $\phi_1 = -19.9^\circ$; $\phi_2 = -8.2^\circ$; $\psi_1 = 14.7^\circ$; and $\psi_2 = 4.1^\circ$

When $\phi < 15^\circ$, the DKP ring is thought to be planar or weakly puckered (Jankowska and Ciarkowski, 1987).

These angles differed from cyclo(L-Trp-L-Pro), in which the following angles were obtained by x-ray crystallography (Grant *et al.*, 1999):

$$\text{Conformer 1: } \psi_1 = -43.739^\circ; \quad \psi_2 = -38.954^\circ$$

$$\text{Conformer 2: } \psi_1 = -43.272^\circ; \quad \psi_2 = -38.056^\circ$$

As can be noted, these angles are all negative in cyclo(L-Trp-L-Pro), whilst being positive in cyclo(D-Trp-L-Pro).

Similarly, the orientation of the side chain of Trp of the 2 conformers of cyclo(D-Trp-L-Pro) were comparable:

$$\text{Conformer 1: } \chi_1^{1A} = -62.9^\circ; \quad \chi_1^{2A} = 88.2^\circ$$

$$\text{Conformer 2: } \chi_1^{1A} = -66.6^\circ; \quad \chi_1^{2A} = 83.9^\circ$$

When one considers the orientation of the side chain of Trp of cyclo(L-Trp-L-Pro), the following results were obtained:

$$\text{Conformer 1: } \chi_1^{1A} = 62.027^\circ; \quad \chi_1^{2A} = 167.964^\circ$$

$$\text{Conformer 2: } \chi_1^{1A} = 60.934^\circ; \quad \chi_1^{2A} = 171.214^\circ$$

As can be seen, the orientation of the side chain in cyclo(L-Trp-L-Pro) and cyclo(D-Trp-L-Pro) differ considerably, where the side chain of cyclo(L-Trp-L-Pro) is folded towards the DKP ring. This folded conformation is also noted for cyclo(Tyr-Pro) ($\chi^1 = 64.1^\circ$) (Milne *et al.*, 1992). The orientations of the aromatic side chain of cyclo(D-Trp-L-Pro) for both conformers ($\chi_1^{1A} = -62.9^\circ$, and -66.6°) are comparable to the aromatic side chain of Phe-Pro ($\chi_1^{1A} = -79.9^\circ$), which occurs as an extended conformation (E_N) away from the DKP ring (Mazza *et al.*, 1984).

When one considers the steric bulk of aliphatic substituents, the unfolded and folded rotameric states exist, where the order of preference is dictated by the steric bulk. The greater the steric bulk, the greater the preference for the extended state (Anteunis, 1978).

The DKP ring of cyclo(D-Trp-L-Pro) for both conformers can be considered to be unusual, with only four atoms in the plane of the ring. These four atoms are considered to be coplanar, with a distance not exceeding 0.02 Å. The fifth atom, C_α or C2, is 0.5 Å

away from the best plane of the ring. At this C, the ring is puckered. This puckering may result from the repulsion between non-ring atoms bonded to adjoining ring atoms, resultant of a planar structure. Furthermore, this planar structure dictates that the non-ring atoms occupy an eclipsed position. Puckering of the C α relieves tension on the ring as it contains the bulky carboxyl group as opposed to the much less bulky H atoms (Mitsui *et al.*, 1969). Our compound may be characterised as an C $_s$ -C^a-exo, envelope symmetry.

This is in contrast to the usual scenario, in which C4 is puckered. This is the case for hydroxyproline (Mitsui *et al.*, 1969). It is well known that the majority of DKPs preferentially adopt a deep boat-like conformation (Jankowska and Ciarkowski, 1987), further illustrating the uniqueness of the cyclo(D-Trp-L-Pro). Furthermore, the DKP ring of cyclo(L-Trp-L-Pro) can be considered to be a typical boat conformation, in which the C α -C β bond of Pro is orientated equatorially. The DKP ring in cyclo(Tyr-Pro) and cyclo(Phe-F-Pro) are considered to be a flattened chair, with the C α -C β bond of Pro positioned equatorially (Grant *et al.*, 1999).

The torsion angles representing the amide bonds of cyclo(D-Trp-L-Pro) are:

$$\omega_1 = 1.9^\circ; \quad \omega_2 = 9.2^\circ \text{ (Conformer 1)}$$

$$\omega_1 = -1.9^\circ; \quad \omega_2 = 10.4^\circ \text{ (Conformer 2).}$$

Such angles are not uncommon to cyclic dipeptides, since values of up to 8° have been found in many of these compounds (Sletten, 1970). In cyclo(L-Trp-L-Pro), the amide bonds were reported as follows:

$$\omega_1 = 0.230^\circ; \quad \omega_2 = 5.649^\circ \text{ (Conformer 1)}$$

$\omega_1 = -1.017^\circ; \quad \omega_2 = 4.816^\circ$ (Conformer 2). The torsion angles for the amide bonds of cyclo(L-Trp-L-Pro) (Grant *et al.*, 1999) are considerably smaller than those reported for cyclo(D-Trp-L-Pro), ω_2 in particular.

The ψ angles indicate whether the dipeptide follows a collagen-type (conformation B) or a α -helix (conformation A) trend.

Conformer 1: $\psi_1 = 14.9^\circ$; $\psi_2 = 8.6^\circ$

Conformer 2: $\psi_1 = 14.7^\circ$; $\psi_2 = 4.1^\circ$

Since collagen-types have characteristically large positive ψ values and α -helix types have small negative ψ values, it is difficult to group cyclo(D-Trp-L-Pro) as either conformation (Garbay-Jaureguiberry *et al.*, 1980).

Additionally, one may consider the θ values in order to group the cyclic dipeptide as either conformation A or B. Positive θ values are characteristic of conformation A, thus one can conclude that both conformers 1 and 2 are characteristically α -helix (conformation A) (Conformer 1 $\theta = 36.2^\circ$; Conformer 2 $\theta = 39.3^\circ$). This is further supported by the χ_4 values i.e. $\chi_4 = -23.8^\circ$ (conformer 1) and $\chi_4 = -18.8^\circ$ (conformer 2) (Benedetti *et al.*, 1974).

The conformation of the pyrrolidine ring of cyclo(L-Trp-L-Pro) was reported as being C_s - C^β -endo) (Conformer 1) and the puckering mode for conformer 2 as an intermediate between C_s and C_2 , with C^β -endo and C^γ -exo with respect to C' (Grant *et al.*, 1999). Since cyclo(D-Trp-L-Pro) so closely resembles the unique conformation of DL-Proline-HCl ($\theta = 33.7^\circ$; $\chi_4 = -18.4^\circ$), further evidence is thus provided for the characterization of our compound as C_s - C^α -exo, which is a particularly rare conformation (where C_s refers to an envelope symmetry) (Mitsui *et al.*, 1969).

Four intermolecular H bonds are responsible for stabilizing the crystal packing (Table 2.13). Interaction between the nitrogen of the indole ring (Conformer 1) and the carbonyl oxygen of the DKP ring (Conformer 2) constitutes the first H bond. A second H bond is formed between the nitrogen of the indole ring (Conformer 2) and the carbonyl oxygen of the DKP ring of conformer 1. Interaction between the carbonyl oxygens of the DKP rings and nitrogens of the DKP rings make up the remaining 2 H bonds.

Table 2. 12: Hydrogen bonding scheme for cyclo(D-Trp-L-Pro).

D-H--A ^a	D-H (Å)	D-A (Å) ^b	H--A (Å) ^b	D-H—A (Angle) ^b
N3-H23-O2A	0.913	2.833 (2.903)	1.978 (2.257)	155.12° (116.4°)
N3A-H23A-O2	0.881	2.877 (2.902)	2.016 (2.244)	165.41° (117.2°)
N1-H1-O1	0.926	2.855 (3.085)	2.017 (2.215)	149.78° (136.1°)
N1A-H1A-O1A	0.930	2.852 (3.094)	1.926 (2.087)	173.68° (147.0°)

^a D-donor, H-hydrogen, A-acceptor.

^b bonding scheme for cyclo(D-Trp-L-Pro), with results obtained for cyclo(L-Trp-L-Pro) in brackets (Grant *et al.*, 1999).

In all cases, the bond lengths obtained for cyclo(D-Trp-L-Pro) are shorter than those obtained for cyclo(L-Trp-L-Pro) (Table 2.12). The D-H—A angles for cyclo(D-Trp-L-Pro) are considerably larger than those obtained for cyclo(L-Trp-L-Pro).

The internal C_α angles follow an expected pattern with conformer 1 (C_α = 114.53° and 110.4°) and conformer 2 (C_α = 112.98° and 114.72°), which is not significantly different from the unsubstituted cyclic dipeptide cyclo(Gly-Gly), which has the internal angle at C_α of 115.1° (Degeilh and Marsh, 1959). Similarly, cyclo(L-Trp-L-Pro) followed this trend with internal angles measuring at 110.4°, 108.6° (conformer 1) and 110.4°, 108.8° (conformer 2) (Grant *et al.*, 1999).

2.1.6 NMR Spectroscopy (Nuclear Magnetic Resonance)

One of the most powerful tools in chemical research is nuclear magnetic resonance (NMR). NMR is based on the magnetic characteristics of atomic nuclei. It is used to determine the structure of unknown samples and in the elucidation of reaction mechanisms in many fields of chemistry (Günther, 1995. Pp. xiii-xix).

^1H Proton (300 MHz) and ^{13}C (75 MHz) spectra were recorded on a Bruker AM-300 MHz spectrophotometer, with DMSO- d_6 as the solvent and TMS as an internal standard. COSY and Hetcor spectra were obtained in order to assist with the ^1H and ^{13}C assignments. An example of a COSY and Hetcor are included in Appendix B (Figure B 1.9 and 1.10, respectively). COSY's are homonuclear two dimensional correlated spectra (Günther, 1995. Pp.xiii-xix), while Hetcor is defined as the heteronuclear two dimensional ^1H , ^{13}C chemical shift correlation (Günther, 1995. Pg. 477). The ^1H and ^{13}C NMR spectra of the isomers are shown in Figures 2.13-2.20. On the ^{13}C NMR spectra, the DMSO- d_6 peak is noted at 39.43 ppm, while in the ^1H spectra, deuterated H_2O (HOD) is noted at 3.3 ppm, while DMSO- d_6 is observed at 2.5 ppm. The ^{13}C NMR data, ^1H NMR data and the coupling constants of the isomers of cyclo(Trp-Pro) are given in Tables 2.14-2.16, respectively.

Table 2. 13: ¹³C NMR data of the isomers of cyclo(Trp-Pro) using DMSO-d₆ as solvent.

Carbon atom	Cyclo(L-Trp-L-Pro) (ppm)	Cyclo(L-Trp-D-Pro) (ppm)	Cyclo(D-Trp-L-Pro) (ppm)	Cyclo(D-Trp-D-Pro) (ppm)
Pro-α	58.301	58.680	58.572	58.287
Pro-β	27.541	30.626	30.557	27.526
Pro-γ	21.729	22.124	22.074	21.719
Pro-δ	44.469	45.448	45.417	44.454
Pro-C=O	165.379	166.402	166.401	165.365
Trp-α	55.130	58.110	58.066	55.115
Trp-β	25.740	29.363	29.316	25.716
Trp-Ar(C ₂)*	124.247	125.583	125.594	124.234
Trp-Ar(C ₃)	109.184	109.397	109.272	109.176
Trp-Ar(C ₄)	118.106	119.232	119.216	118.088
Trp-Ar(C ₅)	118.500	119.283	119.238	118.486
Trp-Ar(C ₆)	120.751	121.894	121.887	120.733
Trp-Ar(C ₇)	111.097	112.211	112.186	111.082
Trp-Ar(C ₈)	127.238	128.194	128.103	127.224
Trp-Ar(C ₉)	135.886	136.991	136.901	135.870
Trp-C=O	168.852	169.259	169.265	168.838

*Ar = aromatic

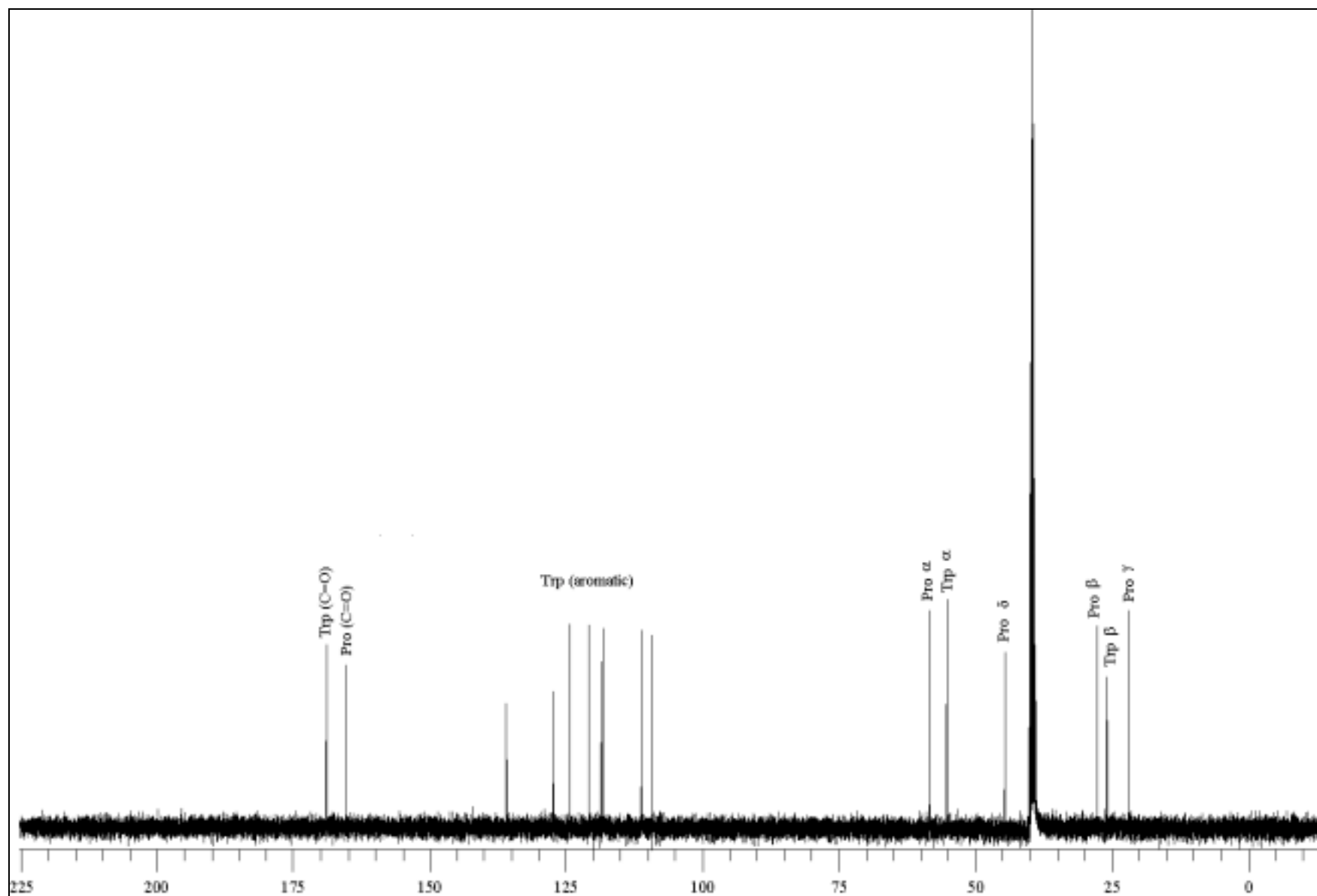


Figure 2. 13: ^{13}C NMR spectrum of cyclo(L-Trp-L-Pro) in DMSO- d_6 .

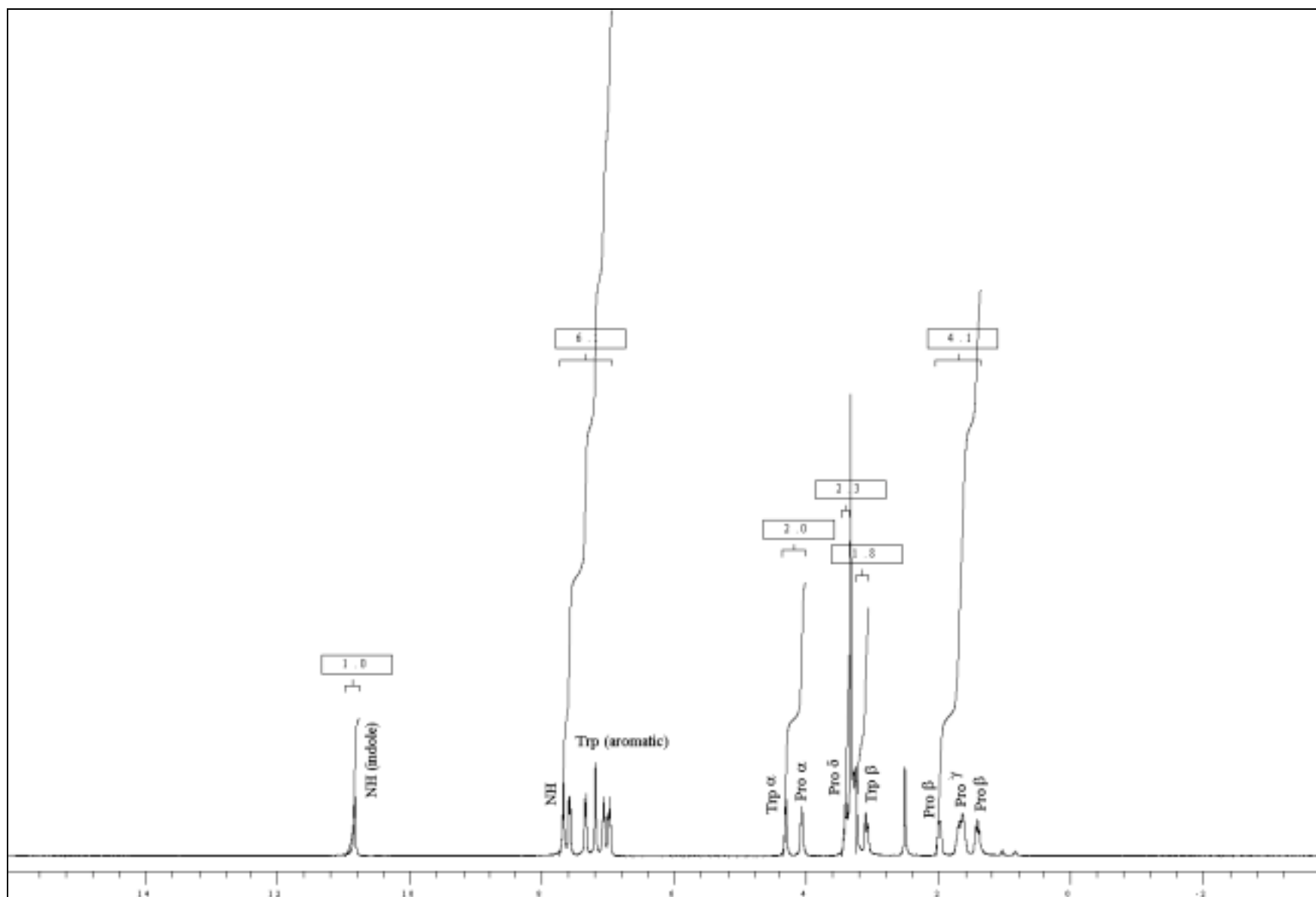


Figure 2. 14: ^1H NMR spectrum of cyclo(L-Trp-L-Pro) in DMSO-d_6 .

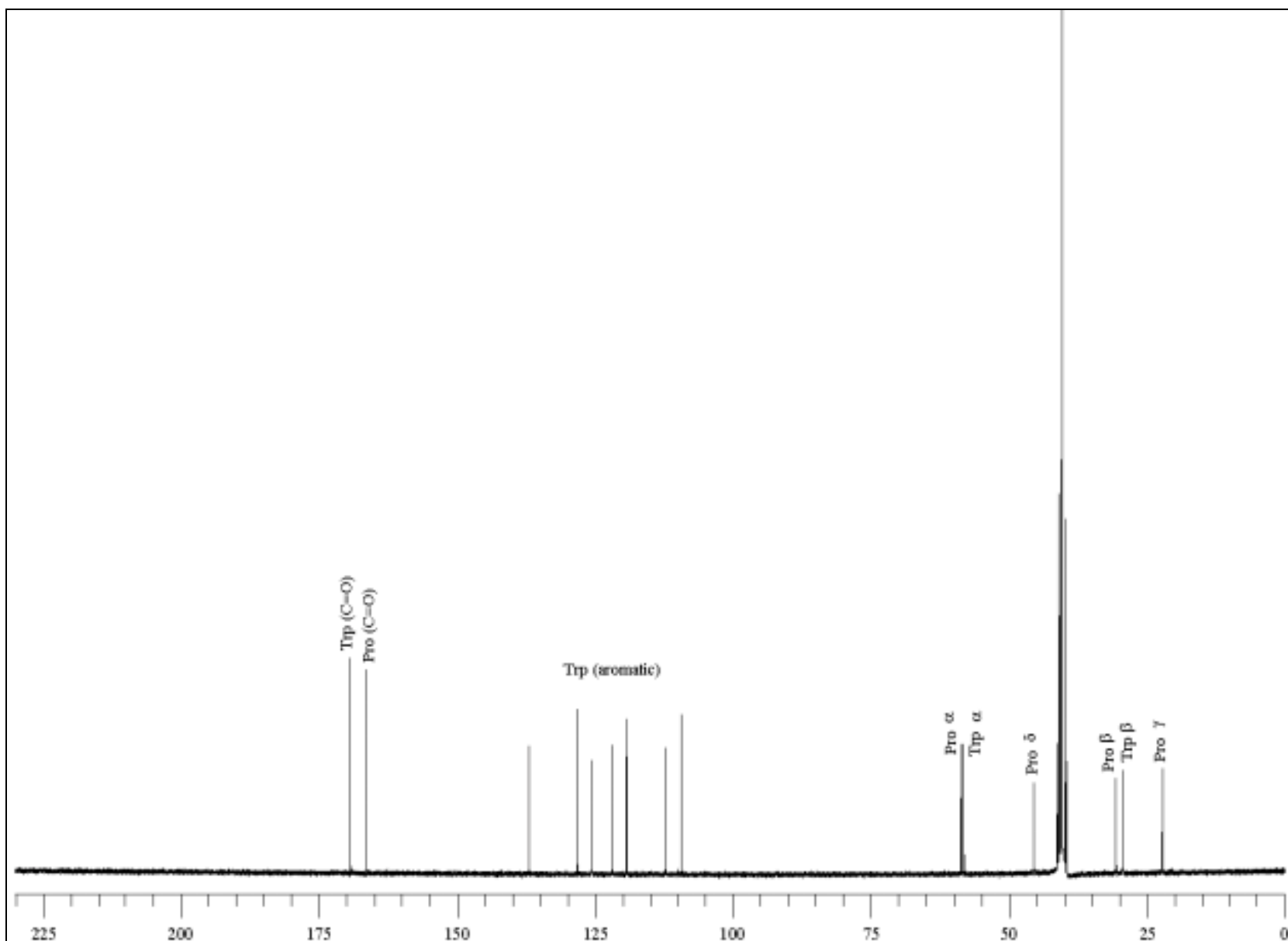


Figure 2. 15: ^{13}C NMR spectrum of cyclo(L-Trp-D-Pro) in DMSO- d_6 .

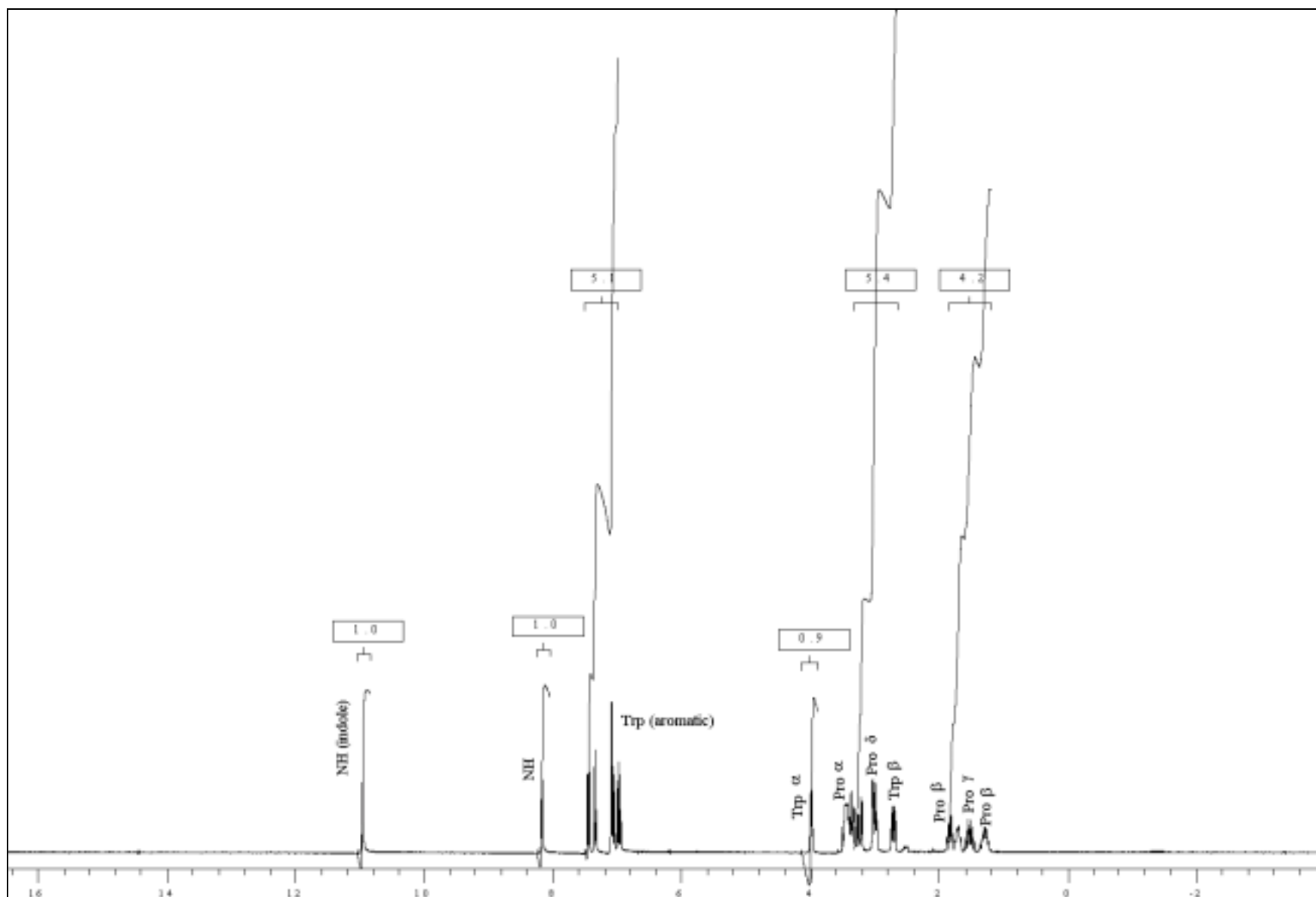


Figure 2. 16: ^1H NMR spectrum of cyclo(L-Trp-D-Pro) in DMSO- d_6 .

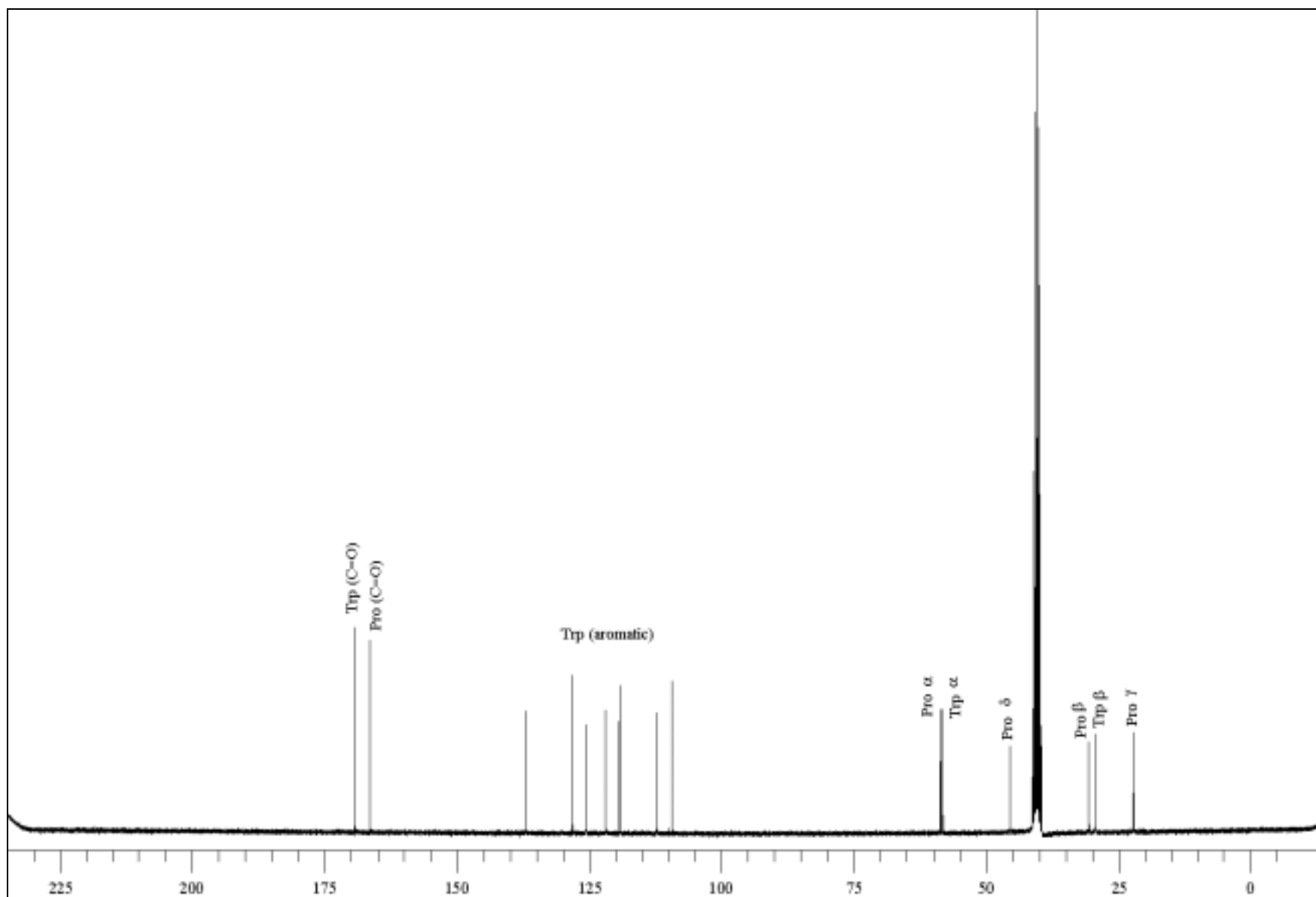


Figure 2. 17: ^{13}C NMR spectrum of cyclo(D-Trp-L-Pro) in DMSO- d_6 .

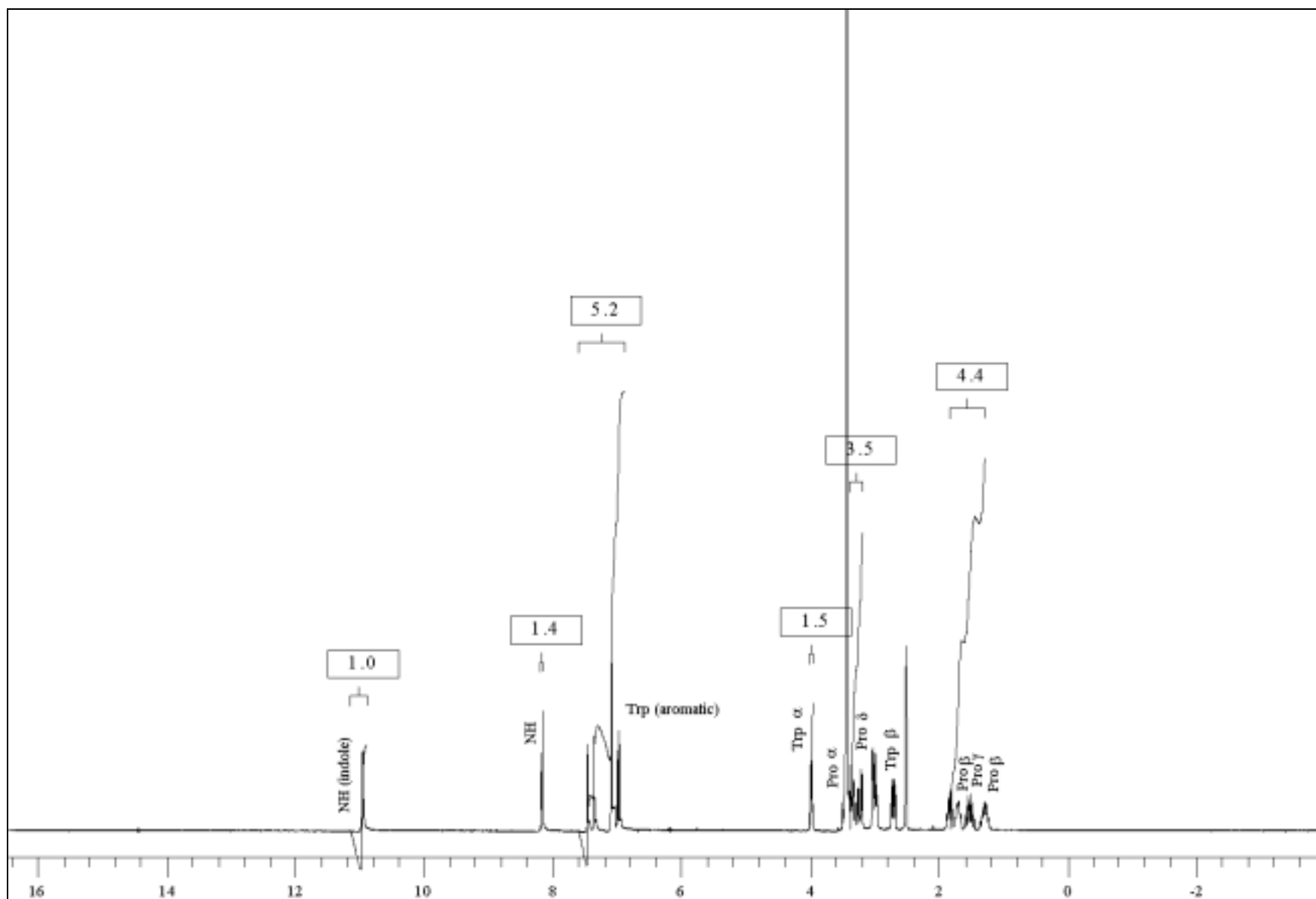


Figure 2. 18: ^1H NMR spectrum of cyclo(D-Trp-L-Pro) in DMSO-d_6 .

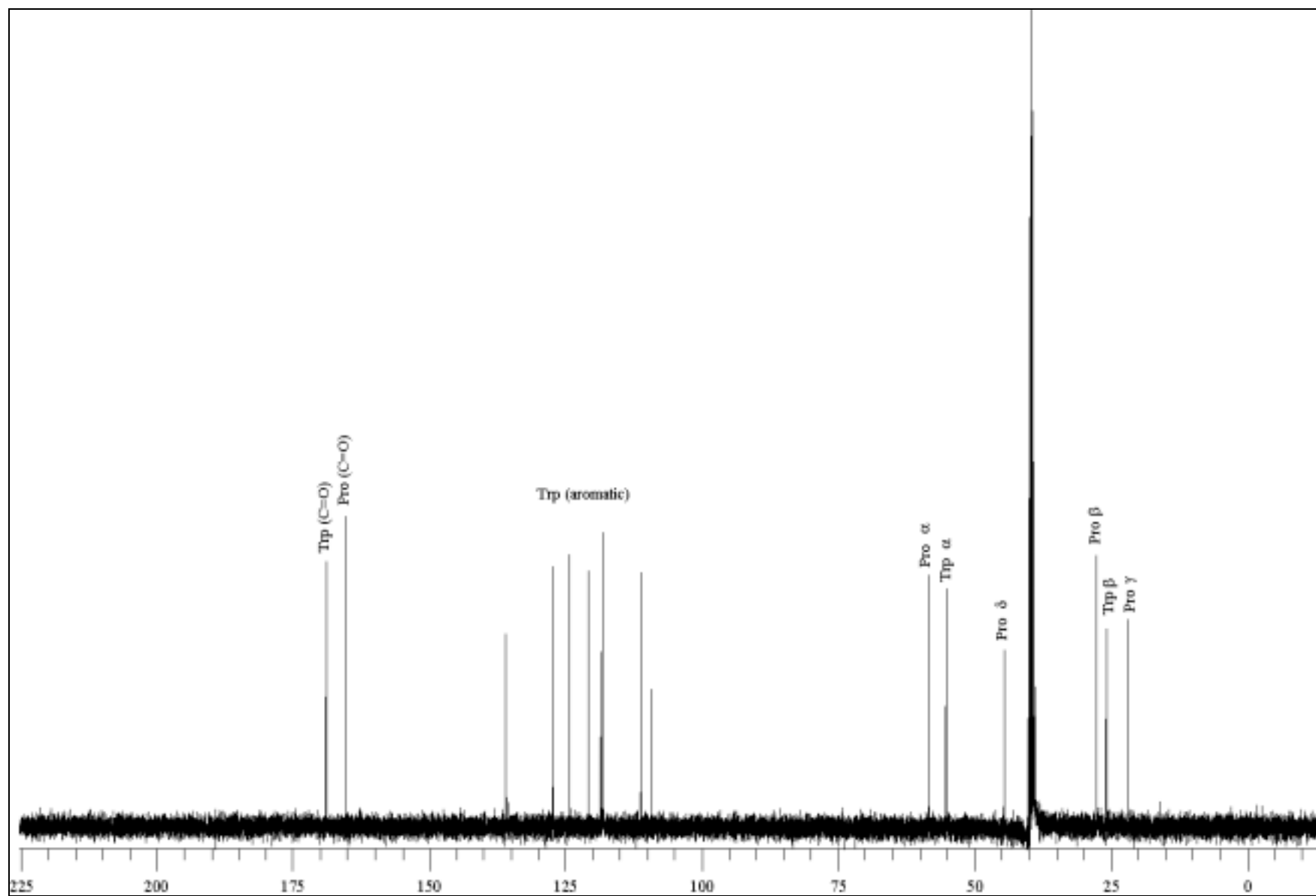


Figure 2. 19: ^{13}C NMR spectrum of cyclo(D-Trp-D-Pro) in DMSO-d_6 .

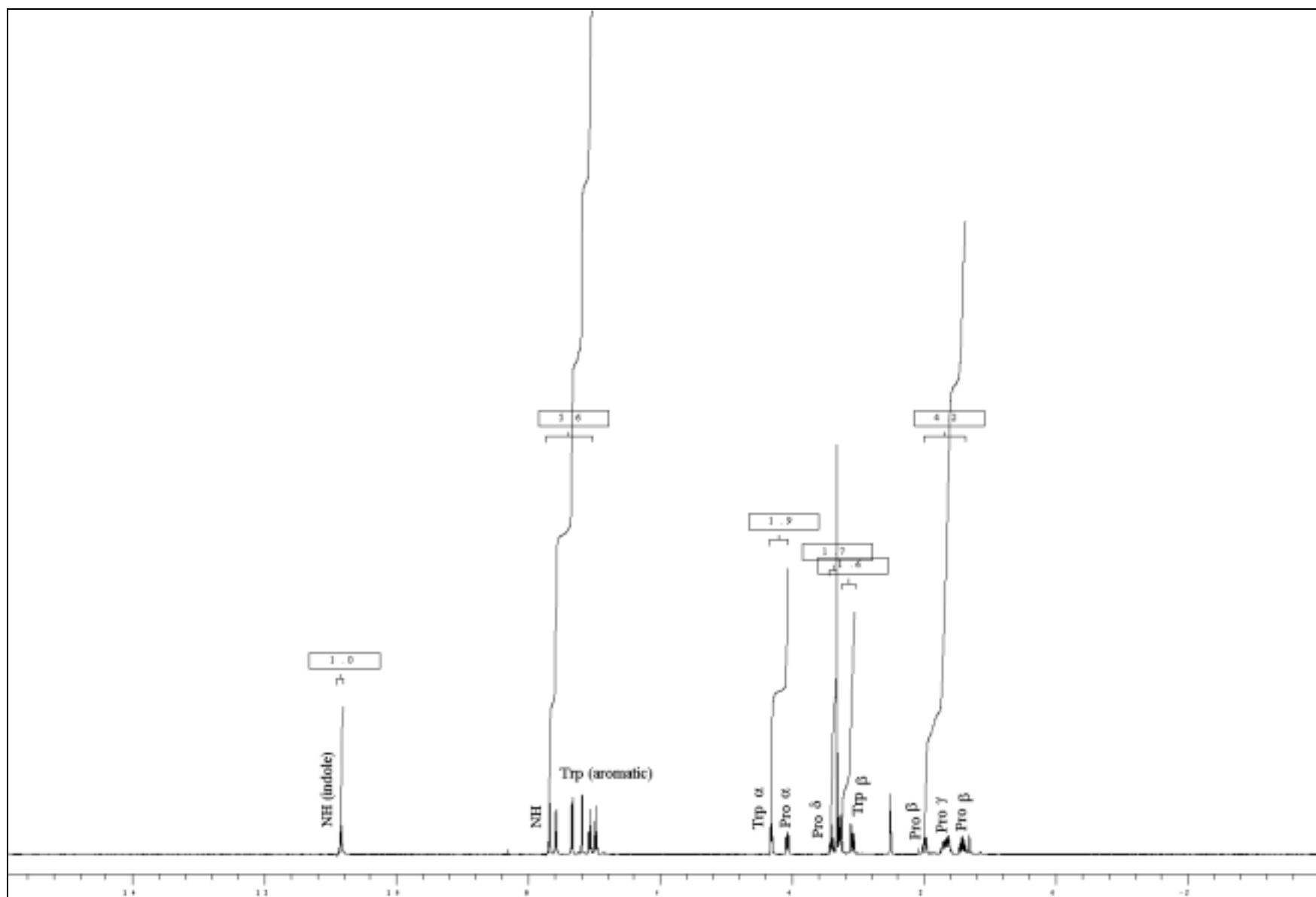


Figure 2. 20: ¹H NMR spectrum of cyclo(D-Trp-D-Pro) in DMSO-d₆.

The C_β resonance of Trp was observed at 25.740 ppm (cyclo(L-Trp-L-Pro)), 29.363 ppm (cyclo(L-Trp-D-Pro)), 29.316 ppm (cyclo(D-Trp-L-Pro)) and 25.716 ppm (cyclo(D-Trp-D-Pro)) (Table 2.14).

When considering the same C_β resonance for cyclo(L-Trp-Gly) (30.7 ppm) and cyclo(L-Leu-L-Trp) (30.7 ppm) (Deslauriers *et al.*, 1975), then it is noted that for the isomers of cyclo(Trp-Pro), the corresponding resonances are shifted upfield by 4.96 ppm (cyclo(L-Trp-L-Pro)), 1.337 ppm (cyclo(L-Trp-D-Pro)), 1.087 ppm (cyclo(D-Trp-L-Pro)), and 4.984 ppm (cyclo(D-Trp-D-Pro)).

For cyclo(L-Trp-L-Pro) (55.13 ppm) and cyclo(D-Trp-D-Pro) (55.115 ppm), C_α resonances of Trp are shifted upfield when compared to the corresponding resonances in cyclo(L-Leu-L-Trp) (57.1 ppm) and cyclo(L-Trp-Gly) (57.0 ppm) (Grant *et al.*, 1999), whereas the C_α-Trp resonances of cyclo(L-Trp-D-Pro) (58.11 ppm) and cyclo(D-Trp-L-Pro) (58.066 ppm) are shifted downfield in comparison.

The $\Delta\delta(\beta\gamma)$ was calculated, as one can assume that this value represents an equilibrium state between the planar and boat forms of the DKP ring (Siemion, 1976). This is expressed by the equilibrium constant K, where $K = [\text{planar form}]/[\text{boat form}]$. It was determined that, for the planar form ($\theta = 60^\circ$), $\Delta\delta(\beta\gamma) = 7.33$ ppm and for the boat form ($\theta = 30^\circ$), $\Delta\delta(\beta\gamma) = 4.90$ ppm. The following equation can be used to determine the amounts of both conformers occurring in the dipeptide:

$$\Delta\delta(\beta\gamma) = 4.90a + 7.33(1-a)$$

where a and (1-a) are molar fractions of the boat and planar forms, respectively. Using this formula, results were only obtained for cyclo(L-Trp-L-Pro) and cyclo(D-Trp-D-Pro). The values of 0.625 (boat) and 0.375 (planar) were obtained for cyclo(L-Trp-L-Pro), while 0.627 (boat) and 0.373 (planar) were obtained for cyclo(D-Trp-D-Pro). Negative results were obtained for cyclo(L-Trp-D-Pro) and cyclo(D-Trp-L-Pro), indicating that these isomers do not assume either a boat or a planar conformation in solution. These results obtained support the stability of the boat conformation for certain cyclic

dipeptides containing Pro residues (Kopple and Marr, 1967). Similar results were obtained for cyclo(L-Trp-L-Pro) in the previous study by Grant *et al.* (1999).

There is a shift in the signal for C α -H (Trp) to a lower field for all the isomers (Table 2.15) in comparison to the corresponding resonance in cyclo(Trp-Trp) (3.87 ppm). The C γ -proton resonance of Pro for the isomers is also shifted upfield in comparison to the same resonance in cyclo(Phe-Pro) and cyclo(Tyr-Pro), which is 1.72 ppm and 1.70 ppm, respectively (Grant *et al.*, 1999).

Table 2. 14: ^1H NMR data of the isomers of cyclo(Trp-Pro) using DMSO-d $_6$ as solvent.

Carbon atom	Cyclo(L-Trp-L-Pro) (ppm)	Cyclo(L-Trp-D-Pro) (ppm)	Cyclo(D-Trp-L-Pro) (ppm)	Cyclo(D-Trp-D-Pro) (ppm)
Pro- α	4.061	3.979	3.980	4.062
Pro- β	1.400	1.250	1.282	1.398
Pro- β	1.971	1.823	1.867	1.982
Pro- γ	1.678	1.693	1.698	1.679
Pro- γ	1.633	1.500	1.519	1.619
Pro- δ	3.405	3.345	3.357	3.409
Trp- α	3.382	3.968	3.949	3.381
Trp- α	4.306	3.979	3.996	4.305
Trp- β	3.101	3.245	3.251	3.104
Trp- β	3.067	3.208	3.203	3.068
Trp-Ar*	7.564	7.486	7.455	7.563
Trp-Ar	7.323	7.326	7.324	7.321
Trp-Ar	7.184	7.079	7.080	7.181
Trp-Ar	7.059	7.060	7.058	7.041
Trp-Ar	6.969	6.968	6.962	6.968
NH (Indole)	10.826	10.826	10.949	10.825
NH	7.667	8.101	8.164	7.671

*Ar = aromatic

The 2 β -protons of the Trp residue differed by 0.034 ppm (cyclo(L-Trp-L-Pro)), 0.037 ppm (cyclo(L-Trp-D-Pro)), 0.048 ppm (cyclo(D-Trp-L-Pro)), and 0.036 ppm (cyclo(D-Trp-D-Pro)) (Table 2.15). In each case, the more shielded β -proton has an apparent coupling to the α -proton of 5.624 Hz (cyclo(L-Trp-L-Pro)), 4.402 Hz (cyclo(L-Trp-D-Pro)), 5.086 Hz (cyclo(D-Trp-L-Pro)), and 5.869 Hz (cyclo(D-Trp-D-Pro)). The less shielded β -proton has an apparent coupling to the α -proton of 4.891 Hz (cyclo(L-Trp-L-Pro)), 4.157 Hz (cyclo(L-Trp-D-Pro)), 4.333 Hz (cyclo(D-Trp-L-Pro)) and 4.891 Hz (cyclo(D-Trp-D-Pro)) (Table 2.16).

These results compare favourably with those reported by Grant *et al.* (1999) for cyclo(L-Trp-L-Pro), whose values were stated as 5.7 Hz (more shielded) and 4.8 Hz (less shielded), respectively. The C_β resonance of Trp in cyclo(Trp-Trp) was reported as 29.88 ppm, where the 2 β -protons differed by 0.51 ppm, with a more shielded coupling of 6.7 Hz, and the less shielded coupling at 4.2 Hz (Grant *et al.*, 1999).

Table 2. 15: Coupling constants of the isomers of cyclo(Trp-Pro) as determined in DMSO- d_6 .

Coupling Constants	Cyclo(L-Trp-L-Pro) (ppm)	Cyclo(L-Trp-D-Pro) (ppm)	Cyclo(D-Trp-L-Pro) (ppm)	Cyclo(D-Trp-D-Pro) (ppm)
$^2J(\text{Trp-}\beta)$	14.427	14.427	13.752	14.627
$^3J(\text{Trp-}\alpha,\beta)$	4.891, 5.624	4.157, 4.402	4.333, 5.086	4.891, 5.869

If one were to consider the α - β coupling values of cyclic dipeptides, the folded conformation would yield equal couplings near 3 Hz, whereas a single, unfolded conformation is presented by one large (14 Hz) and one small (3 Hz) coupling value. Furthermore, if the two couplings are equal and close to 8 Hz, then the two unfolded conformations are populated equally, with the folded conformation being insignificant. If all three conformations are equally populated, then the apparent coupling values should be equal and close to 6.5 Hz (Kopple and Marr, 1967). With this in mind, one could consider all the isomers as having a folded conformation for the aromatic side chain (Table 2.16).

Pachler's analysis (Pachler, 1964) was used to calculate the percentage of the folded conformation (aromatic side chain) for each isomer. An example of the calculation is included in Appendix B. It was determined that cyclo(L-Trp-L-Pro) had a 51.5 %, cyclo(L-Trp-D-Pro) a 59.4%, cyclo(D-Trp-L-Pro) a 52.9 % and cyclo(D-Trp-D-Pro) a 49.3% in the folded conformation.

These results compare favourably with results reported by Grant *et al.* (1999), who showed that cyclo(L-Trp-L-Pro) had a predominance of the folded conformation of 52%. One should however bear in mind that the conformation of the aromatic side chain is dependent on solvent type. In cyclo(Phe-Pro), the side chain favoured an extended conformation in the non-polar solvent cadmium chloride, yet a folded conformation in the polar solvent, DMSO-d₆ (Milne *et al.*, 1992).

2.2 CONCLUSIONS

The isomers of cyclo(Trp-Pro) (cyclo(L-Trp-L-Pro), cyclo(L-Trp-D-Pro), cyclo(D-Trp-L-Pro) and cyclo(D-Trp-D-Pro)) were successfully synthesized ($M_r = 284$), with yields ranging from 70-81% (Table 2.4). Cyclo(L-Trp-L-Pro) and cyclo(D-Trp-D-Pro) were shown to contain *cis*-amide bonds, while cyclo(L-Trp-D-Pro) and cyclo(D-Trp-L-Pro) were shown to contain *trans*-amide bonds (Table 2.7). Endothermic peaks of the isomers were determined by DSC, which showed that the peaks of cyclo(L-Trp-L-Pro) and cyclo(D-Trp-D-Pro) occurred at lower temperatures than cyclo(L-Trp-D-Pro) and cyclo(D-Trp-L-Pro) (Table 2.8). The conformation of the pyrrolidine ring of cyclo(L-Trp-L-Pro) was previously shown as being C_s - C^β -endo (conformer 1) and an intermediate between C_s and C_2 , with C^β -endo and C^γ -exo, with respect to C'. The conformation of the pyrrolidine ring of cyclo(D-Trp-L-Pro) was shown as being a particularly rare conformation, C_s - C^α -exo (envelope symmetry) by X-ray crystallography. NMR analysis indicated that the DKP ring of cyclo(L-Trp-L-Pro) and cyclo(D-Trp-D-Pro) assume a boat/planar conformation, while cyclo(L-Trp-D-Pro) and cyclo(D-Trp-L-Pro) do not. Furthermore, a folded conformation for the side chain of Trp was determined for all the isomers.

CHAPTER 3

SCREEN FOR ANTIMICROBIAL ACTIVITY

3.1 INTRODUCTION

One of the major developments in science has been the discovery and use of antibiotics (Shepherd *et al.*, 1985). As early as 1909, the need for chemical and physical agents that were capable of attacking foreign microorganisms without any adverse effects to the host was recognised as a primary force behind the discovery of chemotherapeutic agents. Since 1935, many such agents have been discovered by screening the metabolic by-products of microorganisms and fungi in the environment. Today, however, these agents are modified and chemically synthesized. A vast number of antibiotics have been discovered and their activity characterised, but as most are toxic to mammalian cells, they are not used in the treatment of infectious diseases (Volk *et al.*, 1996. Pg 258). Bacteria acquire resistance with extreme ease, resulting in species that are multi-drug resistant (Shepherd *et al.*, 1985).

3.1.1 Antibacterial agents

Bacteria are largely grouped into either Gram positive or Gram negative types, based on the cell wall structure. The Gram positive cell wall consists primarily of peptidoglycan that contains peptide interbridges. Within the structure are negatively-charged teichoic and lipoteichoic acids. Attached to the glycerol or ribitol found in lipoteichoic acids are D-alanine, glucose or other molecules. Lipoteichoic acids connect the peptidoglycan layer to the plasma membrane. Examples of Gram positive bacteria include *Staphylococcus*, *Streptococcus*, *Bacillus*, *Enterococcus*, *Lactobacillus* and *Mycobacteria* species (Prescott *et al.*, 1996. Pg. 51).

The Gram negative cell wall is more complex than the Gram positive cell wall. The outer membrane contains lipopolysaccharides (LPS) that contain both lipid and carbohydrates.

LPS contains lipid A, the core polysaccharide and O side chains. Porins, which allow the passage of small molecules, are found embedded in the outer membrane. The plasma membrane lies beneath the periplasmic space and contains integral proteins. The periplasmic space houses a peptidoglycan layer. The outer membrane and peptidoglycan layer are joined by Braun's lipoproteins. In Gram negative cell walls, peptidoglycan contains direct cross-linking whilst Gram positive cell walls contains glycine interbridges. Examples of Gram negative bacteria include *Escherichia*, *Pseudomonas*, *Klebsiella* and *Yersinia* species (Prescott *et al.*, 1996. Pg. 56).

Originally, antibiotic referred to any microbial product that could kill certain microorganisms, but it is now used in a broader sense to include synthetic substances with these properties. No antibiotic is effective against all bacteria though. Antibiotics can be either bactericidal or bacteriostatic, and one that is bactericidal at one concentration may be bacteriostatic at a lower concentration (Singleton, 1992. Pg. 182).

The antibiotic action is usually targeted at a single site, normally a step of macromolecular synthesis in bacteria. These clinically active antibiotics are selectively toxic by inhibiting reactions occurring in bacterial cells but ineffective against the analogous reactions in the host cell. Thus, bacterial targets of antimicrobial activity include peptidoglycan synthesis, synthesis of nucleic acids and proteins. Table 3.1 shows a list of antibiotics and the target site of activity, as well as the spectrum of activity. It is important to bear in mind, however, that inhibiting the synthesis of metabolites available in high quantities in serum or tissue is of little consequence (Volk *et al.*, 1996. Pg. 259). Nevertheless, antibiotic administration in the host is often accompanied by deleterious side effects ranging from rare, lethal reactions (such as irreversible and fatal aplastic anemia) to allergic reactions against the antibiotic (penicillin hypersensitivity), to the growth of drug-resistant opportunistic pathogens as a result of inhibition of microfloral growth (Volk *et al.*, 1996. Pg. 260).

Table 3. 1: Mechanisms of antibacterial actions (Adapted from Volk *et al.*, 1996. Pp. 253-285, 474-495).

Function of cell affected	Antibiotic	Mechanism of action	Spectrum of activity
Cell membranes	Polymyxins	Distorts membrane bilayer thereby interfering with the permeability of the membrane.	<i>Pseudomonas</i>
Nucleic acid synthesis			
Structure and replication of DNA	Metronidazole	Under anaerobic conditions, the nitro group is reduced, producing reactive intermediates or radicals that cause cleavage of DNA.	Anaerobic bacteria.
Supercoiling	Quinolones Nalidixic acid Novobiocin	DNA gyrase activity is affected, thereby resulting in the inhibition of DNA replication, transcription and other activities involving DNA.	Gram negative enteric bacteria. Gram positive bacteria.
Transcription of DNA	Actinomycin Rifamycins	Prevents RNA synthesis by blocking the passage of RNA polymerase to the DNA template. It also complexes with guanine residues in helical DNA. Disturbs the conformation of RNA polymerase.	No selectivity; acts by blocking both eucaryotic and procaryotic transcription. Gram positive bacteria and mycobacteria.
Protein synthesis			
Peptidyl transfer	Chloramphenicol	Binds to the 50S ribosomal subunit and inhibits the peptidyl transfer reaction.	Broad-spectrum antibiotic that is bacteriostatic for most Gram positive and Gram negative bacteria.
Translocation	Fusidic acid	Translational step is inhibited by binding to the elongation factor EF-G.	Gram positive bacteria, in particular staphylococci.
50S ribosomal subunit	Erythromycin Lincomycin and Clindamycin	Interferes with translation by binding to the 50S ribosomal subunit. Binds to the 50S ribosomal subunit and inhibits the peptidyl transfer reaction.	Bacteriostatic for both Gram positive and Gram negative bacteria. Gram positive bacteria (Lincomycin).

30S ribosomal subunit	Streptomycin	Alters membrane permeability. Irreversibly binds to the 30S ribosomal subunit and blocks the movement of the initiation complex. In addition, it also moderately slows transcription and increases misreading.	Bactericidal for Gram positive and Gram negative bacteria.
	Tetracyclines	Inhibits the binding of aminoacyl-tRNA to the acceptor site.	Bacteriostatic against all bacteria except mycobacteria.
Antimetabolites	Sulfonamides	Competitive inhibitor of folic acid biosynthesis by inhibiting the formation of the normal intermediate, dihydropteroic acid in the synthesis of dihydrofolic acid.	<i>Escherichia coli</i>
	Trimethoprim	Inhibits bacterial dihydrofolate reductase.	Broad-spectrum antibiotics effective against rickettsias, chlamydiae and mycoplasmas.
Peptidoglycan biosynthesis			
Precursor synthesis and incorporation	Vancomycin	Blocks transpeptidation by blocking the growth of glycan chains.	Narrow antibacterial activity - Gram positive bacteria.
	D-cycloserine	Inhibits alanine racemase reaction and synthase.	
	Bacitracin	Complexes with undecaprenyl pyrophosphate and prevents its dephosphorylation.	Bactericidal - Gram positive bacteria.
	Fosfomycin	Irreversibly inactivates muramic acid-synthesizing enzyme.	Gram positive and Gram negative bacteria.
	Penicillins	Transpeptidation enzymes responsible for the cross-linking of the	Penicillin G – Gram positive bacteria.

		polysaccharide chains of peptidoglycan are inhibited. Cell wall lytic enzymes are activated.	Ampicillin – Gram negative bacteria
--	--	--	-------------------------------------

The minimal inhibitory concentration (MIC) is defined as the lowest concentration of the drug that effectively prevents the growth of a bacterial culture. MIC values are important in order to establish the levels of antibiotic attained in the serum or tissues on drug administration. An antibiotic cannot be clinically effective unless levels attained at the site of infection surpass the MIC for a sufficient period of time (Volk *et al.*, 1996. Pg. 259).

3.1.2 Antifungal agents

One of the major targets of an antifungal agent is the fungal cell wall. It consists of β -glucans, mannan and chitin. The components of the wall of *Candida albicans* are arranged in layers (fibrillar layer, mannoprotein, β -glucan, β -glucan and chitin, mannoprotein and plasma membrane). Any disruption to the organisation of the cell wall or metabolism of its components would deleteriously affect growth. Included in the functions of the cell wall are: protection against osmotic shock, maintenance of cellular morphology, cytokinesis, prevention from desiccation, it acts as a site of release of enzymes into the exogenous medium, and it provides protection against lytic enzymes and radiation (Debono and Gordee, 1994).

Increased morbidity and mortality among immunocompromised patients are resultant of opportunistic fungal infections. Therapy primarily consists of the azoles and amphotericin B, but is not ideal as only a fungistatic action is obtained with azoles and severe side effects accompany amphotericin B administration (Debono and Gordee, 1994). Eucaryotic fungal cells are similar to human cells, and thus drugs that are toxic to fungal cells are harmful to human cells. In addition, fungi have detoxification systems that modify antibiotics, possibly via hydroxylation. For this reason, antifungal compounds are fungistatic as long as there is repeated application to maintain high levels of the unmodified antibiotics. Antifungal compounds thus have a low therapeutic index. These compounds act by extracting sterols from the cell membranes or by preventing the

synthesis of the sterols. Another target of antifungal compounds is the enzyme chitin synthase, since animal cells do not possess cell walls (Prescott *et al.*, 1996. Pg. 671).

Bioactive cyclic peptides are more stable in acid and are thus more orally bioavailable in comparison to the corresponding linear peptides. In addition, linear peptides are metabolised rapidly. Cyclic peptides containing fatty acyl side chains are important antifungal agents. Echinocandin B and aculeacin A are particularly effective against *C. albicans*. Both these agents contain the same hexapeptide core structure, differing in the fatty acid they are acylated with. Echinocandin B is acylated with linoleic acid, while in aculeacin A, the fatty acid is palmitic acid. These agents act by inhibiting cell wall glucan synthesis (Monaghan and Tkacz, 1990).

Under normal circumstances, *C. albicans*, a dimorphic yeast, is a harmless asymptomatic commensal. Manifestation as a pathogen includes candidoses such as oral and vaginal thrush, myocarditis and septicaemia.

Nucleic acid synthesis in fungi is inhibited by 5-fluorocytosine. It gains entry into *C. albicans* via an energy-dependent process involving cytosine permease that plays an important role in the transport of adenine, cytosine and hypoxanthine. Deamination of 5-fluorocytosine by cytosine permease to 5-fluorouracil is the step that targets the fungal cells, as this enzyme is present at concentrations so low that deamination in other eucaryotic cells is negligible (Shepherd *et al.*, 1985).

Imidazole and triazole derivatives are important azole compounds that exhibit antifungal properties by interfering with sterol synthesis. A new class of antifungal agents is allylamine derivatives. An important example is naftifine, which inhibits ergosterol biosynthesis in dermatophytes, resulting in accumulation of squalene (Shepherd *et al.*, 1985).

3.1.3 Peptide antibiotics

In many biologically active compounds, in particular peptide antibiotics, both L- and D-amino acids are found. In this class of natural products, only a few peptide antibiotics are useful as chemotherapeutic agents. New classes of therapeutic agents have originated from modifications to the amino acids in the peptide-derived antibiotics - included are the β -lactams, glycopeptides and streptogramins. Of the simpler peptides antibiotics, only amino acids joined via the conventional amide bonds are present in the chemical structure, whereas more complex peptide antibiotics may include non-amino acid constituents that are joined in various bonds other than the peptide linkages. Amino acids included in these compounds range from the conventional amino acids to highly modified amino acids not commonly found in various proteins. Finally, the arrangement of the peptide may be linear, cyclic or various combinations thereof (Kirst, 1995. Pg. 498).

A few examples of peptide antibiotics containing both L- and D-amino acids are discussed below.

3.1.3.1 Cycloserine

An antibiotic substance produced by *Streptomyces orchidaceus* is cycloserine in the D(+) isomer form (Figure 3.1). It is a relatively small molecule consisting of a single cyclized D-amino acid. Also active is the L(-) isomer, and more importantly, the D,L mixture is more active than the pure enantiomers. The mechanism of action involves the interference of cell wall synthesis, since it functions as an alanine antimetabolite. Cycloserine readily passes across the blood-brain barrier and is readily absorbed after oral administration (Lemke, 1995. Pg. 754).

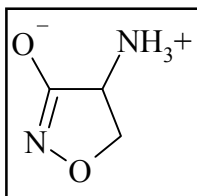


Figure 3. 1: Structure of D-cycloserine (Anand, 1995. Pg. 716).

3.1.3.2 Tryptophan antimetabolites

Microflora, in particular *Bacteroides thetaiotamicron*, are capable of converting tryptophan to toxins and carcinogens. Trp is converted to indole by the action of tryptophanase (Goldin, 1986). When a methyl or fluorine is substituted on the indole moiety of Trp, an effective Trp analogue is produced. 5-Fluorotryptophan (Figure 3.2) and 6-fluorotryptophan prevents the use of anthranilic acid and inhibits the growth of many microorganisms (Lemke, 1995. Pg. 715).

7-Azatriptophan (Figure 3.2) is produced when the 7-C atom of the indole ring is substituted by a N atom, producing a competitive antagonist of Trp. This compound is capable of inhibiting the growth of *Tetrahymena pyriformis*. The growth of *Escherichia coli* and *Bacteroides typhosum* is inhibited by 3-indolylacrylic acid (Figure 3.2) (Lemke, 1995. Pg. 716).

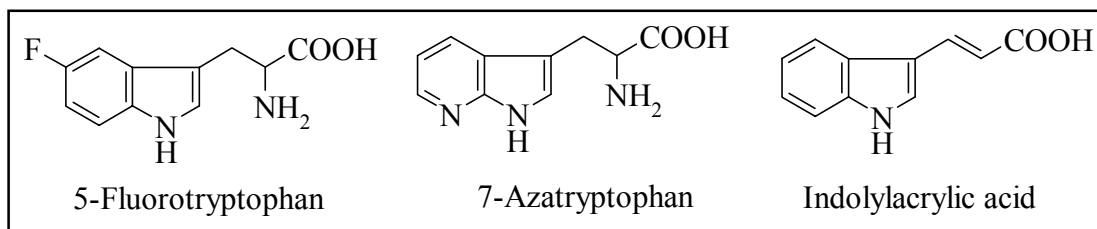


Figure 3. 2: Structures of 5-fluorotryptophan, 7-azatriptophan and indolylacrylic acid. (Lemke, 1995. Pg. 716).

3.1.3.3 Bacitracin

Bacitracin, first isolated from culture broths of *Bacillus licheniformis* in 1943, is active against Gram positive bacteria (Kirst, 1995. Pg. 498). These are commonly used to identify the Lancefield Group A haemolytic streptococci. However, these antibiotics are nephrotoxic when administered parenterally, resulting in haematuria and proteinuria. These drugs are not absorbed by the gut when given orally (Edwards, 1980. Pg. 129). Bacitracin consists of a complex structure (Figure 3.3) - a dodecapeptide that contains an intramolecular hexapeptide ring attached to a thiazoline nucleus (Kirst, 1995. Pg. 498).

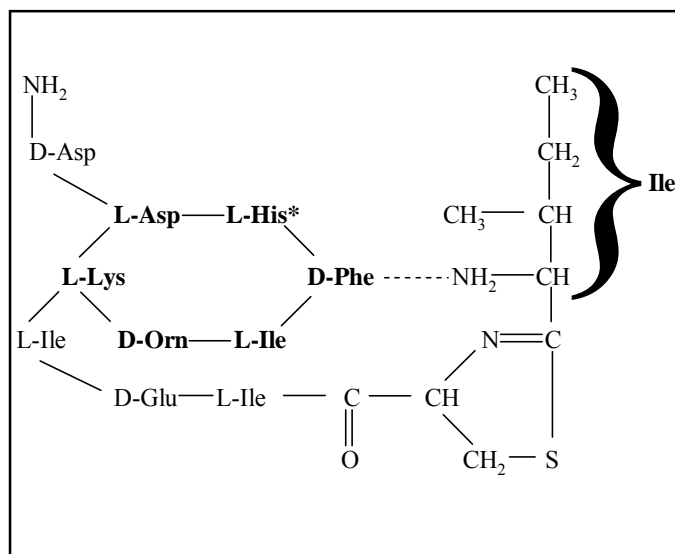


Figure 3.3: Structure of bacitracin. The intramolecular hexapeptide ring is shown in bold-type. L-His*- the amino acid most likely involved in the binding of bacitracin to the pyrophosphate carrier. (Edwards, 1980. Pg. 130).

In Gram positive bacteria, bacitracin complexes with polyisoprenyl pyrophosphate, thereby inhibiting cell wall formation (Kirst, 1995. Pg. 498). This complex formation is dependent on metal ions such as Zn^{2+} and Ca^{2+} and is most likely the property of the histidine side chain (marked with an * in Figure 3.3) (Edwards, 1980. Pg. 130). Another group that may be involved in metal binding is the thiazolidine ring N atom and the amino group of the terminal isoleucine residue as shown in Figure 3.3.1.

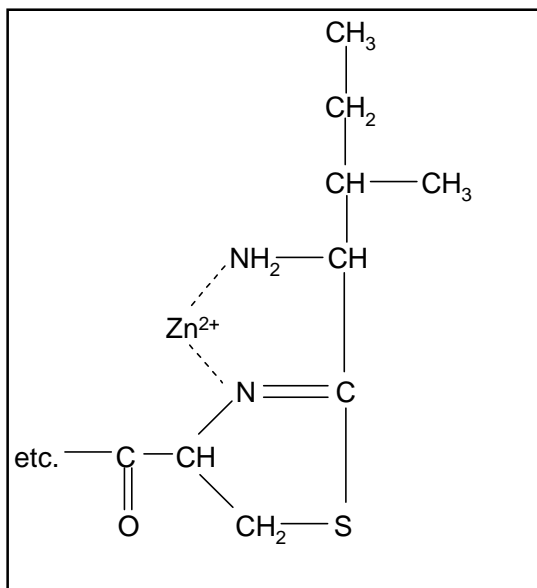


Figure 3.3. 1: Zn^{2+} binding to the amino group of the terminal isoleucine residue and the N atom of the thiazoline ring of bacitracin (Edwards, 1980. Pg. 130).

3.1.3.4 Tyrocidins and the Gramicidins

Bacillus brevis produces a peptide mixture called tyrothricin, which is composed of two compounds, tyrocidin A and gramicidin S. These two compounds occur in a ratio of 4:1, respectively. Gramicidin is a mixture of linear and cyclic peptides, whilst a mixture of three cyclic decapeptides make up the tyrocidin group (Kirst, 1995. Pg. 498). The gramicidin A amino acid sequence (Figure 3.4) consists of alternating D- and L-amino acids (Edwards, 1980. Pg. 145).

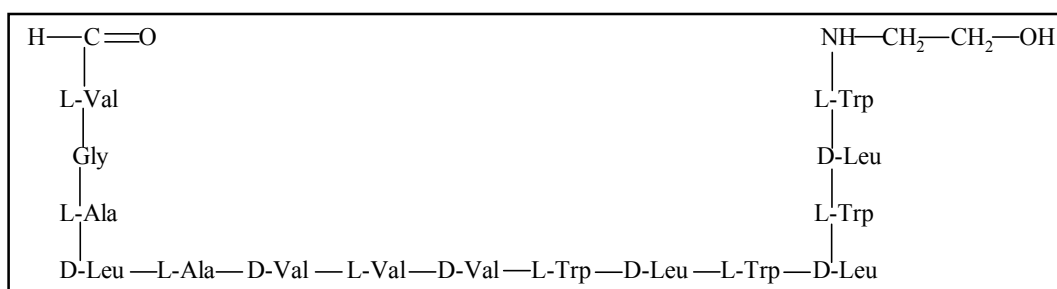


Figure 3.4: Structure of gramicidin A. Abbreviations: Val=valine; Gly=glycine; Ala=alanine; Leu=leucine; Trp=tryptophan. (Edwards, 1980. Pg. 145).

Figure 3.4.1 shows the structure of (a) tyrocidin A and (b) gramicidin S. The left-hand portion of the structure of tyrocidin A (Figure 3.4.1(a)) is found in all tyrocidins, whilst the right-hand portion varies. Gramicidin S (Figure 3.4.1(b)) consists of two identical

pentapeptides that are joined head-to-tail to produce a cyclic decapeptide. This pentapeptide is identical to the left-hand portion of tyrocidin (Gale *et al.*, 1981. Pp. 187-8).

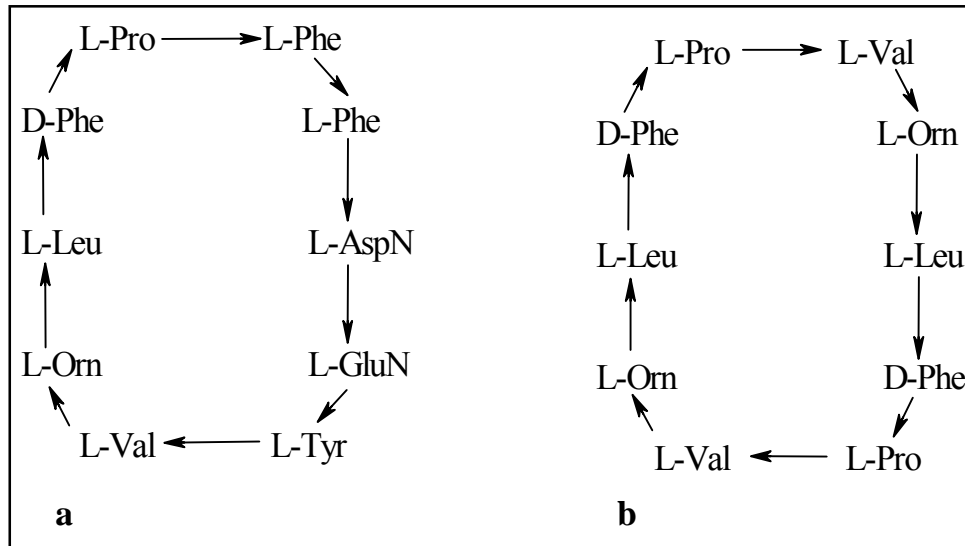


Figure 3.4.1: Structure of (a) tyrocidin A and (b) gramicidin S (Edwards, 1980. Pg. 141).

Gramicidin A (Figure 3.4), B, C, and D differ from gramicidin S (Figure 3.4.1 (b)) in that they are linear pentadecapeptides that are N-formylated. In addition, the C-terminus of these gramicidins forms an amide with ethanolamine (Kirst, 1995. Pg. 499).

The activity of the drug is greatly reduced if the basic amino acids viz. leucine, ornithine, asparagine and glutamine, are replaced (Edwards, 1980. Pg. 141). The importance of the cyclic structure is illustrated in the following experiments. In 1950, the linear pentapeptide of gramicidin S (Val-Orn-Leu-D-Phe-Pro) was produced but showed little antibacterial activity. Four years later, the open-chain decapeptide of gramicidin S was synthesized, but was twelve-fold less effective than gramicidin S under identical conditions. In 1966, an open-chain form of tyrocidin was produced, which showed no activity whatsoever (Gale *et al.* 1981. Pg. 188). It was also shown that the hydrophobic or non-polar residues such as Pro were essential in establishing a bond between drug and membrane, most likely via hydrophobic bonding (Edwards, 1980. Pg. 141).

Both gramicidin and tyrocidin inhibits Gram positive bacteria, although tyrocidin is less potent. In addition, tyrocidin shows activity against Gram negative bacteria. These antibiotics form channels or pores in bacterial membranes, resulting in leakage of cellular contents and loss of the structural integrity of the cell. Gramicidin S interacts with the polar region of the membrane phospholipid via electrostatic interactions that causes membrane disorganisation (Kirst, 1995. Pg. 499). This affects the permeability of the membrane to amino acids and phosphate, eventually resulting in lysis of the cell (Edwards, 1980. Pg. 142).

3.1.3.5 Polymyxin and Octapeptins

Bacillus polymyxa produces five related antibiotics - polymyxin A, B, C, D and E (Figure 3.5). Only polymyxins B and E have been commercially developed. These decapeptides consist of a 9-carbon fatty acid, a cyclic heptapeptide and several units of diaminobutyric acid (Kirst, 1995. Pg. 500).

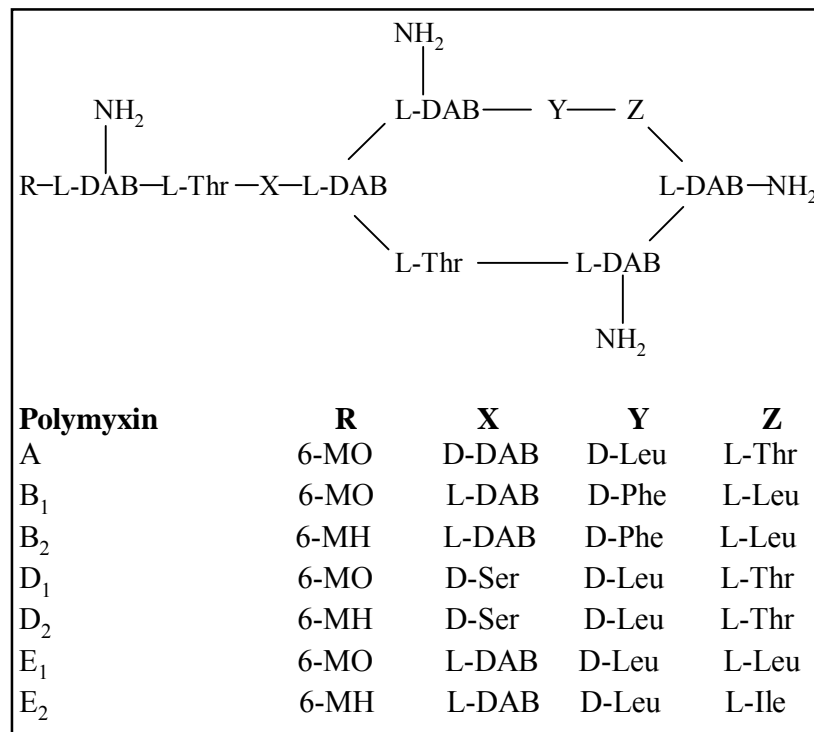


Figure 3. 5: Structure of the polymyxins. 6-MO=6-methyloctanoic acid; 6-MH=6-methylheptanoic acid; DAB=diaminobutyric acid; Thr=threonine; Leu=leucine; Phe=phenylalanine; Ser=serine; Ile=isoleucine (Edwards, 1980. Pg. 142).

Activity is restricted to Gram negative bacteria, in particular against *Pseudomonas*, although ineffective against *Proteus*. These drugs act by binding to membrane phospholipids, thereby disrupting cell membranes in a similar fashion to that of cationic detergents (Kirst, 1995. Pg. 500). Polymyxin is the drug of choice for enteropathogenic infections with *E. coli*. These drugs are administered intravenously or intramuscularly since they are not absorbed by the gut. Other disadvantages of the drug include nephrotoxicity, neuromuscular blockage, dizziness, parasthesias and fever (Edwards, 1980. Pg. 143).

The octapeptins (Figure 3.5.1) differ from the polymyxins in that they contain 8, not 10, amino acid residues and contain a large-chain fatty acid that is linked to the peptide moiety (Edwards, 1980. Pg. 144). These drugs are ten times more effective against Gram positive bacteria than the polymyxins. The octapeptins displace Mg^{2+} and Ca^{2+} from the phosphate groups of the membrane phospholipids in the cell membrane. The fatty acid moiety then interacts with the ordered lipid bilayer. The polar peptide ring then interacts with the phosphate end of the lipids, resulting in the displacement of the divalent cations that are normally present there (Edwards, 1980. Pg. 144).

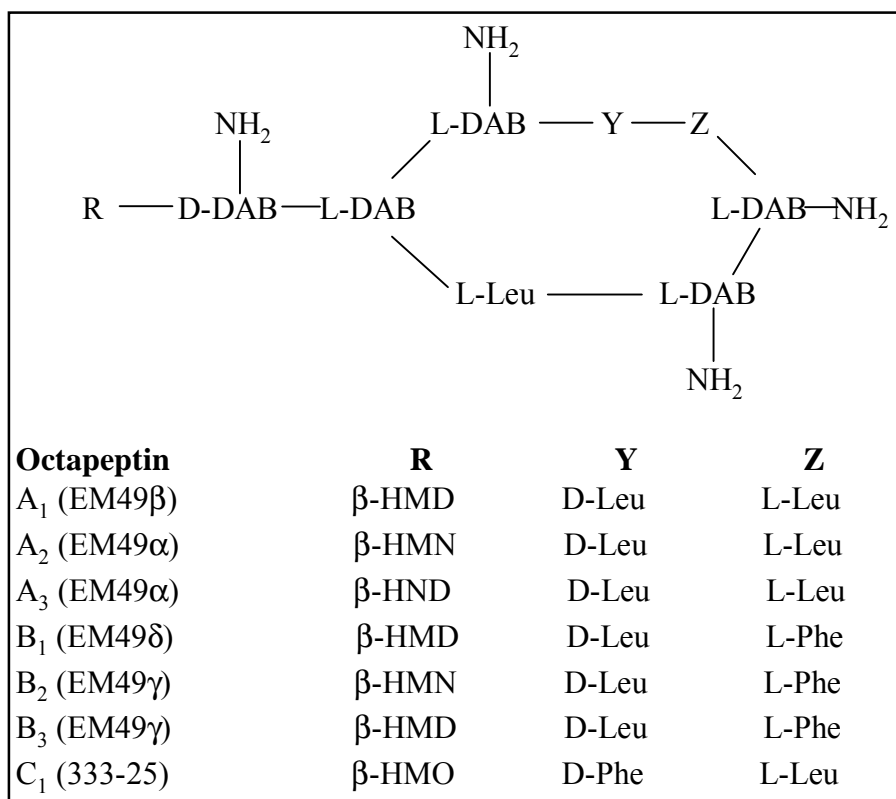


Figure 3.5. 1: Structure of octapeptin. β-HMD=β-hydroxy-8-methyldecanoic acid; β-HND=β-hydroxy-*n*-decanoic acid; β-HMN=β-hydroxy-8-methylnonanoic acid; β-HMO=β-hydroxy-6-methyloctanoic acid; DAB=diaminobutyric acid; Leu=leucine; Phe=phenylalanine. The abbreviation in brackets indicate the alternative name used in literature. (Edwards, 1980. Pg. 142).

3.1.3.6 Valinomycin and Enniatin

This group of cyclic depsipeptides contain 12 (valinomycin) or 6 (enniatin) (Figure 3.6) residues in which amino acids and hydroxyacids alternate (Edwards, 1980. Pg. 146).

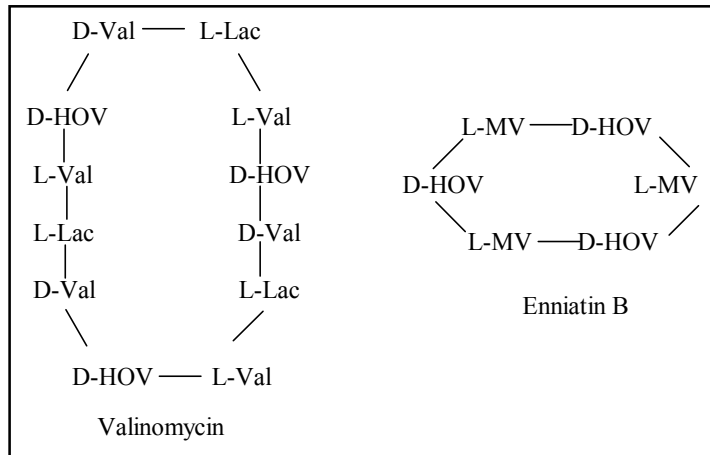


Figure 3. 6: Structures of valinomycin and enniatin. Val=valine; HOV= α -hydroxyisovaleric acid, Lac=lactate; MV=*N*-methylvaline. (Edwards, 1980. Pg. 146).

Valinomycin is produced by *Streptomyces fulvissimus*. It consists of a tetrapeptide (D-Val-L-Lac-L-Val-D-HOV) that is cyclized in a head-to-tail fashion. Enniatin B consists of an alternating sequence of L-*N*-methylvaline and D- α -hydroxyisovaleric acid (D-HOV). Both valinomycin and enniatins are active against Gram positive bacteria and fungi, but have no clinical application (Edwards, 1980. Pg. 146).

3.1.3.7 Enduracidin

Enduracidin, a feed additive in veterinary practice in Japan, is produced by *S. fungicidicus*. This complex consists of 16 aromatic and aliphatic D- and L-amino acids linked via 15 amide bonds and one ester bond with L-threonine, forming a macrocyclic ring. The L-threonine found in the ester bond is N-acylated by L-aspartic acid, which in turn, is N-acylated by an unsaturated 12- or 13-carbon branched-chain fatty acid. It is effective against Gram positive bacteria by inhibiting cell wall synthesis (Kirst, 1995. Pg. 500).

3.1.3.8 Ramoplanin

Isolated from culture broths of *Actinoplanes*, ramoplanin (Figure 3.7) is structurally similar to enduracidin. The ester bond involves β -hydroxyaspartic acid, which is N-acylated by asparagine. Asparagine is in turn N-acylated by an unsaturated 9-carbon branched-chain fatty acid. Another difference is that a *p*-hydroxyphenyl-glycine is glycosylated by 2-*O*-(α -D-mannosyl)- α -D-mannosyl. By blocking the biosynthesis of peptidoglycan components of the bacterial cell wall, it effectively inhibits Gram positive bacteria (Kirst, 1995. Pg. 501).

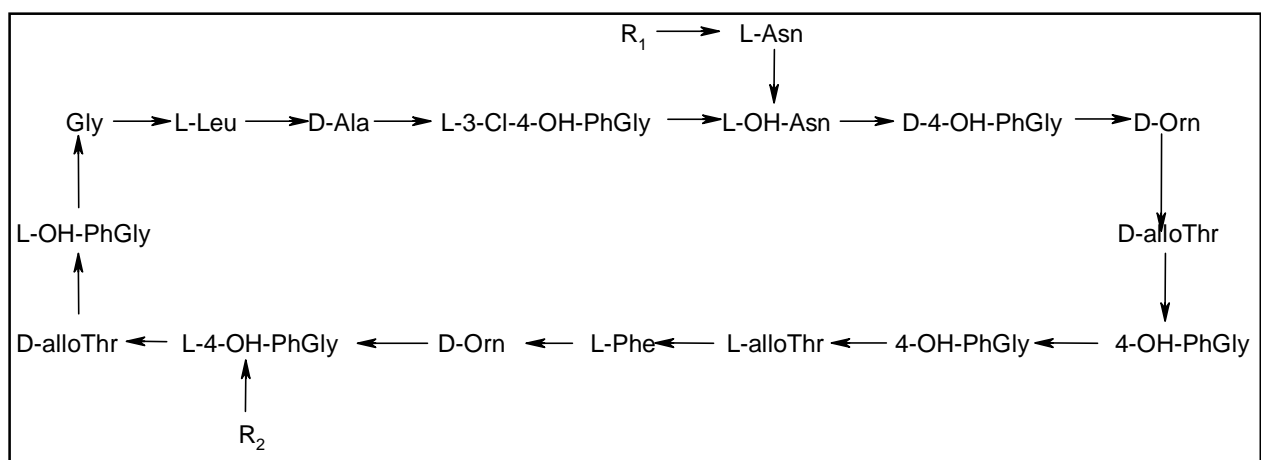


Figure 3. 7: Structure of ramoplanin A₂. R₁=7-methyl-2,4-octadienoyl; R₂= α -D-mannosyl- α -D-mannosyl (Kirst, 1995. Pg. 501).

3.1.3.9 Daptomycin

A foremost example of a semisynthetic peptide antibiotic is daptomycin (Figure 3.8). It is effective in inhibiting Gram positive bacteria. A prerequisite for activity is Ca²⁺. Proposed mechanisms of action include (i) bacterial membrane potential disruption and (ii) lipoteichoic acid synthesis inhibition (Kirst, 1995. Pg. 503).

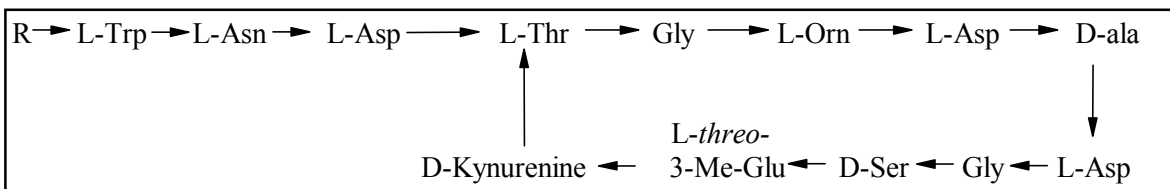


Figure 3. 8: Structure of daptomycin. (Kirst, 1995. Pg. 503).

From the above discussion, it is clear than potential drug entities should be investigated, not only in the L-amino acid configuration, but also in the D-amino acid configuration, including combinations of the two. This will allow the biological activities of the potential drug entities to be fully investigated. Since cyclo(Trp-Pro) is a cyclic peptide, it may prove to be a potential antimicrobial agent.

3.1.4 Determining the level of antimicrobial activity

A critical aspect in drug discovery is the choice of a suitable screening assay. *In vitro* biochemical assays employed in the screening program are supported by secondary or counter assays to provide confirmation for specificity or efficacy (Monaghan and Tkacz, 1990).

The use of agar diffusion techniques is practical only for defined inhibitors, but false positives and negatives are introduced when assessing extracts containing unknown components. The effects noted may be exaggerated by contaminants and MICs cannot be determined. Turbidity testing is the next most widely used assay, but this requires large sample volumes that are often not available. Turbidity readings with microplate readers are inaccurate in that some samples clump at the bottom of the wells, while other organisms stay in suspension (Eloff, 1998). Plate-counting techniques often underestimate microbial biomass as a result of selectivity of growth media, clumping of cells and slow growth rates (Bensaid *et al.*, 2000). This need for a rapid and accurate method in determining cell densities in small culture volumes led to the development of colorimetric assays using tetrazolium salts, such as 3-[4,5-Dimethylthiazol-2-yl]-2,5-diphenyltetrazolium bromide (MTT). Previously, haemocytometer counting and protein content have been used, which are time-consuming and tedious. Wet or dry weight determination is not suitable for small culture volumes and measurement of optical density only applies for regularly shaped cells, as in yeasts (Freimoser *et al.*, 1999).

3.1.4.1 Colorimetric assays using tetrazolium salts

Tetrazolium salts have been used in the identification of various dehydrogenase enzymes at electron transport chain sites and the viability of many biological systems in the form of susceptibility testing (Summanen *et al.*, 1992). MIC values of drugs can be also ascertained by using the National Committee for Clinical Laboratory Standards (NCCLS) recommended microdilution method. This method was compared to the MTT assay. The NCCLS method involves visual MIC determination and is thus objective. Clinical isolates comprising of filamentous fungi were tested against 6 antifungals. A 96% agreement in MIC levels by both methods was determined for MIC-0 (clear wells), with a 92% agreement for MIC-1 (75% growth reduction). Furthermore, the NCCLS method appeared to be more reproducible than MTT for both MIC-0 and MIC-1 determination. Nevertheless, the MTT assay was less time consuming, with results obtainable 24 hr prior to the NCCLS method results (Meletiadiis *et al.*, 2000).

A number of pre-conditions are needed by a tetrazolium-microbe combination for formazan deposition, including the following:

- Diffusion and/or transport of the tetrazolium salt to the reduction site.
- The rate of tetrazolium cation reduction should be at such a pace that formazan is produced at detectable amounts within the reaction time.
- Recognition of formazan within a cell is dependent on localization thereof (Thom *et al.*, 1993).

Some factors affecting the development of cell-associated formazan are listed in Table 3.2 (Adapted from Thom *et al.*, 1993).

Table 3. 2: Factors influencing formazan production in the cell.

Organism-related factors	Reagent-related factors
Structure of the cell envelope	Lipophilicity, charge and molecular size
Physiological state eg. growth rate	Reduction mechanism
Type of oxidative metals	Reducibility of the tetrazolium salt
Types of oxidative enzymes and electron transport activity	Pattern of formazan deposition
Superoxide dismutase activity	Absorbance characteristics of formazan

It should also be noted that some reduction might occur at the surface of the cell. These electrons or species that reduce the tetrazolium salt may diffuse away from the production site and reduce the tetrazolium salt in the medium (Thom *et al.*, 1993).

3.1.4.1.1 3-[4,5-Dimethylthiazol-2-yl]-2,5-diphenyltetrazolium bromide (MTT)

This colorimetric assay is based on the transformation and subsequent colorimetric quantification of the tetrazolium salt, MTT (Figure 3.9). This yellow tetrazolium salt acts as an electron acceptor (Mshana *et al.*, 1998) and in the presence of biologically active organisms, is reduced to insoluble purple MTT formazan crystals (Eloff, 1998). MTT is reduced by the respiratory chain and other electron transport systems. Quantification of the number of crystals can be measured spectrophotometrically. The number of mitochondria (eucaryotic cells) can be estimated and thus the number of viable cells in the sample (Freimoser *et al.*, 1999). The amount of MTT reduction gives a good correlation with the number of colony forming units (CFUs) in the case of bacterial assays (Hjertstedt *et al.*, 1998).

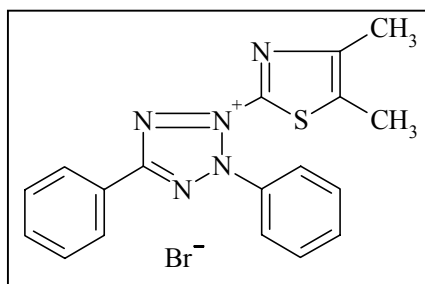


Figure 3. 9: Structure of MTT (Sigma catalogue, 2000-2001. Pg. 686).

Removal of the media prior to extraction of the formazan product with organic solvents such as HCl-isopropanol, dimethyl sulfoxide (DMSO), ethanol or HCl-sodium dodecyl sulfate and mineral oil (Borenfreund *et al.*, 1988), results in improved accuracy and reliability. This is an advantage over the use of 2,3-bis[2-methoxy-4-nitro-5-sulphophenyl]-2H-tetrazolium-5-carboxanilide (XTT), a MTT analogue (Jahn *et al.*, 1995), which forms a water-soluble formazan product (Freimoser *et al.*, 1999).

Menadione, an electron-coupling agent, can be used to increase the rate of MTT reduction (Jahn *et al.*, 1995) thereby decreasing the incubation time required. However, this was found to be unnecessary, as the amount of MTT reduction can be effectively increased by increasing the incubation period to 48 or 72 hrs (Meletiadis *et al.*, 2000). Furthermore, addition of menadione to assays involving fungi resulted in less consistent endpoint determinations, higher MIC values and a decrease in correlation with other reference methods (Clancy and Nguyen, 1997).

Advantages of the MTT assay includes accuracy, sensitivity (Eloff, 1998), reliability, it is time and cost effective, simplicity, small sample sizes are required (Eloff, 1998), large numbers of samples can be tested simultaneously, no radioactive reagents are required (Gomez-Florez *et al.*, 1995; Meshulam *et al.*, 1995) and high levels of skill are not needed. Furthermore, it is considered more accurate than counting since the MTT assay considers all cells in a sample, not just a subsample (Freimoser *et al.*, 1999). A good correlation exists between this assay and the macrodilution method, with easily interpretable endpoint determinations possible when fungi are involved. The assay also

has the potential to be automated (Clancy and Nguyen, 1997). A disadvantage of this assay is that the formazan product must be extracted. When fungi are used, the sensitivity of the assay is reduced, since a high number of fungi are needed to obtain reliable absorbance measurements of MTT reduction (Meshulam *et al.*, 1995). In addition, this method may detect viable organisms that have been damaged by adverse conditions and are unable to proliferate normally (Hjertstedt *et al.*, 1998).

3.1.4.1.2 2,3,5-triphenyltetrazolium chloride (TTC)

Oxidised TTC is a water-soluble tetrazolium salt. Once reduced, TTC acts as a terminal electron acceptor and is transformed to a deep red formazan precipitate (Summanen *et al.*, 1992). In various biological systems at pH values below 11, TTC is reduced to triphenylformazan, a red, water-insoluble product, via respiratory-linked dehydrogenase enzymes that need NAD^+ and NADP^+ . TTC was thought to be reduced at the cytochrome *c* oxidase level where it competes with O_2 for reducing equivalents. It was however found that TTC is reduced by complex I dehydrogenases, possibly by accepting electrons from low potential cofactors. This reduction reaction is reversed by reoxidation by O_2 . Thus, formation of the formazan precipitate only occurs under anaerobic conditions (Rich *et al.*, 2001). For this reason, it is recommended that no shaking occur during incubation, since aeration would interfere with the reduction process. Interference by reducing sugars in this reduction reaction is excluded, as these sugars are only involved at pH values above 11. It has already been proven that a linear relationship exists between cell number and the intensity of red colour produced at a known concentration of TTC (Hurwitz and McCarthy, 1986).

Advantages of the TTC assay include its simplicity and the fact that results can be obtained in a relatively short period of time. The sensitivity of the assay can be increased, however, by prolonging the incubation period. In addition, non-viable cells do not interfere with the assay (Hurwitz and McCarthy, 1986). A good correlation exists between TTC reduction and turbidity (Mattila, 1987). Another advantage stated was that this assay could be widely applied, since a great variety of microbes are capable of

reducing TTC. This was a conclusion drawn by Hurwitz and McCarthy (1986) from data that tested the ability of only *E. coli* to reduce TTC.

3.1.4.1.3 2,3-bis[2-methoxy-4-nitro-5-sulfophenyl]-2H-tetrazolium-5-carboxanilide (XTT)

When H is removed from a substrate by dehydrogenase enzymes, it is delivered to free O₂ or synthetic acceptors along a set of carriers. Free O₂ or the acceptor converts it to a coloured product. Measurement of the dehydrogenase activity of the electron transport system is achieved by the use of artificial electron acceptors such as XTT (Bensaid *et al.*, 2000). XTT (Figure 3.10) is reduced by dehydrogenases to yield a water-soluble formazan product. This reduces assay time since no extraction of the formazan product is necessary (Hawser, 1996). An added advantage of the XTT assay is that highly pathogenic bacteria can be tested safely in bactericidal assays by reducing potential exposure of the researcher to bacterial aerosols. XTT can be substituted for MTT to improve simplicity (no extraction of the formazan product) and increase sensitivity for assays involving fungi. XTT results should be interpreted as fungal damage and not necessarily lethal effects (Meshulam *et al.*, 1995).

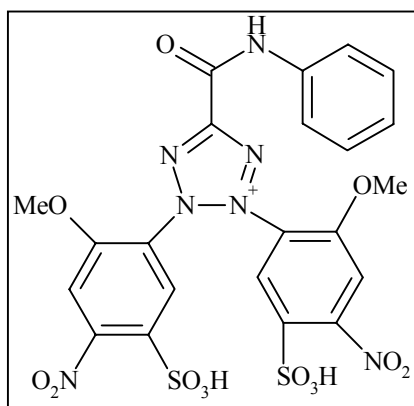


Figure 3. 10: Structure of XTT (Sigma catalogue, 2000-2001. Pg. 1017).

When XTT and MTT were compared in testing for *Mycobacterium bovis* used in live bovine vaccines, XTT was found to detect a lower number of colony forming units (CFU) than MTT (7×10^4 CFU/ml) (Kairo *et al.*, 1999). Stevens and Olsen (1993) reported that bacteria (*S. aureus*, *E. coli*, *Listeria monocytogenes* and *Brucella abortus*) did not reduce

XTT in the absence of coenzyme Q. In addition, the bacteria reduced XTT in the presence of coenzyme Q at a slower rate than they did MTT, resulting in lower absorption readings being obtained. In contrast, when *E. coli*, *Pseudomonas putida*, *Bacillus subtilis* were tested using the XTT assay, it was reduced by all the cultures in the absence of an electron coupling agent. It was thus concluded that the addition of an electron coupler was unnecessary (Roslev and King, 1993). A direct relation between the absorption of the formazan product by XTT reduction and viable bacterial cell number exists (Stevens and Olsen, 1993).

3.2 OBJECTIVES OF THE CHAPTER

3.2.1 Objectives of the present chapter

- ♦ The main objective was to screen the isomers for antimicrobial activity.

In order to satisfy this objective, the following experimental data was collected:

- The susceptibility of both Gram negative and Gram positive bacteria to the isomers at various concentrations were examined using the MTT assay;
- The susceptibility of Gram negative bacteria to the isomers at various concentrations were examined using the TTC assay (Gram positive bacteria did not reduce TTC under experimental conditions used);
- The sensitivity of the MTT assay was compared to that of the TTC assay;
- The susceptibility of the yeast *C. albicans* to the isomers at various concentrations were tested using the MTT and XTT assay;
- The sensitivity of the MTT assay was compared to that of the XTT assay when used in experiments containing yeasts.

3.3 MATERIALS AND METHODS

3.3.1 Microorganisms used in the screen for antimicrobial activity

Pure cultures of *E. coli*, *Pseudomonas aeruginosa* (*P. aeruginosa*), *Streptococcal* sp., *S. aureus* and *C. albicans* were generously donated by the Department of Biochemistry and Microbiology, University of Port Elizabeth. *P. aeruginosa* is a non-fermentative bacillus that causes severe and often fatal infections in immunocompromised patients, targeting burn wound areas and the urinary tract (Prescott *et al.*, 1996. Pg. 423). Virulence factors include two proteases - elastase and alkaline protease. It acts by inhibiting neutrophil chemotaxis and destroys immunoglobulin and complement components (Wick *et al.*, 1990).

A major causative agent of traveller's diarrhea is *E. coli*. Six different strains of diarrheagenic *E. coli* exist. Enterotoxigenic *E. coli* produce heat stable and heat labile enterotoxins. Cytotoxins and enterotoxins are produced by enteroinvasive *E. coli*. Other strains include enterohaemorrhagic, enteropathogenic, enteroaggressive and diffusely adhering *E. coli* (Prescott *et al.*, 1996. Pg. 767).

One of the most common bacterial infections in man is caused by *Streptococcus pneumoniae*. Individuals are only susceptible to such an infection if there is physical injury to the urinary tract, have a viral infection, abuses alcohol or have diabetes (Prescott *et al.*, 1996. Pg. 749). Phagocytosis is inhibited by a capsular polysaccharide, which is the primary virulence factor of this bacterium (Prescott *et al.*, 1996. Pg. 750).

Staphylococcus is found in the microflora of the upper respiratory tract, skin, intestine and vagina. It is the causative agent of a number of pus-forming diseases including carbuncles, boils, folliculitis and scalded-skin syndrome. The bacteria are capable of multiplying and spreading rapidly in tissues. In addition, they produce a number of exotoxins and enzymes such as β -lactamase, exfoliative toxins A and B, hyaluronidase, lipase, nuclease and proteases. Food poisoning may result if enterotoxins, also produced by *Staphylococcal* species, are ingested. (Prescott *et al.*, 1996. Pp. 761, 770).

3.3.1.1 Culturing the microorganisms

Overnight cultures of the bacteria were grown in nutrient broth² (NB) (Biolab, South Africa) at 37°C. An overnight culture of *C. albicans* was grown in sabouraud broth (SAB) (Oxoid, Unipath Ltd., England) and incubated at 28°C. All bacterial cultures were standardised to an absorbance of 0.220 at 540 nm, using NB as a blank. The *C. albicans* culture was also standardised to an absorbance of 0.220 at 600 nm, using SAB as a blank. The cultures were further diluted to obtain a concentration of 0.5×10^6 cells/ml. These dilutions were obtained previously by diluting the 0.220 standardised cultures and plating samples of each on agar plates. The CFUs were counted, from which the concentration of each culture (cells/ml) was calculated (Appendix B, Table B.1).

Linearity curves between absorbance and formazan product for each respective organism and tetrazolium salt were obtained. Serial dilutions of each organism were obtained, of which turbidity readings were taken at the respective wavelengths. To each dilution, MTT, XTT or TTC was added and incubated as described in the assays below. Formazan products were read at the respective absorbances, and correlation between cell number and absorption of the formazan product were obtained (Appendix B, Figures B 2.1 to 2.8).

3.3.2 Solutions tested in the screen for antimicrobial activity

Stock solutions of the isomers were made up in NB containing 0.5 % DMSO to aid dissolution of the isomers. Solutions used in assays involving *C. albicans* were made up in SAB. Stock isomer concentrations of 2 mg/ml, 1 mg/ml, 0.5 mg/ml and 0.25 mg/ml were used in this screen for antimicrobial activity.

In the assays involving the bacteria, 0.1 mg/ml chloramphenicol (Figure 3.11) (Sigma, St. Louis, U.S.A.) was used as a positive control. Chloramphenicol is bacteriostatic and has a broad spectrum of activity against both Gram positive and Gram negative bacteria. It acts by binding to the 50S ribosomal subunit and blocks the formation of peptide linkages by inhibiting peptidyl transferase (Prescott *et al.*, 1996. Pg. 662). Positive controls used in

² Solution list – Appendix C

experiments involving *C. albicans* were 0.25 mg/ml amphotericin B (Figure 3.12) (Sigma, St. Louis, U.S.A.) and fluconazole (Pfizer, South Africa) at stock concentrations of 1 mg/ml and 10 mg/ml. Amphotericin B and fluconazole are both antifungal agents. Amphotericin B binds to the sterols found in the fungal membrane, disrupts membrane permeability and causes cell leakage. Fluconazole is used in the treatment of candidiasis, cryptococcal meningitis and coccidioidal meningitis (Prescott *et al.*, 1996. Pg. 671). Amphotericin B is used in the treatment of deep-seated mycoses, but is very toxic. Fluconazole is less toxic, and its use in the treatment of this disease is thus increasing (Jahn *et al.*, 1995).

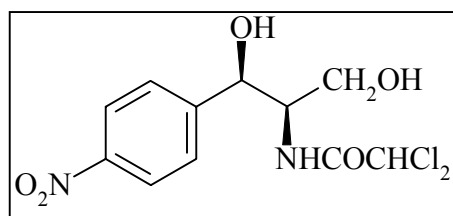


Figure 3. 11: Structure of chloramphenicol (Sigma catalogue, 2000-2001. Pg. 234).

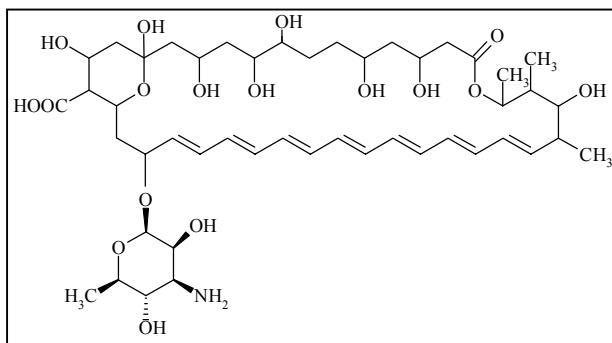


Figure 3. 12: Structure of amphotericin B (Sigma catalogue, 2000-2001. Pg. 113).

3.3.3 Colorimetric assays using tetrazolium dyes

3.3.3.1 MTT assay

A modified version of the MTT assay as described by Freimoser *et al.* (1999) was used. 250 μ l of the 0.5×10^6 cells/ml bacterial cultures were placed in sterile eppendorfs, to which 250 μ l of each concentration of the respective isomers were added. In the case of

C. albicans, 1×10^6 cells/ml were used. This resulted in a two-fold dilution of the isomers. The bacterial samples were incubated overnight at 37°C, while the yeast was incubated at 28°C. After the incubation, 100 µl 0.5 mg/ml MTT was added to each eppendorf and incubated at the respective temperatures for 30 min. In the case of *C. albicans*, this incubation period was extended to 1 hr, since MTT is less sensitive for fungal assays. Following incubation, the cells were pelleted from solution at 8 300 rpm for 5 min. The medium was aspirated from the cells, and 500 µl DMSO was added to extract the formazan product from the cells. Once again, the cells were pelleted from solution. 200 µl of each sample was then read against a DMSO blank at 540 nm using Labsystems Multiskan MS (Multiskan Transmit Program, Rev. 1.3. (1995)). Results are reported as % viability in relation to the negative control samples, which represent 100% viability.

3.3.3.2 TTC assay

The TTC assay was modified from the method employed by Hurwitz and McCarthy (1986). TTC was only tested on Gram negative bacteria, as preliminary tests yielded no results with Gram positive organisms. The same method as used for the MTT assay was used, with the following differences. 100 µl 60 mg/ml TTC was added to each eppendorf and incubated at 37°C for 1 hr. The cells were pelleted from solution and the medium aspirated. The formazan product was extracted from the cells using 500 µl *N,N*-dimethylformamide (Saarchem, South Africa). Once the cells were pelleted from solution, 200 µl of the extracted formazan product was read at 492 nm against a *N,N*-dimethylformamide blank using Labsystems Multiskan MS (Multiskan Transmit Program, Rev. 1.3. (1995)). Results are reported as % viability in relation to the negative control samples, which represent 100% viability.

3.3.3.3 XTT assay

A modified version of the XTT assay as described by Stevens and Olsen (1993) was used. Only *C. albicans* was tested using this tetrazolium dye, as it is said to be more sensitive than the MTT assay for fungi (Meshulam *et al.*, 1995). The same method as used for the MTT assay was used, with the following differences. 100 µl 1 mg/ml XTT

was added to each eppendorf and incubated at 37°C for 2 hrs to increase the amount of XTT reduction, since no electron coupler was added to the assay system. The cells were then pelleted from solution. The coloured medium that resulted was read against a blank consisting of SAB and XTT solution at 492 nm using Labsystems Multiskan MS (Multiskan Transmit Program, Rev. 1.3. (1995)). Results are reported as % viability in relation to the negative control samples, which represent 100% viability.

3.3.4 Statistical analysis

Values are expressed as mean \pm s.d. for the indicated number of experiments. The paired Student's *t* test was used to determine statistical differences in killing of the microorganisms by the isomers and positive controls when using MTT, TTC or XTT to determine % viability (in relation to the negative control samples). A *P* value of less than 0.05 denoted the presence of a statistically significant difference.

3.4 RESULTS AND DISCUSSION

Both *E. coli* and *P. aeruginosa* were capable of reducing TTC under aerobic conditions in the absence of an electron coupling agent, resulting in a formazan product that could be extracted with *N,N*-dimethylformamide. The absorbances of these extracts were comparable to those obtained for the MTT formazan absorbances. The sensitivity of the MTT assay was compared to that of the TTC assay for Gram negative bacteria only.

Cyclo(L-Trp-L-Pro), cyclo(D-Trp-L-Pro) and cyclo(D-Trp-D-Pro) did not show very promising reduction in *E. coli* viability (Figure 3.13), with viability being maintained at between $60.136 \pm 7.822\%$ and $97.172 \pm 11.290\%$ for these isomers at 0.25 to 1 mg/ml. 0.25 mg/ml to 1 mg/ml Cyclo(D-Trp-D-Pro) showed comparable reduction in *E. coli* viability and was not significantly reduced in comparison to 0.125 mg/ml cyclo(L-Trp-L-Pro) ($p=0.2598$). Cyclo(L-Trp-D-Pro) showed the most effective reduction in *E. coli* viability with the MTT assay, resulting in a range of $26.001 \pm 1.451\%$ to $36.011 \pm 3.575\%$ viability in the range of concentrations tested.

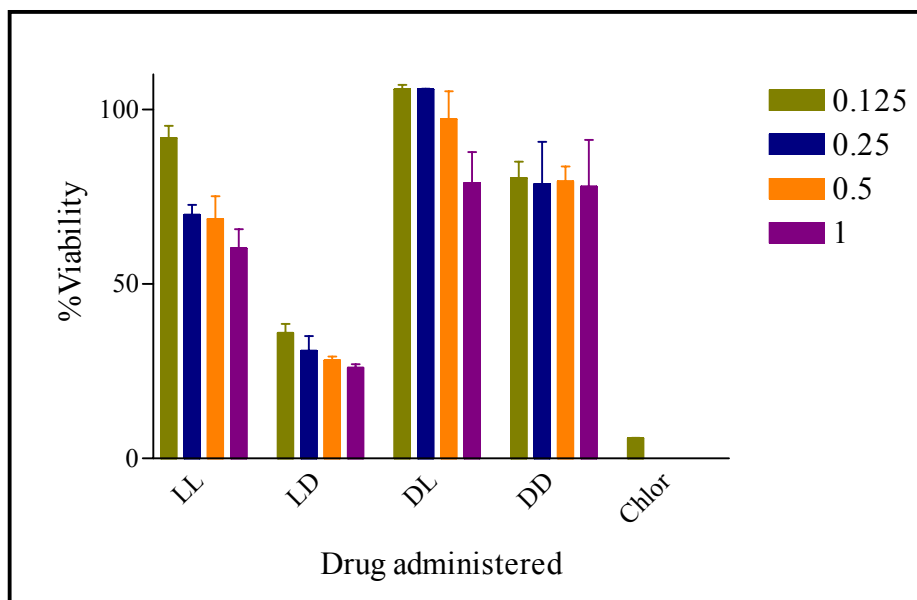


Figure 3. 13: Resultant % viability of 0.5×10^6 cells/ml *E. coli* after exposure to the isomers at various concentrations for 24 hrs, as determined by the MTT assay. The final concentration of Chlor (chloramphenicol) in the eppendorfs was 0.05 mg/ml. The final isomer concentrations (mg/ml) are indicated on the graph. Values indicated are the mean \pm s.d. of quadruplicates.

Only 1 mg/ml cyclo(D-Trp-L-Pro) showed a reduction in *E. coli* viability, with 0.125 mg/ml to 0.5 mg/ml showing no significant effect on *E. coli* survival. Cyclo(D-Trp-D-Pro) did not adversely affect *E. coli* viability for all concentrations tested. 0.05 mg/ml Chloramphenicol resulted in the greatest reduction in viability, resulting in only $5.854 \pm 0.0678\%$ viability after 24 hrs (Figure 3.13).

When the TTC assay was applied to *E. coli*, a reduced viability was noted in the range of 40 – 63% for all concentrations of all the isomers tested (Figure 3.14). Lowered viability of *E. coli* was observed for 0.5 mg/ml cyclo(L-Trp-L-Pro) in comparison to cyclo(L-Trp-L-Pro) at 1 mg/ml, although this was not significantly different ($p=0.0979$). Chloramphenicol showed a $6.235 \pm 0.0672\%$ viability (Figure 3.14) and was significantly lower than any of the results obtained for that of the isomers at all concentrations tested ($p<0.05$).

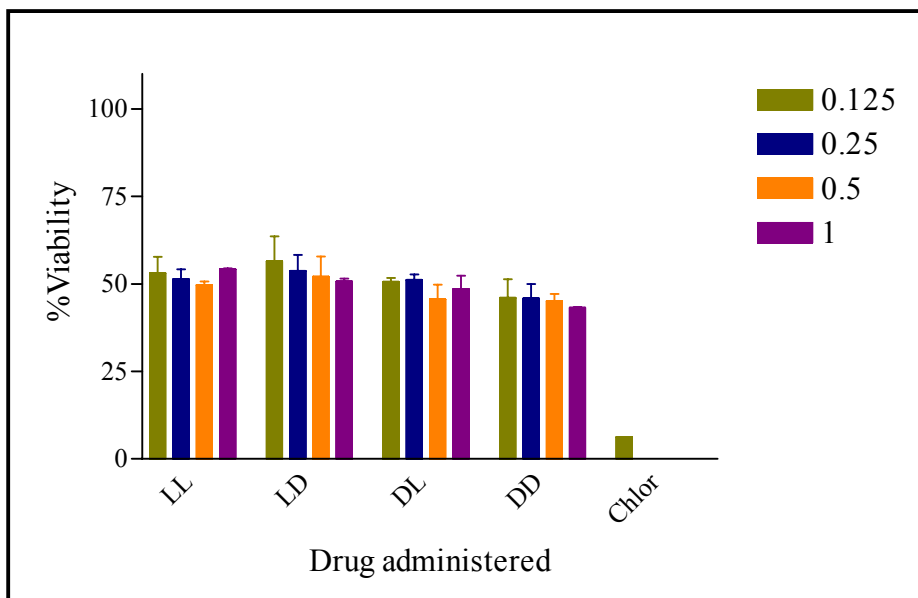


Figure 3. 14: Resultant % viability of 0.5×10^6 cells/ml *E. coli* after exposure to the isomers at various concentrations for 24 hrs, as determined by the TTC assay. The final concentration of Chlor (chloramphenicol) in the eppendorfs was 0.05 mg/ml. The final isomer concentrations (mg/ml) are indicated on the graph. Values indicated are the mean \pm s.d. of quadruplicates.

If one were to compare the results obtained for *E. coli* using the MTT and TTC assays, one would note that TTC shows lowered viability of *E. coli* (Figure 3.14) in the presence

of all the isomers, with the exception of cyclo(L-Trp-D-Pro). One would thus tend towards suggesting that TTC was a more sensitive indicator of cell viability than MTT was. Why MTT reduction in the presence of cyclo(L-Trp-D-Pro) (Figure 3.13) was less than that obtained for TTC reduction is an aspect that would need further investigation.

When *P. aeruginosa* was incubated in the presence of the isomers, MTT reduction showed no drastic effects on viability of these microorganisms (Figure 3.15). Significantly reduced viability was noted in the presence of 1 mg/ml Cyclo(L-Trp-L-Pro) in comparison to 0.125 mg/ml cyclo(L-Trp-L-Pro) ($p < 0.05$). 0.125 and 0.5 mg/ml Cyclo(L-Trp-D-Pro) had no significant effects on *P. aeruginosa* viability, while 1 mg/ml showed a $78.387 \pm 8.952\%$ viability (Figure 3.15). No significant effect on growth was observed in the presence of cyclo(D-Trp-L-Pro) at all concentrations tested. Low levels of inhibition of *P. aeruginosa* growth was observed in the presence of 1 mg/ml cyclo(D-Trp-D-Pro) ($23.641 \pm 11.070\%$). 0.05 mg/ml Chloramphenicol showed an effective $80.846 \pm 0.5487\%$ reduction in the viability of *P. aeruginosa*.

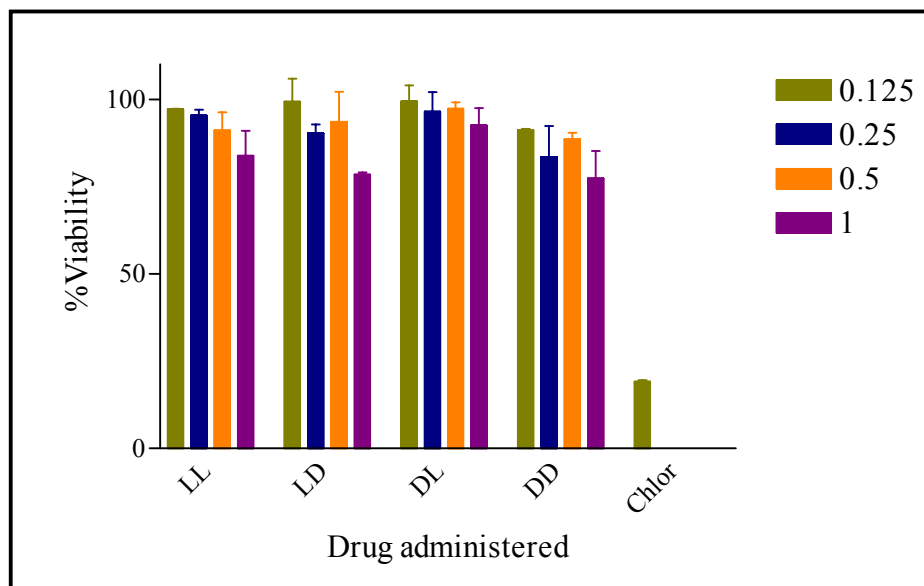


Figure 3. 15: Resultant % viability of 0.5×10^6 cells/ml *P. aeruginosa* after exposure to the isomers at various concentrations for 24 hrs, as determined by the MTT assay. The final concentration of Chlor (chloramphenicol) in the eppendorfs was 0.05 mg/ml. The final isomer concentrations (mg/ml) are indicated on the graph. Values indicated are the mean \pm s.d. of quadruplicates.

When MTT was substituted by TTC as the tetrazolium salt, significantly lowered viability of *P. aeruginosa* was obtained (Figure 3.16) in comparison to the MTT reduction assay. Cyclo(L-Trp-L-Pro) showed no significant differences in its effects on *P. aeruginosa* viability for all concentrations tested. 1 mg/ml Cyclo(L-Trp-D-Pro) showed significantly reduced levels of *P. aeruginosa* growth in comparison to that of 0.125 to 0.5 mg/ml cyclo(L-Trp-D-Pro) ($p < 0.05$).

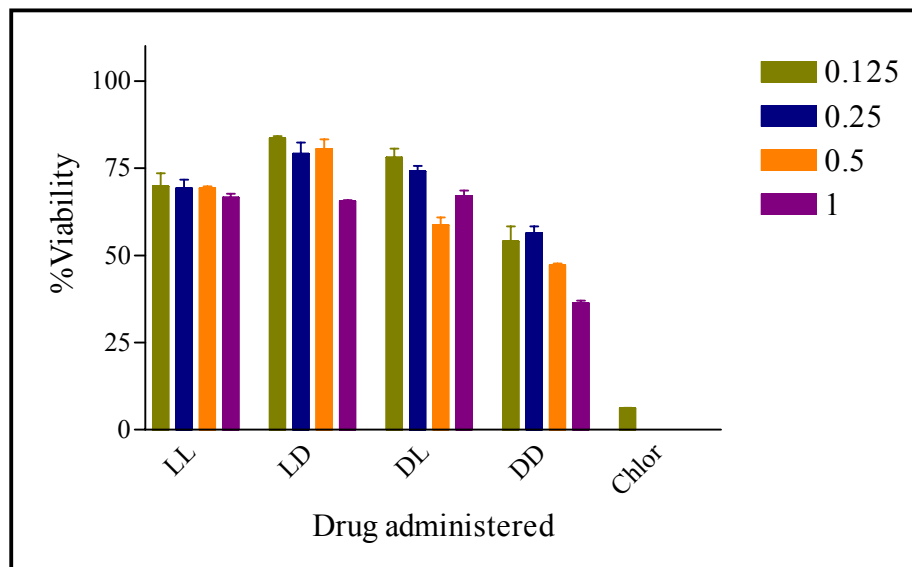


Figure 3. 16: Resultant % viability of 0.5×10^6 cells/ml *P. aeruginosa* after exposure to the isomers at various concentrations for 24 hrs, as determined by the TTC assay. The final concentration of Chlor (chloramphenicol) in the eppendorfs was 0.05 mg/ml. The final isomer concentrations (mg/ml) are indicated on the graph. Values indicated are the mean \pm s.d. of quadruplicates.

Cyclo(D-Trp-L-Pro) showed a $58.692 \pm 3.177\%$ viability in the presence of 0.5 mg/ml and a $67.051 \pm 2.237\%$ viability in the presence of 1 mg/ml (Figure 3.16). The greatest reduction in *P. aeruginosa* viability resulted from the addition of cyclo(D-Trp-D-Pro) to the incubation mixture. 0.125 mg/ml and 0.25 mg/ml Cyclo(D-Trp-D-Pro) showed similar effects on *P. aeruginosa* growth, while both 0.5 mg/ml and 1 mg/ml significantly reduced the viability of the microorganism. 1 mg/ml Cyclo(D-Trp-D-Pro) was most effective, resulting in a $36.309 \pm 1.077\%$ survival rate. 0.05 mg/ml Chloramphenicol had a dramatic effect on *P. aeruginosa* growth, showing a low $6.192 \pm 0.1831\%$ viability after

24 hrs. From these results, one would once again tend towards stating that TTC is a more sensitive assay than MTT.

TTC has been used in assaying the effects of different drugs in the presence of *Mycobacterium tuberculosis*, a Gram positive bacterium. On development of a method for the TTC assay, no reduction of this tetrazolium salt was observed in the presence of the Gram positive bacteria. This may be resultant of the aerobic conditions under which the assay was conducted, or the lack of an electron coupling agent in the reaction mixture. It is for these reasons that all avenues including aerobic vs anaerobic incubation and the presence of or absence of an effective electron coupling agent be examined before parallels between these two assays be drawn.

S. aureus and *Streptococcus* were tested using MTT only, as no formazan product could be extracted with *N,N*-dimethylformamide. A concentration dependent inhibition of *S. aureus* growth was noted for both cyclo(L-Trp-L-Pro) and cyclo(L-Trp-D-Pro), with 1 mg/ml resulting in a reduced viability of $52.60 \pm 0.619\%$ and $53.686 \pm 0.667\%$, respectively (Figure 3.17). No concentration-dependent effect was observed on addition of both cyclo(D-Trp-L-Pro) and cyclo(D-Trp-D-Pro) to the incubation mixture. No significantly different effect was noted in the presence of cyclo(D-Trp-L-Pro) at concentrations ranging between 0.125 to 0.5 mg/ml. Only 1 mg/ml cyclo(D-Trp-L-Pro) resulted in a significantly reduced viability of $66.374 \pm 6.932\%$ ($p < 0.05$). Cyclo(D-Trp-D-Pro) did not show a concentration-dependent effect on *S. aureus* viability, with 0.125 and 0.5 mg/ml showing similar effects on growth. Similarly, 0.25 and 1 mg/ml cyclo(D-Trp-D-Pro) produced similar effects on *S. aureus* growth (Figure 3.17). Chloramphenicol showed significantly lowered viability ($p < 0.05$) in comparison to the isomers at all concentrations tested. These results show that although 1 mg/ml cyclo(L-Trp-L-Pro) and cyclo(L-Trp-D-Pro) are effective in inhibiting *S. aureus* growth by $47.405 \pm 0.8747\%$ and $46.315 \pm 0.667\%$, respectively, they are not nearly as effective as chloramphenicol.

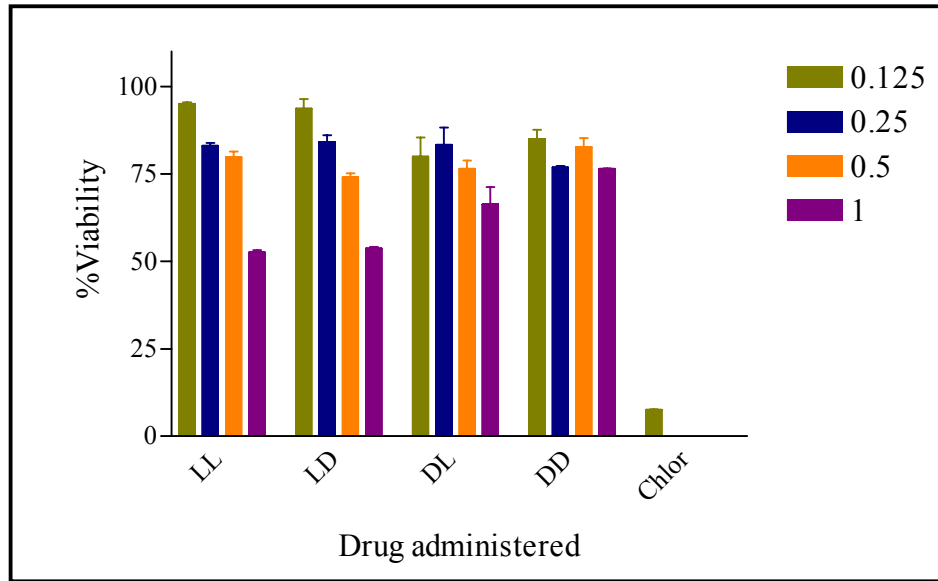


Figure 3. 17: Resultant % viability of 0.5×10^6 cells/ml *S. aureus* after exposure to the isomers at various concentrations for 24 hrs, as determined by the MTT assay. The final concentration of Chlor (chloramphenicol) in the eppendorfs was 0.05 mg/ml. The final isomer concentrations (mg/ml) are indicated on the graph. Values indicated are the mean \pm s.d. of quadruplicates.

The most effective reduction in Streptococcal growth occurred at a concentration of 1 mg/ml cyclo(L-Trp-L-Pro) ($54.539 \pm 1.359\%$) (Figure 3.18). 0.25 and 0.5 mg/ml Cyclo(L-Trp-L-Pro) showed comparable results ($p=0.6473$). 0.125 mg/ml Cyclo(L-Trp-D-Pro) did not adversely affect Streptococcal growth, while both 0.5 and 1 mg/ml significantly reduced the viability thereof.

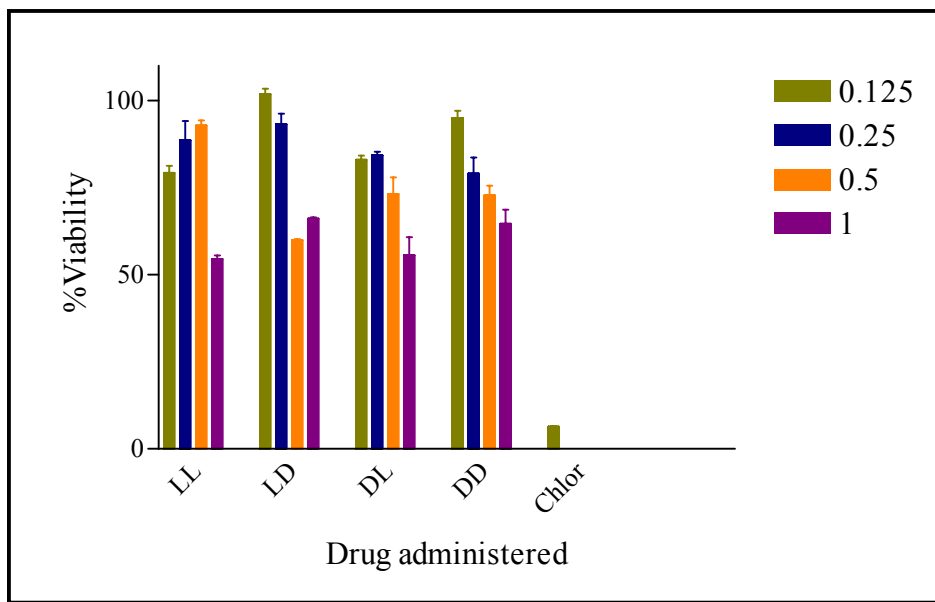


Figure 3. 18: Resultant % viability of 0.5×10^6 cells/ml *Streptococcus* after exposure to the isomers at various concentrations for 24 hrs, as determined by the MTT assay. The final concentration of Chlor (chloramphenicol) in the eppendorfs was 0.05 mg/ml. The final isomer concentrations (mg/ml) are indicated on the graph. Values indicated are the mean \pm s.d. of quadruplicates.

Effects of 0.5 mg/ml cyclo(L-Trp-D-Pro) was comparable to that of 1 mg/ml cyclo(L-Trp-L-Pro) ($p=0.0622$). Significantly reduced viability resulted from the addition of 1 mg/ml cyclo(D-Trp-L-Pro) in comparison to 0.125 and 0.25 mg/ml cyclo(D-Trp-L-Pro). 1 mg/ml resulted in a $55.581 \pm 7.299\%$ viability, which is comparable to the effects of 1 mg/ml cyclo(L-Trp-L-Pro) and 0.5 mg/ml cyclo(L-Trp-D-Pro) ($p=0.8927$). Addition of cyclo(D-Trp-D-Pro) to the culture medium resulted in a concentration-dependent reduction in the viability of Streptococcal growth after 24 hrs (Figure 3.18). 1 mg/ml Cyclo(D-Trp-D-Pro) produced comparable results to 1 mg/ml cyclo(L-Trp-D-Pro) ($p=0.7915$). 0.05 mg/ml Chloramphenicol resulted in dramatically reduced streptococcal viability ($5.597 \pm 0.1089\%$) in comparison to the isomers tested ($p < 0.05$). Once again, this showed that the isomers were not as effective against Streptococcal growth as this drug was.

Effects noted in the above assays may be resultant of the hydrophobic nature of the cyclic dipeptides, which allow them to interfere with the outer membrane in Gram negative bacteria, and the plasma membrane in Gram positive bacteria (Milne *et al.*, 1998).

When 0.01 µg/ml to 1.0 µg/ml rifampin was added to the incubation mixture of *Mycobacterium bovis* (BCG), which is rifampin sensitive, a dose-dependent decrease in MTT reduction resulted. After 48 hrs and 72 hrs incubation periods, MTT reduction was significantly reduced ($p < 0.001$ for each incubation period). In the presence of menadione, an electron coupling agent, an increase in the sensitivity of the MTT assay was observed (Mshana *et al.*, 1998).

The MICs of a number of drugs was tested against *Mycobacterium avium*-*M. intracellulare* complex (MAC), an intracellular pathogen prevalent in AIDS patients. The MTT assay was used to assess the susceptibility of this pathogen to clofazimine, resorcinomycin A and PD 127391, an experimental quinolone. Over a 4-8 day period, the MIC for clofazimine was determined at 3 µg/ml, 15 µg/ml in the case of resorcinomycin A and 31 µg/ml for PD 127391. When clofazimine was tested against *M. avium*, the MIC obtained was less than that obtained for the complex (1.5 µg/ml). When tested against *M. intracellulare* only, the MIC value was 3 µg/ml (Gomez-Flores *et al.*, 1995).

When 0.125 mg/ml and 0.25 mg/ml cyclo(L-Trp-L-Pro) were added to the medium of *C. albicans* (Figure 3.19), viability was reduced to $85.356 \pm 1.947\%$ and $85.795 \pm 2.567\%$, respectively, as determined by the MTT assay. Moreover, 0.5 mg/ml and 1 mg/ml further decreased viability to $69.9155 \pm 0.4207\%$ and $63.141 \pm 4.868\%$, respectively.

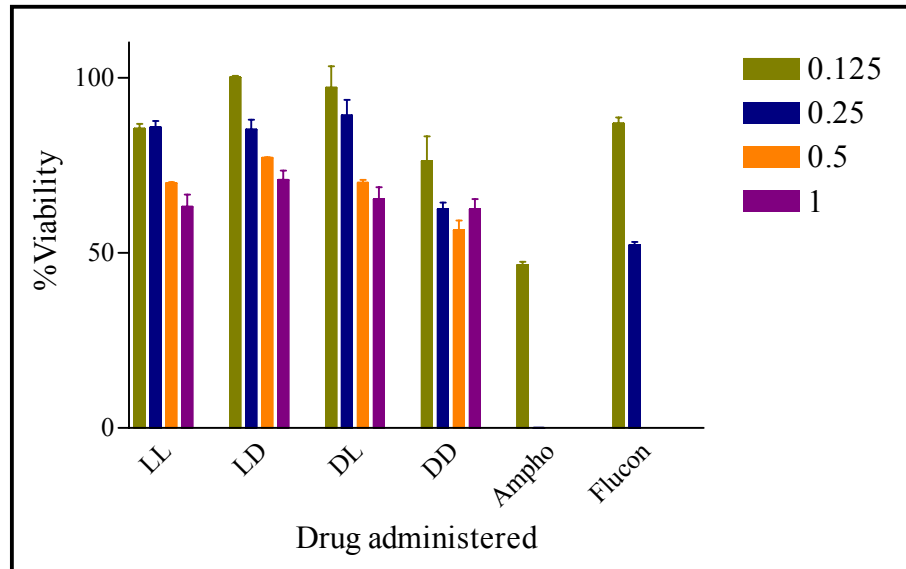


Figure 3. 19: Resultant % viability of 1×10^6 cells/ml *C. albicans* after exposure to the isomers at various concentrations for 24 hrs, as determined by the MTT assay. The final concentration of Ampho (Amphotericin B) in the eppendorfs was 0.125 mg/ml. Flucon (Fluconazole) was tested at final concentrations of 0.5 mg/ml (green bar) and 5 mg/ml (blue bar). The final isomer concentrations (mg/ml) are indicated on the graph. Values indicated are the mean \pm s.d. of quadruplicates.

Cyclo(L-Trp-D-Pro) showed a dose-dependent reduction in *C. albicans* viability, with 0.125 mg/ml having no adverse effect on its growth (Figure 3.19). At 0.125 mg/ml cyclo(D-Trp-L-Pro), no significant effect on *C. albicans* growth was observed. 0.5 and 1 mg/ml cyclo(D-Trp-L-Pro) significantly reduced the viability of this yeast to $69.963 \pm 1.240\%$ and $65.3315 \pm 4.779\%$, respectively. 0.25 mg/ml to 1 mg/ml Cyclo(D-Trp-D-Pro) showed comparative reduction in *C. albicans* growth. 0.125 mg/ml Amphotericin B showed a $53.471 \pm 1.279\%$ reduction in viability (Figure 3.19). Fluconazole at 5 mg/ml was significantly more effective against *C. albicans* growth ($52.219 \pm 1.280\%$ viability) than 0.5 mg/ml fluconazole ($86.8655 \pm 2.441\%$ viability) ($p < 0.0157$). 0.5 mg/ml Fluconazole was shown to be less effective against *C. albicans* than 0.5 mg/ml and 1 mg/ml cyclo(L-Trp-L-Pro), cyclo(L-Trp-D-Pro) and cyclo(D-Trp-L-Pro), and 0.25mg/ml to 1 mg /ml cyclo(D-Trp-D-Pro). 5 mg/ml Fluconazole showed a greater effect on *C. albicans* growth in comparison to the isomers tested.

XTT is commonly used to assess fungal cell damage and should not be used as a viability assay as such, but rather a means by which fungal damage and not necessarily lethal effects, can be evaluated (Meshulam *et al.*, 1995). In addition, a major disadvantage of the MTT assay when applied to fungal cells is that this assay detects viable organisms that have been damaged by adverse conditions, but are unable to proliferate normally (Hjertstedt *et al.*, 1998). On this basis, XTT is said to be a more sensitive assay for *C. albicans* than MTT. The results should be expressed as fungal cell damage and not % viability, as shown in Figure 3.20. This was done, however, to facilitate comparison between the results between the MTT assay and the XTT assay.

Cyclo(L-Trp-L-Pro) at 0.5 mg/ml and 1 mg/ml showed significantly reduced cell viability (Figure 3.20) in comparison to 0.125 mg/ml and 0.25 mg/ml ($p < 0.05$).

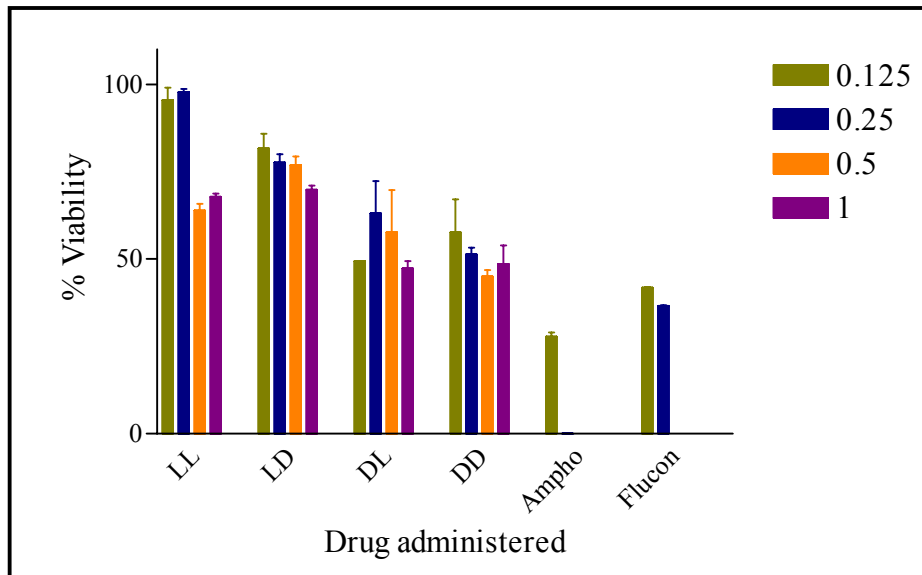


Figure 3. 20: Resultant % viability of 1×10^6 cells/ml *C. albicans* after exposure to the isomers at various concentrations for 24 hrs, as determined by the XTT assay. The final concentration of Ampho (Amphotericin B) in the eppendorfs was 0.125 mg/ml. Flucon (Fluconazole) was tested at final concentrations of 0.5 mg/ml (green bar) and 5 mg/ml (blue bar). The final isomer concentrations (mg/ml) are indicated on the graph. Values indicated are the mean \pm s.d. of quadruplicates.

In the presence of 0.125 mg/ml to 0.5 mg/ml cyclo(L-Trp-D-Pro), approximately 25% of the cells had been adversely affected. 0.125 mg/ml to 1 mg/ml Cyclo(D-Trp-L-Pro) did

not show any significant concentration-dependent effect in its action on *C. albicans*, where viability assessment using MTT showed significantly increased viability in comparison to the TTC assay ($p=0.0451$), with the exception of cyclo(D-Trp-L-Pro) at 0.5 mg/ml (Figure 3.20). Similarly, significantly reduced viability levels in the presence of all concentrations of cyclo(D-Trp-D-Pro) was observed for the XTT assay (Figure 3.20) in comparison to the MTT assay, except at 1 mg/ml ($p=0.1084$). In addition, significantly reduced viability levels were noted for amphotericin B and fluconazole at all concentrations tested when XTT was used as the tetrazolium salt ($p<0.05$). No isomer was shown to be as effective as these drugs were.

Since viability for most of the samples were higher in the MTT assay than the XTT assay, one may conclude that the isomers were capable of causing injury to the fungal cells, but were not necessarily lethal in its action.

Results of research conducted by other researchers are now discussed. The effectivity of tyrothricin was tested against a number of *Candida* species using the MTT assay. Two clinical isolates were tested – *C. albicans* and *C. tropicalis*. MICs obtained for *C. albicans* ranged between 4.8-6.7 mg/l, while *C. tropicalis* was susceptible to this drug in the range of 5.3-7.6 mg/l. *C. albicans* DSM 1386 was also tested. A higher concentration of 6.2 mg/l tyrothricin was needed to yield an MIC value. When XTT was substituted for MTT, significant reduction in the amount of formazan product formed was observed at ≥ 3.125 mg/l tyrothricin in the presence of *C. albicans* DSM 1386 (Kretschmar *et al.*, 1996).

In the development of a microtiter method for susceptibility testing of fungi, fluconazole and amphotericin B were added to the incubation mixture of *Aspergillus fumigatus* and *C. albicans* strains. Four different *C. albicans* strains were tested, including two wild-type strains (0815 and 8166), an amphotericin B-resistant strain (R64) and a fluconazole-resistant strain (3059). When amphotericin B was added to the incubation reaction, 0.16 to 0.32 $\mu\text{g/ml}$ resulted in a 90 % inhibition of growth in the strains 0815, 3059 and 8166. Strain R64 was susceptible to 1.25 to 2.5 $\mu\text{g/ml}$ amphotericin B, resulting in a 90%

inhibition of growth. Application of fluconazole ranging from 0.4 to 3.2 µg/ml resulted in a 90% inhibition of growth in the strains R64, 0815 and 8166. Strain 3059 was not affected by fluconazole up to 50 µg/ml (Jahn *et al.*, 1995). This indicates that the strain of *C. albicans* tested was more resistant to these drugs than the strains used in the study by Jahn *et al.* (1995). In addition, incubation conditions differed to the ones used in this study. This suggests that culture conditions may influence the results of susceptibility studies.

MICs for fluconazole as applied to *Candida* strains were determined by Clancy and Nguyen (1997). Excellent agreement of the MIC values was obtained by the MTT assay and the microdilution method. *C. albicans* was susceptible to 0.125 to 32 µg/ml fluconazole, which represented the MIC₅₀ value. The MIC₅₀ value for *C. neoformans* was determined at 0.5 to 32 µg/ml fluconazole. These values were identical to that as determined by the microdilution method. The MTT assay had the advantage of producing results in a shorter time frame than the microdilution method (Clancy and Nguyen, 1997). Once again, these results were obtained under culture conditions that differed vastly from the ones employed in our study.

The MIC values for adherent and planktonic *C. albicans* cells were assessed by use of the XTT assay. A time-dependent decrease in the MIC value of amphotericin B was noted with planktonic cells. After 5 hrs, the IC₅₀ value of amphotericin B was 0.009 µg/ml in the presence of 1.5 x 10³ cells/well. This value decreased to 0.006 µg/ml after 24 hrs, with a further decrease to 0.003 µg/ml after 48 hrs. Similarly, in the presence of ketoconazole, another antifungal agent, a time-dependent decrease in the IC₅₀ value was detected. After 5 hrs, the MIC value was 0.009 µg/ml. At 24 hrs, the value had decreased to 0.008 µg/ml, with a further decrease to 0.005 µg/ml after 48 hrs. Significantly different MIC values were obtained with the adherent yeast. After 24 hrs, the MIC value had increased to 1.4 µg/ml (p<0.05), with a greater increase occurring after 48 hrs (4.8 µg/ml). Similarly, in the presence of ketoconazole, the adherent cells appeared to be more resistant to the antifungal agent, with an increase in the MIC value to 1.6 µg/ml (p<0.05) after 24 hrs. A further increase to 4.9 µg/ml (p<0.001) was observed after a 48 hr

incubation period (Hawser, 1996). This indicated that culture conditions may influence the concentrations at which a MIC value is obtained.

The MICs of other cyclic dipeptides have been assessed using the Kirby-Bauer disc-diffusion method (Milne *et al.*, 1998). The susceptibility of *E. coli*, *P. aeruginosa*, *Klebsiella pneumoniae*, *S. aureus*, *B. subtilis* and *Streptococcus pneumoniae* to cyclo(Phe-Pro), cyclo(Trp-Pro), cyclo(Trp-Trp) and cyclo(Tyr-Pro) were examined. The cyclic dipeptides were dissolved in 100% DMSO. It was found that all the dipeptides tested were active against the Gram negative bacteria. With the exception of cyclo(Tyr-Pro), all the dipeptides were also active against the Gram positive bacteria. The MIC values thus obtained are tabulate in Table 3.3.

Table 3. 3: MIC values of selected cyclic dipeptides against bacteria using the Kirby Bauer disc-diffusion method (Milne *et al.*, 1998).

Cyclic dipeptide	MICs for Gram positive bacteria	MICs for Gram negative bacteria
Cyclo(Phe-Pro)	0.06 μ M	0.03 μ M
Cyclo(Trp-Pro)	0.035 μ M	8.125 nM
Cyclo(Trp-Trp)	22.5 nM	45 nM
Cyclo(Tyr-Pro)	-	0.13 μ M

As can be noted, the MIC for cyclo(Trp-Pro) as determined by Milne *et al.* (1998) and the values obtained by the MTT and TTC do not correlate. This may be resultant of the fact that the dipeptide was dissolved in 100% DMSO, which in itself may adversely affect bacterial growth.

3.5 CONCLUSIONS

If one were to use MTT assay as a basis for comparison, it is clear that cyclo(L-Trp-L-Pro) is most effective against the Gram positive bacteria at 1 mg/ml (Figures 3.17 and 3.18). Cyclo(L-Trp-D-Pro) was highly effective against *E. coli* (Figure 3.13) at all concentrations tested, but not against the other Gram negative bacteria, *P. aeruginosa* (Figure 3.15). Cyclo(D-Trp-L-Pro) was most effective at inhibiting growth of *Streptococcus* at 1 mg/ml (Figure 3.18), while cyclo(D-Trp-D-Pro) proved effective against *C. albicans* at all concentrations tested (Figure 3.19).

As this study was done as a primary screen for antimicrobial activity, further testing is needed, possibly including the use of multi-drug resistant clinical isolates. Higher concentrations of these isomers should also be tested to fully evaluate the potential of these isomers as antimicrobials. In addition, different culture conditions should be compared in the determination of MIC values.

CHAPTER 4

ANTICANCER STUDIES

4.1 INTRODUCTION

Cancer is a disease of the cells resultant of a shift in control mechanisms that rule cell proliferation and differentiation (Salmon and Sartorelli, 1989. Pg. 685). During embryogenesis, growth, tissue repair and remodeling after injury, cell growth and maturation occur in a normal sequence of events. When regulation over these processes becomes disordered, control over growth, differentiation and spatial confinement is lost. Abnormal growth and invasion of cells characterises human neoplasia (Figure 4.1). With any given patient, the nature of cellular alteration, clinical presentation and course of the disease varies. Precursor lesions such as colon polyps may show signs of abnormal cell proliferation without any invasiveness. This may or may not progress to cancer (Tripathy, 1995. Pg. 49).

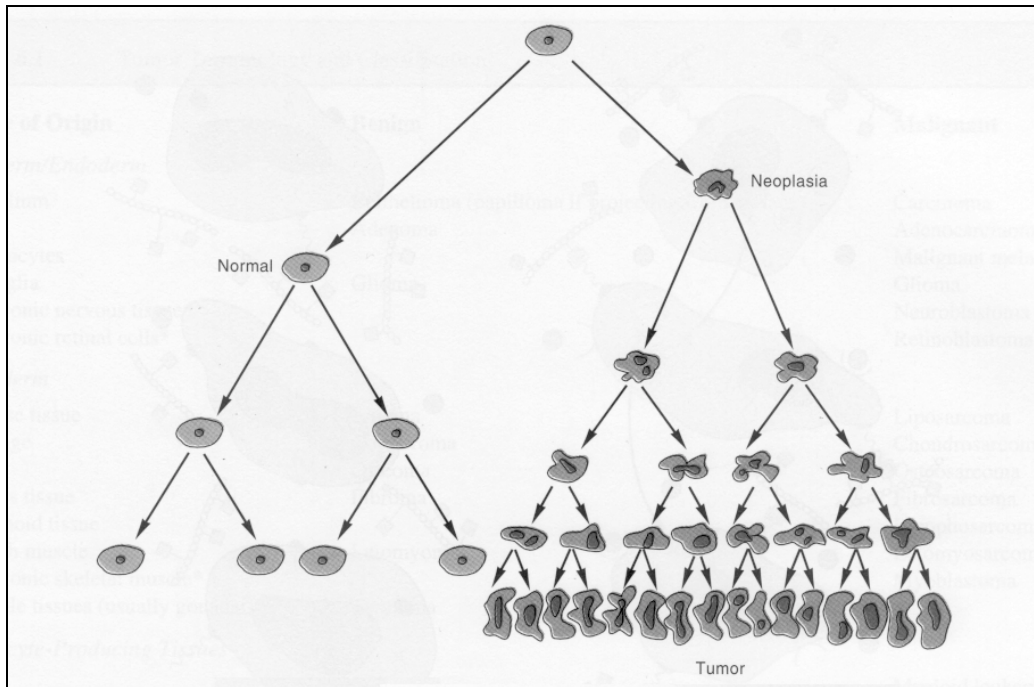


Figure 4. 1: Growth of a neoplasia. Tumour growth overtakes that of normal tissue as a result of a loss in regulation mechanisms that control cell growth. A neoplastic mass is formed (Nowak and Handford, 1999. Pg. 121).

4.1.1 The cell cycle

Cellular proliferation is under the control of the cell cycle, in which cyclins and maturation-promoting factors play a key role in the progression of the cell into the mitosis (M) phase (Karp, 1996. Pp. 604-5).

The cell cycle is divided into two parts, mitosis and interphase (Figure 4.2). Interphase can further be subdivided into three phases:

- i) G₁ (gap) - a duplicate set of chromosomes occur in the cell. This phase occurs after mitosis.
- ii) S (DNA replication)- the cells contain 2n-4n amounts of DNA.
- iii) G₂- the cells contain 4n amounts of DNA and occur between S and M (Cooper, 1997. Pg. 564).

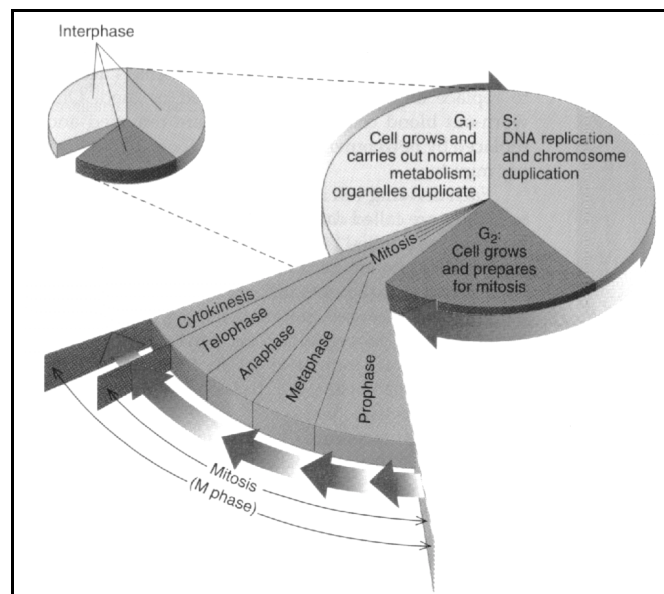


Figure 4. 2: The eucaryotic cell cycle. The phases through which the cell must pass from one division to the next is shown (Karp, 1996. Pg. 602).

The rate of proliferation is controlled by the passage through the G₁ phase (Pardee *et al.*, 1978). The proliferative event's success is dependent on both karyokinesis (nuclear division) and cytokinesis (cytoplasmic division), both of which occur during and at the

end of mitosis. It is felt that neoplasia originates during karyokinesis, where incorrect duplication or separation of the cells' chromosomes occur (Alderson, 1982).

Cell cycle control is a necessity to guarantee that the cell does not enter mitosis before DNA replication has been completed. The first control point, at the transition between the G₁ and S phases, is at the initiation of DNA synthesis (Cooper, 1997. Pg. 565). It is here that the cells become committed irreversibly to cell division (Nurse, 1987). The second control point occurs at the initiation of mitosis, the transition between G₂ and M phases (Cooper, 1997. Pg. 565).

4.1.1.1 Cellular differentiation

Cellular differentiation is a process whereby single cells or cell groups undergo ultrastructural and metabolic modifications that distinguishes them functionally from other cells in the developing organism (Smith and Wood, 1991).

Morphologically and/or functionally altered cells result from a change in gene expression, which results from the initiation of the differentiation pathway induced by external stimulants (De Robertis and De Robertis, 1987).

Cellular differentiation may be considered mutually exclusive to cell proliferation. A cell may divide a limited number of times once it has entered the differentiation pathway before it loses this ability (Potten, 1980). The growth rate of a fully differentiated cell equals zero, since fully differentiated cells are not known to undergo mitosis.

Neoplasia results when differentiation and proliferation become uncoupled, i.e. the cell divides but does not enter into or complete the pathway of differentiation; or completes the differentiative process, but continues proliferating. These cells may metastasize, thereby spreading the neoplasm to other tissues in the body (Vile, 1990). To metastasize means to spawn cells that break away from the parent mass, enter the lymphatic or vascular circulation and spread to distant sites in the body, where the cells establish secondary tumours that cannot be removed by surgery (Karp, 1996. Pg. 694).

Differentiation may be controlled at the molecular level by 8 possible mechanisms: (1) transcriptional control via the action of repressors, transducers or activators; (2) post-transcriptional control by differential RNA processing; (3) post-transcriptional modification of mRNA and ribosome binding factors that affect translational control; (4) post-translational modification of proteins including glycosylation and methylation; (5) gene amplification at genome level, production of homogeneous staining regions and double minutes due to external selection pressures; (6) gene transposition; (7) accessibility of tissue-specific genes to transcriptional enzymes as a result of genomic rearrangement; and (8) changes in gene expression as a result of non-reversible changes in DNA methylation (De Robertis and De Robertis, 1987).

4.1.2 Molecular and biochemical basis of neoplasia

A number of alterations to cellular functions such as proliferation, invasiveness and metastatic potential are characteristic of cancer. It has been suggested that cellular and biochemical alterations accountable for malignant phenotype are triggered by genetic alterations (Tripathy, 1995. Pg. 49).

4.1.2.1 Genetic changes in neoplasia

Due to the inherent genetic instability of malignant cells, any changes occurring at the genome level occur randomly. Oncogenes result from altered genes, resulting in functional gain. Tumour suppressor genes result in a loss of function due to deletions or mutations. *In vitro* cell culture methods have shown that oncogene activation and loss of tumour suppressor genes causes cancer. Oncogenes can be activated by point mutations, chromosomal translocation or amplification of genetic material. Point mutations, frameshift mutations or a deletion within a gene or of a large chromosomal segment may result in a loss of tumour suppressor gene function (Tripathy, 1995. Pg. 49).

Genetic alterations introduced during cell division make haemopoietic and epithelial cells most susceptible. Human papilloma viruses (HPVs) are associated with cervical cancer. Genetic abnormalities may bear strong ties to malignancy, and may be caused by inherited allelic alterations of tumour suppressor genes (Tripathy, 1995. Pg. 49).

4.1.2.2 Oncogenes and tumour suppressor genes in normal physiology and neoplasia

Proto-oncogenes encode proteins that function in various physiological cellular processes. Altered or excessive proteins, encoded by oncogenes (*ras*), have abnormal functions that confer proliferative or invasive properties on the cell. Tumour suppressor genes encode for regulatory proteins, adhesion proteins and cytoplasmic proteins. These proteins keep proliferative and invasive potential of cells in check. Examples of tumour suppressor genes include p53 (cell cycle regulator), WT-1 (transcription factor), DCC (cell adhesion) and hMSH2 (DNA repair) (Tripathy, 1995. Pg. 50).

4.1.2.3 Hormones, growth factors and growth inhibitors

These proteins result in a number of cellular effects, such as mitogenesis, growth inhibition, differentiation and induction of a set of secondary genes. A factor that is secreted by cell type or tissue may influence adjacent cells or a set of distant cells. The signaling end effect may be altered by a changed factor concentration or mutations of the receptor.

4.1.2.4 Cellular changes in neoplasia

At both the cellular and tissue levels, molecular and biochemical changes are accompanied by functional and morphologic changes. The abnormal growth and invasive capacity of malignant cells disrupt normal tissue architecture. The tumour cells at both the sites of origin of the tumour and distant metastases proliferate abnormally and destroy tissue boundaries (eg. basement membrane).

In rare, inherited malignancies, alterations occurring initially may be preprogrammed. Mutations resulting from environmental exposure or a mutation occurring during normal cell division will thus be acquired (Tripathy, 1995. Pg. 52).

4.1.3 Pathophysiology of neoplasia

Common to all neoplasia is uncontrolled growth and invasion. Benign tumours grow faster than normal tissue, but at a decreased pace in comparison to malignant tumours (Figure 4.3). A regular tumour mass is formed by the orderly pattern of expansion

characteristic of benign tumours. The tumour mass is surrounded by a fibrous connective tissue capsule, thereby isolating it from the surrounding normal tissue. The slower growth rate implies that less damage occurs to the surrounding tissue. Surgical removal of the tumour is facilitated by the presence of the capsule (Nowak and Handford, 1999. Pg. 125).

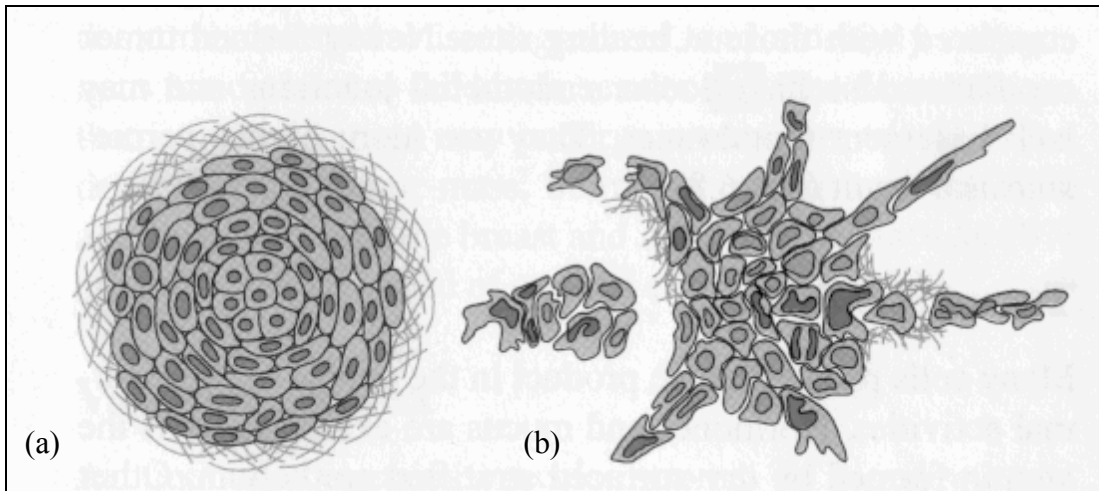


Figure 4.3: Typical tumour structure. (a) A benign tumour (b) A malignant tumour (Nowak and Handford, 1999. Pg. 126).

A larger tumour mass is produced by the faster growing malignant tumour (Figure 4.3 (b)). In contrast to the benign tumour, the pattern of growth of malignant cells is aggressively invasive. The structure and function of adjacent cells are disrupted by the columns of cells that project into it from the tumour. A capsule surrounding the tumour is very rare, but if present, is usually incomplete and irregular. Surgical removal is thus complicated by indistinct borders between tumour cells and normal tissue cells. The single characteristic that clearly distinguishes between benign and malignant tumours is the ability of malignant tumours to metastasize (Nowak and Handford, 1999. Pg. 126).

4.1.3.1 Colon carcinoma

Colon carcinomas progress through three stages of development. In the first stage, a small benign tubular type of adenoma or polyp occurs that increases in size and becomes more villous. Initially, a point mutation in the *ras* gene occurs. This results in increased

cytoplasmic signaling. Then, a part of or all of the DCC gene is lost. This gene encodes for an adhesive protein, resulting in a loss of cell cohesion and a tendency to metastasize. The earliest sign is hyperplasia (increase in cell number) on the luminal epithelial surface.

In the second stage, patches of frank carcinoma tissue become evident. This stage is more aggressive than the first one. An adenoma is produced that consists of gland-forming cells that show enhancement in size and cell number but no invasion of surrounding structures occur. Cell cycle control is thus lost. Mucin production may cease and cell polarity may be changed. Microscopic bleeding occurs from newly developed, fragile vessels, or from existing vessels that have been destroyed (Tripathy, 1995. Pg. 56).

Lastly, the patches grow out and are then referred to as an invasive carcinoma (Bos, 1989). Invasive malignant cells can gain entry to regional lymphatics, entering the bloodstream, from where it can spread throughout the body (Tripathy, 1995. Pg. 56).

4.1.3.2 Breast carcinoma

Epithelial and stroma cells contained within breast tissue are controlled by various growth factors like insulin-like growth factor I. Pre-ovulatory estrogen causes hypertrophy of breast epithelial cells and hyperplasia occurring during pregnancy are examples of normal physiologic responses. Benign proliferative changes such as adenosis or apocrine metaplasia may give an early indication of disordered growth, through loss of cell cycle control or abnormalities in hormonal or growth factor response. Increased risk includes prolonged use of exogenous estrogen (at high doses) and a positive family history (Tripathy, 1995. Pg. 57).

In situ carcinoma of the breast is a preinvasive lesion in which increased proliferation and malignant cell morphology are observed. At this stage, no lymph nodal or distant metastasis occurs. In addition, a mutation of the p53 tumour suppressor gene occurs. Occasionally, a dense reaction of fibroblasts and extracellular matrix by the tumour is observed. This response may be mediated by soluble factors such as tissue growth factor- β and platelet derived growth factor. This dense reaction may isolate the tumour, or

facilitate growth and cell migration. Metastases of breast cancer to bone, lung or liver may be due to cell surface recognition proteins, changes in malignancy and may facilitate invasion and distant metastases (Tripathy, 1995. Pg. 58).

4.1.3.2 Cervical carcinoma

Benign or malignant tumours of the endometrium or myometrium would result in structural lesions that cause abnormal vaginal bleeding. The risk of cervical cancer is increased by multiple sexual partners and the onset of sexual intercourse before 20 years of age. Predisposition to the development of cervical cancer is also increased by infection with HPV, herpes simplex virus (HSV) type II, and other sexually transmitted diseases. Adjacent to the areas of severe dysplasia, condylomas (viral warts), caused by HPV, are often found. Cervical cancer can easily be detected by the Papanicolaou (Pap) smear, which has decreased the mortality rate associated with cervical cancer. The Pap smear detects preneoplastic changes and cancer prior to metastasis, at which point it is curable. Left untreated, it will spread to the pelvis with death resulting through haemorrhage, infection or renal failure secondary to ureteral obstruction (Lingappa, 1995. Pg. 466).

4.1.4 Anticancer drug development

Over the past four decades, increased effort has gone into the development of anticancer agents by empirical screening and rational design of new compounds. Measurement of drug sensitivity of human tumour stem cells has lead to the augmentation and shortening of the testing program. Once a compound is found to have potential as an anticancer agent, animals are used to carry out preclinical toxicologic and limited pharmacologic studies. If the agent is found to have minimal toxicology, then phase I clinical trials are tested in patients with advanced cancer (Salmon and Sartorelli, 1989. Pg. 684).

Ideally, the anticancer agent should target only the neoplastic cells, without adversely affecting normal tissues. To date, no such agent has been discovered (Salmon and Sartorelli, 1989. Pg. 684).

A new intracellular target for cancer therapeutics is DNA topoisomerase I, which is responsible for DNA metabolism. Three metabolites isolated from the broths of *Microsphaeropsis* sp. FL-16144 have shown topoisomerase I inhibition activity. These metabolites, TAN-1496 A, C and E, are diketopiperazine antibiotics belonging to the *epi*-oligothiadiketopiperazine class of fungal metabolites. The growth of tumour cells is effectively suppressed and apoptosis is induced by these metabolites (Funabashi *et al.*, 1994).

Classes of anticancer agents include:

- ◆ Inducers of differentiation: neoplastic cells are forced past the maturation block to produce endstage cells that exhibit little or no proliferative capacity.
- ◆ Antimetastatic drugs: these agents act by disrupting the surface characteristics of tumour cells, thereby altering their invasive and metastatic potential.
- ◆ Hypoxic tumour stem cell-specific agents: these agents target the elevated capacity for reductive reactions created by a lack of oxygen in solid tumours.
- ◆ Tumour radiosensitizing and normal tissue radio-protecting drugs: the point of these agents is to increase the therapeutic effectiveness of radiation therapy.
- ◆ Biologic response modifiers: the tumour-host metabolic and immunologic relationships are altered (Salmon and Sartorelli, 1989. Pg. 684).

4.1.4.1 Resistance to cytotoxic drugs

Resistance to drugs poses a major problem to cancer chemotherapy. Primary resistance by non-small cell lung and colon cancers is common i.e. these cancers do not respond to the first exposure of currently available standard drugs. In a number of drug-sensitive tumours, acquired resistance develops. Drug resistance can develop against a single drug, resultant of an alteration in the tumour cell's genome with amplification or enhanced expression of one or more specific genes. A multi-drug resistant phenotype may occur in other instances, developing after exposure to a single agent. Associated with this type of resistance is an increased expression of the gene that encodes for the P-170 protein (a cell surface glycoprotein) that is involved in drug efflux (Salmon and Sartorelli, 1989. Pg. 686).

4.1.5 Antitumour therapy

The main aim of any antitumour agent is the removal of and destruction of the tumour. Antitumour therapy includes surgery, radiation therapy, chemotherapy, immunotherapy and combination therapy.

4.1.5.1 Surgery

Surgery involves the physical removal of the tumour. It is an effective form of therapy if the tumour did not metastasize prior to treatment (Salmon and Sartorelli, 1989. Pg 686). Where the tumour is benign, removal of the well-defined encapsulated tumour poses minimal complications and risk. In contrast, removal of the irregular, invasive growth of malignant tumours presents increased complications. Since the edge of the tumour is not well defined, it is necessary to remove some surrounding normal tissue that may contain tumour cells. If the tumour is present in nervous tissue or if a small gland is involved, removal of any normal tissue presents significant difficulties. Surgical removal of the tumour may result in the formation of a number of tumour emboli, which can metastasize, resulting in secondary growths (Nowak and Handford, 1999. Pg. 148).

4.1.5.2 Radiation therapy

Radiation therapy is used to deliver ionizing radiation to the tumour mass. A major drawback to this therapy is that normal tissue is also susceptible to damage. Rapidly dividing cells are most susceptible to radiation. Heat produced when radiation passes through the skin may cause burns (Nowak and Handford, 1999. Pg. 149).

4.1.5.3 Chemotherapy

Toxic chemicals are used to destroy the tumour. These chemicals are not selective for the tumour cells and damage normal cells to varying degrees. Initially, an antitumour effect is noted in that the growth of the tumour may slow down. After this initial period of up to several months, the tumour resumes its previous high growth rate (Nowak and Handford, 1999. Pg. 149).

4.1.5.3.1 Chemotherapeutic drugs

4.1.5.3.1.1 Fluorouracil

Fluorouracil (5-FU), a pyrimidine antagonist, is the drug of choice for colon cancer sufferers. It is biotransformed to ribosyl and deoxyribosyl nucleotide metabolites. One such metabolite formed is 5-fluoro-2'-deoxyuridine 5'-phosphate (FdUMP). FdUMP combines with thymidylate synthetase and its cofactor N^{5,10}-methylenetetrahydrofolate, to form a covalently bound ternary complex. This reaction is essential for the synthesis of thymine nucleotides. This causes inhibition of DNA synthesis due to a lack of thymine. When 5-FU is converted to 5-fluorouridine triphosphate, it is incorporated into RNA, thereby interfering with RNA processing and function. 5-FU cytotoxicity is therefore due to its effects on both DNA and RNA. 5-FU is the drug of choice for colon cancer, and is usually administered intravenously. Side effects of this drug include myelosuppression and mucositis (Salmon and Sartorelli, 1989. Pg. 692).

4.1.5.3.1.2 Mitomycin

Mitomycin is isolated from *Streptomyces caespitosus*. Its activity is contributed by the quinone, carbamate and aziridine groups contained in the molecule. It is a bioreductive, alkylating agent that is activated via a cytochrome P450 reductase-mediated reaction, producing an alkylating agent that cross-links DNA. Hypoxic tumour stem cells of solid tumours are more susceptible to the cytotoxic actions of mitomycin than normal and oxygenated tumour cells. It is used in combination chemotherapy for squamous cell carcinoma of the cervix and stomach, pancreas and lung adenocarcinomas. It is also a useful second-line agent for metastatic colon cancer. It causes severe myelosuppression with late toxicity against all three formed elements from bone marrow. Shortly after injection, nausea, vomiting and anorexia occur. Renal toxicity and interstitial pneumonitis have also been reported to occur occasionally (Salmon and Sartorelli, 1989. Pg. 696).

4.1.5.3.1.3 Estrogen and androgen inhibitors

Tamoxifen, an estrogen inhibitor, is the treatment of choice in breast cancer. Estrogen-stimulated increases in uterine weight and vaginal cornification are inhibited by tamoxifen. It acts as a competitive inhibitor of estrogen by binding to estrogen receptor

(ER) proteins of estrogen-sensitive tissue and tumours. Since the affinity of tamoxifen is 10 times lower for ER proteins than estradiol, ablation of endogenous estrogen is important for optimal antiestrogen effects. Mild adverse effects are noted, including hot flushes and occasional nausea (Salmon and Sartorelli, 1989. Pg. 699).

4.1.5.4 Immunotherapy

The immune system is used to combat the growing tumour. A substance with potent antigenic properties is administered, resulting in a strong, general stimulus to the immune system. It was hoped that the antitumour activity of host defenses would increase, thereby increasing tumour destruction. However, its effectiveness is disappointing. Side effects include nausea, fever, liver damage and inflammation and abscess formation at antigen injection sites. Autoimmune destruction of normal tissue may also be induced by such a strong stimulus (Nowak and Handford, 1999. Pg. 150).

4.1.5.5 Combination therapy

Combination therapy involves the use of two or more modes of therapy in combination. Side effects are kept to a minimum, as the dose of each agent can be decreased while still maintaining a lethal effect on the tumour. The tumour mass is reduced by surgery, followed by chemotherapy or radiation to kill tumour cells that were not removed (Nowak and Handford, 1999. Pg. 150). If micrometastasis has occurred, systemic therapy such as chemotherapy, in conjunction with surgery or radiation is needed. This is an effective combination for early stage breast cancer and osteogenic sarcoma (Salmon and Sartorelli, 1989. Pg. 686).

4.2 OBJECTIVES OF THE CHAPTER

4.2.1 Objectives of the present chapter

- ◆ The main aim was to perform a primary screen to determine whether cyclo(L-Trp-L-Pro), cyclo(L-Trp-D-Pro), cyclo(D-Trp-L-Pro) and cyclo(D-Trp-D-Pro) show potential as anticancer agents.

In order to satisfy this aim, the following experimental data was collected:

- The relationship between cell number and MTT-formazan product was determined.
- Growth curves were obtained using the MTT assay to determine the optimal concentrations of cells to give maximal absorbance with the MTT assay.
- The effects of the isomers on cell viability were tested using the MTT assay.
- Expression of alkaline phosphatase was determined using a modified assay of Bergmeyer (1984).

4.3 MATERIALS AND METHODS

Interest in human tissue was encouraged by the demonstration that human tumours could give rise to continuous cell lines eg. HeLa (Alley *et al.*, 1988). Many biological assays need the assessment of surviving and/or proliferating mammalian cells in the presence of various chemicals. Several methods can be used to achieve this, including counting cells that include or exclude dye, measuring released ^{51}Cr -labeled protein after cell lysis and measuring incorporated radioactive nucleotides during cellular proliferation. Vital dyes such as trypan blue, eosin, crystal violet and neutral red have been used in the predictive screening of drugs in general and the assessment of efficacy of antitumour agents selected for chemical use (Löwik *et al.*, 1993). These staining methods can be used to measure viable cell numbers, but processing time increases and sample variation results from washing steps (Mosmann, 1983).

4.3.1 Cell lines

Cell cultures present a simplified, valid biological model in *in vitro* screening of cytotoxicity of different compounds. *In vitro* models are often used as they are simplistic and represent fewer inherent variations than the corresponding *in vivo* model (Briske-Anderson *et al.*, 1997). Cellular models are also used as an alternative to animal studies, since the use of animals is limited by their expense and ethical issues. *In vitro* methods are used to quantitatively define toxicity of chemicals, using human cellular models. This eliminates extrapolation of animal data to human due to species differences in biotransformation or target organs (Jover *et al.*, 1992).

The cell lines are extremely useful in cell research, as they provide large numbers of cells of a uniform type. Furthermore, these cells can be stored at -70°C until needed, and are still viable when thawed. The effects of the compounds on development, apparent toxicity levels for humans, mechanisms of toxicity, identification of markers in order to monitor potential side effects *in vivo*, and the determination of ways to circumvent any adverse reactions to the drug can be predicted (Vickers, 1997).

The HT-29, HeLa and MCF-7 cell lines were chosen to represent the effects of the isomers on colon, cervical and breast cancer, respectively.

4.3.1.1 The HT-29 cell line

The cells were originally isolated from a carcinoma of the colon from a Caucasian female in 1975 by Fogh and Trempe (Forgue-Lafitte *et al.*, 1989). Until recently, the human colon carcinoma cell line HT-29, has been used mainly for studies related to glucose metabolism and hormone receptors (Rousset, 1986). Undifferentiated HT-29 cells have an impaired glucose metabolism, high rates of glucose consumption and lactic acid production. Functional receptors for insulin, epidermal growth factor and catecholamines have been found to be present on these undifferentiated cells (Rousset, 1986). They grow in a multilayer of unpolarised undifferentiated cells under standard culture conditions i.e. with glucose and serum. In this state, no characteristics of the intestinal epithelial cells are found (Pinto *et al.*, 1982).

If glucose is omitted from the medium, these cells express enterocytic differentiation. In the differentiated state, the cells form a polarised monolayer with tight junctions and a brush border. Villin, a protein associated with the cytoskeleton of the intestinal brush border microvilli, is also found. Hydrolases and sucrase-isomaltase, which are not normally found in the healthy colon, have been found associated with the differentiated colonic cells. These enzymes, including dipeptidyl peptidase and alkaline phosphatase, are found at activities much lower than those observed in the small intestine. When the cells are cultured without serum, large amounts of lysozyme are secreted and about 50% of the cells differentiate into goblet-like cells. Mucin is present, which reacts with antibodies raised against normal human colonic mucins (Rousset, 1986).

Changes occurring in non-neoplastic cell lines are not represented by the changes occurring in HT-29 cells, as this cell line is neoplastic. All the same, HT-29 is the only cell line available for modeling *in vitro* gastrointestinal epithelial differentiation (Huet *et al.*, 1987).

4.3.1.2 The HeLa cell line

In 1951, the HeLa cell was isolated from the cervical carcinoma of Henrietta Lacks. This cell line has been used in various fields from virology, molecular biology to cellular biology. AK (1-1) for adenylate kinase, ADA (1-1) for adenosine deaminase, PGM (1-1) for phosphoglucomutase, 6PGD(A) for 6-phosphogluconate dehydrogenase and G6PD (A) for glucose-6-phosphate dehydrogenase are the enzyme phenotypes expressed, including the M, N, S, s, Tja, and HLA antigens (Akiyama, 1987).

4.3.1.3 The MCF-7 cell line

The MCF-7 cell line was derived from a metastatic pleural effusion of a human breast cancer. Many properties of *in vivo* human mammary epithelium are retained *in vitro* by the MCF-7 line. The survival of the cells seems to be dependent on the presence of hormones. It grows in medium supplemented with insulin, transferrin, epidermal growth factor, prostaglandin F₂α and Clg. The growth rate does not differ in medium containing or lacking fetal calf serum. The growth rate of the cells is reduced if any of the five supplements are omitted from the medium. When grown in serum-free medium, the cells are most susceptible to damage from proteases, extremes in pH and centrifugation. Cells grown in serum-free medium are round in shape and grow as aggregates, without spreading over the surface of the plate. In medium supplemented with serum, the MCF-7 cells take on the characteristic epithelial shape. Under serum-free conditions, estradiol is noted to stimulate MCF-7 growth (Barnes *et al.*, 1981). It was later established that these cells are capable of growing in Dulbecco's medium, as used in the experiments.

4.3.2 Routine cell culture

The HT-29, MCF-7 and HeLa cells were routinely maintained in 25 cm² flasks (Corningware, Cambridge, U.S.A.) in Dulbecco's modification of Eagle's minimal essential medium³ (DMEM) (Highveld Biological, Lyndhurst, South Africa) supplemented with 10% heat inactivated fetal calf serum (FCS) (Highveld Biological, Lyndhurst, South Africa), 1 mM sodium pyruvate (Highveld Biological, Kelvin, South Africa), and 60 mg/l Benzyl-Penicillin and 100 mg/l Streptomycin (100X concentration)

³ Solution list – Appendix C

(Highveld Biological, Lyndhurst, South Africa), at 37°C. The medium was replaced every 24 hrs. The cells were sub-cultured at 75% confluence with 0.25% trypsin (Highveld Biological, Johannesburg, South Africa) and 1 mM EDTA (BDH Chemicals, Poole, England) in 1 mM phosphate-buffered saline (PBS) at pH 7.4.

4.3.3 The 3-[4,5-Dimethylthiazol-2-yl]-2,5-diphenyltetrazolium bromide (MTT) assay

Viable cells are able to reduce the tetrazolium-based compound MTT to a blue formazan dye by cleavage of the tetrazolium ring (Mosmann, 1983). Large numbers of samples can be analysed simply and rapidly. It gives comparable results with clonogenic and dye exclusion assays for lung cancer and Chinese hamster cells. MTT is reduced by mitochondrial succinic dehydrogenases of viable cells (Carmichael *et al.*, 1987). It has wide applicability, since a number of cell types are capable of reducing MTT (Mosmann, 1983). The MTT assay exhibits good signal-to-noise ratios (Monks *et al.*, 1991). MTT reduction correlates well with cellular protein, dye exclusion and clonogenic assay methodologies under various culture and assay conditions

Strong reducing agents cause MTT reduction in solution, but do not affect interpretation of the assay when the supernatant is removed prior to solubilization of the formazan crystals (Carmichael *et al.*, 1987).

One major disadvantage of this assay is that the blue formazan crystals produced by the reduction reaction is insoluble and must be extracted from the cell. This increases the assay time considerably (Löwik *et al.*, 1993), and is potentially error prone (Monks *et al.*, 1991).

A potential limitation of the assay is that it does not distinguish between cytostatic and cytotoxic effects. Furthermore, some compounds tested may exhibit peaks in the 500-600 nm range. This can be circumvented with the aspiration of the medium from adherent cells, but still poses a problem for cells in suspension (Carmichael *et al.*, 1987).

4.3.3.1 Linearity for MTT assay

The relationship between cell number and MTT formazan crystal production was determined by counting 200 μ l aliquot of different dilutions of each cell suspension stained with 0.4% trypan blue solution. These dilutions were incubated with 0.5% MTT to correlate cell number to MTT absorbance.

A modified method as described by Carmichael *et al.* (1987) was used. 50 μ l 0.5 % MTT solution was added to 200 μ l cell suspension in an eppendorf and incubated at 37 °C for 2 hrs. After the incubation period, the cells were pelleted from solution by microcentrifugation and resuspended in 200 μ l DMSO. After a 5 min incubation period with mild agitation, the cells were pelleted from solution. The extracted formazan product was then read at 540 nm using Labsystems Multiskan MS (Multiskan Transmit Program, Rev. 1.3. (1995)).

4.3.3.2 Growth curves

Growth curves of the cell lines were obtained over a 7 day period. 25 000 cells/ml were seeded into 96-well plates and were incubated at 37°C under standard culture conditions. Each day, the MTT assay was performed to obtain a growth curve of each cell line in culture.

On the assay day, 50 μ l 0.5% MTT solution was added to each well, and incubated at 37°C for 2 hrs. After the incubation period, the solution was aspirated from the cells, and 200 μ l DMSO was added to each well. A 5 min reaction period was allowed with mild agitation. The resultant formazan products were removed from the plate and put into a clean 96-well plate. The absorbance at 540 nm was read against a DMSO blank using Labsystems Multiskan MS (Multiskan Transmit Program, Rev. 1.3. (1995)).

4.3.3.3 Effects of the isomers on cell viability

The effect of the isomers at stock concentrations of 10^{-7} M to 10^{-3} M was determined. Each cell line was seeded at a density of 25 000 cells/ml. The cells were allowed 24 hrs for attachment, after which the medium was aspirated from the cells, and replaced by

isomer-containing medium. Melphalan (Figure 4.4) was used as a positive control at stock concentrations in the range of 10^{-7} M to 10^{-3} M. Melphalan is an antineoplastic agent, which creates DNA intrastrand crosslinks through bifunctional alkylation in 5'-GGC sequences (Sigma catalogue, 2000-2001). It is effective against ovary carcinomas, multiple myelomas, macroglobulinemias and thyroid carcinomas (Salmon and Sartorelli, 1989. Pg. 702). The number of viable cells was assessed using the MTT assay as described in Section 4.3.3.2. The % viability of each sample was calculated in relation to the negative control samples, where the negative control samples represent 100% viability.

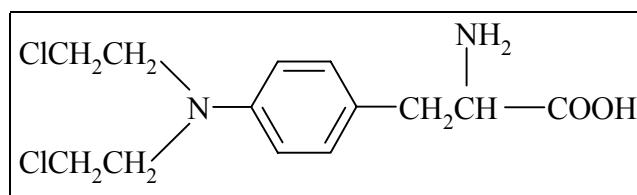


Figure 4. 4: Structure of melphalan (Salmon and Sartorelli, 1989. Pg. 686).

4.3.4 Alkaline phosphatase (AP) activity

AP (E.C. 3.1.3.1) is expressed in all cells (Herz *et al.*, 1973), and is the most commonly used marker of small intestinal differentiation. Pinto *et al.* (1982) found the presence of this enzyme at low levels in undifferentiated cells, but at increased levels in differentiated cells. This metalloenzyme is anchored to the cell membrane via glycoposphatidylinositol. They are capable of hydrolysing a number of monophosphate esters at alkaline pHs. The determination of expression levels is based on the use of *p*-nitrophenyl phosphate (*p*NPP) as a substrate of AP. In the enzymatic reaction, *p*NPP is converted to yellow *p*-nitrophenyl, which absorbs light maximally at 410 nm (Bergmeyer, 1984).

4.3.4.1 Alkaline phosphatase assay

A modification of the AP assay by Bergmeyer (1984) was used. The cells were grown in 96-well plates (Corningware, Cambridge, U.S.A.). One day after seeding, the cells were exposed to the isomers at varying concentrations (10^{-7} to 10^{-3} M). 10^{-7} to 10^{-3} M Melphalan was added as a positive control. On the assay days (24 hrs and 72 hrs), the

medium was aspirated from the cells. The cells were washed twice with 1 mM PBS (pH 7.4) in order to remove any traces of medium. To each well, 26 μ l 1 mM MgCl_2 (Saarchem, Krugersdorp, South Africa) and 200 μ l glycine (BDH Chemicals, Poole, England) buffer (0.1 M, pH 10.5, 1 mM MgCl_2 (Saarchem, Krugersdorp, South Africa), 0.1 mM ZnCl_2) were added. At zero time, 40 μ l 0.03 M *p*NPP (Merck, Germany) was added to each well. A 5 min incubation period at room temperature was allowed for the reaction to occur, after which the absorbance was read at 410 nm using Labsystems Multiskan MS (Multiskan Transmit Program, Rev. 1.3. (1995)). The blank consisted of reagent mixture without cells. A standard curve was constructed from the results of different concentrations of commercial AP (Appendix B, Figure B 3.1) (Merk, Darmstadt, Germany). The activity is expressed as mU/ml.

4.3.5 Statistical analysis

Values are expressed as mean \pm s.d. for the indicated number of experiments. Results were analysed using the software package GraphPad Prism Version 2.0 and GraphPad InStat (GraphPad Software, Inc., San Diego, U.S.A.). All tests were performed on raw data obtained from the experiments (n=4). The effect of a single qualitative factor on a single response variable was determined by univariate ANOVA test. *P* values <0.05 were accepted as evidence of a statistically significant difference.

4.4 RESULTS AND DISCUSSION

A primary screen was performed to assess the potential of the isomers as anticancer agents. To determine the relationship of cell number to MTT formazan crystal formation, increasing cell numbers of HT-29, HeLa and MCF-7 cells were incubated in the presence of MTT. Linearity was obtained between MTT and HT-29 cells (Figure 4.5) in the range of 15000 to 563000 cells/ml ($R^2=0.9994$).

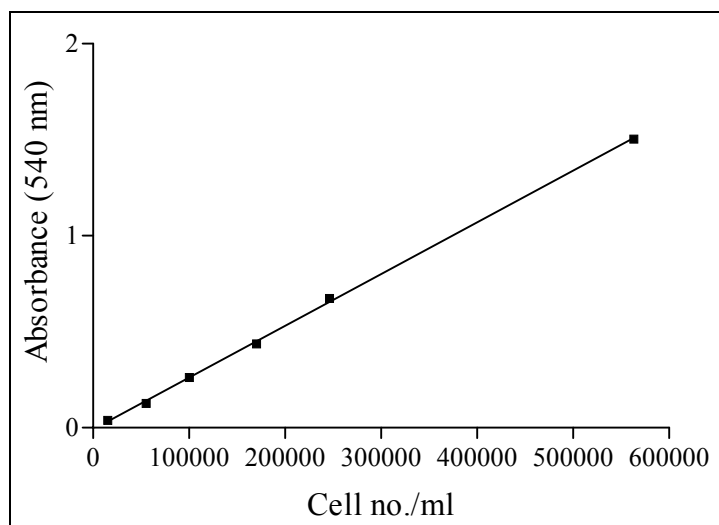


Figure 4. 5: Correlation between HT-29 cell number and MTT formazan crystal production. $R^2=0.9994$. Values indicated are the mean \pm s.d. of quadruplicates.

Similarly, linearity was obtained in the 5000 to 260000 cells/ml range for MCF-7 cells (Figure 4.6) ($R^2=0.9954$).

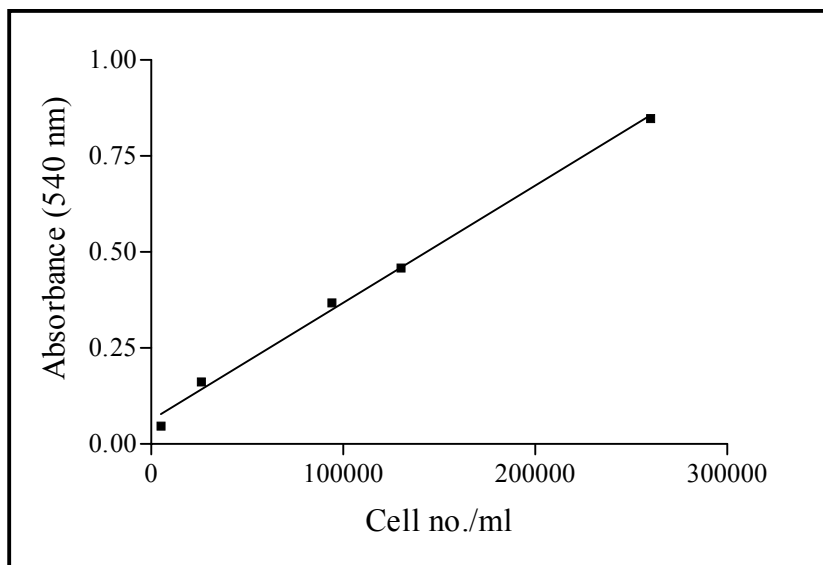


Figure 4. 6: Correlation between MCF-7 cell number and MTT formazan crystal production. $R^2=0.9954$. Values indicated are the mean \pm s.d. of quadruplicates.

When HeLa cells in the range of 2600 to 250000 cells/ml were tested with MTT (Figure 4.7), a linear relationship was obtained ($R^2=0.9935$).

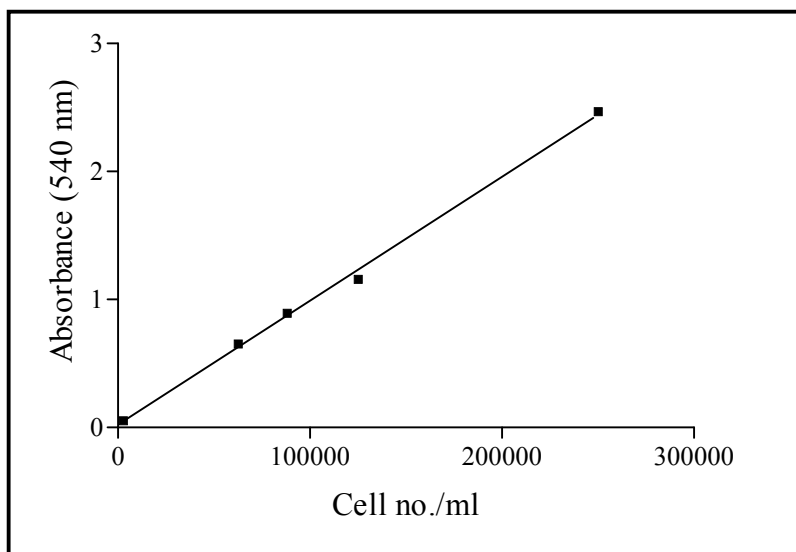


Figure 4. 7: Correlation between HeLa cell number and MTT formazan crystal production. $R^2=0.9935$. Values indicated are the mean \pm s.d. of quadruplicates.

These results are in agreement with Carmichael *et al.* (1987), who stated that the amount of cell number and formazan product are proportional. Linearity was obtained for MTT

with EL₄.3 lymphoma cells in the 200 to 50000 cells/well range (Mosmann, 1983).

Twenty-five thousands cells/ml was chosen as a common seeding density for all the cells, as they are able to proliferate in culture, without limitation to growth space. If the seeding density chosen was too high, not all the cells would be able to attach to the relatively small surface area of the well of a 96-well plate. Cells in suspension would then be removed by aspiration before the addition of the drug-containing medium. This would have lead to variability in the initial cell number present per well at the addition of the isomers.

Growth rates of the cell lines in microtiter plates were determined using the MTT assay. Cell numbers were measured daily over a 7 day period. MTT-labeled cells were lysed using DMSO as a formazan crystal solvent. Solubility of the crystals in acid/isopropyl alcohol was found to be poor. Isopropanol/HCl resulted in colour fading of product as well as a rapid, irreversible shift in absorbance maxima as a result of the low pH. The solvent of choice is DMSO, since formazans are quickly mobilized from sites within thick cell layers by DMSO. The absorbance of the MTT formazan product solubilized in DMSO is 6.2 times higher than in the acid/isopropanol system. DMSO also rapidly solubilizes serum and has improved extraction and detection of the formazan product within cultured cells. With DMSO extraction, stable spectrophotometric characteristics are obtained for several days. (Alley *et al.*, 1988).

After seeding, the cells were allowed to recover from the trypsin-treatment during detachment for 24 hrs in the wells. The medium was then changed, and the growth curve started. The first reading was thus taken 48 hrs after seeding, and is reported as a day 1 reading on the graphs.

Exponential growth started at day 2 for HT-29 cells (Figure 4.8), MCF-7 cells (Figure 4.9) and HeLa cells (Figure 4.10).

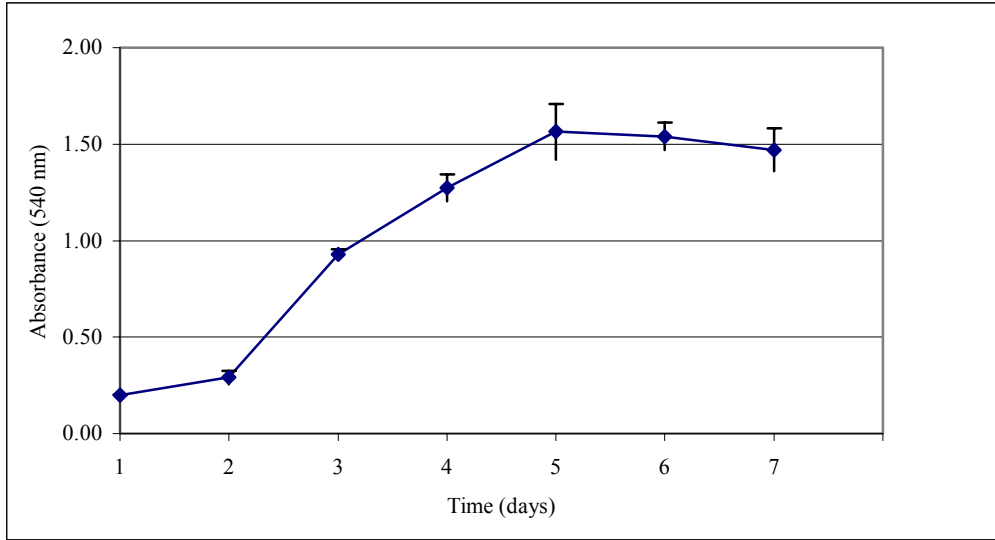


Figure 4. 8: Growth curve of HT-29 cells in a microtiter plate over a 7 day period. Values indicated are the mean \pm s.d. of quadruplicates.

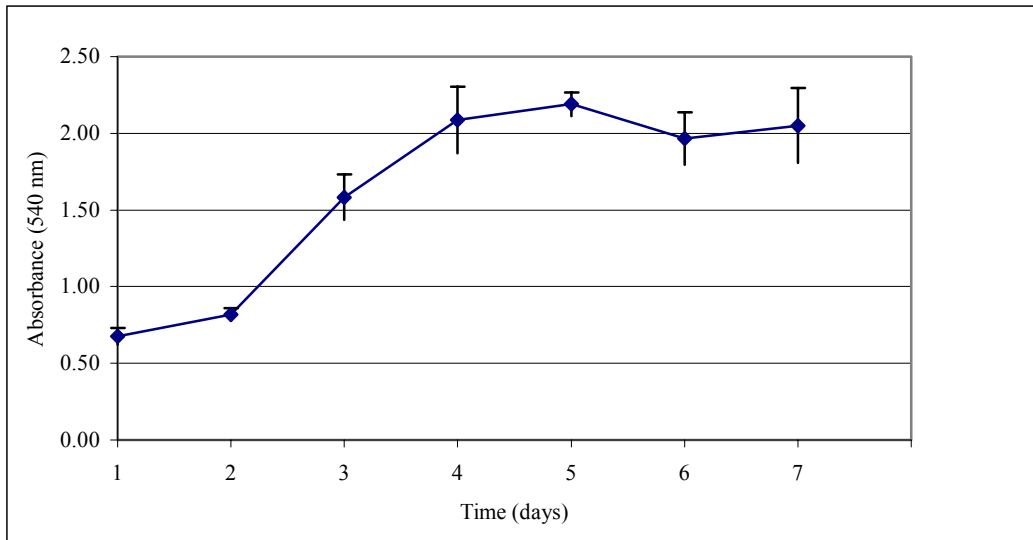


Figure 4. 9: Growth curve of MCF-7 cells in a microtiter plate over a 7 day period. Values indicated are the mean \pm s.d. of quadruplicates.

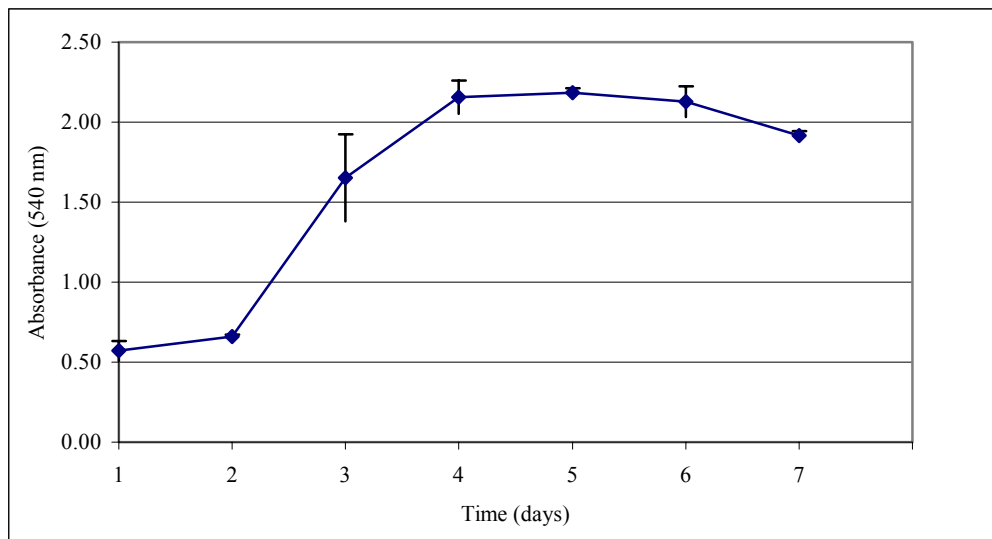


Figure 4. 10: Growth curve of HeLa cells in a microtiter plate over a 7 day period. Values indicated are the mean \pm s.d. of quadruplicates.

The effects of the isomers over a short-term exposure to the cells were determined at 24 hrs and 72 hrs. These periods were chosen to determine the effects on exponentially growing cells (Figures 4.8-4.10). Erroneous results could be obtained if the control cells reach the stationary phase of growth, while the treated cells continue to grow at an exponential rate, or vice versa (Carmichael *et al.*, 1987). This would lead to erroneous estimation of the potential of the isomers as anticancer agents, as the results are expressed as % viability in relation to the control samples, where the control samples represent 100% viability.

No great adverse effects were noted in the viability of the cells in the presence of cyclo(L-Trp-L-Pro) at all concentrations tested after 24 hrs (Figure 4.11). At 10^{-3} M, cyclo(L-Trp-L-Pro) significantly reduced the growth of MCF-7 cells to $90.205 \pm 1.872\%$ ($p < 0.05$).

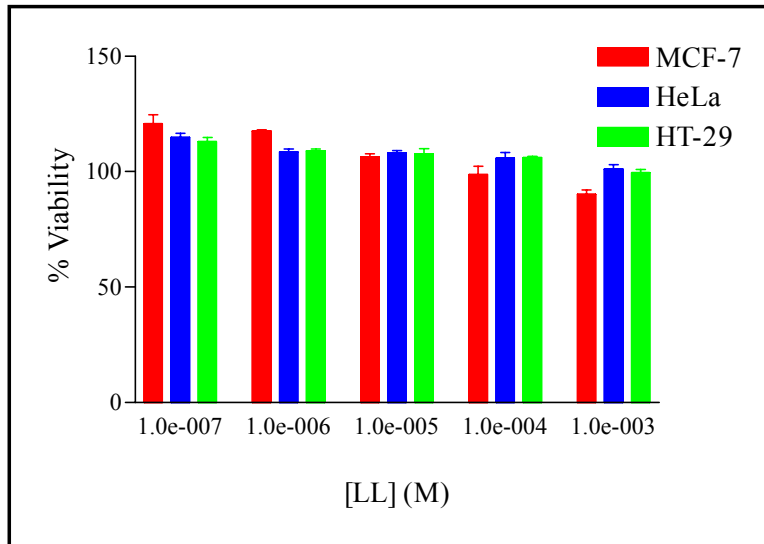


Figure 4. 11: The effect of cyclo(L-Trp-L-Pro) on HT-29, MCF-7 and HeLa growth after a 24 hr exposure period. Final concentrations of cyclo(L-Trp-L-Pro) are indicated. Values indicated are the mean \pm s.d. of quadruplicates.

After 72 hrs, the effects of 10^{-7} to 10^{-3} M cyclo(L-Trp-L-Pro) (Figure 4.12) did not differ significantly from the corresponding effects at 24 hrs ($p > 0.05$) in HT-29 cells. Significant reduction in MCF-7 and HeLa cell viability was noted after 72 hrs in comparison to the 24 hrs effects at all concentrations of cyclo(L-Trp-L-Pro) tested ($p < 0.05$). This indicated that a long exposure period is needed to induce cell death in MCF-7 and HeLa cells.

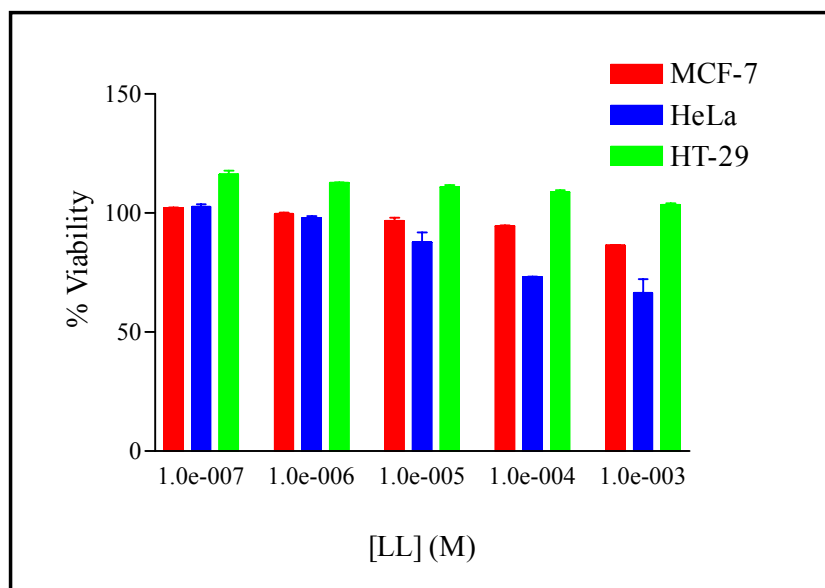


Figure 4. 12: The effect of cyclo(L-Trp-L-Pro) on HT-29, MCF-7 and HeLa growth after a 72 hr exposure period. Final concentrations of cyclo(L-Trp-L-Pro) are indicated. Values indicated are the mean \pm s.d. of quadruplicates.

No significant reduction in cell viability was observed in the presence of cyclo(L-Trp-D-Pro) after 24 hrs (Figure 4.13), with the exception of 10^{-3} M cyclo(L-Trp-D-Pro) applied to HeLa cells.

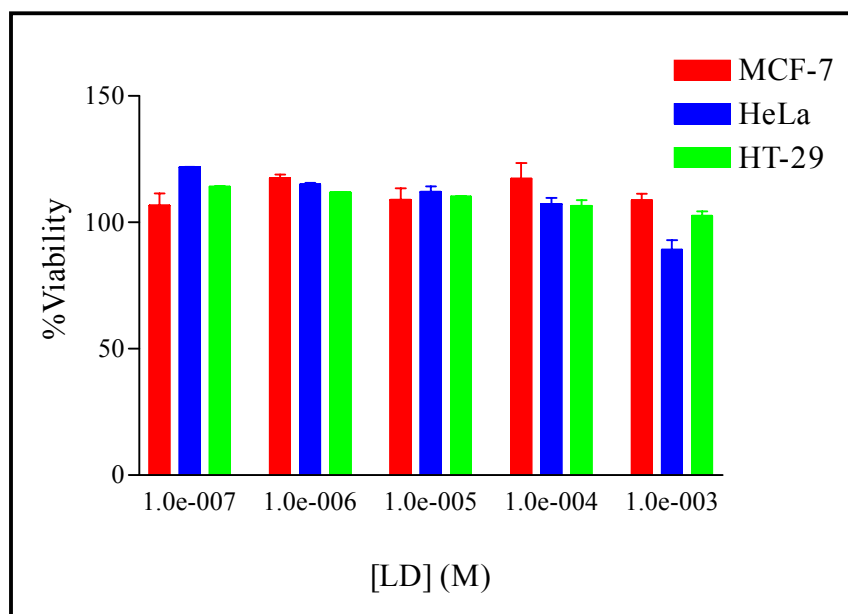


Figure 4. 13: The effect of cyclo(L-Trp-D-Pro) on HT-29, MCF-7 and HeLa growth after a 24 hr exposure period. Final concentrations of cyclo(L-Trp-D-Pro) are indicated. Values indicated are the mean \pm s.d. of quadruplicates.

After 72 hrs, significantly reduced viability ($p < 0.05$) in comparison to the negative control sample was noted for cyclo(L-Trp-D-Pro) in the range of 10^{-6} M to 10^{-3} M (Figure 4.14). This effect was more pronounced for the HeLa cells. In addition, a dose-dependent reduction in cell viability is noted for both HT-29 and HeLa cells.

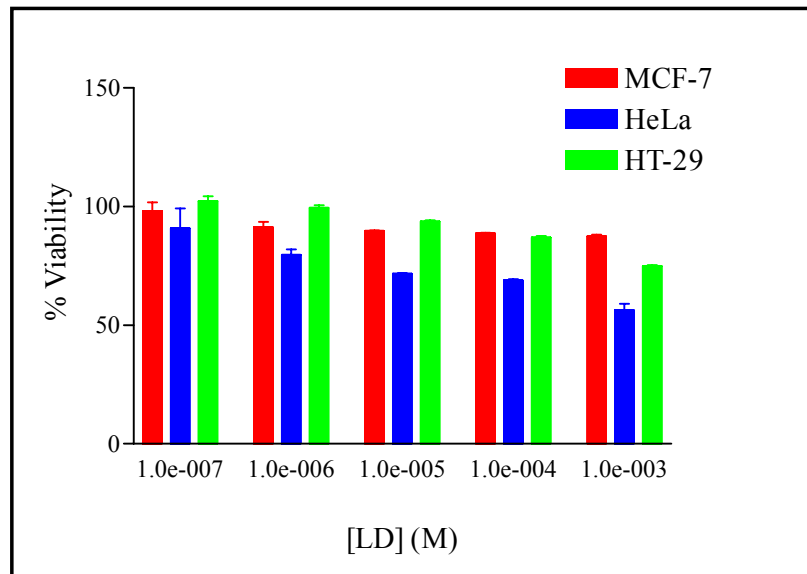


Figure 4. 14: The effect of cyclo(L-Trp-D-Pro) on HT-29, MCF-7 and HeLa growth after a 72 hr exposure period. Final concentrations of cyclo(L-Trp-D-Pro) are indicated. Values indicated are the mean \pm s.d. of quadruplicates.

After 24 hrs exposure to cyclo(D-Trp-L-Pro) at 10^{-7} M to 10^{-3} M, significantly reduced viability was noted for MCF-7 and HeLa cells ($p < 0.05$) at 10^{-3} M cyclo(L-Trp-D-Pro) (Figure 4.15). No adverse effects on HT-29 cell viability were observed.

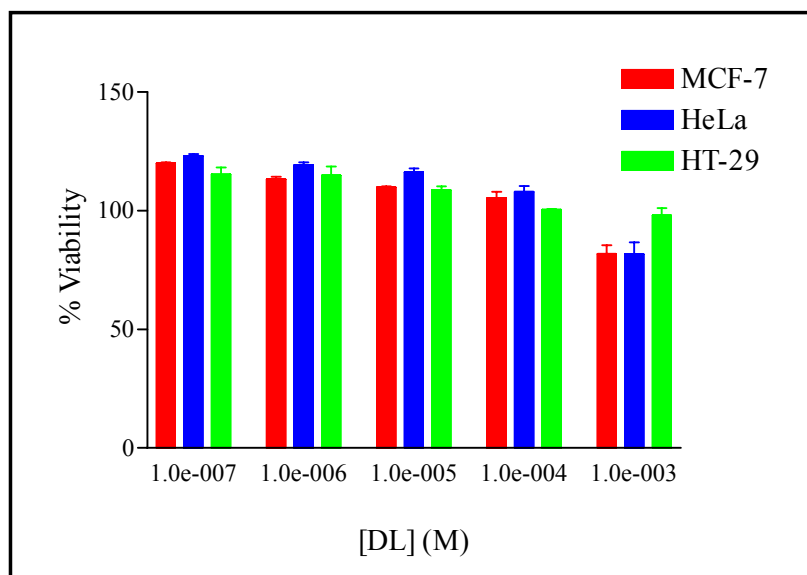


Figure 4. 15: The effect of cyclo(D-Trp-L-Pro) on HT-29, MCF-7 and HeLa growth after a 24 hr exposure period. Final concentrations of cyclo(D-Trp-L-Pro) are indicated. Values indicated are the mean \pm s.d. of quadruplicates.

When the exposure period was prolonged to 72 hrs (Figure 4.16), pronounced decreases in cell viability were noted for all the cell lines in comparison to the 24 hr effects ($p < 0.05$) in the presence of cyclo(D-Trp-L-Pro). The effects were most pronounced in the MCF-7 and HeLa cells. Viability of HeLa cells was reduced to $49.064 \pm 2.465\%$ in the presence of 10^{-3} M cyclo(D-Trp-L-Pro).

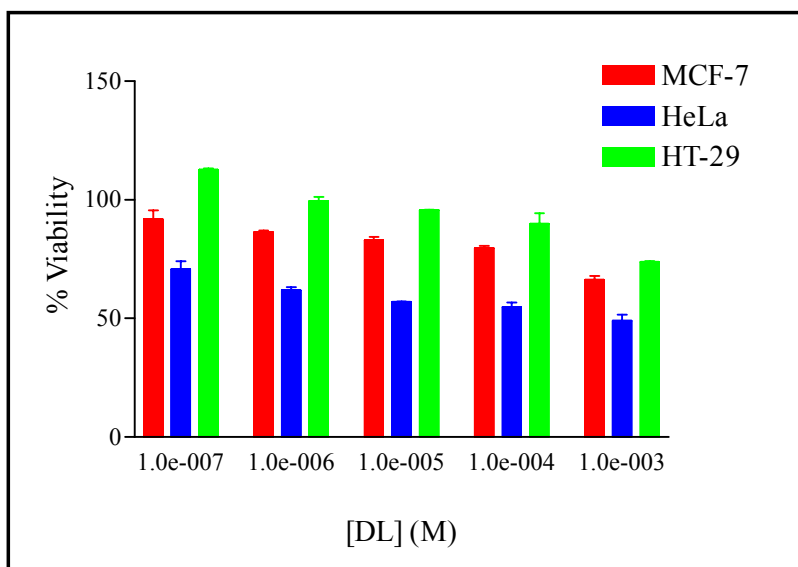


Figure 4. 16: The effect of cyclo(D-Trp-L-Pro) on HT-29, MCF-7 and HeLa growth after a 72 hr exposure period. Final concentrations of cyclo(D-Trp-L-Pro) are indicated. Values indicated are the mean \pm s.d. of quadruplicates.

No adverse effects on cell growth were noted in the presence of 10^{-7} to 10^{-5} M cyclo(D-Trp-D-Pro) after 24 hrs (Figure 4.17). At 10^{-4} M cyclo(D-Trp-D-Pro), HeLa and MCF-7 cell viability was significantly reduced in comparison to the viability of HT-29 cells ($p < 0.05$). At 10^{-3} M, no effect on HT-29 cell viability was noted. However, similar reduction in MCF-7 and HeLa cell viability was noted at this concentration ($p > 0.05$).

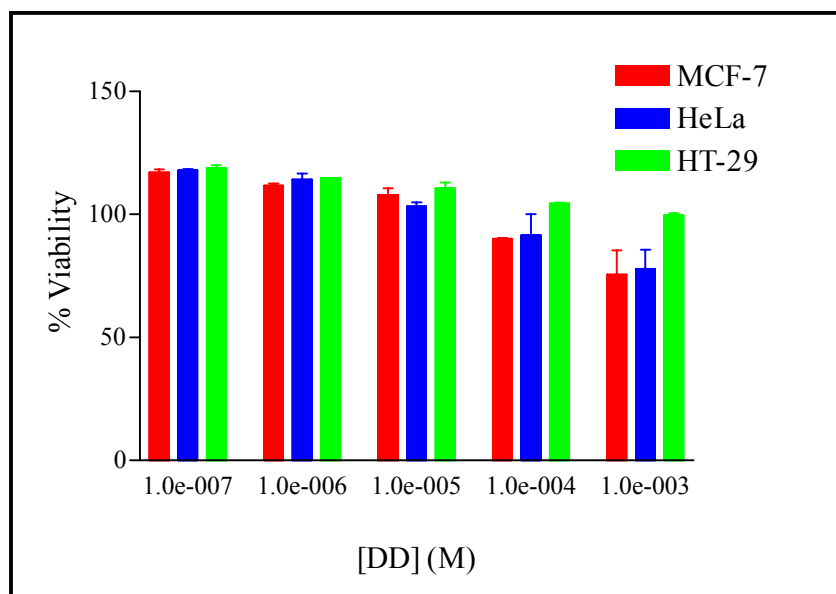


Figure 4. 17: The effect of cyclo(D-Trp-D-Pro) on HT-29, MCF-7 and HeLa growth after a 24 hr exposure period. Final concentrations of cyclo(D-Trp-D-Pro) are indicated. Values indicated are the mean \pm s.d. of quadruplicates.

Significantly reduced HT-29 cell viability was observed after 72 hrs (Figure 4.18) in the presence of 10^{-3} M cyclo(D-Trp-D-Pro) ($p < 0.05$). Similar effects on HT-29 cells growth was observed for 10^{-7} M to 10^{-4} M cyclo(D-Trp-D-Pro) at 24 and 72 hrs. Significantly lowered cell viability was observed for MCF-7 and HeLa cells in the range of 10^{-7} to 10^{-3} M cyclo(D-Trp-D-Pro). This decrease in cell viability was more pronounced for the HeLa cells. This indicates that a long exposure period is needed for drug-induced cell death to occur.

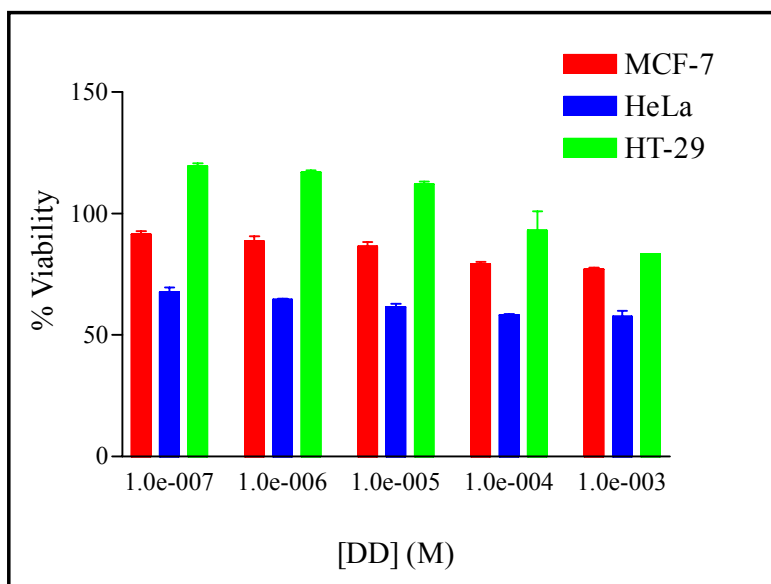


Figure 4. 18: The effect of cyclo(D-Trp-D-Pro) on HT-29, MCF-7 and HeLa growth after a 72 hr exposure period. Final concentrations of cyclo(D-Trp-D-Pro) are indicated. Values indicated are the mean \pm s.d. of quadruplicates.

As a positive control, the antineoplastic agent, melphalan (10^{-7} M to 10^{-3} M) was incubated with the cells for 24 hrs (Figure 4.19) and 72 hrs (Figure 4.20). After a 24 hr exposure period, significant reduction in cell viability ($p < 0.05$) was only observed for 10^{-3} M melphalan for all the cells tested (Figure 4.19). At 10^{-4} M and 10^{-3} M, decreased viability was also observed in the HeLa cell culture.

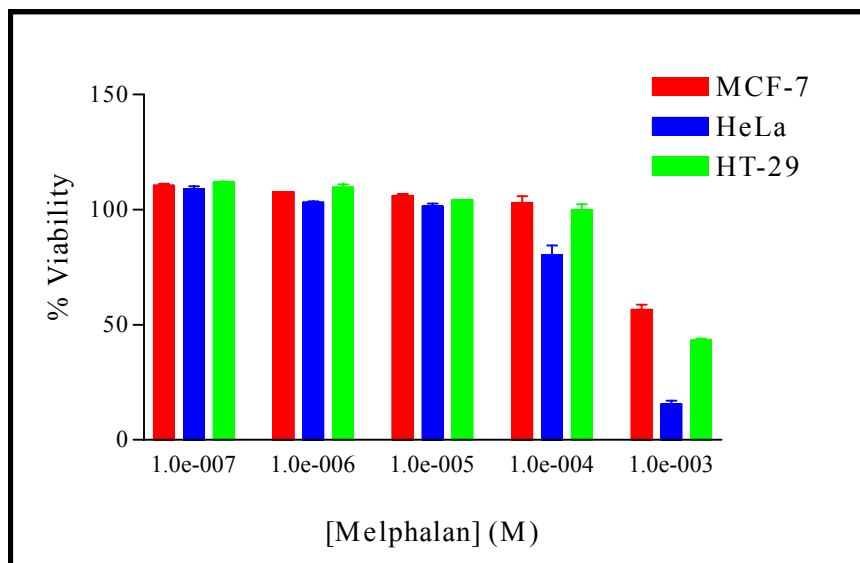


Figure 4. 19: The effect of melphalan on HT-29, MCF-7 and HeLa growth after a 24 hr exposure period. Final concentrations of melphalan are indicated. Values indicated are the mean \pm s.d. of quadruplicates.

This suggests that high concentrations of melphalan are effective over a short exposure period, where lower concentrations produced little or no antineoplastic effects.

Pronounced effects on HeLa cell viability ($p < 0.05$) was observed in the presence of 10^{-7} to 10^{-3} M melphalan after 72 hrs (Figure 4.20). Significant effects on HT-29 cell growth were also observed ($p < 0.05$). Melphalan exerted its effects on MCF-7 viability to a lesser degree than on the HT-29 and HeLa cells. 10^{-6} M Melphalan showed similar effects on HeLa and HT-29 cell viability ($p > 0.05$). Less than 50% viability remained after a 72 hr exposure of HT-29, MCF-7 and HeLa cells to 10^{-3} M melphalan.

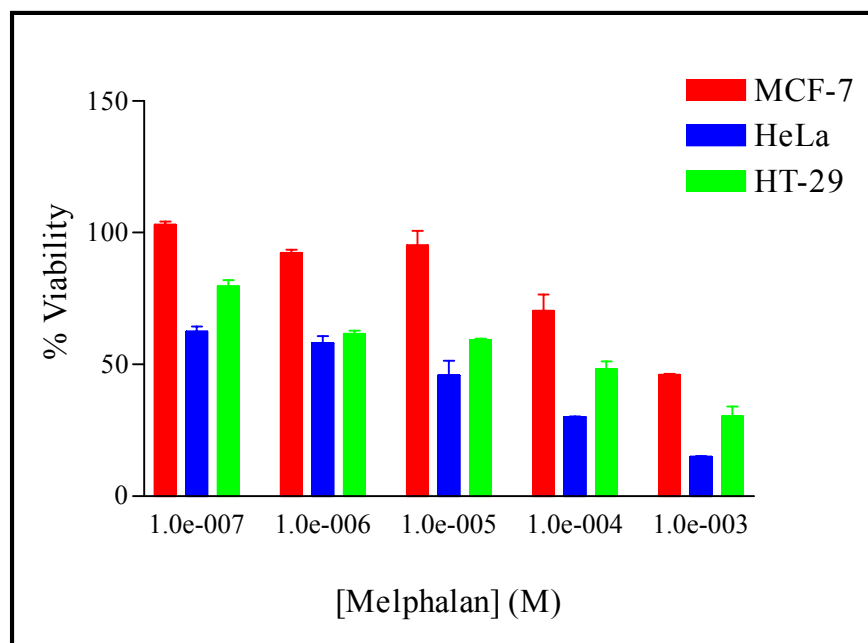


Figure 4. 20: The effect of melphalan on HT-29, MCF-7 and HeLa growth after a 72 hr exposure period. Final concentrations of melphalan are indicated. Values indicated are the mean \pm s.d. of quadruplicates.

As can be seen, no isomer showed as adverse an effect on cell viability as did 10^{-4} M to 10^{-3} M melphalan after 72 hrs. Similarities of effects of the isomers and melphalan on cell viability are shown in Table 4.1.

Table 4. 1: Concentrations of isomers producing similar effects as melphalan after a 72 hr exposure period.

Isomer (M)	Melphalan (M)	Cell line
Cyclo(L-Trp-L-Pro)		
No similarity to melphalan		HT-29
10^{-7} to 10^{-4}	10^{-7} to 10^{-5}	MCF-7
10^{-3}	10^{-7}	HeLa
Cyclo(L-Trp-D-Pro)		
10^{-3}	10^{-7}	HT-29
10^{-7} to 10^{-3}	10^{-7} to 10^{-5}	MCF-7
10^{-3}	10^{-7} to 10^{-6}	HeLa
Cyclo(D-Trp-L-Pro)		
10^{-3}	10^{-7}	HT-29
10^{-3}	10^{-4}	MCF-7
10^{-3}	10^{-5}	HeLa
Cyclo(D-Trp-D-Pro)		
10^{-3}	10^{-7}	HT-29
10^{-4} to 10^{-3}	10^{-4}	MCF-7
10^{-6} to 10^{-3}	10^{-7} to 10^{-6}	HeLa

10^{-3} M Cyclo(D-Trp-L-Pro) and cyclo(D-Trp-D-Pro) showed the greatest potential as anticancer agents against HeLa cells, as they produced the greatest decrease in cell viability in comparison to the other isomers (Figures 4.16 and 4.18) after 72 hrs.

The effects of various drugs on cell viability are now discussed. The ID_{50} value of adriamycin, melphalan, cisplatin and vinblastine on application to Chinese hamster ovary (CHO) cells were determined by Carmichael *et al.* (1987). A wild type CHO line (AuxB1) and a pleiotropic mutant line ($CH^R C5$) were used. The mutant line exhibits resistance towards colchicines. ID_{50} values were determined, where ID_{50} is defined as a 50% reduction in MTT formazan product absorbance compared to the control values. In

the wild type line, adriamycin had an ID₅₀ of 45 nM, melphalan an ID₅₀ of 28 nM, cisplatin an ID₅₀ of 1100 nM and vinblastine an ID₅₀ of 9.5 nM. Adriamycin, melphalan, cisplatin and vinblastine exhibited ID₅₀ values of 10000 nM, 300 nM, 2800 nM and 435 nM, respectively, when applied to the CH^RC5 line (Carmichael *et al.*, 1987).

The IC₅₀ value of a number of well known drugs were tested using the MTT assay against mouse 3T3 cells and human hepatocytes (Jover *et al.*, 1992). The IC₅₀ value is defined as the concentration of the drug at which a 50% inhibitory effect is noted. The results obtained are tabulated in Table 4.2.

Table 4. 2: IC₅₀ values of a number of commonly used drugs (Adapted from Jover *et al.*, 1992).

Drug tested	Mouse 3T3 cells	Human Hepatocytes
Paracetamol	13.60 mM	6.60 mM
Acetylsalicylic acid	15.00 mM	4.97 mM
Diazepam	0.26 mM	0.23 mM
Methanol	>1500 mM	819 mM

A separate study was undertaken by Arnould *et al.* (1990) to investigate the IC₅₀ values of three chemotherapeutic agents against different mouse cells using the MTT assay. Mouse melanoma cells (B16-BL6), a mouse macrophage-like cell line (P388D1) and a mouse renal carcinoma cell line (RC) were used. The IC₅₀ values of these drugs were tested after a 48 hr exposure period. The results are tabulated in Table 4.3.

Table 4. 3: IC₅₀ values of 3 chemotherapeutic agents against selected mouse cells (Adapted from Arnould *et al.*, 1990).

Drug	B16-BL6	P388D1	RC
Melphalan	216.2 μ M	28.6 μ M	11.9 μ M
Hexamethylmelamine	>2.38 mM	>2.38 mM	>2.38 mM
Daunorubicin	0.568 μ M	0.44 μ M	0.227 μ M

Alkaline phosphatase, a marker of small intestinal differentiation, is found at elevated levels in differentiated HT-29 cells (Pinto *et al.*, 1982). It is also expressed at low levels in many cell types. A decreased level in AP expression would indicate a decreased cell number due to cell death. Elevated levels in HT-29 cells would indicate the potential of the compound being tested as an inducer of differentiation. The expression of AP in the presence of 10^{-3} M isomer or melphalan was tested on the cell lines after a one and three day exposure periods.

In HT-29 cells, the levels of AP expression did not differ significantly ($p > 0.05$) from that of the control sample (Figure 4.21) after 24 hrs. This indicated that no differentiation in HT-29 cells was induced by these compounds. This also showed that the viability of the cells is similar to that of the control sample.

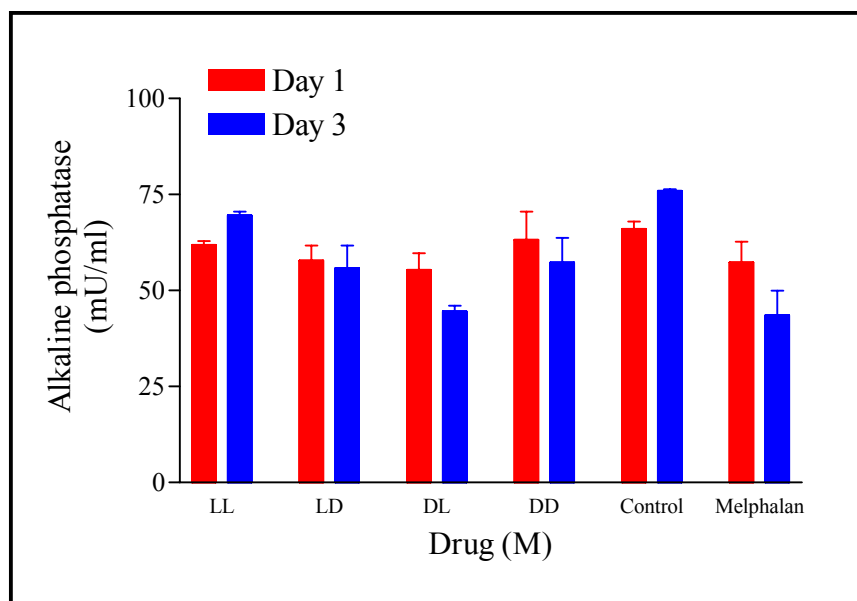


Figure 4. 21: Alkaline phosphatase activity in HT-29 cells, as a result of exposure to the isomers or melphalan at 10^{-3} M. Values indicated are the mean \pm s.d. of quadruplicates.

This reduction in the expression of AP in HT-29 cells agree with those results obtained for HT-29 cell viability in the presence of 10^{-3} M isomer or melphalan after 24 hrs. Decreased levels of AP expression are noted in melphalan-treated cells (Figure 4.21), which correlates well with the decreased viability of HT-29 cells in the presence of 10^{-3} M melphalan after 24 hrs (Figure 4.19).

After 72 hrs, decreased levels of AP expression ($p < 0.05$) are noted (Figure 4.21). This suggests that the isomers are not inducers of differentiation, as no elevation in expression is observed. The effect of the isomers on these cells after 72 hrs is thus resultant of cell death. Similarly, melphalan does not induce cell differentiation in HT-29 cells, as decreased levels of AP were noted.

Levels of AP expression in MCF-7 cells were determined in the presence of 10^{-3} M isomer or melphalan (Figure 4.22). Decreased levels were observed in the presence of cyclo(L-Trp-L-Pro) and melphalan. Cyclo(L-Trp-D-Pro), cyclo(D-Trp-L-Pro) and cyclo(D-Trp-D-Pro) did not show significant differences in the expression of AP in comparison to the control samples ($p > 0.05$) at day 1. These results are in agreement with the levels of cell viability obtained at 24 hrs (Figures 4.13, 4.15 and 4.17). Decreased

levels of AP expression in cyclo(L-Trp-L-Pro)- and melphalan-treated cells ($p < 0.05$) indicate cell death, as can be seen from the decrease in MCF-7 cell viability (Figures 4.11 and 4.19). Furthermore, no change in AP expression was observed in MCF-7 cells treated with 10^{-3} M cyclo(L-Trp-D-Pro), cyclo(D-Trp-L-Pro) and cyclo(D-Trp-D-Pro) from 24 hrs to 72 hrs ($p > 0.05$).

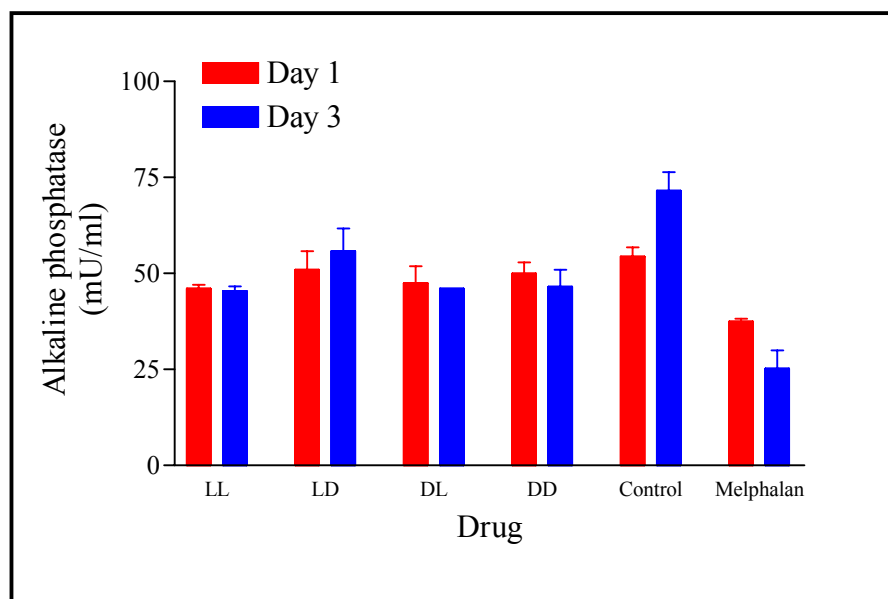


Figure 4. 22: Alkaline phosphatase activity in MCF-7 cells, as a result of exposure to the isomers or melphalan at 10^{-3} M. Values indicated are the mean \pm s.d. of quadruplicates.

After 72 hrs, decreased levels of AP expression ($p < 0.05$) were noted for all the isomer- and melphalan-treated MCF-7 cells in comparison to the control sample (Figure 4.22).

Slightly lowered levels of AP expression were observed in the presence of cyclo(L-Trp-L-Pro) with HeLa cells (Figure 4.23) in comparison to the control sample ($p > 0.05$). Significantly decreased levels of AP expression were observed for cyclo(L-Trp-D-Pro), cyclo(D-Trp-L-Pro), cyclo(D-Trp-D-Pro) and melphalan-treated cells after 24 hrs in comparison to the control. This indicates cell death in the presence of these compounds.

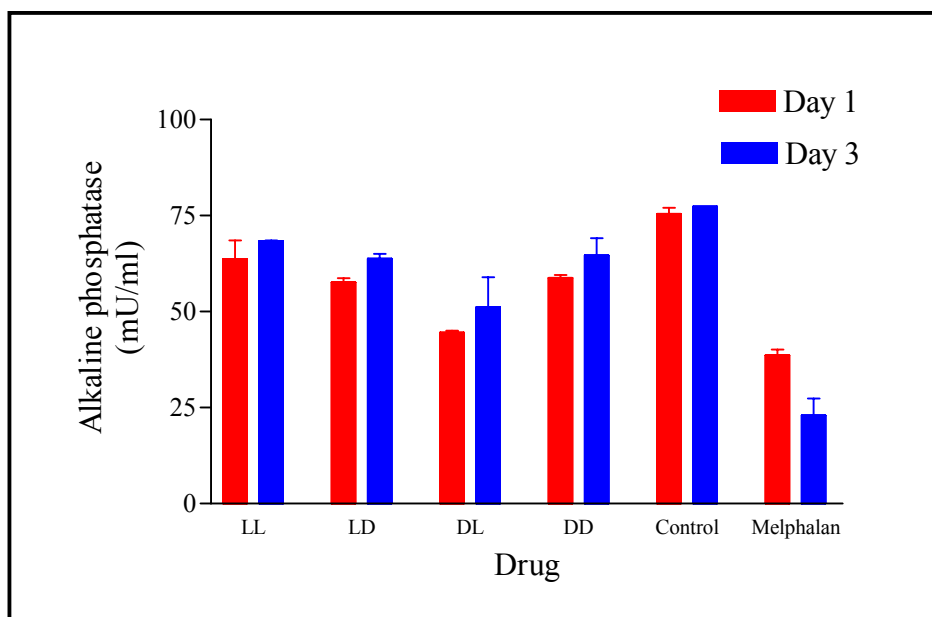


Figure 4. 23: Alkaline phosphatase activity in HeLa cells, as a result of exposure to the isomers or melphalan at 10^{-3} M. Values indicated are the mean \pm s.d. of quadruplicates.

Significantly decreased levels of AP expression ($p < 0.05$) were observed after 72 hrs in the presence of all the compounds tested (Figure 4.23). This is a result of decreased HeLa viability in the presence of these compounds after 72 hrs (Figures 4.12, 4.14, 4.16, 4.18 and 4.20).

These results suggest that MTT should be used in conjunction with different assays in order to distinguish between cell death as a result of differentiation or cell death induced by the drug via a different mechanism. This would be particularly useful in cells that can be induced to differentiate under varying culture conditions, such as the HT-29 cell line.

The effects of other cyclic dipeptides (125 $\mu\text{g/ml}$), cyclo(Trp-Trp), cyclo(Phe-Pro), cyclo(Tyr-Pro) and cyclo(L-Trp-L-Pro), on differentiation induction have been reported. It was found that only cyclo(Trp-Trp), cyclo(Phe-Pro) and cyclo(Tyr-Pro) significantly increased the expression of AP, and was thus capable of inducing differentiation in HT-29 cells. It was also noted that no significant changes in AP expression resulted after incubation with 125 $\mu\text{g/ml}$ cyclo(L-Trp-L-Pro) over a 10 day period (Milne *et al.*, 1998). This result is in agreement with results obtained in this study.

4.5 CONCLUSIONS

If 99.9% of clonogenic tumour cells can be killed by tolerable doses of an effective drug, the neoplasm will go into remission, accompanied by symptomatic improvement. However, 0.1% of tumour cells would still remain viable, including some that, due to heterogeneity, would be inherently resistant to the drugs. Other tumour cells may be harboured in pharmacological havens (eg. central nervous system) where effective drug concentrations may be difficult to attain. Host mechanisms are generally ineffective in clearing the system of a moderate number of tumour cells. To overcome this, combination chemotherapy is used, combining agents with different toxicities and mechanisms of action (Salmon and Sartorelli, 1989. Pg. 684).

For these reasons, it is clear that the only potential antitumour agents are 10^{-3} M cyclo(L-Trp-D-Pro) and cyclo(D-Trp-L-Pro) against HeLa cells over a 72 hr period. These isomers only result in <50% reduction in viability, and should thus be used in conjunction with other therapeutic agents in a combination therapy strategy. Furthermore, none of the compounds tested was capable of inducing differentiation in HT-29 cells.

CHAPTER 5

HEPATOTOXICITY

5.1 INTRODUCTION

5.1.1 The liver

Two to five percent of the body weight is contributed by the liver occupying a position that is central to the body's metabolism (Vickers, 1997). It is the largest gland in the body consisting of four lobes: right, left, caudate and quadrate. The right and left lobes are separated by a mesentery cord – the falciform ligament (Figure 5.1). On the inferior surface of the right lobe rests the gallbladder. Bile produced in the liver exits it via several bile ducts that fuse, thereby forming a hepatic duct. The common bile duct is formed by the fusion of the hepatic and cystic ducts that drain the gallbladder (Marieb, 1989. Pg. 772).

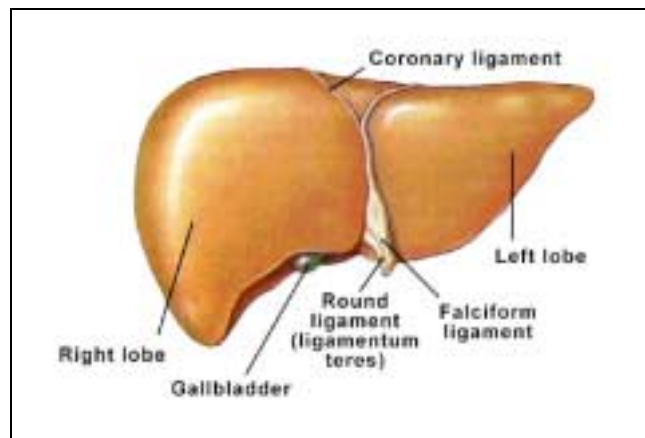


Figure 5. 1: The anterior surface of the liver, showing the right and left lobes, as well as the falciform ligament (Martini, 1995. Pg. 910).

The major cells of the liver, the hepatocytes, make up 70% of the liver cells. The remaining 30% of the cells comprises of Kupffer cells, endothelial cells, fat storage cells, pit cells and bile duct epithelial cells (Vickers, 1997). Hepatocytes, contained within a liver lobule (Figure 5.2), form a number of plates. Each plate consists of a single cell

layer. Hepatocytes, whose surfaces are exposed, are covered by microvilli. Situated between adjacent plates are sinusoids, which empty out into a central vein (Martini, 1995. Pg. 909).

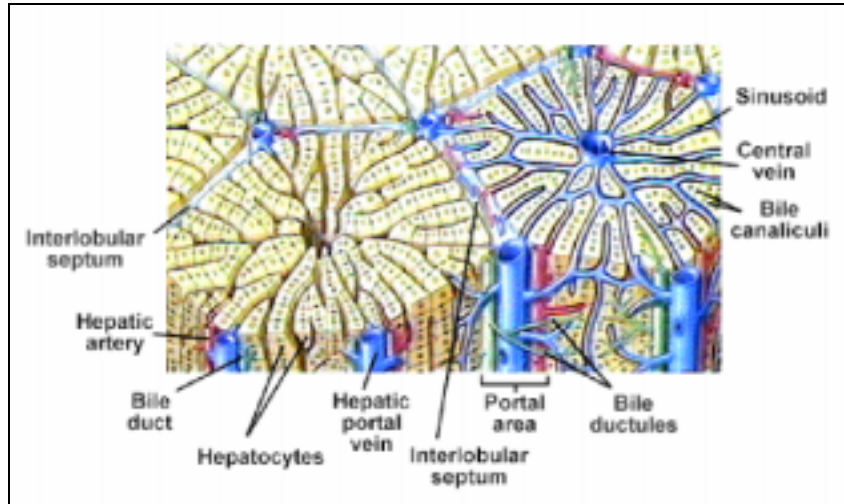


Figure 5. 2: Diagrammatic view of lobular organization (Martini, 1995. Pg. 911).

The major functions of the hepatocytes are to:

- 1) produce bile;
- 2) canvas nutrients from the passing blood;
- 3) store fat-soluble vitamins eg. Vitamins A, E, D and K; and
- 4) partake in detoxification

(Marieb, 1989. Pg. 772).

As a result, the blood exiting the liver via the hepatic veins contains less nutrients and waste material than the blood that enters the liver. About 500-1000 ml bile is produced daily by hepatocytes, a process that is enhanced by secretin and high concentrations of bile salts in the blood (Marieb, 1989. Pg. 775).

5.1.1.1 General metabolic functions

A brief summary of the metabolic functions of the liver is listed below:

- 1) It packages fatty acids into storage or transportation forms;

- 2) It forms plasma proteins, non-essential amino acids by transamination and converts ammonia to urea;
- 3) Regulates blood sugar homeostasis by storing glucose as glycogen; and
- 4) Iron released from worn-out red blood cells is salvaged and substances such as drugs and alcohol are detoxified.

Amino acids derived from dietary proteins are used to synthesize proteins in the liver. The amount of protein in serum is valuable in determining a number of diseases, including those affecting the liver. If the concentration of protein within the plasma is decreased, a disruption in the water balance occurs, resulting in, amongst others, edema. Three main groups of protein are found in plasma: albumin, fibrinogen and globulin. Serum does not, however, contain fibrinogen (Kirk *et al.*, 1975. Pg. 300).

A number of changes in protein composition (Table 5.1) are found with the various disease states.

Table 5. 1: Disease states associated with various protein compositions (Baron, 1982, Pp. 116-7).

Disease state	Albumin	α_2 -globulin	β -globulin	γ -globulin
Obstructive jaundice	NC	+	NC	NC
Acute infective hepatitis	-	+	+	+
Chronic hepatitis and cirrhosis	--	+	++	++

NC = no change; + = slight increase; - = slight decrease; -- = large decrease; ++ = large increase

Changes in plasma concentration may result from any of three changes: a) rate of synthesis; b) rate of removal; and c) in volume of distribution (Kirk *et al.*, 1975. Pg. 300).

Albumin, with a $M_r = 70\ 000$ Da, contributes 80% towards the oncotic pressure of plasma. Oncotic pressure is defined as the osmotic pressure resultant of the presence of proteins. Increases in albumin levels are associated with loss of plasma water that may result from local stasis, such as burns. A decrease in albumin levels or hypoalbuminemia

may result from decreased synthesis, associated with various liver diseases. In addition, decreases are also seen with low protein intake, inadequate digestion or absorption, increased catabolism of proteins, increased loss of protein and haemodilution. Albumin has a relatively long half-life in plasma, about 15 days (Baron, 1982, Pg. 107).

Urea, an end product of protein metabolism, is synthesized in the liver and excreted from the body via the kidneys. Decreases in blood urea concentrations, however rare the case may be, are associated with severe liver disease (Kirk *et al.*, 1975. Pg. 286).

One of the functions of the liver is to produce bile, which is stored and concentrated in the gallbladder. Bile is released into the duodenum, where it acts to emulsify dietary fat. Bilirubin is an important component of bile (Kirk *et al.*, 1975. Pg. 297). When effete red cells are removed from circulation by the reticuloendothelial system (RES), the haeme portion of the haemoglobin molecule is liberated. Once the globin and haeme are separated, the porphyrin ring is opened (Baron, 1982. Pg. 192). The RES consists of cells found in the spleen, liver, lymphoid tissue and bone marrow (Kirk *et al.*, 1975. Pg. 297). Bilirubin is derived mainly from the tetrapyrrole ring of the haeme portion, while the iron portion is reused. Other sources include myoglobin and cytochromes. Lipid-soluble, unconjugated bilirubin is bound to albumin, and transported in the bloodstream. Once it reaches the liver, the unconjugated bilirubin is taken up, minus the albumin, via carrier proteins. Once the bilirubin is transported to the RES, it undergoes conjugation, primarily with glucuronic acid, forming a diglucuronide, a reaction catalysed by bilirubin-uridyl diphosphate glucuronyl transferase (Marshall, 1997. Pp. 72-4).

Conjugated bilirubin, which is water-soluble, is transported to the small intestines via the biliary ducts, where it is deconjugated. Once in the small intestines, bilirubin is converted into colourless urobilinogen by bacterial action. Two fates of urobilinogen exist: firstly, most may be absorbed into the portal blood or is excreted in urine. Secondly, it may be oxidized in the gut, forming urobilin, the brown pigment excreted in feces (Marshall, 1997. Pp. 72-4).

If any abnormalities occur at the hepatocellular level, it may result in defective bilirubin transport into the cell, defective conjugation or defective excretion into bile canaliculi (Baron, 1982. Pg. 193).

Hepatogenous jaundice is directly related to liver parenchymal damage, resulting in decreased bile excretion. Concomitantly, blood levels of bilirubin will increase. Obstructive jaundice is caused by a blocked biliary tract, which inhibits the proper flow of bile. This results in bile flowing into the bloodstream (Bauer *et al.*, 1974. Pg. 435).

5.1.2 Liver injury-hepatotoxicity

The safety evaluation of novel compounds of potential medical applicability must undergo a number of tests using animal models to determine its general toxicity and mutagenicity (Castell *et al.*, 1985).

Injury to the liver can be evaluated through the determination of a number of parameters of the cell, including synthesis and secretion of albumin, synthesis of cholesterol, transportation of bilirubin, ureogenesis, glutathione levels, adenosine-5'-triphosphate (ATP) levels, concentration of Ca^{2+} , membrane leakage of cytosolic enzymes such as lactate dehydrogenase, protein synthesis and morphological changes (Vickers, 1997).

In the detection of liver disease, the most commonly assayed enzymes are aspartate transaminase (AST) and alanine transaminase (ALT). In acute liver disease, higher values of ALT are found in plasma as compared to AST. A continuing rise in the plasma transaminase concentration may be detected as a result of hypersensitivity hepatocellular damage as a result of drugs (Baron, 1982. Pg. 198).

Increased AST levels may result from a number of causes. If levels are increased by greater than 10 times the upper limit of normal (ULN), this may indicate severe tissue damage, including acute hepatitis and liver necrosis. Accompanying any change in the concentration of AST, ALT levels also increase, but to a lesser degree. However, in hepatitis, ALT levels may surpass AST levels. Measurement of AST levels is however

the preferred enzyme, as it is used primarily in the management of liver disease. Here, a raised level indicates hepatocellular damage (Marshall, 1997. Pp. 231-2).

If levels of AST are increased 5-10 times the ULN range, it may indicate chronic hepatitis, and other liver diseases if levels are below 5 times the ULN range (Marshall, 1997. Pp. 231-2).

Alkaline phosphatase is found in high concentrations in the liver, osteoblasts, placenta and the intestinal epithelium. In the case of liver cholestasis, alkaline phosphatase synthesis is stimulated in a type of enzyme-induction mechanism. The cholestasis induces excess enzyme synthesis stimulation in the cells of the liver lining the bile canaliculi, to greater than 5 times the ULN (Marshall, 1997. Pp. 230-1).

Raised alkaline phosphatase levels and plasma bilirubin are seen with primary or metastatic malignant deposits in the liver, as well as cirrhosis of the liver, even in the absence of obstruction. Increased levels are also an early indication of cholestatic liver damage resultant of certain drugs such as chlorpromazine (Baron, 1982. Pg. 197).

Lactate dehydrogenase (LDH) is found widely distributed in the tissues, with high activities being found in the liver, kidneys, skeletal and cardiac muscle (Baron, 1982. Pg. 120). In body tissues, LDH exists as a tetramer consisting of two monomers, H and M. These monomers combine in varying proportions to give rise to 5 isoenzymes (LD1-5). Increases in total LDH concentration is seen in various conditions such as acute liver damage and haemolytic anemias (Marshall, 1997. Pg. 232). In hepatitis, the total LDH content increase is due mainly to LD-5 increases (Baron, 1982. Pg. 105).

A complex sequence of events resulting in cell death can be induced by chemicals and other noxious stimuli. This type of cell damage can lead to necrosis- a process resulting from the failure of endogenous systems to compensate – or the initiation of apoptosis or programmed cell death (Boobis *et al.*, 1989).

One of the first morphological changes occurring on exposure of hepatocytes to a wide variety of toxins, is blebs. Blebs are protrusions at the surface of the plasma membrane. Initially, blebbing is reversible, eventually becoming irreversible. Once large membrane blebs rupture, cellular contents are lost, resulting in cell death (Boobis *et al.*, 1989).

Examples of hepatotoxicity mechanisms include:

- Metabolic activation (free radical) and covalent binding;
- Metabolic activation, reduced glutathione, and covalent binding;
- Metabolic activation, polypeptide antigen formation;
- Disruption of Ca^{2+} -homeostasis;
- Disruption of tissue repair mechanisms;
- Inhibition of transport;
- Inhibition of cellular energy; and
- Loss of cell volume homeostasis

(Vickers, 1997).

Liver injury can take on one of three forms: 1) hepatocellular necrosis; 2) cholestatic disease and 3) disease of mixed pattern. Lethal injury to hepatocytes may result from cellular function impairment, while bile secretory dysfunction may lead to cholestasis (Aw, 1986).

Acute hepatocellular necrosis is characterised by elevated serum transaminase levels. This is caused by the release of the enzymes from dying cells. Clinically, this type of necrosis resembles viral or ischaemic disease. Cholestasis results from the alteration in the ability of the liver to secrete bile. Changes in the chemical and physical properties of the hepatocytes membrane may effect this disease state. Any drug-induced liver disease that cannot be classified as either acute hepatitis or cholestasis pattern is termed as a mixed pattern disease (Aw, 1986).

5.1.3 Drug-induced hepatic injury

Drug-induced hepatic injury has been noted with the administration of drugs such as phenytoin, chlorpromazine, halothane and tienilic acid (Castell *et al.*, 1997).

5.1.3.1 Idiosyncratic and intrinsic toxicity

Hepatotoxins are defined as substances that specifically produce hepatocyte damage. Intrinsic hepatotoxins exert their effects in a predictable manner in all individuals. Idiosyncratic hepatotoxins exert their effects in certain individuals only, often in an unpredictable way (Castell *et al.*, 1997). This may be due to genetic differences in the pathways of either drug toxification or detoxification. Toxicity risks may also be increased by environmental conditions and exposure to other drugs that induce certain enzymes (Aw, 1986).

Intrinsic toxins can be either active or latent. If the toxins act directly on the cells, it is active. On the other hand, a toxin may become toxic after hepatocyte biotransformation - these are referred to as latent hepatotoxins. Idiosyncratic hepatotoxicity results from either unusual drug metabolism (metabolic idiosyncrasy) or an immune-mediated response (sensitization) (Castell *et al.*, 1997).

The damages induced in the hepatocytes are divided into three groups: cytotoxic, genotoxic or metabolic. Cytotoxic injury, a common feature of intrinsic hepatotoxins, is characterised by morphological changes in the hepatocytes in combination with increased serum levels of hepatic enzymes. DNA damage is produced by genotoxins, which show potential as tumour promoters. Metabolic damage results from altered cellular metabolism without causing the death of the cell (Castell *et al.*, 1997).

5.1.3.2 Cell toxicity as a consequence of drug bioactivation

The liver metabolizes foreign compounds, xenobiotics, mostly via redox reactions that are catalysed by cytochrome P450-dependent mono-oxygenases. One atom of the molecular oxygen is oxidized, while the cytochrome P450 reductase electron reduces the other atom. In this way, new metabolites are formed that are then conjugated with

endogenous molecules (such as glutathione), forming derivatives that are more water soluble and usually less toxic. In some cases, however, this biotransformation of the xenobiotic produces a derivative that is far more toxic and reactive than the parent compound. Defence against such derivatives takes the form of enzymes, reduced glutathione, and DNA and protein repair mechanisms (Castell *et al.*, 1997).

5.1.4 Drug-induced cell death: necrosis and apoptosis

Necrosis is a pathological and accidental death of the cell, while apoptosis is a physiological process referred to as programmed cell death. Apoptosis is said to be gene-directed. Necrosis is characterised by rapid disruptions of the internal homeostasis of the cell, characterised by cellular content release. In addition, DNA is fragmented by the action of lysosomal enzymes (Vickers, 1997). A mechanism distinct from necrosis is apoptosis, a process requiring active RNA and protein synthesis. It is characterised by DNA fragmentation and cell shrinkage that leads to loss of membrane contact with adjacent cells and formation of apoptotic bodies. DNA fragmentation is caused by the activation of non-lysosomal enzymes (Vickers, 1997). The extent of apoptosis appears to be dependent on the concentration of the toxic agent. While moderate concentrations may induce apoptosis, higher concentrations may cause cell necrosis. This scenario may not always be the case in the liver (Castell *et al.*, 1997).

5.1.5 Molecular mechanisms of toxicity

5.1.5.1 Impairment of cellular metabolism

The energetic balance of the cells may be indirectly altered by many hepatotoxins by increasing the energy demand, reducing ATP production, or both. A common event in cellular damage is the depletion of ATP. Increased energy demand may take the form of the *de novo* synthesis of glutathione (GSH). Oxidised GSH (GSSG) is normally reused after it is reduced by GSH reductase, a reaction that is dependent on the reduced form of nicotinamide adenine dinucleotide phosphate (NADPH). Intracellular levels of GSSG cannot however, drop below a certain threshold level (Ross, 1989). If this does occur, GSH disulfide is expelled from the cell, thereby decreasing the GSH pool, thus creating an important ATP demand (Castell *et al.*, 1997).

Alternatively, hepatocyte ATP production may be altered by the xenobiotic or its metabolites. Energy is derived from β -oxidation of lipids, amino acid oxidation and glycolysis of hexose monophosphates. ATP is largely produced from acetyl CoA via the Krebs cycle and oxidative phosphorylation of NADPH in mitochondria. Any substance that interferes with these processes may result in decreased ATP production. All cellular anabolic processes are thus disrupted, as well as hepatocyte functions (gluconeogenesis, ureogenesis, bile acid transport). To counter this imbalance, glycolysis is increased, resulting in lactic acid overproduction (Castell *et al.*, 1997).

During hypoxia and cyanide toxicity, lethal cell injury in isolated liver and rat cells is prevented by the glycolytic substrate fructose. Fructose preserves cellular ATP levels by glycolysis. This is in preference to the preservation of mitochondrial membrane potential, which also decreases. Thus, it was determined that any mechanism that decreases the amount of cellular ATP formation would have a pivotal role in the progression of irreversible cell injury (Nieminen *et al.*, 1994).

An important target of hepatotoxins is the mitochondria. Mechanisms involved in mitochondrial injury include: (a) direct inhibition of the metabolism of mitochondria, (b) alteration of the mitochondrial membrane resultant of oxidative damage, (c) diminished membrane potential, and (d) mitochondrial DNA damage (Castell *et al.*, 1997). Cytotoxic compounds such as carbon tetrachloride, menadione and benzoquinones result in the oxidation of mitochondrial NADPH, as well as the depletion of ATP. This in turn causes the release of mitochondrial Ca^{2+} (Boobis *et al.*, 1989).

5.1.6 Drug-induced lipid peroxidation

Lipid peroxidation, a free radical-mediated process, results in oxidative degradation of the component lipids found in the cell membranes. Several cardiovascular, pulmonary and hepatic diseases are affected by peroxidised lipids present in animal tissues (Uchiyama and Mihara, 1978). A complex process, lipid peroxidation involves the reaction between unsaturated lipid material and molecular oxygen, generating lipid hydroperoxides (Porter, 1984). In this reaction, a peroxy radical abstracts hydrogen from

the lipid and molecular oxygen is added to this carbon radical. The hydroperoxides in turn are degraded to a number of products including alkanals, alkenals and ketones. Substances may become metabolically activated within cells to produce toxic free radical intermediates that induces lipid peroxidation, resulting in cell injury by disorganisation of membrane structure and membrane function disruption (Slater, 1984). In addition, enzyme inhibition, release of lysosomal enzymes and protein-protein cross-linking may result (Smith *et al.*, 1982). Lipid peroxidation levels may also increase due to the depletion of normal cellular protective mechanisms (eg. GSH).

5.1.6.1 Drug-derived radicals and active oxygen species

Lipophilic drugs are converted into more polar, aqueous soluble forms in the liver, so that they can be eliminated in the bile or urine. This may be achieved by cytochrome P450 or conjugation reactions. The action of cytochrome P450 results in reactive, toxic metabolites including electrophiles and free radicals as end-products (Aw, 1986).

Electrophiles thus produced covalently bind to nucleophilic sites, the principal one being the thiol group of cysteine, which is found in abundance in GSH. Thus, the detoxification action of GSH is to bind these toxins. If the toxin levels exceed the glutathione levels, toxicity may result (Aw, 1986).

Drug radicals produced by cytochrome P450 metabolism initiate lipid peroxidation. Protection from lipid peroxidation includes inactivation of the active oxygen species, trapping of radicals (superoxide dismutase, catalase, GSH peroxidase and reduced GSH), inhibition of radical chain propagation (Vitamin E) and repair of damaged lipids (Castell *et al.*, 1997).

5.1.7 Drug-induced oxidative stress

Biomolecule oxidation plays an integral role in the development of disease such as cancer and cardiovascular disorders. Nutritional imbalances, irradiation, injury or existing disease states may produce or aggravate existing oxidative stress. Counteracting this, a number of physiological antioxidant defences are offered by enzymes and molecules

capable of breaking chains eg. ascorbic acid, α -tocopherol and GSH. If the amount of reactive oxygen species outweighs the defence mechanisms, synthetic or natural antioxidants (such as guaiiazulene) may be administered (Kourounakis *et al.*, 1997).

Oxidative stress has been defined as a disturbance in the balance between pro-oxidant and antioxidant of the cell. This results when there is an increased production of active oxygen species with concurrent loss of GSH, placing the cell in a state of favoured oxidative damage, immediately resulting in increased lipid peroxidation (Castell *et al.*, 1997).

5.1.7.1 Drug redox cycling as a cause of oxidative stress

Substances capable of undergoing repeated oxidation and reduction cycles within a cell are responsible for eliciting oxidative stress. Examples of such compounds include quinones, chatecols, pyridinium derivatives, aromatic nitro and nitroso compounds (Castell *et al.*, 1997).

5.1.7.2 Glutathione and oxidative stress

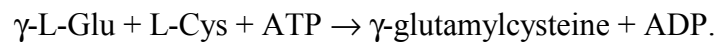
Glutathione is widely distributed in the cytosol. It exists in both a reduced (sulfhydryl) form (GSH) and as GSSG. It is however maintained *in vivo* primarily as the reduced form by glutathione reductase (Tietze, 1969).

In most mammalian cells, glutathione concentration is very high (> 4 mM), with 98% being present in the reduced form (Boobis *et al.*, 1989). The rest is present as the oxidized form, mixed disulfides (GSS proteins) and as thioethers (Deleve and Kaplowitz, 1990).

The three amino acids making up the tripeptide (L-gamma-glutamyl-L-cysteinyl-glycine) dictates the metabolism and functioning of GSH. Firstly, the γ -carbonyl group of glutamate is used to link the N-terminal glutamyl and cysteinyl moieties, as opposed to the more common α -carbonyl peptide linkage. This γ bond is resistant to all peptidases except γ -glutamyltranspeptidase, which is only found on the external surface of certain cell membranes. This γ -linkage thus confers the intracellular stability of GSH. Protection

against cleavage by intracellular γ -glutamylcystotransferase is provided by the C-terminal glycine. The reactive thiol group is provided by the cysteinyl moiety and is primarily responsible for the many functions of GSH. These include: detoxification of both exogenous and endogenous compounds; maintenance of the thiol status of proteins and other molecules by reducing disulfide linkages; storage and transport form of cysteine; and plays key roles in leukotriene and prostaglandin metabolism and reduction of ribonucleotides (Deleve and Kaplowitz, 1990).

Synthesis of the tripeptide requires two molecules of ATP per mole of GSH and occurs in the cytosol in a two-step reaction. The first step is the rate-limiting step. Cysteine and γ -glutamate are linked via an amide bond. This reaction is catalysed by γ -glutamylcysteine synthetase.



This reaction is under non-allosteric competitive inhibition by GSH.

The second step is catalysed by GSH synthetase:



Since GSH synthesis is ATP-dependent, any condition that decreases the ATP concentration may result in the depletion of GSH levels. This would impair antioxidant defence mechanisms of the cell (Deleve and Kaplowitz, 1990).

GSH, a nucleophile, protects the cells against electrophilic damage by reducing phenol and amine-derived radicals back to the original compounds. It also serves as a cofactor for GSH peroxidase, the enzyme responsible for the removal of hydroperoxides produced during oxidative processes (Ross, 1989). Levels of GSH may decrease for the following reasons: (a) oxidation of GSH to GSSG, (b) formation of conjugates with metabolites or endogenous proteins and (c) a reduction in the *de novo* synthesis.

GSSG is the toxic form of GSH. If it accumulates in the cell, it is exported and lost from the cell. Formation of conjugates ensures that other tissues, including the kidney, recover glutamate and glycine. Mercapturic acid derivatives thus formed are excreted via the urine. In this manner, GSH is irreversibly lost and can only be replenished by *ex novo*

synthesis. This depletion may result in modification of the sulfhydryl groups of target proteins, producing S-thiolation (Castell *et al.*, 1997).

5.1.8 Calcium- and drug-induced cell injury

Ca^{2+} plays an integral role in signal transduction as a second messenger. It regulates many enzymes and acts as an effector for hormones and growth factors, controlling a broad range of physiological processes. It accumulates in dying cells, and is thus involved in many pathological and toxicological processes (Orrenius *et al.*, 1989). Intracellular Ca^{2+} -levels are approximately 1000 times lower than in the extracellular fluids (Castell *et al.*, 1997). Influx of Ca^{2+} occurs passively due to the electrochemical gradient that exists between the extra- and intercellular milieus. This passive influx is countered by active efflux of Ca^{2+} or a Na^+ - Ca^{2+} exchange in excitable tissues (Orrenius *et al.*, 1989). The major inlets of extracellular Ca^{2+} into the cell are via voltage-gated channels and receptor-operated channels. Ca^{2+} -homeostasis is maintained by Ca^{2+} -extrusion via an outward-directed membrane Ca^{2+} -ATPase. In addition, Ca^{2+} -sequestration into intracellular stores such as the mitochondria and endoplasmic reticulum, also plays a role in maintaining a balance (Castell *et al.*, 1997). Ca^{2+} is also sequestered by binding to intracellular proteins such as calmodulin (Orrenius *et al.*, 1989).

The major reservoirs of Ca^{2+} in the hepatocytes are the mitochondria and the endoplasmic reticulum, both of which are involved in xenobiotic-induced cytotoxicity. An increase in intracellular Ca^{2+} in isolated hepatocytes causes a rapid depletion of mitochondrial GSH, possibly due to mitochondrial Ca^{2+} -cycling. This suggests that any change in Ca^{2+} -homeostasis may induce oxidative stress (Chacon and Acosta, 1991). The mechanisms involving cell killing are shown in Figure 5.3 (Orrenius *et al.*, 1989).

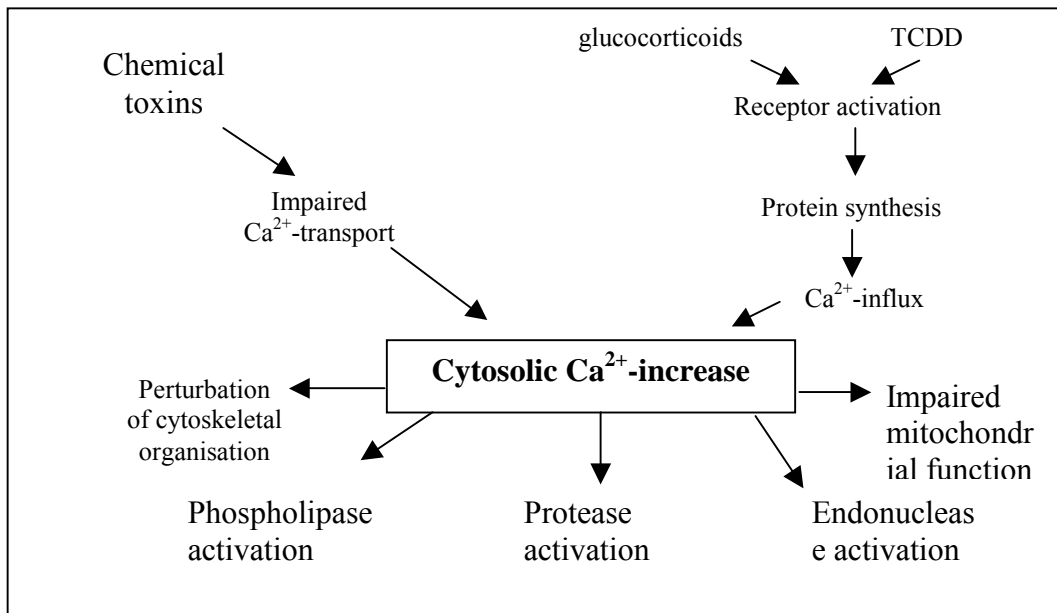


Figure 5. 3: Mechanisms involved in Ca^{2+} -mediated cell killing (Adapted from Orrenius *et al.*, 1989). TCDD = 2,3,7,8-tetrachlorodibenzo-*p*-dioxin.

Toxins may increase the external influx of Ca^{2+} or release from intracellular stores, impair the uptake of Ca^{2+} by organelles or its extrusion into the external environment. Catalytic mechanisms of many enzymes, including the Ca^{2+} -ATPases, rely on free SH groups. Thus, any disruption in intracellular GSH and resultant thiolation or oxidation of SH groups lead to alterations in Ca^{2+} -homeostasis. Accompanying this disruption is lipid peroxidation of mitochondria that results in Ca^{2+} -release. In summary, three factors are responsible for the increase in Ca^{2+} -concentration: (i) reduction of GSH and modification of proteins; (ii) an increased demand for NADPH; and (iii) a decrease in the production of ATP (Castell *et al.*, 1997).

The toxic action of xenobiotics may cause a sustained rise in cytosolic levels of Ca^{2+} . Resultant of such a rise is plasma membrane blebbing. This is as a direct consequence of disruption of the cytoskeletal organisation and/or cleavage of proteins regulated by intracellular Ca^{2+} or Ca^{2+} -dependent proteases (Castell *et al.*, 1997).

Increased Ca^{2+} -levels may also activate phospholipases and non-lysosomal proteases, which cause irreparable damage and functional injury to the components of the cell (Castell *et al.*, 1997).

GSH concentration, Ca^{2+} -levels, ATP content and lipid peroxidation are interdependent biochemical parameters that become altered prior to cell death. The time course of each parameter may however differ, depending on the type of toxic mechanism involved.

5.1.9 Covalent binding

Stable drug adducts may form when chemical intermediates react with cell macromolecules, such as DNA, RNA and proteins. In this context, covalent binding refers to the irreversible binding between drug and macromolecule. The most common target is protein, such as carboxyl esterases and GSH transferases. If a compound were to bind to regulatory proteins and enzymes, cellular function would be disrupted, leading to cell death. The incidence and severity of hepatotoxicity is directly linked to the presence of covalent binding to protein (Hinson *et al.*, 1994).

5.1.9.1 Mechanisms of drug-protein adduct formation

The mechanisms of bioactivation of the drug largely govern the extent of drug binding. Glucuronides, a group of reactive molecules, covalently bind macromolecules. A drug that contains a free carboxyl group may conjugate with glucuronic acid, producing acyl glucuronides that are unstable towards other hydroxyl and amino groups (Castell *et al.*, 1997).

5.1.9.2 Covalent binding and hepatotoxicity

In most cases, covalent binding is usually necessary for triggering an immune response. Binding is dependent on the amount of reactive intermediate formed, its half-life as well as its reactivity with cell macromolecules (Castell *et al.*, 1997).

5.1.10 Immunological mechanisms of drug hepatotoxicity

Unless bound to a macromolecule (hapten), drugs are unable to illicit an immune response. The binding of drug to macromolecule is thus an important step of the mechanism, but it cannot trigger the immune response as such. The subsequent step is thus accessibility of the neoantigen to the immune response. This process may occur as either (a) the adduct would be transported to the cell membrane, thereby exposing it to the external surface, or (b) the metabolite would react with molecules that are transported to the membrane (Castell *et al.*, 1997).

5.1.11 Screening for potential hepatotoxicity for new drugs

Novel drugs are examined for hepatotoxic effects as part of routine tests to which compounds are normally subjected.

The first step in determining the effects of the drug on the biological system is to determine whether the drug is hepatocyte-specific. Concentration-toxicity curves should be assessed in primary cultured hepatocytes, in non-hepatic cells and in non-metabolising hepatocytes. This would give an indication as to whether the drug is toxic preferentially on hepatocytes, or whether bioactivation of the drug is necessary to cause cellular damage. The effects of the drug on hepatocyte-specific functions such as ureogenesis, plasma protein synthesis and gluconeogenesis, should be assessed to determine whether these functions are altered in the presence of the drug. Of particular interest is the decrease in plasma protein synthesis, which is one of the earliest and most sensitive signs of cellular hepatocyte damage (Castell *et al.*, 1997).

Parameters measured often give an indication of the damage induced, eg. LDH leakage from the cell indicates cell membrane damage and ATP-mediated uptake of neutral red for lysosomal damage. Metabolic parameters measured render information on the ability of the cells to carry out its normal functions, such as lactate production or lipid metabolism. For all intents and purposes, measuring the end product of a metabolic process will give an indication as to the potential effects of the drug on the hepatocyte function (Castell *et al.*, 1997).

Early cell membrane alterations can be detected by measuring the culture medium concentrations of enzymes that, under normal circumstances, are found in the cytoplasm, such as LDH. Enzyme measurements of mitochondrial enzymes eg. AST and ALT, indicate the extent of the damage as well as the organelle involved in the injury. Included in this aspect is the MTT assay, which measures the survival of the cells in the presence of the drug. Less often, parameters measured include cell extension, monolayer formation and cell survival. The main goal of measuring cytotoxicity is to determine the maximal non-toxic concentration of the drug (Castell *et al.*, 1997).

The potential toxicity of the drug can be measured by determining the effects of the drug on metabolic parameters including gluconeogenesis, ureogenesis, plasma protein synthesis and glycogen metabolism.

5.2. OBJECTIVES OF THE CHAPTER

5.2.1 Objectives of the present chapter

- ◆ The primary aim was to determine whether cyclo(L-Trp-L-Pro), cyclo(L-Trp-D-Pro), cyclo(D-Trp-L-Pro) and cyclo(D-Trp-D-Pro) have any hepatotoxic effects;
- ◆ to determine the bioavailability of the isomers;
- ◆ to determine the rate of blood absorption of cyclo(L-Trp-L-Pro) and cyclo(L-Trp-D-Pro) only (to reduce the number of rats needed for the experiment);
- ◆ to determine whether any hepatotoxic effects are hepatocyte-specific or not; and
- ◆ to determine the metabolic/physiological functions affected by the presence of the isomers in the rat.

In order to satisfy these objectives, the following experimental data was collected:

- albumin-binding of the isomers was determined by equilibrium dialysis;
- *in vitro* blood absorption of cyclo(L-Trp-L-Pro) and cyclo(L-Trp-D-Pro) were determined by measuring the amount of isomer present in the bloodstream at various time intervals;
- the effect on cell viability was tested on cultured, isolated rat hepatocytes, the Chang liver cell line (a hepatoma) and a neuronal cell line, the N-2-alpha cells;
- metabolic and physiological functioning of the liver was assessed by using various biochemical assays in order to determine serum levels of LDH, alkaline phosphatase, AST, ALT, ATP, Ca²⁺, GSH, urea nitrogen, albumin and bilirubin. The amount of lipid peroxidation was assessed on liver samples.

5.3 MATERIALS AND METHODS

The use of rats for this study was approved by the Animal Ethics Committee, University of Port Elizabeth. The rats were housed in a well-ventilated room and were fed *ad lib*.

In vivo and *in vitro* methods have been used to study the specificity of hepatotoxins. The integrity of the liver and its natural biochemical and physiological environment is maintained in *in vivo* examination. A large number of experimental animals are needed and for this reason is limited by various ethical and economic constraints. *In vivo* screening systems are thus looked at as an alternative form of investigation. Mechanistic studies at cellular levels are permitted with *in vitro* studies using isolated rat hepatocytes. A major disadvantage, however, is that the anatomical basis of the functional heterogeneity of the liver is lost. Collagenase, used in the isolation procedure, causes cellular damage, loss of stratification and identity (Bhattacharya *et al.*, 1996).

A primary function of the liver is the metabolism of xenobiotics. In assessing the toxicological potential of new drugs or environmental studies, the assessment of hepatotoxicity by both *in vivo* and *in vitro* methods plays a major role (Bhattacharya *et al.*, 1996).

5.3.1 *In vitro* examination of hepatotoxicity

Binding of drug to plasma protein differs from one drug to another. Pharmacological effects are thus related to the concentration of free drug available (Hudson and Walker, 1990). The bioavailable dose is the amount of unchanged drug of the administered dose and thus, the amount of intact drug that reaches the systemic circulation and the rate at which this occurs is defined as the bioavailability of that particular drug (Proudfoot, 1988). If drugs are not injected directly into the blood circulation, the drug must be absorbed in a sufficient quantity and rate to achieve a specific circulation concentration (Proudfoot, 1988). Albumin is the major protein in serum and is at a much lower concentration in interstitial fluid. When drugs bind to albumin, a temporary storage of the drug is formed. Binding is usually reversible, consisting of ionic interactions, van der Waals forces, hydrogen bonding and/or hydrophobic interactions (Gibaldi, 1984). Drugs

that have bound to plasma proteins cannot diffuse across capillaries because of the high molecular weights and is restricted from moving across cell membranes due to the low lipid solubility of proteins (Gibaldi, 1984). Once free drug has been metabolised and excreted, it is released. If one were to increase drug concentration or decrease albumin concentration, an increase in the free drug concentration in the circulation would result (Gennaro *et al.*, 1980).

Equilibrium dialysis is the most common method of drug-binding determination. Briefly, a protein solution is enclosed within a membrane that is permeable to small molecular species, but impermeable to the protein or protein-complex. The protein solution within the membrane is inserted into an equal volume of solution containing the small molecule, and is agitated until equilibrium is reached. Concentrations of the small molecular species on both sides of the membrane is then determined, from which the amount of binding to the protein can be calculated (Gennaro *et al.*, 1980).

5.3.1.1 Albumin-binding assay (Modified method of Taki *et al.*, 1998).

Each isomer (1 mg/ml) was dissolved in 0.5% DMSO, and brought to volume in Krebs-Henseleit bicarbonate buffer (KHBB) containing 3% BSA, constituting a final concentration of 1.761 mM (pH 7.4)⁴. Each isomer solution was dialysed against an equal volume of KHBB for 8 hrs, with shaking, at 37°C. Characteristics of the dialysis tubing (Spectrum Laboratory Products) used are as follows: flat width = 10 mm; diameter = 14.3 mm; volume/length = 0.32 ml/m; and M_r capacity = 12 000 – 14 000 Da. After the 8 hr incubation, the solution on both sides of the membrane was mixed with equal volumes of a 10% aqueous trichloroacetic acid (TCA) solution in order to precipitate free BSA out of solution. The KHBB-TCA solutions were incubated overnight at 4°C to facilitate precipitation. After incubation, the solutions were centrifuged at 3 000 rpm for 15 min and the supernatants were retained for high-performance liquid chromatography (HPLC) analysis. In a separate set of experiments, the isomers were mixed with the TCA solution to determine whether any compound was precipitated with the TCA, but no precipitation

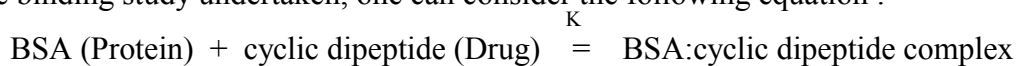
⁴ Solution list – Appendix C

occurred. It was thus concluded that only the BSA-isomer complex was precipitated out of solution, leaving only the free isomers in solution.

5.3.1.1.1 HPLC of compounds

Standard curves for each respective isomers were obtained by making a 750 μM stock solution of each isomer in 0.5% DMSO, and brought to volume in KHBB. 4 dilutions of these stocks were made to give final concentrations of 1.875 μM ; 3 μM ; 3.75 μM and 7.5 μM , respectively. Samples were analysed on a reverse-phase C-18 column (W5 C18-RS), at a flow rate of 0.7 ml/min. The wavelength used for analysis was 220 nm. The mobile phase used was made up of 94.95% MilliQ H_2O (MQ H_2O); 5% methanol and 0.05% phosphoric acid, all of HPLC grade. All solutions were degassed by means of ultrasonication for 1 hr, and filtered via a 0.45 μm syringe filter before being applied to the column. Each serum sample was analysed and the concentration of free isomer in each sample was determined using the standards curves obtained (Appendix B, Figures B 4.1-4.4).

In the binding study undertaken, one can consider the following equation :



where K = association constant. A mass law expression can be applied where

$$K = [\text{binding complex}] / ([\text{unbound protein}] \times [\text{unbound drug}])$$

For experimental simplicity, r can be defined as the average number of drug bound per mole of BSA. This was applied to the binding of caffeine to albumin, as is thus applied here, where $r = [\text{drug bound}] / [\text{albumin}]$ (Gennaro *et al.*, 1980).

5.3.1.2 Blood absorption of the drugs

When peptide drugs are administered orally, the systemic bioavailability is limited by extremely low absorption from the gastro-intestinal tract. This is as a result of the low permeation through the intestinal membrane as well as the high affinity of the drug for proteolytic enzymes. In addition, first-pass extraction by the liver is high, resulting in

lowered drug concentrations that enter the systemic circulation (Taki *et al.*, 1998). For these reasons, parenteral administration of drug, eg. the intraperitoneal route, remains the more viable route for peptide and a few other drugs (Martin, 1993).

In order for peptide and protein drugs to exert their pharmacological action, they must reach their target site without metabolic degradation. Intestinal absorption of these drugs is severely limited by the action of peptidases. Cyclo(Gly-Phe) was stably transported in any region of the small intestine, whereas linear Gly-Phe and Phe-Gly were too unstable and could not be transported. Also, cyclo(Tyr-Arg) is a more effective analgesic than the corresponding linear form. A study conducted on cyclo(Ser-Tyr), cyclo(Asp-Phe), cyclo(His-Phe) and cyclo(His-Pro) inferred that the cyclic form was stable against the peptidases as opposed to the corresponding linear forms in the intestine. In the case of cyclo(Ser-Tyr), it was found that the oligopeptide transporter played a major role in the transportation of this peptide across the intestinal wall, but played minor roles in the case of cyclo(Asp-Phe) and cyclo(His-Phe) (Mizuma *et al.*, 1998).

5.3.1.2.1 Determination of blood absorption of cyclo(L-Trp-L-Pro) and cyclo(L-Trp-D-Pro)

Male Long Evans rats, weighing between 250 g and 350 g, were injected intraperitoneally with a 7.1 mg/50 ml saline solution of the respective isomers, representing a final concentration of 500 μ M (pH 7.4). 0.5% Glycerol was used to facilitate dissolution of the isomer in saline. All solutions were filter sterilised with a 0.45 μ m filter unit (Millipore) before use. Seven groups of rats (corresponding to 10 min, 20 min, 30 min, 60 min, 2 hr, 4 hr and 24 hr) were injected simultaneously. At the respective time intervals after injection, rats were subjected to light ether anaesthesia. Blood was collected by cardiac puncture into empty vacutainer tubes and placed at 4°C to allow for clot formation. Serum was obtained by centrifugation at 3 000 rpm for 15 min. The serum was retained and equal volumes of a 10% TCA solution were added to precipitate proteins from the serum. After the overnight incubation at 4°C, the solution was centrifuged at 3 000 rpm for 15 min and the supernatant was collected. The concentrations of the isomers were

determined by HPLC as described in Section 5.3.1.1.1. Blanks consisted of rat serum collected from rats that were injected with a saline solution containing 0.5% glycerol.

5.3.1.3 Isolation of hepatocytes

Over the past decade, there has been an increase in the use of cellular models as a partial alternative to whole animal studies (Jover *et al.*, 1992). Intact cellular systems such as hepatocytes have been used as *in vitro* models in the investigation of biotransformation of a number of drugs. Supporting the use of primary cultured hepatocytes is the fact that the cells retain most specific functions, as opposed to established cell lines, such as Hep-G2, which have been manipulated to such an extent that some of the characteristics of this cell line has been lost (Jover *et al.*, 1992). The researcher is able to predict the effects of the compounds on development, as well as apparent toxicity levels for humans, mechanisms of toxicity, identification of markers in order to monitor potential side effects *in vivo*, and the determination of ways to circumvent any adverse reactions to the drug (Vickers, 1997). Freshly isolated hepatocytes have, however, shown impaired functions although they do recover these functions during primary culture. Also, decreased rates of protein synthesis, ATP concentrations and low activity for amino acid and ion transport have been noted (Tanaka *et al.*, 1978).

The most commonly used method for the isolation of hepatocytes from the rat liver is that of a two-step collagenase perfusion method, which yields the highest number of viable hepatocytes. In earlier isolation methods, enzymes including hyaluronidase, lysozyme and trypsin were used, but were ineffective as liver-dispersing agents (Seglen, 1973). Immature liver cells with few liver functions contaminated the isolated hepatocyte culture when trypsin was used as a digesting agent (Tanaka *et al.*, 1978). These isolated cells survived for at least 5 days in culture as a non-replicating, cell monolayer (Vickers, 1997). On attachment, the cells appear to flatten out, and monolayer formation occurs as a result of cell aggregation (Tanaka *et al.*, 1978).

The first perfusion buffer containing ethylene glycol-bis(β -aminoethyl ether)-N,N,N',N'-tetraacetic acid (EGTA), a Ca^{2+} -chelator, has three basic functions. It is used to clear the

liver of blood, and also acts to cleave hepatocyte desmosomes. In addition, it facilitates in the removal of Ca^{2+} -dependent adhesion factors (Seglen, 1973). Calcium is added to the second buffer containing collagenase to facilitate its action (Vickers, 1997). Hypoxic conditions introduced during enzymatic treatment do not affect the viability of the cells, and thus oxygenation of buffers was omitted to facilitate sterile preparation of the primary isolates (Seglen, 1973).

Several aspects of the isolation procedure contained potential pitfalls. The anaesthesia had to be maintained at light levels to ensure that the liver maintained a healthy light red appearance, as opposed to a dark red or purple colour, indicative of poor liver circulation. Heparin injection had to be done carefully so as not to sever the thin-walled femoral vein. Once the liver was removed, the next potential pitfall was the insertion of the cannula. This had to be done rapidly to avoid the collapse of the portal vein and any complication by bleeding, which would have resulted in poor visibility for cannulation. Also, cannulation had to be done in such a manner as not to rupture the vein. Since hepatocytes are structurally fragile, the suspension of cells was handled gently. Vigorous pipetting, shearing with the comb and foaming of the suspension were avoided (Seglen, 1994).

5.3.1.3.1 Isolation procedure

A modified method as used by Seglen (1994) was employed. All solutions were made up in MQH₂O and sterilised accordingly. All procedures were carried out with the utmost sterility. Perfusion tubing was sterilised by recirculation of 70% ethanol. Figure 5.4 illustrates a similar apparatus as used in the isolation procedure.

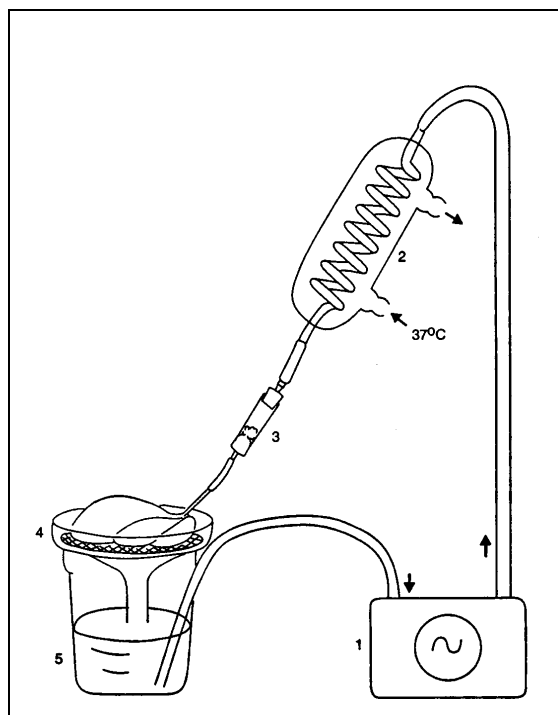


Figure 5. 4: An illustration of the perfusion apparatus. (1) perfusion pump; (2) heating unit; (3) cannula unit; (4) liver support dish (in this instance, a sterilized wire mesh covered with sterile gauze was used); (5) perfusate reservoir (in the set-up used, the perfusate reservoir consisted of a perspex block that allowed drainage of perfusate for recirculation) (Adapted from Seglen, 1994. Pg. 97).

Male Long Evans rats weighing between 250-350 g were used for hepatocyte isolation. Rats were subjected to a light ether anaesthesia to a loss of blink and pain reflexes. The abdominal cavity was opened and the liver lobes were removed without puncturing. Perfusion buffers were maintained at 37°C using a water bath (Not shown in Figure 5.4). Before cannulation, the lobes were washed gently in perfusion buffer to remove most of the blood. The portal vein was cannulated so that there was uniform blanching of the lobe. During cannulation, an EGTA-containing solution was recirculated. Once perfusion of the liver was established, the perfusion solution was changed to a second EGTA-containing solution and recirculated for 15 min using a Watson Marlow 302S perfusion pump. During this period, the liver was covered with a piece of sterile gauze soaked in perfusion buffer. After the 15 min EGTA-perfusion, the buffer solution was changed to the collagenase- and Ca^{2+} -containing perfusion buffer. This solution was recirculated for approximately 15 min, or until the lobes were soft but not mushy. The lobes were carefully removed and placed in 20 mls of perfusion buffer, after which the

liver cells were dispersed by gentle stroking of the cell mass with a sterile plastic comb. The cell suspension was filtered through gauze and divided into plastic tubes for centrifugation at 600 rpm for 1.5 min. The supernatant was removed and the cell pellet was resuspended in 10 ml perfusion buffer. The suspension was then re-centrifuged at 600 rpm for 1.5 min. The cells were resuspended in 4.5 ml culture medium, to which 5 ml Percoll (Sigma, St. Louis, U.S.A.) solution was added, followed by a 10 min centrifugation step at 600 rpm. The supernatant was removed, the pellet resuspended in 5 ml serum-containing culture medium and centrifuged once more at 600 rpm for 1.5 min. The cells were then suspended in culture medium and counted to determine both yield and viability.

5.3.1.3.2 Cell yield and viability

A 100 µl aliquot of the cell suspension was diluted with 100 µl aliquot of a 0.4% trypan blue (BDH Chemicals, Poole, England) solution. Yields between 80-95% were routinely obtained. The MTT assay was used to correlate cell number to MTT absorbance. The linear relationship that exists between cell number and formazan production for each cell type used is shown in Appendix B (Figures B 4.5-4.7).

5.3.1.3.2.1 MTT assay for cells in suspension

50 µl 0.5 % MTT solution was added to 200 µl cell suspension in an eppendorf. The cells were incubated at 37 °C for 2 hrs. After the incubation period, the cells were pelleted from solution and resuspended in 200 µl DMSO. Ethanol was not used as it causes precipitation of some serum proteins (Mosmann, 1983). After a 5 min incubation period with mild agitation, the cells were pelleted from solution. The extracted formazan product was then read against a DMSO blank at 540 nm using Labsystems Multiskan MS (Multiskan Transmit Program, Rev. 1.3. (1995)).

5.3.1.3.3 Culture medium and conditions

Hepatocytes were seeded in 96-well cell culture plates (Corningware, Cambridge, U.S.A.) at 75 000 cells per well and incubated at 37°C in an atmosphere of 95% O₂ and 5% CO₂ (Afrox, South Africa). Prior to seeding, the wells were coated with newborn calf

serum (NCS) (BioWhittaker, Walkersville) to facilitate attachment of the cells to the plate. For the first 24 hrs of incubation, serum-supplemented Hams F-12 medium (Highveld Biologicals, Lyndhurst, South Africa) was used (Jover *et al.*, 1992). This medium was replaced after 24 hrs, to a serum- and antibiotic-free Hams F-12 medium, supplemented with 10^{-8} M dexamethasone (Sigma, St. Louis) (Jover *et al.*, 1992). This hormone was added to enhance cell attachment and maintain cultures for about 1 week (Tanaka *et al.*, 1978). After the 24 hrs incubation, the cells were exposed to 200 μ M of each isomer (pH 7.4), respectively. The control solution consisted of Hams F-12 medium containing 0.5% glycerol. As a positive control, the cells were exposed to 1 mg/ml isoniazid dissolved in Hams F-12 medium containing 0.5% glycerol. Use of isoniazid may result in allergic reactions that manifest as skin rashes, fever, and hepatitis. Isoniazid has also been associated with hepatotoxicity over long periods of administration. Liver functions become impaired, jaundice may result and multilobular necrosis may occur (Jawetz, 1989). The cells were incubated in the presence of the compounds for a total of 5 days; each day the MTT assay (Section 4.3.3.2) was used to determine viability of the cells of the treated cells, as well as of the controls. Results are expressed as a percentage of the control cell viability, which was taken as 100%. In order to determine whether any effects exerted on the isolated hepatocytes were hepatocyte-specific or not, Chang Liver cells and N-2-alpha cells were also exposed to 200 μ M of each compound, made up in DMEM containing 0.5% glycerol. These cells were treated in the same manner as that of the isolated hepatocytes, with the exception that these cells were seeded at a density of 25 000 cells per well, as these cell lines undergo proliferation in culture. No coating of the wells was necessary as these cells readily adhere to the wells.

5.3.2 *In vivo* examination of hepatotoxicity

5.3.2.1 Treatment of animals

Male Long Evans rats (250 – 350g) were housed in a well-ventilated room at 24 °C, 12 hr light. Fasting and starvation may adversely affect biotransformation of oxidising agents as well as the antioxidant state of the liver, and therefore, animals were fed *ad lib.* (Tanaka *et al.*, 1978) and not fasted prior to experimentation. The rats were injected intraperitoneally with a 7.1 mg/50 ml saline solution of the respective compounds,

representing a final concentration of 500 μM . 0.05 % Glycerol was used to facilitate dissolution of the isomers in saline. All solutions were filter sterilised with a 0.45 μm filter unit (Millipore) before use. The rats were separated into 2 sets of 6 groups of rats. Rats in set 1 were injected only once and sacrificed after 24 hrs, while the rats in set 2 were subjected to injections every alternate day for a period of 5 days before being sacrificed. Group 1 of each set served as the control group, receiving normal saline injections containing 0.05 % glycerol. Groups 2-5 received injections of the 500 μM solution of the respective cyclic dipeptide in saline containing 0.05 % glycerol. Group 6, the positive control group, received saline injections containing isoniazid at a concentration of 1 mg/ml.

Rats were subjected to light ether anaesthesia to a loss of blink and pain reflexes. The entire liver was removed and rinsed in 0.15 M KCl solution. The livers were then weighed (wet mass obtained). The livers were placed in 0.15 M KCl solution and frozen at -20°C until lipid peroxidation was assessed. Blood was collected by cardiac puncture into empty vacutainer tubes and placed at 4°C to allow for clot formation. Serum was obtained by centrifugation at 3 000 rpm for 15 min. The serum was retained for the assessment of hepatotoxicity by various enzymatic and biochemical assays.

5.3.2.2 Determination of serum LDH levels

The interconversion of lactate and pyruvate is catalysed by LDH. Of the 5 LDH isoenzymes, the liver and kidneys contain the highest proportion of LD-5. Elevated levels of LDH activity are associated with various pathological conditions including myocardial infarction, pernicious anemia and various liver diseases (Sigma package insert, 2000).

Determination of LDH depends on either the oxidation of lactate to pyruvate, or the reverse reaction, i.e. pyruvate to lactate. The Sigma Diagnostics kit determination is based on the following reaction:



Along with the oxidation of lactate to pyruvate, NAD^+ is reduced to NADH. This production of NADH results in an increased absorbance at 340 nm. This rate of change in the absorbance at 340 nm is directly proportional to the activity of LDH in the sample.

5.3.2.2.1 LDH Assay

10 μl of the serum sample was placed into a 96-well plate (Corningware, Cambridge, U.S.A.) to which 200 μl LDH reagent was added. An initial absorbance at 340 nm was read using Labsystems Multiskan MS (Multiskan Transmit Program, Rev. 1.3. (1995)), after which the reaction was followed at 340 nm for 1 min. The change in absorbance/min was determined. LDH activity was calculated using the following formula (Sigma Diagnostics, St. Louis, U.S.A. (2000)):

$$\text{LDH activity} = (\Delta \text{ Abs/min} \times \text{TV} \times 1000) / (6.22 \times \text{SV} \times \text{LP})$$

Where:

$\Delta \text{ Abs/min}$ = change in absorbance at 340 nm per min

TV = total reaction volume

1000 = converts units per ml to units per liter

6.22 = millimolar absorptivity of NADH at 340 nm

LP = light path (1.33 for a 96-well plate (Walkowiak *et al.*, 1997))

SV = sample volume

Thus, LDH activity = $\Delta \text{ Abs/min} \times 3376 \text{ U/L}$ at 25 °C.

5.3.2.3 Determination of alkaline phosphatase levels

The main function of this alkaline phosphatase is to hydrolyse phosphate monoesters, such as inorganic pyrophosphates. Specificity for substrate is not high, with a number of phosphate monoesters being used as substrate. Increases in alkaline phosphatase levels are associated with liver disease and conditions affecting bone (Kirk *et al.*, 1975. Pg. 308). Alkaline phosphatase measurement is a more specific indicator of liver dysfunction than AST (Marshall, 1997. Pg. 76).

The determination of alkaline phosphatase activity is based on the use of *p*-nitrophenol phosphate (*p*NPP) (Merck, Germany) as a substrate. In this enzymatic reaction, *p*NPP is converted to *p*-nitrophenol, which absorbs light maximally at 410 nm (Bergmeyer, 1984).

5.3.2.3.1 Alkaline phosphatase assay

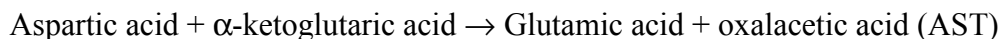
A microtiter version of the alkaline phosphatase assay by Bergmeyer (1984) was used, which makes use of 96-well plates (Corningware, Cambridge, U.S.A.). To each well, 26 µl serum sample/standard, 26 µl 1 mM ZnCl₂ and 200 µl glycine buffer (0.1 M (pH 10.5), 1 mM MgCl₂, 0.1 mM ZnCl₂) were added. At zero time, 40 µl of 0.03 M *p*-nitrophenyl phosphate (Merck, Germany) was added to each well. 5 min at room temperature were allowed for the reaction to occur, after which the absorbance was read at 410 nm, using Labsystems Multiskan MS (Multiskan Transmit Program, Rev. 1.3. (1995)). The blank consisted of reagent mixture without serum. A standard curve (Appendix B, Figure B 4.8) was constructed from the results of different concentrations of commercial alkaline phosphatase (Merk, Darmstadt, Germany). The activity is expressed as mU/ml.

5.3.2.4 Serum transaminases

Aspartate transaminase [(AST) EC 2.6.1.1.] and alanine transaminase [(ALT) EC 2.6.1.2.] are normally found in the blood at low concentrations, with higher levels present in the liver and heart muscles. AST is essentially a cytoplasmic and mitochondrial enzyme, while ALT is found only in the cytoplasm. If the liver is destroyed, the enzymes are released into the blood stream, where it will be present at elevated levels (Baron, 1982. Pg. 198). Both AST and ALT are found widely distributed in body tissues. It is only in the liver that both ALT and AST are found in equal amounts; in the rest of the body, AST levels are considerably lower than ALT levels (Marshall, 1997. Pp. 231-2).

The transaminases catalyse the intraconversion of amino acids and keto acids, whereby the amino group is transferred from one molecule to another. This results in the disappearance of one amino acid and the formation of another.

The following reactions are catalysed by the respective enzymes:



Once 2,4-dinitrophenylhydrazine (DNPH) is added, the respective reactions are stopped and the corresponding hydrazones of oxalacetic acid and pyruvic acid are formed in the reactions. The colour reaction is intensified by the addition of sodium hydroxide (Faulkner and King, 1970. Pg. 84).

5.3.2.4.1 Determination of serum AST and ALT content

A modified version of the assay by Bauer *et al.* (1974) was used. To each set of tubes, 250 μl AST/ALT substrate (37°C) was added. To the experimental tubes, 50 μl serum was added, whilst to the blank tube, 50 μl H₂O was added. The tubes were mixed and incubated at 37°C for 30 min for ALT determination, while a longer incubation of 1 hr was needed for AST determination. 250 μl 1 mM DNPH was added, mixed and the solution was incubated at room temperature for 20 min. 2.5 ml 0.4 N NaOH was then added and allowed to incubate at room temperature for 5 min. The solution was diluted twice with 0.4 N NaOH and the absorbance was read at 505 nm using a Shimadzu UV-160A UV-Visible recording spectrophotometer, against a blank consisting of reaction mixture. Calibration curves were set-up as described in Table 5.2 (Bauer *et al.*, 1974. Pp. 493-4).

Table 5. 2: Reaction mixtures for ALT and AST calibration curves.

Tube No.	Pyruvate std (μl)	ALT substrate (μl)	Corresponding ALT units (U)	H ₂ O (μl)	AST substrate	Corresponding AST units (U)
1	0	250	0	50	250	0
2	25	225	24	50	225	48
3	50	200	61	50	200	122
4	75	175	114	50	175	228
5	100	150	190	50	150	380

Once the corresponding substrates and H₂O were added to the tubes, the method was followed as described above. Smooth, not linear, calibration curves (Appendix B, Figures B 4.9 and 4.10) were obtained for both AST and ALT (Bauer *et al.*, 1974. Pp. 493-4). The activities are expressed as U/ml.

5.3.2.5 Lipid peroxidation determination

Lipid peroxidation is seen in several cardiovascular and hepatic diseases (Uchiyama and Mihara, 1978). Increased levels result from damage by toxic free radical intermediates, as well as a reduction in cellular protective mechanisms, leading to cell injury, disorganisation of membrane structure and membrane function (Smith *et al.*, 1982).

Lipid peroxidation was assayed by determining malondialdehyde concentration as thiobarbituric acid (TBA) reactive material (Souza *et al.*, 1999). Free malondialdehyde reacts with TBA reagent in an acidic medium, produced by the addition of phosphoric acid. On reaction, a red-coloured pigment is produced, aided by heating on a boiling water bath.

The method as described by Souza *et al.* (1999) was used. 0.2 g Wet liver tissue was homogenised by the loose plunge of a Dounce homogeniser in 2 ml ice-cold 0.15 M KCl solution. To each test tube, 3 ml 1% H₃PO₄, 1 ml 0.6% aqueous TBA solution and 0.5 ml homogenate were added. The solutions were mixed and heated on a boiling water bath for 45 min. The reaction mixtures were then cooled to room temperature. 4 ml n-butanol was added and the reaction mixtures thoroughly vortexed. The n-butanol layer was separated by centrifugation at 1200 rpm for 15 min. The absorbances of the n-butanol layers were read at both 535 nm and 520 nm (Shimadzu UV-160A UV-Visible recording spectrophotometer), against a blank consisting of reaction mixture only. The difference between the 2 readings was taken as the TBA value and the malondialdehyde content of the liver homogenates was calculated on the basis of a molar coefficient of 153 000 M⁻¹cm⁻¹ (Esterbauer *et al.*, 1984), using the equation :

$$A = \epsilon cl$$

Where

A = absorbance

ϵ = molar extinction coefficient

c = concentration

l = light path length

Malondialdehyde content of the liver homogenates is expressed as $\mu\text{mol}/0.2 \text{ g}$ wet tissue.

5.3.2.6 Assessment of the state of energy metabolism

ATP, the major energy source in cells, plays important roles in amino acid activation, CO_2 fixation and DNA replication, among others. Any mechanism whereby cellular ATP levels are decreased plays a pivotal role in the progression of irreversible cellular injury (Nieminen *et al.*, 1994). The adenosine-5'-triphosphate kit from Sigma Diagnostics was used according to manufacturers specifications.

The assay is based on the following reaction, which is catalysed by phosphoglycerate kinase (PGK):



A second enzyme, glyceraldehyde phosphate dehydrogenase (GAPD), is also present in the reaction mixture, and catalyses the following reaction:



When NADH is oxidised to NAD^+ , there is a resultant decrease in absorbance at 340 nm. By measuring this decrease, the amount of ATP originally in the sample was obtained (Sigma Diagnostics, 1995).

5.3.2.6.1 ATP concentration assay

300 μl of each serum sample was transferred to a clean eppendorf, to which 300 μl 12% (w/v) TCA was added. The mixture was vortexed for 7 s and left on ice for 5 min. The mixture was then centrifuged at 12 000 rpm for 7 min. 50 μl of the serum from each sample was then transferred to a 96-well plate (Corningware, Cambridge, U.S.A.). To each well, 250 μl of a 1 mg/ml NADH solution in 18 mM buffered solution was added.

The samples were mixed and an initial absorbance (A) reading at 340 nm was taken using Labsystems Multiskan MS (Multiskan Transmit Program, Rev. 1.3. (1995)). 4 μ l of the GAPD/PGK enzyme mix was added to each well, the solutions rapidly mixed, and the absorbance at 340 nm was read over a period of 10 min, until the minimum absorbance reading was reached. The blood ATP concentration (μ mol) was calculated using the following equation:

$$\Delta A = \text{Initial A} - \text{Final A}$$

$$[\text{ATP}] = \Delta A \times 977.492$$

The factor 977.492 was calculated as follows:

$$977.492 = (0.304 \times 1000)/(6.22)(0.05)$$

0.304 = volume of liquid in well

1000 = conversion of concentration per ml to concentration per l

6.22 = millimolar absorptivity of NADH at 340 nm

0.050 = sample volume

5.3.2.7 Serum calcium determination

There are two common pathways of Ca^{2+} -release, Na^{+} -dependent (antiporter) and Na^{+} -independent pathways. A common viewpoint has been that Ca^{2+} -release via the Na^{+} -independent pathway is accompanied by an increase in permeability of the inner mitochondrial membrane. Once Ca^{2+} -levels are decreased by the introduction of EGTA, permeabilisation of the membrane is reversed. This increase in Ca^{2+} -concentration of hepatocytes causes a rapid depletion of mitochondrial GSH, possibly due to mitochondrial Ca^{2+} -cycling. This suggests that any change in Ca^{2+} -homeostasis may induce oxidative stress (Boobis *et al.*, 1989; Chacon and Acosta, 1991).

The basis of the reaction is the interaction of Ca^{2+} (the cation) with the chromogenic agent, *o*-cresolphthalein-complexone. In alkali medium, this complex produces a red colour, with absorbance maxima at 575 nm. Interference with Mg^{2+} is prevented by the presence of 8-hydroxyquinoline, while interference from any heavy metals is negligible (Sigma package insert, 1997).

$\text{Ca}^{2+} + o\text{-cresolphthalein-complexone} \rightarrow \text{Ca}^{2+}\text{-cresolphthalein-complexone complex}$.

Serum was removed from the blood sample without delay as red blood cell membranes are permeable to Ca^{2+} .

5.3.2.7.1 Ca^{2+} -concentration assay

1 ml Ca^{2+} -reagent was added to a set of eppendorfs. 10 μl double distilled H_2O (dd H_2O) was added as a blank, 10 μl 10 g/l Ca^{2+} -standard was added to a separate eppendorf, while to the rest, 10 μl serum was added. The solutions were mixed by gentle inversion, and the reaction was allowed to proceed at room temperature for 5 min. 200 μl of each sample was placed in a 96-well plate (Corningware, Cambridge, U.S.A.). The absorbance was read within 30 min at 600 nm using Labsystems Multiskan MS (Multiskan Transmit Program, Rev. 1.3. (1995)). Ca^{2+} -content in the serum samples was determined by using the following equation (Sigma, St. Louis, U.S.A. (1997)):

$$[\text{Ca}^{2+}] \text{ (g/l) of sample} = \Delta A \text{ sample} / \Delta A \text{ standard} \times [\text{std}]$$

5.3.2.8 Assessment of protective mechanisms

Glutathione is kept primarily in the reduced form (GSH) *in vivo* by GSH reductase. GSSG, the oxidized form, is toxic to the cell. GSH removes toxic peroxides from the cell by acting as a cofactor for GSH peroxidase. In this reaction, GSH is converted to GSSG. GSH levels are then maintained by the conversion of GSSG to GSH by the action of GSSG reductase (Ross, 1989).

The principle of this assay is based on the reaction of GSH with the sulfhydryl reagent, the Ellman reagent (5,5'-dithiobis-(2-nitrobenzoic acid)) (DTNB). GSH reacts with DTNB to form a chromophoric product, 2-nitro-5-thiobenzoic acid, which absorbs light optimally at 410 nm (Tietze, 1969).

5.3.2.8.1 Reduced glutathione assay

To a 96-well plate (Corningware, Cambridge, U.S.A.), 210 μl Hanks balanced salt solution (HBSS) (pH 7.4) and 20 μl of serum/standard sample were added. At zero time,

20 µl 0.625 mM DTNB (Sigma, St. Louis, U.S.A.) was added to each well. The reaction was followed at 410 nm over a period of 6 min using Labsystems Multiskan MS (Multiskan Transmit Program, Rev. 1.3. (1995)). A standard curve (Appendix B, Figure B 4.11) was constructed from the results of differing concentrations of GSH (Sigma, St. Louis, U.S.A.). Changes in absorbance over a 3 min period were plotted against the corresponding reduced GSH concentrations. The concentration of GSH is expressed as mM.

5.3.2.9 Assessment of ureogenesis

Urea, a product of protein metabolism is passed via the bloodstream to the kidneys, where it is excreted into urine. Decreases in urea concentration will thus reflect negatively on protein metabolism (Kirk *et al.*, 1975. Pg. 286).

The principle of the assay is based on the following reaction, catalysed by urease:



Ammonia, later released by alkali, forms a blue indophenol product on reaction with phenol and hypochlorite (Faulkner and King, 1970, Pg. 86).

5.3.2.9.1 Urea nitrogen assay

To each test tube, 0.25 ml buffered urease solution (30 mg/100 ml) was added, into which 10 µl std/serum was mixed. The reaction mixture was incubated at 37°C for 15 min. 0.5 ml alkaline hypochlorite solution was added, followed by 0.5 ml 0.53 M phenol reagent. After each addition, the solutions were thoroughly vortexed. The reaction mixtures were then incubated at 37°C for 15 min, after which 5 ml H₂O was added to each test tube. The reaction mixture was left at room temperature for 1 min, after which the absorbance at 620 nm was read using a Shimadzu UV-160A UV-Visible recording spectrophotometer, against a reaction mixture blank. For each experiment, the absorbance of a standard urease solution (60 mg/100 ml) was also determined. This absorbance was used in the calculation to determine urea nitrogen content of the serum samples (Bauer *et al.*, 1974. Pp. 393-4).

The formula used is as follows:

$$\text{Abs sample/Abs std} \times \text{conc std} = \text{mg/100 ml urea nitrogen}$$

5.3.2.10 Assessment of protein synthesis

Albumin functions as a transport protein for many substances including thyroid hormones, Ca^{2+} and fatty acids. In the blood stream, many drugs bind to albumin, thereby decreasing free albumin concentrations. This has important pharmacokinetic consequences as free drug concentrations may increase, thus increasing the risk of toxicity (Marshall, 1997. Pp. 203-4).

A modification of the albumin assay by Bauer *et al.* (1974) was used. A solution containing albumin was added to a buffered solution of an indicator dye (bromocresol green). Subsequently, albumin bound some of the dye, changing the colour of the solution. Other serum proteins such as the globulins do not react with the dye. A surface active agent, succinate buffer containing Brij-35 (Sigma, St. Louis, U.S.A.), was added to facilitate proper colour changes (Bauer *et al.*, 1974. Pg. 403).

5.3.2.10.1 Albumin assay

To a set of test tubes, 5 ml working reagent solution was added, to which 25 μl sample/albumin standard was added, mixed and left to incubate at room temperature for 10 min. The absorbance was read at 630 nm using a Shimadzu UV-160A UV-Visible recording spectrophotometer against a blank consisting of working reagent. A 10 g/100 ml albumin standard was used. Albumin content in serum samples were calculated using the following formula:

$$\text{Abs sample/Abs std} \times \text{conc. std} = \text{conc sample g/100 ml}$$

5.3.2.11 Determination of bilirubin content in serum

If the concentration of bilirubin in the blood stream is increased, it results in jaundice. This may be resultant of a number of different causes. If haemoglobin breakdown is increased, the liver may not be able to cope with the greater load of pigment present and the bilirubin concentration in the blood will increase (haemolytic jaundice), which does not reflect on impaired liver functioning.

Serum bilirubin is treated with diazotised sulphanilic acid (diazo reagent) in a HCl solution. Bilirubin and albumin are separated, with the former being split into two 2-pyrrole portions. Each pyrrole portion then couples with the diazo reagent, forming a purple-pigment, azobilirubin. With the substitution of methanol for water, the lipid-soluble unconjugated bilirubin reacts with the diazo reagent, providing a measure of the total bilirubin present in the serum (Bauer *et al.*, 1974. Pg. 435).

5.3.2.11.1 Bilirubin assay

A modification of Malloy and Evelyn (1937) was used. In test tubes, the following were added in order, mixing after each addition:

50 μ l serum/bilirubin std, 0.95 ml H₂O, 0.2 ml diazo reagent (freshly prepared), and 1.25 ml methanol. The reaction was allowed to proceed in the dark at room temperature for 30 min. The absorbance was read at 540 nm using a Shimadzu UV-160A UV-Visible recording spectrophotometer against a blank consisting of reagent mixture only. A standard curve was constructed from the results of differing concentrations of bilirubin (Sigma, St. Louis, U.S.A.) standards. The concentrations of bilirubin in the serum samples were derived from the standard curve (Appendix B, Figure B 4.12), and are expressed as μ mol.

5.3.3 Statistical analysis

Results are expressed as mean \pm s.d. for the indicated number of experiments. Results were analysed using the software package GraphPad Prism Version 2.0 and GraphPad InStat (GraphPad Software, Inc., San Diego, U.S.A.). All tests were performed on raw data obtained from the experiments (n=6). The effect of a single qualitative factor on a single response variable was determined by univariate ANOVA using the Mann-Whitney test. *P* values <0.05 were accepted as evidence of a statistically significant difference.

5.4 RESULTS AND DISCUSSION

5.4.1 *In vitro* examination of hepatotoxicity

An *in vitro* protein-binding study of the isomers was performed at 37°C by equilibrium dialysis (Taki *et al.*, 1998). In an *in vivo* experiment, different proteins present in blood (such as albumin) may affect the hepatic metabolism of peptide drugs by interacting with them. Table 5.3 shows the amount (%) of isomer bound by BSA (3% w/v) as estimated by equilibrium dialysis.

Table 5. 3: Percentage binding of albumin to the isomers as determined by equilibrium dialysis. Values indicated are the mean \pm s.d. of 6 experiments.

Cyclic Dipeptide (Concentration = 1760.563 μ M)	Concentration recovered in KHHB (μ M)	Concentration recovered in BSA medium (μ M)	Total Concentration recovered (μ M)	% Binding
Cyclo(L-Trp-L-Pro)	396.91 \pm 0.287	268.23 \pm 0.621	665.14 \pm 2.04	62.22 \pm 1.269
Cyclo(L-Trp-D-Pro)	441.08 \pm 0.284	299.99 \pm 0.340	741.07 \pm 1.32	57.91 \pm 0.767
Cyclo(D-Trp-L-Pro)	428.00 \pm 0.365	296.45 \pm 0.534	724.54 \pm 1.93	58.85 \pm 1.133
Cyclo(D-Trp-D-Pro)	430.12 \pm 0.213	276.54 \pm 0.393	706.65 \pm 1.31	59.86 \pm 0.784

The interaction between BSA and cyclo(L-Trp-L-Pro) resulted in a \pm 62% binding (Table 5.3), the greatest amount for all the isomers. Binding of BSA to cyclo(L-Trp-L-Pro) was significantly higher than binding to the other isomers ($p < 0.05$), which did not show any significant differences in their extent of binding by BSA.

In studies undertaken by Taki *et al.* (1998), the binding of metkephamid (a stable analogue of methionine enkephalin) that contains both L- and D-amino acids, to BSA by equilibrium dialysis and liver perfusion were examined. Under dialysis conditions, it was found that BSA bound to metkephamid by 50%. At 5 μ M and 50 μ M metkephamid, approximately 50% and 37% (respectively) was taken out of solution by BSA-binding. Furthermore, it was noted that an increase in concentration of metkephamid resulted in decreased binding by BSA. A number of Ca^{2+} -channel blockers are readily bound to plasma protein after oral administration. Greater than 90% verapamil and nifedipine and

between 70-90% diltiazem is bound by plasma protein (Katzung and Chatterjee, 1989). Three typical cardiac glycosides are bound by plasma protein to varying degrees: ouabain (0%), 20-40% digoxin and greater than 90% of digitoxin is bound by plasma protein (Katzung and Parmley, 1989).

The average number of drug bound per mole of albumin (r) was calculated for each isomer. Results are shown in Table 5.4.

Table 5. 4: Average number of isomer bound per mole of albumin.

Isomer	Calculated r value
Cyclo(L-Trp-L-Pro)	2.556
Cyclo(L-Trp-D-Pro)	2.547
Cyclo(D-Trp-L-Pro)	2.418
Cyclo(D-Trp-D-Pro)	2.459

As can be noted in Table 5.4, the average number of isomer per mole of albumin does not differ greatly from one isomer to the next. This is much greater than the r value obtained for the binding of caffeine by BSA, which is reported to be 0.143 (Gennaro *et al.*, 1980).

An *in vivo* study of blood absorption of cyclo(L-Trp-L-Pro) and cyclo(L-Trp-D-Pro) was performed in rats. Only two isomers were tested due to limitations in the number of rats available. It was suggested by Mizuma *et al.* (1998) that any drug entering the small intestine would do so stably. Intraperitoneal injection was chosen as a route of administration in order to avoid low oral absorption of these peptide entities (Martin, 1993). Blood was collected by cardiac puncture, as there was not enough pressure in the hepatic portal vein. Blood was collected from 7 groups of rats at 10 min, 20 min, 30 min, 1 hr, 2 hr, 4 hr and 24 hr intervals ($n=3$ for each time interval).

Within 30 min, the maximum amount of drug was detected in the blood stream (Figure 5.5). The rest could be lost to protein-binding or absorption into the small intestine.

Within an hour, the blood levels of both cyclo(L-Trp-L-Pro) and cyclo(L-Trp-D-Pro) had decreased, with the greatest decrease occurring for cyclo(L-Trp-D-Pro). By 4 hrs, the concentrations of cyclo(L-Trp-L-Pro) and cyclo(L-Trp-D-Pro) were below 300 μM , and may be resultant of albumin-binding. After 24 hrs, the concentrations of both the isomers had reached levels below 200 μM , resultant of BSA binding and/or hepatic metabolism.

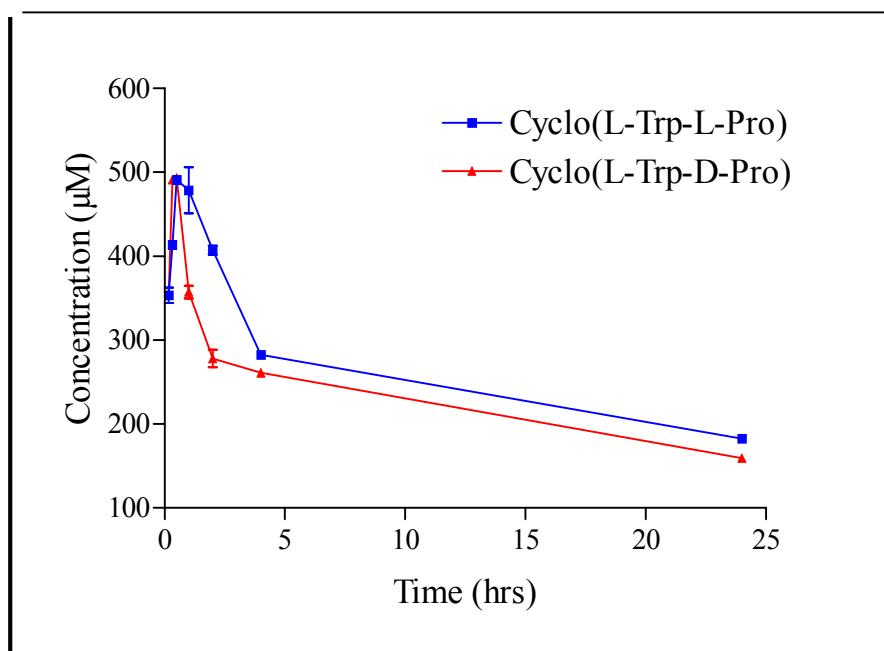


Figure 5. 5: Rates of blood absorption of cyclo(L-Trp-L-Pro) and cyclo(L-Trp-D-Pro) in the rat. Values indicated are the mean \pm s.d. of triplicates.

In a liver perfusate study, 40% metkephamid was recovered after 30 min in the BSA-free system. When the same experimental conditions were applied in the presence of BSA, the amount of metkephamid recovered increased to approximately 75%, suggesting that BSA may protect metkephamid from degradation in the liver (Taki *et al.*, 1998).

In the past decade, the use of cellular models as a partial alternative to whole animal experimentation as a model of toxicity testing has increased. Cell cultures present a simplified, valid biological model in *in vitro* screening of hepatotoxicity of different compounds and their respective metabolites (Jover *et al.*, 1992). In the assessment of cytotoxicity of the isomers and isoniazid, three different cell types were chosen in such a manner as to determine the specificity of toxicity, i.e. if any toxicity is detected, whether

it is hepatocyte-specific or not. The primary isolated hepatocytes from rats (Figure 5.6), Chang liver cells, a hepatoma cell line (transfected with a cervical carcinoma) and N-2-alpha cells (a neuronal cell line) were used. Results are depicted as % viability of the negative control cultures, which represent 100% viability.

A normal internal infrastructure is characteristic of the isolated cells. Using scanning electron micrographs, microvilli that cover the entire surface of the cell is evident. The shapes may vary from highly irregular (initially) to rounded (in suspension) or spread (on attachment to surface). Deep constrictions may develop that may appear as cleavage furrows. When the cell-to-cell contacts are released, the latent cleavage potential of these polyploid cells may be initiated (Seglen, 1973). Isolated human hepatocytes show glycogen particles in a rosette pattern, distributed throughout the cytoplasm. The rough endoplasmic reticulum is well-defined and visible exocytotic vesicles are seen with the Golgi apparatus. Different sized lipid droplets, lysosomes and peroxisomes are also found within the cytoplasm (Gomez-Lechon *et al.*, 1997).



Figure 5. 6: Liver cells in suspension (stained with trypan blue) prepared by the two-step collagenase perfusion method (The photograph was taken at a magnification of 272x, using a phase contrast filter 2 and $\frac{1}{8}$ s shutter speed).

In the isolated hepatocytes (Figure 5.7), isoniazid was the only treatment that favoured the growth of the cells, and thus differed significantly from the other treatments ($p < 0.05$).

All isomers resulted in decreased growth in comparison to the control culture over the 5 day period and did not differ significantly from each other ($p>0.05$). The greatest inhibition of growth was noted for cyclo(L-Trp-L-Pro) and cyclo(L-Trp-D-Pro) (60% and 62% inhibition, respectively), while cyclo(D-Trp-L-Pro) and cyclo(D-Trp-D-Pro) only resulted in a decrease of 53.5% and 55% (respectively), in comparison to the control.

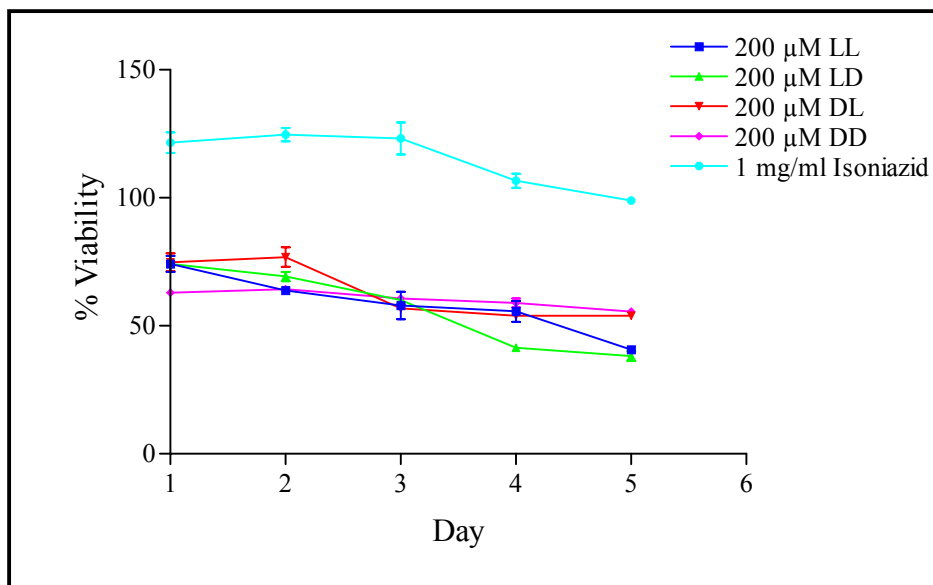


Figure 5. 7: Effects of the compounds on the viability of isolated rat hepatocytes. LL = cyclo(L-Trp-L-Pro); LD = cyclo(L-Trp-D-Pro); DL = cyclo(D-Trp-L-Pro); DD = cyclo(D-Trp-D-Pro). Values indicated are the mean \pm s.d. of 6 experiments per day per treatment.

When the isomers were applied to the Chang liver cells (Figure 5.8), isoniazid resulted in decreased growth over a 2 day period (~30% inhibition of growth). After that, growth appeared to increase slightly (from 70 to 78%). Cyclo(D-Trp-L-Pro) also resulted in an initial decrease in cell growth, but not to the same extent of isoniazid. This was also followed by a slight increase in cell growth.

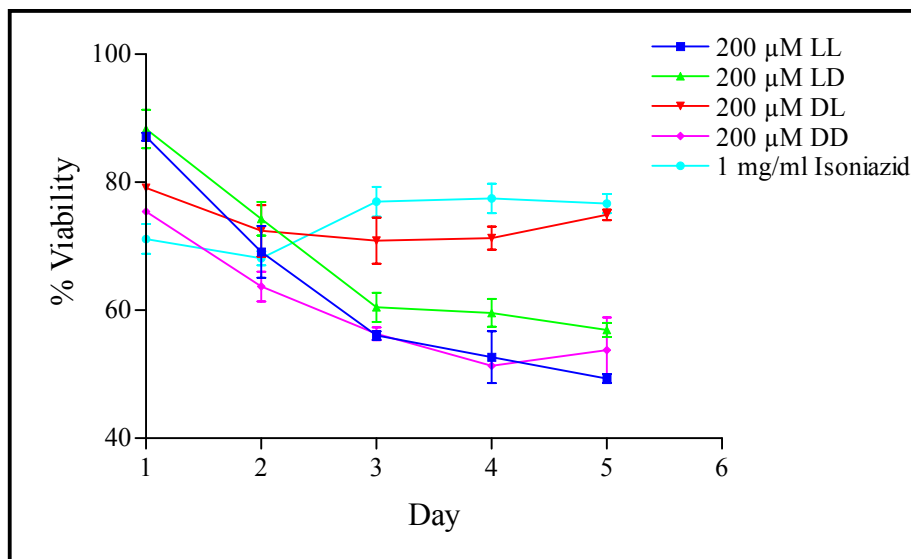


Figure 5.8: Effects of the compounds on the viability of Chang liver cells. LL = cyclo(L-Trp-L-Pro); LD = cyclo(L-Trp-D-Pro); DL = cyclo(D-Trp-L-Pro); DD = cyclo(D-Trp-D-Pro). Values indicated are the mean \pm s.d. of 6 experiments per day per treatment.

Cyclo(L-Trp-L-Pro), cyclo(L-Trp-D-Pro) and cyclo(D-Trp-D-Pro) greatly inhibited cell growth over the 5 day period ($p < 0.05$) (Figure 5.8), with cyclo(L-Trp-L-Pro) being the most cytotoxic isomer, resulting in a 50% inhibition of cell growth.

Cyclo(D-Trp-L-Pro) did not adversely affect the growth of N-2-alpha cells (Figure 5.9), indicating that any hepatotoxic effects noted in *in vivo* studies were hepatocyte-specific. However, in the presence of cyclo(L-Trp-L-Pro), cyclo(L-Trp-D-Pro), cyclo(D-Trp-D-Pro) and isoniazid, the growth of N-2-alpha decreased over the 5 day period to approximately 75% of the control growth. This indicated that the cytotoxicity noted for these compounds were not hepatocyte-specific, and may be capable of exerting their cytotoxic effects on a number of different cell types.

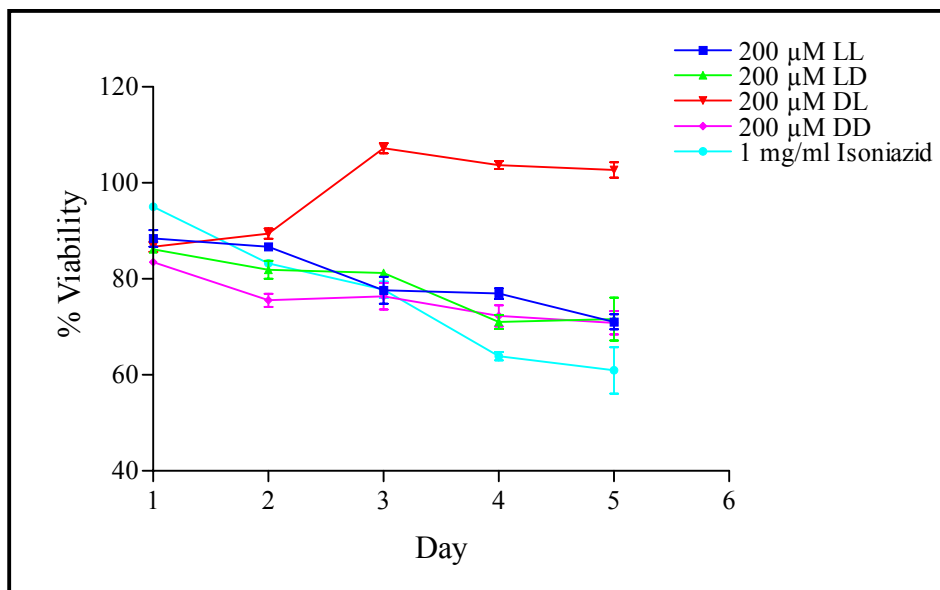


Figure 5. 9: Effects of the compounds on the viability of N-2-alpha cells. LL = cyclo(L-Trp-L-Pro); LD = cyclo(L-Trp-D-Pro); DL = cyclo(D-Trp-L-Pro); DD = cyclo(D-Trp-D-Pro). Values indicated are the mean \pm s.d. of 6 experiments per day per treatment.

In studies conducted by other researchers, the concentrations of pesticides that resulted in a 50% inhibition of cell growth by the MTT assay were determined on BALB/c mouse 3T3 fibroblasts. It was found that 60 μ M trimethyltin hydroxide, 2 μ M triethyltin bromide, 0.2 μ M tricyclohexyltin bromide and 0.06 μ M triphenyltin hydroxide all caused a 50% inhibition of cell growth. Similarly, it was reported that 13 μ M oligomycin, 66 μ M antimycin and 1419 μ M L-ascorbic acid produced the same results (Borenfreund *et al.*, 1988).

This toxicity was divided into four categories. If a 50% inhibition of growth was noted by the MTT assay, the following would apply:

- < 100 μ M – highly toxic,
- \geq 100 μ M < 1000 μ M – moderately toxic,
- > 1000 μ M < 2000 μ M – slightly toxic, and
- > 2500 μ M – nontoxic.

(Borenfreund *et al.*, 1988).

In terms of this categorization, it can be said that no compound applied to the N-2-alpha cells were highly toxic; cyclo(L-Trp-L-Pro) was moderately toxic for Chang liver cells, and cyclo(L-Trp-L-Pro) and cyclo(L-Trp-D-Pro) was moderately toxic for the isolated rat hepatocytes.

In a study on freshly isolated rat hepatocytes in suspension, it was determined that 0.1 µg/ml oligomycin caused a maximal cell killing after 210 min exposure. An ~90% viability was lost during this exposure period. At 0.1 and 1 µg/ml oligomycin, 55% viability resulted after a 2 hr exposure period. In cultured hepatocytes, viability of the cells decreased to just 10% within 2 hrs of exposure to 0.1 µg/ml oligomycin (Nieminen *et al.*, 1994). In a separate study, no effect on cell viability was noted in the presence of the non-steroidal anti-inflammatory drugs (NSAIDs) ibuprofen (10^{-4} M), flurbiprofen (5×10^{-5} M) and butibufen (2×10^{-4} M) (Castell *et al.*, 1988).

Furthermore, a study on the concentration of well known drugs that produced a 50% reduction in the viability of cells was tested on human and rat hepatocytes, as well as mouse 3T3 cells. The following results (Table 5.5) were reported (Jover *et al.*, 1992):

Table 5. 5: Concentrations of drugs resulting in a 50% reduction in cell viability (MTT₅₀) in three different cell types.

Drug tested	Human hepatocytes	Rat hepatocytes	Mouse 3T3 cells
Paracetamol	6.60 mM	5.00 mM	13.60 mM
Acetylsalicylic acid	4.97 mM	2.30 mM	15.00 mM
Diazepam	0.23 mM	0.41 mM	0.26 mM

5.4.2 In vivo examination of hepatotoxicity

In the *in vivo* assessment of the metabolic effects of the compounds on the liver, the rats were injected intraperitoneally with drug solutions of 500 µM (0.5% glycerol in saline), to effect a final concentration of 200 µM in the blood stream. Isoniazid was injected at a concentration of 1 mg/ml saline containing 0.5% glycerol. After injection, the rats were

sacrificed under light ether anaesthesia, blood collected by cardiac puncture and the livers removed. For the long-term study, rats were injected over a period of 5 days, after which blood and livers were collected.

The hepatic weight (% of body weight) was determined for all the experimental rats (Figure 5.10). After a 24 hr exposure, the hepatic weight of cyclo(L-Trp-L-Pro) and cyclo(D-Trp-L-Pro) was significantly decreased ($p < 0.05$) in comparison to the control sample, with no significant difference being noted for any of the other compounds ($p > 0.05$). After a 5 day exposure, the hepatic weights for cyclo(L-Trp-L-Pro), cyclo(D-Trp-L-Pro) and cyclo(D-Trp-D-Pro) increased significantly ($p < 0.05$) from the control. Significant differences between the day 1 and day 5 groups were noted for cyclo(L-Trp-L-Pro) and cyclo(D-Trp-L-Pro) only, with day 1 hepatic weights being lower than the day 5 weights ($p = 0.0286$ for both compounds). Isoniazid did not affect liver weight at either day 1 or day 5.

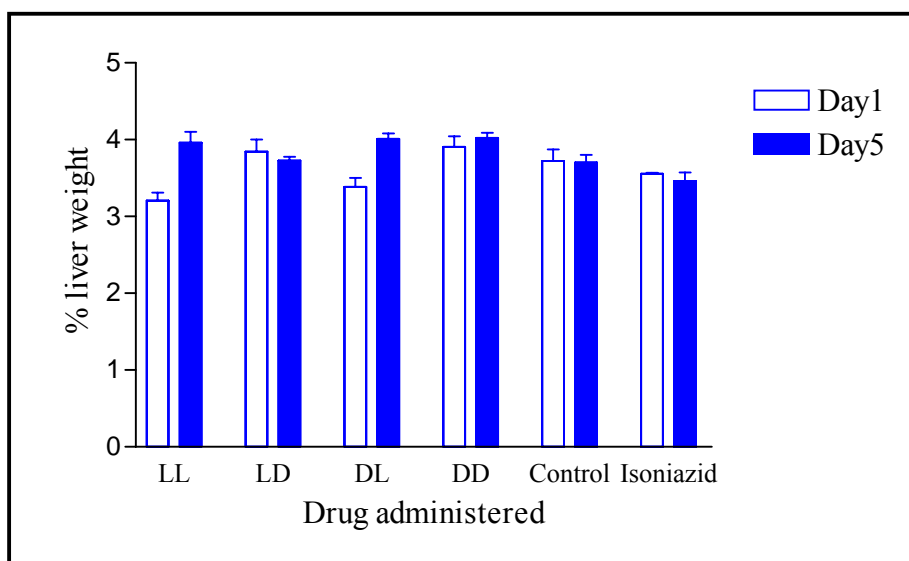


Figure 5. 10: Effects of the compounds on wet liver weight, represented as a % of the total body weight. LL = cyclo(L-Trp-L-Pro); LD = cyclo(L-Trp-D-Pro); DL = cyclo(D-Trp-L-Pro); DD = cyclo(D-Trp-D-Pro). Values indicated are the mean \pm s.d. of 6 experiments per day per treatment.

Guaiazulene, an antioxidant, did not change the hepatic weight of rats when administered at a concentration of 250 mg/kg. Paracetamol, administered at a hepatotoxic dosage of

600 mg/kg, did not, however, produce any significant effect on hepatic weight (Kourounakis *et al.*, 1997). In a study carried out by Herdson *et al.* (1964), 0.1% w/w Naphendoarbital introduced into the diet of young rats induced liver enlargement, a function of parenchymal cell hyperplasia, in that hepatocytes were of normal size with an abnormally large number of mitoses.

One of the most common assays used in the assessment of hepatotoxicity of a drug is LDH activity, which gives an indication of cell membrane integrity. Increased LDH activity is associated with disruption of cell membrane structure (Vickers, 1997). Significantly increased ($p < 0.05$) levels of LDH were determined for all the compounds in comparison to the control after 24 hrs (Figure 5.11). These levels increased significantly for cyclo(L-Trp-L-Pro) and cyclo(L-Trp-D-Pro) ($p < 0.05$), decreased for cyclo(D-Trp-L-Pro) and isoniazid ($p < 0.05$), with no changes noted for the control and cyclo(D-Trp-D-Pro) groups ($p = 0.5602$ and $p = 0.6857$, respectively) when day 1 and day 5 levels were compared. At day 5, levels detected for cyclo(L-Trp-L-Pro) and cyclo(L-Trp-D-Pro) increased in comparison to the control group ($p < 0.05$) while no differences were noted for any other compound in comparison to the control group. It appears that cyclo(L-Trp-L-Pro) and cyclo(L-Trp-D-Pro) induced the greatest disruption in cell membrane integrity, which resulted in the greatest leakage of LDH from the cell.

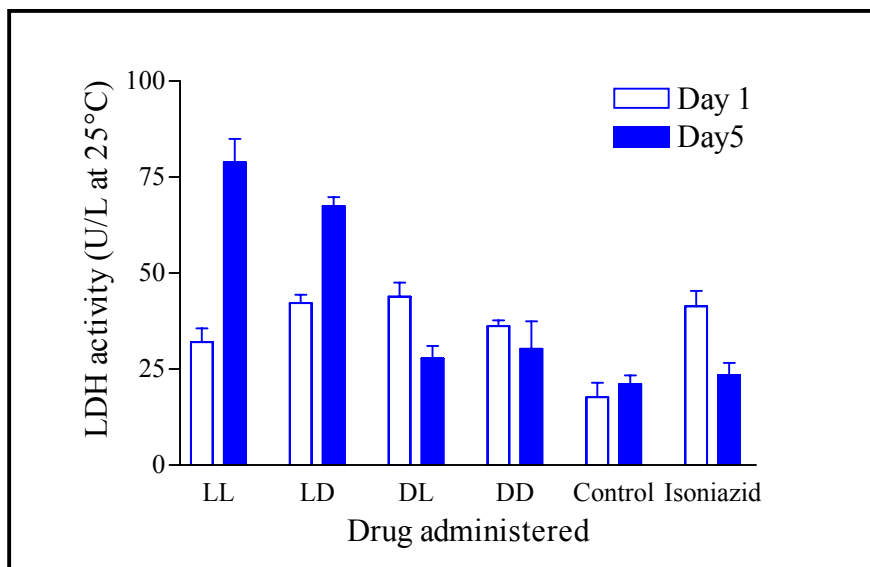


Figure 5. 11: Effects of the compounds on lactate dehydrogenase activity in the blood stream. LL = cyclo(L-Trp-L-Pro); LD = cyclo(L-Trp-D-Pro); DL = cyclo(D-Trp-L-Pro); DD = cyclo(D-Trp-D-Pro). Values indicated are the mean \pm s.d. of 6 experiments per day per treatment.

In data adapted from Castell *et al.* (1988), LDH activity of control cultures was 76 ± 2 U/ml and 11 ± 2 U/ml at 24 hrs and 48 hrs respectively. Significantly increased levels of LDH leakage ($p < 0.001$) from the cells were noted for ibuprofen, flurbiprofen and butibufen at the therapeutic plasma concentrations (10^{-6} to 10^{-3} M). Massive cell membrane damage occurred at 10^{-4} M of these NSAID's (Castell *et al.*, 1988). It is thus possible that a 5 day exposure to cyclo(L-Trp-L-Pro) and cyclo(L-Trp-D-Pro) could result in massive cell membrane damage, resultant of the high levels of LDH leakage in these samples. An approximate 300% increase in LDH levels are noted for these compounds (Figure 5.11), which compare favourably with LDH leakage in the presence of 5×10^{-4} M ibuprofen.

Studies of the effect of the microcystin toxin in mice showed a 20 fold increase in LDH concentration (an increase from 2.7 ± 0.3 U/ml to 38.0 ± 3.3 U/ml) 45 min after the injection was administered (Falconer *et al.*, 1981). In a separate study on isolated rat hepatocytes, a dose- and time-dependant LDH leakage occurred in the presence of diclofenac, with maximal leakage occurring in the presence of 500 μ M and 1 mM ($p < 0.01$) diclofenac. In addition, ATP levels rapidly decreased in the presence of 500 μ M diclofenac ($p < 0.05$). Decreases in ATP levels are known to precede LDH leakage,

although marked decreases in ATP levels are not necessarily followed by LDH leakage (Masubuchi *et al.*, 1998).

Measurement of alkaline phosphatase levels as an indicator of liver damage is a much more sensitive indicator than measurement of AST levels (Marshall, 1997. Pg. 76). An increase in alkaline phosphatase levels indicates liver disease. With a disruption in cell membrane integrity (Figure 5.11), it is expected that alkaline phosphatase levels be elevated for both the cyclo(L-Trp-L-Pro) and cyclo(L-Trp-D-Pro) groups. Significantly increased alkaline phosphatase levels (Figure 5.12) were noted after a 24 hr exposure to cyclo(L-Trp-D-Pro), cyclo(D-Trp-D-Pro) and isoniazid ($p=0.0286$), with no alterations noted when dosed with cyclo(L-Trp-L-Pro) and cyclo(D-Trp-L-Pro) in comparison to the control samples. These increased levels indicate that liver damage had been induced by the administration of cyclo(L-Trp-D-Pro), cyclo(D-Trp-D-Pro) and isoniazid. Over the 5 day period, decreases in all levels were noted for cyclo(L-Trp-L-Pro), cyclo(L-Trp-D-Pro), cyclo(D-Trp-D-Pro) and isoniazid ($p<0.05$), with an increase occurring in the presence of cyclo(D-Trp-L-Pro) ($p<0.05$) in comparison to the day 1 levels. This decrease in alkaline phosphatase may indicate a repair mechanism employed by the cells to counter the liver damage. This would however not be the case for cyclo(L-Trp-L-Pro) and cyclo(L-Trp-D-Pro), as a disrupted cell membrane would result in irreversible damage to the cell. Increased alkaline phosphatase levels were noted for cyclo(D-Trp-L-Pro) and isoniazid ($p<0.05$) in comparison to the control group at day 5. These levels did not differ significantly from each other ($p=0.700$).

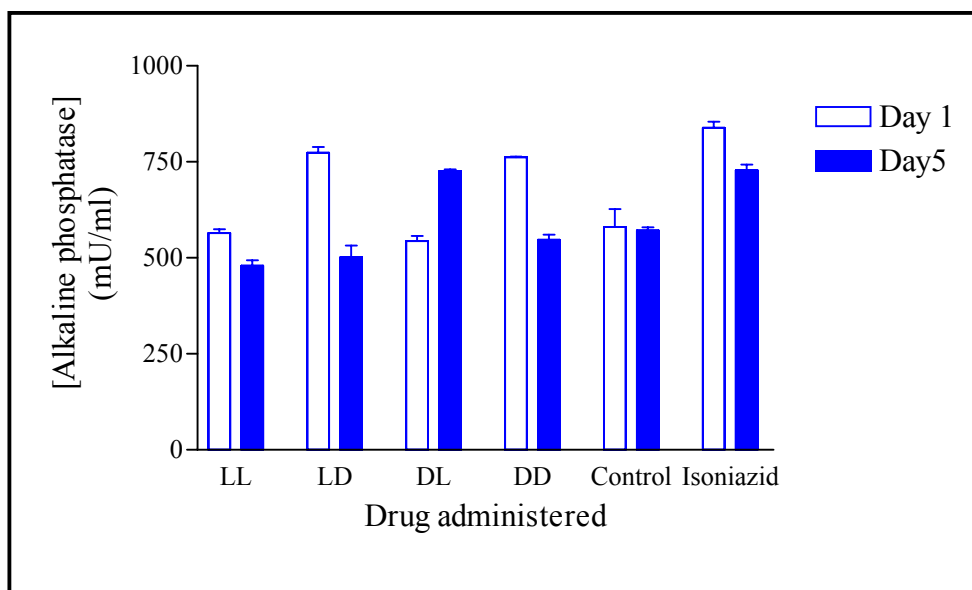


Figure 5. 12: Effects of the compounds on the levels of alkaline phosphatase in the serum. LL = cyclo(L-Trp-L-Pro); LD = cyclo(L-Trp-D-Pro); DL = cyclo(D-Trp-L-Pro); DD = cyclo(D-Trp-D-Pro). Values indicated are the mean \pm s.d. of 6 experiments per day per treatment.

Significantly decreased levels of alkaline phosphatase were noted when rats were dosed with 1 mg/kg endotoxin from *Klebsiella pneumoniae* (Nadai *et al.*, 1998).

Once intracellular liver enzymes leak into extracellular fluid and blood, alterations in hepatocyte permeability are indicated. Primarily, ALT leakage occurs from damaged hepatocytes. In man, these levels are expected to peak within 20-48 hrs, after which normal levels are attained after a period of 2-3 weeks (Towner *et al.*, 2000).

AST serum levels are normally low (2-20 IU/l in humans). An increase in serum activity is resultant of damage to organs that involve necrosis of cells or increased cell permeability. For this reason, it was expected that AST levels in the cyclo(L-Trp-L-Pro) and cyclo(L-Trp-D-Pro) groups would have elevated AST levels (LDH leakage, Figure 5.11). This was, however, not observed, with cyclo(L-Trp-L-Pro) showing significantly lowered levels ($p=0.0286$) and cyclo(L-Trp-D-Pro) not showing any difference to the control group ($p=0.1143$) (Figure 5.13). On day 1, no drug produced any significantly increased AST concentrations, while significantly decreased levels were noted on day 5 for all the compounds (with the exception of isoniazid) in comparison to the control

group ($p < 0.05$). After 5 days, significantly elevated levels of AST were only noted in the isoniazid-treated group ($p = 0.0286$).

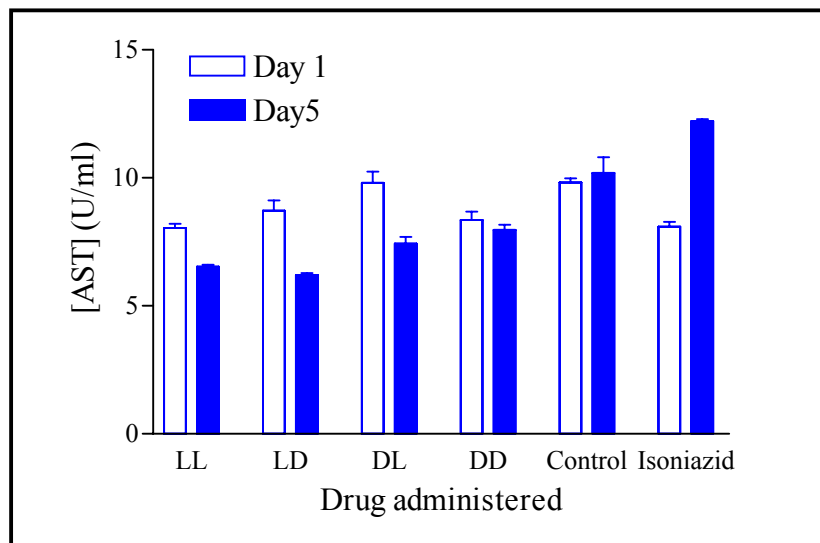


Figure 5. 13: Effects of the compounds on the concentration of aspartate transaminase in the blood stream. LL = cyclo(L-Trp-L-Pro); LD = cyclo(L-Trp-D-Pro); DL = cyclo(D-Trp-L-Pro); DD = cyclo(D-Trp-D-Pro). Values indicated are the mean \pm s.d. of 6 experiments per day per treatment.

In the presence of aflatoxin B₁, a metabolite of *Aspergillus flavus*, significantly increased levels of AST were noted ($p < 0.001$) after a 22 hr exposure to 1 mg/kg toxin. Ternatin, a bioflavonoid, showed no alteration in AST levels. However, when both ternatin and aflatoxin B₁ were administered to the rats, significantly increased levels of AST was observed (Souza *et al.*, 1999). Similarly, treatment of rats with *K. pneumoniae* endotoxin produced significantly increased levels of AST ($p < 0.05$) (Nadai *et al.*, 1998). Investigations into the effect of the Microcystin toxin (23 μ g) in mice resulted in a 50 fold increase in the expression of AST after an exposure of 45 min. This heptapeptide hepatotoxin is derived from the cyanobacterium *Microcystis aeruginosa*, and contains both L- and D-amino acids. Levels increased from 0.13 ± 0.04 U/ml to 9.7 ± 0.9 U/ml (Falconer *et al.*, 1981).

Serum ALT concentrations (Figure 5.14) were significantly increased after a 24 hr exposure to cyclo(D-Trp-L-Pro) and cyclo(D-Trp-D-Pro) ($p < 0.05$), with no significant alteration in the cyclo(L-Trp-L-Pro) and isoniazid groups ($p = 0.1143$ and $p = 0.1478$,

respectively). Significant decreases in ALT levels were noted for all groups (with the exception of cyclo(L-Trp-L-Pro)) from day 1 to day 5, the greatest decrease noted for cyclo(D-Trp-D-Pro) ($p < 0.05$). No significant changes in ALT activity occurred for cyclo(L-Trp-L-Pro). However, in relation to the control (day 5), serum levels of ALT in all the treated groups were significantly elevated ($p < 0.05$), indicating altered hepatocyte permeability.

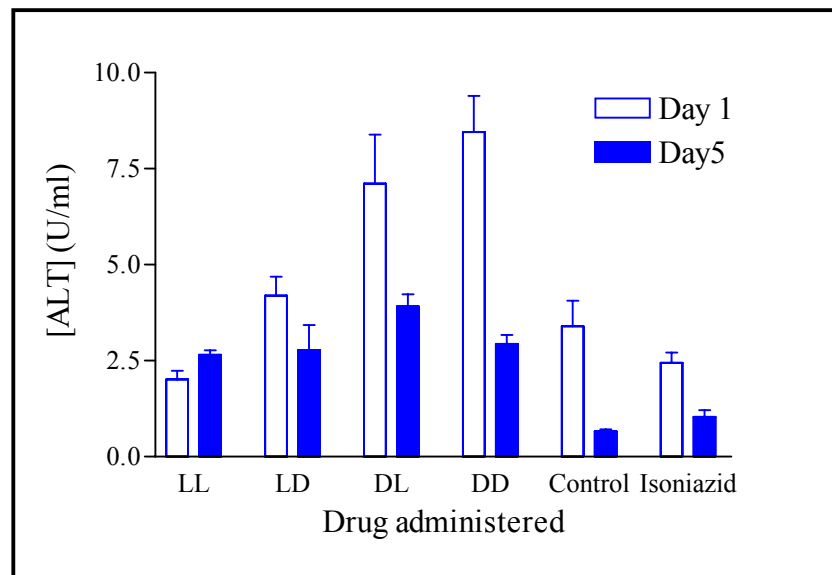


Figure 5. 14: Effects of the compounds on alanine transaminase levels in the blood stream. LL = cyclo(L-Trp-L-Pro); LD = cyclo(L-Trp-D-Pro); DL = cyclo(D-Trp-L-Pro); DD = cyclo(D-Trp-D-Pro). Values indicated are the mean \pm s.d. of 6 experiments per day per treatment.

Significant elevation in ALT levels was also noted in the rats treated with a *K. pneumoniae* endotoxin, from 44.2 ± 4.3 IU/L (international units per liter) to 69.6 ± 12.1 IU/L, representing a 1.5 fold increase (Nadai *et al.*, 1998). An enormous increase in ALT concentration was observed in rats treated with aflatoxin B₁ ($p < 0.001$) with levels increasing to 5071.4 ± 763 IU/L in comparison to the control group of 129.3 ± 17.6 IU/L (a 39 fold increase) (Souza *et al.*, 1999).

Levels of AST and ALT as measured by Towner *et al.* (2000) in rats showed that liver damage had been induced in the presence of 3 mg/kg aflatoxin B₁ after a 24 hr exposure period ($p < 0.01$). Elevated levels of these liver enzymes were also reported by Guzman and Solter (1999) when rat liver slices were exposed to 32 $\mu\text{g}/\text{kg}/\text{day}$ and 48 $\mu\text{g}/\text{kg}/\text{day}$

microcystin hepatotoxin after as little as 2 hrs. In a separate study, 80 µg/kg of a different microcystin toxin, YR, produced maximal levels of these enzymes in serum collected 9 hrs after the rats were injected intraperitoneally. When this concentration was increased to 800 µg/kg, all rats died as a result of intrahepatic haemorrhage (Nishiwaki-Matsushima *et al.*, 1992).

Oxidative degradation of component lipids on the cell membrane is caused by lipid peroxidation. This process would obviously disrupt the integrity of the cell membrane. The TBA reaction of liver homogenates in rats showed significant elevations of malondialdehyde concentrations after a single intraperitoneal injection of cyclo(L-Trp-L-Pro), cyclo(D-Trp-L-Pro) and cyclo(D-Trp-D-Pro), indicating the occurrence of lipid peroxidation ($p < 0.05$) (Figure 5.15). No significant elevation in malondialdehyde levels was observed for cyclo(L-Trp-D-Pro) ($p = 0.667$) and isoniazid ($p = 0.333$). However, after 5 days, malondialdehyde levels increased dramatically for cyclo(L-Trp-D-Pro) and isoniazid-treated groups ($p < 0.05$). This significant increase was also noted for the other compounds in relation to the control ($p < 0.05$), indicating lipid peroxidation.

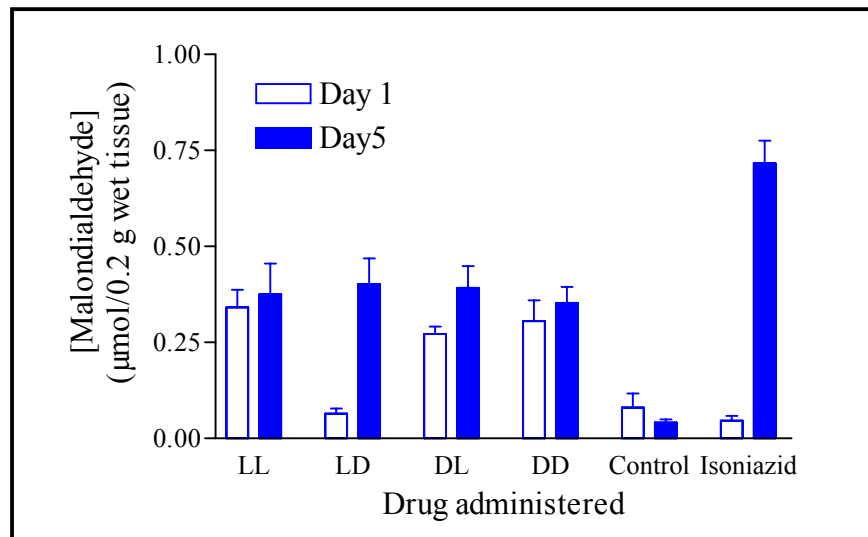


Figure 5. 15: Effects of the compounds on lipid peroxidation, as measured in terms of malondialdehyde concentrations in the serum of the rats. LL = cyclo(L-Trp-L-Pro); LD = cyclo(L-Trp-D-Pro); DL = cyclo(D-Trp-L-Pro); DD = cyclo(D-Trp-D-Pro). Values indicated are the mean \pm s.d. of 6 experiments per day per treatment.

In the treatment of rats with aflatoxin B₁, a 5 fold increase in malondialdehyde concentration was observed (Souza *et al.*, 1999). When aflatoxin B₁ and ternatin were simultaneously administered to the rats, a 50% decrease in malondialdehyde concentration was detected (Souza *et al.*, 1999), showing that ternatin effectively inhibited aflatoxin B₁-induced lipid peroxidation. *In vitro* testing of D- α -tocopherol acetate inhibited lipid peroxidation by 100% at 1 mM, where the IC₅₀ was calculated at 9.8 μ M for guaiazulene (Kourounakis *et al.*, 1997). A 3 and 4 fold increase in malondialdehyde concentration was reported by Guzman and Solter (1999) when liver slices isolated from the rat were exposed to 32 μ g/kg/day and 48 μ g/kg/day (respectively) microcystin LR toxin.

In the presence of hepatotoxins, ATP levels may be decreased by an increase in energy demand, a common event in cell injury (Ross, 1989). The energy metabolism, in terms of ATP levels in serum, was also assessed. Similar levels were noted for the control and isoniazid groups on both days 1 and 5 ($p > 0.05$), indicating that isoniazid did not induce any changes in energy metabolism in the cells. After 24 hrs (Figure 5.16), significantly decreased levels of ATP was observed in the cyclo(L-Trp-D-Pro), cyclo(D-Trp-L-Pro) and cyclo(D-Trp-D-Pro) groups ($p < 0.05$), while no difference was noted for cyclo(L-Trp-L-Pro) ($p = 0.6857$) in relation to the control group. This decrease in ATP would thus indicate a greater energy demand in those cells treated with cyclo(L-Trp-D-Pro), cyclo(D-Trp-L-Pro) and cyclo(D-Trp-D-Pro), or mitochondrial dysfunction. This was however ruled out as, at day 5 (Figure 5.16), significantly increased levels were observed for all the isomers ($p < 0.05$) when compared to the respective day 1 levels. At day 5, the highest level was noted for cyclo(D-Trp-L-Pro) ($p < 0.01$), followed by cyclo(D-Trp-D-Pro), cyclo(L-Trp-L-Pro) and cyclo(L-Trp-D-Pro). This increase may be as a result of increased rates of glycolysis (Castell *et al.*, 1997). However, no significant difference was noted between the day 5 cyclo(L-Trp-L-Pro) and cyclo(L-Trp-D-Pro) levels ($p = 0.2469$).

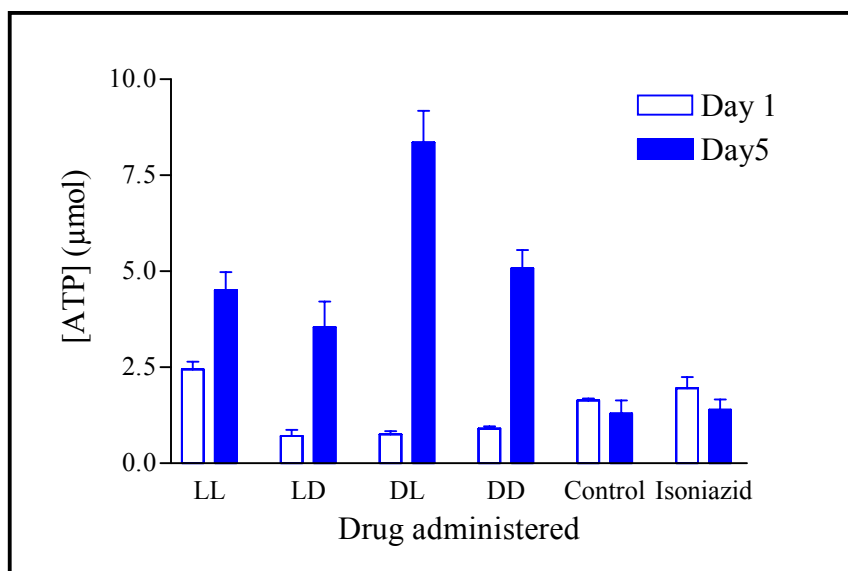


Figure 5. 16: Effects of the compounds on energy metabolism in rat hepatocytes, measured in terms of ATP concentrations in the blood stream. LL = cyclo(L-Trp-L-Pro); LD = cyclo(L-Trp-D-Pro); DL = cyclo(D-Trp-L-Pro); DD = cyclo(D-Trp-D-Pro). Values indicated are the mean \pm s.d. of 6 experiments per day per treatment.

Investigations into the effects of a H_1 receptor antagonist, methapyrilene (200 μ M) on isolated rat hepatocytes indicated significant decreases in ATP synthesis within 2 hrs, indicating mitochondrial dysfunction (Ratra *et al.*, 1998).

Ca^{2+} accumulates in dying cells and is thus involved in toxicological processes (Orrenius *et al.*, 1989). Significantly decreased levels of Ca^{2+} were obtained in the cyclo(L-Trp-L-Pro) and cyclo(L-Trp-D-Pro) samples ($p < 0.05$) (Figure 5.17), whereas cyclo(D-Trp-L-Pro), cyclo(D-Trp-D-Pro) and isoniazid did not show any significantly different levels ($p > 0.05$) in comparison to the control group. The only group to show any significant difference in Ca^{2+} -levels from day 1 to day 5 was the isoniazid-treated group ($p = 0.0286$). Cyclo(L-Trp-L-Pro), cyclo(L-Trp-D-Pro), cyclo(D-Trp-L-Pro) and cyclo(D-Trp-D-Pro)-treated groups showed significantly diminished Ca^{2+} -levels in comparison to the control on day 5 ($p < 0.05$) with no significance between the control and isoniazid-treated groups ($p = 0.6857$). These changes in Ca^{2+} -homeostasis would adversely affect signal transduction of the cell, as Ca^{2+} plays a vital role as a second messenger.

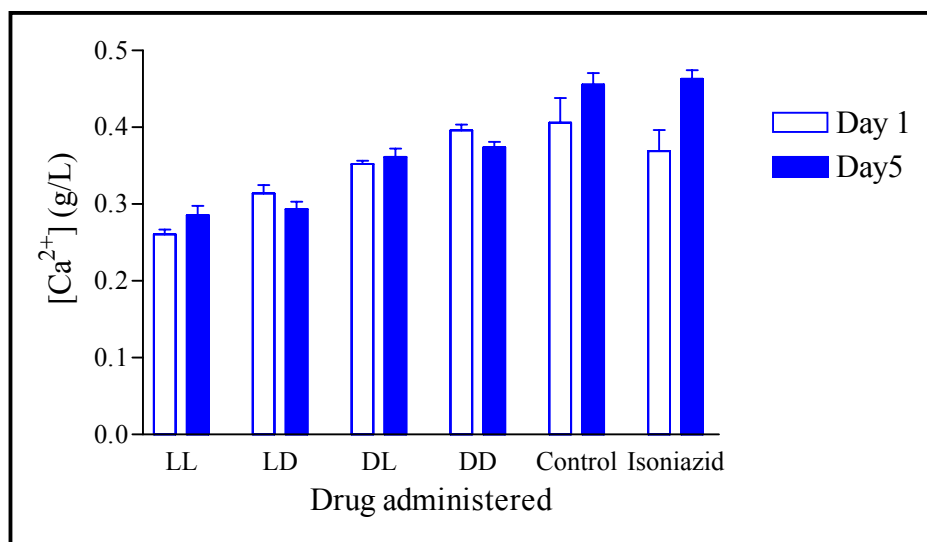


Figure 5. 17: Effects of the compounds on Ca²⁺-levels in the blood stream. LL = cyclo(L-Trp-L-Pro); LD = cyclo(L-Trp-D-Pro); DL = cyclo(D-Trp-L-Pro); DD = cyclo(D-Trp-D-Pro). Values indicated are the mean \pm s.d. of 6 experiments per day per treatment.

Poisoning with carbon tetrachloride and dimethylnitrosamine resulted in a massive influx of Ca²⁺ into the liver (Reynolds, 1964). In a separate study, 200 μ M of methapyrilene caused oxidative stress in rat hepatocytes. However, when these cells were preincubated with a Ca²⁺-channel blocker, verapamil, the cell death induced by methapyrilene was significantly reduced after 8 hrs of incubation (Ratra *et al.*, 1998).

The most efficient way of direct protection against induced hepatotoxicity is the prevention of GSH depletion and the induction of glutathione transferase and glutathione reductase. The amount of GSH was determined to give an indication of the hepatoprotective levels in the cells. Elevated GSH levels would indicate increased protective mechanisms, whereas a decreased level would indicate increased oxidation of GSH to GSSG, conjugate formation with metabolites or decreased *de novo* synthesis of GSH (Castell *et al.*, 1997). After a 24 hr exposure to cyclo(L-Trp-L-Pro) and cyclo(L-Trp-D-Pro), significantly increased levels of GSH were determined ($p < 0.05$) (Figure 5.18). No significant difference was noted for cyclo(D-Trp-L-Pro) and cyclo(D-Trp-D-Pro) ($p > 0.05$), while the isoniazid-treated group showed significantly decreased levels of GSH ($p = 0.0286$) in comparison to the control. Elevated levels of GSH were only noted after a 5 day exposure (Figure 5.18) to cyclo(D-Trp-L-Pro) and cyclo(D-Trp-D-Pro) ($p < 0.05$),

where no significant changes in cyclo(L-Trp-L-Pro) ($p=0.2$) and cyclo(L-Trp-D-Pro) ($p=0.6857$) were noted in comparison to the control. Although the concentration of GSH in the presence of isoniazid increased from day 1 to day 5 ($p=0.0286$), no significant difference between this level and the control group level on day 5 was noted ($p=0.4857$).

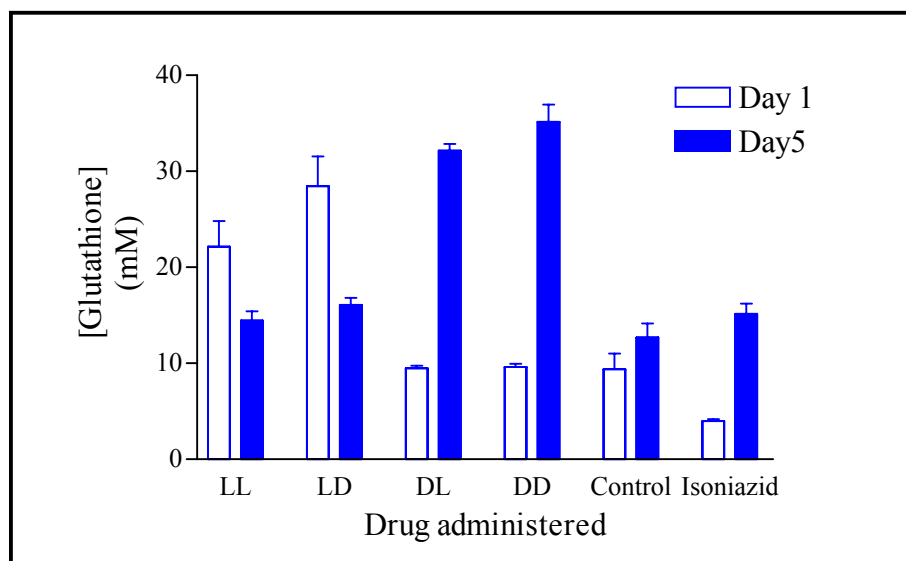


Figure 5. 18: Effects of the compounds hepato-protective mechanisms, as measured by the levels of reduced glutathione present in the blood stream. LL = cyclo(L-Trp-L-Pro); LD = cyclo(L-Trp-D-Pro); DL = cyclo(D-Trp-L-Pro); DD = cyclo(D-Trp-D-Pro). Values indicated are the mean \pm s.d. of 6 experiments per day per treatment.

No significant alteration in glutathione reductase activity was noted at hepatotoxic levels of paracetamol (600 mg/kg). In combination with guaiazulene, the glutathione reductase levels decreased further, but still not to levels significantly lower than the control group (Kourounakis *et al.*, 1997). A decrease in the acid-soluble thiol GSH levels was observed within 10 min of exposure of cultured hepatocytes to the microcystin toxin. Maximal results were noted at a concentration of 300 nM that diminished the GSH content from 32 nmol/10⁶ cells to 5 nmol/10⁶ cells (Runnegar *et al.*, 1987).

Ureogenesis may be disrupted as a result of decreased ATP levels (Castell *et al.*, 1997). One would thus expect a disruption in ureogenesis in the cyclo(L-Trp-D-Pro), cyclo(D-Trp-L-Pro) and cyclo(D-Trp-D-Pro)-treated rats, as a result of the decreased ATP levels in these samples (Figure 5.16). Significantly elevated levels of urea nitrogen in serum

(Figure 5.19) was detected in cyclo(D-Trp-L-Pro), cyclo(D-Trp-D-Pro) and isoniazid-treated groups ($p < 0.05$), with no effect on cyclo(L-Trp-L-Pro) and cyclo(L-Trp-D-Pro)-treated groups in relation to the control. After 5 days (Figure 5.19), significantly increased urea nitrogen concentrations was noted for both cyclo(L-Trp-L-Pro) and cyclo(L-Trp-D-Pro) ($p < 0.05$) in comparison to the day 1 values. In addition, these values were also significantly elevated in comparison to the control group. For the cyclo(D-Trp-L-Pro), cyclo(D-Trp-D-Pro) and isoniazid-treated groups, a significant decrease in levels of urea nitrogen was noted when compared to the respective levels ($p < 0.05$) on day 1. However, only cyclo(D-Trp-L-Pro) was significantly lower than the control value ($p < 0.05$), while both cyclo(D-Trp-D-Pro) and isoniazid did not differ significantly from the control value ($p = 0.2718$ and $p = 0.1143$, respectively). Elevated levels indicate a stimulation of ureogenesis on day 1, immaterial of the low ATP levels detected in the samples.

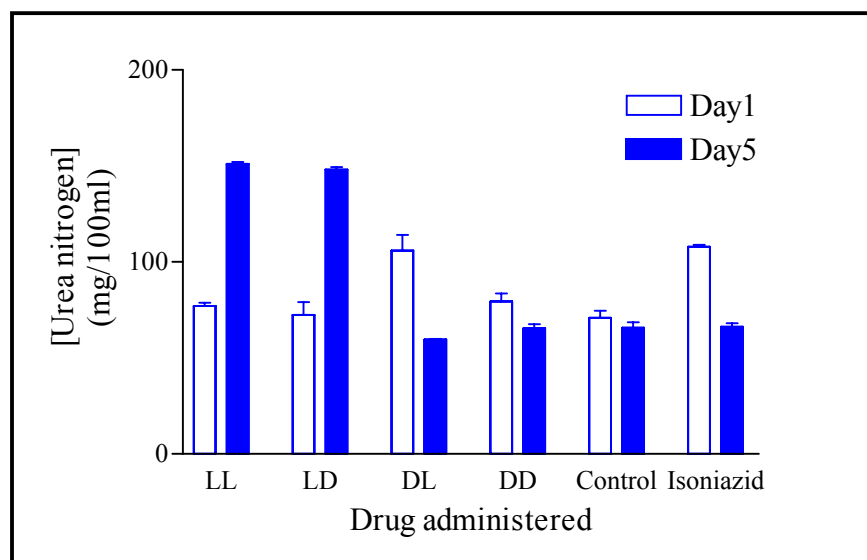


Figure 5. 19: Effects of the compounds on ureogenesis, as measured by urea nitrogen levels in the blood stream. LL = cyclo(L-Trp-L-Pro); LD = cyclo(L-Trp-D-Pro); DL = cyclo(D-Trp-L-Pro); DD = cyclo(D-Trp-D-Pro). Values indicated are the mean \pm s.d. of 6 experiments per day per treatment.

Urea production measured in culture media of hepatocytes after 4 hrs exposure to benorylate, a potent antirheumatic agent, at concentrations varying from 1.5×10^{-7} to 1.5×10^{-3} M diminished the rate of urea production by 20%, while impacina, a liver protective drug, produced no adverse effects on urea production (Castell *et al.*, 1985). In

the presence of 10^{-3} M ibuprofen, 5×10^{-4} M flurbiprofen and 2×10^{-4} to 4×10^{-4} M butibufen, urea production was significantly decreased after hepatocytes were exposed for a period of 24 hrs, indicating an inhibition of ureogenesis (Castell *et al.*, 1988).

Free albumin concentration may decrease due to binding to drugs or as a result of decreased protein synthesis (Marshall, 1997. Pp. 203-4). As a result, free drug concentration may increase which may increase toxicity risks. In addition, Ca^{2+} -homeostasis may be disrupted by changes in protein synthesis (Orrenius *et al.*, 1989). Decreased protein synthesis is one of the earliest and most sensitive signs of cellular hepatocytes damage (Castell *et al.*, 1997). After a 24 hr exposure (Figure 5.20) to the isomers and isoniazid, the levels of albumin in the serum were significantly decreased in comparison to the control value ($p < 0.05$), indicating decreased protein synthesis and hepatocyte damage. Cyclo(D-Trp-L-Pro) produced the largest decrease in albumin synthesis ($p = 0.0286$). However, after 5 days (Figure 5.20), the serum levels of albumin in all the treated-groups had decreased, including that of the control group, with only cyclo(D-Trp-D-Pro) differing significantly from the control sample ($p = 0.0286$). From the results, it is clear that the compounds (including isoniazid) resulted in an initial decrease in protein synthesis, with no significant effects noted over a longer period (5 days).

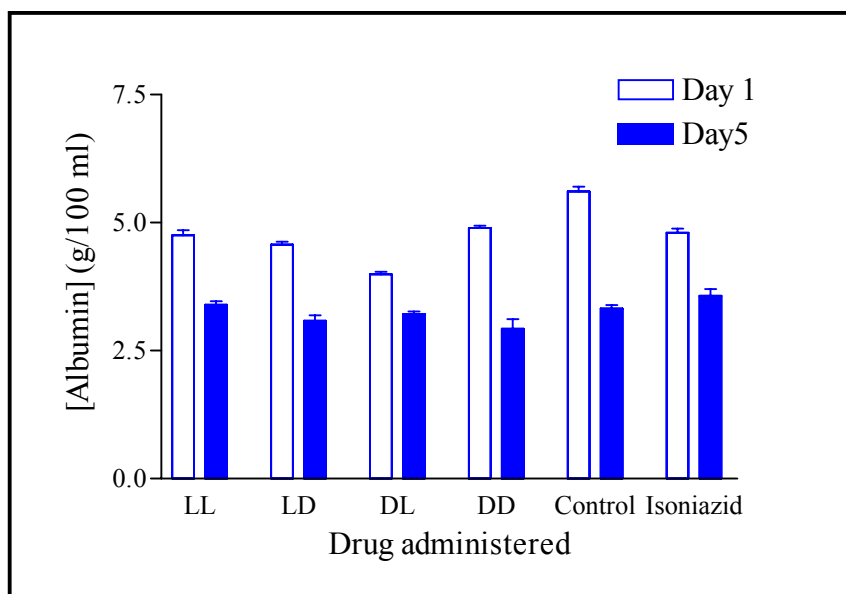


Figure 5. 20: Effects of the compounds on protein synthesis, as measured by albumin concentrations in the blood stream. LL = cyclo(L-Trp-L-Pro); LD = cyclo(L-Trp-D-Pro); DL = cyclo(D-Trp-L-Pro); DD = cyclo(D-Trp-D-Pro). Values indicated are the mean \pm s.d. of 6 experiments per day per treatment.

No changes in total protein content were noted when rats were treated with the endotoxin isolated from *K. pneumoniae* ($p > 0.05$) (Nadai *et al.*, 1998). Interestingly, impacina was capable of stimulating albumin synthesis at a concentration of 10^{-5} M. A 25% increase ($p < 0.05$) in albumin synthesis was noted between 3-4 hrs exposure of the cells to impacina. The use of impacina in liver patients was thus suggested, since the increase in plasma protein content would result in a sensible edema reduction (Castell *et al.*, 1985).

If any abnormalities occur at a hepatocellular level, it may result in defective bilirubin transport to the cell, defective conjugation or defective excretion into bile canaliculi (Baron, 1982. Pp. 192-3), resulting in increased bilirubin levels in the liver. This may be as a direct result of a disruption in cellular anabolic processes caused by a decrease in ATP production (Castell *et al.*, 1997). After 24 hrs, significantly increased bilirubin levels were obtained for rats treated with cyclo(L-Trp-L-Pro) ($p = 0.0427$) and cyclo(D-Trp-D-Pro) ($p = 0.0286$); no difference for isoniazid ($p = 0.6599$) and cyclo(L-Trp-D-Pro) ($p < 0.999$), while cyclo(D-Trp-L-Pro) showed significantly decreased levels ($p < 0.05$) in comparison to the control group (Figure 5.21). From day 1 to day 5, significantly increased levels were noted for cyclo(L-Trp-D-Pro) and cyclo(D-Trp-L-Pro) ($p < 0.05$);

significantly decreased levels for cyclo(L-Trp-L-Pro) and cyclo(D-Trp-D-Pro) ($p < 0.05$) while no significant changes in bilirubin concentration was noted for both the control ($p = 0.6625$) and isoniazid-treated ($p = 0.7722$) groups.

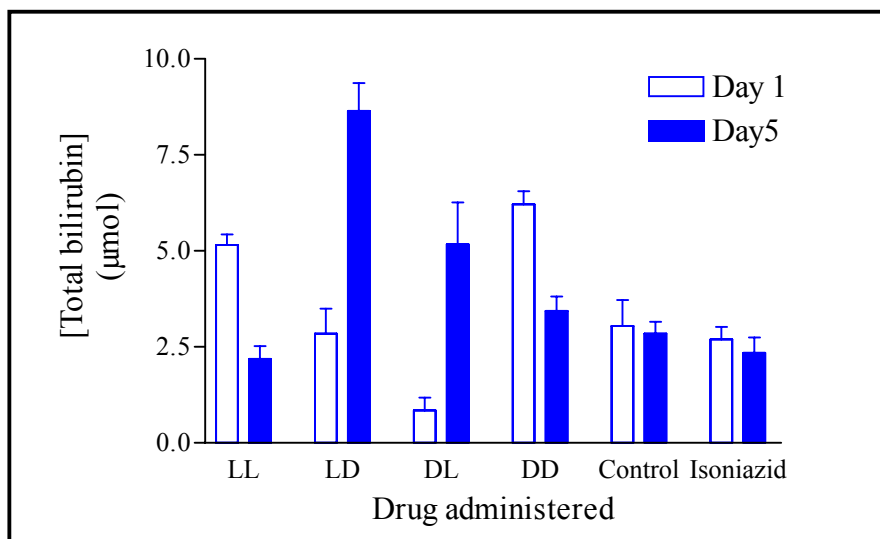


Figure 5. 21: Effects of the compounds on the total bilirubin content in the blood stream. LL = cyclo(L-Trp-L-Pro); LD = cyclo(L-Trp-D-Pro); DL = cyclo(D-Trp-L-Pro); DD = cyclo(D-Trp-D-Pro). Values indicated are the mean \pm s.d. of 6 experiments per day per treatment.

On day 5 (Figure 5.21), significantly increased levels of bilirubin were noted for cyclo(L-Trp-D-Pro) and cyclo(D-Trp-L-Pro) ($p < 0.05$) while significantly decreased levels were observed for cyclo(L-Trp-L-Pro) ($p = 0.0427$) in comparison to the control sample. These increases in bilirubin content in the bloodstream indicate that no blockage of bile canaliculi occurred.

5.5 CONCLUSIONS

Approximately 60% of the isomers are bound by BSA (Table 5.3), effectively taking them out of circulation in the bloodstream, with an average 2.4 drug bound per mole of albumin (Table 5.4). The isomers were maximally absorbed into the bloodstream within 30 min (Figure 5.5), after which the concentrations decreased, possibly as a result of BSA binding (Table 5.3).

A summary of the effects of the isomers and isoniazid on liver metabolism is tabulated in Table 5.6.

Table 5. 6 : A summary of the effects of the isomers and isoniazid on liver metabolism. Significant changes indicated show alterations that would adversely affect liver metabolism.

Function	LL		LD		DL		DD		Isoniazid	
	1	5	1	5	1	5	1	5	1	5
<i>In vitro</i> cytotoxicity on isolated rat hepatocytes	+++		+++		+++		++		-	
Chang liver cells	+++		++		+		+++		+	
N-2-alpha cells	+		+		-		+		++	
Hepato-specificity	No		No		Yes		No		No	
Day Number	1	5	1	5	1	5	1	5	1	5
↑/↓ Liver weights	✓	✗	✗	✗	✓	✓	✗	✓	✗	✗
↑ [LDH]	✓	✓	✓	✓	✓	✗	✓	✗	✓	✗
↑ [AP]	✗	✗	✓	✗	✗	✓	✓	✗	✓	✓
↑ [AST]	✗	✗	✗	✗	✗	✗	✗	✗	✗	✓
↑ [ALT]	✗	✓	✗	✓	✓	✓	✓	✓	✗	✓
↑ Lipid peroxidation	✓	✓	✗	✓	✓	✓	✓	✓	✗	✓
↓ [ATP]	✗	✗	✓	✗	✓	✗	✓	✗	✗	✗
↑/↓ [Ca ²⁺]	✓	✓	✓	✓	✗	✓	✗	✓	✗	✗
↓ [GSH]	✗	✗	✗	✗	✗	✗	✗	✗	✓	✗
↑ Ureogenesis	✗	✓	✗	✓	✓	✓	✓	✗	✓	✗
↓ Protein synthesis	✓	✗	✓	✗	✓	✗	✓	✗	✓	✗
↑ [Total bilirubin]	✓	✗	✗	✓	✗	✓	✓	✗	✗	✗

LL = cyclo(L-Trp-L-Pro); LD = cyclo(L-Trp-D-Pro); DL = cyclo(D-Trp-L-Pro); DD = cyclo(D-Trp-D-Pro)

- = No adverse effect on cell viability

+ = A decrease in cell viability by 20-35 %

++ = A decrease in cell viability by 36-45 %

+++ = A decrease in cell viability by 46-65 %

✗ = No significant change

✓ = Significant change

As can be seen from the summary of results, it is difficult to predict the effect of any of the isomers on the different metabolic and physiological parameters measured. It is however clear that isoniazid exerts its cytotoxic effect by producing lipid peroxidation. Only cyclo(D-Trp-L-Pro) is hepatocyte-specific in its cytotoxicity while cyclo(L-Trp-L-Pro), cyclo(L-Trp-D-Pro) and cyclo(D-Trp-D-Pro) are cytotoxic for other cell types too.

CHAPTER 6

HAEMATOLOGICAL STUDIES

6.1 INTRODUCTION

Blood, the only liquid connective tissue, consists of plasma and various cells and cell fragments. It has three general functions, including the transportation of O₂ from lungs to body cells, and CO₂ from the cells to lungs. Nutrients, hormones, heat and waste products are also transported. Water content of the cells and pH are regulated, as well as body temperature. Protective functions include formation of blood clots to prevent excessive blood loss. White blood cells, transported by blood, carry out phagocytosis and produces antibodies. Protection against disease is also achieved by carrying interferons and complement proteins (Tortora and Grabowski, 2000. Pp. 610-11). Bleeding and thrombosis are distorted states of haemostasis. Thrombus formation is resultant of stimulated haemostasis, while impaired haemostasis results in spontaneous bleeding (O'Reilly, 1989).

6.1.1 Platelets

Platelets are disc-shaped, 4 µm in diameter and approximately 1 µm thick. The life span of a platelet ranges from 9 to 12 days, after which they are removed from circulation by phagocytes, especially in the spleen (Martini, 1995. Pg. 667). The average concentration of platelets is 350 000/µl of circulating blood. One third of these platelets are held in reserve in the spleen and other vascular organs, and are mobilized when a circulatory crisis occurs e.g. severe bleeding (Martini, 1995. Pg. 669).

Excessive platelet destruction or insufficient production leads to abnormally lowered platelet counts (80 000/µl or less), a condition called thrombocytopaenia (Bessman, 1989). Excessive platelet formation as a result of infection, inflammation or cancer may increase platelet concentration to above 1000000/µl – this condition is referred to as

thrombocytosis. Platelets function to transport chemicals necessary for the clotting process; to form a temporary platelet plug in the wall of the damaged blood vessel; and to contract after clot formation to reduce the size of the break in the wall (Martini, 1995. Pg. 670).

6.1.1.1 Counting of platelets

Various methods are employed to count platelets, including phase microscopy, electronic particle analyzers and Coulter counter-type semi-automated platelet counters. Phase microscopy involves the use of a haemocytometer, although duplicate errors in counting may be as much as 23%. This method is only used for lack of a better automated one (Bessman, 1989).

Platelet counts using the photometric method are limited by the number of samples that can be analyzed simultaneously. This increase in time before sampling results in altered properties of a sample, making proper interpretation of results difficult. A major disadvantage of using an aggregometer is that inconsistent results are obtained as a result of varying time lapses between blood collection and experimentation. In addition, as the number of donors and agonists or inhibitors is increased, use of the aggregometer becomes very time consuming. Employing a microplate reader allows up to 96 samples to be analyzed simultaneously (Walkowiak *et al.*, 1997)

6.1.2 Haemostasis

The process of haemostasis is a series of steps that prevent the loss of blood through the walls of ruptured vessels. This process must be quick, localized and controlled. Blood loss is reduced by three mechanisms: (a) vascular spasm; (b) platelet plug formation; and (c) blood coagulation (Tortora and Grabowski, 2000. Pg. 622). This is then followed by (d) clot retraction and (e) fibrinolysis.

(a) Vascular spasm

If the wall of a blood vessel is damaged, smooth muscle fibres in the vessel wall are triggered to contract, thereby decreasing vessel diameter at the site of injury (Figure 6.1).

A number of changes in the endothelium occur during this phase. The basement membrane of the vessel wall is exposed to the bloodstream by contraction of the endothelial cells. Chemical factors, such as ADP, tissue factor and prostacyclin, are released along with endothelins. These peptide hormones activate smooth muscle contraction, thereby promoting vascular spasms. Endothelial cells, smooth muscle fibres and fibroblasts are stimulated to divide, thereby accelerating the repair process. The membranes of the endothelial cells become sticky (Martini, 1995. Pg. 671).

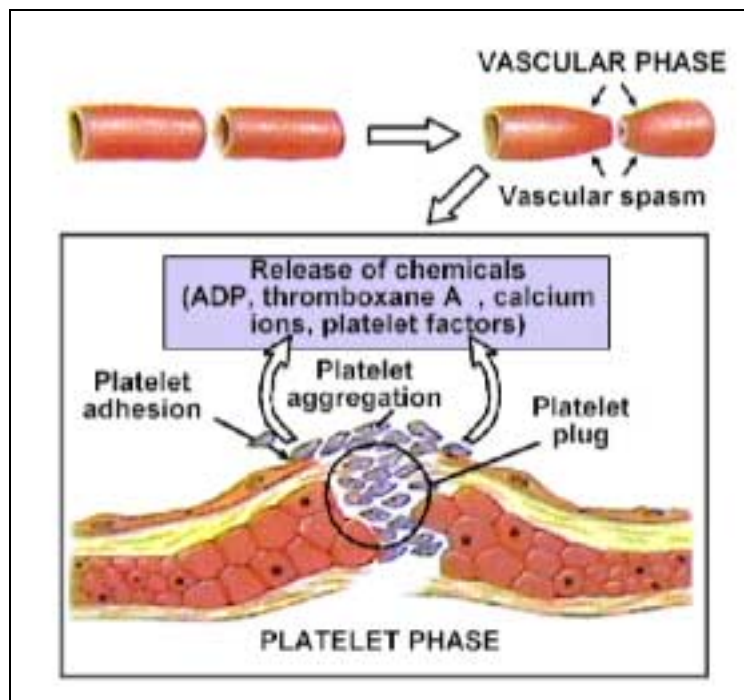


Figure 6. 1: The vascular and platelet phases of haemostasis (Martini, 1995. Pg. 671).

(b) The platelet phase

Unstimulated platelets are disc-shaped. The platelets contact and attach to the sticky endothelial surfaces, the basement membrane as well as exposed collagen fibres. This process is referred to as platelet adhesion (Figure 6.1). A platelet plug is formed as more and more platelets arrive at the site of injury and aggregate (Figure 6.1). Once adhesion occurs, platelets become activated. Adhesion is receptor-mediated, as platelets possess receptors for proteins such as collagen, fibrinogen, sialic acid-containing glycoproteins, laminin, and vitronectin. ADP, collagen and thrombin, which are physiological platelet

agonists, are capable of activating stimulus-response coupling pathways that enhance either the amount or the ligand affinity of specific adhesion receptors. The platelets become spherical in shape and develop cytoplasmic processes that enable them to interact with other platelets. Thromboxanes and prostaglandins are formed and membrane sites are made available that participate in two steps of the intrinsic coagulation pathway (Mustard *et al.*, 1989). The contents of their granules are released in a process called the platelet-release reaction (Figure 6.1). Two types of granules occur: alpha granules and dense granules (Tortora and Grabowski, 2000. Pg. 622). Alpha granules include clotting factors, as well as platelet-derived growth factor (PDGF) and dense granules contain ADP, ATP, Ca^{2+} and serotonin.

ADP stimulates platelet aggregation by binding to aggregin. Once bound, activation of adenylate cyclase results, which in turn activates cAMP that stimulates a number of cytoplasmic enzymes. ADP release makes other platelets sticky, causing them to attach to originally activated platelets (Martini, 1995. Pg. 671).

Thromboxane A_2 activates nearby platelets and function as a vasoconstrictor, enhancing the vascular spasm that decreases blood flow through the damaged vessel (Tortora and Grabowski, 2000. Pg. 622).

Serotonin acts with thromboxane A_2 to stimulate vasoconstriction. Ca^{2+} , needed for platelet aggregation and the clotting process, is also released. Procoagulants and PDGF are also released (Martini, 1995. Pg. 672). Initially the platelet plug formed is loose. During clotting, it is reinforced by fibrin threads and becomes quite tight.

(c) Blood coagulation

The process of gel formation is called coagulation, which results in the formation of fibrin threads. Several coagulation factors are involved in clotting. Each coagulation factor activates the next one in a specific sequence, resulting in a complex cascade of reactions (Tortora and Grabowski, 2000. Pg. 623).

The coagulation factors include Ca^{2+} and eleven different proteins. These enzymes are released as inactive proenzymes. The procoagulation factors are listed in Table 6.1.

Ca^{2+} is also referred to as factor IV. With the exception of factors III, IV, VIII, all procoagulation factors are synthesized in the liver. During the platelet phase, factors III, IV, V, VIII and XIII are released by activated platelets. During coagulation, proenzymes interact, creating enzymes that interact with second proenzymes, and so forth, in a cascade (Figure 6.2). This cascade is divided into the extrinsic, intrinsic and common pathways (Martini, 1995. Pg. 672).

Table 6.1: Procoagulation factors (Tortora and Grabowski, 2000. Pg. 626).

Number	Name(s)	Source	Pathway(s) of activation
I	Fibrinogen	Liver	Common
II	Prothrombin	Liver	Common
III	Tissue factor (thromboplastin)	Damaged tissue and activated platelets	Extrinsic
IV	Ca^{2+}	Diet, bones, and platelets	All
V	Proaccelerin, labile factor	Liver and platelets	Extrinsic and intrinsic
VII	Proconvertin	Liver	Extrinsic
VIII	Antihemophilic factor	Platelets and endothelial tissue	Intrinsic
IX	Christmas factor	Liver	Intrinsic
X	Stuart-Prower factor, thrombokinase	Liver	Extrinsic and intrinsic
XI	Plasma thromboplastin antecedent	Liver	Intrinsic
XII	Hageman factor, contact factor	Liver	Intrinsic
XIII	Fibrin-stabilising factor	Liver and platelets	Common

(i) The extrinsic pathway

Once tissue factor (TF) is released by damaged endothelial cells or peripheral tissue, the extrinsic pathway begins. It occurs rapidly. TF combines with Ca^{2+} and factor VII to form factor III (tissue thromboplastin). Ultimately, factor X is activated (Figure 6.2), which then combines with factor V to produce prothrombinase. This reaction occurs in the presence of Ca^{2+} . This marks the completion of this pathway (Tortora and Grabowski, 2000. Pg. 625).

(ii) The intrinsic pathway

This pathway occurs more slowly than the extrinsic pathway. When proenzymes come into contact with exposed collagen fibres at the site of injury, the intrinsic pathway is activated (Figure 6.2). Factor XII is activated, resulting in a series of reactions involving factors VIII, IX and XI, which ultimately result in the activation of factor X. The intrinsic pathway is completed when active factor X combines with factor V, forming active prothrombinase (Martini, 1995. Pg. 673).

(iii) The common pathway

The common pathway follows prothrombinase formation. Prothrombinase, in conjunction with Ca^{2+} , catalyses the activation of prothrombin to thrombin (Figure 6.2). In the presence of Ca^{2+} , thrombin converts soluble fibrinogen to insoluble, loose fibrin threads. Factor XIII is also activated by thrombin, which reinforces and stabilizes the fibrin threads into a strong clot (Tortora and Grabowski, 2000. Pg. 625).

Two positive feedback effects for thrombin exist (Figure 6.2). The first loop involves factor V, which increases the rate at which prothrombinase is formed. Prothrombinase thus increases thrombin production and so forth. Secondly, thrombin may activate platelets, reinforcing the aggregation and platelet phospholipid release (Tortora and Grabowski, 2000. Pg. 625).

Inhibition or removal of procoagulants restricts the coagulation process. Several enzymes called anticoagulants are contained in normal plasma. Antithrombin III inactivates factors

XII, XI, IX, X and II (Tortora and Grabowski, 2000. Pg. 627). Mast cells and basophils release heparin that binds to antithrombin III, thereby increasing its effectiveness. Thrombomodulin, secreted by endothelial cells, binds to thrombin. Once bound, thrombin is converted to the anticoagulant. Once bound, protein C is activated. Protein C inactivates factors V and VIII and stimulates plasmin formation. Plasmin acts by breaking down fibrin strands. Platelet adhesion and release is inhibited by prostacyclin, which opposes the action of thrombin, ADP and thromboxane A₂. Alpha-2-macroglobin, a plasminogen activator, inhibits thrombin and plasmin, while alpha-1-antitrypsin inactivates factor XI (Martini, 1995. Pg. 674).

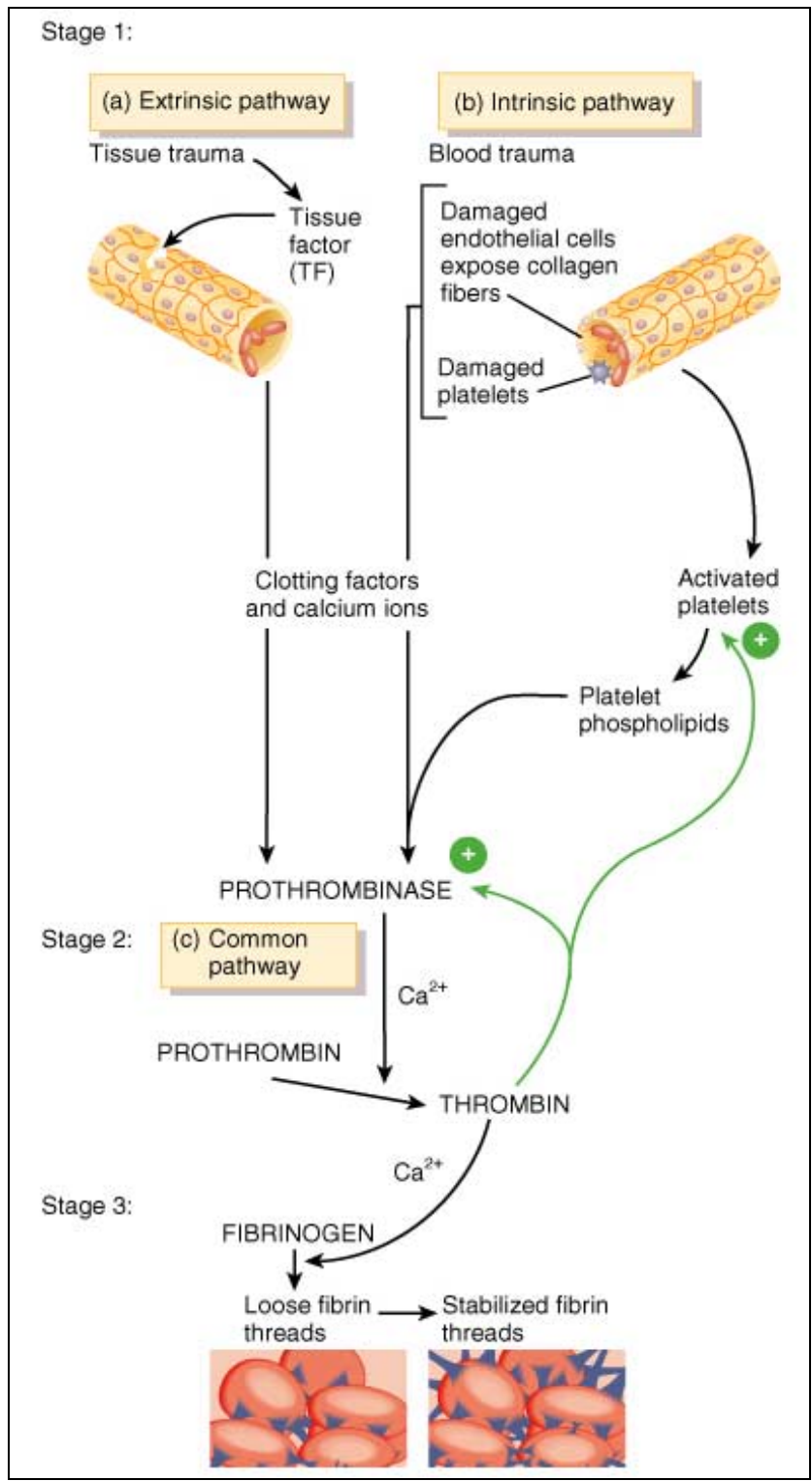


Figure 6. 2: The blood coagulation cascade, showing the extrinsic, intrinsic and common pathways. The green arrows indicate the positive feedback effects of thrombin (Tortora and Grabowski, 2000. Pg. 625).

All three pathways require Ca^{2+} , thus any decrease in Ca^{2+} -concentration will impair blood coagulation. Vitamin K is required by the liver for the synthesis of factors II, VII, IX and X. Vitamin K is a fat-soluble vitamin, absorbed from the large intestine along with lipids. If there is a deficiency of vitamin K, the common pathway will be adversely affected, resulting in inactivation of the clotting system (Martini, 1995. Pg. 674).

(d) Clot retraction

Once a fibrin meshwork occurs, platelets and red blood cells adhere to the strands. The platelets contract, pulling the fibrin thread with them, resulting in clot retraction (syneresis). The torn edges of the damaged vessel are pulled closer together, stabilizing the injury site and reduces the risk of further damage. The size of the injury is thus reduced, making repair easier (Martini, 1995. Pg. 675).

(e) Fibrinolysis

The clot will gradually dissolve as the repair proceeds. Fibrinolysis is initiated by the activation of plasminogen by thrombin and tissue plasminogen activator. Plasminogen is activated to form plasmin, that dissolves fibrin strands and inactivates factors I, II, V, VIII and XII (Tortora and Grabowski, 2000. Pg. 627).

6.1.3 Disorders of haemostasis

Uncontrolled bleeding may result from the synthesis of insufficient platelet numbers, defective platelets or absence of functional coagulation factors (Russell *et al.*, 1982. Pg. 125).

Herpes simplex virus-infected (HSV-infected) endothelial cells express a virus-encoded membrane glycoprotein C receptor, which binds factor X. This results in increased procoagulant activity. HSV-infected endothelial cells are a major risk for vascular injury and atherosclerotic disease. Thrombin generated under these conditions mediate fibrin formation and also acts as a potent leukocyte chemoattractant and increases monocyte attachment to viral-infected endothelium. This leads to vascular injury and monocyte

accumulation in arterial intima, increasing the risk of atherosclerotic risk (Altieri, 1997. Pp. 51-2).

Central to all thromboembolic disease is the platelet. In high-pressure arteries, circulating platelets adhere to the arterial wall, initially forming a white thrombus. Aggregation increases, resulting in reduced arterial flow as the thrombus enlarges. Fibrin formation is then initiated, and a red thrombus surrounding the nidus white thrombus is produced. This red thrombus forms in low-pressure veins. A long red tail is formed from the bulk of the thrombus, which consists of red blood cells enmeshed in a fibrin network. These tails detach and enter the circulation as emboli. An arterial thrombus consists primarily of the platelet nidus, while the venous thrombus is dominated by the fibrin tail. Local occlusive ischaemia is produced by arterial thrombi, while distant embolization is resultant of venous thrombi (O'Reilly, 1989).

Antithrombotic therapy is divided into 3 forms: prevention of platelet aggregation; anticoagulatory therapy and thrombolytic therapy.

In the prevention of platelet aggregation, the most effective agents are those that prevent arterial thrombosis by altering platelet properties. Agents include aspirin, sulphinpyrazone, dipyridamole and dextran. Aspirin inhibits platelet aggregation secondary to inhibition of thromboxane synthesis. Since thromboxane accelerates platelet aggregation, aspirin effectively reduces aggregation. In this way, the incidence of transient ischaemic attacks and unstable angina in men are reduced. In addition, aspirin is also known to reduce the incidence of thrombosis in coronary artery bypass grafts (Payan and Shearn, 1989). Sulphinpyrazone inhibits platelet cyclo-oxygenase, which catalyses prostaglandin G₂ synthesis from arachidonic acid (Russell *et al.*, 1982. Pg. 129). Dipyridamole reduces platelet adhesion to thrombogenic surfaces by inhibiting platelet phosphodiesterase and platelet prostaglandin production (O'Reilly, 1989).

Anticoagulant agents, used in the prevention and treatment of venous thrombosis, are administered to patients who are susceptible to blood clot formation (Tortora and

Grabowski, 2000. Pg. 627). These agents interfere with fibrin formation and do not affect platelet function. Examples of such agents include warfarin and heparin. Warfarin prevents production of functional clotting factors VII, IX, X and prothrombin. Heparin is used in haemodialysis and cardiac surgery (Russell *et al.*, 1982. Pg. 129), to prevent pulmonary emboli in patients with established venous thrombi (O'Reilly, 1989).

Agents that dissolve blood clots to restore circulation are termed thrombolytic agents. Thrombolytic agents act to increase fibrin dissolution, either directly or indirectly. Streptokinase is isolated from haemolytic streptococci, while urokinase is purified from male urine. Streptokinase binds to plasminogen, which then undergoes conformational changes. Other plasminogen molecules are activated, which leads to rapid plasmin production. When plasmin binds to fibrin, the thrombus is dissolved. Urokinase activates plasminogen by cleaving two peptide bonds within the molecule (Russell *et al.*, 1982. Pg. 129).

Thrombocytopenia results in spontaneous bleeding all over the body from small blood vessels. Widespread haemorrhage may be caused by normal movement, forming purple patches, called petechiae, on the skin. Suppression or destruction of myeloid tissue, such as malignancy of bone marrow, exposure to ionizing radiation or certain drugs results in reduced platelet numbers. Treatment with whole blood transfusion is a temporary relief from bleeding (Marieb, 1989. Pg. 587).

Simultaneous bleeding and unregulated blood clotting and haemorrhage throughout the body characterize disseminated intravascular clotting. Spontaneous bleeding or bleeding after a minor trauma is characteristic of the inherited deficiency of clotting disorder called haemophilia. Haemophilia A is characterised by the absence of factor VIII, while a lack of factor IX is called haemophilia B. Haemophilia A and B are sex-linked recess disorders and are found primarily among males. Haemophilia C, affecting both males and females, results from the absence of factor XI. Factor XI activates factor IX, which can also be activated by factor VII. For this reason, haemophilia C is less severe than haemophilia A or B. Haemophilia is associated with traumatic subcutaneous and

intramuscular bleeding, nosebleeds, blood in urine and painful haemorrhages in the joints. Treatments include transfusion with plasma and replacement of deficient clotting factors (Tortora and Grabowski, 2000. Pg. 631).

6.1.4 Thrombosis and cancer

There is increasing evidence that a link between cancer and thrombosis exists. Many reports have described thrombosis in malignancy, which have claimed (i) deposition of fibrin in and around tumour cells; (ii) small cell lung cancer patients have an increased survival with warfarin treatment; and (iii) mortality rates of patients have decreased with heparin treatment (Arkel, 2000).

Coagulation factors V, VIII, IX and XI have been shown to be present at increased levels in malignancy. Furthermore, increased levels of the coagulation activation markers (prothrombin fragment 1.2, thrombin antithrombin and fibrinogen/fibrin degradation products) have also been noted. Protein C, protein S and antithrombin III, natural inhibitory proteins of coagulation, are decreased in some cancer patients. As a result, chemotherapy may induce thrombosis (Arkel, 2000).

It was thus hoped that the isomers show potential as antithrombotic agents, in order to eliminate any complications of thrombosis in cancer patients, as no pronounced anticancer potential was noted for the isomers (Chapter 4).

6.2 OBJECTIVES OF THE CHAPTER

6.2.1 Objectives of the present chapter

- ◆ The primary aim was to determine whether cyclo(L-Trp-L-Pro), cyclo(L-Trp-D-Pro), cyclo(D-Trp-L-Pro) and cyclo(D-Trp-D-Pro) have any effect (inhibitory or stimulatory) on platelet aggregation;
- ◆ to determine the effect of the isomers on thrombin activity; and
- ◆ to determine the effect of the isomers on adhesion to a coated artificial surface.

In order to satisfy these aims, the following experimental data was collected:

- effects of the isomers on platelet aggregation was determined using washed platelets, activated by thrombin;
- effects of the isomers on platelet aggregation was determined using platelets in suspension, activated by ADP;
- the effect of the isomers on thrombin activity was determined by following a thrombin-substrate S2238 reaction in the presence of the isomers; and
- the internal acid phosphatase activity of platelets was used in order to assess the effects of the isomers on platelet adhesion to a coated, artificial surface.

6.3 MATERIALS AND METHODS

The use of human blood for experimentation purposes was approved by the Human Ethics Committee at the University of Port Elizabeth⁵.

6.3.1 Platelet count

Isolation procedures for platelets should not stimulate the platelets, providing platelet suspensions that react to stimuli as platelets in circulation do. Anticoagulants such as heparin result in some aggregation of platelets; hirudin only blocks thrombin and no other activated coagulation factors; ethylenediaminetetraacetic acid (EDTA) adversely affects glycoproteins in the membrane that participates in aggregation. Two weeks prior to blood collection, the donor should not use drugs, as these may affect platelet reactions (Mustard *et al.*, 1989).

Fatty meals prior to experimentation (6-8 hrs) should be avoided, since the plasma will appear turbid irrespective of platelet aggregation. Contamination of plasma with red blood cells will result in decreased sensitivity, as these cells remain suspended in plasma (Zucker, 1989).

Blood was donated by a healthy donor who had abstained from medication for a minimum period of two weeks. Blood was collected in vacutainer tubes containing 0.105 M sodium citrate (BD Vacutainer Systems, Preanalytical Solutions). Aggregation of platelets is supported by citrated plasma, whereas plasma collected from EDTA-containing tubes does not support aggregation (Zucker, 1989). Platelet rich plasma (PRP) was obtained by centrifugation at 300 g for 10 min. The plasma was removed and recentrifuged at 1100 g for 15 min, to obtain a platelet pellet. The pellet was then resolubilised in buffer A⁶ (145 mM NaCl, 5 mM KCl, 10 mM HEPES, 6 mM Na₂HPO₄·12H₂O and 0.2% (w/v) BSA) to a final volume of 1 ml, after which the absorbance was adjusted to 0.220 at 540 nm. Addition of albumin to the suspension medium prevents interaction of the platelets with foreign surfaces such as glass, and

⁵ Human Ethics Approval Letter – Appendix D

⁶ Solution list – Appendix C

binds to arachidonic acid or its products that may be released from the platelets (Zucker, 1989). This solution represented the stock platelet solution. The suspension was kept at room temperature and used within the hour. A 1000 times dilution of this stock was obtained using buffer A as a diluent. The amount of platelets per ml in this sample was then counted using a Neubauer Improved Bright Line Chamber (Superior, Germany). Prior to counting, the platelets were allowed to settle on the chamber for 30 min. Several such dilutions were made and the number of platelets per ml was determined for the construction of a standard curve (Figure 6.3). The absorbance of each platelet dilution was read at 540 nm using Labsystems Multiskan MS (Multiskan Transmit Program, Rev. 1.3. (1995)).

6.3.2 Platelet aggregation

Routine coagulology studies include the simplistic and sensitive platelet aggregation test and fibrinogen clotting or cleavage tests. Use of a microplate reader has minimized variability in results due to time differences before analysis, since changes in transmission in as many as 96 samples can be monitored simultaneously. Aggregation was triggered by the addition of ADP or thrombin (Walkowiak *et al.*, 1997).

6.3.2.1 Thrombin-induced platelet aggregation

This aggregating agent acts via a primary effect, via secretion through the cyclooxygenase pathway and possibly by diacylglycerol-mediated protein kinase C activation. Thrombin is an extremely potent agonist, and is able to induce this secretion in the absence of cell-to-cell contacts (Hawiger, 1989). Effective thrombin concentrations are approximately 0.25 U/ml, since lower levels (0.15 U/ml) are negated by the presence of thrombin inhibitors found in plasma. At levels exceeding 0.25 U/ml, aggregation is followed by clotting. Washed platelets were used in order to avoid interference by components of plasma, such as thrombin inhibitors, with the assay (Zucker, 1989).

A modified method as used by Bednar *et al.* (1995) was employed. A platelet suspension, standardised to an absorbance of 0.220 at 540 nm, was prepared as described above (approximately 89.72×10^6 platelets/ml). Ten minutes prior to use, the platelet suspension

was warmed to 37°C. 75 µl of buffer A (standard curve) or 75 µl 3 mM of each isomer solution was added to a 96-well plate and prewarmed to 37°C. Once the platelet suspension had reached 37°C, 75 µl was placed into each well. A 10 min incubation period at room temperature was allowed for interaction between the isomers and platelets. For the standard curve (Figure 6.4), 75 µl of prewarmed thrombin (Sigma, St. Louis, U.S.A.) was added at stock concentrations of 3.75 U/ml, 3 U/ml, 2.25 U/ml and 1.5 U/ml to the wells, representing final concentrations of 1.25 U/ml, 1.0 U/ml, 0.75 U/ml and 0.5 U/ml. In the assay, 75 µl prewarmed thrombin at a stock concentration of 3.75 U/ml was added. This agonist was prepared fresh in buffer A, supplemented with 3 mM MgSO₄·7H₂O and 3 mM CaCl₂ (Buffer B). The reaction was followed over a 60 min period at 410 nm using Labsystems Multiskan MS (Multiskan Transmit Program, Rev. 1.3. (1995)). Between readings, the plate was maintained at 37°C. Percentage transmission was calculated using the absorbance obtained for platelet poor plasma (PPP) (150 µl buffer A and 75 µl buffer B) as 100% transmission. Zero percent transmission was obtained by the absorbance of PRP (75 µl PRP, 75 µl buffer A and 75 µl buffer B). As cyclo(L-Trp-D-Pro) was the only isomer to show any activity, a dose-response curve was also obtained at the following stock concentrations: 0.375 mM, 0.75 mM and 1.5 mM, using the method as described above.

6.3.2.2 ADP-induced platelet aggregation

ADP causes platelet aggregation at 37°C, resulting in secretion that is dependent on low Ca²⁺-concentrations in citrated plasma. No secretion occurs at physiological ionized Ca²⁺-levels and close contact between platelets is needed before secretion can be initiated (Hawiger, 1989). Platelet aggregation with ADP is readily lost with isolated platelets; therefore PRP was used for the assay. A minimal response to ADP is noted when it is applied to washed platelets (Zucker, 1989).

A modified version of the method employed by Bednar *et al.* (1995) was used. The assay was performed as the thrombin assay (Section 6.3.2.1), with the following modifications. Platelets in suspension were used. PPP was obtained by centrifugation at 1100 g for 15 min. For the standard curve (Figure 6.7), 100 µl PRP and 10 µl distilled H₂O (dH₂O) was

added to a 96-well plate, which was then incubated at 37°C for 10 min. After the incubation period, 10 µl ADP (Boehringer Mannheim, Darmstadt, Germany) at stock concentrations of 5 µM, 10 µM, 15 µM, 25 µM and 50 µM, representing final concentrations of 0.417 µM, 0.833 µM, 1.25 µM, 2.08 µM and 4.167 µM, respectively, were added to the wells. The reaction was followed at 540 nm for 65 min. Percentage transmission was calculated using the absorbance obtained for PRP (100 µl PRP and 20 µl dH₂O) as 0% transmission. One hundred percent transmission was obtained from the absorbance of PPP (100 µl PPP and 20 µl dH₂O). In the case of the isomer assays, the method was followed as described, with the following changes: 10 µl of 0.125 mg/ml, 0.25 mg/ml, 0.5 mg/ml or 1 mg/ml isomer solution (final concentrations) was added to the plate instead of 10 µl dH₂O. The 10 µM ADP solution was used in the assay, which was followed over a 30 min period at 540 nm.

6.3.3 Thrombin assay

Thrombin, a serine protease with a M_r of 36 000, catalyses the conversion of the plasma glycoprotein fibrinogen to fibrin in the presence of Ca^{2+} , effectively ending the coagulation process (Tortora and Grabowski, 2000. Pg. 625).

A modified method as employed by Rob *et al.* (1997) was used to determine the direct effects of the isomers on thrombin activity. 10 µl of a thrombin solution at 50 U/ml, 40 U/ml, 30 U/ml 20 U/ml and 10 U/ml were added to a 96-well plate. 50 µl buffer containing 50 mM Tris-HCl (pH 8.4), 7.4 mM EDTA and 175 mM NaCl was added. 190 µl 0.456 mM substrate S2238 (H-D-Phe-Pip-Arg-NH- ϕ -NO₂·2HCl) (Chromogenix Instrumentation Lab., SpA, Sweden) was added and the reaction was followed every 10 sec for 5 min at 410 nm using Labsystems Multiskan MS (Multiskan Transmit Program, Rev. 1.3. (1995)). In the assay containing the isomers, 10 µl 30 U/ml thrombin was added to each well. 50 µl of each isomer at 3 mM, 1 mM, 0.5 mM, and 0.25 mM was added. A 10 min incubation period at room temperature was allowed for the interaction between the enzyme and the isomers to occur. 190 µl of the substrate was then added and the reaction followed every 10 sec for 5 min at 410 nm using Labsystems Multiskan MS (Multiskan Transmit Program, Rev. 1.3. (1995)). The change in

absorbance per min was determined to obtain progress curves (Figures 6.11-6.14). The change in absorbance over the linear portion of the curve was then determined and plotted against the molar ratios of thrombin:isomer at the different concentrations of isomer tested, to determine any significant effects.

6.3.4 Platelet adhesion

The *in vivo* use of artificial materials is limited by platelet adhesion and subsequent thrombus formation. Individual platelet adherence to a surface is dependent on receptor-mediated recognition of specific sites or chemical moieties on absorbed proteins. Platelet adhesion is enhanced when some proteins e.g. γ -globulin, fibrinogen and von Willebrand factor, are preabsorbed on surfaces. Platelet adhesion and thrombogenesis are minimized by albumin. It was found that the amount of fibrinogen on the surface dictates the platelet adhesion and aggregation in some *in vitro* and *in vivo* experiments (Park *et al.*, 1989).

The method as employed by Bellavite *et al.* (1994) was used. This method makes use of the internal acid phosphatase activity contained in platelets as a marker of platelet number. Citrated plasma was obtained by centrifugation of blood at 1100 g for 15 min. A 1:1 dilution of the plasma with PBS (pH 7.4) was made. 100 μ l of this diluted plasma was placed into a 96-well plate and incubated overnight at 4°C. Before use, the plate was washed twice with saline.

PRP was obtained by centrifugation of blood at 300 g for 10 min. The PRP was pooled and recentrifuged at 1100 g for 15 min to obtain a platelet pellet. This pellet was then resuspended in buffer A and adjusted to 1 966 000 platelets/ml.

6.3.4.1 Adhesion in the presence of ADP

25 μ l ADP at 100 μ M, 50 μ M, 25 μ M and 12.5 μ M was added to the plate. After the addition of 25 μ l buffer B, the plate was warmed to 37°C. 50 μ l prewarmed platelet suspension was added to the plate. The plate was then incubated at 37°C for 1 hr. After the incubation period, the plate was washed twice with PBS (pH 7.4). Excess PBS was removed from the plate by inversion and gentle shaking. The wells were then

supplemented with 150 μ l 0.1 M citrate buffer (pH 5.4), containing 5 mM *p*NPP (Sigma, St. Louis, U.S.A.) and 0.1% Triton X-100 (Sigma, St. Louis, U.S.A.). An incubation period at room temperature for 1 hr followed. The colour was then developed by the addition of 100 μ l 2 N NaOH. The *p*-nitrophenol produced by this reaction was read at 410 nm using Labsystems Multiskan MS (Multiskan Transmit Program, Rev. 1.3. (1995)) after a 5 min incubation period at room temperature. The control consisted of 150 μ l citrate buffer and 100 μ l 2 N NaOH.

6.3.4.1.1 Adhesion, stimulated by ADP, in the presence of the isomers

The reaction as described in Section 6.3.4.1 was used, with the following changes. For this assay, 25 μ M ADP was used. Buffer B was replaced by 25 μ l of the isomers at stock concentrations of 4 mM, 2 mM, 1 mM and 0.5 mM.

6.3.4.2 Adhesion in the presence of thrombin

The method was followed as described in Section 6.3.4.1, with the following changes. Instead of ADP, thrombin was added at stock concentrations of 2.5 U/ml, 1.25 U/ml, 0.625 U/ml and 0.3125 U/ml, respectively.

6.3.4.2.1 Adhesion, stimulated by thrombin, in the presence of the isomers

The reaction was followed as described in Section 6.3.4.2, with the following changes. 0.625 U/ml Thrombin was used. Buffer B was replaced by 25 μ l of the isomers at stock concentrations of 4 mM, 2 mM, 1 mM and 0.5 mM.

6.3.5 Statistical analysis

Results are expressed as mean \pm s.d. for the indicated number of experiments. Results were analysed using the software package GraphPad Prism Version 2.0 and GraphPad InStat (GraphPad Software, Inc., San Diego, U.S.A.). All tests were performed on raw data obtained from the experiments (n=4). Paired *t* tests were used to determine the statistical significance of the effects of the isomers on aggregation and adhesion. *P* values <0.05 were accepted as evidence of a statistically significant difference. Reciprocal plots were used to determine significance of effects on thrombin activity.

6.4 RESULTS AND DISCUSSION

Thrombin, a powerful platelet agonist, stimulates shape changes, degranulation and aggregation. When thrombin interacts with its protease-activated receptor, several intracellular changes occur in the platelets, including a rapid rise in cytosolic free Ca^{2+} -concentrations (Grenegård *et al.*, 1996). In order to eliminate possible fibrin production induced by thrombin, aggregation studies were conducted on washed platelets (Sugidachi *et al.*, 2000). It should however be noted that washing of platelets always result in some degree of damage, in addition to a loss of plasma cofactors. Thus, the pharmacological behaviour of these platelets differs from the platelets in their native plasma (Cusack and Hourani, 1982).

A linear relationship exists between the number of platelets and absorbance (Figure 6.3) measured at 540 nm ($R^2=0.9912$).

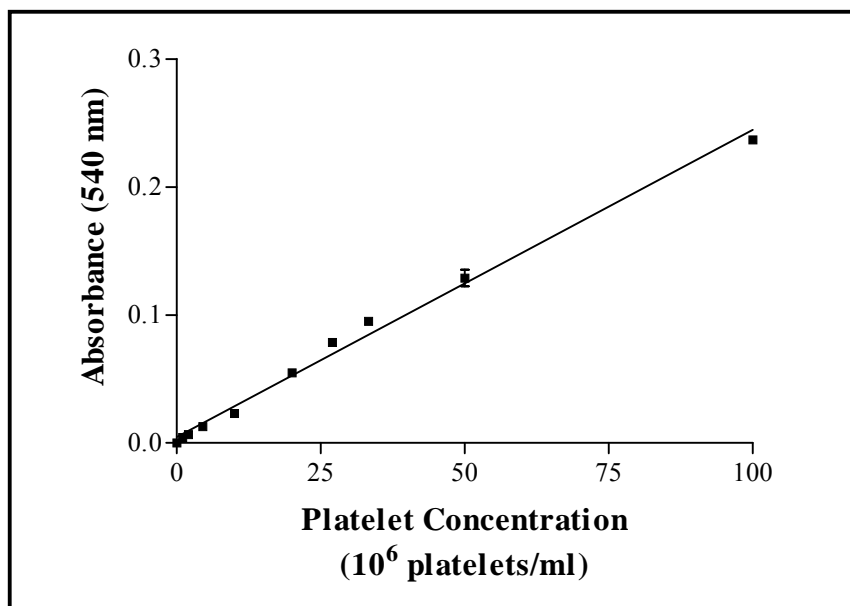


Figure 6. 3: Linear relationship between platelet number and optical density. $R^2 = 0.9912$; $y=0.0024x + 0.004669$. Values indicated are the mean \pm s.d. of quadruplicates.

Once stimulated by agonists, platelets become sticky. Suspended platelets come into contact with one another, which is visually noted by formation of visible clumps and

clearing of the suspension. Analysis of platelet aggregation was recorded by following absorbance changes throughout the reaction. Controls for 100% transmission (PPP or buffer) and 0% transmission (PRP or platelet suspension) were also monitored throughout the experiments. These absorbance values were used to convert the data obtained to % transmission, from which aggregation curves were drawn.

When platelets are exposed to picomolar concentrations of α -thrombin, immediate granule release occurs and irreversible aggregation in PRP or washed platelets in suspension supplemented with fibrinogen results. Thrombin interacts with a seven transmembrane domain functional thrombin receptor on platelets, resulting in an immediate increase in cytosolic free Ca^{2+} , inositol triphosphate generation and tyrosine kinase phosphorylation of a number of platelets proteins (Altieri, 1997. Pg. 118). A concentration-dependent increase in platelet aggregation was observed when washed platelets were exposed to various concentrations of thrombin (Figure 6.4). 1.25 U/ml Thrombin was chosen as a standard concentration, since it resulted in approximately 50% light transmission within 30 min.

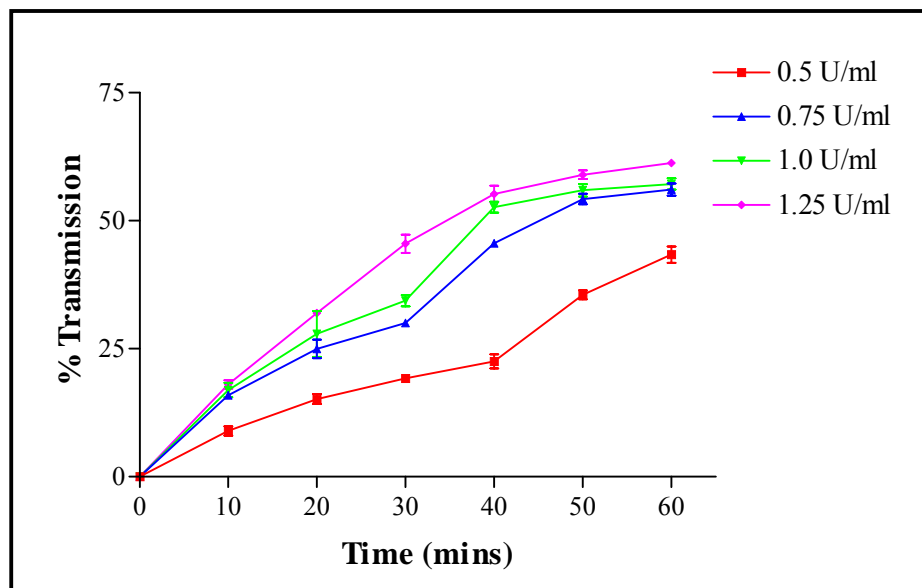


Figure 6. 4: Aggregation curves of washed platelets stimulated with varying concentrations of thrombin. Final concentrations of thrombin in the wells are indicated on the graph. Values indicated are the mean \pm s.d. of quadruplicates.

The isomers were tested at a final concentration of 1 mM (Figure 6.5). In the presence of the isomers, there is an initial decrease in light transmission. This may be as a result of platelet shape change from disc-shaped to spherical. An increase in light transmission is then noted, resultant of aggregation, as light is now able to pass through the platelet suspension (Zucker, 1989).

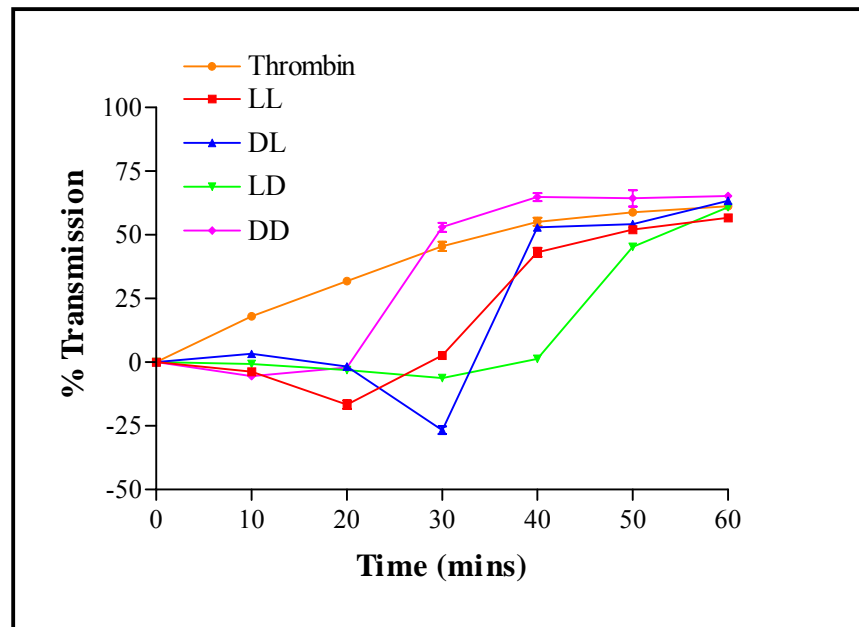


Figure 6. 5: Aggregation curves obtained when washed platelets, stimulated by thrombin at a final concentration of 1.25 U/ml, were exposed to each isomer at a final concentration of 1 mM. Values indicated are the mean \pm s.d. of quadruplicates.

Only cyclo(L-Trp-D-Pro) showed potential in inhibiting thrombin-receptor stimulated platelet aggregation significantly ($p < 0.05$). Further testing was then conducted at final concentrations of 0.125 mM, 0.25 mM and 0.5 mM cyclo(L-Trp-D-Pro) (Figure 6.6). The effect of these three concentrations on platelet aggregation induced by thrombin did not differ significantly from each other, possibly due to saturation of the receptor with the isomer. A significant decrease in aggregation was however noted when cyclo(L-Trp-D-Pro) was compared to that of 1.25 U/ml thrombin ($p < 0.05$). This indicated that 0.125 mM, 0.25 mM, 0.5 mM (Figure 6.6) and 1 mM cyclo(L-Trp-D-Pro) (Figure 6.5) were capable of decreasing thrombin-receptor stimulated aggregation. This effect could be due to the conformation of cyclo(L-Trp-D-Pro), which differs from that of cyclo(D-Trp-L-

Pro) in the orientation of the side chain of tryptophan. Cyclo(L-Trp-D-Pro) may thus be useful in the prevention of pulmonary emboli in patients with established venous thrombi, since aggregation is significantly decreased. Nonfatal myocardial infarction may also be reduced by the administration of cyclo(L-Trp-D-Pro) as a prophylaxis. Furthermore, platelets may also be inhibited, thereby resulting in a decreased risk of arterial thrombi formation (O'Reilly, 1989). The potential usage of cyclo(L-Trp-D-Pro) to decrease complications associated with thrombosis in cancer patients is also shown.

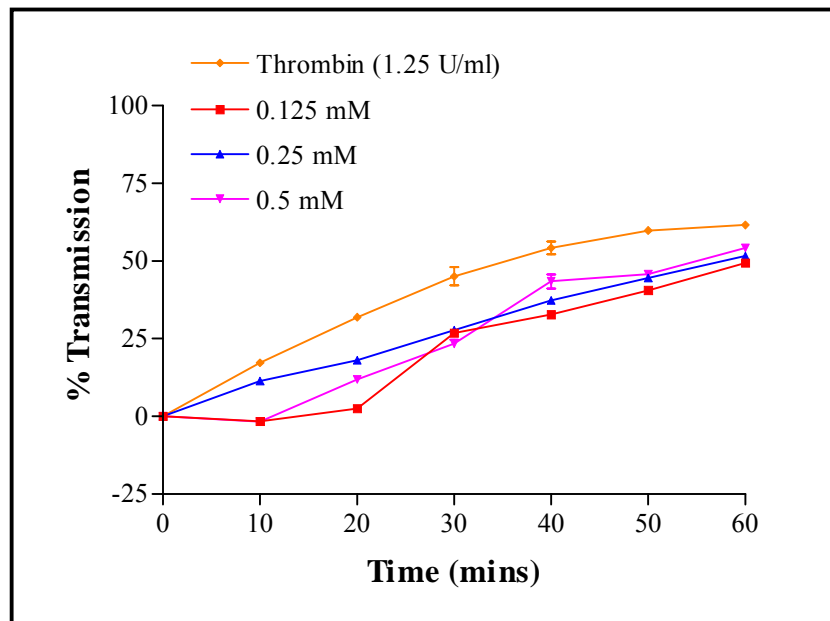


Figure 6. 6: The effect of differing concentration of cyclo(L-Trp-D-Pro) on aggregation stimulated by thrombin at a final concentration of 1.25 U/ml. Concentrations of cyclo(L-Trp-D-Pro) indicated are the final concentrations in the wells. Values indicated are the mean \pm s.d. of quadruplicates.

ADP has been recognized as a platelet-activating agent as early as the 1960s. ADP was thus implicated as an important mediator in haemostasis and thrombosis (Jarvis *et al.*, 2000). When vascular injury occurs, ADP is released from damaged cells and activated platelets into the bloodstream. This in turn acts on other platelets. A number of changes in platelets are induced by ADP, including shape change, aggregation, granule content secretion, increased cytosolic Ca^{2+} -concentrations and inhibition of stimulated adenylate cyclase (Sugidachi *et al.*, 2000).

Platelet aggregation in PRP was triggered by the addition of ADP. A standard curve was obtained by the addition of various concentrations of ADP to the suspension (Figure 6.7). A concentration-dependent increase in light transmission was observed for ADP ranging from 0.417 μM to 2.08 μM . No significant difference was noted between the aggregation curve obtained in the presence of 2.08 μM and 4.167 μM ADP ($p>0.05$).

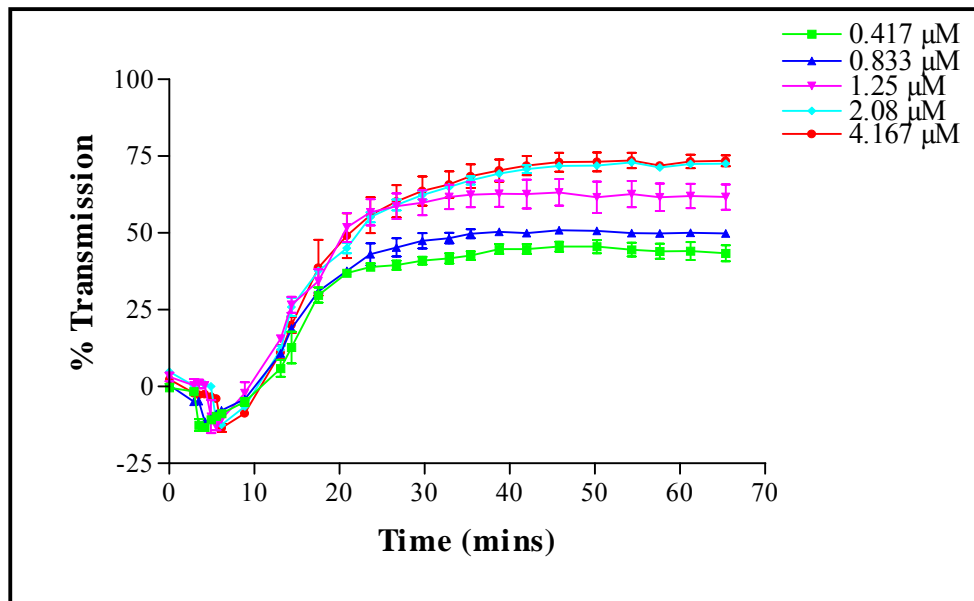


Figure 6. 7: Aggregation curves of PRP stimulated with varying concentrations of ADP. Final concentrations of ADP in the wells are indicated on the graph. Values indicated are the mean \pm s.d. of quadruplicates.

Initially, light transmission decreased (Figure 6.7) following the addition of ADP, when platelets change shape from discoid to spherical. As the platelets aggregate, there is a gradual increase in light transmission as light can now pass through the platelet suspension (Zucker, 1989).

In the assays to assess the effects of the isomers on aggregation stimulated by ADP, ADP at a final concentration of 0.833 μM was chosen, as it resulted in a $\pm 50\%$ transmission within the 65 min incubation period (Figure 6.7). The isomers were added at final concentrations of 0.125, 0.25, 0.5 and 1 mg/ml (Figure 6.8-6.11). At all concentrations tested, cyclo(L-Trp-L-Pro) resulted in approximately 32% transmission, about 10% less than ADP.

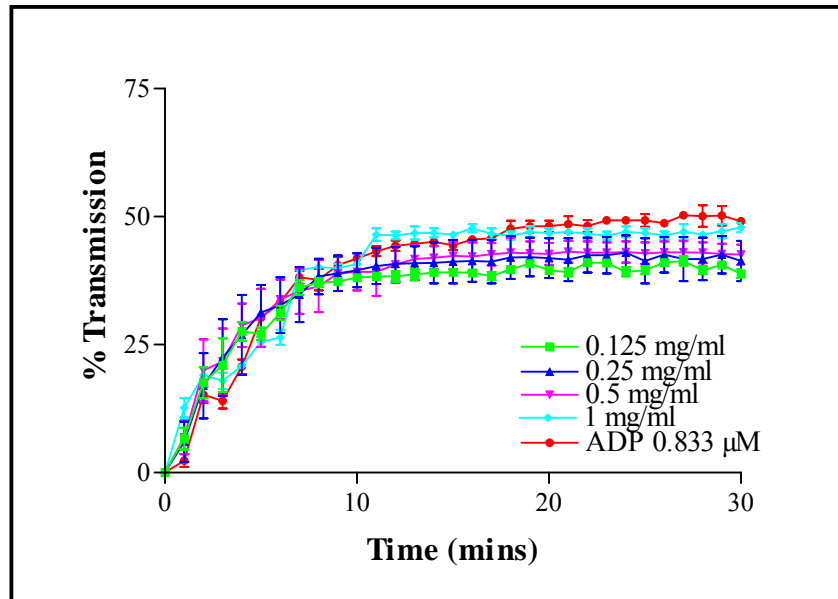


Figure 6. 8: Aggregation curves of ADP-stimulated platelets in plasma with varying concentrations of cyclo(L-Trp-L-Pro). The respective final concentrations in the wells are indicated on the graph. Values indicated are the mean \pm s.d. of quadruplicates.

Similarly, cyclo(L-Trp-D-Pro) (Figure 6.9), cyclo(D-Trp-L-Pro) (Figure 6.10) and cyclo(D-Trp-D-Pro) (Figure 6.11) resulted in approximately 45%, 45.5% and 44% transmissions, respectively. These decreases in light transmission were not significant ($p > 0.05$), indicating that the isomers did not affect aggregation of platelets induced by ADP.

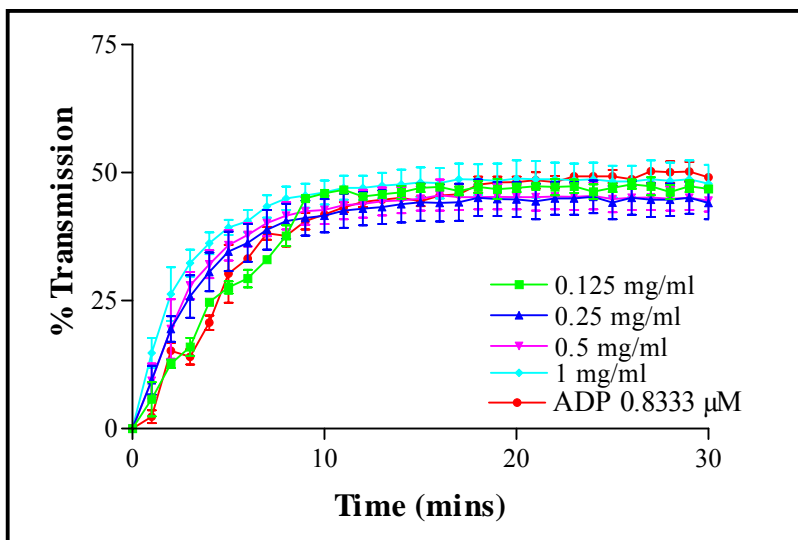


Figure 6. 9: Aggregation curves of ADP-stimulated platelets in plasma with varying concentrations of cyclo(L-Trp-D-Pro). The respective final concentrations in the wells are indicated on the graph. Values indicated are the mean \pm s.d. of quadruplicates.

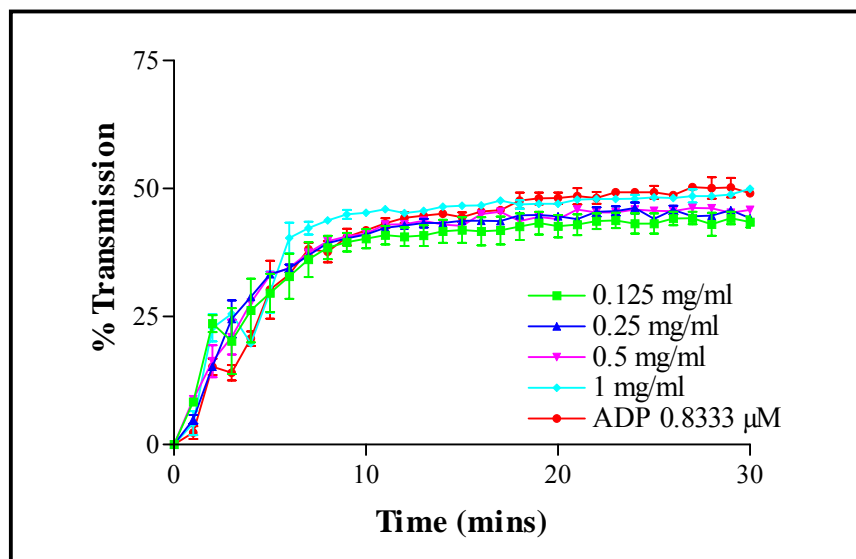


Figure 6. 10: Aggregation curves of ADP-stimulated platelets in plasma with varying concentrations of cyclo(D-Trp-L-Pro). The respective final concentrations in the wells are indicated on the graph. Values indicated are the mean \pm s.d. of quadruplicates.

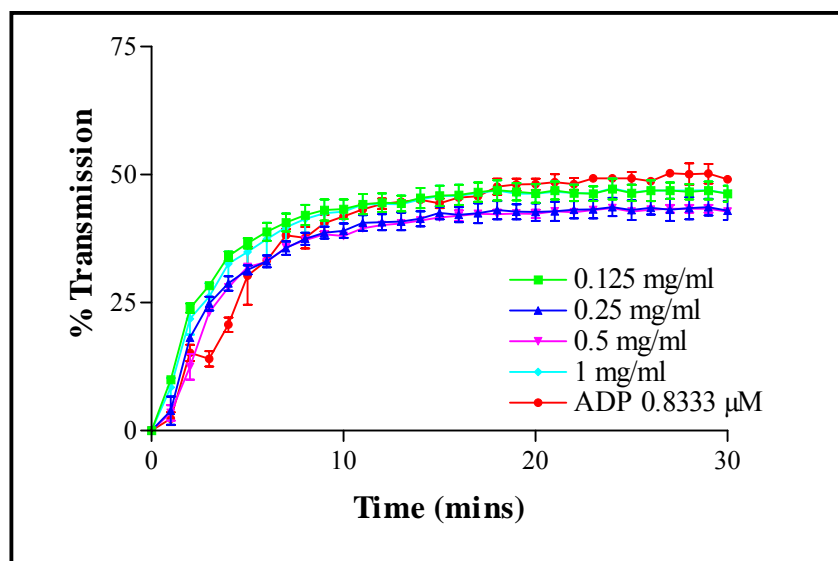


Figure 6. 11: Aggregation curves of ADP-stimulated platelets in plasma with varying concentrations of cyclo(D-Trp-D-Pro). The respective final concentrations in the wells are indicated on the graph. Values indicated are the mean \pm s.d. of quadruplicates.

The shapes of the aggregation curves observed in the presence of ADP and thrombin are characteristic of each agonist and compares well with those obtained by Bednar *et al.* (1995).

Similar research conducted by other researchers will now be discussed. 5-Hydroxytryptamine (HT) ($M_r = 176.26$), a major product of platelet aggregation contains an indole ring. 10 μ M 5-HT resulted in a significant increase in platelet aggregation in the presence of either 0.1 μ M ADP ($p < 0.01$) or 1 μ g/ml collagen ($p < 0.01$). 1 μ M U-46619 (9,11 dideoxy-11 α ,9 α -epoxymethano-prostaglandin $F_{2\alpha}$), a thromboxane A_2 mimetic, significantly increased this response to ADP and collagen in rat blood. With a M_r of 350.5, it is larger than the isomers. Blood was then collected from rats that had previously received 1 mg/kg ICI 170,809 (2-2-[dimethylamino-2-methylpropylthio]-3-phenylquinoline hydrochloride), a 5-HT $_2$ antagonist or 1 mg/kg/min ICI 192,605 (4(Z)-6-(2,4,5 *cis*)[2-chlorophenyl]-4-(2-hydroxyphenyl)1,3-dioxan-5-yl] hexenoic acid), a thromboxane A_2 antagonist. The PRP was then treated with ADP as a primary aggregating agent. It was found that the ability of U-46619, in the absence of or in

combination with 5-HT to increase this primary response was limited by ICI 192,605 and a combination of ICI 192,605 and ICI 170,809 (Shaw *et al.*, 1997).

In human PRP, aggregation induced by the addition of 2 μM ADP or 2 $\mu\text{g/ml}$ thrombin was completely inhibited by both 5 μM EP 035 and 0.5 μM EP 157, which are both prostaglandin endoperoxide analogues (Armstrong *et al.*, 1986).

1 μM 5'-N-Ethylcarboxamidoadenosine (NECA), an adenosine analogue, inhibited aggregation of human platelets that were stimulated with either 1 μM ADP, 10 μM 5-HT, 10 μM adrenaline or 5 U/ml thrombin. NECA also proved to be 5 times more potent than adenosine in its action with aggregation induced with 5 μM ADP (Cusack and Hourani, 1981).

3 mg/kg CS-747 (2-acetoxy-5(α -cyclopropylcarbonyl-2-fluorobenzyl)-4,5,6,7-tetrahydrothieno[3,2-c]pyridine), a novel antiplatelet agent that produced an active metabolite *in vivo*, significantly reduced aggregation induced by 0.3-30 μM ADP. A moderate reduction in aggregation induced by 0.06 U/ml thrombin resulted from the addition of CS-747 (Sugidachi *et al.*, 2000).

The effect of the isomers on thrombin activity was also determined. In addition to ending the coagulation process, thrombin-dependent signaling could trigger immediate responses in vascular and inflammatory cells. It can influence cell division in fibroblasts and other mesenchymal cell cultures. Cell cycle progression and cell division of avian fibroblasts are also induced in a growth factor-like reaction. Thrombin is therefore also capable of triggering nonhaemostatic mesenchymal cell responses, relevant to wound healing and tissue repair processes. In endothelial cells, thrombin stimulates phosphatidic acid metabolism, an increase in Ca^{2+} -levels and an increase in the expression of the *c-sis* gene product, PDGF. Up-regulated expression of urokinase receptor, increased cell migration through a protein synthesis-dependent mechanism and induced cell proliferation resulted from vascular smooth muscle cells in response to thrombin. Thrombin also acts as a

potent mitogen for vascular smooth muscle cells, thereby contributing to the proliferative aspect of atherosclerotic lesions and vascular re-occlusion (Altieri, 1997. Pg. 121).

Progress curves were obtained by following the absorbance at 410 nm over a 5 min period. The addition of increasing concentrations of thrombin resulted in progress curves with increasing slopes in the linear portion of the graphs (Figure 6.12). Validation of the method was achieved by plotting the slope of these linear portions against the concentration of thrombin added to the assay (Figure 6.13).

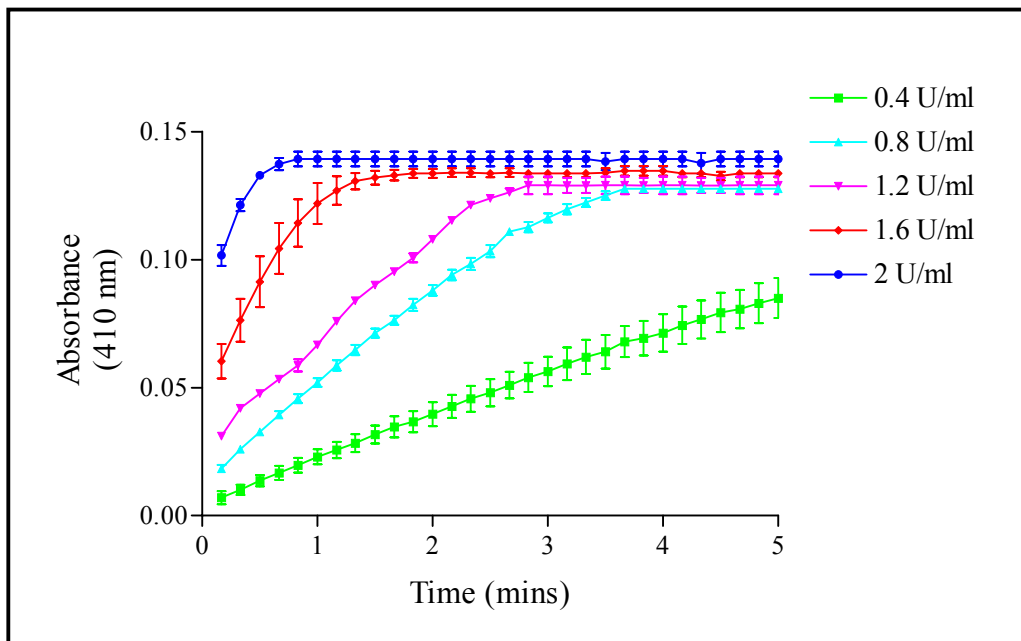


Figure 6. 12: Progress curves obtained in the presence of varying concentrations of thrombin. Final concentrations of thrombin in the wells are indicated on the graph. Values indicated are the mean \pm s.d. of quadruplicates.

A good correlation between thrombin concentration and change in absorbance was obtained ($R^2=0.9905$). This indicates that with increasing concentrations of thrombin, there is a linear increase in the rate at which the substrate is cleaved.

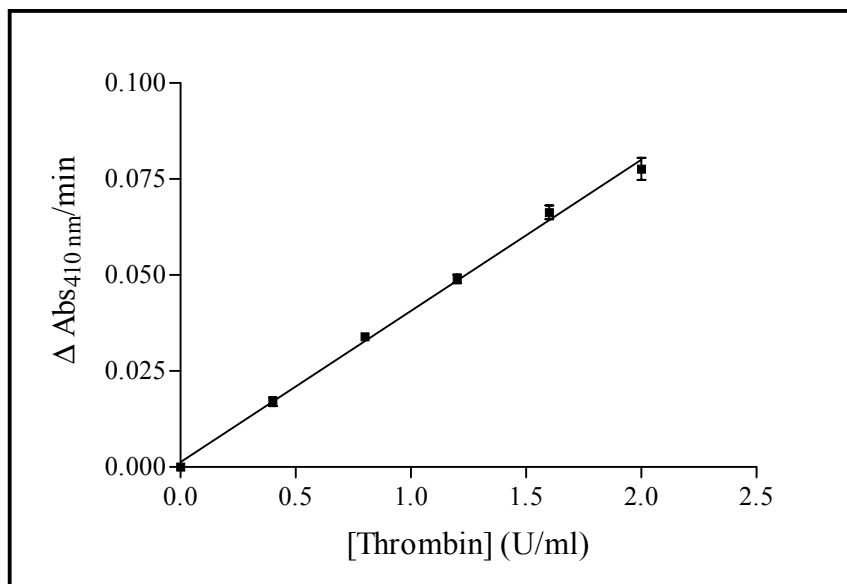


Figure 6. 13: Correlation between thrombin concentration and change in absorbance over the linear portion of the progress curves. $R^2=0.9905$. Final concentrations of thrombin in the wells are indicated. Values indicated are the mean \pm s.d. of quadruplicates.

Thrombin at a final concentration of 1.2 U/ml was used as a standard concentration in the assays involving the isomers, as this concentration resulted in a 0.050 change in absorbance per min of the reaction (Figure 6.13). The isomers were tested at a range of stock concentrations, from 0.25 mM to 3 mM. In the presence of cyclo(L-Trp-L-Pro), the reaction reached a stationary phase quicker than thrombin at 1.2 U/ml (Figure 6.14). These results were not significant however, since no linearity exists between the change in absorbance over the reaction period ($R^2=0.6332$)

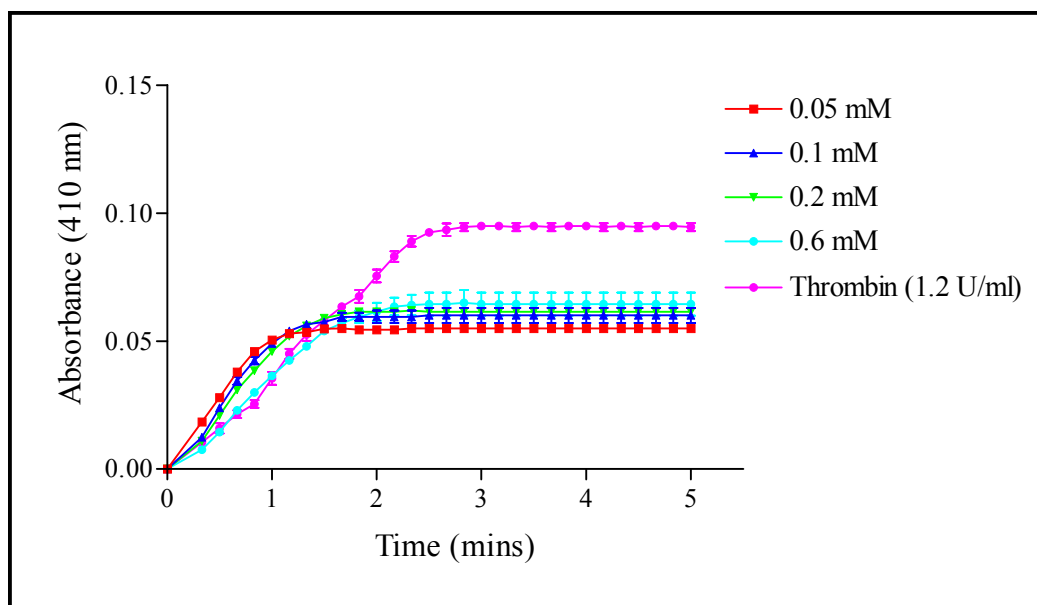


Figure 6. 14: Progress curves in the presence of cyclo(L-Trp-L-Pro). Final concentrations of the respective compounds are indicated on the graph. Values indicated are the mean \pm s.d. of quadruplicates.

Similarly, progress curves were drawn from data obtained for the assay in the presence of cyclo(L-Trp-D-Pro) (Figure 6.15), cyclo(D-Trp-L-Pro) (Figure 6.16) and cyclo(D-Trp-D-Pro) (Figure 6.17). Once again, the data was analysed by determining the change in absorbance over the reaction period. No significant effect on thrombin activity was noted for cyclo(L-Trp-D-Pro) ($R^2=0.07623$), cyclo(D-Trp-L-Pro) ($R^2=0.6624$) and cyclo(D-Trp-D-Pro) ($R^2=0.7029$).

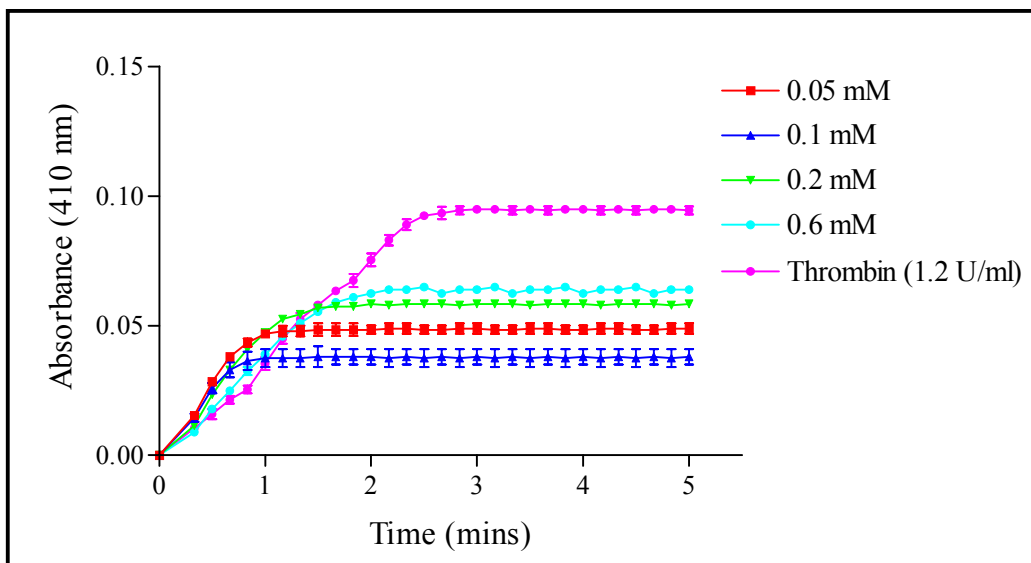


Figure 6. 15: Progress curves in the presence of cyclo(L-Trp-D-Pro). Final concentrations of the respective compounds are indicated on the graph. Values indicated are the mean \pm s.d. of quadruplicates.

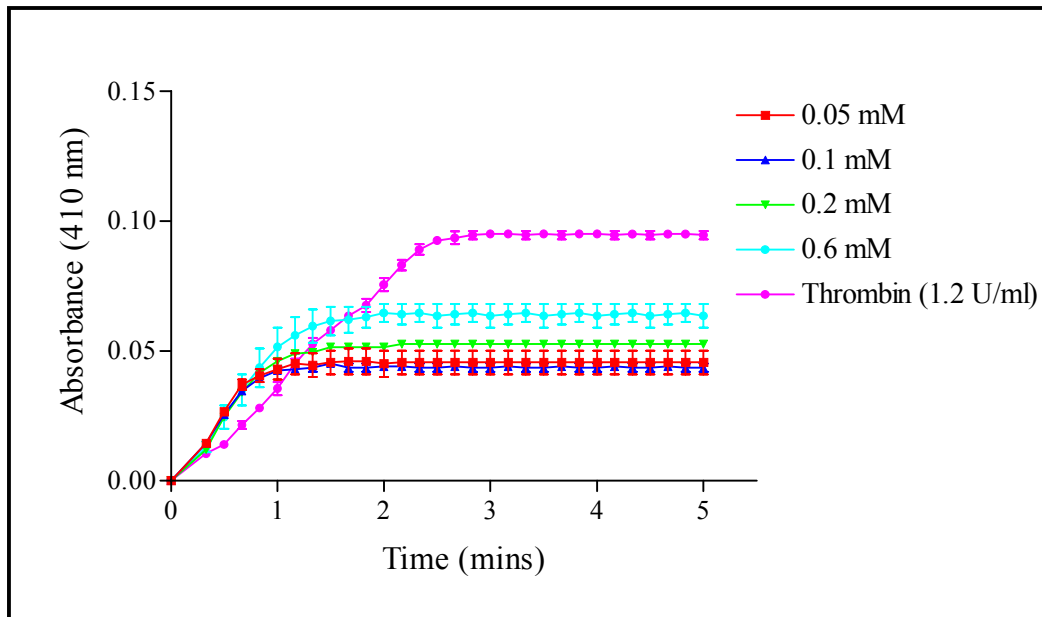


Figure 6. 16: Progress curves in the presence of cyclo(D-Trp-L-Pro). Final concentrations of the respective compounds are indicated on the graph. Values indicated are the mean \pm s.d. of quadruplicates.

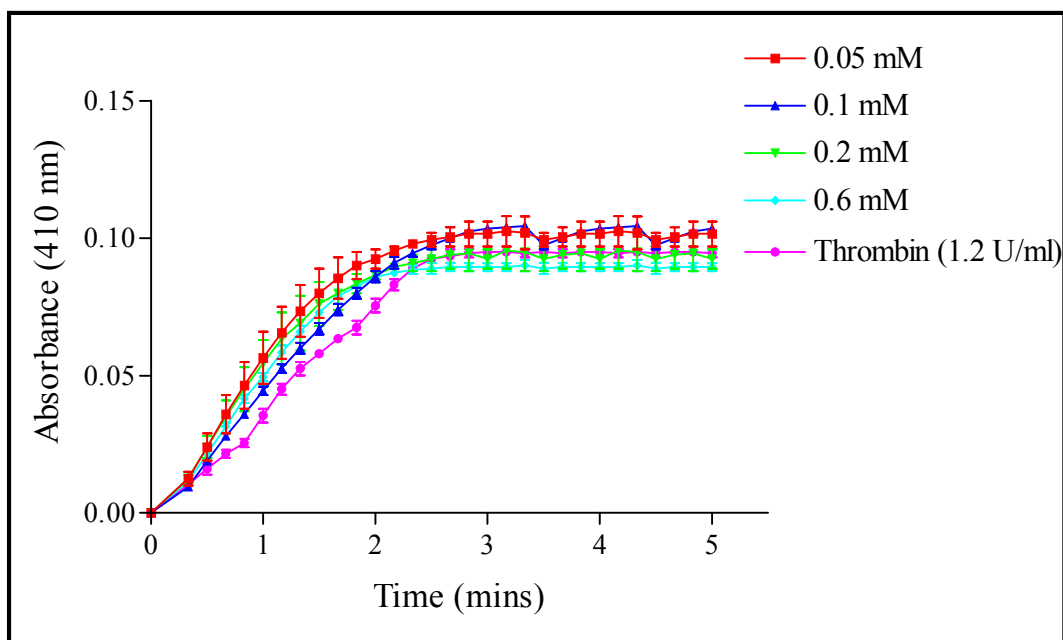


Figure 6. 17: Progress curves in the presence of cyclo(D-Trp-D-Pro). Final concentrations of the respective compounds are indicated on the graph. Values indicated are the mean \pm s.d. of quadruplicates.

No further analyses, such as K_i determination, could be performed, since no significant effect on thrombin activity was detected. Thus, it is suggested that the decrease in aggregation in the presence of cyclo(L-Trp-D-Pro) (Figures 6.5 and 6.6) is not due to direct inhibition of thrombin, but via a different mechanism. This could possibly be by inhibition of any factor involved in the activation of thrombin (eg. prothrombinase).

As the results suggest, the isomers do not interact with thrombin to any significant degree, neither inhibiting nor enhancing its action. It is therefore suggested that patients infected with HSV would be more susceptible to vascular injury and atherosclerotic disease as a result of thrombotic action. Thrombin-dependent signaling of coagulation and nonhaemostatic mesenchymal cell responses in terms of wound healing and tissue repair mechanisms would thus not be adversely affected by the administration of these isomers.

α -Thrombin is inhibited by the synthetic peptide MDL 28 050 (N^α -succinyl-Tyr-Glu-Pro-Ile-Pro-Glu-Glu-Ala-Cha-D-Glu-OH), which acts at a site separate from the catalytic site of thrombin. Under *in vitro* conditions, MDL 28 050 has a potency of 29 nM against

α -thrombin, while a decreased potency against bovine α -thrombin was determined at 150 nM. Hirudin was determined to have a potency of 34 000 nM in the presence of bovine α -thrombin, indicating that MDL 28 050 is more potent than hirudin. Furthermore, MDL 28 050 does not need any cofactors, and has a reduced hemorrhagic potential (Krstensky *et al.*, 1990).

Platelets play a vital role in adhering to an injured vessel wall. This crucial step in the haemostatic process can be compromised by both acquired and genetic defects of adhesion. On the other hand, enhanced adhesion may culminate in an increased risk of vascular disorders. Binding of plasma and subendothelial tissue components to different membrane glycoproteins forms part of adhesion. Characterization of the platelet-substrate interaction mechanism is thus dependent on the determination of adhesion to different surfaces in the presence of different agonists.

In vivo testing of platelet interactions with artificial surfaces is limited by the expense, numerous variables that are often difficult or impossible to control and may not allow for comparison with different materials, and species differences in behaviour and composition of blood. With *in vitro* testing, human blood can be used, different materials can be tested and compared and large numbers of variables can be tested simultaneously (Lindon *et al.*, 1989).

Adhesion of platelets to a coated surface may lead to morphological and functional alterations in the platelet. Activated platelets take on a more spherical configuration and may form several pseudopods. Platelet aggregates form and storage granule contents may be released into the media. Testing of compounds for effects on platelet adhesion to artificial surfaces is beneficial in that adverse effects of thrombi formation in a prosthetic device include blood flow impairment and dysfunction of the device, thrombocytopenia, platelet function alteration or embolization resultant of thrombi detachment (Lindon *et al.*, 1989). The assay was thus conducted to determine whether the isomers would induce aggregation to an artificial surface, thereby increasing the risk of complications where prosthetic devices are present.

It has been reported that acid phosphatase activity is contained within platelets and was thus used as an indicator of platelet concentration in the well. Precoating of the wells with plasma prevented non-specific adhesion. Addition of Triton X-100 resulted in platelet lysis and did not affect acid phosphatase activity. The assay employed is capable of detecting adhesion of unstimulated and ADP-stimulated platelets to coated wells in the absence of aggregation. When thrombin is added to stimulate platelets, small aggregates of platelets also adhere to the wells. Overall, binding of platelets to the surface is not affected but does render this method less sensitive for adhesion. (Bellavite *et al.*, 1994)

Addition of a protective protein such as albumin (0.35-4%) prevents platelet adhesion to containers, reducing the chances of activation during isolation and handling. The pH is to be maintained at that of plasma (pH 7.35). Tris buffers should be avoided as some platelet responses are inhibited, whilst others are potentiated. Ca^{2+} in the suspending medium is important, since omission thereof results in activation of the arachidonate pathway, formation of thromboxane A_2 , some granule contents are released and second phase aggregation results (Mustard *et al.*, 1989).

The effects of the isomers on platelet adhesion to plasma-coated microtiter plates were determined using the internal acid phosphatase activity of platelets as a marker of platelet number. This assay has an increased sensitivity for platelet concentration in comparison to turbidity readings. A linear relationship exists between acid phosphatase activity and the number of platelets present (Figure 6.18), determined using *p*NPP as a substrate ($R^2=0.9906$).

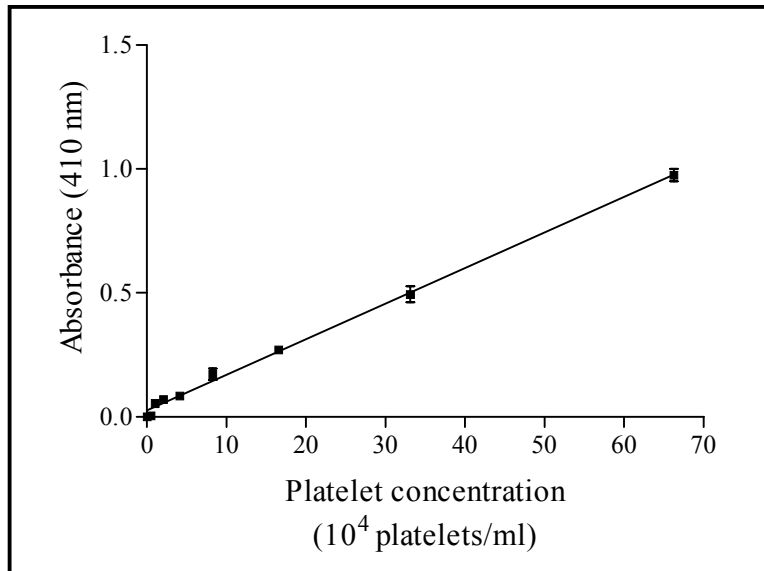


Figure 6. 18: Linear relationship between acid phosphatase activity and platelet number. Values indicated are mean \pm s.d. of quadruplicates. $R^2=0.9906$.

During incubation, no shaking occurred to prevent detachment of the platelets from the wells. The amount of adhesion of ADP- and thrombin-stimulated platelets was determined in the presence of various concentrations of either ADP or thrombin. At low concentrations of both thrombin and ADP, similar degrees of adhesion were observed (Figures 6.19 and 6.20).

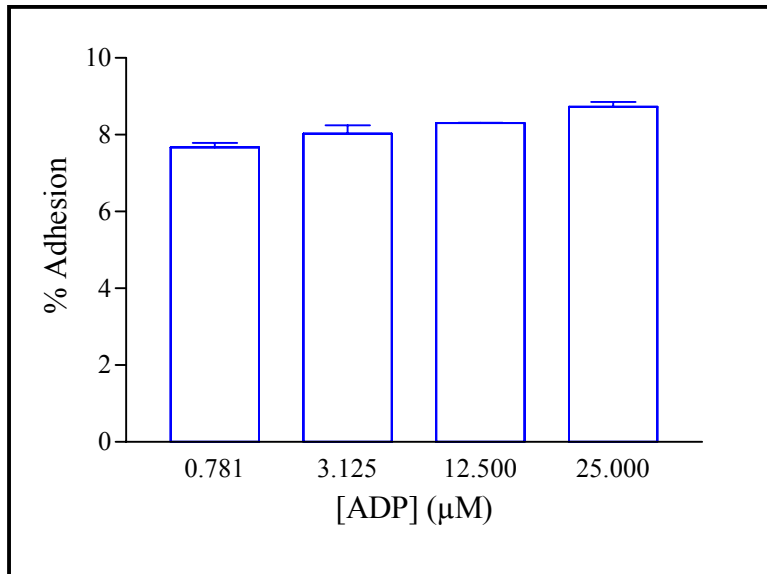


Figure 6. 19: The effects of various concentrations of ADP on platelet adhesion to a plasma-coated surface. Final concentrations of ADP in the wells are indicated on the graph. Values indicated are mean \pm s.d. of quadruplicates.

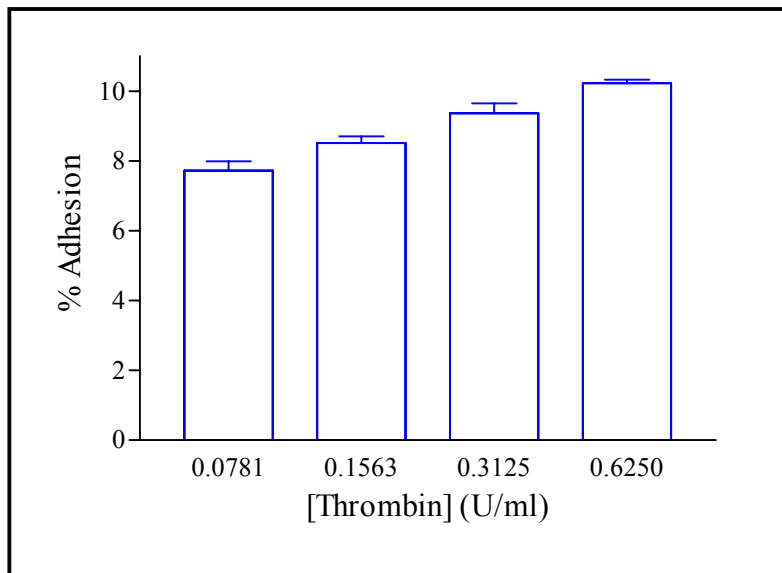


Figure 6. 20: The effects of various concentrations of thrombin on platelet adhesion to a plasma-coated surface. Final concentrations of thrombin in the wells are indicated on the graph. Values indicated are mean \pm s.d. of quadruplicates.

At 0.625 U/ml thrombin, the degree of adhesion was slightly greater than that of 25 μ M ADP. These low levels of adhesion of platelets to the plasma-coated plates are supported by findings of Bellavite *et al.* (1994).

When platelets were stimulated by 3.125 μ M ADP, elevated levels of adhesion (Figure 6.21) were noted, particularly in the presence of cyclo(L-Trp-D-Pro), cyclo(D-Trp-L-Pro) and cyclo(D-Trp-D-Pro) ($p < 0.05$). Adhesion resultant from the addition of the isomers to ADP-stimulated platelets was significantly higher ($p < 0.05$) than the adhesion obtained with thrombin-stimulated platelets for all the concentrations of all the isomers tested (Figure 6.22).

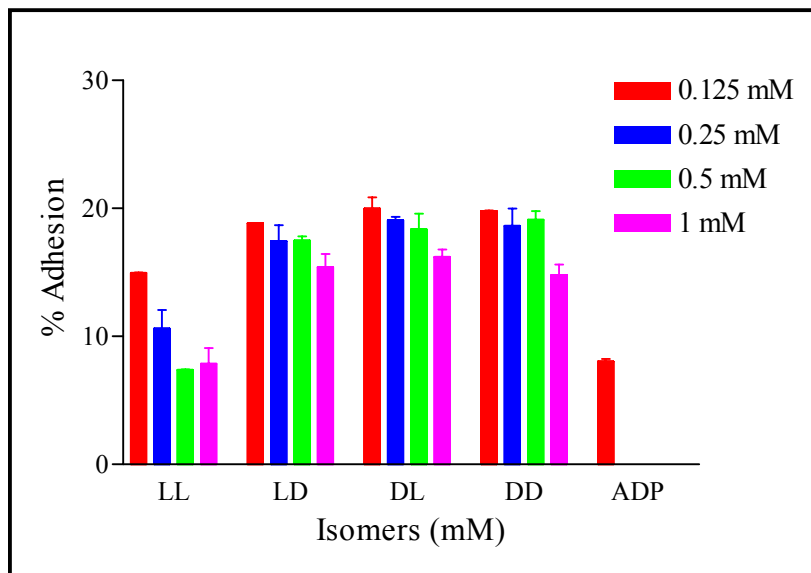


Figure 6. 21: Percentage adhesion of platelets, stimulated with 3.125 μ M ADP, in the presence of cyclo(Trp-Pro) isomers at final concentrations as indicated on the graph. Values indicated are mean \pm s.d. of quadruplicates.

0.125 mM Cyclo(L-Trp-L-Pro) resulted in a higher degree of adhesion in comparison to the other concentrations tested for cyclo(L-Trp-L-Pro) (Figure 6.21), which did not differ significantly from the amount of adhesion induced by 3.125 μ M ADP ($p > 0.05$). As the concentration of cyclo(L-Trp-D-Pro), cyclo(D-Trp-L-Pro) and cyclo(D-Trp-D-Pro) increased, the amount of adhesion was decreased.

This increase in adhesion induced by the isomers could result in thrombi formation in a prosthetic device, which would lead to complications in that blood flow would be impaired. Prosthetic valves may become blocked by the platelet adhesion, resulting in

dysfunction of the device. Furthermore, the thrombi formed may detach, resulting in embolization, thrombocytopenia or platelet function alteration (Lindon *et al.*, 1989).

Adhesion, induced by the addition of 0.1563 U/ml thrombin, was significantly reduced ($p < 0.05$) in the presence of all the isomers at all concentrations tested (Figure 6.22). The greatest reduction in adhesion was noted for both cyclo(L-Trp-L-Pro) and cyclo(L-Trp-D-Pro) at 1 mM. The decrease in adhesion did not appear to be concentration-dependent. Once again, the highest concentrations of isomer resulted in the greatest reduction of adhesion.

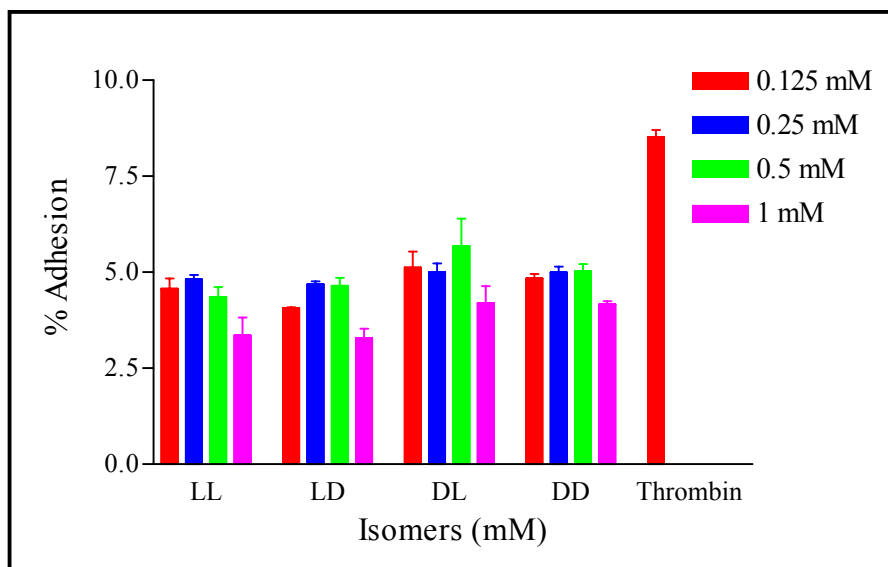


Figure 6. 22: % Adhesion of platelets, stimulated with 0.1563 U/ml thrombin, in the presence of cyclo(Trp-Pro) isomers at final concentrations as indicated on the graph. Values indicated are mean \pm s.d. of quadruplicates.

This difference in the effect of the isomers on ADP- and thrombin-induced adhesion may be caused by the binding of the isomers to the proteins in the plasma (Chapter 5) with which the wells were coated. This binding of the isomers to the protein may not interfere with the binding of ADP to the affinity binding sites on the platelets, but may interfere with the binding of thrombin to these binding sites. This would then result in decreased binding in the presence of thrombin.

These isomers, in the presence of thrombin, would thus be beneficial to a patient fitted with a prosthetic device, as no increase in adhesion to the device is induced, reducing the risk of complications. Since thrombin is a more potent agonist than ADP (Hawiger, 1989), the decrease in adhesion (Figure 6.22) to the plasma-coated microtiter plate would be the overall effect of the isomers.

This method bypasses the problem with distinguishing between platelet-surface and platelet-platelet interactions. Any suspension formed by platelet-platelet interactions are removed by aspiration and washing. Aggregation is also discouraged by minimizing membrane contacts in the absence of stirring or mixing during incubation. Once platelet numbers fall below 10^8 /ml, *in vitro* aggregation is reduced. The concentration of platelets used in the assay was 1 966 000 platelets/ml. Fibrinogen, that bridges gaps between platelets, thereby enhancing platelet-platelet interactions, was not included in the buffer systems used (Bellavite *et al.*, 1994).

The assay is more sensitive when ADP is used to assess adhesion, since thrombin-stimulated platelets secrete fibrinogen, which may lead to erroneous results or interpretations thereof. Aggregation is needed before secretion occurs with ADP-stimulation of platelets, thus rendering the assay more sensitive in the sense that it would detect adhesion in the absence of aggregation. Stimulation using thrombin would thus be less specific for adhesion (Bellavite *et al.*, 1994).

It should be remembered that albumin, a major plasma protein, binds to the isomers to a large degree. Albumin binds to cyclo(L-Trp-L-Pro) by $62.22 \pm 1.269\%$, to cyclo(L-Trp-D-Pro) by $57.91 \pm 0.767\%$, to cyclo(D-Trp-L-Pro) by $58.85 \pm 1.133\%$ and to cyclo(D-Trp-D-Pro) by $59.86 \pm 0.784\%$ (Chapter 5, Table 5.3). This effectively reduces the amount of free isomer available to interact with the platelets, and thus adherence to wells coated with a substance devoid of albumin may result in larger percentages of adhesion. The concentrations of the isomers administered for clinical purposes should therefore take this into account in order to achieve the concentration needed to exhibit an effect.

In a study conducted by Hirafuji and Shinoda (1993), endothelial cells were pretreated with 500 μM aspirin for 15 min. The cells were then incubated with platelets in the presence of sonicates of platelet-activating factor-stimulated polymorphonuclear leukocytes. No significant platelet adhesion to endothelial cells was noted. When the cells were pretreated with both aspirin and 300 μM N^{G} -nitro-L-arginine, a significant increase in adhesion was induced by sonicates of platelet-activating factor-stimulated polymorphonuclear leukocytes ($p < 0.01$). Adhesion increased from $2.8 \pm 0.3\%$ to $8.4 \pm 0.6\%$. When aspartate, N^{G} -nitro-L-arginine and 1 mM L-arginine was applied to the cells, significantly reduced adhesion resulted ($p < 0.05$). Adhesion was inhibited by $20.5 \pm 5.1\%$ (Hirafuji and Shinoda, 1993).

6.5 CONCLUSIONS

No effect on aggregation induced by thrombin (Figure 6.5) or ADP (Figure 6.7) was noted in the presence of the isomers at the concentrations tested. The only effect resulted from the addition of cyclo(L-Trp-D-Pro) at final concentrations of 0.125 mM, 0.25 mM, 0.5 mM (Figure 6.6) and 1 mM (Figure 6.5), to washed platelets stimulated with thrombin. Furthermore, the isomers produced no significant effects on thrombin activity (Figures 6.14-6.17), indicating that the aggregation effects noted with cyclo(L-Trp-D-Pro) was not resultant of thrombin inhibition. The isomers induced greater adhesion to plasma-coated microtiter plates in the presence of ADP (Figure 6.21), which would not benefit a patient fitted with a prosthetic device. When thrombin was used to induce adhesion (Figure 6.22), however, the isomers caused decreased levels of adhesion, thereby reducing the risk of thrombi formation, thrombocytopenia or platelet function alteration (Lindon *et al.*, 1989).

CHAPTER 7
EFFECT OF THE ISOMERS ON HEART
AND ION CHANNEL ACTIVITY

7.1 INTRODUCTION

The heart (Figure 7.1), blood and blood vessels make up the cardiovascular system. The heart pumps blood through the blood vessels at about 14 000 litres per day and beats approximately 100 000 times per day (Martini, 1995. Pg. 682). The heart is situated in the mediastinum, with two thirds of its mass lying to the left of the midline. It is protected by a pericardium that confines the heart to its position in the mediastinum. The heart wall consists of three layers: the epicardium, the myocardium and the endocardium. The epicardium is the thin, transparent outer layer, while the middle layer is termed the myocardium, which consists of cardiac muscle tissue. The innermost layer is the endocardium that is continuous with the endothelial lining of the blood vessels that are attached to the heart. The heart is divided into four chambers; two atria and two ventricles (Tortora and Grabowski, 2000. Pp. 636-639).

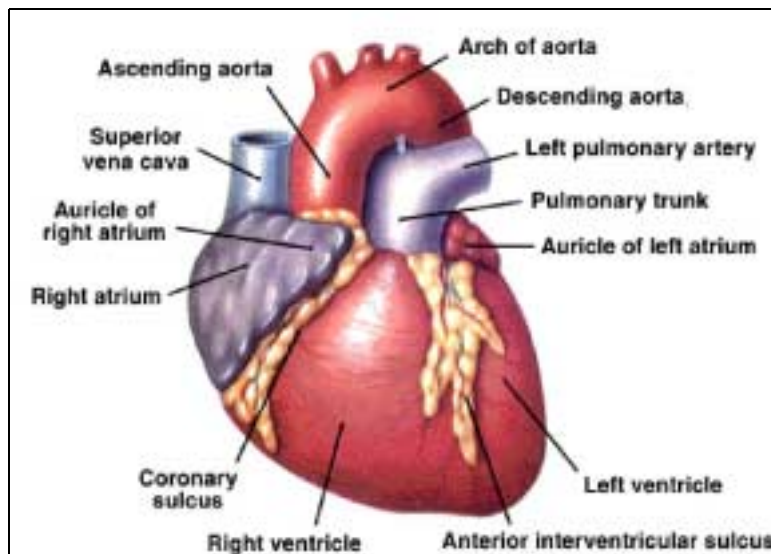


Figure 7. 1: The anterior view of the heart, showing major anatomical features (Martini, 1995. Pg. 685).

7.1.1 Electrophysiology of the heart

Any electrical impulses originating from the sinoatrial node results in a normal cardiac contraction. The impulse is propagated through the atria, where it enters the atrioventricular node. The impulse then moves to the rest of the ventricles via the His-Purkinje system. Propagation of this impulse is dependent on transmembrane potential, which is produced by the concentrations of Ca^{2+} , K^+ and Na^+ (Sperelakis and Norwell, 1989. Pg. 1009). Movement across the cell membrane occurs along a concentration gradient, in conjunction with energy-dependent transport pumps. Any disturbance in the generation or propagation of these impulses results in arrhythmias.

When oxygen requirements are not adequately supplied by cardiac output, congestive heart failure occurs. The principal therapeutic effect is an increase in cardiac contractility or positive inotropic action. In some types of congestive failure, vasodilators have been used with considerable success by reducing vascular tone, thereby decreasing any stress placed on the myocardium (Katzung and Parmley, 1989). Very rarely, high-output failure occurs. This happens when even an increased cardiac output is insufficient in meeting the demands on the body.

For all cases of congestive heart failure, the primary signs and symptoms include tachycardia, a decrease in tolerance to exercise and shortness of breath, cardiomegaly, as well as peripheral and pulmonary edema (Katzung and Parmley, 1989).

7.1.2 Cardiac performance

Cardiac performance is dependent on four factors:

1) Preload

Pulmonary congestion results if preload exceeds 20-25 mm Hg. In heart failure, preload is usually increased due to increased blood volume and venous tone. Salt restriction and diuretic therapy are administered in order to reduce high filling pressure. Preload may also be reduced by decreasing venous return, which is the action of venodilator drugs

(Katzung and Parmley, 1989).

2) Afterload

Afterload, characterised by aortic impedance and systemic vascular resistance, is defined as the resistance against which the heart must pump blood. In coronary heart failure, systemic vascular resistance is usually increased. This in turn may reduce cardiac output as a result of increased resistance to ejection.

3) Contractility

Contractility is defined as the dynamism of heart muscle contraction. If contractility decreases, the velocity of muscle shortening is decreased and there is a reduction in the rate of intraventricular pressure development (Katzung and Parmley, 1989).

4) Heart rate

A major determinant of cardiac output is heart rate. The first compensatory mechanism used to maintain cardiac output is the use of β -adrenoceptor activation that results in an increased heart rate (Katzung and Parmley, 1989).

7.1.3 Movement of ions during an action potential

In the contractile fibres, an action potential (Figure 7.2) occurs in 3 stages:

1) Rapid depolarization

Close to -90 mV, contractile fibres have a resting membrane potential. If neighbouring fibres are excited, these fibres are brought to threshold. Depolarization of the membrane occurs once the impulse reaches the muscle fibre, as a result of the rapid influx of Na^+ through opened voltage-gated fast Na^+ -channels (Figure 7.2), along the electrochemical gradient. The voltage-gated fast Na^+ -channels inactivate within milliseconds and the concentration of Na^+ decreases (Tortora and Grabowski, 2000. Pg. 651).

2) Plateau

At $+30$ mV, voltage-regulated Na^+ -channels close. Voltage-gated slow Ca^{2+} -channels in the sarcolemma and sarcoplasmic reticulum membrane open, increasing Ca^{2+} -

permeability (Figure 7.2). The amount of Ca^{2+} in the cytosol increases by passing through the sarcolemma or pouring out of the sarcoplasmic reticulum within the fibre. The transmembrane potential is maintained near 0 mV for approximately 175 ms. (Tortora and Grabowski, 2000. Pg. 651).

3) Repolarization

After a delay, the membrane permeability to K^+ increases as voltage-gated slow K^+ -channels open (Figure 7.2). Simultaneously, Ca^{2+} -channels close. The negative resting membrane potential is restored as more K^+ leave the fibre and less Ca^{2+} enters. Any substance that alters Ca^{2+} movement via the channels would influence heart contraction. The contraction force is enhanced by Ca^{2+} -influx caused by epinephrine (Tortora and Grabowski, 2000. Pg. 651).

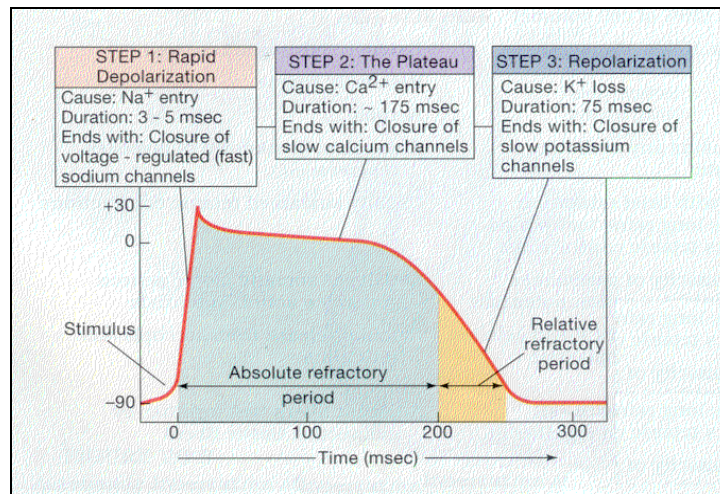


Figure 7. 2: The three stages of an action potential in cardiac muscle (Martini, 1995. Pg. 696).

The rate of ion passage across the cell membrane is associated with various phases of cardiac action potential and varies with cell membrane permeability. The intracellular $[\text{K}^+]$ exceeds the extracellular $[\text{K}^+]$, consistent with other cell types. The opposite is true for both Na^+ and Ca^{2+} - the respective intracellular concentrations are much less than the extracellular concentrations. In the resting cell, K^+ tends to diffuse out of the cell along the concentration gradient (Figure 7.3), since the membrane tends to have a high permeability to K^+ , with lower permeability levels towards Ca^{2+} and Na^+ . Countering this

diffusion is the negative potential (or high concentration of anions) that exists in the interior of the cell, which attract the K^+ (Sperelakis and Norwell, 1989. Pg. 1009).

Progressive depolarization of the resting cell membrane would result from the steady leak of Na^+ into the cell were it not countered by the Na^+K^+ -ATPase pump (Figure 7.3). This pump acts to extrude Na^+ from the interior of the cell, while allowing K^+ to enter the cell. Any increase in either the $[Na^+/K^+]$ would result in increased pump activity. The number of Na^+ leaving the cell does not equal the number of K^+ entering the cell, thus the pump creates a potential difference across the cell membrane (Martini, 1995. Pg. 83).

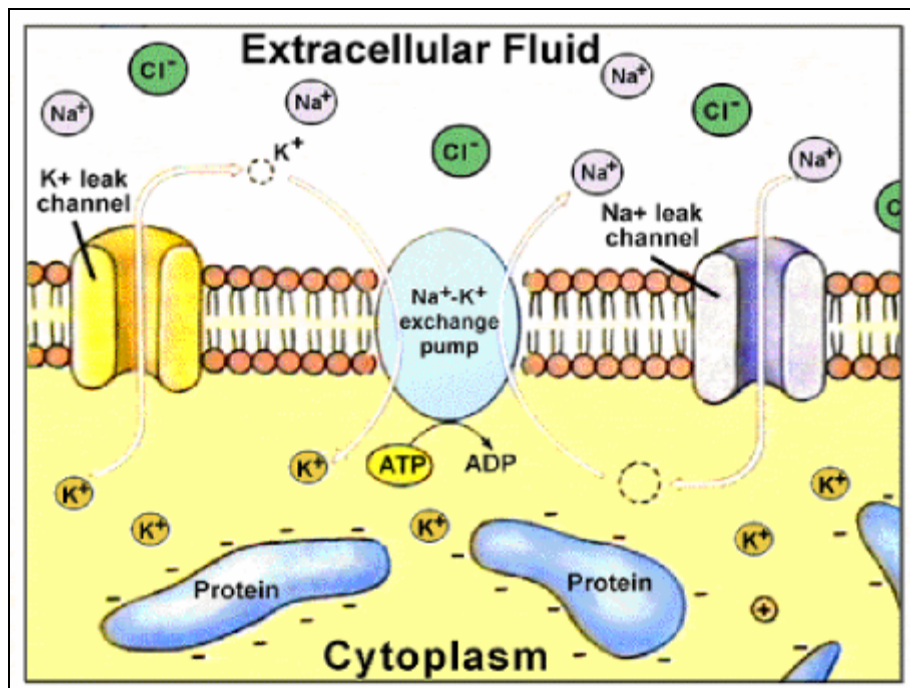


Figure 7. 3: Ion distribution across the cell membrane. At the resting potential, 3 Na^+ enter the cell for every 2 K^+ that leave the cell. These movements are countered by the Na^+K^+ exchange pump (Martini, 1995. Pg. 83).

Since action potential depends on extracellular Na^+ , the heart is not excitable and thus will not beat if there is an absence of Na^+ . On the other hand, the resting membrane potential is independent of Na^+ . Insignificant effects on myocardial excitation and contraction are produced at reduced K^+ -concentrations. If large increases in this concentration occur, depolarization may result, as well as a loss of excitability. Another important ion in cardiac contraction is Ca^{2+} , where a decreased extracellular Ca^{2+} causes a

decrease in contractile force. In contrast, increased extracellular Ca^{2+} results in enhance contractile force (Berne and Levy, 1986. Pg. 57).

A rise in extracellular K^+ initiates ischaemia and reperfusion-induced arrhythmias. This rise may result from cellular damage that causes K^+ to leak from the cell. Partial depolarization or a loss in resting potential in myocardial cells may result. This extracellular increase may cause a shortening of action potential and an increase in K^+ -conductance. Thus, Ca^{2+} -channel blockers may be used to increase refractory periods (Dipiro *et al.*, 1997).

7.1.4 Voltage-dependent calcium channels

Using physiological and pharmacological properties, voltage-dependent or voltage-operated Ca^{2+} -channels (VOCCs) (Figure 7.4) have been divided into 6 classes i.e. L, N, P, T, R and Q.

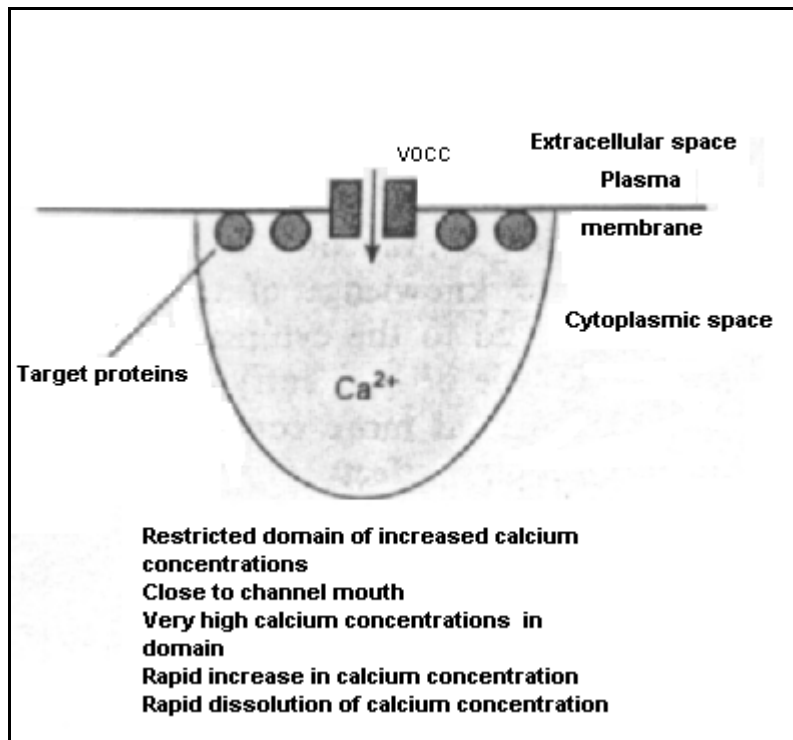


Figure 7. 4: Voltage-operated Ca^{2+} -channel (Barritt, 1999).

The function of VOCCs (Figure 7.4) is to deliver large quantities of Ca^{2+} to the subplasmalemmal space. This distribution occurs at specific locations, which are determined by the arrangement of VOCCs in the plasma membrane. When Ca^{2+} enters the cell via VOCCs, only a small region in the cytoplasmic space called the Ca^{2+} -domain receives the Ca^{2+} . This effect can be negated by cytoplasmic Ca^{2+} -buffers and the inactivation of open VOCCs. This delivery of rapid and large amounts of Ca^{2+} is thought to activate Ca^{2+} -responsive target enzymes, such as calmodulin. VOCCs may also act to restore endoplasmic reticulum Ca^{2+} -stores (Barritt, 1999).

Long-lasting Ca^{2+} -currents are mediated by the L-type channels, which are dihydropyridine-sensitive channels. It consists of 5 different subunits ($\alpha 1$, $\alpha 2$, β , γ and δ), with the binding site for Ca^{2+} -channel antagonists located on the $\alpha 1$ subunit. A functional channel can be formed by the association of $\alpha 1$ and β subunits, the function of which is modulated by phosphorylation. In vascular smooth muscle cells, this phosphorylation is modulated by protein kinase A (PKA), protein kinase C and tyrosine kinases (Godfraind and Govoni, 1995).

The major entry pathway for Ca^{2+} is the L-type Ca^{2+} -channels, which can be blocked by Ca^{2+} -channel antagonists. Three classes have been identified:

- i) phenylalkylamines eg. verapamil,
- ii) benzothiazepines eg. diltiazem, and
- iii) 1,4-dihydropyridines eg. nifedipine (Yasui and Palade, 1995).

The therapeutic effectiveness of L-type Ca^{2+} -channel antagonists in cardiovascular pathologies is based on the inhibition of Ca^{2+} -influx in depolarized smooth muscle (Godfraind and Govoni, 1995). Ca^{2+} -channel antagonists are known to exhibit the following effects on the heart:

1) Negative inotropic effects

During cardiac muscle contraction, Ca^{2+} is essential for interaction with troponin. Thus, any event that leads to a decrease in Ca^{2+} -levels will result in decreased interaction with

troponin, and hence a decreased force of contraction. A concurrent decrease in cardiac output is experienced (Nayler, 1988).

2) Relative vasodilatory activity

Similarly, a decreased force of contraction is noted for smooth muscles in the presence of Ca^{2+} -channel blockers. If vascular smooth muscle is relaxed, blood vessels will dilate, increasing the coronary flow rate (Nayler, 1988). These drugs have also been noted to increase membrane permeability to K^+ , resulting in hyperpolarization of the membrane. This leads to an inhibition of action potential generation (Cook, 1998).

3) Inhibitory effect on heart rate

Ca^{2+} -channel blockers decrease heart rate by inhibiting the slow influx of Ca^{2+} into the cell, thereby decreasing the rate of stimulation of the heart (Nayler, 1988).

4) Antiarrhythmia effects

Arrhythmia is characterised by abnormal conductances. Ca^{2+} -channel blockers cause stabilization of the conductance patterns of the heart, thereby stopping arrhythmias (Nayler, 1988). Class IV antiarrhythmia agents act by blocking Ca^{2+} -channels (Dupuis and Adamantidis, 1995).

7.1.5 Potassium channels

K^+ -channels, found in most cells, are integral membrane proteins. Two subunits occur, α and β . Domains for a channel pore, a voltage sensor, an activation gate and an inactivating domain are located on the α subunit. Four such subunits may associate to form a functional channel. Different K^+ -channels may be formed when the peripheral membrane β subunit associates with the cytoplasmic domain of the α subunit (Godfraind and Govoni, 1995). K^+ -channels are also the target in the treatment of various disease states such as non-insulin dependent diabetes mellitus (NIDDM), asthma and cardiac arrhythmias. If the K^+ -current is inhibited, electrical events in the myocardial cells will be affected (Sensch *et al.*, 2000). In NIDDM, K^+ -channels in pancreatic β cells are closed due to increases in ATP production, resultant of rises in plasma glucose concentrations.

As a result, membrane depolarization causes Ca^{2+} -influx into the cell with subsequent insulin secretion. Drugs used in hypoglycaemia target these ATP-sensitive K^+ -channels (Rang and Dale, 1991).

Bronchodilators are widely used in the treatment of asthma. β agonists act by stimulating β -receptors in smooth muscles of the airways. Cyclic AMP levels increase, resulting in the activation of cAMP-dependent PKA, which causes muscle relaxation via several mechanisms. One such mechanism involves hyperpolarization of the cell membrane by opening Ca^{2+} -activated K^+ -channels (Barnes and Mueller, 1995).

K^+ -channel blockers (Class III antiarrhythmia drugs) are useful in the treatment of cardiac arrhythmias (Dupuis and Adamantidis, 1995). The cell can be driven into a resting state by repolarizing currents that are generated by the opening of voltage-gated K^+ -channels under normal conditions. These drugs prolong the repolarization phase (Godfraind and Govoni, 1995).

7.1.6 The electrocardiogram

Electrical activities occurring in the heart can be detected by electrodes and the recording thereof constitutes an electrocardiogram (ECG). An ECG can indicate and monitor specific nodal performances, conductance and contractile components (Martini, 1995. Pg. 700).

The important features of an ECG (Figure 7.5) include:

P wave

Depolarization of the atria is accompanied by a small P wave.

QRS complex

As the ventricles depolarize, the QRS complex appears. Shortly after the peak of the R wave, the ventricles start contracting. The QRS complex is also referred to as the intraventricular conduction time.

T wave

Ventricular repolarization is characterised by the smaller T wave. No deflection relating to atrial repolarization is detected, since it occurs during ventricular depolarization. In addition, the QRS complex masks these electrical events (Martini, 1995. Pg. 701).

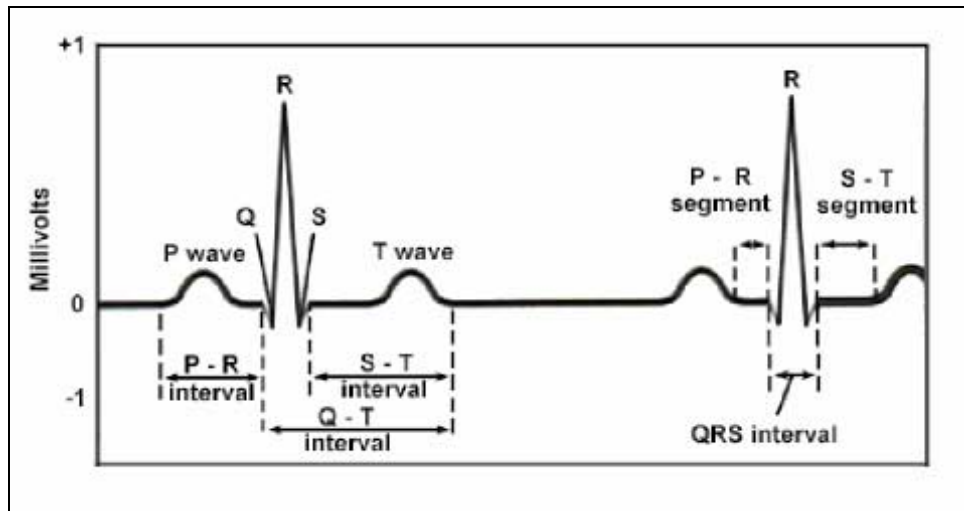


Figure 7. 5: An electrocardiogram, indicating the major components and the measurements most often taken during clinical analysis (Martini, 1995. Pg. 701).

7.1.6.1 ECG analysis

When examining an ECG, the amount of depolarization occurring during the P wave and QRS complex is of particular importance. An enlarged QRS complex may indicate an enlarged heart. Conditions such as coronary ischaemia or altered ion concentrations will result in a decreased T wave (Martini, 1995. Pg. 700). Cardiac arrhythmias are indicated by abnormal patterns of cardiac electrical activity.

The time between waves are reported as intervals. The PR, QT and ST intervals are shown in Figure 7.5. The interval between the onset of atrial depolarization to the onset of the QRS complex, and not to the R peak is referred to as the PR interval. The QT interval gives an indication of the time taken to undergo a single cycle of depolarization and repolarization. Measurement begins where the PR interval ends to the end of the T wave. A prolonged QT interval may indicate conduction problems, coronary ischaemia or myocardial damage (Martini, 1995. Pg. 701). The ST interval extends from the end of the

S wave to the start of the T wave. During this time, ventricular contractile fibres are fully depolarized (Tortora and Grabowski, 2000. Pg. 654).

7.1.7 The need for new antiarrhythmic agents

Despite intensive research, ischaemic heart disease remains a serious problem. Death and cardiac arrhythmias are often associated. Antiarrhythmia drugs are generally classified as having a relatively low therapeutic index and are further limited in their use by producing intolerable side effects (Hashimoto *et al.*, 1986). Antiarrhythmic agents devoid of serious side effects are thus needed. Rational treatment of cardiac arrhythmias is therefore in need of an absolute understanding of pharmacokinetic and pharmacodynamic properties of potential cardiac disease agents (Hashimoto *et al.*, 1986). These drugs may be developed rationally by drug design in terms of high selective cellular action. This, however, needs prior knowledge that the selective action is beneficial in antiarrhythmic activity (Rees and Curtis, 1993). Screening of antiarrhythmic agents for anti-ventricular fibrillation activity is important since ventricular fibrillation (VF) is a major cause of death in acute myocardial infarction. In studies performed by Lubbe *et al.* (1978), it was found that the concentration of potassium in the perfusate was a major factor in the incidence of VF. Also, at any K⁺-concentration, provocation of reperfusion arrhythmias occurred to a larger extent than ischaemic arrhythmias (Lubbe *et al.*, 1978).

7.1.8 The use of the rat model

Since the introduction of the rat model for myocardial infarction studies by coronary artery ligation in 1946, a number of different features such as the detection and assessment of antiarrhythmic activity of a number of different drug types such as β -adrenoreceptor inhibitors and Ca²⁺-channel antagonists have been investigated. The rat is a suitable model in the evaluation of potential antiarrhythmic drugs as this model is relatively simple and low cost in terms of time and expense (Hashimoto *et al.*, 1986). Advantages and disadvantages of this model are set out in Table 7.1.

Table 7. 1: Advantages and disadvantages of the use of the rat model in myocardial infarction studies (Curtis *et al.*, 1987).

Advantages of rats	Disadvantages of rats
- reproducible occluded zones as a result of a uniform lack of effective coronary collaterals.	- absolute clinical relevance is unclear, a disadvantage that is shared by all animal species, since rat cardiac anatomy and cardiac electrophysiology is not identical to man.
- rats are relatively cheap and easy to maintain and are readily available.	- the rat has a higher drug metabolism rate, and may therefore require comparatively larger drug doses to achieve a particular blood concentration.
- diabetes, hypertension and obesity, diseases that can occur with myocardial ischaemia and infarction, can easily be produced with myocardial ischaemia in rats.	- rats are susceptible to lung infection.
- biochemical and physiological data bases exist for rats.	

7.1.9 Patch-clamp techniques-A brief overview

In an attempt to record currents through individual ion channels in biological membranes, patch-recording techniques were developed. Once a gigaseal has formed, five patch configurations are possible. A gigaseal, which provides mechanical stability, is essential to eliminate problems such as resolution limitations. The gigaseal is formed by applying slight suction within a pipette. This increases resolution and allows for local voltage stimulation on the cell by applying potentials across the seal. The pipettes used are fire-

polished glass pipettes with resistances of 1-10 M Ω (Cahalan and Neher, 1992). The patch-clamp configurations (Figure 7.6) include:

1) *Cell-attached patch recording*

This configuration is created on gigaseal formation. Part of the cell membrane is trapped within the pipette tip. No breakage of the cell occurs, although limited deformation of the membrane occurs due to seal formation. Only the extracellular surface of the patch is exposed to the pipette solution.

2) *Inside-out configuration*

After seal formation, an isolated patch of the membrane is torn from the cell by withdrawing the pipette. In this way, the cytoplasmic membrane surface is exposed to the bath solution.

3) *Outside-out configuration*

This configuration is obtained by drawing a tether of cell membrane that breaks off and forms a seal over the pipette tip. In comparison to the whole-cell recording, there is a reduction in the membrane surface area, permitting subpicoampere resolution of the current.

4) *Perforated-patch configuration*

Loss of cytoplasmic ions, nucleotides and other cell constituents is an unavoidable consequence of whole-cell recording. Electrical continuity between pipette and cytoplasm is achieved by adding pore-forming antibiotic molecules (nystatin) to the pipette solution after the seal has been formed. This will result in the formation of conducting channels that are selective for monovalent cations. This reduces the electrical resistance of the patch, and current through the patch that is permeabilised can be recorded.

5) *Whole-cell recording*

In this configuration, the patch of membrane that is trapped within the pipette tip is ruptured deliberately by applying a voltage pulse of a few hundred millivolts. This leads

to electrical and diffusional continuity from cytoplasm to pipette allowing for exchange of pipette contents with cytoplasmic constituents.
(Cahalan and Neher, 1992).

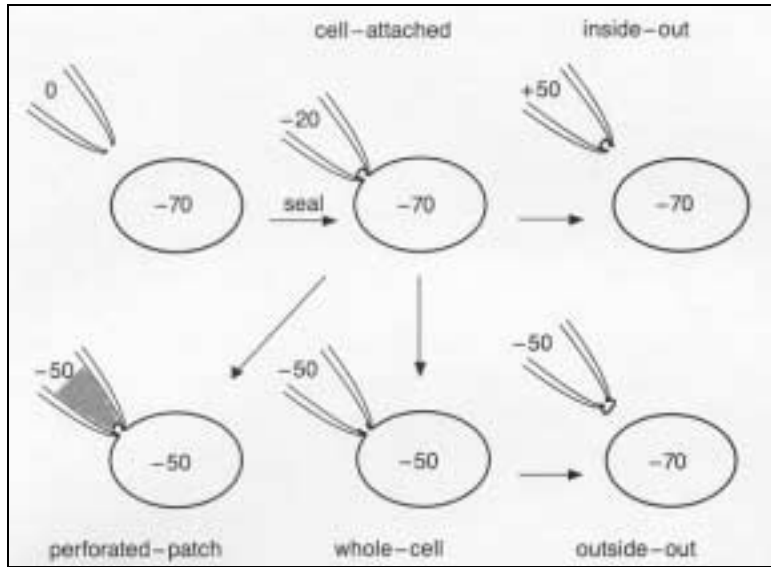


Figure 7. 6: Patch-clamp configurations (Cahalan and Neher, 1992).

7.2 OBJECTIVES OF THE CHAPTER

7.2.1 Objectives of the present chapter

- ♦ The primary aim was to study the effects of the isomers on heart and ion channel activities.

In order to satisfy these objectives, the following experimental data was collected:

- The effect of the isomers on Ca^{2+} -channel activity was determined using the whole-cell patch-clamp technique on ventricular myocytes isolated from the guinea-pig.
- The voltage-dependence of the effects of the isomers determined on Ca^{2+} -channel activity was determined using the whole-cell patch-clamp technique.
- The effect of the isomers on the inward rectifier K^{+} -current was determined using the whole-cell patch-clamp technique.
- A modified Langendorff method was used to determine the effects of the isomers on heart rate and coronary flow in the isolated, perfused rat heart.
- The time to stop ischaemia-induced arrhythmias and ventricular fibrillation, as well as the time taken for the heart rate to return to normal sinus rhythm was also determined.
- The ECG was examined to determine effects of the isomers on the QRS complex.

7.3 MATERIALS AND METHODS

The use of guinea-pigs for this study was approved by the Animal Ethics Committee, Potchefstroom University, Potchefstroom. The use of rats for this study was approved by the Animal Ethics Committee, University of Port Elizabeth.

7.3.1 Whole-cell patch-clamp method

7.3.1.1 Ca²⁺-channel activity

Replenishment of the intracellular milieu with Ca²⁺-influx may result from activation of voltage-operated Ca²⁺-channels. This influx of Ca²⁺ was determined by blocking Mg²⁺, while negating the effects of Na⁺-fluxes. The whole-cell patch-clamp technique was performed on excitable, ventricular cells, isolated from guinea-pigs. The guinea-pigs were killed by a sharp blow to the base of the skull. After the heart was removed, it was perfused via a constant perfusion system, with the addition of 6 mg collagenase (Type II, Sigma, St Louis) and 4.5 mg protease (Type 14, Sigma, St Louis) per 40 ml. This was done to aid the dispersion of the ventricular cells. The cells were resuspended in the resuspension buffer containing 138 mM Tris, 20 mM CsCl, 0.5 mM MgCl₂, 10 mM HEPES-NaOH, 5.4 mM CaCl₂ and 5 mM glucose (pH 7.2)⁷. The whole-cell patch-clamp technique (Hamil *et al.*, 1981) was used to determine the effects of the compounds on L-type Ca²⁺-channels. The pipettes (electrodes) were pulled with a Narishige PP 83 model pipette puller. The ionic currents were recorded (Dagan, model 8800, Total Clamp Amplifier) under voltage-clamp conditions, using the following pipette solution : 125 mM CsCl, 2 mM MgCl₂, 5 mM EGTA, 10 mM HEPES, 1 mM CaCl₂, 10 mM glucose and 3 mM Mg-ATP (pH 7.2). The holding potential was changed from -80 mV to -45 mV for 3 s to inactivate the Na⁺-channels, after which the inward Ca²⁺-currents were recorded. The cells were then exposed to 100 μM solutions (pH 7.4) of the respective isomers. Two protocols were used. In the first protocol (A), the inward Ca²⁺-currents were recorded after changing the holding potential of -90 mV to different test potentials for 100 ms. The test potentials were increased in 5 mV steps from -50 mV to +20 mV. Inward Ca²⁺-currents were recorded at a holding potential of -45 mV for the second protocol (B). The aim of the two protocols was to determine if the effect of the isomers

⁷ Solution list – Appendix C

on the Ca²⁺-channel was voltage-dependent or not. Data was analysed using the Microsoft Origin Scientific Graphic System, Version 4. The isomers were washed out of the system using the resuspension solution.

Blockage or opening of the peak inward current was measured from the current-voltage relationship as the % change from the control at the membrane potential where the current reached a maximum (eg. at 10 mV for cyclo (L-Trp-L-Pro), Figure 7.9).

7.3.1.2 Potassium channel activity

The whole-cell patch-clamp technique was used to record ionic currents under voltage clamp conditions from single cells isolated with enzymatic dispersion from the ventricles of guinea-pig, as described for the Ca²⁺-channel activities. The resuspension buffer contained 130 mM NaCl, 4 mM KCl, 1 mM MgCl₂, 10 mM HEPES-NaOH, 1.8 mM CaCl₂ and 10 mM glucose (pH 7.2). The cells were then exposed to 100 μM solutions (pH 7.4) of the respective compounds. The ionic currents were recorded under voltage-clamp conditions, using the following pipette solution: 140 mM KCl, 2 mM MgCl₂, 11 mM EGTA, 10 mM HEPES, 1 mM CaCl₂, 10 mM glucose and 5 mM Na₂-ATP (pH 7.2). Currents were recorded during 500 ms hyperpolarizing steps from a holding potential of –80 mV (to inactivate Na⁺-channel activity) to different potentials between –140 mV and –50 mV. The isomers were washed out of the system using resuspension buffer. Data was analysed using the Microsoft Origin Scientific Graphic System, Version 4.

7.3.2 Isolated heart perfusion

Retrogradely perfused rat heart allows for the association of biochemical and mechanical events. In this technique, oxygen supply meets the demands of the working heart, stability of the preparation is maintained, and all factors (such as temperature and oxygen tension of the media) influencing heart performance can be measured. KHBB contains half the usual concentration of Ca²⁺, with glucose as substrate. Major lactate build-up is avoided by equilibrating the buffer at atmospheric pressure with carbogen (95% O₂, 5% CO₂, Afrox, South Africa) (Fallen *et al.*, 1967).

A modified Langendorff method (Figure 7.7) was used to study the effects of the isomers on heart rate, coronary flow and reperfusion-induced arrhythmias in rat hearts (Langendorff, 1895). Induction of arrhythmia was accomplished by occlusion of the left descending coronary artery, producing a zone of ischaemia. This was followed by reperfusion of the ischaemic area, using a low K^+ -buffer to start the development of reperfusion arrhythmia (Curtis *et al.*, 1987).

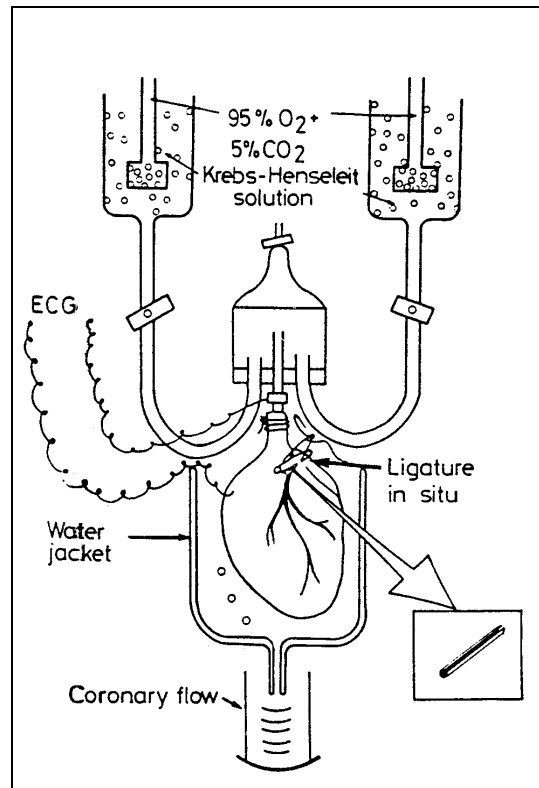


Figure 7. 7: The Langendorff perfusion apparatus. Two perfusate reservoirs are shown with a single bubble-trap situated above the aortic cannula. In this set-up, the atria are left intact (Lubbe *et al.*, 1978).

Male Long Evans rats (250 – 350g) were placed under light ether anaesthesia to a loss of blink and pain reflexes. Prior to dissection, heparin sodium (200 I.U., Intramed, South Africa) was injected into the femoral vein to prevent blood clot formation in the coronary blood vessels. In order to open the abdomen, a transverse cut at the base of the rib cage was used. By transection of the diaphragm and parallel incisions along the sides of the rib cage, the heart was revealed. The pericardium and filamentous tissue were removed from the heart, after which the heart was removed by a cut through the blood vessels at the

base of the heart. Once removed, the hearts were arrested in ice-cold KHBB (pH 7.4), to prevent metabolic activity. Once the heart was positioned on the aortic cannula, retrograde perfusion was commenced, using an IKA-PA-SF 5 peristaltic pump (Laboratory and Scientific Equipment, (Pty.), Ltd.). The heart was perfused via an aortic cannula, held in position by means of an arterial clamp and silk thread (Clinisut, South Africa). Bipolar ECG leads were used to record ECGs. The cathode electrode was placed into the epicardium of the anterior portion of the right ventricle for heart rate recording. The anode electrode was attached to the steel aortic cannula of the perfusion apparatus. Occlusion was achieved by using a silk suture (Clinisut, South Africa) and a rigid polyvinyl occluder (5 mm x 1 mm), which was pulled tightly to effect ligation. Successful occlusions were characterised by a 50% decrease in coronary flow rate. On occlusion, a region of ischaemia develops, causing K^+ to accumulate on one side of the heart. This essentially causes a K^+ -gradient to form across the heart. A larger gradient is induced by using buffer containing low K^+ -concentrations, thereby increasing the probability of ventricular tachycardia and arrhythmias. Reperfusion of the infarcted area of the left ventricle occurred once the tension on the occluder was removed. Acceptable reperfusion was characterised by a 90% increase in coronary flow rate. The heart was kept in a 37°C environment by means of a warming jacket. The perfusion pressure was maintained at 1 m water pressure, and aeration of the perfusate was achieved by carbogen. Coronary flow was measured throughout the experiment at 5 min intervals.

Prior to experimentation, a 15 min stabilization period was allowed, during which time the heart was perfused with KHBB containing 5.9 mM K^+ (normal K^+ -levels). After this period, the isomer solution (200 μ M isomer dissolved in 0.5% DMSO) was perfused into the heart for 15 min. During this period, the heart rate and coronary flow were monitored every 5 min. The heart rate was displayed on a digital heart rate monitor (Microplex Electronics). Following this, the perfusion buffer was changed to a KHBB containing a lower concentration of K^+ (3.3 mM). At the same time, the left descending coronary artery was occluded for a period of 10 min, allowing for the development of ischaemia. The occluder was then released and the heart reperfused with the low K^+ -containing KHBB and isomer. Ventricular tachycardia (VT) and arrhythmia (VA) were monitored

until the occurrence of a regular sinus rhythm (SR) or the termination of the experiment occurred. These ECGs were monitored and stored on a storage oscilloscope (Telequipment DM63). Control samples were perfused with KHBB containing 0.5 % DMSO.

A summary of the experimental protocol is set out in Figure 7.8.

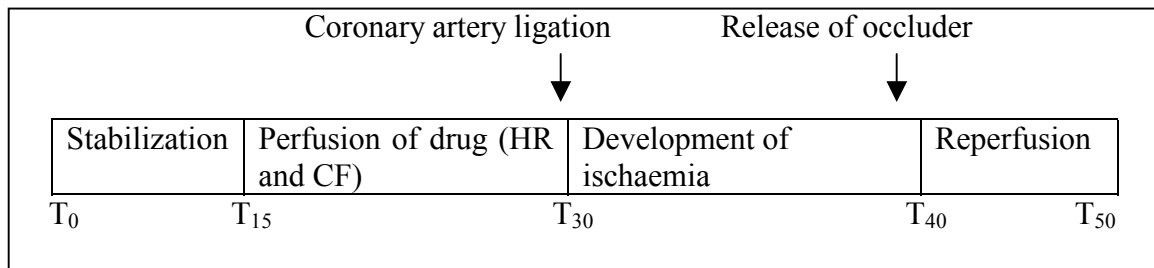


Figure 7. 8: The experimental protocol for the isolated rat heart perfusion. T= time in minutes, HR= heart rate, CF= coronary flow.

7.3.2.1 Measurement of ventricular tachycardia and arrhythmia, time to sinus rhythm and QRS interval

ECGs recorded on PolyView Data Acquisition and Analysis System (Version 2.0, 1997) were examined for duration of VT and VA, time to SR, as well as duration of QRS complexes. The QRS complexes were measured by manual positioning of the screen markers. At least four complexes were measured and averaged at each time point.

7.3.3 Statistical analysis

The values of parameters measured are presented as mean \pm s.d. for the indicated number of experiments. Results were analysed using the software package GraphPad Prism Version 2.0 and GraphPad InStat (GraphPad Software, Inc., San Diego, U.S.A.). All tests were performed on raw data obtained from the experiments. The effect of a single qualitative factor on a single response variable was determined by univariate ANOVA using the Mann-Whitney test. *P* values <0.05 were accepted as evidence of a statistically significant difference.

7.4 RESULTS AND DISCUSSION

In recent years, there has been increased favour in the use of Ca^{2+} -antagonists in the treatment of cardiovascular disorders, such as cardiac arrhythmias. Their use is largely based on the disruption of voltage-dependent Ca^{2+} -channels in both the cardiac muscle and vascular smooth muscle (Dong *et al.*, 1993). Some substances that inhibit Ca^{2+} -channels may have a lowered negative inotropic effect, possibly as a result of influences on other ion channels (Sensch *et al.*, 2000). For this reason, the effect of the isomers on inwardly rectifying K^{+} -channels was also determined.

On exposure to 100 μM cyclo(L-Trp-L-Pro) to the isolated guinea-pig myocyte, an increased current was observed after a 1 min exposure period in protocol A, with maximal effects noted after a 5 min exposure period (Figure 7.9). The effect was not completely reversible, since the current did not return to the control current value after either the 1 min or 7 min washout period, although it did move in the direction of the current. The maximal increase for the 1 min exposure was 22 %, while a 77% increase in current was noted for the 5 min exposure.

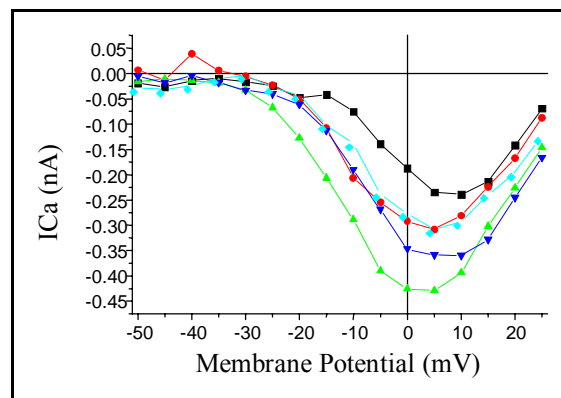


Figure 7. 9: The current-voltage relationship of inward currents recorded with the addition of 100 μM cyclo (L-Trp-L-Pro). (■) = Control after 10 min (to ensure stable current). (●) = 100 μM cyclo(L-Trp-L-Pro) for 1 min. (▲) = 100 μM cyclo(L-Trp-L-Pro) for 5 min. (▼) = Washout period of 1 min. (◆) = Washout period of 7 min. I_{Ca} = inward current flow. Values indicated are the mean \pm s.d of duplicates.

Determination of the dependence on voltage was determined by using protocol B. When a holding potential of -45 mV was applied to the cells, the peak inward current

decreased. This was noted in 2 different cells (Figure 7.10). After the 1 min washout period, it was noted that the effect was not totally reversible, as the currents did not return to that of the control value.

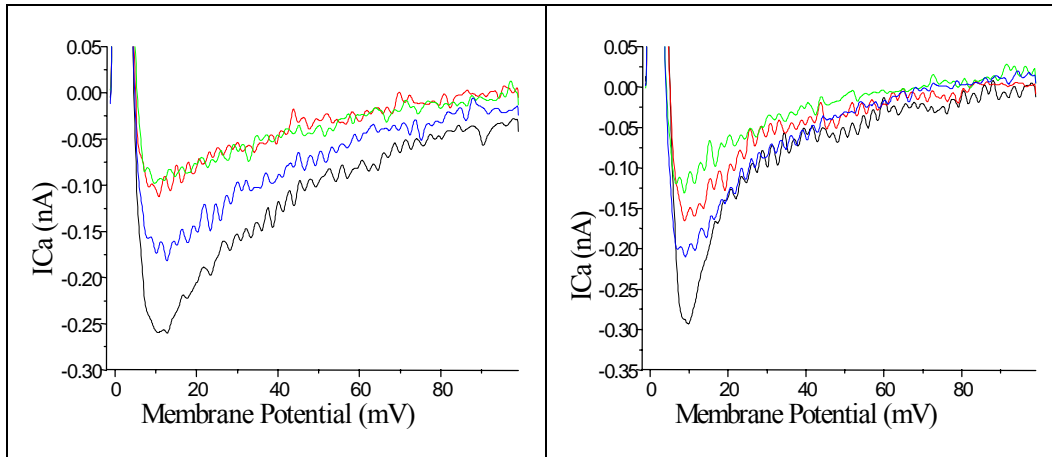


Figure 7. 10: The current-voltage relationship of inward currents recorded with the addition of 100 μM cyclo(L-Trp-L-Pro). (—) = Control after 10 min (to ensure stable current). (—) = 100 μM cyclo(L-Trp-L-Pro) for 1 min. (—) = 100 μM cyclo(L-Trp-L-Pro) for 5 min. (—) = Washout period of 1 min.

It is interesting to note that with protocol B (Figure 7.10), antagonism is noted (blockage of peak inward current), whereas with protocol A (Figure 7.9) agonism of the Ca^{2+} -channel activity is noted. This suggests that the effect of the compound on the cell is dependent on membrane potential.

Two control currents (A and B) were recorded for K^{+} -channel activity (Figure 7.11) to ensure that a stable current amplitude was achieved before applying cyclo(L-Trp-L-Pro) to the cell. After 1 min and 3 min exposure periods, an insignificant decrease ($p > 0.05$) in the inward current was observed. The effect was totally reversible, with the current returning to both control A and B value after a 3 min washout period.

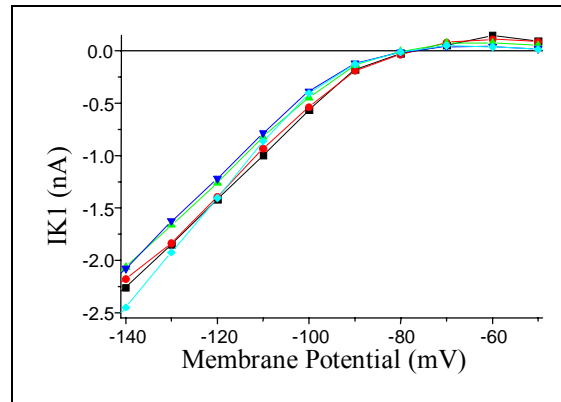


Figure 7. 11: The current-voltage relationship of inward currents recorded with the addition of 100 μM cyclo(L-Trp-L-Pro). (■) = Control after 10 min (to ensure stable current). (●) = Second control current. (▲) = 100 μM cyclo(L-Trp-L-Pro) for 1 min. (▼) = 100 μM cyclo(L-Trp-L-Pro) for 3 min. (◆) = Washout period of 3 min. IK_1 = inward rectifier K^+ -current. Values indicated are the mean \pm s.d of duplicates.

100 μM cyclo(L-Trp-D-Pro) was tested on 2 different cells using protocol A (Figure 7.12). Cell A (Figure 7.12) was exposed to both a 1 min and 5 min period to the compound, while cell B (Figure 7.12) was only exposed for 1 min. In cell A, the current was increased in the presence of the compound by 90%, with the maximal effect being noted after 5 min (a 92% increase in the peak inward current).

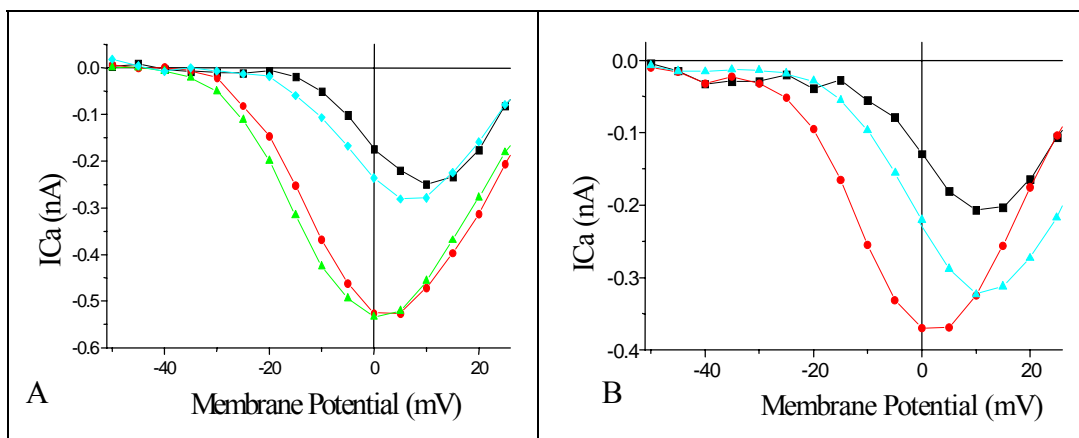


Figure 7. 12: The current-voltage relationship of inward currents recorded with the addition of 100 μM cyclo(L-Trp-D-Pro). (■) = Control after 10 min (to ensure stable current). (●) = 100 μM cyclo(L-Trp-D-Pro) for 1 min. (▲) = 100 μM cyclo(L-Trp-D-Pro) for 5 min. (◆) = Washout period of 4 min. ICa = inward current flow. (n=2)

The same effect was noted in cell B, showing a 63% increase in the peak inward current. In cell A, the effect was almost completely reversible, while only partially reversible in cell B after a 4 min washout period.

Protocol B was also tested on two cells (A and B) (Figure 7.13), showing a decrease in the peak inward current after both a 1 min and 5 min exposure period to cyclo(L-Trp-D-Pro). After approximately 8 ms, a 55% blockage (1 min exposure) and 86% blockage (5 min exposure) was noted in cell A, while a 70% blockage (1min exposure) and a 100% blockage (5 min exposure) was observed in cell B. In both cells, the effects were not completely reversible after a 7 min washout period. Once again, it is seen that for protocol A (Figure 7.12), the compound is agonistic, while in protocol B (Figure 7.13), an antagonistic effect is observed, suggesting that the effect of the drug on the Ca^{2+} -channel is dependent on the membrane potential.

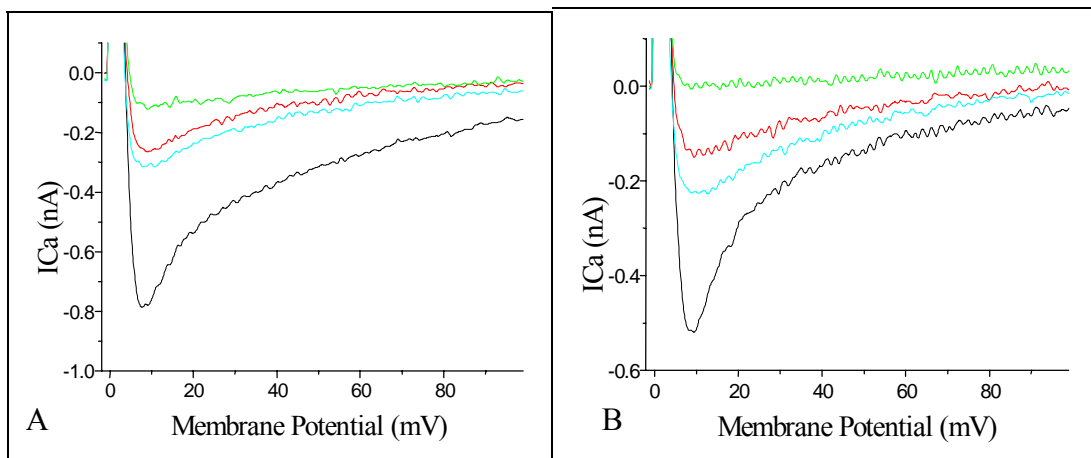


Figure 7. 13: The current-voltage relationship of inward currents recorded with the addition of 100 μM cyclo(L-Trp-D-Pro). (-) = Control after 10 min (to ensure stable current). (-) = 100 μM cyclo(L-Trp-D-Pro) for 1 min. (-) = 100 μM cyclo(L-Trp-D-Pro) for 5 min. (-) = Washout period of 7 min. I_{Ca} = inward current flow. (n=2)

Testing of the effects of cyclo(L-Trp-D-Pro) on the K^{+} -channel for both a 1 min and 3 min exposure period showed an insignificant effect on the inward rectifier K^{+} -channel (Figure 7.14). A 3 min washout period returned the current to that of the control current.

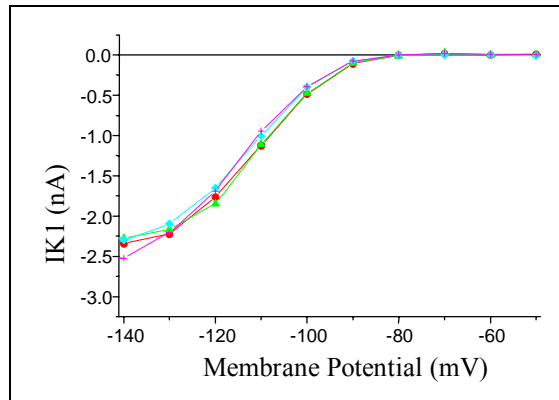


Figure 7. 14: The current-voltage relationship of inward currents recorded with the addition of 100 μM cyclo(L-Trp-D-Pro). (●) = Control after 10 min (to ensure stable current). (▲) = 100 μM cyclo(L-Trp-D-Pro) for 1 min. (◆) = 100 μM cyclo(L-Trp-D-Pro) for 3 min. (-+-) = Washout period of 3 min. IK1 = inward rectifier K^+ -current. Values indicated are the mean \pm s.d of duplicates.

Before the application of 100 μM cyclo(D-Trp-L-Pro) to the cells, two control currents were recorded to ensure stability of the current (Figure 7.15). After both a 1 min and a 5 min exposure period, a blockage in the peak inward current was observed, with a maximal effect after 5 min. For the 1 min exposure, blockages of 23% and 25% were noted for control 1 and control 2, respectively. Blockages of 32% and 34%, respectively, were noted for the 5 min exposure period. Similarly, a decrease in the current was also noted for protocol B (Figure 7.16).

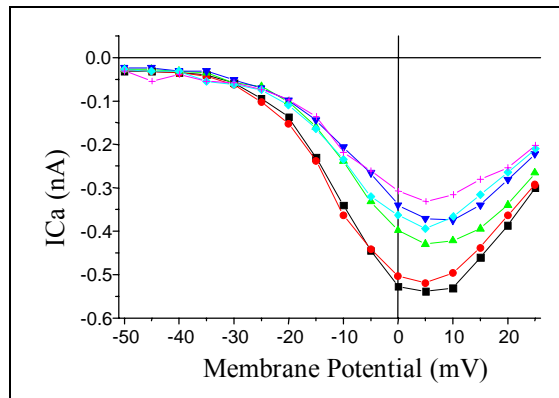


Figure 7. 15: The current-voltage relationship of inward currents recorded with the addition of 100 μM cyclo(D-Trp-L-Pro). (■) = Control 1 current after 10 min (to ensure stable current). (●) = Control 2 current. (▲) = 100 μM cyclo(D-Trp-L-Pro) for 1 min. (▼) = 100 μM cyclo(D-Trp-L-Pro) of 5 min. (◆) = Washout period of 1 min. (-+-) = Washout period for 5 min. ICa = inward current flow. Values indicated are the mean \pm s.d of duplicates.

For both protocols A and B, the effects were not reversible, since the washout currents did not return to that of the controls. Unlike cyclo(L-Trp-L-Pro) and cyclo(L-Trp-D-Pro), it appears that the effect of cyclo(D-Trp-L-Pro) is independent of membrane potential, since antagonism of the Ca^{2+} -channels was noted for both protocol A and B.

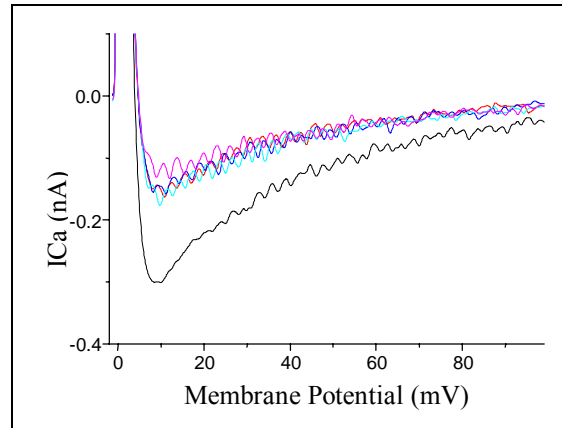


Figure 7. 16: The current-voltage relationship of inward currents recorded with the addition of 100 μM cyclo(D-Trp-L-Pro). (-) = Control after 10 min (to ensure stable current). (-) = 100 μM cyclo(D-Trp-L-Pro) for 1 min. (-) = 100 μM cyclo(D-Trp-L-Pro) for 5 min. (-) = Washout period of 1 min. (-) = Washout period of 5 min. I_{Ca} = inward current flow.

The inward rectifier K^{+} -current was decreased between -140 mV and -120 mV after a 3 min exposure to cyclo(D-Trp-L-Pro) (Figure 7.17). However, the effect was almost completely reversible, as the current almost returned to that of the control current after a 3 min washout period.

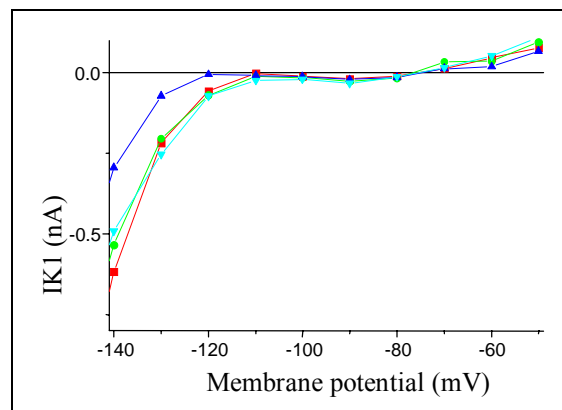


Figure 7. 17: The current-voltage relationship of inward currents recorded with the addition of 100 μM cyclo(D-Trp-L-Pro). (■) = Control after 10 min (to ensure stable current). (●) = 100 μM cyclo(D-Trp-L-Pro) for 1 min. (▲) = 100 μM cyclo(D-Trp-L-Pro) for 3 min. (▼) = Washout period of 3 min. I_{K1} = inward rectifier K^{+} -current. Values indicated are the mean \pm s.d of duplicates.

A slight increase (17%) in the peak inward was observed after a 1 min exposure period to cyclo(D-Trp-D-Pro) (Figure 7.18). The effect was not reversible although the current moved in the direction of the control current. At a holding potential of -45 mV (protocol B) (Figure 7.19), the current increased slightly (10%) after 1 min, but decreased by 24% in relation to the control current value after a 5 min exposure period. The effect was not completely reversible after a 5 min washout period.

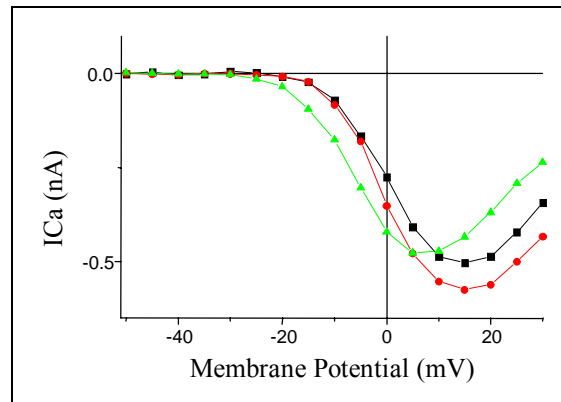


Figure 7. 18: The current-voltage relationship of inward currents recorded with the addition of $100 \mu\text{M}$ cyclo(D-Trp-D-Pro). (■) = Control after 10 min (to ensure stable current). (●) = $100 \mu\text{M}$ cyclo(D-Trp-D-Pro) for 1 min. (▲) = Washout period of 5 min. I_{Ca} = inward current flow. Values indicated are the mean \pm s.d of duplicates.

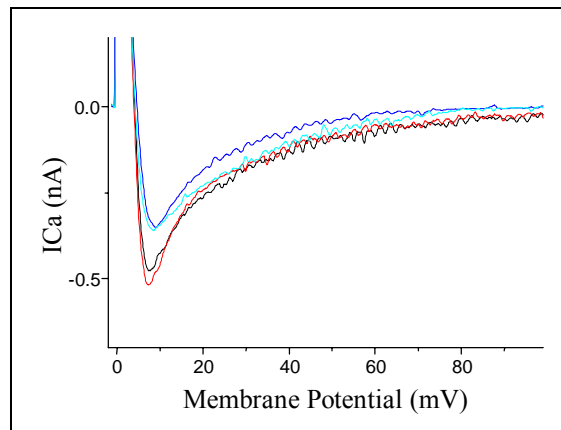


Figure 7. 19: The current-voltage relationship of inward currents recorded with the addition of $100 \mu\text{M}$ cyclo(D-Trp-D-Pro). (-) = Control after 10 min (to ensure stable current). (-) = $100 \mu\text{M}$ cyclo(D-Trp-D-Pro) for 1 min. (-) = $100 \mu\text{M}$ cyclo(D-Trp-D-Pro) for 5 min. (-) = Washout period of 5 min. I_{Ca} = inward current flow.

No significant effect on the inward rectifier K^+ -channels (Figure 7.20) was noted after a 3 min exposure period to 100 μ M cyclo(D-Trp-D-Pro), since the currents for the 1 min and 3 min exposure period did not deviate from the control current.

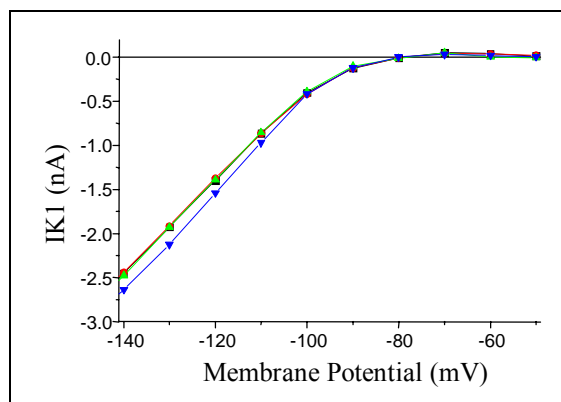


Figure 7. 20: The current-voltage relationship of inward currents recorded with the addition of 100 μ M cyclo(D-Trp-D-Pro). (■) = Control after 10 min (to ensure stable current). (●) = 100 μ M cyclo(D-Trp-D-Pro) for 1 min. (▲) = 100 μ M cyclo(D-Trp-D-Pro) for 3 min. (▼) = Washout period of 3 min. IK_1 = inward rectifier K^+ -current. Values indicated are the mean \pm s.d of duplicates.

A summary of the results as determined for L-type Ca^{2+} -channel activity is tabulated in Table 7.2.

Table 7. 2: Effects of the isomers on L-type Ca^{2+} -channel activity.

Compound (100 μ M)	Ca^{2+} -channel activity (Protocol A)	Ca^{2+} -channel activity (Protocol B)	Dependence on membrane potential	K^+ -channel activity
Cyclo (L-Trp-L-Pro)	Agonist (77%)	Antagonist	Dependent	No significant effect
Cyclo (L-Trp-D-Pro)	Agonist (92%)	Antagonist	Dependent	No significant effect
Cyclo (D-Trp-L-Pro)	Antagonist (32%)	Antagonist	Independent	No significant effect
Cyclo (D-Trp-D-Pro)	Agonist (17%)	Antagonist	Dependent	No significant effect

Studies on another cyclic dipeptide, cyclo(Trp-Trp), showed antagonistic activity towards Ca^{2+} -channel activity, with a 45% blockage after 1 min exposure to 100 μM solution of the dipeptide. This blockage increased by 2% to 47% after a 3 min exposure and was found to be faster acting than cyclo(L-Trp-L-Pro) in isolated guinea-pig ventricular myocytes (Milne *et al.*, 1998).

Other non-peptidic compounds, such as acetoacetate and butyrate, both C4 compounds, showed antagonistic activity towards the Ca^{2+} -channel activity in isolated myocytes from the rat. Acetoacetate was a more effective antagonist, showing a 63% blockage vs 50% blockage for butyrate. The effect of both these compounds were reversible (Jamie *et al.*, 2001).

The initial study on the effects of cyclo(L-Trp-L-Pro), cyclo(Tyr-Pro), cyclo(Phe-Pro) and cyclo(Trp-Trp) on K^+ -channel activity was conducted by Milne *et al.* (1998). They found that cyclo(L-Trp-L-Pro) and cyclo(Tyr-Pro) inhibited the delayed-rectifier K^+ -channels, with cyclo(Tyr-Pro) exhibiting a greater effect (65% as opposed to 38% after a 2 min exposure period). Cyclo(Trp-Trp) and cyclo(Phe-Pro) had no effect on the current. It was further concluded that these compounds did not affect other K^+ -channels, such as the inward rectifier current (Milne *et al.*, 1998). This statement supports results obtained in the present study.

In a study on cardiac ventricular cells of the guinea-pig, a 50% reduction in the inward Ca^{2+} -current was noted with the following concentrations of drug: $0.318 \pm 0.006 \mu\text{mol/l}$ nifedipine, $29 \pm 1 \mu\text{mol/l}$ β -caryophyllene oxide and $226 \pm 17 \mu\text{mol/l}$ eugenol. The only drug that inhibited K^+ -channel activity was reported to be β -caryophyllene oxide at a concentration of $30 \mu\text{mol/l}$ (Sensch *et al.*, 2000). In a separate study, ranolazine, an antifungal agent, was tested agonist Ca^{2+} -channel activity. It was found that 10 μM and 100 μM of this agent inhibited the channel activity by 2.4 and 11.3%, respectively. When the channel was activated by the application of 20 nM isoprenaline, a β -adrenoceptor activator, the inhibition of Ca^{2+} -channel activity in the presence of 100 μM ranolazine increased to 88%. When the channel was pretreated with 200 nM histamine, only 30%

inhibition was noted (Allen and Chapman, 1996). 50 μM Norbormide, a vasoactive compound, inhibited inward current flow by $49.6 \pm 3.9\%$ in guinea-pig ventricular myocytes, with a maximum effect after 5-7 min. This effect was not completely reversible, as after a 8min washout period, the current returned to only $65.6 \pm 5.1\%$ of the control current (Bova *et al.*, 1997). The effect of protopine, an isoquinoline alkaloid isolated from *Corydalis tubers*, was studied on ventricular myocytes isolated from the guinea-pig. The inward current amplitude was reduced to 85.6, 62.1 and 48.9% of the control in the presence of 25, 50 and 100 μM protopine, respectively. 100 μM Protopine resulted in a 55% decrease in the inward rectifier K^+ -current (Song *et al.*, 2000).

Ca^{2+} -channel antagonists such as nifedipine and verapamil are known to cause antiarrhythmic action against ischaemic arrhythmias, thus protecting the ischaemic heart (Allen and Chapman, 1996). If the influx of Ca^{2+} is inhibited, the initiation and maintenance of VF does not occur if the drug is capable of binding to the dihydropyridine-sensitive Ca^{2+} -channels. In addition, this blockage would also result in the inhibition of activities related to Ca^{2+} -influx, such as heart rate. In the incidence of an ischaemic myocardium, a diminished heart rate would be beneficial in that the demand for oxygen by the myocardium is reduced (Dong *et al.*, 1993). Vascular smooth muscle relaxes as a result of Ca^{2+} -influx inhibition. In cardiac muscle, reduced Ca^{2+} -inward current plays a crucial role in the antiarrhythmic properties of these Ca^{2+} -channel antagonists i.e. it always leads to a negative inotropic effect (Sensch *et al.*, 2000).

As a result of the agonistic effect of cyclo(L-Trp-L-Pro), cyclo(L-Trp-D-Pro) and cyclo(D-Trp-D-Pro) on Ca^{2+} -channel activity, the effect on the heart rate was investigated, as it was suggested that these agonists would possess positive chronotropic activity i.e. cause an increase in heart rate. On the other hand, due to the antagonistic effect of the DL isomer on Ca^{2+} -channel activity, it was expected that it would possess negative chronotropic activity i.e. result in a decreased heart rate. In addition, an increase in the coronary flow is expected with the application of cyclo(D-Trp-L-Pro) (Cook, 1998).

There was a slight decrease in heart rate in the control sample (Figure 7.21), which is to be expected, since experimental conditions are not ideal. Cyclo(L-Trp-L-Pro) and cyclo(D-Trp-D-Pro) did not show any significant difference in heart rate when compared to the control ($p=0.1$) whereas cyclo(L-Trp-D-Pro) significantly increased the heart rate in relation to the control ($p= 0.004$). As expected, cyclo(D-Trp-L-Pro) decreased the heart rate ($p=0.0238$).

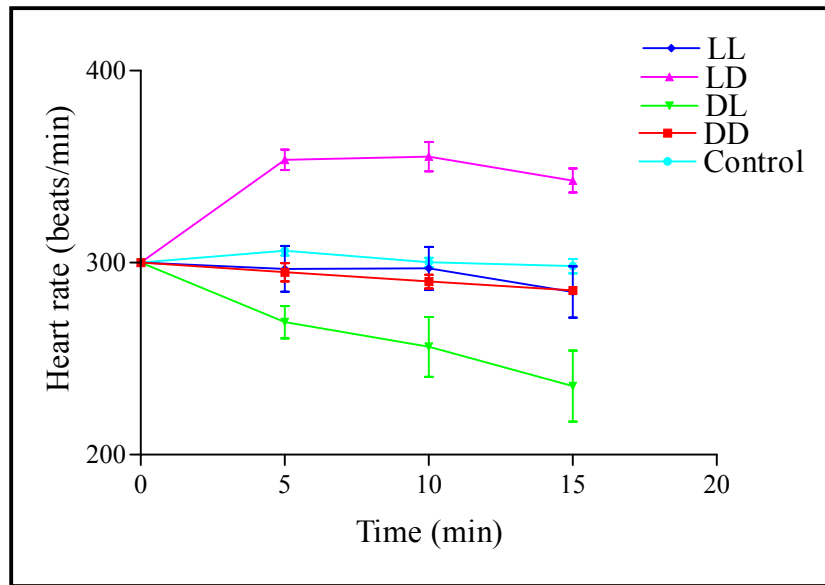


Figure 7. 21: Effect of the isomers on the heart rate in isolated, rat heart. Values indicated are the mean \pm s.d of 6 experiments.

Statistical analysis on the correlation between the different isomers is shown in Table 7.3.

Table 7. 3: Correlation data of the effects of the isomers on heart rate in the isolated, perfused rat heart.

Isomers compared	P value	Significant difference
Cyclo(L-Trp-L-Pro) and cyclo(L-Trp-D-Pro)	P < 0.0001	Yes
Cyclo(L-Trp-L-Pro) and cyclo(D-Trp-L-Pro)	P = 0.0239	Yes
Cyclo(L-Trp-L-Pro) and cyclo(D-Trp-D-Pro)	P = 0.3639	No
Cyclo(L-Trp-D-Pro) and cyclo(D-Trp-L-Pro)	P = 0.0045	Yes
Cyclo(L-Trp-D-Pro) and cyclo(D-Trp-D-Pro)	P = 0.0016	Yes
Cyclo(D-Trp-L-Pro) and cyclo(D-Trp-D-Pro)	P = 0.0346	Yes

As can be noted from Table 7.3, cyclo(L-Trp-D-Pro) and cyclo(D-Trp-L-Pro) differ significantly from each other, while cyclo(L-Trp-L-Pro) and cyclo(D-Trp-D-Pro) do not.

In isolated perfused hearts of the guinea-pig, a neuropeptide termed Substance P, showed that it had negative inotropic effects in the left ventricle and right atria by resulting in a negative change in heart rate at concentrations ranging between 3×10^{-10} to 3×10^{-5} M (Chiao and Caldwell, 1995).

In a study on the effects of the endogenous cannabinoid, arachidonylethanolamide (AEA) in the rat, it was found that 3 mg/kg, 10 mg/kg and 30 mg/kg resulted in significantly decreased heart rates within a minute in comparison to the control group ($p < 0.05$). No significant change was noted 30 min post drug. When an AEA metabolite, arachidonic acid, was administered to the rats at 10 mg/kg, a significant decrease in heart rate resulted within a minute. When the heart rate was monitored over a 30 min period, significant decreases in heart rate was also noted in rats treated with 1 mg/kg and 3 mg/kg arachidonic acid (Stein *et al.*, 1996).

In experiments carried out on isolated, perfused rat hearts, decreases in heart rate were noted in the presence of 10^{-7} M nifedipine, 3×10^{-6} M diltiazem and 10^{-5} M CPU-23 ((1-{1-[(6-methoxy)-naphth-2-yl]}-propyl-2-(1-piperidine)-acetyl-6,7-dimethoxy-1,2,3,4-

tetra-hydroisoquinoline) (a substituted tetrahydroisoquinoline) (Dong *et al.*, 1993). 0.3 mg/kg ICI 170,809 (5-HT₂ antagonist) significantly reduced the heart rate in anaesthetized rats from 388±12 beats/min (control) to 345±6 beats/min (p<0.05). A thromboxane antagonist, ICI 192,605, also resulted in a reduction in heart rate to 347±12 beats/min (p<0.05) (Shaw and Coker, 1996). The effects of lidocaine, a standard ischaemia-selective drug, and tedisamil, a class III antiarrhythmia agent, on heart rate in anaesthetized rabbits were determined by Barrett *et al.* (2000). It was found that 2.5 µmol/kg/min lidocaine reduced heart rate by 14±5% (p<0.05), while 0.125 µmol/kg/min and 0.25 µmol/kg/min tedisamil resulted in 15±2% and 27±5% decreases in heart rate, respectively (Barrett *et al.*, 2000).

During all experiments, coronary flow rates were determined. Common to all Ca²⁺-antagonists is dilation of coronary vessels, i.e. an increase in coronary flow (Bova *et al.*, 1997). It was thus expected that cyclo(D-Trp-L-Pro) produce increased rates of coronary flow as a result of its antagonist action against Ca²⁺-channels (Figure 7.15). From Figure 7.22, it is clear that cyclo(L-Trp-L-Pro) and cyclo(D-Trp-D-Pro) did not produce any significant effects on the coronary flow in relation to the control (p = 0.4326, p=0.7228, respectively). Both cyclo(L-Trp-D-Pro) and cyclo(D-Trp-L-Pro) increased coronary flow (p = 0.0296 and p = 0.0071, respectively) when compared to the control samples. This increase in coronary flow for cyclo(D-Trp-L-Pro) was expected, although a decrease in coronary flow for cyclo(L-Trp-D-Pro) was anticipated. Of particular interest is the fact that cyclo(L-Trp-L-Pro) and cyclo(D-Trp-D-Pro) did not produce any significant effects on cardiac vascular smooth muscle (from coronary flow rate results). This indicates that cyclo(L-Trp-D-Pro) and cyclo(D-Trp-L-Pro) resulted in relaxed vascular smooth muscle, which caused blood vessels in these regions to dilate, resulting in an increased coronary flow (Nayler, 1988). Disease states such as angina and myocardial infarction are often accompanied by arrhythmias, which may be aggravated by drugs that cause vasoconstriction. It is thus of particular interest that none of the isomers tested resulted in vasoconstriction i.e. a decrease in coronary flow rate.

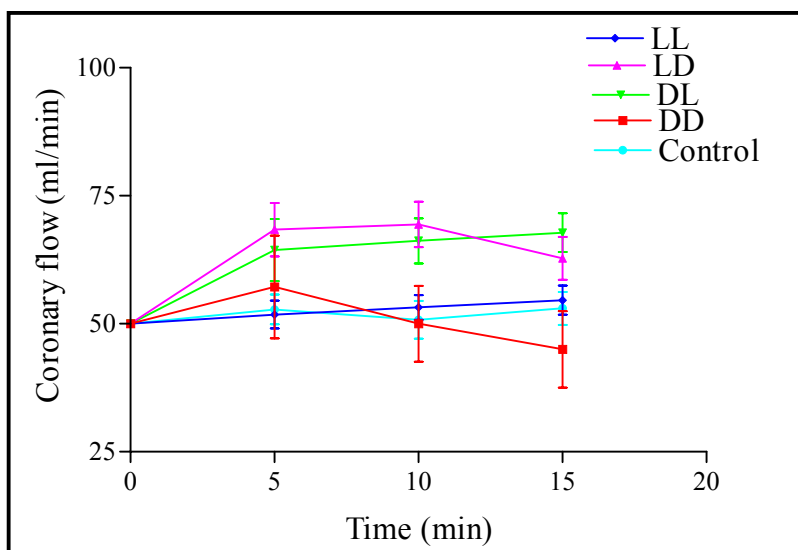


Figure 7. 22: The effects of the isomers on coronary flow rate as determined in the isolated rat heart. Values indicated are the mean \pm s.d of 6 experiments.

Statistical analysis of the correlation between the different isomers is shown in Table 7.4.

Table 7. 4: Correlation data of the effects of the isomers on coronary flow in the isolated, perfused rat heart.

Isomers compared	P value	Significant difference
Cyclo(L-Trp-L-Pro) and cyclo(L-Trp-D-Pro)	P = 0.6275	No
Cyclo(L-Trp-L-Pro) and cyclo(D-Trp-L-Pro)	P = 0.0378	Yes
Cyclo(L-Trp-L-Pro) and cyclo(D-Trp-D-Pro)	P = 0.0764	No
Cyclo(L-Trp-D-Pro) and cyclo(D-Trp-L-Pro)	P = 0.0234	Yes
Cyclo(L-Trp-D-Pro) and cyclo(D-Trp-D-Pro)	P = 0.0002	Yes
Cyclo(D-Trp-L-Pro) and cyclo(D-Trp-D-Pro)	P = 0.8226	No

Similar to the effects on heart rate (Table 7.3), the effects of cyclo(L-Trp-D-Pro) and cyclo(D-Trp-L-Pro) differ significantly from each other, while cyclo(L-Trp-L-Pro) and cyclo(D-Trp-D-Pro) do not differ significantly in the effect on coronary flow (Table 7.4).

In the isolated guinea-pig heart, $0.23 \pm 0.04 \mu\text{M}$ sumatriptan (an anti-migraine drug) resulted in a decreased coronary flow. No effect on coronary flow was detected in the presence of 3 and 10 nM GR 127935 (N-[4-methoxy-3-(4-methyl-1-piperazinyl)phenyl]-2'-methyl-4'-(5-methyl-1,2,4-oxadiazol-3-yl)[1,1-biphenyl]-4-carboxamide), a selective $5\text{HT}_{1\text{D}}$ receptor antagonist (Ellwood and Curtis, 1997). In the isolated, perfused rat heart, 20 ng/ml tumour necrosis factor significantly reduced the coronary flow within 5 min ($p < 0.01$) (Edmunds *et al.*, 1999).

The effect of cyclosporin (used in graft rejection) and cremophor EL (a vehicle used as an intravenous preparation) on perfused rat heart was examined by Mankod *et al.* (1992). 500 ng/ml Cremophor EL and cyclosporin caused a $9.2 \pm 0.7\%$ and a $12.7 \pm 2\%$ decrease in coronary flow, respectively. When the concentration was increased to 1000 ng/ml, cremophor EL and cyclosporin caused a $24.8 \pm 2.2\%$ and a $48.7 \pm 0.6\%$ decrease, respectively. The coronary flow was also determined in the presence of 5-HT and nitroglycerine (GTN). In both cases, an increase in coronary flow was noted. An increase of $33.3 \pm 2.5\%$ was recorded for 5-HT and a $34.3 \pm 2.5\%$ increase for GTN. When 500 ng/ml and 1000 ng/ml cremophor EL was applied to the heart after 5-HT pretreatment, the coronary flow decreased significantly for both cases. However, no effect was noted in coronary flow with pretreatment of the heart with GTN. When cyclosporin was substituted for cremophor EL, the coronary flow was decreased significantly with either the 5-HT or the GTN pretreatments. It was therefore concluded that cyclosporin dissolved in cremophor EL may aggravate vascular smooth muscle injury (Mankod *et al.*, 1992).

A major cause of morbidity and mortality is ventricular arrhythmias, which are associated with myocardial ischaemia. No complete therapeutic solution is available as yet (Barrett *et al.*, 2000). In all experiments, the coronary flow decreased to less than 40% during occlusion and returned to normal after reperfusion. Following short periods of ischaemia, VA occur upon reperfusion, partially attributed to the production of oxygen-derived free radicals and other reactant oxygen intermediates (Loesser *et al.*, 1991). Ischaemia-induced arrhythmias started within a few seconds of occlusion release around the coronary artery and then progressed to VF and finally to SR. Segments of ECGs recorded

during experimentation are shown, illustrating SR (Figure 7.23 A), VT (Figure 7.23 B), arrhythmia (Figure 7.23 C), SR changing to VT (Figure 7.23 D), VT to VA (Figure 7.23 E) and VT to SR (Figure 7.23 F).The time spent in VT, VA and the time to SR (Figure 7.24) were determined by studying the ECGs.

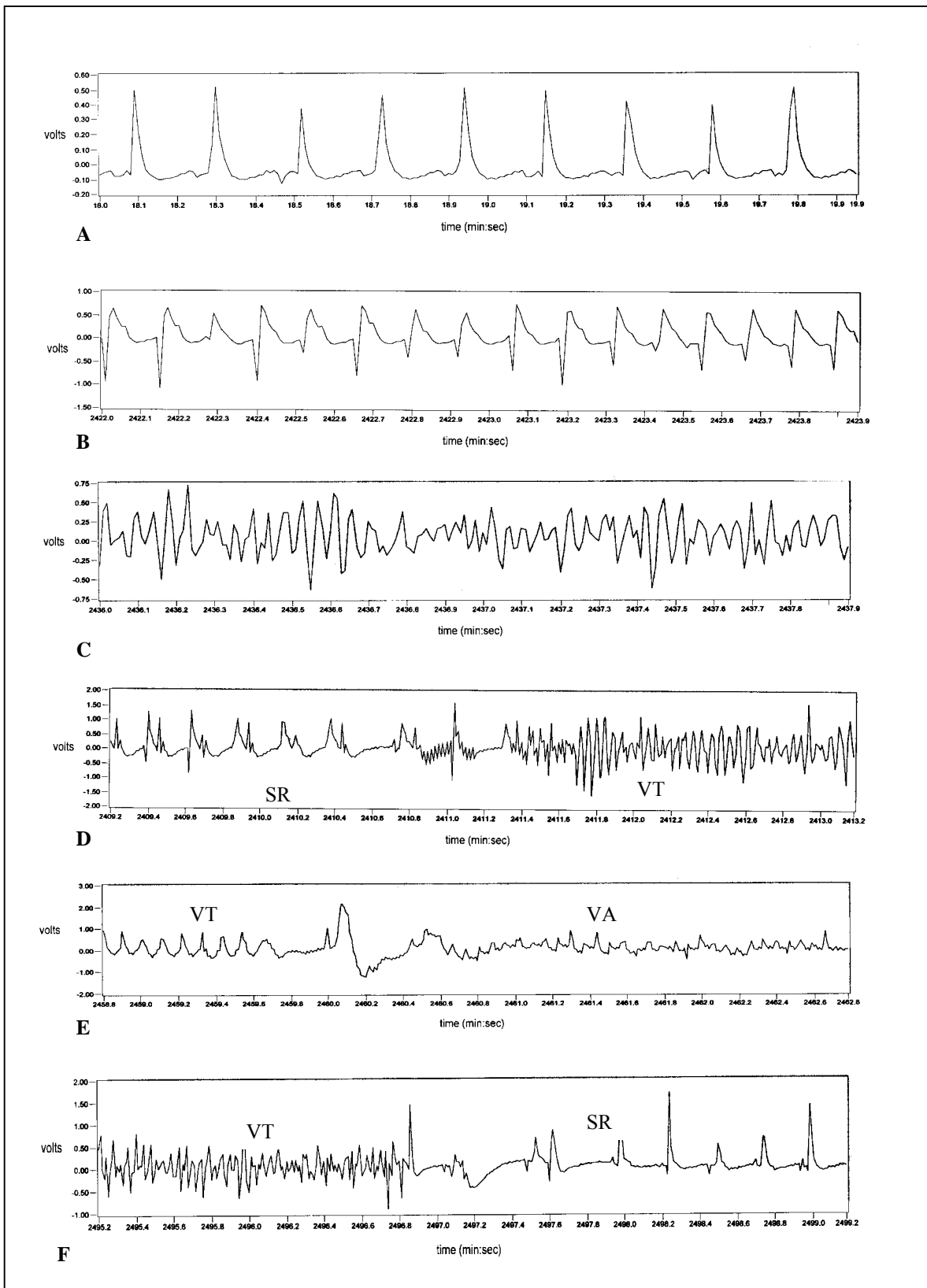


Figure 7. 23 A-F: Segments of ECGs showing (A) normal sinus rhythm (SR); (B) ventricular tachycardia (VT); (C) arrhythmias; (D) SR changing to VT; (E) VT changing to VA; and (F) VT changing to sinus rhythm, as recorded in the rat isolated heart.

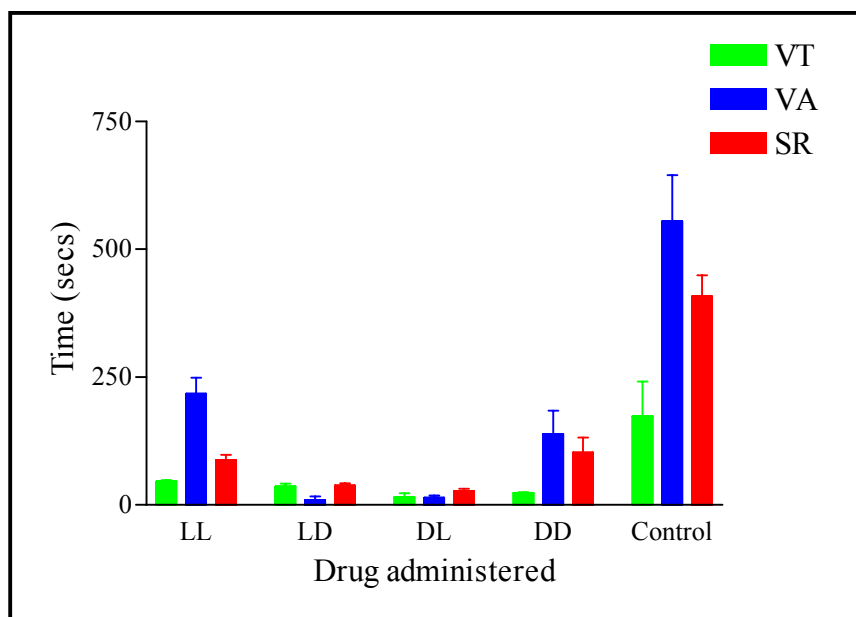


Figure 7. 24: The time to stop VT (ventricular tachycardia), VA (ventricular arrhythmias) and time to return to SR (normal sinus rhythm) in the presence of 200 μ M LL (cyclo(L-Trp-L-Pro)), LD (cyclo(L-Trp-D-Pro)), DL (cyclo(D-Trp-L-Pro)) and DD (cyclo(D-Trp-D-Pro)). Values indicated are the mean \pm s.d of 6 experiments.

The time spent in VT (Figure 7.24) was significantly reduced in the presence of all the isomers in comparison to the control ($p < 0.05$ for all the isomers). Similarly, time spent in VA was also significantly reduced for all the isomers ($p < 0.01$ for cyclo(L-Trp-L-Pro), and $p < 0.001$ for cyclo(L-Trp-D-Pro), cyclo(D-Trp-L-Pro) and cyclo(D-Trp-D-Pro)). In addition, the time taken to return to SR was greatly reduced in comparison to the control group ($p < 0.001$ for all the isomers). These results show that significant reduction in the severity of arrhythmias that result from coronary artery ligation can be achieved with cyclo(L-Trp-L-Pro), cyclo(L-Trp-D-Pro), cyclo(D-Trp-L-Pro) and cyclo(D-Trp-D-Pro).

The duration of VT in the control group of anaesthetized rats was 95 ± 19 s in a study conducted by Shaw and Coker (1996). In the presence of 1 mg/kg ICI 170,809, the duration of VT was decreased to 39 ± 15 s. When 1 mg/kg ICI 192,605 was administered to the rats, the time spent in tachycardia was increased to 48 ± 24 s. However, when both these agents were applied simultaneously to the rats, the time spent in tachycardia was significantly reduced ($p < 0.05$) to 27 ± 10 s (Shaw and Coker, 1996).

CPU-23 reduced the duration and incidence of VT and VF in the first 30 min at 2.5 mg/kg and 5 mg/kg in the isolated, perfused rat heart. At all concentrations of CPU-23 tested, the incidence of VT decreased from 70% (control) to 13% for 1 mg/kg and 0% for 2.5 mg/kg and 5 mg/kg. The duration of tachycardia was also significantly decreased (Dong *et al.*, 1993). No effect on the incidence of ischaemia-induced arrhythmias was noted in the presence of 0.3 and 1 μ M UK 66,914 ((N-(4-{1-hydroxy-2-[4-(4-pyridinyl)-1-piperazinyl]ethyl}phenyl)methanesulphonamide) (a specific and selective blocker of the delayed rectifying K⁺-current) when applied to the rat heart (Rees and Curtis, 1993).

In 1984, Fagbemi *et al.* conducted a comparative study of the effects of the Ca²⁺-channel antagonists verapamil, prenylamine, flunarizine and cinnarizine. Varying concentrations of these drugs were applied to anaesthetized rat. The duration of VT decreased from 82 \pm 18 s (control) to 18 \pm 8 s ($p < 0.05$) in the presence of 0.05 mg/kg verapamil, to 49 \pm 15 s with 0.01 mg/kg verapamil and to 17 \pm 4 s ($p < 0.05$) with 0.5 mg/kg verapamil. Time spent in VF also decreased significantly from the control (81 \pm 38 s) to 2.8 \pm 0.5 s in the presence of 0.01 mg/kg verapamil, while no incidence of VF was noted in the presence of 0.05 mg/kg verapamil.

Significant reduction in the duration of VT was noted in the presence of 0.5 mg/kg prenylamine. Time was reduced from 98 \pm 23 s (control) to 40 \pm 10 s, with a further decrease noted when 5 mg/kg prenylamine was administered (10 \pm 7 s). Time spent in VF was increased from 2 \pm 7 s in the control to 26 s in the presence of 0.5 mg/kg prenylamine, whereas no incidence of VF occurred in the presence of 5 mg/kg prenylamine (Fagbemi *et al.*, 1984).

0.25 mg/kg, 0.5 mg/kg and 1 mg/kg Flunarizine significantly reduced the duration of VT when administered to the anaesthetized rat, with a significant reduction in VF also occurring in the presence of 0.25 mg/kg and 2.5 mg/kg flunarizine. No incidence of VF was noted in the presence of 0.5 mg/kg and 1 mg/kg flunarizine (Fagbemi *et al.*, 1984).

Cinnarizine administered at 0.1 mg/kg, 0.25 mg/kg, 0.5 mg/kg and 1 mg/kg all reduced the duration of VT significantly ($p < 0.05$) when compared to the control rat (Fagbemi *et al.*, 1984).

Time to SR was greatly increased in the presence of 1 μM ceruloplasmin, a reactive oxygen species scavenger, when applied to the isolated rat heart during post ischaemia reperfusion (Wang *et al.*, 1999). An increase to 263 ± 10 s from 25 ± 12 s in the control was noted, while increases were also seen with urea (the end product of protein catabolism) at concentrations of 30 mM (not significant), 150 mM (134 ± 54 s) and 300 mM (200 ± 14 s). Also, 30 mM and 150 mM urea resulted in a 75% and 50% (respectively) incidence of irreversible VF (Wang *et al.*, 1999).

QRS intervals (Figure 7.25) were determined for all experiments, during perfusion of the isolated heart with isomer-containing perfusion buffer. No significant alterations in the duration of the QRS intervals were observed for all the isomers in comparison to the control samples ($p > 0.05$). However, cyclo(D-Trp-L-Pro) showed a significant decrease in QRS complex duration in comparison to the other isomers ($p < 0.05$), indicating a decreased intraventricular conduction time.

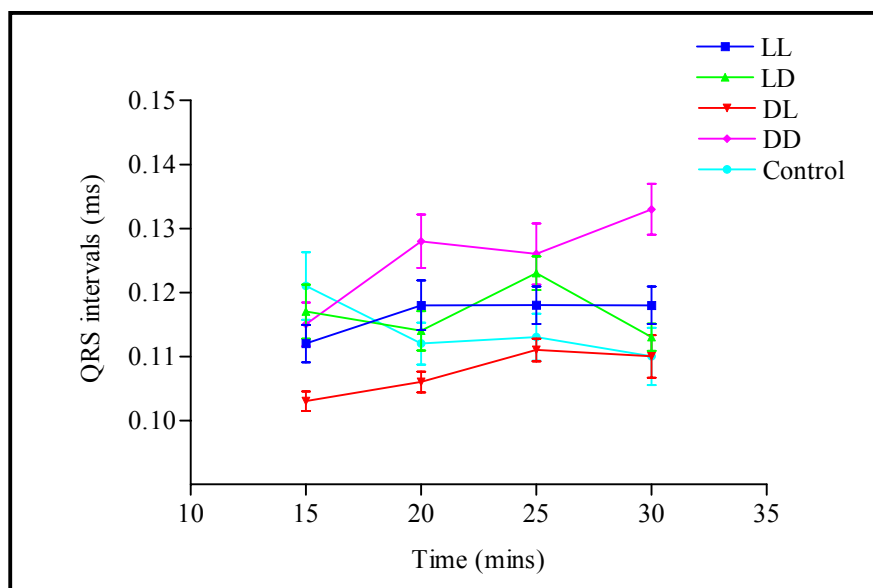


Figure 7. 25: QRS intervals as measured with perfusion of the isomers, from 15 min to 30 min. Values indicated are the mean \pm s.d of 6 experiments.

A rate-dependent enlargement of the intraventricular interval was noted when norbamide was administered to isolated guinea-pig hearts. This action was similar to that of class I antiarrhythmic agents. Verapamil was however found not to alter the QRS interval (Bova *et al.*, 1997). Other class I antiarrhythmic agents, viz. lidocaine, tedisamil and RSD 1019 ((\pm)-*trans*-[2-(4-morpholinyl)cyclohexyl](4-bromophenyl) acetate monohydrochloride), were tested on pentobarbital anaesthetized rats (Barrett *et al.*, 2000). A dose-dependent increase in the QT interval was observed with tedisamil at concentrations ranging from 0.063 $\mu\text{mol/kg/min}$ to 0.25 $\mu\text{mol/kg/min}$, whereas no significant alterations in the QT intervals were observed in the presence of lidocaine (2.5 – 10 $\mu\text{mol/kg/min}$). RSD 1019 administered at concentrations of 4 and 8 $\mu\text{mol/kg/min}$ resulted in significantly prolonged QT intervals (Barrett *et al.*, 2000).

Prolonged QT intervals in the rabbit are seen with the administration of UK 66,914, but not in the rat. This occurrence in the rabbit is explained by and evidence of I_K blockage in rabbits. The absence of a prolonged QT interval in rats is explained by and evidence of an absence of I_K blockage (Rees and Curtis, 1993). This may be related to our study, where it was found that the isomers had no significant effects on K^+ -channels, although this study was examined in the guinea-pig myocytes, and not in the rat model.

Further testing on quinidine, mexiletine and flecainide, all class I antiarrhythmic agents were conducted by Yang *et al.* (1995). It was found that 10 μM quinidine, 15 μM mexiletine and 3 μM flecainide all resulted in significantly prolonged QRS intervals when applied to isolated guinea-pig hearts. In the presence of quinidine, the QRS interval was prolonged from 35.9 ± 2.0 ms to 55.4 ± 3.3 ms ($p < 0.001$); mexiletine caused an increase to 52.5 ± 2.5 ms ($p < 0.001$); and flecainide resulted in a prolonged QRS interval of 58.6 ± 1.4 ms ($p < 0.005$). Furthermore, pinacidil, a K^+ -channel opener, was applied to the hearts. At concentrations of 10, 30 and 50 μM , no significant effect on the QRS intervals was observed. When these different concentrations of pinacidil were applied in conjunction with 15 μM mexiletine, a significant decrease in the QRS interval was noted (-17%). Similarly, when pinacidil was combined with 10 μM quinidine, an 8% decrease in the QRS interval was noted. No alteration in the QRS interval was observed when pinacidil was combined with 3 μM flecainide. It was thus concluded that pinacidil could antagonize the QRS widening effect of class I antiarrhythmic agents (Yang *et al.*, 1995).

7.5 CONCLUSIONS

Arrhythmias are of particular concern, as contractions that are too fast, asynchronous or too slow will reduce cardiac output. Arrhythmias may precipitate further complications in the form of VFs. Any agent capable of reducing the duration of VA and VF are of considerable importance in the sense that the agent is capable of modifying critically impaired conduction. This is most commonly noted with Ca^{2+} -channel blockers. Of the isomers tested, only cyclo(D-Trp-L-Pro) showed potential as a Ca^{2+} -channel antagonist. Cyclo(L-Trp-L-Pro), cyclo(L-Trp-D-Pro) and cyclo(D-Trp-D-Pro) all showed Ca^{2+} -channel agonism. Only cyclo(D-Trp-L-Pro) showed independence of the membrane potential. No effect on the inward rectifier K^+ -current was noted for any of the isomers. This may explain why none of the isomers showed a prolonged QRS complex (Rees and Curtis, 1993).

In relation to the control group, cyclo(L-Trp-L-Pro) and cyclo(D-Trp-D-Pro) showed no significant effect on the heart rate, while cyclo(L-Trp-D-Pro) showed a positive chronotropic effect, with cyclo(D-Trp-L-Pro) exhibiting negative chronotropic effects. Clinical research has shown that vasodilative agents are capable of relieving the stressed myocardium by reducing the vascular tone, and have thus shown considerable success in the treatment of some types of congestive failure (Hondeghe and Mason, 1989). This increase in coronary flow was observed on treatment of the hearts with cyclo(L-Trp-D-Pro) and cyclo(D-Trp-L-Pro), with no significant increase noted for both cyclo(L-Trp-L-Pro) and cyclo(D-Trp-D-Pro) in relation to the control group. Cyclo(L-Trp-D-Pro) was expected to decrease the coronary flow, since it showed positive chronotropic effects. To clarify this, it is suggested that the heart studies be conducted on isolated, guinea-pig hearts, to eliminate any discrepancies as far as species differences are concerned.

Furthermore, it was found that all the isomers were capable of reducing the time spent in both VA and VF, as well as reducing the time taken for the heart to return to a normal SR. These isomers show potential as antiarrhythmic agents and should be investigated

further, as coronary flow is not decreased on application, and will thus not place extra strain on the heart.

CONCLUSIONS

The isomers of cyclo(Trp-Pro) have shown a range of biological activity, differing both quantitatively and qualitatively from each other. This may be as a result of the difference in conformation amongst the isomers, due to a difference in amide bond types and orientations of the tryptophan side chain. Furthermore, one cannot generalize by saying that any particular combination of isomer (eg. cyclo(L-Trp-L-Pro) and cyclo(L-Trp-D-Pro)) will result in any specific activity, which is governed by the interaction of the compounds with the receptor. Screening of other novel cyclic dipeptides for biological activity in the future will therefore have to include the different isomers of the given compounds, to fully define its potential as a biological agent.

FURTHER RECOMMENDATIONS

The major role that peptides play as central modulators of various biological functions is being recognized more and more. The determination of the conformation of a linear peptide has been hindered by the many conformations that exist in solution. This problem is circumvented by cyclization of the peptide, which introduces structural rigidity to the molecule.

The isomers of cyclo(Trp-Pro) has shown potential as a drug entity. Solubility is however restricted to polar solvents such as DMSO, with limited solubility in glycerol. As DMSO usage as a solvent poses toxicity risks at high concentrations, it is recommended that the solubility of these isomers in aqueous solvents be increased. This can be achieved by chlorination of the molecule i.e. produce the chloride salts of the isomers. Furthermore, optimization of the interaction between the isomers and any given receptor can be achieved by chemical modification (such as methylation, phosphorylation or acetylation) in combination with computational chemistry. In this manner, any potential activity shown can be enhanced to yield greater specificity of activity, thereby decreasing the risk of adverse reactions with other receptors. Different stereoisomers should also be investigated for activity.

Cyclization of tripeptides based on cyclo(Trp-Pro) should be included in further investigations. The third amino acid should contain a site that would impart activity to the molecule, such as the sulfhydryl group of cysteine or the thioether group of methionine. From here, the biological relevance of the molecule can be related to the relative structural simplicity of the molecule, thereby increasing our understanding of both pharmacokinetic and pharmacodynamic properties of the molecule.

RESEARCH OUTPUT

Presentations

Jamie, H., Kilian, G., Milne, P.J. and Dyason, K. (2001) The effect of the isomers of cyclic dipeptide (L-Trp-L-Pro) on heart and ion channel activity. IUBMB/SASBMB Special Meeting on The Biochemical and Molecular Basis of Disease. Cape Town (Poster).

Graz, C.J.M., Grant, G.D., Brauns, S.C.A., Haywood, A.L., Jamie, H., Milne, P.J. (2000) Cyclic dipeptides in the induction of maturation for cancer therapy. Academy of Pharmaceutical Sciences 21st Annual Congress. Rhodes University. Grahamstown. (General Scientific Paper)

Articles that have been submitted – Appendix E.

Journal of Pharmacy and Pharmacology

Submitted January 2002

The effect of the isomers of cyclo(Trp-Pro) on heart and ion channel activity

¹Hajierah Jamie, ¹Gareth Kilian, ²Karin Dyason, ¹*Pieter J. Milne

¹Cyclic Dipeptide Research Unit, Department of Pharmacy, Box 1600, University of Port Elizabeth, Port Elizabeth, 6000, South Africa

²Department of Physiology, Potchefstroom University of C.H.E., Potchefstroom, 2520, South Africa

Die Pharmazie

Submitted January 2002

Hepatotoxicity of the isomers of cyclo(Trp-Pro)

Jamie, H., Kilian, G. and *Milne, P.J.

Cyclic Dipeptide Research Unit, Department of Pharmacy, Box 1600, University of Port Elizabeth, Port Elizabeth, 6000, South Africa

REFERENCE LIST

- Alderson, M. (1982) The causes of cancer, Pp. 20-29, In: Alderson, M. (Ed.), The Prevention of Cancer, Edward Arnold, London.
- Allen, T.J.A. and Chapman, R.A. (1996) Effects of ranolazine on L-type calcium channel currents in guinea-pig single ventricular myocytes, *Br. J. Pharmacol.*, 118:249-254.
- Alley, M.C., Scudiero, D. A., Monks, A., Hursey, M.L., Czerwinski, M.J., Fine, D.L., Abbott, B.J., Mayo, J.G., Shoemaker, R.H. and Boyd, M. (1988) Feasibility of drug screening with panels of human tumour cell lines using a microculture tetrazolium assay, *Cancer Res.*, 48:589-601.
- Altieri, D.C. (1997) Coagulation-inflammation interface: Coagulation assembly on leukocytes, Pp. 51-2, 118, 121, Chapman and Hall, New York, U.S.A.
- Akiyama, S. (1987) HeLa cell lines, *Met. Enz.*, 151:38-39.
- Anand, N. (1995) Antimetabolite antagonism, In: Foye, W., Lemke, T. and Williams, D., Principles of Medicinal Chemistry, Pp. 716, Williams and Wilkins, Baltimore.
- Anderson, G.W. and McGregor, A. (1957) *t*-Butylcarbonylamino acids and their use in peptide synthesis, *J. Am. Chem. Soc.*, 79:6180-6183.
- Anteunis, M.J.O. (1978) The cyclic dipeptides. Proper model compounds in peptide research, *Bull. Soc. Chim. Belg.*, 87:626-650.
- Arkel, Y.S. (2000) Thrombosis and cancer, *Semin. Oncol.*, 27:362-374.
- Armstrong, R.A., Jones, R.L., MacDermot, J. and Wilson, N.H. (1986) Prostaglandin endoperoxide analogues which are both thromboxane receptor antagonists and prostacyclin mimetics, *Br. J. Pharmacol.*, 87:534-551.
- Arnould, R., Dubois, J., Abikhalil, F., Libert, A., Ghanem, G., Atassi, G., Hanocq, M. and Lejeune, F.J. (1990) Comparison of two cytotoxicity assays – Tetrazolium derivative reduction (MTT) and tritiated thymidine uptake- on three malignant mouse cell lines using chemotherapeutic agents and investigational drugs, *Anticancer Res.*, 10:145-154.
- Ashida, T. and Kakudo, M. (1974) Conformations of prolyl residues in oligopeptides, *Bull. Chem. Soc. Jpn.*, 47:1129-1133.
- Aw, T.Y. (1986) Hemaprotection by glutathione and acetaminophen toxicity, Pp. 830, 831, In: Kaplowitz, N. Drug-induced hepatotoxicity. *Ann. Intern. Med.*, 104:826-839.
- Barnes, D., van der Bosch, J., Masui, H., Miyazaki, K. and Sato, G. (1981) Culture of human tumour cells in serum-free medium, *Met. Enz.*, 79:368-391.
- Barnes, P.J. and Mueller, R.A. (1995) Bronchodilators. Principles of Pharmacology-Basic concepts and clinical applications, Pg. 586. Chapman and Hall, New York.
- Baron, D.N. (1982) A short textbook of Chemical Pathology, 4th Ed., Pp. 105, 107, 116-117, 120, 192-193, 197-198, Hodder and Stoughton, London.
- Barrett, T.D., MacLeod, A. and Walker, M.J. (2000) RSD1019 suppresses ischaemia-induced monophasic action potential shortening and arrhythmias in anaesthetized rabbits, *Br. J. Pharmacol.*, 131:405-414.

- Barritt, G. (1999) Receptor-activated Ca^{2+} -inflow in animal cells: a variety of pathways tailored to meet different intracellular Ca^{2+} -signalling requirements, *Biochem. J.*, 337:153-169.
- Bauer, J.D., Ackermann, P.G. and Toro, G. (1974) Clinical Laboratory methods, 8th edition, Pp. 393-4, 403, 435, 493-4, CV Mosby Co., St. Louis, U.S.A.
- Bednar, B., Condra, C., Gould, R. and Connolly, T.M. (1995) Platelet aggregation monitored in a 96 well microplate reader is useful for evaluation of platelet agonists and antagonists, *Thromb. Res.*, 77:453-463.
- Bellamy, L.J. (1957) The infrared spectra of complex molecules, Pp. 1-1876, Methuen and Co., Ltd., London.
- Bellavite, P., Andrioli, G., Guzzo, P., Arigliano, P., Chirumbolo, S., Manzata, F. and Santonastaso, C. (1994) A colorimetric method for the measurement of platelet adhesion in microtiter plates, *Anal. Biochem.*, 216:444-450.
- Bender, D. A. (1995) Amino acid metabolism, Pg. 523, John Wiley and Sons, New York.
- Benedetti, E., Ciajolo, M.R. and Maisto, A. (1974) The crystal structure of *N*-(*t*-Butylcarbonyl-L-proline, *Acta Cryst.*, B30, 1783-1788.
- Bensaid, A., Thierie, J. and Penninckx, M. (2000) The use of tetrazolium salt XTT for the estimation of biological activity of activated sludge cultivated under steady-state and transient regimes, *J. Microbiol. Methods*, 40:255-263.
- Bergmeyer, H.U. (1984) *Methods in Enzymatic Analysis*, Pp. 75-82, Verlag Chemie, Weinheim.
- Berne, R. M. and Levy, M.N. (1986) Cardiovascular Physiology, 5th Ed., Pg. 57, C.V. Mosby Co., St. Louis, U.S.A.
- Bessman, D. (1989) Determination of platelet volume and number, *Met. Enz.*, 169:164-172.
- Bhattacharya, R., Lakshmana Rao, P.V., Bhaskar, A.S.B., Pant, S.C. and Dube, S.N. (1996) Liver slice culture for assessing hepatotoxicity of freshwater cyanobacteria, *Hum. Exp. Toxicol.*, 15:105-110.
- Bodanzsky, M., Klausner, Y.S. and Ondetti, M.A. (1976) Peptide Synthesis, 2nd Ed., Pp. 1-169, John Wiley and Sons, U.S.A.
- Boobis, A. R., Fawthrop, D. J. and Davies, D.S. (1989) Mechanisms of cell death, *TiPS*, 10:275-280.
- Borenfreund, E., Babich, H. and Martin-Alguacil, M. (1988) Comparisons of two *in vitro* cytotoxicity assays-the neutral red (NR) and tetrazolium MTT tests, *Toxic. In Vitro*, 2:1-6.
- Bos, J. (1989) *Ras* Oncogenes in human cancer: A review, *Cancer Res.*, 49:4682-4689.
- Bova, S., Cargnelli, G., D'Amato, E., Forti, S., Yang, Q., Trevisi, L., Debetto, P., Cima, L., Luciani, S. and Padriani, R. (1997) Calcium-antagonist effects of norbomide on isolated perfused heart and cardiac myocytes of guinea-pig: a comparison with verapamil, *Br. J. Pharmacol.*, 120:19-24.
- Branden, C. and Tooze, J. (1991) Introduction to protein structure, Pg. 14, Garland Publishing Inc., New York.
- Briske-Anderson, M., Finley, J. and Newman, S. (1997) The influence of culture time and passage number on the morphological and physiological development of Caco-2 cells, *P.S.E.B.M.*, 214:248-257.

- Bull, S.D., Davies, S.G., Parkin, R.M. and Sanchez-Sancho, F. (1998) The biosynthetic origin of diketopiperazines derived from D-proline, *J. Chem. Soc., Perkin Trans.1.*, 2313-2319.
- Cahalan, M. and Neher, E. (1992) Patch-clamp techniques: An overview, *Met. Enz.*, 207:3-10.
- Capasso, S., Vergara, A. and Mazzarella, L. (1998) Mechanism of 2,5-dioxopiperazine formation, *J. Am. Chem. Soc.*, 120:1990-1995.
- Carmichael, J., DeGraff, W.G., Gazdar, A.F., Minna, J.D. and Mitchell, J.B. (1987) Evaluation of a tetrazolium-based semiautomated colorimetric assay: assessment of chemosensitivity testing, *Cancer Res.*, 47:936-942.
- Castell, J.V.M., Montoya, A., Larrauri, A., Lopez, P. and Gomez-L. J. (1985) Effects of benorylate and imipacina on the metabolism of cultured hepatocytes, *Xenobiotica*, 15:743-749.
- Castell, J.V., Larrauri, A. and Gomez-Lechon, M.J. (1988) A study of the relative hepatotoxicity *in vitro* of the non-steroidal anti-inflammatory drugs ibuprofen, flurbiprofen and butibufen, *Xenobiotica*, 18:737-745.
- Castell, J.V., Gomez-Lechon, M., Ponsoda, X. and Bort, R. (1997) In Vitro investigation of the molecular mechanisms of hepatotoxicity, In: In Vitro methods in pharmaceutical research. Pp. 375-397. Academic Press, San Diego.
- Chacon, E. and Acosta, D. (1991) Mitochondrial regulation of superoxide by Ca^{2+} : an alternate mechanism for the cardiotoxicity of Doxorubicin, *Toxicol. Appl. Pharmacol.*, 107:117-128.
- Chiao, H. and Caldwell, R.W. (1995) Local cardiac effects of substance P: roles of acetylcholine and noradrenaline, *Br. J. Pharmacol.*, 114:283-288.
- Clancy, C.J. and Nguyen, M.H. (1997) Comparison of a photometric method with standardized methods of antifungal susceptibility testing of yeasts, *J. Clin. Microbiol.*, 35:2878-2882.
- Cook, N.S. (1988) The pharmacology of potassium channels and their therapeutic potential, *TiPS*, 9:21-28.
- Cooper, G. (1997) The cell: A molecular approach, Pp., 564-565, ASM Press, U.S.A.
- Cotrait, M., Ptak, M., Busetta, B. and Heitz, A. (1976) Crystal structure and conformation of the cyclic dipeptide *cyclo*-(L-Threonyl-L-histidyl) dihydrate, *J. Am. Chem. Soc.*, 98:1073-1076.
- Crescenzi, V., Cesaro, A. and Russo, E. (1973) On some physico-chemical properties of diketopiperazines in water, *Int. J. Peptide Protein Res.*, 5:427-434.
- Cromer, D.T. and Liberman, D. (1974) International tables for X-ray crystallography, *J. Chem. Phys.*, 4:1891.
- Curtis, M.J., MacLeod, B.A. and Walker, M.J.A. (1987) Models for the study of arrhythmias in myocardial ischaemia and infarction: the use of the rat, *J. Mol. Cell Cardiol.*, 19:399-419.
- Cusack, N.J. and Hourani, S.M.O. (1981) 5'-N-Ethylcarboxamidoadenosine: A potent platelet inhibitor of human platelet aggregation, *Br. J. Pharmacol.*, 72:443-447.
- Cusack, N.J. and Hourani, S.M.O. (1982) Adenosine 5'-diphosphate antagonists and human platelets: No evidence that aggregation and inhibition of stimulated adenylate cyclase are mediated by different receptors, *Br. J. Pharmacol.*, 76:221-227.
- Deber, C.M., Madison, V., Blout, E.R. (1976) Why cyclic peptides? Complementary approaches to conformations, *Acc. Chem. Res.*, 9:106-113.

- Debono, M. and Gordee, R. (1994) Antibiotics that inhibit fungal cell wall development, *Ann. Rev. Microbiol.*, 48:471-497.
- Degeilh, R. and Marsh, R.E. (1959) Cyclo(Gly-Gly) (c/Gly)₂, *Acta Cryst.*, 12:1007.
- Deleve, L. D. and Kaplowitz, N. (1990) Importance and regulation of hepatic glutathione, *Semin. Liver Dis.*, 10:251-266.
- De Robertis, E. and De Robertis, E. (1987) Cell and Molecular Biology, 8th Edition, Pp. 623-38, Lea and Febiger, Philadelphia.
- Deslauriers, R., Grzonka, Z., Schaumburg, K., Shiba, T. and Walter, R. (1975) Carbon-13 Nuclear Magnetic Resonance studies of the conformations of cyclic dipeptides, *J. Am. Chem. Soc.*, 97:5093-5099.
- Dipiro, J.T., Talbert, R.L., Yee, G.C., Matzke, G.R., Wells, B.G., Conn, A.E.L. and Posey, L.M. (1997) Pharmacotherapy: A pathophysiologic Approach, 3rd Ed., Pg. 2886, Academic Press, London.
- Dong, H., Sheng, J., Lee, C. and Wong, T. (1993) Calcium antagonistic and antiarrhythmic actions of CPU-23, a substituted tetrahydroisoquinoline, *Br. J. Pharmacol.*, 109:113-119.
- Dupuis, B.A. and Adamantidis, M.M. (1995) Antiarrhythmic drugs: Principles of Pharmacology-Basic concepts and Clinical applications, Pg. 518, Chapman and Hall, New York.
- Edelhoch, H., Bernstein, R. and Wilchek, M. (1968) The fluorescence of tyrosyl and tryptophanyl diketopiperazines, *J. Biol. Chem.*, 243:5985-5992.
- Edmunds, N.J., Lal, H. and Woodward, B. (1999) Effects of tumour necrosis factor- α on left ventricular function in the rat isolated perfused heart: possible mechanisms for a decline in cardiac function, *Br. J. Pharmacol.*, 126:189-196.
- Edwards, D. (1980) Antimicrobial drug action, Pp. 129-130, 140-146, Macmillan Press Ltd., London.
- Ellwood, A.J. and Curtis, M.J. (1997) Mechanism of actions of sumatriptan on coronary flow before and after endothelial dysfunction in guinea-pig isolated heart, *Br. J. Pharmacol.*, 120:1039-1048.
- Eloff, J.N. (1998) A sensitive and quick microplate method to determine the minimal inhibitory concentration of plant extracts for bacteria, *Planta Medica*, 64:711-713.
- Esterbauer, H., Lang, J., Zadavec, S. and Slater, T. (1984) Detection of malonaldehyde by high-performance liquid chromatography, *Met. Enz.*, 105: 319-328.
- Fagbemi, O., Kane, K.A., McDonald, F.M., Parrat, J.R. and Rothaul, A.L. (1984) The effects of verapamil, prenylamine, flunarizine and cinnarizine on coronary artery occlusion-induced arrhythmias in anaesthetized rats, *Br. J. Pharmacol.*, 83:299-304.
- Falconer, R., Jackson, A.R.B., Langley, J. and Runnegar, M.T. (1981) Liver pathology in mice poisoning by the blue-green alga *Microcystis aeruginosa*, *Aust. J. Biol. Sci.* 34:179-187.
- Fallen, E.L., Elliot, W.C. and Gorlin, R. (1967) Apparatus for study of ventricular function and metabolism in the isolated perfused rat heart, *J. Appl. Physiol.*, 22:836-839.
- Faulkner, W.R. and King, J.W. (1970) Manual of Clinical Laboratory Procedures, Pp. 84, 86, Chemical Rubber Co., Ohio.
- Fischer, E. (1906) Untersuchungen über Aminosäuren, Polypeptide und Proteine, *Chem. Ber.*, 39: 530-610.

- Forgue-Lafitte, M., Coudray, A., Breant, B. and Mester, J. (1989) Proliferation of the human colon carcinoma cell line HT-29: autocrine growth and deregulated expression of the *c-myc* oncogene, *Cancer Res.*, 49:6566-6571.
- Freimoser, F.M., Jakob, C.A., Aebi, M. and Tuor, U. (1999) The MTT [3-(4,5-Dimethylthiazol-2-yl)-2,5-diphenyltetrazolium bromide] assay is a fast and reliable method for colorimetric determination of fungal cell densities, *Appl. Environ. Microbiol.*, 65:3727-3729.
- Funabashi, Y., Horiguchi, T., Iinuma, S., Tanida, S. and Harada, S. (1994) TAN-1496 A, C and E, diketopiperazine antibiotics with inhibitory activity against mammalian DNA topoisomerase I, *J. Antibiot.*, 47:1202-1215.
- Gale, E. F., Cundliffe, E., Reynolds, P., Richmond, M. H. and Waring, M. (1981) The molecular basis of antibiotic action, 2nd Ed., Pp. 187-8, J. Wiley and Sons, London.
- Garbay-Jaureguiberry, C., Arnoux, B., Prange, T., Wehri-Altenburger, S., Pascard, C. and Roques, B. (1980) X-ray and NMR studies of L-4-Hydroxyproline conformation in oligopeptides related to collagen, *J. Am. Chem. Soc.*, 102:1827-1836.
- Gennaro, A.R., Chase, G.D., Gibson, M.R., Granberg, C.B., Zink, G.L., Harvey, S.C., King, R.E., Martin, A.N. and Swinyard, E.A. (1980) Remington Pharmaceutical Sciences, 16th Ed., Pp. 188-9, Mack Publishing Co., Easton, Pennsylvania.
- Gibaldi, M. (1984) Biopharmaceutics and Clinical Pharmacokinetics, 3rd Ed., Pg. 173, Lea and Febiger, Philadelphia.
- Godfraind, T. and Govoni, S. (1995) Recent advances in the pharmacology of Ca²⁺ and K⁺ channels, *TiPS*, 16:1-4.
- Goldin, B.R. (1986) In situ bacterial metabolism and colon mutagens, *Ann. Rev. Microbiol.*, 40:367-393.
- Gomez-Flores, R., Gupta, S., Tamez-Guerra, R. and Mehta, R.T. (1995) Determination of MICs for *Mycobacterium avium*-M. intracellulare complex in liquid medium by a colorimetric method, *J. Clin. Microbiol.*, 33:1842-1846.
- Gomez-Lechon, M.J., Donata, T., Ponsoda, X., Fabra, R., Trullenque, R. and Castell, J.V. (1997) Isolation, culture and use of human hepatocytes in drug research, In: In Vitro methods in pharmaceutical research. Pp. 129-153. Academic Press, San Diego.
- Grant, G.D., Hunt, A.L., Milne, P.J., Roos, H.M. and Joubert, J. A. (1999) The structure and conformation of the tryptophanyl diketopiperazines cyclo(Trp-Trp)C₂H₆SO and cyclo(Trp-Pro), *J. Chem. Crystallogr.*, 29:435-447.
- Grenegård, M., Gustafsson, M.C., Andersson, R. and Bengtsson, T. (1996) Synergistic inhibition of thrombin-induced platelet aggregation by the novel nitric oxide-donor GEA 3175 and adenosine, *Br. J. Pharmacol.*, 118:2140-2144.
- Günther, H. (1995) NMR Spectroscopy. Basic Principles, concepts and applications in chemistry, 2nd Ed., Pp. xiii-xix, 477, John Wiley and Sons, New York, U.S.A.
- Guzman, R.E., and Solter, P.F. (1999) Hepatic oxidative stress following prolonged sublethal microcystin LR exposure, *Toxicol. Pathol.*, 27:582-588.
- Hamil, P., Marty, A., Neher, E., Sakman, B., Sigworth, F. (1981) Improved patch-clamp techniques for high-resolution current recording from cells and cell-free membrane patches, *Pflügers Arch.*, 391:85-100.

- Hashimoto, Y., Hori, R., Okumura, K. and Yasuhara, M. (1986) Pharmacokinetics and antiarrhythmic activity of ajmaline in rats subjected to coronary artery occlusion, *Br. J. Pharmacol.*, 88:71-77.
- Hawiger, J. (1989) Platelet secretory pathways: An overview, *Met. Enz.*, 169:191-195.
- Hawser, S. (1996) Comparisons of the susceptibilities of planktonic and adherent *Candida albicans* to antifungal agents: a modified XTT tetrazolium assay using synchronized *C. albicans* cells, *J. Med. Vet. Mycol.*, 34:149-152.
- Haywood, A. (2000) The Medicinal Chemistry of the Tryptophan-containing cyclic dipeptide : Cyclo(Trp-Pro), PhD Thesis, U.P.E., Port Elizabeth.
- Herdson, P.B., Garvin, P.J. and Jennings, R. (1964) Fine structural changes in rat liver induced by Phenobarbital, *Lab. Invest.*, 13:1032-1037.
- Herz, F., Kaplan, E. and Fineman, E. (1973) Regulation of alkaline phosphatase activity in B cells: Influence of serum, *Biochim. Biophys. Acta*, 304:660-668.
- Hider, R.C. (1998) Science in action: Development of a novel treatment for renal failure, *Pharm. J.*, 261:393-399.
- Hinson, J.A., Pumford, N.R. and Nelson, S.D. (1994) The role of metabolic activation in drug toxicity, *Drug Metab. Rev.*, 26:395-412.
- Hirafuji, M. and Shinoda, H. (1993) Roles of prostacyclin, EDRF and active oxygens in leukocyte-dependent platelet adhesion to endothelial cells induced by platelet-activating factor *in vitro*, *Br. J. Pharmacol.*, 109:524-529.
- Hjertstedt, J., Hanh, B.L., Kos, W. and Sohnle, P.G. (1998) Comparison of fungal viability assays using *Candida albicans* yeast cells undergoing prolonged incubation in the absence of nutrients, *Mycoses*, 41:487-492.
- Hondeghem, L.M. and Mason, J.W. (1989) Agents used in Cardiac Arrhythmias, Pg. 165, In: Basic and Clinical Pharmacology, 4th Ed., Ed. Katzung, B.G., Prentice-Hall International, U.S.A.
- Hudson, S.A. and Walker, R.W. (1990) In: Pharmaceutical Practice, Ed. Collett, D.M. and Aulton, M.E., Pg. 400, Churchill Livingstone, London.
- Huet, C., Sahuquillo-Merino, C., Coudrier, E. and Louverd, D. (1987) Absorptive and mucus-secreting subclones from a multipotent cell line (HT-29) provide new models for cell polarity and differentiation, *J. Cell. Biol.*, 105:345-357.
- Hurwitz, S.J. and McCarthy, T.J. (1986) 2,3,5-Triphenyltetrazolium chloride as a novel tool in germicide dynamics, *J. Pharm. Sci.*, 75:912-916.
- Indelicato, T.M., Norvilas, T.T. and Wheeler, W.J. (1972) Intramolecular nucleophilic attack in 7 (α -amino) phenylcephalosporanic esters, *JCS Chem. Commun.*, 1162.
- Jahn, B., Martin, E., Stueben, A. and Bhakdi, S. (1995) Susceptibility testing of *Candida albicans* and *Aspergillus* species by a simple microtiter menadione-augmented 3-(4,5-Dimethyl-2-thiazolyl)-2,5-diphenyl-2H-tetrazolium bromide assay, *J. Clin. Microbiol.*, 33:661-667.
- Jamie, H., Dyason, K., Milne, P.J. and Graz, C.J.M. (2001) The influence of acetoacetate and butyrate on calcium influx and ATP concentrations in HT-29 cells, *Pharmazie*, 56:332-336.

- Jankowska, R. and Ciarkowski, J. (1987) Conformation of dioxopiperazines, *Int. J. Peptide Protein Res.*, 30:61-78.
- Jarvis, G.E., Humphries, R.G., Robertson, M.J. and Leff, P. (2000) ADP can induce aggregation of human platelets via both $PY2_1$ and P_{2T} receptors, *Br. J. Pharmacol.*, 129:275-282.
- Jawetz, E. (1989) Antimycobacterial Drugs, Pg. 579, In: Basic and Clinical Pharmacology, 4th Ed, Ed.: Katzung, B.G., Prentice-Hall International, U.S.A.
- Jover, R., Ponsoda, X., Castell, J.V. and Gomez-Lechon, M.J. (1992) Evaluation of the cytotoxicity of ten chemicals on human cultured hepatocytes: Predictability of human toxicity and comparison with rodent cell culture systems, *Toxic. in Vitro*, 6:47-52.
- Kairo, S.K., Bedwell, J., Tyler, P.C., Carter, A. and Corbel, M.J. (1999) Development of a tetrazolium salt assay for rapid determination of viability of BCG vaccines, *Vaccine*, 17:2423-2428.
- Karp, G. (1996) Cell and Molecular Biology, Pp. 602, 604, 605, 694, John Wiley and Sons, New York.
- Katzung, B. G. and Chatterjee, K. (1989) Vasodilators and the treatment of angina pectoris, Pg. 146, In: Basic and Clinical Pharmacology, 4th Ed., Ed.: Katzung, B.G., Prentice-Hall International, U.S.A.
- Katzung, B.G. and Parmley, W. (1989) Cardiac Glycosides and other drugs used in congestive heart failure, Pg. 154, In: Basic and Clinical Pharmacology, 4th Ed., Ed.: Katzung, B.G., Prentice-Hall International, U.S.A.
- Kirk, C.J.C., Peel, R.N., James, R.R. and Kershaw, Y. (1975) Basic Medical Laboratory Technology, Pp. 286, 297, 300, 308, Pitman Medical Publishing Co., Great Britain.
- Kirst, H. (1995) Aminoglycoside, macrolide, glycopeptide and miscellaneous antibacterial antibiotics, In: Wolff, M., Burgers Medicinal Chemistry and Drug Discovery, Pp. 498, 499, 500, 501, 503, John Wiley and Sons, New York.
- Kopple, K.D. and Marr, D.H. (1967) Conformations of cyclic dipeptides: The folding of cyclic dipeptides containing an aromatic side chain, *J. Am. Chem. Soc.*, 89:6193-6200.
- Kourounakis, A.P., Reka, E.A. and Kourounakis, P.N. (1997) Antioxidant activity of guaiazulene and protection against paracetamol hepatotoxicity in rats, *J. Pharm. Pharmacol.*, 49:938-942.
- Kretschmar, M., Nichterlein, T., Nebe, C.T., Hof, H. and Burger, K.J. (1996) Fungicidal effect of tyrothricin on *Candida albicans*, *Mycoses*, 39:45-50.
- Krstenansky, J.L., Owen, T.J., Payne, M., Broersma, R.J., Yates, M. and Mao, S. (1990) MDL 28 050, a representative of a new class of anticoagulant: Development, in-vitro and in-vivo actions, Pp. 92-3, In: Peptides: Chemistry, Structure, and Biology, Eds: Rivier, J.E. and Marshall, G.R., Escom, Leiden.
- Lambert, J.N., Mitchell, J.P. and Roberts, K.D. (2001) The synthesis of cyclic peptides, *J. Chem. Soc. Perkin Trans. I*, 471-484.
- Langendorff, O. (1895) Untersuchungen am uberlebenden saugethierhergen, *Arch. Geo. Physiol.* 61:291-332.
- Lehninger, A., Nelson, D. and Cox, M. (1993) Principles of Biochemistry, Pg. 124, Worth Publishers, U.S.A.
- Lehninger, A., Nelson, D. and Cox, M. (2000) Principles of Biochemistry, Pp. 118, 120, 128, 169, Worth Publishers, U.S.A.

- Lemke, T. L. (1995) Antimycobacterial agents, Pp. 715, 716, 754, In: Foye, W., Lemke, T. and Williams, D., Principles of Medicinal Chemistry, Williams and Wilkins, Baltimore.
- Lindon, J.N., Kushner, L. and Salzman, E.W. (1989) Platelet interaction with artificial surfaces: *in vitro* evaluation, *Met. Enz.*, 169:104-117.
- Lingappa, V. (1995) Disorders of the female reproductive tract, Pg. 466, In: Pathophysiology of disease: An introduction to clinical medicine, 1st Ed., Eds: McPhee, S.J., Lingappa, V.R., Ganong, W. and Lange, J., Prentice-Hall International Inc., U.S.A.
- Loesser, K.E., Kukreja, R.C., Kazzuha, S.Y., Jesse, R.L. and Hess, M.L. (1991) Oxidative damage to the myocardium: A fundamental mechanism of myocardial injury, *Cardioscience*, 2:199-216.
- Löwik, C.W.G.M., Albas, M.J., van de Ruit, M., Papapoulos, S.E. and van der Pluijm, G. (1993) Quantification of adherent and nonadherent cells cultured in 96-well plates using the supravital stain neutral red, *Anal. Biochem.*, 213:426-433.
- Lubbe, W.F., Davies, P.S. and Opie, L.H. (1978) A model for assessment of antifibrillatory action of antiarrhythmic agents, *Cardiovasc. Res.*, 12:212-220.
- Malloy, H.T. and Evelyn, K.A. (1937) The determination of bilirubin with a photoelectric colorimeter, *J. Biol. Chem.*, 119:481.
- Mankod, P., Spatenka, J., Slavik, Z. O'Neil, G. Chester, A. and Yacoub, M. (1992) Acute effects of cyclosporin and Cremophor EL on endothelial function and vascular smooth muscle in the isolated rat heart, *Cardiovasc. Drugs Ther.*, 6:77-84.
- Marieb, E.N. (1989) Human Anatomy and Physiology, Pp. 587, 772, 775, Benjamin Cummings Publishing CO., U.S.A.
- Marshall, W. (1997) Clinical Chemistry, 3rd Ed., Pp. 72-74, 76, 203-204, 230-232. Mosby, Great Britain.
- Martin, A. (1993) Physical Pharmacy, 4th Ed. Pg. 546, Lea and Febiger, Philadelphia.
- Martini, F.H. (1995) Fundamentals of Anatomy and Physiology, Pp. 83, 667, 669-75, 682, 685, 696, 700-701, 909-911, Prentice Hall, New Jersey, U.S.A.
- Masubuchi, Y., Saito, H. and Horie, T. (1998) Structural requirements for the hepatotoxicity of non-steroidal anti-inflammatory drugs in isolated rat hepatocytes, *J. Pharmacol. Exp. Ther.*, 287:208-213.
- Mathison, I.W., Solomons, W.E. and Tidwell, R.R. (1996) Structural features and pharmacologic activity, In: Foye, W., Lemke, T. and Williams, D., Principles of Medicinal Chemistry, Pp. 25, 31-32, Williams and Wilkins, Baltimore.
- Mattila, T. (1987) A modified Kelsey-Sykes method for testing disinfectants with 2,3,5-triphenyltetrazolium chloride reduction as an indicator of bacterial growth, *J. Appl. Bacteriol.*, 62:551-554.
- Mazza, F., Lucente, G., Pinnen, F. and Zanotti, G. (1984) Cyclic dipeptides containing proline. Structure and conformation of cyclo(L-Phe-L-Pro), C₁₄H₁₆N₂O₂, *Acta Cryst.*, C40:1974-1976
- Meletiadiis, J., Meis, J.F., Mouton, J.W., Donnelly, J.P. and Verweij, P.E. (2000) Comparison of NCCLS and 3-(4,5-dimethyl-2-Thiazyl)-2,5-diphenyl-2H-tetrazolium bromide (MTT) methods of *in vitro* susceptibility testing of filamentous fungi and development of a new simplified method, *J. Clin. Microbiol.*, 38:2949-2954.

- Meshulam, T., Levitz, S., Christin, L. and Diamond, R.D. (1995) A simplified new assay for assessment of fungal cell damage with the tetrazolium dye, (2,3)-bis-(2-methoxy-4-nitro-5-sulphenyl)-(2H)-tetrazolium-5-carboxanilide (XTT), *J. Infect. Dis.*, 172:1153-1156.
- Milne, P.J., Oliver, D.W. and Roos, H.M. (1992) Cyclodipeptides: Structure and conformation of cyclo(tyrosyl-prolyl), *J. of Crystallog. and Spectros. Res.* 22(6):644-650.
- Milne, P.J., Hunt, A.L., Rostoll, K., van der Walt, J.J. and Graz, C.J.M. (1998) The biological activity of selected cyclic dipeptides, *J. Pharm. Pharmacol.*, 50:1331-1337.
- Minamiura, N., Matsumura, Y. and Yamamoto, T. (1972) Bitter peptides in the casein digests with bacterial proteinase, *J. Biochem.*, 72:841-848.
- Mitsui, Y., Tsuboi, M. and Iitaka, Y. (1969) The crystal structure of DL-proline hydrochloride, *Acta Cryst.*, B25:2182-2192.
- Mizuma, T., Masubuchi, S. and Awazu, S. (1998) Intestinal absorption of stable cyclic dipeptides by the oligopeptide transporter in rat, *J. Pharm. Pharmacol.*, 50:167-172.
- Monaghan, R. and Tkacz, J. (1990) Bioactive microbial products: Focus upon mechanism of action, *Annu. Rev. Microbiol.*, 44:271-301.
- Monks, A., Scudiero, D., Skehan, P., Shoemaker, R., Paull, K., Vistica, D., Hose, C., Langley, J., Cronise, P., Valgro-Wolff, A., Gray-Goodrich, M., Campbell, H., Mayo, J. and Boyd, M. (1991) Feasibility of a high-flux anticancer drug screen using a diverse panel of cultured human tumour cell lines, *J. Natl. Cancer. Inst.*, 83:757-766.
- Mosmann, T. (1983) Rapid colorimetric assay for cellular growth and survival: Application to proliferation and cytotoxicity assays, *J. Immunol. Met.*, 65:55-63.
- Mshana, R.N., Tadesse, G., Abate, G. and Miorner, H. (1998) Use of 3-(4,5-dimethylthiazol-2-yl)-2,5-diphenyltetrazolium bromide for rapid detection of rifampin-resistant *Mycobacterium tuberculosis*, *J. Clin. Microbiol.*, 36:1214-1219.
- Mustard, J. F., Kinlough-Rathbone, R.L. and Packman, M.A. (1989) Isolation of human platelets from plasma by centrifugation and washing, *Met. Enz.*, 169:3-11.
- Myers, P.L. (1997) Will combinatorial chemistry deliver real medicines? *Curr. Opin. Biotech.*, 8:701-707.
- Nadai, M., Sekido, T., Matsuda, I., Li, W., Kitaichi, K., Itoh, A., Nabeshima, T. and Hasegawa, T. (1998) Time-dependent effects of *Klebsiella pneumoniae* endotoxin on hepatic drug-metabolising enzyme activity in rats, *J. Pharm. Pharmacol.*, 50:871-879.
- Nayler, W.G. (1988) Calcium antagonists, Pg. 347, Academic Press, London.
- Nieminen, A., Saylor, A., Herman, B. and Lemasters, J. (1994) ATP depletion rather than mitochondrial depolarization mediates hepatocyte killing after metabolic inhibition, *Am. J. Physiol.*, 267:C64-C74
- Nishiwaki-Matsushima, R., Ohta, T., Nishiwaki, S., Suganuma, M., Kohyama, K., Ishikawa, T., Carmichael, W. and Fujiki, H. (1992) Liver tumour promotion by the cyanobacterial cyclic peptide toxin microcystin LR, *J. Cancer Res Clin Oncol.*, 118:420-424.
- Nitecki, D.E., Halpern, B. and Westley, J.W. (1968) A simple route to sterically pure diketopiperazines, *J. Org. Chem.*, 33:864-866.

- North, A.C.T., Phillips, D.C. and Matthews, F.S. (1968) Standard intensity checks and orientation control for diffraction measurements, *Acta Cryst.*, A24:351.
- Nowak, T.J. and Handford, A. G. (1999) Essentials of Pathophysiology: Concepts and Applications for Health Care Professionals, 2nd Ed., Pp. 121, 125, 126, 148-150, WCB McGraw-Hill, Boston.
- Nurse, P. (1987) Cell reproduction, *Brit. Med. J.*, 295:1037-1038.
- O'Reilly, R.A. (1989) Drugs used in disorders of coagulation, Pp. 406-418, In: Basic and Clinical Pharmacology, 4th Ed., Ed.: Katzung, B.G., Prentice-Hall International, U.S.A.
- Orrenius, S., McConkey, D., Bellomo, G. and Nicotera, P. (1989) Role of Ca²⁺ in toxic cell killing, *TiPS*, 10:281-285.
- Ovchinnikov, Y.A. and Ivanov, V.T. (1975) Conformational states and biological activity of cyclic peptides, *Tetrahedron*, 31:2177-2209.
- Pachler, K.G.R. (1964) Nuclear magnetic resonance study of some α -amino acids. II. Rotational isomerism, *Spectrochim. Acta.*, 20:581-587.
- Pardee, A., Dubrow, R., Hamlin, J. and Kletzien, R. (1978) Animal cell cycle, *Ann. Rev. Biochem.*, 47:715-750.
- Park, K., Mosher, D.F. and Cooper, S.L. (1989) *Ex vivo* measurement of platelet adhesion to polymeric surfaces, *Met. Enz.*, 169:91-117.
- Payan, D.G. and Shearn, M. (1989) Nonsteroidal anti-inflammatory drugs; nonopioid analgesics; drugs used in gout, Pp. 431-450, In: Basic and Clinical Pharmacology, 4th Ed., Ed.: Katzung, B.G., Prentice-Hall International, U.S.A.
- Pinto, M., Appay, M., Simon-Assmann, S., Chevalier, G., Dracopoli, N., Fogh, J. and Zweibaum, A. (1982) Enterocytic differentiation of cultured human colon carcinoma cells by replacement of glucose by galactose in the medium, *Biol. Cell*, 44:193-196.
- Porter, N. (1984) Chemistry of Lipid Peroxidation, *Met. Enz.*, 105:273-282.
- Potten, S. (1980) Stem cells in small-intestinal crypts, In: Appleton, D., Sunter, J. and Watson, A. (Eds.) Cell proliferation in the gastrointestinal tract, Pp. 143-145, Pitman Medical, Tunbridge Wells.
- Prasad, C. (1995) Bioactive cyclic dipeptides, *Peptides*, 16:151-164.
- Prescott, L.M., Harley, J. P. and Klein, D.A. (1996) Microbiology, 3rd Ed., Pp. 51, 56, 423, 662, 671, 749, 750, 761, 767, Wm. C. Brown Publishers, U.S.A.
- Proudfoot, S.G. (1988) Biopharmaceutics, In: Pharmaceutics: The science of dosage form design, Ed. Aulton, M.E. , Pg. 132, Churchill Livingstone, London.
- Ramachandran, G.M. and Mitra, A.K. (1976) An explanation for the rare occurrence of cis peptide units in proteins and polypeptides, *J. Mol. Biol.*, 107:85-92.
- Ramani, R., Sasisekharan, V. and Venkatesan, K. (1977) Conformational studies on cyclic dipeptides, *Int. J. Peptide Protein Res.*, 9:277-292.
- Rang, H.P. and Dale, M.M. (1991) Pharmacology, 2nd Ed., Pg. 355, Churchill Livingstone, Tokyo.

- Ratra, G., Morgon, W., Mullervy, J., Powell, C.J. and Wright, M.C. (1998) Methapyrilene hepatotoxicity is associated with oxidative stress, mitochondrial dysfunction and is prevented by the Ca²⁺-channel blocker verapamil, *Toxicology*, 130:79-93.
- Rees, S.A. and Curtis, M.J. (1993) Selective I_K blockade as an antiarrhythmic mechanism: effects of UK 66,914 on ischaemia and reperfusion arrhythmias in rat and rabbit hearts, *Br. J. Pharmacol.*, 108:139-145.
- Reynolds, E.S. (1964) Liver parenchymal cell injury, *Lab. Invest.*, 13:1457-1470.
- Rich, P.R., Mischis, L.A., Purton, S. and Wiskich, J.T. (2001) The sites of interaction of triphenyltetrazolium chloride with mitochondrial respiratory chains, *FEMS Microbiol. Lett.*, 202:181-187.
- Rob, J., Tollefsen, S. and Helgeland, L. (1997) A rapid and highly sensitive chromogenic microplate assay for quantification of rat and human prothrombin, *Anal. Biochem.*, 245:222-225.
- Roskoski R. (1996) *Biochemistry*, Pp. 224, 225, 232, 233, 234, 240, 409, 410, W.B. Saunders Co., Philadelphia.
- Roslev, P. and King, G.M. (1993) Application of a tetrazolium salt with a water-soluble formazan as an indicator of viability in respiring bacteria, *Appl. Environ. Microbiol.*, 59:2891-2896.
- Ross, D. (1989) Mechanistic Toxicology: A radical perspective, *J. Pharm. Pharmacol.*, 41:505-511.
- Rousset, M. (1986) The human colon carcinoma cell lines HT-29 and Caco-2: two *in vitro* models for the study of intestinal differentiation, *Biochimie*, 68:1035-1040.
- Runnegar, M.T.C., Andrews, J., Gerdes, R. and Falconer, I. (1987) Injury to hepatocytes induced by a peptide toxin from the cyanobacterium *Microcystis aeruginosa*, *Toxicon.*, 25:1235-1239.
- Russell, N.J., Powell, G.M., Jones, G., Winterburn, P. and Basford, J.M. (1982) *Blood biochemistry*, Pp. 125, 129, Croom Helm, London.
- Salmon, S.E. and Sartorelli, A.C. (1989) Cancer chemotherapy, Pp. 684, 685, 686, 692, 696, 699, 702, In: *Basic and Clinical Pharmacology*, 4th Ed., Ed.: Katzung, B.G., Prentice-Hall International, U.S.A.
- Sammes, P. G., (1975) Naturally occurring 2,5-Dioxopiperazines and related compounds, *Forts. Chem. Organ. Naturst.*, 32:51-118.
- Seglen, P.O. (1973) Preparation of rat liver cells, *Exp. Cell Res.*, 82:29-83.
- Seglen, P.O. (1994) Isolation of hepatocytes, In: *Cell Biology: A laboratory handbook*, Ed.: Pp. 96-102, Academic Press.
- Sensch, O., Vierling, W., Brandt, W. and Reiter, M. (2000) Effects of inhibition of calcium and potassium currents in guinea-pig cardiac contraction: comparison of β-caryophyllene oxide, eugenol and nifedipine, *Br. J. Pharmacol.*, 131:1089-1096.
- Shaw, L.A. and Coker, S.J. (1997) Suppression of reperfusion-induced arrhythmias with combined administration of 5-HT₂ and thromboxane A₂ antagonists, *Br. J. Pharmacol.*, 117:817-822.
- Sheldrick, G. M. (1986) SHELX86 – A program for the solution of crystal structures, University of Gottingen.
- Shepherd, M.G., Poulter, R.T.M. and Sullivan, P.A. (1985) *Candida albicans*: Biology, genetics and pathogenicity, *Ann. Rev. Microbiol.*, 39:579-614.

- Shiba, T. and Nunami, K. (1974) Structure of a bitter peptide in casein hydrolyzate by bacterial proteinase, *Tetrahedron Lett.*, 6:509-512.
- Siemion, I.Z. (1976) Conformational investigations on cyclic dipeptides containing a proline residue by means of ¹³C NMR spectroscopy, *Org. Magn. Reson.*, 8:432-435.
- Sigma catalogue (2000-2001) Biochemicals and Reagents for Life Science Research, Pp. 113, 234, 686, 1017.
- Sigma Diagnostics (ATP) (1995) St. Louis, MO.
- Sigma Diagnostics (Ca²⁺) (1997) St. Louis, MO.
- Sigma Diagnostics (LDH) (2000) St. Louis, MO.
- Silverman, R.B. (1992) The organic chemistry of drug design and drug action, Pg. 286, Academic Press, San Diego.
- Singleton, P. (1992) Introduction to bacteria, Pg. 182, Wiley Publishers, New York.
- Slater, T.F. (1984) Overview of methods used for detecting lipid peroxidation, *Met Enz.*, 105:283-293.
- Sletten, E. (1970) Conformation of cyclic dipeptides: The crystal and molecular structures of cyclo-D-alanyl-L-alanyl (3,6-dimethylpiperazine-2,5-dione), *J. Am. Chem. Soc.*, 92:172-177.
- Smith, M., Thor, H., Hartzell, P. and Orrenius, S. (1982) The measurement of lipid peroxidation in isolated hepatocytes, *Biochem. Pharmacol.*, 31:19-26.
- Smith, C. and Wood, E. (1991) Molecular and Cell Biochemistry: Cell Biology, Pg. 323, Chapman and Hall, London.
- Song, L., Ren, G., Chen, Z., Chen, Z., Zhou, Z. and Cheng, H. (2000) Electrophysiological effects of protopine in cardiac myocytes: inhibition of multiple cation channel currents, *Br. J. Pharmacol.*, 129:883-900.
- Souza, M.F., Tome, A.R. and Rao, V.S.N. (1999) Inhibition by the bioflavonoid ternatin of Aflatoxin B₁-induced lipid peroxidation in rat liver, *J. Pharm. Pharmacol.* 51:125-129.
- Sperelakis, N. and Norwell, K. (1989) Physiology and Pathophysiology of the heart, 2nd Ed., Pg. 1009, Academic Press, London.
- Stein, E.A., Fuller, S.A., Egemond, W.S. and Campbell, W.B. (1996) Physiological and behavioural effects of the endogenous cannabinoid, arachidonylethanolamide (anandamide), in rat, *Br. J. Pharmacol.*, 119:107-114.
- Stevens, M.G., and Olsen, S.C. (1993) Comparative analysis using MTT and XTT in colorimetric assays for quantitating bovine neutrophil bactericidal activity, *J. Immunol. Methods*, 157:225-231.
- Stryer, L. (1988) Biochemistry, Pp. 17, 18, 503, 505, 579, W. H. Freeman and Co., New York.
- Sugidachi, A., Asai, F., Ogawa, T., Inoue, T. and Koike, H. (2000) The *in vivo* pharmacological profile of CS-747, a novel antiplatelet agent with platelet ADP receptor antagonist properties, *Br. J. Pharmacol.*, 129:1439-1446.

- Summanen, P., Wexler, H.M and Finegold, S.M. (1992) Antimicrobial susceptibility testing of *Biophila wadsworthia* by using triphenyltetrazolium chloride to facilitate endpoint determination, *Antimicrob. Agents Chemother.*, 36:1658-1664.
- Suzuki, K., Sasaki, Y., Endo, N. and Mihara, Y. (1981) Acetic acid-catalysed diketopiperazine synthesis, *Chem. Pharm. Bull.*, 29:233-237.
- Svec, H.J. and Junk, G.A. (1964) The mass spectra of dipeptides, *J. Am. Chem. Soc.*, 86:2278-2282.
- Szafranek, J., Palacz, Z. and Grzonka, Z. (1976) A comparison of electron impact and field ionisation spectra of some 2,5-diketopiperazines, *Org. Mass Spectrom.*, 11:920-930.
- Taki, Y., Sakane, T., Nadai, T., Sezaki, H., Amidon, G., Langguth, P. and Yamashita, S. (1998) First-pass metabolism of peptide drugs in rat perfused liver, *J. Pharm. Pharmacol.*, 50:1013-1018.
- Tanaka, K., Sato, M., Tomita, Y. and Ichichara, A. (1978) Biochemical studies on liver function in primary cultured hepatocytes of adult rats – hormonal effects on cell viability and protein synthesis, *J. Biochem.*, 84:937-948.
- Thom, S., Horobin, R., Seidler, E. and Barer, M.R. (1993) Factors affecting the selection and use of tetrazolium salts as cytochemical indicators of microbial viability and activity, *J. Appl. Bacteriol.*, 74:433-443.
- Tietze, F. (1969) Enzymatic method for quantitative determination of nanogram amounts of total and oxidized glutathione: applications to mammalian blood and other tissues, *Anal. Biochem.*, 27:502-522.
- Tortora, G. J. and Grabowski, S.R. (2000) Principles of Anatomy and Physiology, 9th Ed., Pp. 610-11, 622, 623, 625-7, 631, 636-639, 651, 654, John Wiley and Sons, Inc., New York.
- Towner, R.A., Hashimoto, H. and Summers, P. (2000) Non-invasive *in vivo* magnetic resonance imaging assessment of acute aflatoxin B₁ hepatotoxicity in rats, *Biochim. Biophys. Acta.* 1475:314-320.
- Triggle, D.J. (1996) The transition from agonist to antagonist activity: Symmetry and other considerations, In: Wermuth, C.G., Practice in Medicinal Chemistry, Pg. 550, Academic Press, London.
- Tripathy, D. (1995) Neoplasia, Pp. 49, 50, 52, 56-8, In: Pathophysiology of disease: An introduction to clinical medicine, 1st Ed., Eds: McPhee, S.J., Lingappa, V.R., Ganong, W. and Lange, J., Prentice-Hall International Inc., U.S.A.
- Uchiyama, M. and Mihara, M. (1978) Determination of malonaldehyde precursor in tissues by thiobarbituric acid test, *Anal. Biochem.*, 86:271-278.
- Varughese, K. I., Lu, C.T. and Kartha, G. (1981) Crystal structure and conformation of cyclo-L-cystine, *Int. J. Peptide Protein Res.*, 18:88-102.
- Vickers, A.E. (1997) Experimental In Vitro models to evaluate hepatotoxicity, In : In Vitro methods in pharmaceutical research. Pp.103-123. Academic Press, San Diego.
- Vile, R. (1990) Cancer and oncogenes, Inside Science 32, *New Scientist*, Pp. 25-30.
- Volk, W.A., Gebhardt, B.M., Hammarskjold, M.T. and Kadner, R.J. (1996) Essentials of Medical Microbiology, Pp. 253-285, 474-495, Lippincott-Raven, Philadelphia.
- Walkowiak, B., Keşy, A. and Michalec, L. (1997) Microplate reader – A convenient tool in studies of blood coagulation, *Thromb. Res.*, 87:95-103.

- Wang, X., Wu, L., Aoufflen, M., Mateescu, M., Nadeau, R. and Wang, R. (1999) Novel cardiac protective effects of urea: from shark to rat, *Br. J. Pharmacol.*, 128:1477-1484.
- Wick, M.J., Frank, D.W., Storey, D.G. and Iglewski, B.H. (1990) Structure, function and regulation of *Pseudomonas aeruginosa*, *Ann. Rev. Microbiol.*, 44:335-363.
- Willard, H.H., Merritt, L.L., Dean, J.A., Settle, F.A. (1988) Instrumental methods of analysis, Pp. 287-288, 465, 473, 762, 7th Ed., Wadsworth Publishing Co., California.
- Yajima, H., Ogawa, H. and Fuji, N.F.S. (1977) Studies on peptides. LXIX. Selective removal of acid-labile α -amino protecting groups with dilute sulfonic acids, *Chem. Bull.*, 25:740-747.
- Yamazaki, T., Nunami, K. and Goodman, M. (1991) Cyclic retro-inverso dipeptides with two aromatic side chains. II. Conformational analysis, *Biopolymers*, 31:1513-1528.
- Yang, Q., Padrini, R., Bova, S., Piovan, D. and Magnolfi, G. (1995) Electrocardiographic interactions between pinacidil, a potassium channel opener and class I antiarrhythmic agents in guinea-pig isolated perfused heart, *Br. J. Pharmacol.*, 114:1745-1749.
- Yasui, K. and Palade, P. (1995) Inhibitory action of SR 33557 on L-type calcium current in single ventricular myocytes of rat, *Br. J. Pharmacol.*, 114:468-474.
- Zucker, M.B. (1989) Platelet aggregation measured by the photometric method, *Met. Enz.*, 169:117-134.

APPENDIX A

AMINO ACID TABLE

Table A. 1: Abbreviations and symbols of the amino acids as used in the text (Lehninger *et al.*, 2000. Pg. 118).

Amino acid	Abbreviation	Symbols
Alanine	Ala	A
Arginine	Arg	R
Asparagine	Asn	N
Aspartate	Asp	D
Cysteine	Cys	C
Glutamate	Glu	E
Glutamine	Gln	Q
Glycine	Gly	G
Histidine	His	H
Isoleucine	Ile	I
Leucine	Leu	L
Lysine	Lys	K
Methionine	Met	M
Phenylalanine	Phe	F
Proline	Pro	P
Serine	Ser	S
Threonine	Thr	T
Tryptophan	Trp	W
Tyrosine	Tyr	Y
Valine	Val	V

APPENDIX B

SPECTRA, GRAPHS, ETC.

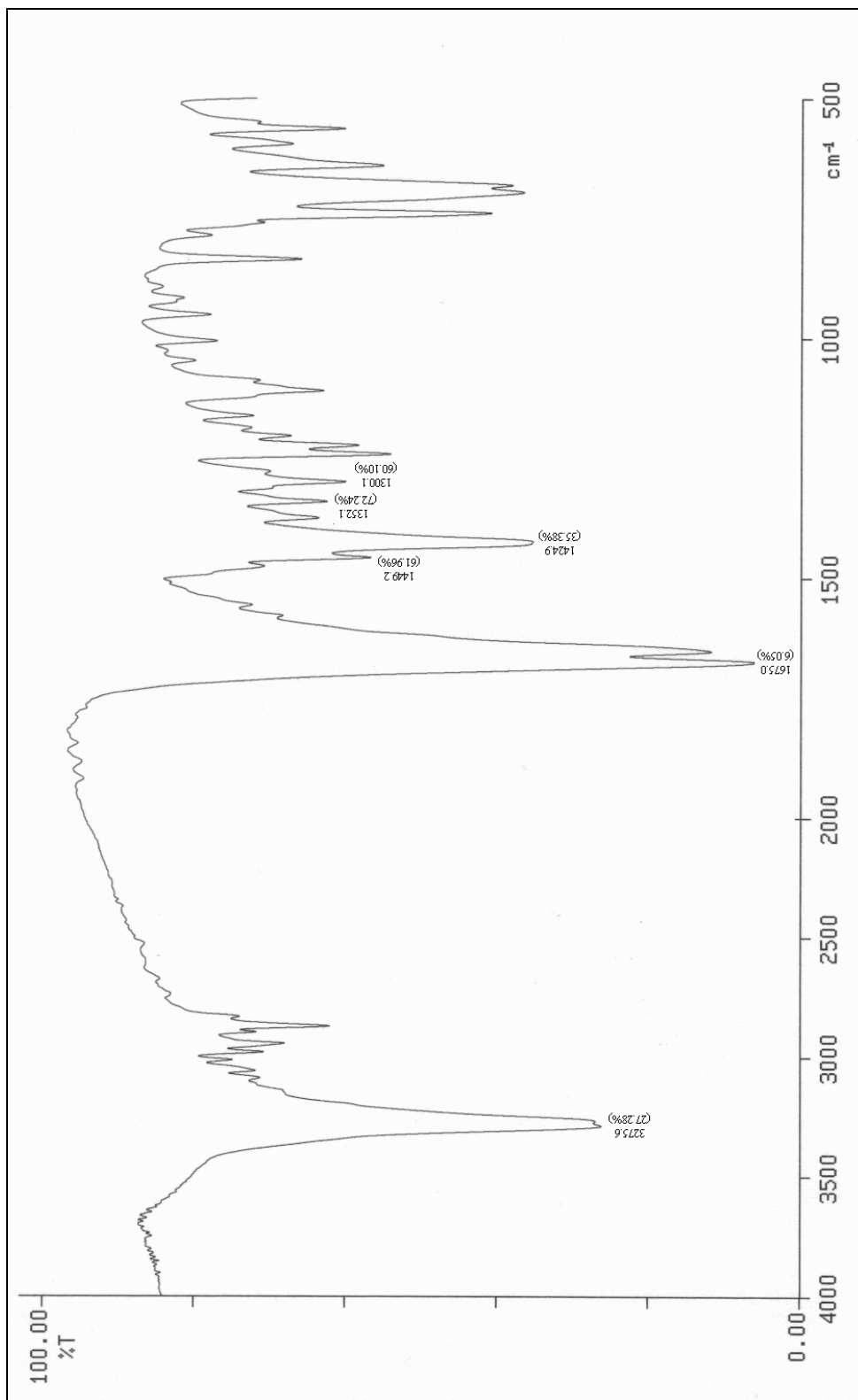


Figure B1. 1: IR spectrum of cyclo(L-Trp-L-Pro).

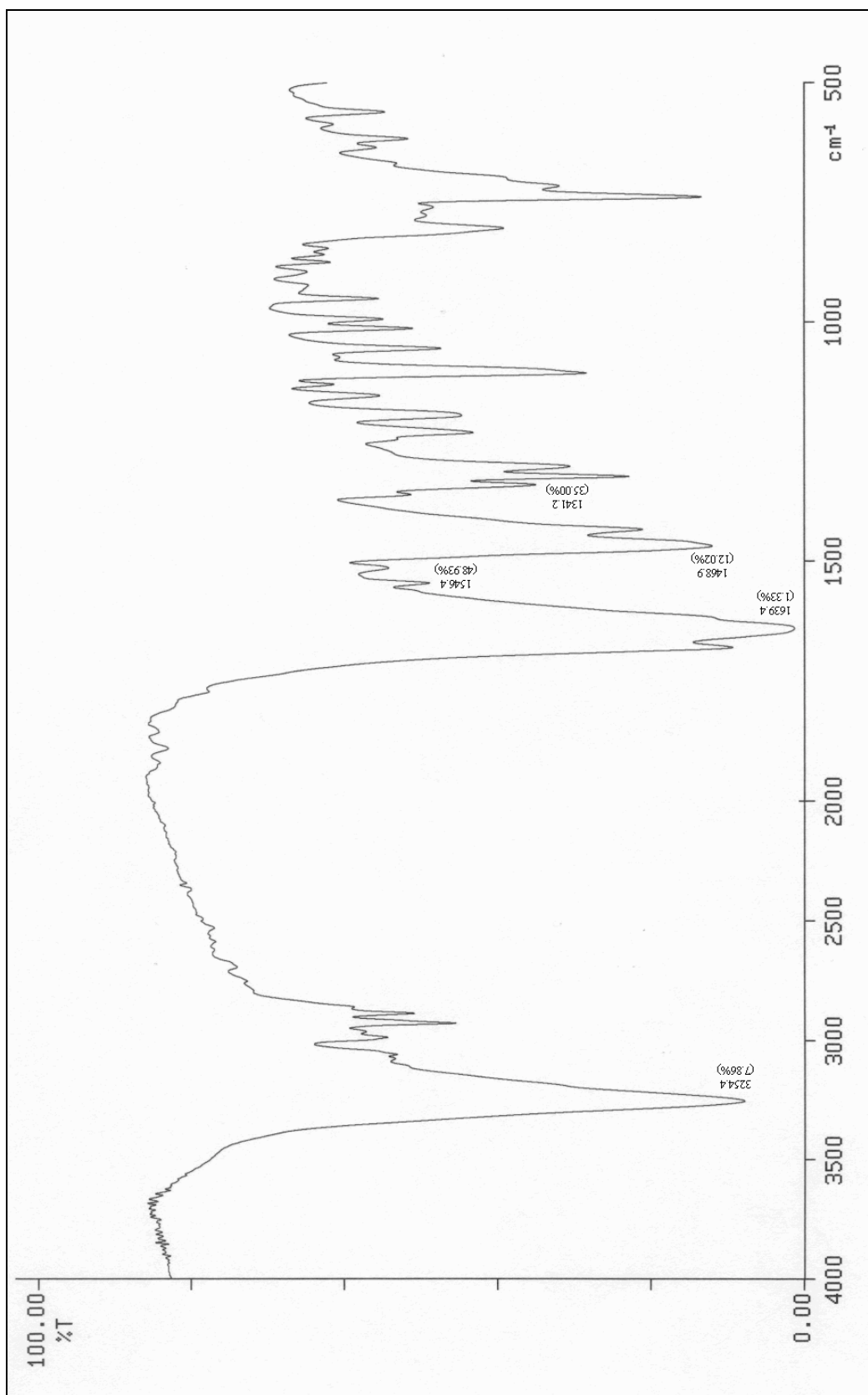


Figure B1. 2: IR spectrum of cyclo(L-Trp-D-Pro).

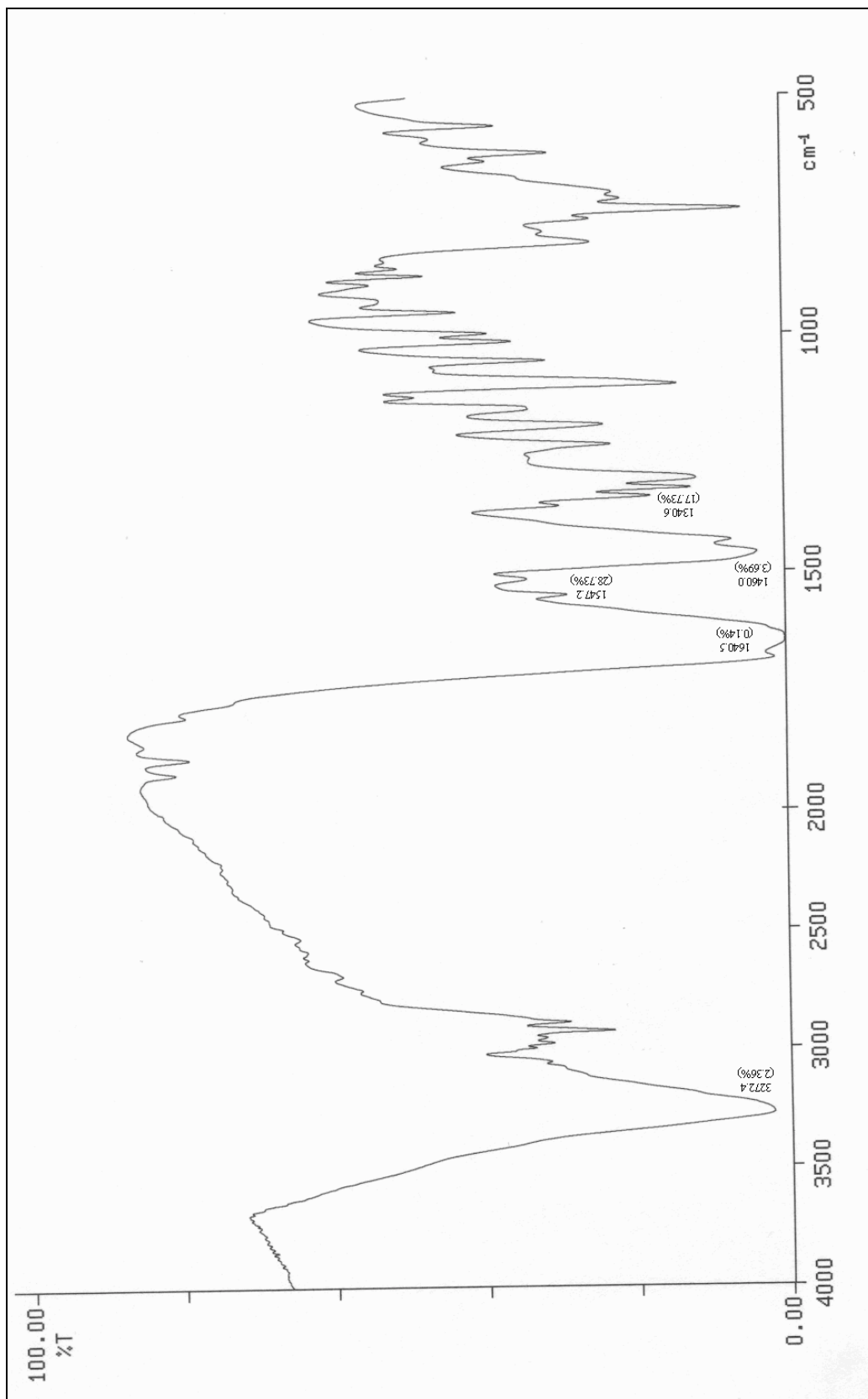


Figure B1. 3: IR spectrum of cyclo(D-Trp-L-Pro).

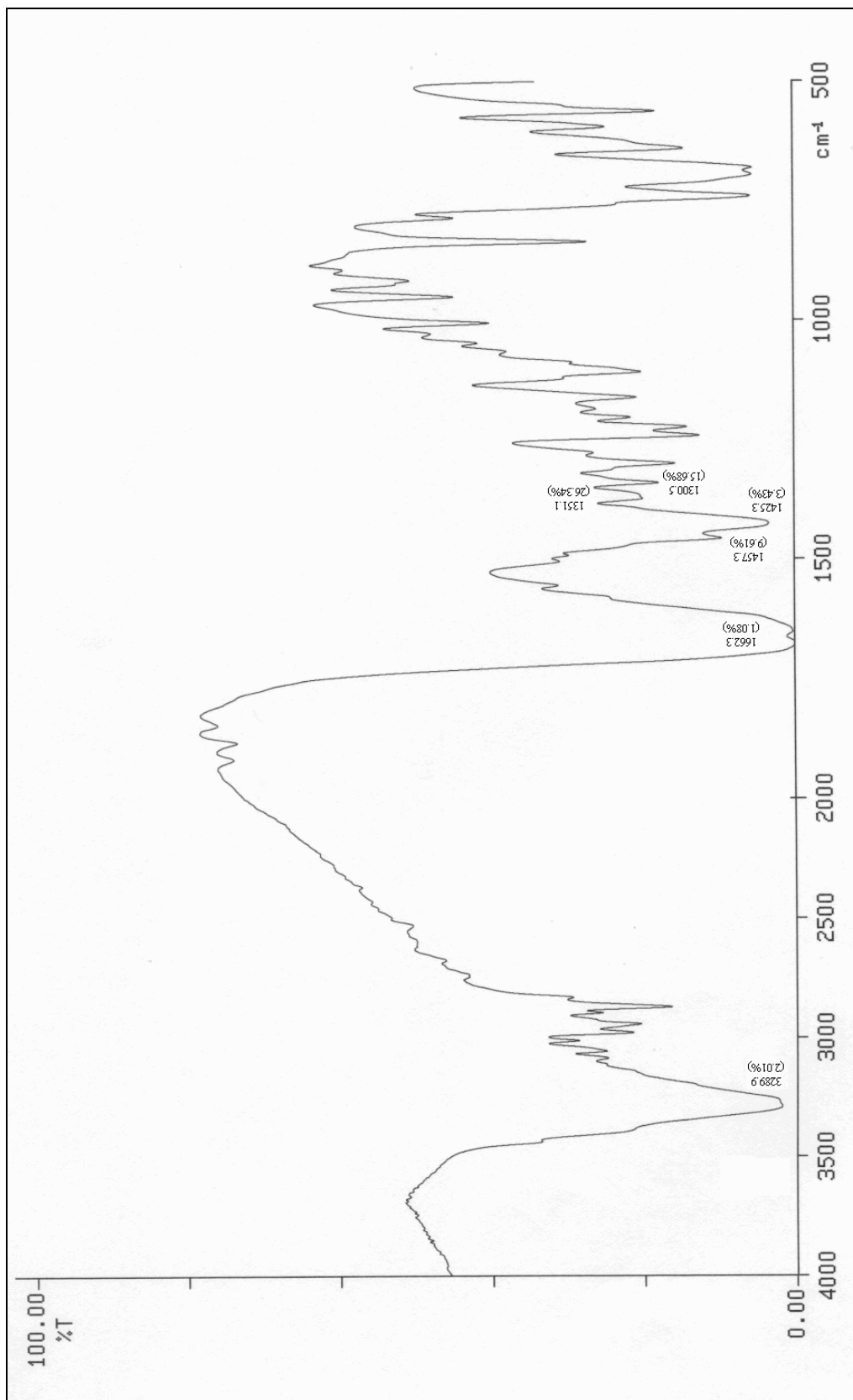


Figure B1. 4: IR spectrum of cyclo(D-Trp-D-Pro).

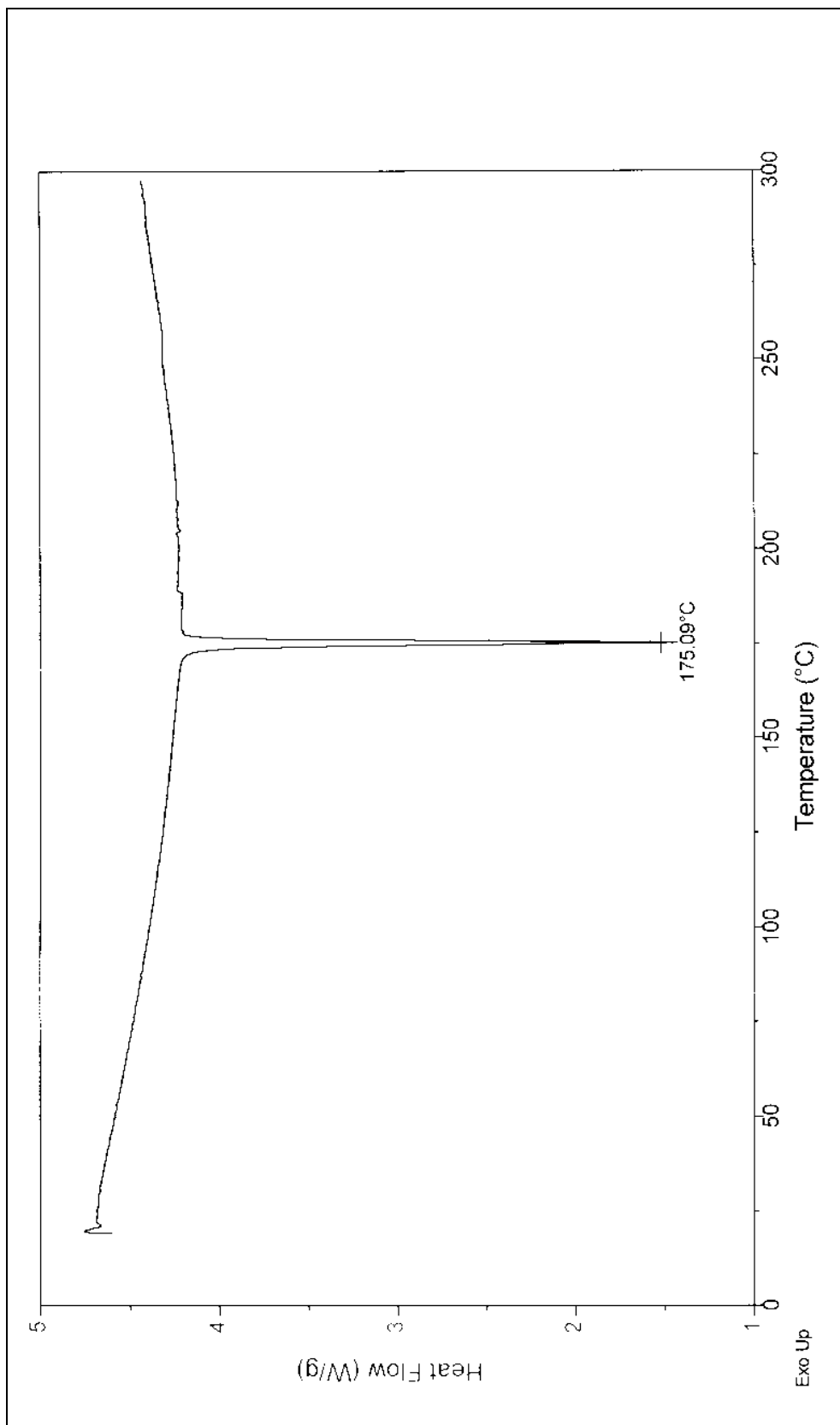


Figure B1. 5: DSC thermogram for cyclo(L-Trp-L-Pro).

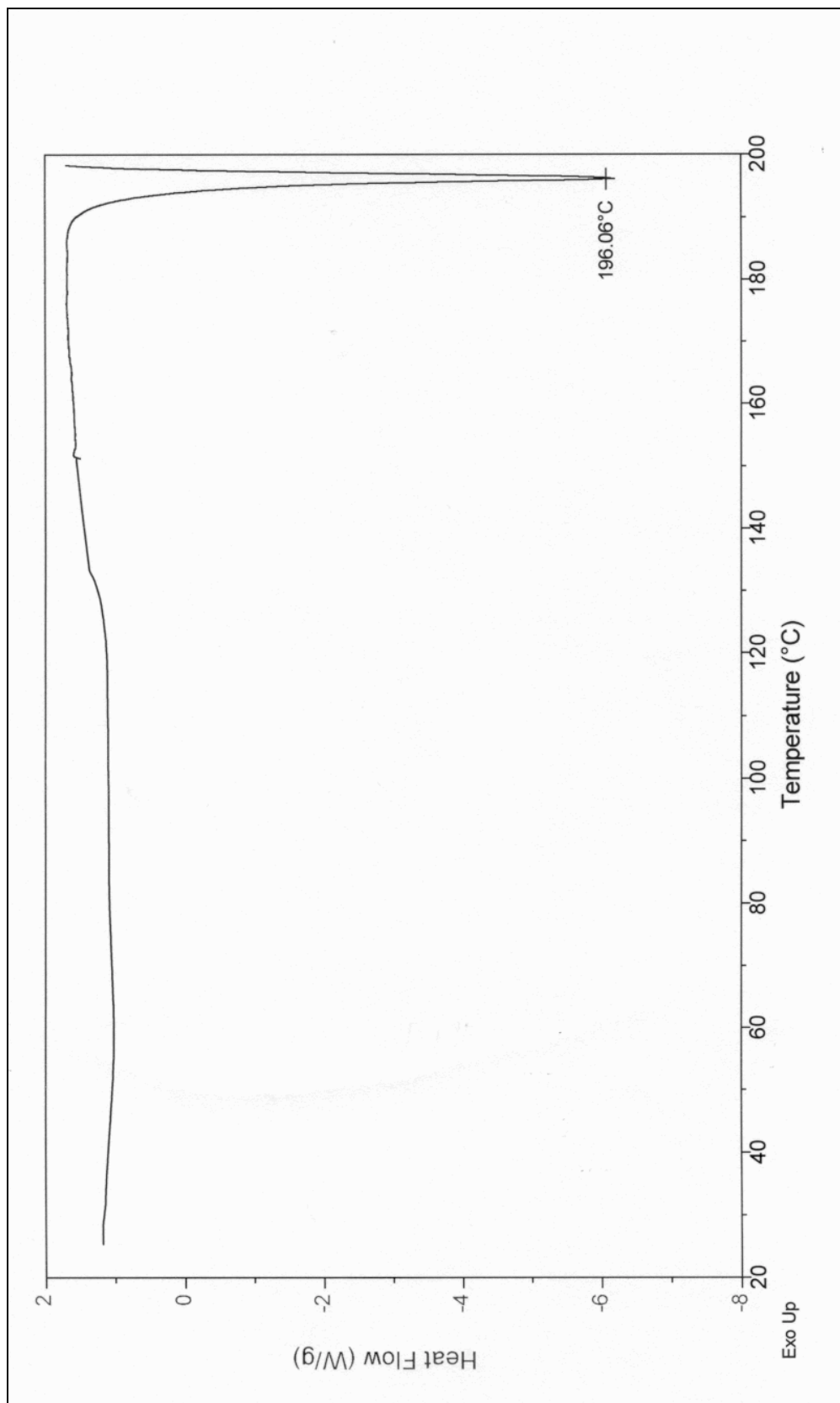


Figure B1. 6: DSC thermogram for cyclo(L-Trp-D-Pro).

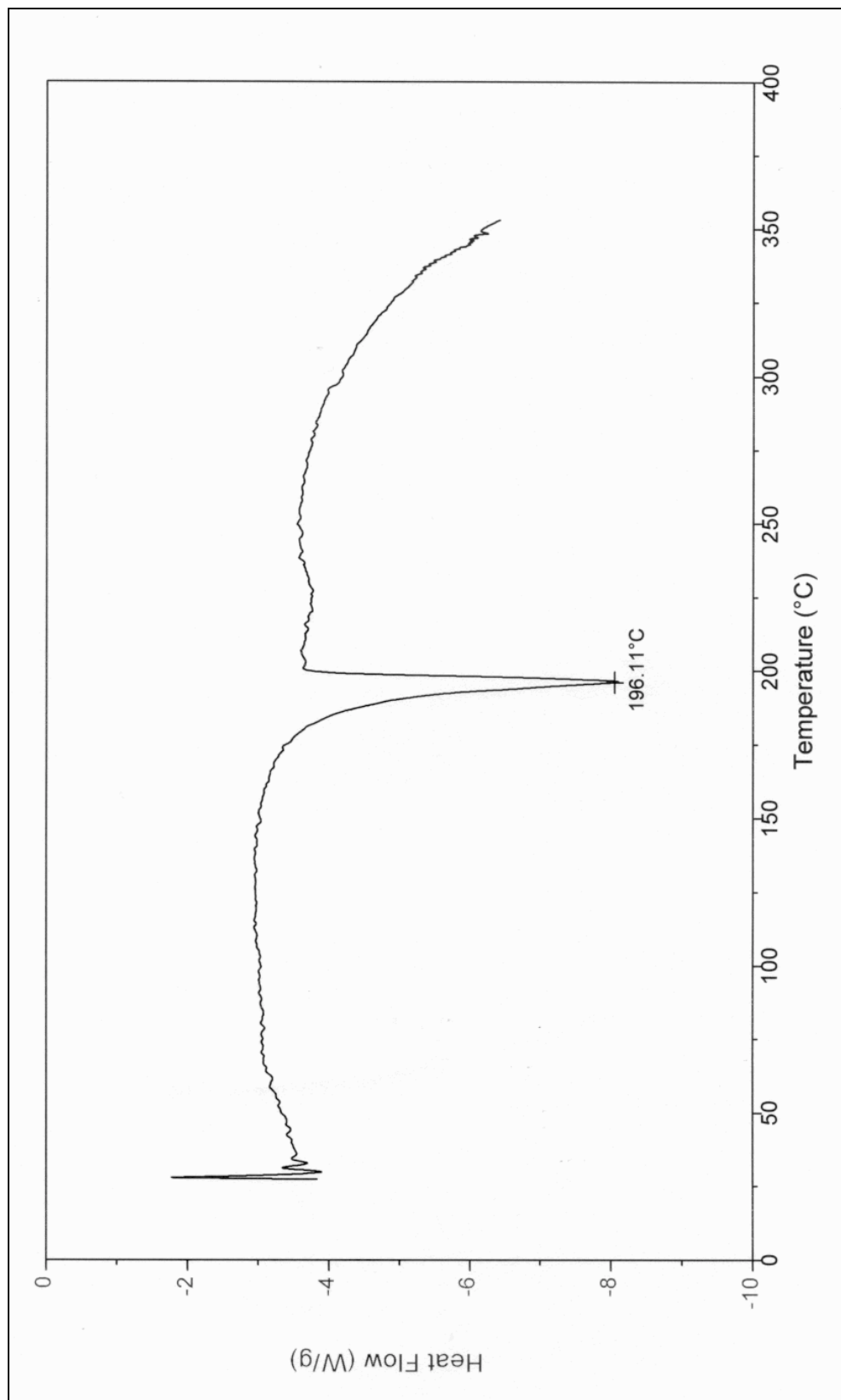


Figure B1. 7: DSC thermogram for cyclo(D-Trp-L-Pro).

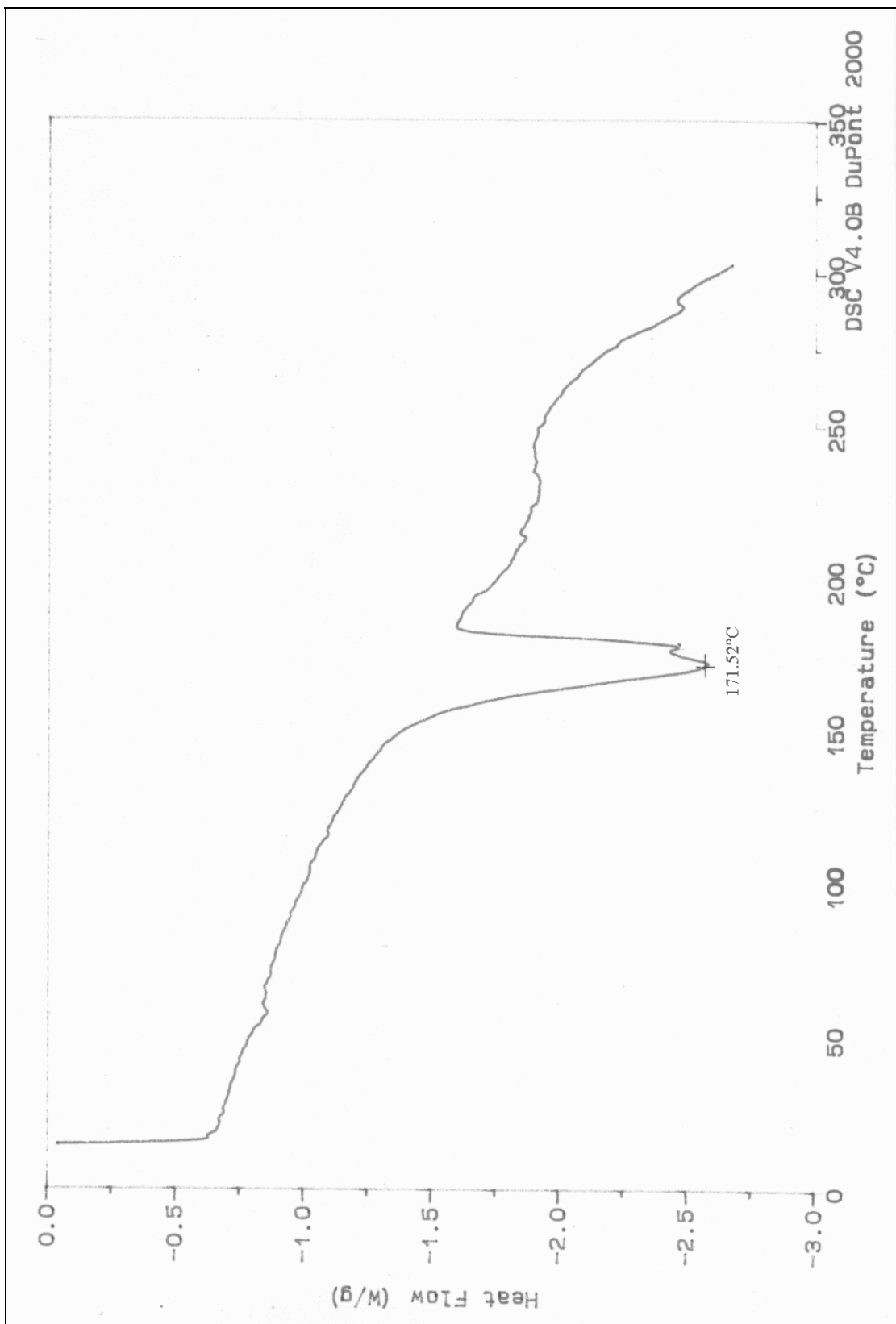


Figure B1. 8: DSC thermogram for cyclo(D-Trp-D-Pro).

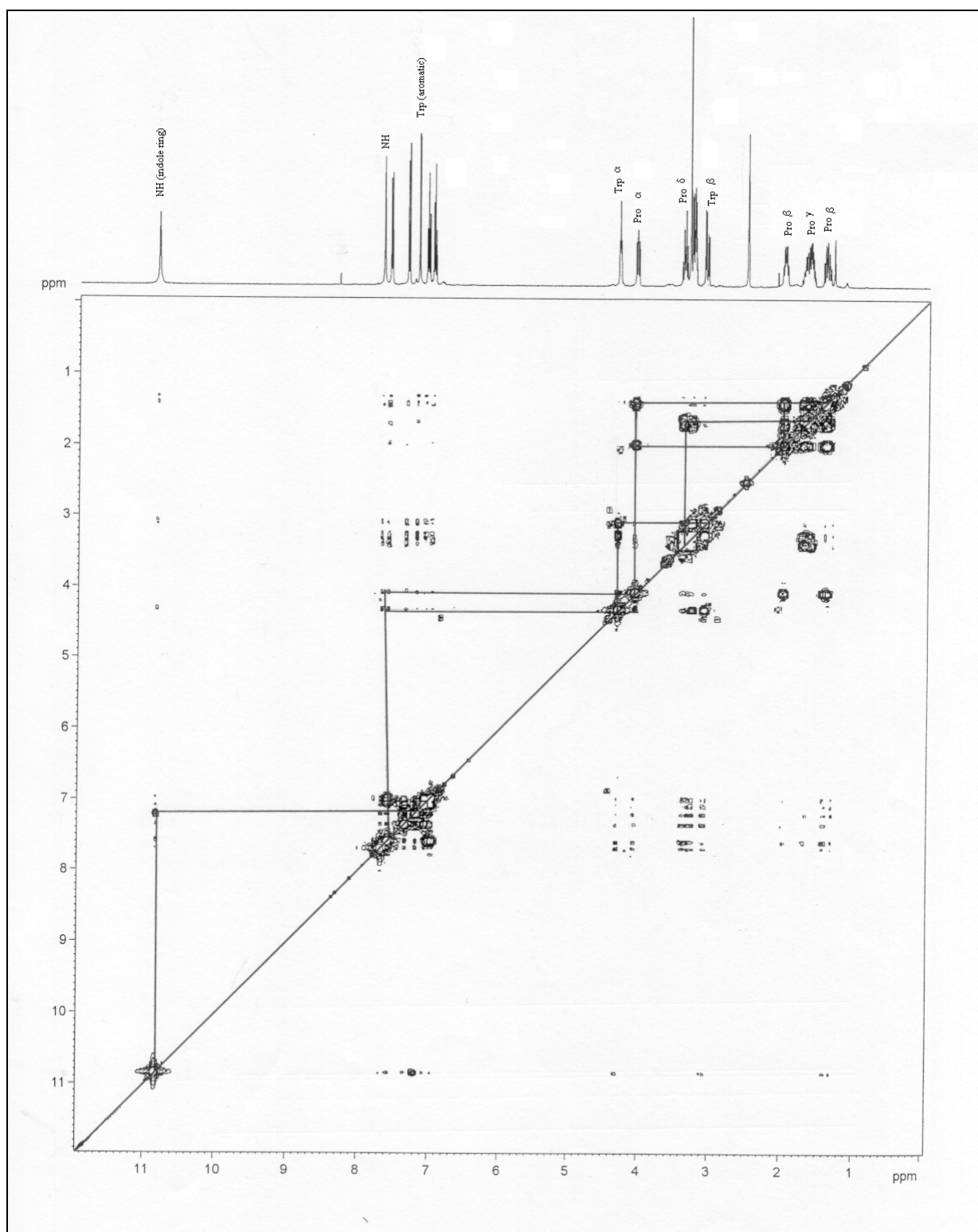


Figure B1. 9: COSY spectrum of cyclo(D-Trp-D-Pro) in DMSO-d₆.

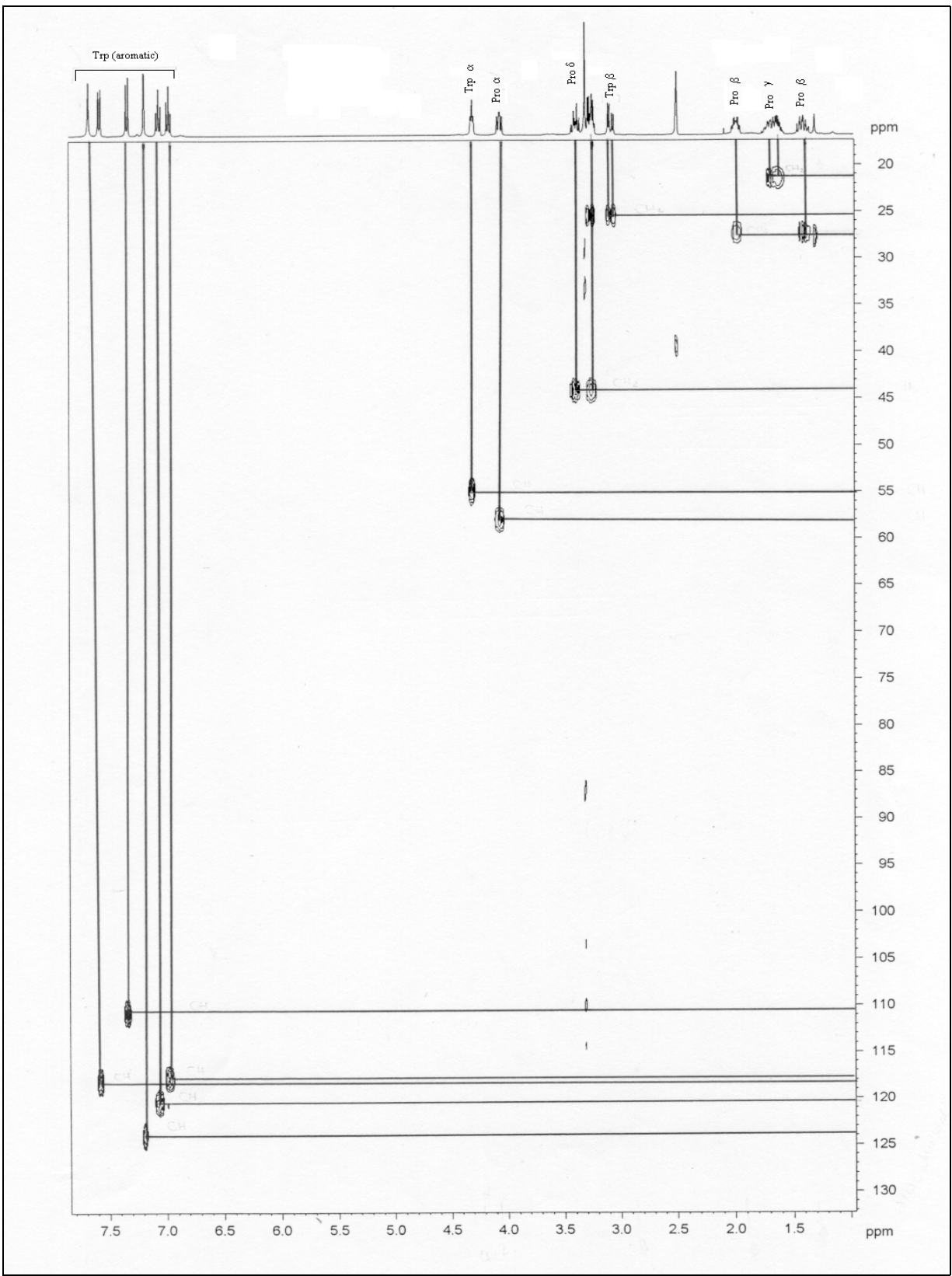


Figure B1. 10: Hetcor spectrum of cyclo(D-Trp-D-Pro) in DMSO-d₆.

CALCULATION

Calculation using Pachler's analysis (Pachler, 1964)

$$a = (J_{13} - J_g) / (J_r - J_g)$$

$$b = (J_{12} - J_g) / (J_r - J_g)$$

$$c = 1 - (a + b)$$

For cyclo(L-Trp-L-Pro), $J_{13} = 5.624$ ppm

$$J_{12} = 4.891$$

By substitution,

$$a = (5.624 - 2.60) / (13.56 - 2.60) = 0.276 \text{ (unfolded 27.6\%)}$$

$$b = (4.891 - 2.60) / (13.56 - 2.60) = 0.209 \text{ (unfolded 20.9\%)}$$

Thus, $c = 1 - (0.276 + 0.209) \times 100\%$

$$= 51.5 \% \text{ (folded)}$$

Table B. 1: Dilutions of the different microbial cultures.

Microorganism	Cells/ml as determined from CFUs (Absorbance of 0.220 at 540/600 nm)	Dilution to obtain 0.5×10^6 cells/ml ($*1 \times 10^6$ cells/ml)
<i>E. coli</i>	8×10^7	62.5 μ l to 10 ml
<i>P. aeruginosa</i>	5×10^8	10 μ l to 10 ml
<i>S. aureus</i>	5.7×10^8	8.8 μ l to 10 ml
<i>Streptococcus</i>	8.45×10^8	5.9 μ l to 10 ml
<i>C. albicans</i>	4.2×10^8	*13.2 μ l to 10 ml

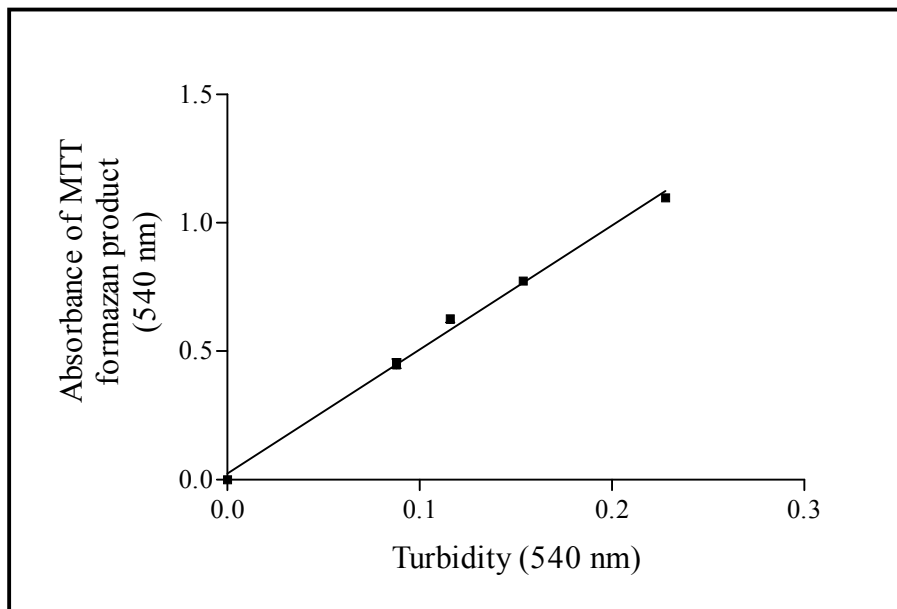


Figure B2. 1: Correlation between turbidity of *E. coli* (540 nm) and MTT formazan production, measured at 540 nm. $R^2=0.9936$. Values indicated are the mean \pm s.d. of triplicates.

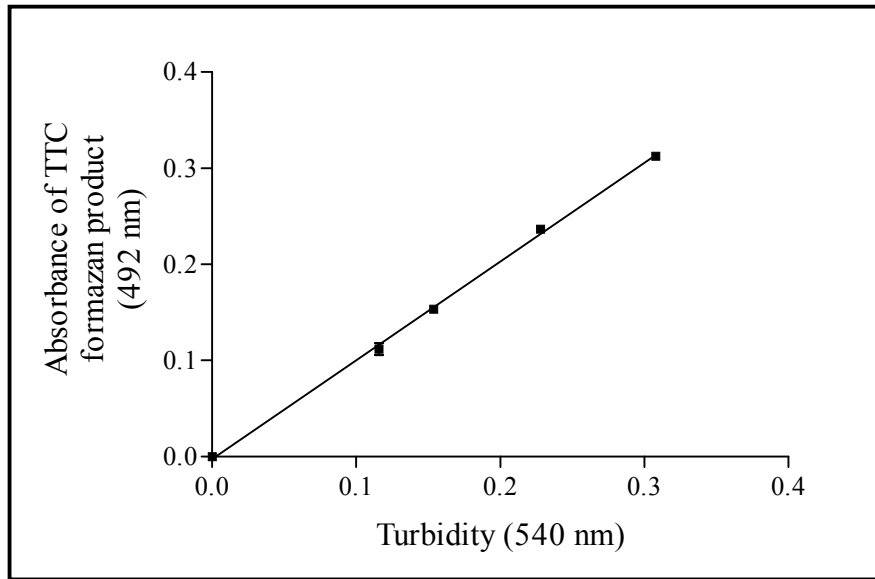


Figure B2. 2: Correlation between turbidity of *E. coli* (540 nm) and TTC formazan production, measured at 492 nm. $R^2=0.9975$. Values indicated are the mean \pm s.d. of triplicates.

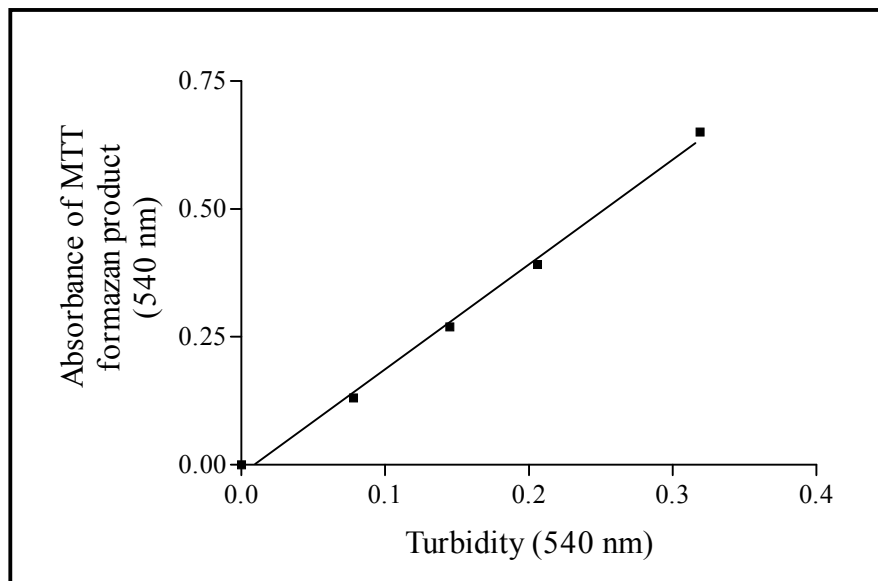


Figure B2. 3: Correlation between turbidity of *P. aeruginosa* (540 nm) and MTT formazan production, measured at 540 nm. $R^2=0.9958$. Values indicated are the mean \pm s.d. of triplicates.

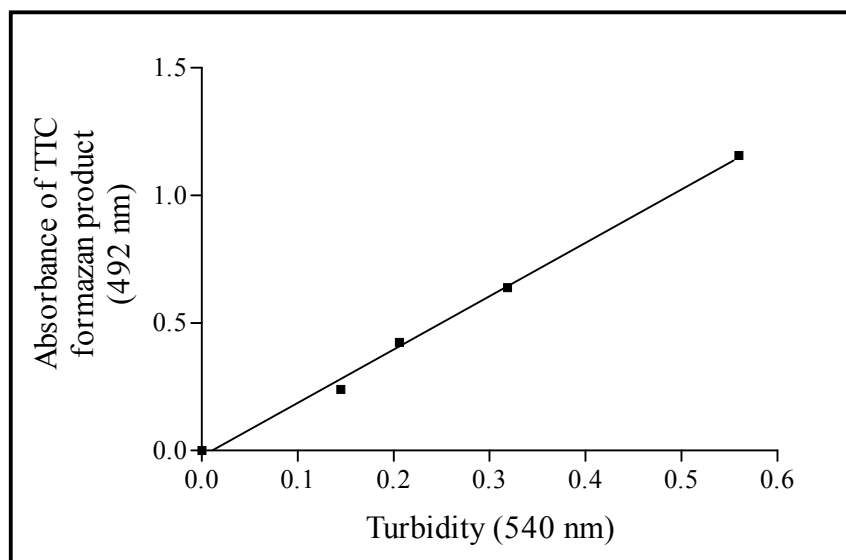


Figure B2. 4: Correlation between turbidity of *P. aeruginosa* (540 nm) and TTC formazan production, measured at 492 nm. $R^2=0.9967$. Values indicated are the mean \pm s.d. of triplicates.

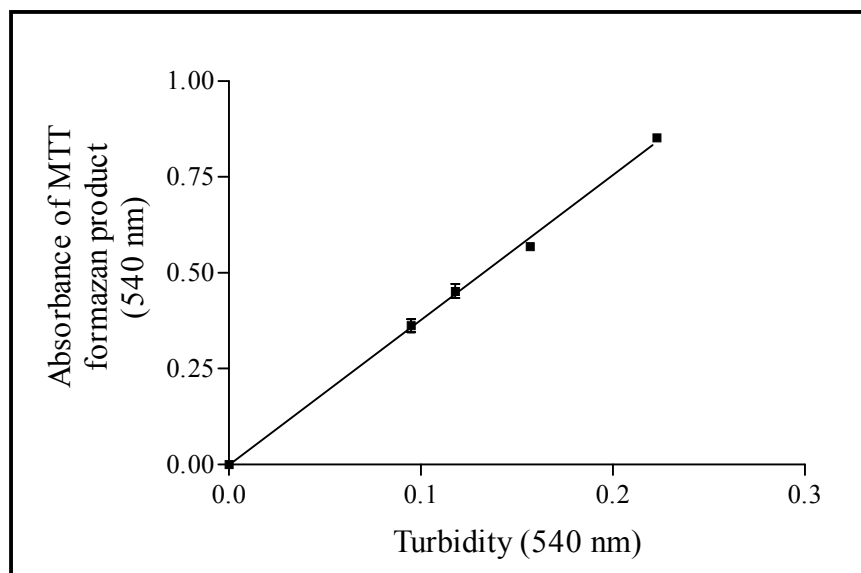


Figure B2. 5: Correlation between turbidity of *S. aureus* (540 nm) and MTT formazan production, measured at 540 nm. $R^2=0.9945$. Values indicated are the mean \pm s.d. of triplicates.

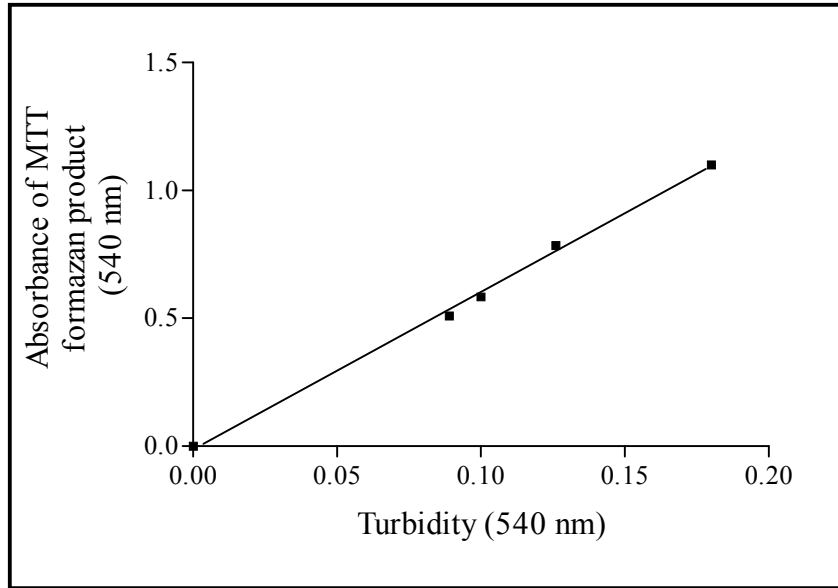


Figure B2. 6: Correlation between turbidity of *Streptococcus* (540 nm) and MTT formazan production, measured at 540 nm. $R^2=0.9973$. Values indicated are the mean \pm s.d. of triplicates.

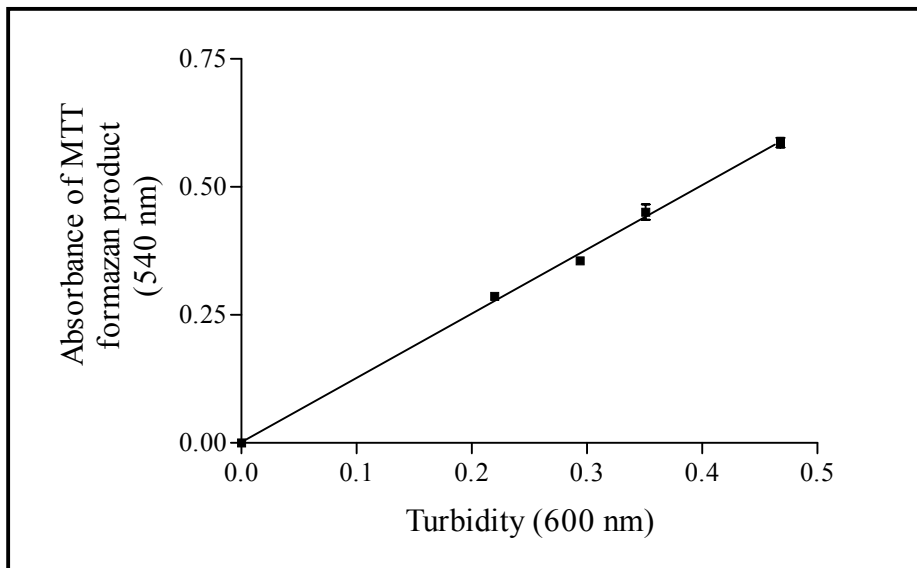


Figure B2. 7: Correlation between turbidity of *C. albicans* (600 nm) and MTT formazan production, measured at 540 nm. $R^2=0.9943$. Values indicated are the mean \pm s.d. of triplicates.

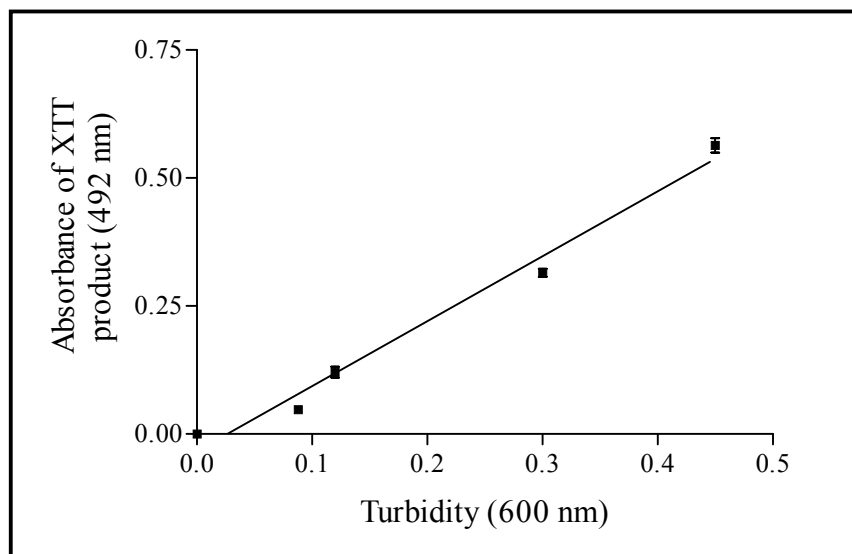


Figure B2. 8: Correlation between turbidity of *C. albicans* (600 nm) and XTT formazan production, measured at 492 nm. $R^2=0.9790$. Values indicated are the mean \pm s.d. of triplicates.

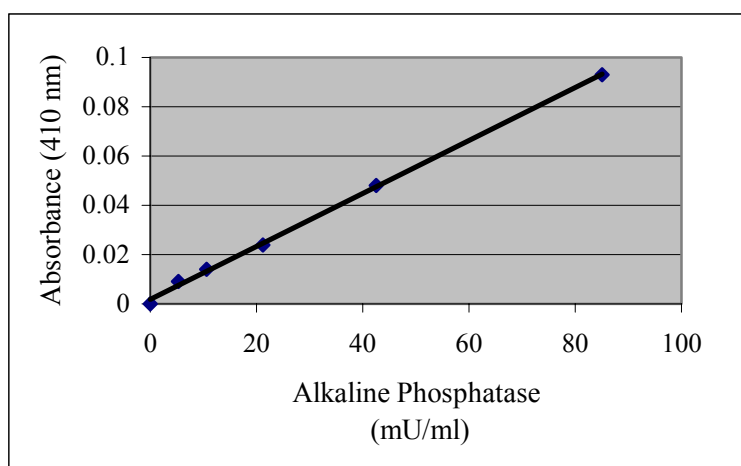


Figure B3. 1: Alkaline phosphatase standard curve (anticancer study). $R^2=0.9989$.

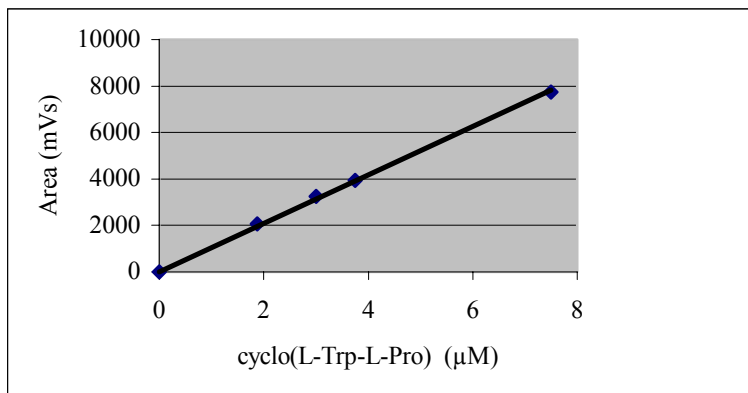


Figure B4. 1: Standard curve of cyclo(L-Trp-L-Pro) vs area (HPLC). $R^2=0.9988$.

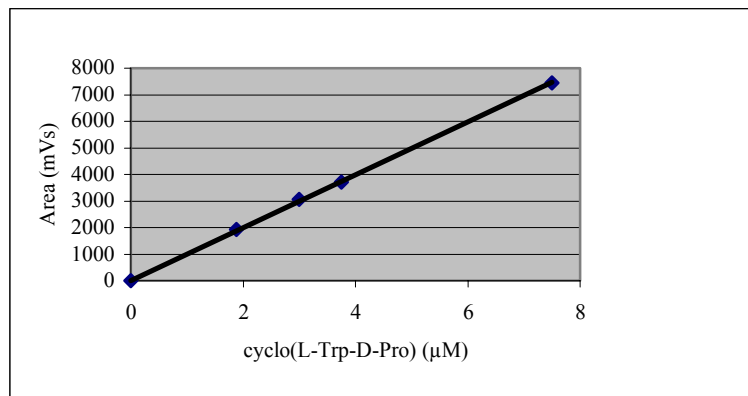


Figure B4. 2: Standard curve of cyclo(L-Trp-D-Pro) vs area (HPLC). $R^2=0.9996$.

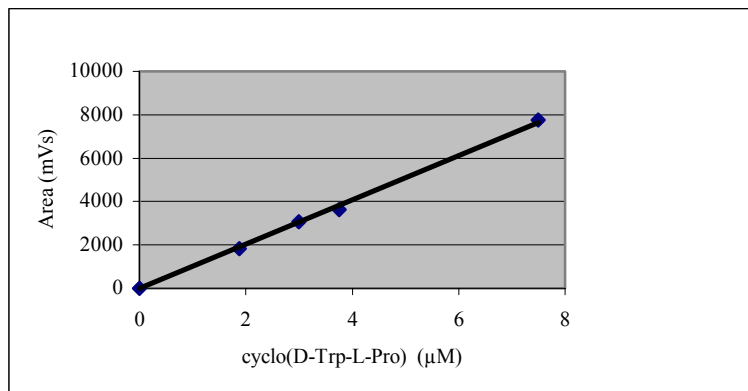


Figure B4. 3: Standard curve of cyclo(D-Trp-L-Pro) vs area (HPLC). $R^2=0.9983$.

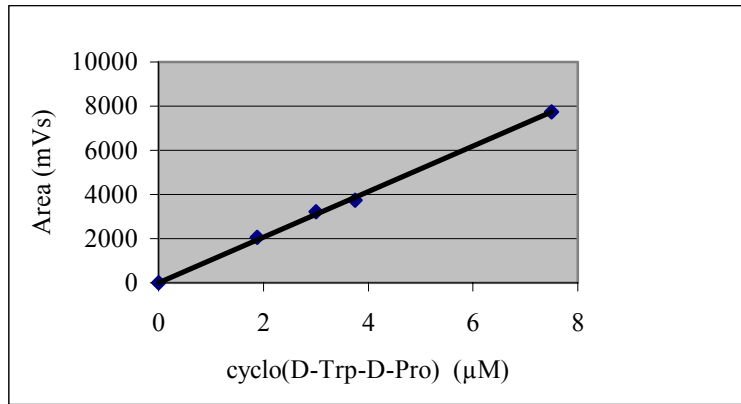


Figure B4. 4: Standard curve of cyclo(D-Trp-D-Pro) vs area (HPLC). $R^2=0.9985$.

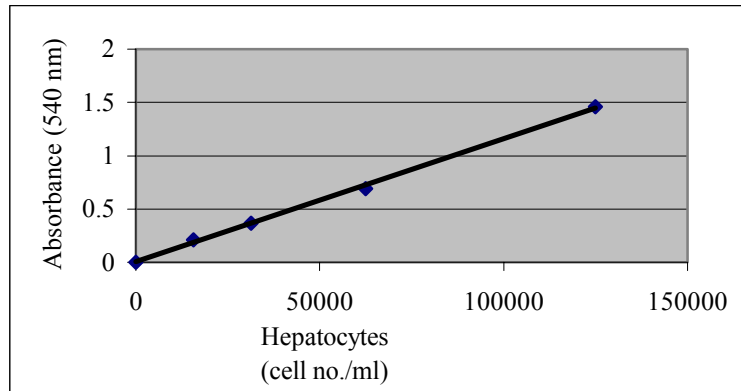


Figure B4. 5: Standard curve of isolated hepatocyte cell number vs MTT absorbance. $R^2=0.9985$.

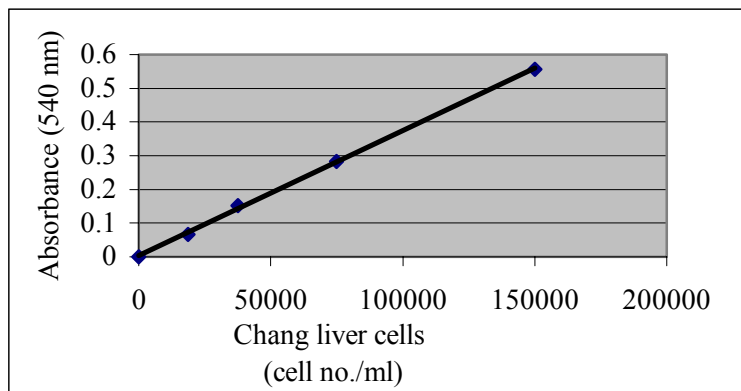


Figure B4. 6: Standard curve of Chang liver cell number vs MTT absorbance. $R^2=0.9993$.

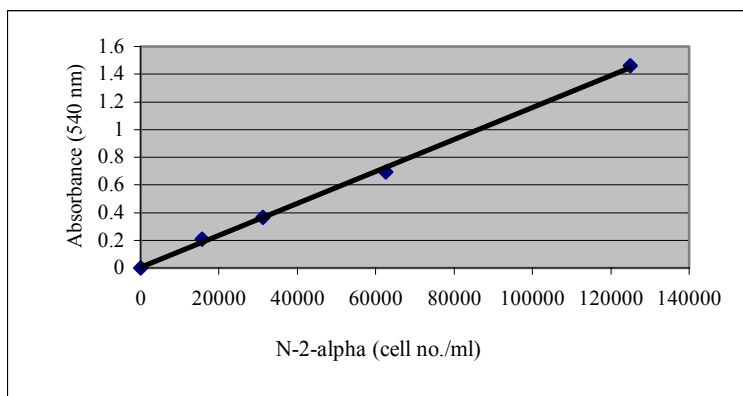


Figure B4. 7: Standard curve of N-2-alpha cell number vs MTT absorbance. $R^2=0.9985$.

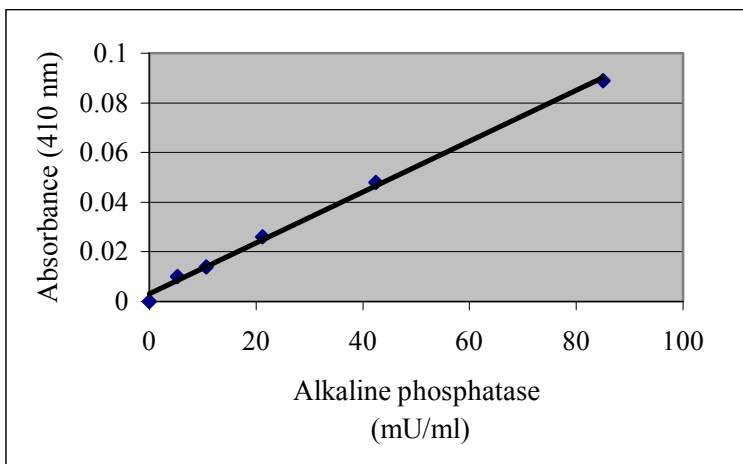


Figure B4. 8: Alkaline phosphatase standard curve (hepatotoxicity study). $R^2=0.9970$.

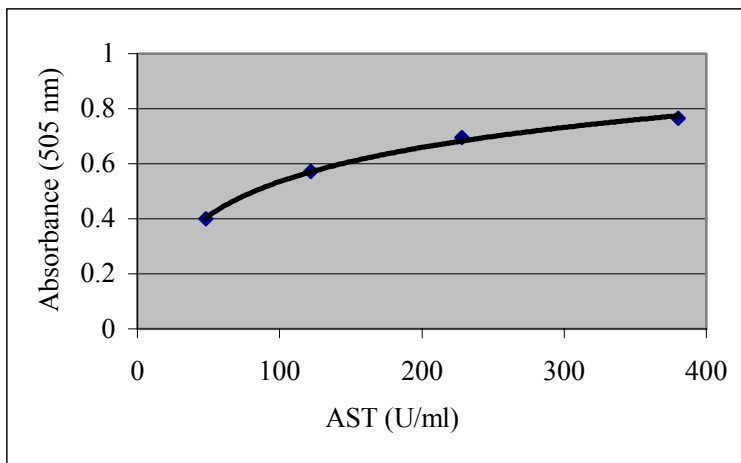


Figure B4. 9: Aspartate transaminase standard curve. $R^2=0.9968$.

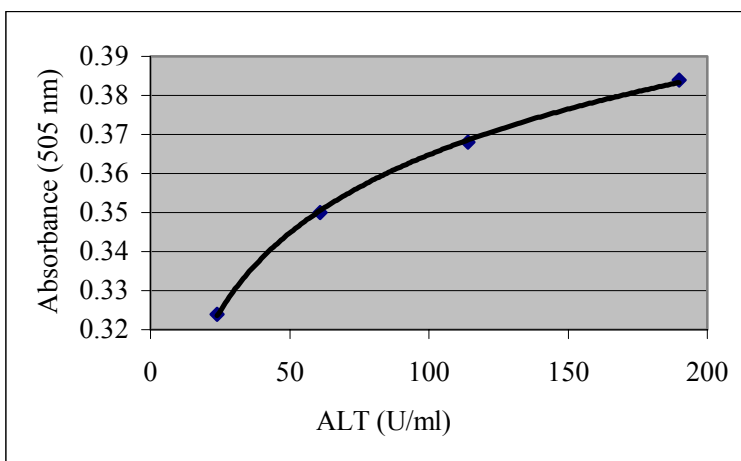


Figure B4. 10: Alanine transaminase standard curve. $R^2=0.9994$.

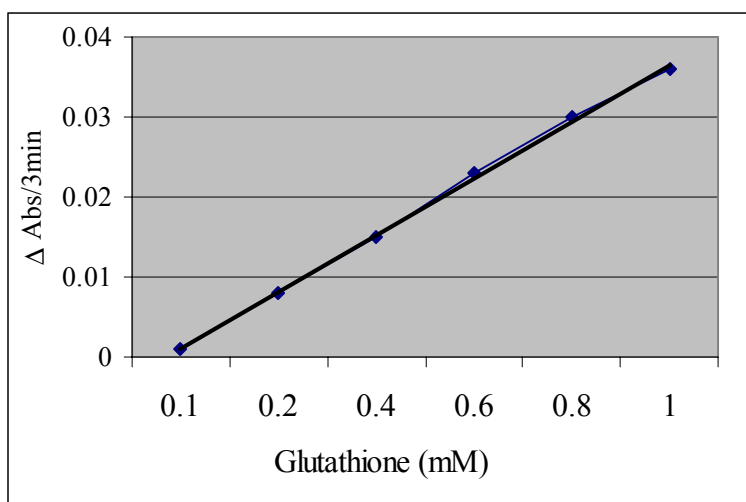


Figure B4. 11: Glutathione standard curve. $R^2=0.9988$.

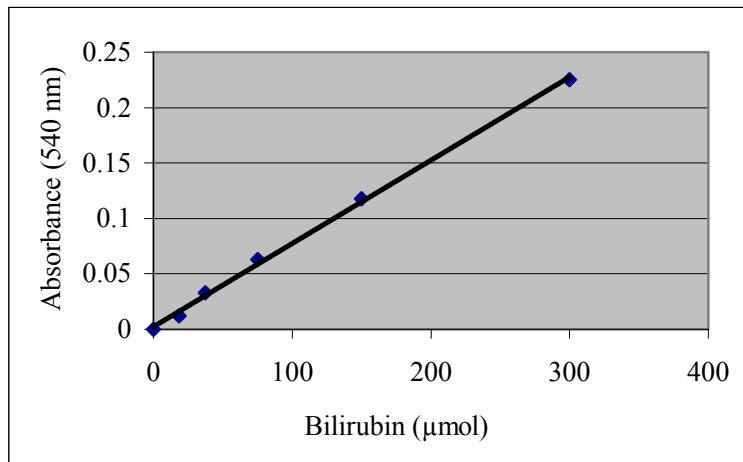


Figure B4. 12: Bilirubin standard curve. $R^2=0.9983$.

APPENDIX C
SOLUTION LIST

CHAPTER 3

Nutrient broth

31 g NB was dissolved in 1 l dH₂O. The NB was then autoclaved for 15 min to ensure sterility.

Sabouraud's broth

30 g SAB was dissolved in 1 l dH₂O and autoclaved for 15 min to sterilize the medium before use.

1 mM Phosphate-buffered saline (PBS)

8 g NaCl (Saarchem, Krugersdorp, South Africa), 0.2 g KH₂PO₄ (Protea Laboratory Services, Johannesburg, South Africa), 1.44 g Na₂HPO₄.12H₂O (Unilab Saarchem, Chamdor, Krugersdorp), 0.2 g KCl (Unilab, Saarchem, Krugersdorp), 0.2 g EDTA (BDH Chemical Ltd., Poole, England) were added to 900 ml H₂O, the pH adjusted to 7.4 and the volume was adjusted to 1 l.

0.5 mg/ml MTT solution

5 mg MTT was dissolved in 10 ml 1 mM PBS, and filtered through a 0.22 µm syringe filter unit, thereby removing any crystals from the solution.

60 mg/ml TTC solution

0.6 g TTC was dissolved in 10 ml 1 mM PBS, and filtered through a 0.22 µm syringe filter unit to sterilize the solution.

1 mg/ml XTT solution

10 mg was dissolved in 10 ml 1mM PBS. The solution was heated at 60°C for 10 min to aid dissolution of the powder. The solution was then filter sterilized, using a 0.22 µm syringe filter unit.

0.1 mg/ml Chloramphenicol

1 mg Chloramphenicol was dissolved in 10 ml NB for bacterial studies, and filter sterilized using 0.22 µm syringe filter unit.

0.25 mg/ml Amphotericin B

2.5 mg Amphotericin B was dissolved in 10 ml SAB. The solution was filter sterilized and stored at 4°C until use.

1 mg/ml Fluconazole

10 mg Fluconazole was dissolved in 10 ml SAB, filter sterilized and stored at 4°C until use.

10 mg/ml Fluconazole

0.1 g fluconazole was dissolved in 10 ml SAB and filtered through a 0.22 µm syringe filter unit.

Isomer solutions

20 mg of each isomer was dissolved in 50 µl DMSO (0.5%). The volumes were then adjusted to 10 ml with either NB for bacterial studies or 10 ml SAB for *C. albicans* studies. This represented a 2 mg/ml solution. Two fold dilutions of each isomer were then made to 1 mg/ml, 0.5 mg/ml and 0.25 mg/ml, using either NB or SAB as a diluent. The solutions were all filtered through a 0.22 µm syringe filter unit and stored at 4°C until use.

CHAPTER 4

All solutions were made with MQH₂O (MilliQ Plus Millipore, Molsheim, France).

DMEM (Dulbecco's modification of Eagles essential minimal media)

13.44 g DMEM powder was dissolved in 1 l H₂O. Once dissolved, 3.7 g NaHCO₃ (Merck, Darmstadt, Germany) was added. The media was filtered through a 0.22 µm filter (Micron Separations Inc., Elabtec, Port Elizabeth). 2 ml 1 mM sodium pyruvate and 1 ml Penicillin/Streptomycin (100X concentration) (Highveld Biological, Lyndhurst, South Africa) were added to 500 ml media.

10⁻³ M isomer solutions

2.83 mg of each isomer was diluted in 10 ml serum-supplemented DMEM. This represented a 10⁻³ M solution. A ten-fold solution was made to obtain a 10⁻⁴ M. Further dilutions were made to obtain 10⁻⁵ to 10⁻⁷ M solutions.

10⁻³ M Melphalan

3.05 mg melphalan was dissolved in 10 ml DMEM, supplemented with 10% FCS. This represented a 10⁻³ M solution. A ten-fold solution was made to obtain a 10⁻⁴ M. Further dilutions were made to obtain 10⁻⁵ to 10⁻⁷ M solutions.

0.5% MTT solution

0.05 g MTT was dissolved in 10 ml serum-free DMEM. The solution was filtered through a 0.22 µm syringe filter unit in order to remove any MTT crystals. The solution was stored in the dark at 4°C for a maximum of 2 weeks.

Alkaline phosphatase for standard

0.00179 mg alkaline phosphatase was dissolved in 1 ml H₂O; this represented 700 mU/ml. This stock solution was diluted 10X to obtain a 70 mU/ml solution. This was serially diluted to obtain the concentrations needed for the standard curve.

1 mM MgCl₂

0.10165 g MgCl₂ was dissolved in 50 ml H₂O.

Glycine Buffer

0.3754 g Glycine was dissolved in 40 ml H₂O, the pH was adjusted to 10.5 with 1 M NaOH (BDH Chemicals, Poole, England); 0.10165 g MgCl₂ and 0.6814 g ZnCl₂ were added and the volume was adjusted to 50 ml.

0.03 M pNPP

0.05565 g *p*-nitrophenylphosphate was dissolved in 5 ml H₂O

CHAPTER 5

Albumin-binding assay

Krebs-Henseleit Bicarbonate Buffer (KHBB)

6.9 g NaCl, 2.1 g NaHCO₃, 0.354 g KCl, 0.161 g KH₂PO₄, 0.291 g MgSO₄·7H₂O and 0.368 g CaCl₂·2H₂O were dissolved in 1 l H₂O.

Buffer containing isomers

10 mg of each isomer was dissolved in 10 ml KHBB containing 0.5% DMSO to facilitate dissolution of the isomers. 0.3 g bovine serum albumin (BSA) (Sigma, St. Louis, U.S.A.) was added to the buffer, constituting a 3% concentration.

10% TCA

10 g TCA was dissolved in 100 ml H₂O.

HPLC solutions

Isomer stock solutions

21.255 mg of each isomer was dissolved in 500 µl DMSO (Riedel-de Haen, Germany). The volume was adjusted to 100 ml with H₂O. A 100 x dilution of these 750 µM stock solutions were made to produce a 7.50 µM solution. Further dilutions were made to 3.75 µM, 3 µM and 1.875 µM for the standard curves.

Mobile phase

5 ml methanol (BDH Laboratory Supplies, Poole, England) and 50 μ l phosphoric acid were added to 94.95 ml MQH₂O. All solutions were degassed before being applied to the column.

Blood absorption study solutions

Saline

0.9 g NaCl was dissolved in 100 ml H₂O.

Isomer solutions

7.1 mg of each isomer was dissolved in 40 ml saline. Dissolution of each isomer was facilitated by the addition of 250 μ l glycerol. The pH was adjusted to 7.4 and the volume brought up to 50 ml. Each solution was filter sterilized through a 0.22 μ m syringe filter unit and stored at 4°C until use.

Hepatocyte isolation

10X Hanks-Hepes buffer (pH 7.4) (HH)

80 g NaCl, 0.6 g KH₂PO₄, 1.2 g Na₂HPO₄·7H₂O, 4 g KCl, 47.6 g HEPES (*N*-2-Hydroxyethylpiperazine-*N'*-2-ethanesulfonic acid) (Sigma, St. Louis, U.S.A.), 0.1 g phenol red (Sigma, St. Louis, U.S.A.) and 4 g NaOH were added to 900 ml H₂O, the pH adjusted to 7.4 and the volume brought up to 1 l.

1X HH buffer

The 10X HH buffer was diluted 1:10 with H₂O in 500 ml aliquots. The buffer was sterilized by autoclaving and stored at 4°C until use.

25 mM EGTA solution

0.48 g EGTA, dissolved in 25 ml 1x HH buffer was mixed with 2.5 ml 1 M NaOH. The volume was brought up to 50 ml with 1X HH buffer, filter sterilized through a 0.22 μ m syringe filter unit and stored at 4°C until use.

250 mM CaCl₂ solution

1.84 g dihydrate CaCl_2 was dissolved in 50 ml H_2O , filter sterilized through a 0.22 μm syringe filter unit and stored at 4°C until use.

MBG solution

3.1 g NaHCO_3 , 2.5 g glucose and 0.75 g methionine (Sigma, St. Louis) were dissolved in 50 ml H_2O . The solution was filter sterilized and stored in 10 ml aliquots at -20°C.

10X Hanks Balanced Salt Solution (HBSS)

0.8g NaCl , 0.4 g KCl , 0.06 g KH_2PO_4 , 0.06 g $\text{Na}_2\text{HPO}_4 \cdot 12\text{H}_2\text{O}$ and 1 g glucose were dissolved in 10 ml H_2O , filter sterilized and stored at -20°C until use.

Percoll

Percoll was dissolved in 10X HBSS at a ratio of 9:1, filter sterilized and stored in 5 ml aliquots at 4°C.

Perfusion buffer

10 ml MBG solution was added to 500 ml 1X HH under sterile conditions.

Perfusion buffer containing EGTA

2 ml EGTA solution was added to 100 ml perfusion buffer

Collagenase-containing perfusion buffer

10 000 units (17 mg) Collagenase Type IV and 2 ml CaCl_2 solution were dissolved in 100 ml perfusion buffer.

Hams F-12 medium

10.69 g Hams F-12 (Highveld Biological, Lyndhurst, South Africa) and 1.18 g NaHCO_3 were dissolved in 1 l H_2O . The media was filtered through a 0.22 μm filter.

Serum-supplemented culture medium

100 ml Hams F-12 medium was supplemented with 2 ml newborn calf serum (NCS), 0.2 g BSA (Sigma, St. Louis), 60 mg/l Benzyl-Penicillin and 100 mg/l Streptomycin (100X concentration) and 18.0 mg glucose (1 mM). The media was filtered through a 0.22 µm filter.

Hormone-supplemented culture medium

A 1 µM stock solution of dexamethasone was made by dissolving 39.25 ng dexamethasone in 100 ml Hams F-12 medium. 1 ml of this stock solution was dissolved in 99 ml Hams F-12 medium, constituting a final dexamethasone concentration of 1×10^{-8} M. The media was filtered through a 0.22 µm filter.

Trypan blue solution

Trypan blue stock solution

400 mg trypan blue (Gürr Microscopy Materials, BDH Chemical, Poole, England) was dissolved in 90 ml 1 mM PBS.

Working trypan blue solution

1 ml trypan blue stock solution was diluted with 4 ml PBS.

200 µM isomer solutions

0.5686 mg of each isomer was dissolved in 50 µl glycerol. The volume was brought up to 10 ml with either Hams F-12 or DMEM. The solutions were filter sterilized through a 0.22 µm syringe filter and stored at 4 °C until use.

1 mg/ml Isoniazid solution

10 mg isoniazid was dissolved in 10 ml Hams F-12 or DMEM containing 50 µl glycerol. The solution was filter sterilized and stored at 4°C until use.

Solutions for albumin assay

Stock succinate buffer (0.1 M, pH 4.0)

11 g succinic acid (Saarchem, Krugersdorp) was dissolved in 800 ml H₂O. The pH was adjusted to 4.0 with approximately 20 ml 10% NaOH and the volume was adjusted to 1 l. The solution was stored at 4°C until use.

Stock bromocresol green (0.6 mM)

419 mg bromocresol green (Riedel de-Haen, Germany) was dissolved in 10 ml 0.1 N NaOH. The solution was then diluted to 1 l and stored at 4°C until use.

Working reagent

1 volume of stock bromocresol green solution was mixed with 3 volumes of succinate buffer. 1.4 ml 30% Brij-35 solution (Sigma, St. Louis, U.S.A.) was added and the pH was adjusted to 4.2. The solution was stored at 4°C until use.

Albumin standards

10g of albumin was dissolved in a solution containing 0.9 g NaCl and 0.05 g sodium azide (Riedel de-Haen, Germany) per 100 ml H₂O. The albumin was dissolved and allowed to stand at 4°C until dissolved. Occasionally, the dissolution of albumin was aided by swirling, while excess foaming was avoided. Serial dilutions to 5, 4 and 3 g/100 ml of albumin were then prepared.

Solutions for urease assay

Alkaline hypochlorite

12.5 g NaOH was dissolved in 400 ml H₂O and allowed to cool. 20 ml commercial sodium hypochlorite solution (Dyna Chemicals, Port Elizabeth, South Africa) was added and the volume brought up to 500 ml. The solution was stored at 4°C until use.

Phenol reagent

25 g phenol (BDH Chemical Ltd., Poole, England) and 0.13 g sodium nitroprusside (Riedel de-Haen, Germany) was dissolved in 500 ml H₂O. The solution was stored in a brown bottle at 4°C until use.

Buffer

5 g EDTA was dissolved in 200 ml glycerin (Merck, Darmstadt). 250 ml H₂O was added and the pH was adjusted to 6.5 with approximately 10 ml 4% NaOH. The volume of the solution was then adjusted to 500 ml.

Buffered urease

30 mg urease (Miles Laboratory, Pty.) was dissolved in 100 ml of buffer. The solution was stored at 4°C until use.

Benzoic acid solution

2 g benzoic acid (Hopkin and Williams, AnalR, England, Essex) was dissolved in 1 l H₂O, to which 0.8 ml conc. H₂SO₄ (Merck, Darmstadt) was added.

Standard urease solutions

0.644 g urea (Riedel de-Haen, Germany) was dissolved in 500 ml benzoic acid solution. This represented a 60 mg/ml urea nitrogen solution.

Materials for bilirubin assay

Bilirubin standard

0.0087 g bilirubin (Sigma, St. Louis, U.S.A.) was dissolved in 4% NaOH. The solution was transferred to a volumetric flask and diluted to 100 ml with FCS diluent. This solution was serially diluted with serum diluent to make up the different concentrations for the standard curve.

Serum diluent

1 ml FCS was dissolved in a 0.85 % NaCl solution.

Diazo reagent

A. 10% NaNO₂ stock

10 g NaNO₂ (NT Laboratory Supplies, Johannesburg) was dissolved in 100 ml H₂O and stored at 4°C.

B. Working solution of NaNO₂

0.5 ml solution A was dissolved in 0.9 ml H₂O.

C. Sulfanilic acid (M & B Laboratory Chemicals, Dagenham, England)

1 g sulfanilic acid was dissolved in 15 ml conc HCl (Merck, Darmstadt), and diluted to 1 l with H₂O.

Diazo reagent = 5 ml C + 0.15 ml B. This reagent was prepared fresh for each experiment.

Materials for ALT and AST assays

0.1 M Phosphate buffer (pH 7.4)

420 ml 0.1 M disodiumphosphate solution (Unilab Saarchem, Chamdor, Krugersdorp) was mixed with 80 ml potassium dihydrogen phosphate solution.

(7.098g disodium phosphate was dissolved in 500 ml H₂O (pH 7.4); 1.316g potassium dihydrogen phosphate was dissolved in 100 ml H₂O (pH 7.4)).

ALT substrate (pH 7.4)

1 N NaOH was added to 0.0292 g α -ketoglutaric acid (Boehringer Mannheim, Germany) and 1.78 g DL-alanine (Sigma, St. Louis, U.S.A.) to effect solution. The pH was adjusted to pH 7.4 with 1 N HCl. The solution was transferred to a 100 ml volumetric flask and diluted to 100 ml with the phosphate buffer.

AST substrate (pH 7.4)

1 N NaOH was added to 0.0292g α -ketoglutaric acid (Boehringer Mannheim, Germany) and 2.66 g DL-aspartatic acid (BDH Chemicals, Poole, England) to effect solution. The pH was adjusted to pH 7.4 with 1 N HCl. The solution was transferred to a 100 ml volumetric flask and diluted to 100 ml with phosphate buffer.

2,4-Dinitrophenylhydrazine solution

0.0198 g dinitrophenylhydrazine was dissolved in 100 ml 1 N HCl. The solution was stored in the fridge.

0.4 N NaOH

16 g NaOH pellets was dissolved in 1 l H₂O.

Materials for Ca²⁺-assay

Calcium reagent working solution

1 part calcium binding reagent (Sigma, St. Louis, U.S.A.) was combined with 1 part calcium buffer (Sigma, St. Louis, U.S.A.).

10 g/l Ca²⁺-standard

10 g CaCl₂ was dissolved in 1 l MQH₂O.

Material for LDH assay

LDH reagent

LDH reagent (Sigma, St. Louis, U.S.A.) was reconstituted with 20 ml MQH₂O, and used within 2 weeks.

Solutions for Lipid peroxidation

0.15 M KCl solution

5.591 g KCl was dissolved in 500 ml H₂O.

1% H₃PO₄

1 ml H₃PO₄ (B. Owen Jones, Johannesburg, South Africa) was dissolved in 99 ml H₂O, producing a 1% solution.

0.6% aqueous TBA solution

0.6 g TBA was dissolved in 100 ml H₂O by boiling until dissolved.

Solutions for Glutathione assay

HBSS (pH 7.4)

0.14 g CaCl₂ (anhydrous), 0.4 g KCl, 0.06 g KH₂PO₄, 0.1 g MgSO₄·7H₂O, 8 g NaCl, 0.35 g NaHCO₃, 0.09 g Na₂HPO₄·7H₂O and 1 g Glucose were dissolved in 800 ml H₂O. The pH was adjusted to 7.4 with HCl. The volume was then brought up to 1 l.

Reduced Glutathione solution

0.0307 g reduced glutathione (Sigma, St. Louis, U.S.A.) was dissolved in 10 ml H₂O. 0.5 ml of this stock solution was then dissolved in 4.5 ml H₂O, producing a 1 mM solution. This 1 mM solution was further diluted, producing different concentrations for the standard curve.

DTNB solution

0.0396 g 5,5'-dithio-bis(2-nitrobenzoic acid) (DTNB) (Sigma, St. Louis, U.S.A.) was dissolved in 10 ml DMSO, producing a stock solution of 10 mM. For the assay, 7.5 ml DMSO was added to 0.5 ml stock DTNB solution, resulting in a 0.625 mM solution.

CHAPTER 6

Platelet count

Buffer A

0.2118 g NaCl, 9.32 mg KCl, 0.0596 g HEPES, 0.0267 g Na₂HPO₄·12H₂O and 0.05 g BSA were dissolved in 25 ml dH₂O.

Buffer B

To 25 ml Buffer A, 0.0208 g CaCl₂ and 0.0226 g MgSO₄·7H₂O were added.

Aggregation - Thrombin assay

Thrombin solutions

30 μl of a 50 U/ml stock was diluted to 370 μl with buffer A. This represented a 3.75 U/ml solution. Dilutions were then made to obtain the other concentrations used, i.e. 3 U/ml, 2.25 U/ml and 1.5 U/ml.

3 mM Isomer solutions

8.5 mg of each isomer was dissolved in 50 μl DMSO, to aid dissolution of the isomers. The volume was then adjusted to 10 ml with buffer A. Dilutions of cyclo(L-Trp-D-Pro) were made to 1.5 mM, 0.75 mM and 0.375 mM.

Aggregation - ADP assay

ADP solutions

0.2356 g ADP was dissolved in 10 ml dH_2O , representing a 50 mM stock solution. A 1000 times dilution of this stock was made to produce a 50 μM solution. Dilutions of this 50 μM stock solution were made to obtain 25 μM , 15 μM , 10 μM , and 5 μM solutions.

1 mg/ml Isomer solutions

In order to obtain a final concentration of 1 mg/ml isomer in the well, a 12x stock solution of each isomer was made as follows: 33.96 mg of each isomer was dissolved in 50 μl DMSO, to aid dissolution of the isomers. The volume was then adjusted to 10 ml with dH_2O . Dilutions of these solutions were made to 6 mg/ml, 3 mg/ml and 1.5 mg/ml. These dilutions represented 0.5 mg/ml, 0.25 mg/ml and 0.125 mg/ml final concentrations (respectively) in the wells.

Thrombin assay

Buffer (pH 8.4)

0.3025 g Tris was dissolved in 40 ml dH_2O . The pH was adjusted to 8.4 with 1 N HCL, after which the volume was adjusted to 50 ml. 0.108 g EDTA and 0.511 g NaCl was then dissolved in the Tris-HCl solution.

0.456 mM S2238

5.712 mg S2238 was dissolved in 20 ml buffer (pH 8.4).

Thrombin solutions

32 μ l of a 50 U/ml thrombin stock was diluted to 80 μ l in buffer (pH 8.4), representing a 40 U/ml solution. This solution was double diluted to obtain a 20 U/ml solution. 12 μ l of the stock was diluted to 40 μ l in order to obtain a 30 U/ml solution. The 50 U/ml solution was diluted 5 times to obtain a 10 U/ml solution.

Isomer solutions

8.5 mg of each isomer was dissolved in 50 μ l DMSO, to aid dissolution of the isomers. The volume was then adjusted to 10 ml with buffer (pH 8.4). This represented a 3 mM solution. 4 ml of this stock was then diluted to 6 ml, to obtain a 2 mM solution. This solution was then double diluted to obtain 1 mM, 0.5 mM, 0.25 mM and 0.125 mM, using buffer (pH 8.4).

Platelet adhesion assay

0.1 M Citrate buffer (pH 5.4)

2.1014 g citric acid was dissolved in 100 ml H₂O. 7.1628 g Na₂HPO₄·12H₂O was dissolved in 100 ml H₂O. 44.7 ml of citric acid solution was added to 50 ml sodium phosphate solution. The pH was adjusted to 5.4, after which the volume was adjusted to 100 ml with the sodium phosphate solution.

0.1 M citrate buffer, 5 mM pNPP, 0.1% Triton X-100

0.1855 g pNPP and 100 μ l Triton X-100 was dissolved in 100 ml citrate buffer (pH 5.4).

2 N NaOH

1.6 g NaOH was dissolved in 20 ml H₂O.

ADP solutions

0.342 mg ADP was dissolved in 4 ml buffer B, representing a 100 μM solution. This solution was then double diluted to obtain 50 μM , 25 μM and 12.5 μM .

Thrombin solutions

100 μl of the 50 U/ml stock solution was dissolved in 1.9 ml buffer B. This represented a 2.5 U/ml solution. This solution was then double diluted to 1.25 U/ml, 0.625 U/ml and 0.3125 U/ml.

Isomer solutions

11.34 mg of each isomer was dissolved in 50 μl DMSO. The volumes were then adjusted to 10 ml with buffer A. This solution was then double diluted to 2 mM, 1 mM, 0.5 mM and 0.5 mM.

CHAPTER 7

Whole-cell patch-clamp technique

Ca²⁺-channel studies

Resuspension buffer

16.698 g Tris, 3.368 g CsCl, 0.0476 g MgCl₂, 2.383 g HEPES-NaOH, 0.794 g CaCl₂ and 0.901 g glucose were dissolved in 900 ml H₂O. The pH was adjusted to 7.2 with HCl, after which the volume was adjusted to 1 l.

Pipette solution

21.050 g CsCl, 0.190 g MgCl₂, 1.902 g EGTA, 2.383 g HEPES, 0.147 g CaCl₂, 1.802 g glucose and 1.522 g Mg-ATP were dissolved in 900 ml H₂O. The pH was adjusted to 7.2 with HCl, after which the volume was adjusted to 1 l.

K⁺-channel studies

Resuspension buffer

7.597 g NaCl, 0.298 g KCl, 0.095 g MgCl₂, 2.383 g HEPES-NaOH, 0.265 g CaCl₂ and 1.802 g glucose were dissolved in 900 ml H₂O. The pH was adjusted to 7.2 with KOH, after which the volume was adjusted to 1 l.

Pipette solution

10.437 g KCl, 0.1904 g MgCl₂, 4.184 g EGTA, 2.383 g HEPES, 0.147 g CaCl₂, 1.802 g glucose and 2.756 g Na₂-ATP were dissolved in 900 ml H₂O. The pH was adjusted to 7.2 with HCl, after which the volume was adjusted to 1 l.

100 μM solution of isomers (pH 7.4)

1.417 mg of each isomer was dissolved in 25-50 μl DMSO with heating. Once dissolved, it was introduced into the resuspension buffer (pH 7.2) of each respective study.

Langendorff perfusion buffers

Krebs-Henseleit Bicarbonate Buffer (KHBB)-low K⁺-concentration

6.9 g NaCl, 2.1 g NaHCO₃, 0.158 g KCl, 0.161 g KH₂PO₄, 0.291 g MgSO₄·7H₂O and 0.368 g CaCl₂·2H₂O were dissolved in 1 l H₂O.

Control perfusion buffer

1.25 ml DMSO was dissolved in 248.75 ml KHBB. For each experiment, the control solutions were made up in KHBB containing the normal K⁺-concentration, as well as KHBB containing the lower K⁺-concentration.

200 μM isomer solutions for heart studies

14.15 mg of each isomer was dissolved in 1.25 ml DMSO, after which the volume was adjusted to 250 ml with KHBB. For each experiment, the isomer solutions were made up in KHBB containing the normal K⁺-concentration, as well as KHBB containing the lower K⁺-concentration.

APPENDIX D

HUMAN ETHICS LETTER OF APPROVAL



Universiteit van Port Elizabeth
University of Port Elizabeth

HUMAN ETHICS COMMITTEE

3 December 2001

Dr C Frost
Biochemistry and Microbiology Department

Dear Dr Frost

PROPOSAL FOR APPROVAL

Your proposal entitled "Screening and Investigating Potential antithrombotic compounds" was circulated to all members of the Human Ethics Committee. The proposal was accepted, but with some concerns being expressed about voluntary participation by subjects used in this investigation. These comments have been given to you personally.

We wish you well with this project. We have informed the Research Office of these findings as well.

A handwritten signature in black ink, appearing to read "Isobel Lemmer".

ISOBEL LEMMER
SECRETARY

Cc: Prof B Robertson, Director, Research Office UPE

APPENDIX E

ARTICLES THAT HAVE BEEN SUBMITTED FOR PUBLICATION

Article 1

Title : The effect of the isomers of cyclo(Trp-Pro) on heart and ion channel activity

¹Hajierah Jamie, ¹Gareth Kilian, ²Karin Dyason, ¹*Pieter J. Milne

¹Cyclic Dipeptide Research Unit, Department of Pharmacy, Box 1600, University of Port Elizabeth, Port Elizabeth, 6000, South Africa

²Department of Physiology, Potchefstroom University of C.H.E., Potchefstroom, 2520, South Africa

*Author for correspondence:

E-mail : pmapjm@upe.ac.za

Short title Heart and ion channel activity of cyclo(Trp-Pro)

Summary

Cyclo(L-Trp-L-Pro) has shown potential for use in the treatment of cardiovascular dysfunction. The aim of the study was to determine the effects of the isomers of cyclo(Trp-Pro) (cyclo(L-Trp-L-Pro), cyclo(L-Trp-D-Pro), cyclo(D-Trp-L-Pro) and cyclo(D-Trp-D-Pro)) on heart and ion channel activity. The effects on L-type Ca^{2+} channel and inward rectifier K^+ channel activity were determined by using the whole-cell patch-clamp technique on myocytes of guinea-pig origin. Dependence on the membrane potential in terms of Ca^{2+} channel activity was also investigated. A modified Langendorff method was used to determine the effects of the isomers on heart rate, coronary flow, duration of ventricular tachycardia and arrhythmia, time to sinus rhythm, and QRS interval on the isolated rat heart. 100 μM Cyclo(L-Trp-L-Pro), cyclo(L-Trp-D-Pro) and cyclo(D-Trp-D-Pro) showed antagonism towards Ca^{2+} channel activity, while cyclo(D-Trp-L-Pro) caused a blockage of the current. The action of cyclo(D-Trp-L-Pro) was shown to be dependent on membrane potential. No significant effect ($p > 0.05$) on the inward rectifier K^+ current was observed in the presence of the isomers. A positive chronotropic effect was observed in the presence of 200 μM cyclo(L-Trp-D-Pro) ($p = 0.004$), while negative chronotropic action was observed in the presence of cyclo(D-Trp-L-Pro) ($p = 0.0238$). 200 μM Cyclo(L-Trp-D-Pro) and cyclo(D-Trp-L-Pro) significantly increased ($p = 0.0296$, $p = 0.0071$, respectively) the coronary flow rate in rat heart. All isomers significantly reduced the duration of ventricular tachycardia and arrhythmia, as well as the time to sinus rhythm. Furthermore, no change in the QRS intervals was noted in the presence of the isomers. The isomers thus show antiarrhythmic potential and may manifest as novel agents in the treatment of cardiovascular dysfunction.

Introduction

Despite intensive research, ischaemic heart disease remains a serious problem. Death and cardiac arrhythmias are often associated, particularly ventricular fibrillation (VF), which may be initiated by ischaemia and reperfusion. Antiarrhythmic agents devoid of serious side effects are thus needed. Rational treatment of cardiac arrhythmias is therefore in need of an absolute understanding of pharmacokinetic and pharmacodynamic properties of potential cardiac disease agents (Hashimoto *et al.*, 1986). These drugs may be developed rationally by drug design in terms of high selective cellular action. This, however, needs prior knowledge that the selective action is beneficial in antiarrhythmic activity (Rees and Curtis, 1993). Screening of antiarrhythmic agents for anti-ventricular fibrillation activity is important since VF is a major cause of death in acute myocardial infarction.

The therapeutic effectiveness of L-type Ca^{2+} -channel antagonists in cardiovascular pathologies is based on the inhibition of Ca^{2+} -influx in depolarized smooth muscle (Godfraind and Govoni, 1995). Ca^{2+} -channel antagonists are known to exhibit antiarrhythmic activity, negative inotropic effects, inhibit heart rate, and show relative vasodilatory activity.

K^{+} channels are also the target in the treatment of various disease states such as non-insulin dependent diabetes mellitus, asthma and cardiac arrhythmias (Sensch *et al.*, 2000). K^{+} channel blockers (Class III antiarrhythmia drugs) are useful in the treatment of cardiac arrhythmias (Dupuis and Adamantidis, 1995). The cell can be driven into a resting state by repolarizing currents that are generated by the opening of voltage-gated K^{+} channels under normal conditions. These drugs prolong the repolarization phase (Godfraind and Govoni, 1995).

Research in our laboratories have shown the potential of the cyclic dipeptide cyclo(Trp-Pro) as an antimicrobial substance, as well as potential usage in the treatment of cardiovascular dysfunction (Milne *et al.*, 1998). Investigation of the activities of the isomers may result in the formulation of a drug entity with greater activity and/or

specificity than the L-form, or as the case may be, the isomers may show reduced or no activity at all.

In this study, we determined the effect of the isomers on inward rectifier K^+ current and Ca^{2+} channel activity using the whole-cell patch-clamp technique on ventricular myocytes isolated from the guinea-pig. A modified Langendorff method was used to determine the effects of the isomers on heart rate and coronary flow in the isolated, perfused rat heart. The time to stop ischaemia-induced arrhythmias and ventricular tachycardia, as well as the time taken for the heart rate to return to normal sinus rhythm was also determined. The ECG was examined to determine effects of the isomers on the QRS complex.

Methods

Isomer solutions

The method of Grant *et al.* (1999) was used to synthesize the isomers of cyclo(Trp-Pro). The isomers ($M_r = 284$) were stored at 4°C until use. All compounds used were of analytical grade. The isomers were dissolved in 0.5% dimethylsulfoxide (DMSO), to aid dissolution of the isomers.

Whole-cell patch-clamp method

Ca²⁺ channel activity

The whole-cell patch-clamp technique was performed on excitable, ventricular cells, isolated from guinea pigs, as described previously (Hamil *et al.*, 1981), to determine the effects of the compounds on Ca^{2+} channel activity. The cells were exposed to 100 μ M solutions (pH 7.4) of the respective isomers. Two protocols were used. In the first protocol (A), the inward Ca^{2+} currents were recorded after changing the holding potential of -90 mV to different test potentials for 100 ms (-50 to +20 mV in 5 mV steps every 6 secs). Inward Ca^{2+} currents were recorded at a holding potential of -45 mV for the second protocol (B). The aim of the two protocols was to determine if the effect of the isomers on the Ca^{2+} channel was voltage-dependent or not.

Potassium channel activity

The whole-cell patch-clamp technique was used to record inward rectifier K⁺ currents under voltage clamp conditions from single cells isolated with enzymatic dispersion from the ventricles of guinea pig, as described for the Ca²⁺ channel activities. The cells were then exposed to 100 μM solutions (pH 7.4) of the respective compounds. Currents were recorded during 500 ms hyperpolarizing steps from a holding potential of –80 mV to different potentials between –140 mV and –50 mV.

Isolated heart perfusion

A modified Langendorff method was used to study the effects of the isomers on heart rate, coronary flow and reperfusion-induced arrhythmias in rat hearts (Langendorff, 1895). Male Long Evans rats (250 – 350g) were placed under light ether anesthesia to a loss of blink and pain reflexes. Once removed, the hearts were arrested in ice-cold Krebs Henseleit Bicarbonate Buffer (KHBB) (pH 7.4). The heart was perfused via an aortic cannula. Occlusion was achieved by using a silk suture (Clinisut, South Africa) and a rigid polyvinyl occluder (5 mm x 1 mm). Successful occlusions were characterized by a 50% decrease in coronary flow rate. Reperfusion of the infarcted area of the left ventricle occurred once the tension on the occluder was removed. Acceptable reperfusion was characterized by a 90% increase in coronary flow rate.

After a 15 min stabilization period, the isomer solution (200 μM isomer dissolved in 0.5% glycerol) was perfused into the heart for 15 min. During this period, the heart rate and coronary flow were monitored every 5 min. Following this, the perfusion buffer was changed to a KHBB containing a lower concentration of K⁺ (3.3 mM). At the same time, the left descending coronary artery was occluded for a period of 10 min, allowing for the development of ischaemia. The occluder was then released and the heart reperfused with the low K⁺-containing KHBB and respective isomer. Control samples were perfused with KHBB containing 0.5 % DMSO.

A summary of the experimental protocol is set out in Figure 1.

Measurement of ventricular tachycardia and arrhythmia, time to sinus rhythm and QRS interval

ECGs recorded on PolyView Data Acquisition and Analysis System (Version 2.0, 1997) were examined for duration of VT and VA, time to SR, as well as duration of QRS complexes. The QRS complexes were measured by manual positioning of the screen markers. At least four complexes were measured and averaged at each time point.

Statistical analysis

The values of parameters measured are presented as mean \pm s.d. for the indicated number of experiments. Results were analysed using the software package GraphPad Prism Version 2.0 and GraphPad InStat (GraphPad Software, Inc., San Diego, U.S.A.). All tests were performed on raw data obtained from the experiments (n=6). The effect of a single qualitative factor on a single response variable was determined by univariate ANOVA using the Mann-Whitney test. *P* values <0.05 were accepted as evidence of a statistically significant difference.

Results and Discussions

Whole-cell patch-clamp method

Ca²⁺ channel activity

In recent years, there has been increased favour in the use of Ca²⁺ antagonists in the treatment of cardiovascular disorders, such as cardiac arrhythmias. Their use is largely based on the disruption of voltage-dependent Ca²⁺ channels in both the cardiac muscle and vascular smooth muscle (Dong *et al.*, 1993). Some substances that inhibit Ca²⁺ channels may have a lowered negative inotropic effect, possibly as a result of influences on other ion channels (Sensch *et al.*, 2000). For this reason, the effect of the isomers on inward rectifying K⁺ channels was also determined.

On exposure to 100 μ M cyclo(L-Trp-L-Pro) to the isolated guinea-pig myocyte, an increased current was observed after a 1 min exposure period in protocol A, with maximal effects noted after a 5 min exposure period (Figure 2 I a). The effect was not completely reversible, since the current did not return to the control current value after

either the 1 min or 7 min washout period. The maximal increase for the 1 min exposure was 22 %, while a 77% increase in current was noted for the 5 min exposure.

Determination of the dependence on voltage was determined by using protocol B. When a holding potential of -45 mV was applied to the cells, the peak inward current decreased (Figure 2 I b). After the 1 min washout period, it was noted that the effect was not totally reversible, as the currents did not return to that of the control value.

It is interesting to note that with protocol B (Figure 2 I b), antagonism is noted (blockage of peak inward current), whereas with protocol A (Figure 2 I a) agonism of the Ca^{2+} channel activity is noted. This suggests that the effect of the compound on the cell is dependent on membrane potential.

When $100 \mu\text{M}$ cyclo(L-Trp-D-Pro) was applied to the cell using protocol A (Figure 2 II a), the current was increased in the presence of the compound by 90%, with the maximal effect being noted after 5 min (a 92% increase in the peak inward current). The effect was almost completely reversible.

Using protocol B (Figure 2 II b), a decrease in the peak inward current after both a 1 min and 5 min exposure period to cyclo(L-Trp-D-Pro) was observed. After approximately 8 ms, a 55% blockage (1 min exposure) and 86% blockage (5 min exposure) was noted. The effect was not completely reversible after a 4 min washout period. Once again, it is seen that for protocol A, the compound is agonistic, while in protocol B, an antagonistic effect is observed, suggesting that the effect of the drug on the Ca^{2+} channel is dependent on the membrane potential.

On application of $100 \mu\text{M}$ cyclo(D-Trp-L-Pro) to the cell (Figure 2 III a), a blockage in the peak inward current was observed, with a maximal effect after 5 min. For the 1 min exposure, blockages of 23% and 25 % were noted for control 1 and control 2, respectively. Blockages of 32% and 34%, respectively, were noted for the 5 min exposure period. Similarly, a decrease in the current was also noted for protocol B (Figure 2 III b).

For both protocols A and B, the effects were not reversible, since the washout currents did not return to that of the controls. Unlike cyclo(L-Trp-L-Pro) and cyclo(L-Trp-D-Pro), it appears that the effect of cyclo(D-Trp-L-Pro) is independent of membrane potential, since antagonism of the Ca²⁺ channels was noted for both protocol A and B.

A slight increase (17%) in the peak inward was observed after a 1 min exposure period to cyclo(D-Trp-D-Pro) (Figure 2 IV a). The effect was not reversible although the current moved in the direction of the control current. At a holding potential of -45 mV (Figure 2 IV b) (protocol B), the current increased slightly (10%) after 1 min, but decreased by 24% in relation to the control current value after a 5 min exposure period. The effect was not completely reversible after a 5 min washout period.

In a previous study, the effect of cyclo(Trp-Pro) on Ca²⁺ channel activity was determined and it was found that this compound resulted in a 45% blockage of the inward Ca²⁺ current after 1 min exposure. This was increased to 50% after a 3 min exposure. Furthermore, cyclo(Trp-Trp) showed antagonistic activity towards Ca²⁺ channel activity, with a 45% blockage after 1 min exposure to 100 µM solution of the dipeptide. This blockage increased by 2% to 47% after a 3 min exposure and was found to be faster acting than cyclo(L-Trp-L-Pro) (Milne *et al.*, 1998).

Potassium channel activity

Two control currents (A and B) were recorded for K⁺ channel activity (Figure 3 I) to ensure that a stable current amplitude was achieved before applying the 100 µM cyclo(L-Trp-L-Pro) to the cell. After 1 min and 3 min exposure periods, an insignificant decrease ($p > 0.05$) in the inward current was observed. The effect was totally reversible, with the current returning to both control A and B value after a 3 min washout period.

Testing of the effects of cyclo(L-Pro-D-Trp) on the K⁺-channel (Figure 3 II) for both a 1 min and 3 min exposure period showed an insignificant effect on the inward rectifier K⁺ channel. A 3 min washout period returned the current to that of the control current. The inward rectifier K⁺ current was decreased between -140 mV and -120 mV after a 3 min

exposure to cyclo(D-Trp-L-Pro) (Figure 3 III). However, the effect was almost completely reversible, as the current almost returned to that of the control current after a 3 min washout period. No significant effect on the inward rectifier K^+ channels was noted after a 3 min exposure period to 100 μ M cyclo(D-Trp-D-Pro) (Figure 3 IV), since the currents for the 1 min and 3 min exposure period did not deviate from the control current.

The effects of the isomers on Ca^{2+} channel and K^+ channel activity are summarized in Table 1.

The initial study on the effects of cyclo(Trp-Pro), cyclo(Tyr-Pro), cyclo(Phe-Pro) and cyclo(Trp-Trp) on K^+ channel activity was conducted by Milne *et al.* (1998). They found that cyclo(Trp-Pro) and cyclo(Tyr-Pro) inhibited the delayed-rectifier K^+ channels, with cyclo(Tyr-Pro) exhibiting a greater effect (65% as opposed to 38% after a 2 min exposure period). Cyclo(Trp-Trp) and cyclo(Phe-Pro) had no effect on the current. It was further concluded that these compounds did not affect other K^+ channels, such as the inward rectifier current (Milne *et al.*, 1998). This statement supports results obtained in the present study.

Heart rate

As a result of the agonistic effect of cyclo(L-Trp-L-Pro), cyclo(L-Trp-D-Pro) and cyclo(D-Trp-D-Pro) on Ca^{2+} channel activity, the effect on the heart rate was investigated, as it was suggested that these agonists would possess positive chronotropic activity i.e. cause an increase in heart rate. On the other hand, due to the antagonistic effect of the DL isomer on Ca^{2+} channel activity, it was expected that it would possess negative chronotropic activity i.e. result in a decreased heart rate. In addition, an increase in the coronary flow is expected with the application of cyclo(D-Trp-L-Pro) (Cook, 1998).

There was a slight decrease in heart rate in the control sample (Figure 4), which is to be expected, since experimental conditions are not ideal. Cyclo(L-Trp-L-Pro) and cyclo(D-Trp-D-Pro) did not show any significant difference in heart rate when compared to the

control ($p=0.1$) whereas cyclo(L-Trp-D-Pro) significantly increased the heart rate in relation to the control ($p= 0.004$). As expected, cyclo(D-Trp-L-Pro) decreased the heart rate ($p=0.0238$).

Coronary flow

During all experiments, coronary flow rates were determined. Common to all Ca^{2+} antagonists is dilation of coronary vessels, i.e. an increase in coronary flow (Bova *et al.*, 1997). It was thus expected that cyclo(D-Trp-L-Pro) produce increased rates of coronary flow as a result of its antagonist action against Ca^{2+} channels (Figure 5). From Figure 5, it is clear that cyclo(L-Trp-L-Pro) and cyclo(D-Trp-D-Pro) did not produce any significant effects on the coronary flow in relation to the control ($p = 0.4326$, $p=0.7228$, respectively). Both cyclo(L-Trp-D-Pro) and cyclo(D-Trp-L-Pro) increased coronary flow ($p = 0.0296$ and $p = 0.0071$, respectively) when compared to the control samples. This increase in coronary flow for cyclo(D-Trp-L-Pro) was expected, although a decrease in coronary flow for cyclo(L-Trp-D-Pro) was anticipated. Of particular interest is the fact that cyclo(L-Trp-L-Pro) and cyclo(D-Trp-D-Pro) did not produce any significant effects on cardiac vascular smooth muscle (from coronary flow rate results) (Figure 5). This indicates that cyclo(L-Trp-D-Pro) and cyclo(D-Trp-L-Pro) resulted in relaxed vascular smooth muscle, which caused blood vessels in these regions to dilate, resulting in an increased coronary flow (Nayler, 1988). Disease states such as angina and myocardial infarction are often accompanied by arrhythmias, which may be aggravated by drugs that cause vasoconstriction. It is thus of particular interest that none of the isomers tested resulted in vasoconstriction i.e. a decrease in coronary flow rate.

Duration in VT and VA, and time to SR

A major cause of morbidity and mortality is ventricular arrhythmias, which are associated with myocardial ischaemia. No complete therapeutic solution is available as yet (Barrett *et al.*, 2000). In all experiments, the coronary flow decreased to less than 40% during occlusion and returned to normal after reperfusion. The time spent in VT, VA and the time to SR (Figure 6) were determined by studying the ECGs.

The time spent in VT (Figure 6) was significantly reduced in the presence of all the isomers in comparison to the control ($p < 0.05$ for all the isomers). Similarly, time spent in VA was also significantly reduced for all the isomers ($p < 0.01$ for cyclo(L-Trp-L-Pro), and $p < 0.001$ for cyclo(L-Trp-D-Pro), cyclo(D-Trp-L-Pro) and cyclo(D-Trp-D-Pro)). In addition, the time taken to return to SR was greatly reduced in comparison to the control group ($p < 0.001$ for all the isomers). These results show that significant reduction in the severity of arrhythmias that result from coronary artery ligation can be achieved with all the isomers of cyclo(Trp-Pro).

QRS intervals

No significant alterations in the duration of the QRS intervals (Figure 7) were observed for all the isomers in comparison to the control samples ($p > 0.05$). However, cyclo(D-Trp-L-Pro) showed a significant decrease in QRS complex duration in comparison to the other isomers ($p < 0.05$), indicating a decreased intraventricular conduction time.

Conclusions

Arrhythmias are of particular concern, as contractions that are too fast, asynchronous or too slow will reduce cardiac output. Arrhythmias may precipitate further complications in the form of VFs. Any agent capable of reducing the duration of VA and VF are of considerable importance in the sense that the agent is capable of modifying critically impaired conduction. Of the isomers tested, only cyclo(D-Trp-L-Pro) showed potential as a Ca^{2+} channel antagonist. Cyclo(L-Trp-L-Pro), cyclo(L-Trp-D-Pro) and cyclo(D-Trp-D-Pro) all showed Ca^{2+} channel agonism. Only cyclo(D-Trp-L-Pro) showed independence of membrane potential. No effect on the inward rectifier K^+ current was noted for any of the isomers. This may explain why none of the isomers showed a prolonged QRS complex (Rees and Curtis, 1993).

Cyclo(L-Trp-L-Pro) and cyclo(D-Trp-D-Pro) showed no significant effect on the heart rate, while cyclo(L-Trp-D-Pro) showed a positive chronotropic effect, with cyclo(D-Trp-L-Pro) exhibiting negative chronotropic effects. Clinical research has shown that vasodilative agents are capable of relieving the stressed myocardium by reducing the

vascular tone, and have thus shown considerable success in the treatment of some types of congestive failure (Hondegem and Mason, 1989). This increase in coronary flow was observed with cyclo(L-Trp-D-Pro) and cyclo(D-Trp-L-Pro), with no significant increase noted for both cyclo(L-Trp-L-Pro) and cyclo(D-Trp-D-Pro). Cyclo(L-Trp-D-Pro) was expected to decrease the coronary flow, since it showed positive chronotropic effects. To clarify this, it is suggested that the heart studies be conducted on isolated, guinea-pig hearts, to eliminate any discrepancies as far as species differences are concerned.

Furthermore, it was found that all the isomers were capable of reducing the time spent in both VA and VT, as well as reducing the time taken for the heart to return to SR. These isomers show potential as antiarrhythmic agents and should be investigated further, as coronary flow is not decreased on application, and will thus not place extra strain on the heart.

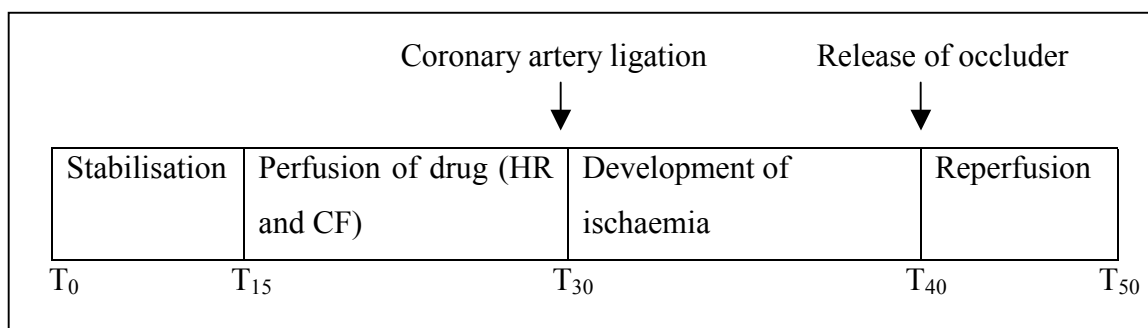
Acknowledgements

The authors would like to acknowledge the National Research Foundation for funding this research.

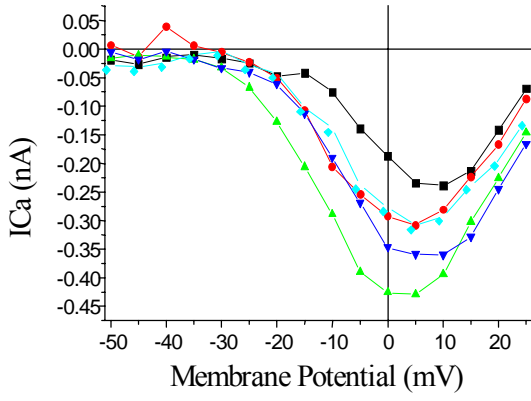
References

- Barrett, T.D., MacLeod, A. and Walker, M.J. (2000) RSD1019 suppresses ischaemia-induced monophasic action potential shortening and arrhythmias in anaesthetized rabbits, *Br. J. Pharmacol.* **131**:405-414.
- Bova, S., Cargnelli, G., D'Amato, E., Forti, S., Yang, Q., Trevisi, L., Debetto, P., Cima, L., Luciani, S., Padrini, R. (1997) Calcium-antagonist effects of norbomide on isolated perfused heart and cardiac myocytes of guinea-pig: a comparison with verapamil. *Br. J. Pharmacol.* **120**:19-24.
- Cook, N.S. (1998) The pharmacology of potassium channels and their therapeutic potential. *TiPS.* **9**:21-28.
- Dong, H., Sheng, J., Lee, C., Wong, T. (1993) Calcium antagonistic and antiarrhythmic actions of CPU-23, a substituted tetrahydroisouinolone. *Br. J. Pharmacol.* **109**:113-119.
- Dupuis, B.A., Adamantidis, M.M. (1995) Antiarrhythmic drugs: Principles of Pharmacology-Basic concepts and Clinical applications, Chapman and Hall, New York., pg. 518.
- Godfraind, T., Govoni, S. (1995) Recent advances in the pharmacology of Ca²⁺ and K⁺ channels. *TiPS.* **16**:1-4.
- Grant, G.D., Hunt, A.L., Milne, P.J., Roos, H.M. and Joubert, J. A. (1999) The structure and conformation of the tryptophanyl diketopiperazines cyclo(Trp-Trp)C₂H₆SO and cyclo(Trp-Pro), *J. Chem. Crystallogr.* **29**:435-447.
- Hamil, P., Marty, A., Neher, E., Sakman, B., Sigworth, F. (1981) Improved patch-clamp techniques for high-resolution current recording from cells and cell-free membrane patches. *Pflügers Arch.* **391**:85-100.
- Hashimoto, Y., Hori, R., Okumura, K., Yasuhara, M. (1986) Pharmacokinetics and antiarrhythmic activity of ajmaline in rats subjected to coronary artery occlusion. *Br. J. Pharmac.* **88**:71-77.
- Hondeghem, L.M., Mason, J.W. (1989) Agents used in Cardiac Arrhythmias, In: Katzung, B.G. (ed) *Basic and Clinical Pharmacology*, 4th Edn. Prentice-Hall International, U.S.A., pg. 165.
- Langendorff, O. (1895) Untersuchungen am überlebenden saugethierhergen. *Arch. Geo. Physiol.* **61**:291-332.
- Milne, P.J., Hunt, A.L., Rostoll, K., van der Walt, J.J., Graz, C.J.M. (1998) The biological activity of selected cyclic dipeptides. *J. Pharm. Pharmacol.* **50**:1331-1337.
- Nayler, W.G. (1988) *Calcium antagonists*, Academic Press, London, pg. 347.
- Rees, S.A., Curtis, M.J. (1993) Selective I_K blockade as an antiarrhythmic mechanism: effects of UK 66,914 on ischaemia and reperfusion arrhythmias in rat and rabbit hearts. *Br. J. Pharmacol.* **108**:139-145.
- Sensch, O., Vierling, W., Brandt, W., Reiter, M. (2000) Effects of inhibition of calcium and potassium currents in guinea-pig cardiac contraction: comparison of β-caryophyllene oxide, eugenol and nifedipine. *Br. J. Pharmacol.* **131**:1089-1096.

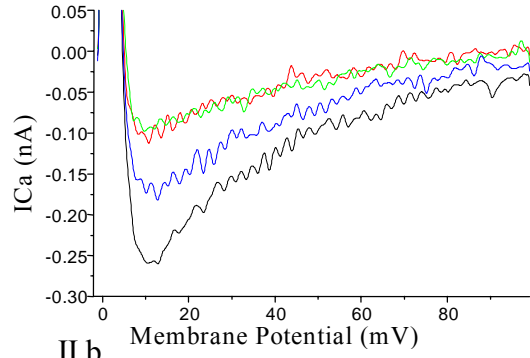
Compound (100 μM)	Ca²⁺-channel activity (Protocol A)	Ca²⁺ channel activity (Protocol B)	Dependence on membrane potential	K⁺ channel activity
Cyclo (L-Trp-L-Pro)	Agonist (77%)	Antagonist	Dependent	No significant effect
Cyclo (L-Trp-D-Pro)	Agonist (92%)	Antagonist	Dependent	No significant effect
Cyclo (D-Trp-L-Pro)	Antagonist (32%)	Antagonist	Independent	No significant effect
Cyclo (D-Trp-D-Pro)	Agonist (17%)	Antagonist	Dependent	No significant effect



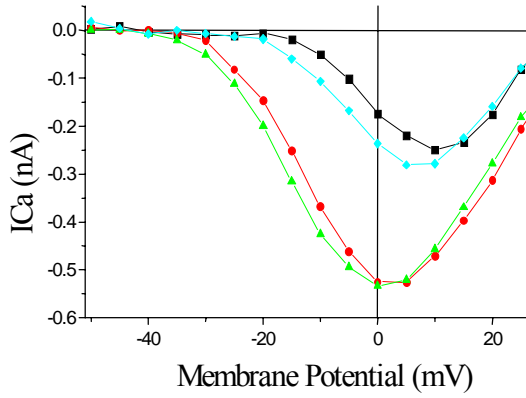
I a



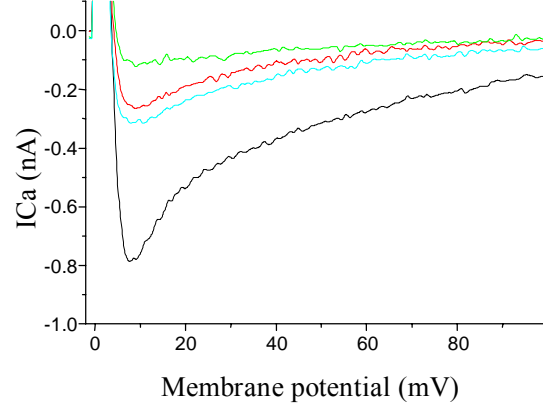
I b



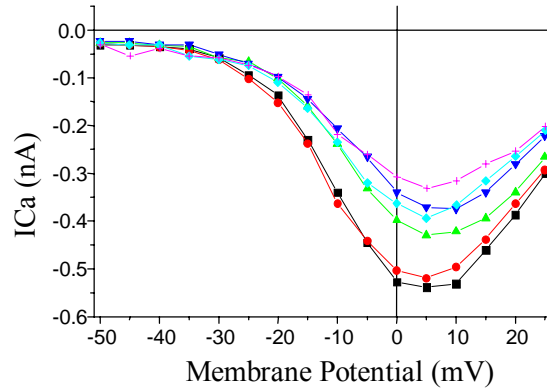
II a



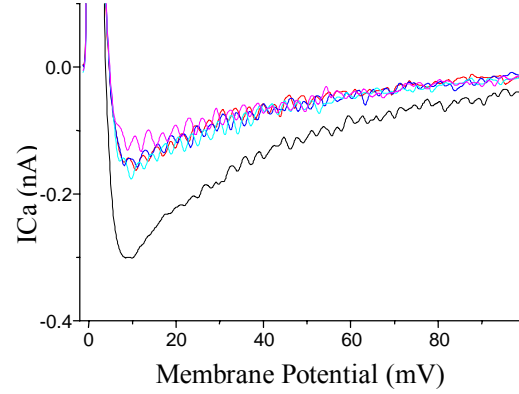
II b



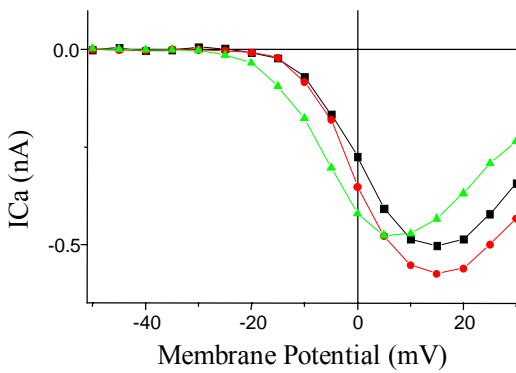
III a



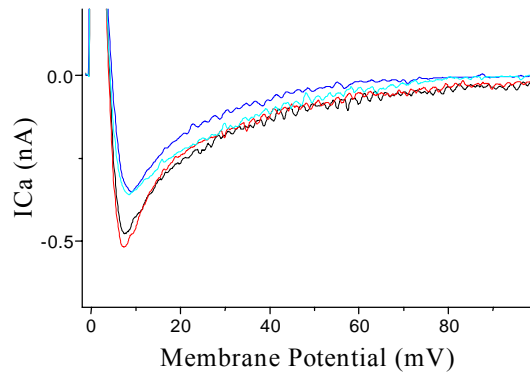
III b



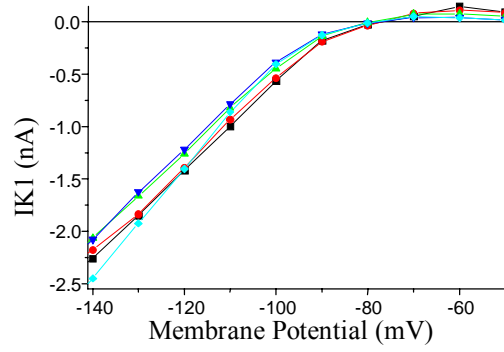
IV a



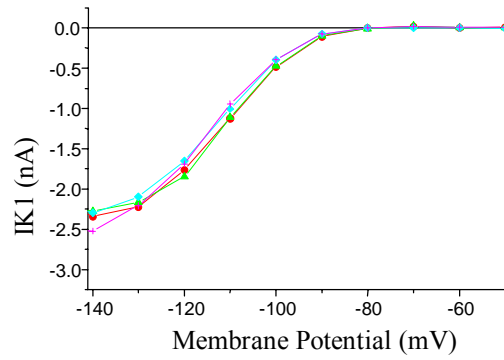
IV b



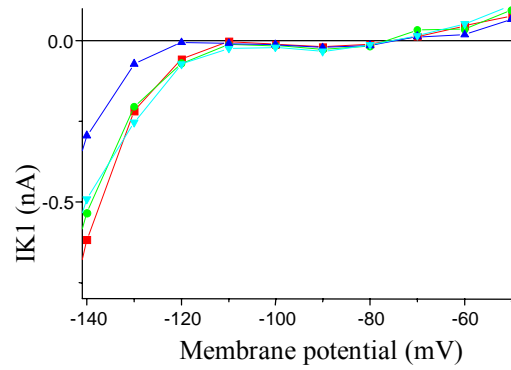
I



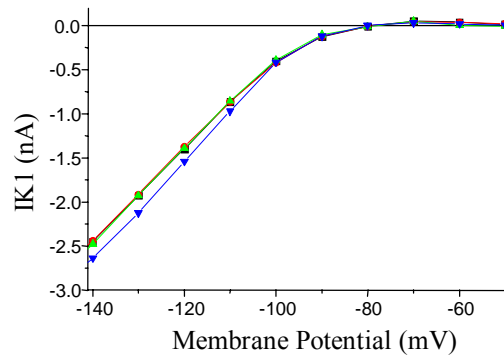
II

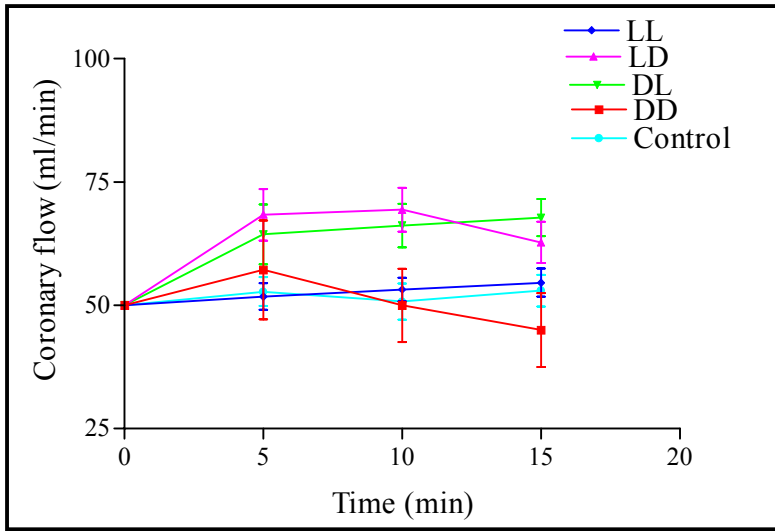
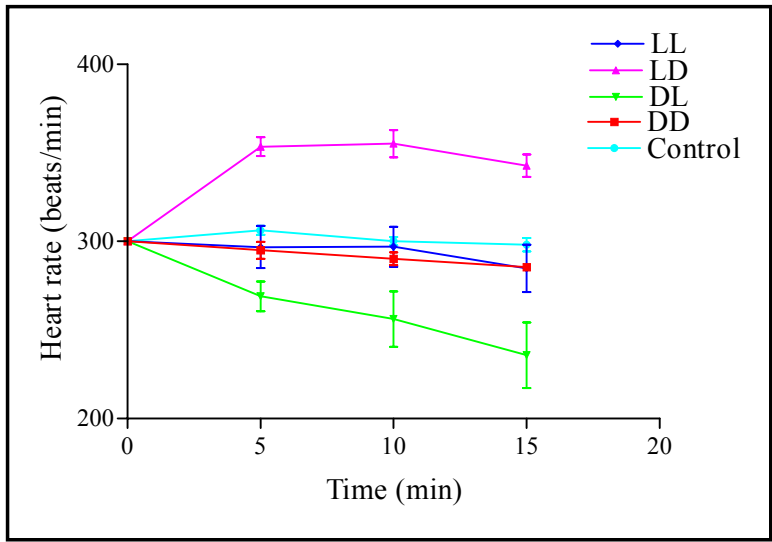


III



IV





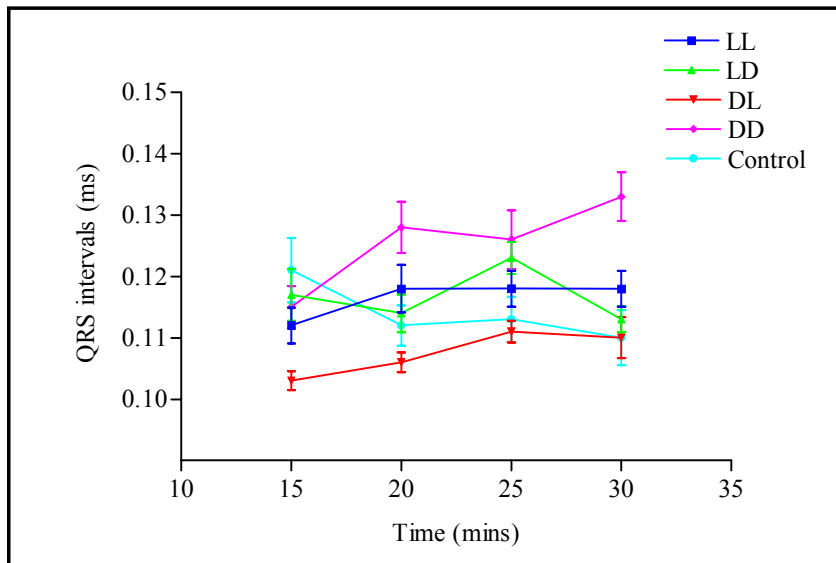
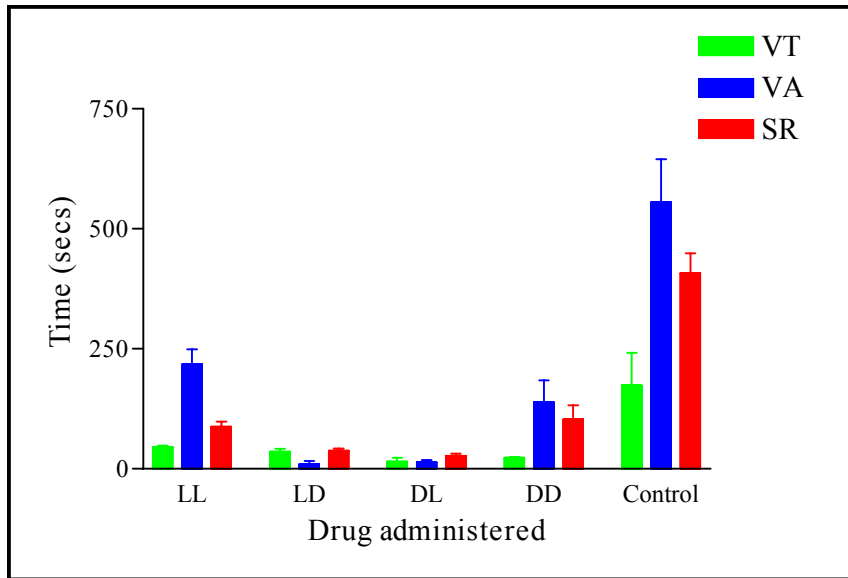


Table 1: Effects of the isomers on L-type Ca^{2+} and K^{+} channel activity.

Figure 1: The experimental protocol for the isolated rat heart perfusion. T= time in minutes, HR= heart rate, CF= coronary flow.

Figure 2 I a: The current-voltage relationship of inward currents recorded with the addition of 100 μM cyclo(L-Trp-L-Pro). (■) = Control after 10 min (to ensure stable current). (●) = 100 μM cyclo(L-Trp-L-Pro) for 1 min. (▲) = 100 μM cyclo(L-Trp-L-Pro) for 5 min. (▼) = Washout period of 1 min. (◆) = washout period of 7 min. I_{Ca} = inward current flow. (n=2) **2 I b:** The current-voltage relationship of inward currents recorded with the addition of 100 μM cyclo(L-Trp-L-Pro). (-) = Control after 10 min (to ensure stable current). (-) = 100 μM cyclo(L-Trp-L-Pro) for 1 min. (-) = 100 μM cyclo(L-Trp-L-Pro) for 5 min. (-) = Washout period of 1 min. (n=2) **2 II a:** The current-voltage relationship of inward currents recorded with the addition of 100 μM cyclo(L-Trp-D-Pro). (■) = Control after 10 min (to ensure stable current). (●) = 100 μM cyclo(L-Trp-D-Pro) for 1 min. (▲) = 100 μM cyclo(L-Trp-D-Pro) for 5 min. (◆) = washout period of 4 min. I_{Ca} = inward current flow. (n=2) **2 II b:** The current-voltage relationship of inward currents recorded with the addition of 100 μM cyclo(L-Trp-D-Pro). (-) = Control after 10 min (to ensure stable current). (-) = 100 μM cyclo(L-Trp-D-Pro) for 1 min. (-) = 100 μM cyclo(L-Trp-D-Pro) for 5 min. (-) = washout period of 7 min. I_{Ca} = inward current flow. (n=2) **2 III a:** The current-voltage relationship of inward currents recorded with the addition of 100 μM cyclo(D-Trp-L-Pro). (■) = Control 1 current after 10 min (to ensure stable current). (●) = Control 2 current. (▲) = 100 μM cyclo(D-Trp-L-Pro) for 1 min. (▼) = 100 μM cyclo(D-Trp-L-Pro) for 5 min. (◆) = washout period of 1 min. (-+-) = washout period of 5 min. I_{Ca} = inward current flow. (n=2) **2 III b:** The current-voltage relationship of inward currents recorded with the addition of 100 μM cyclo(D-Trp-L-Pro). (-) = Control after 10 min (to ensure stable current). (-) = 100 μM cyclo(D-Trp-L-Pro) for 1 min. (-) = 100 μM cyclo(D-Trp-L-Pro) for 5 min. (-) = washout period of 1 min. (-) = Washout period of 5 min. I_{Ca} = inward current flow. (n=2) **2 IV a:** The current-voltage relationship of inward currents recorded with the addition of 100 μM cyclo(D-Trp-D-Pro). (■) = Control after 10 min (to ensure stable current). (●) = 100 μM cyclo(D-Trp-D-Pro) for 1 min. (▲) = Washout period of 5 min. I_{Ca} = inward current flow. (n=2) **2 IV b:** The current-voltage relationship of inward currents recorded with the addition of 100 μM cyclo(D-Trp-D-Pro). (-) = Control after 10 min (to ensure stable current). (-) = 100 μM cyclo(D-Trp-D-Pro) for 1 min. (-) = 100 μM cyclo(D-Trp-D-Pro) for 5 min. (-) = washout period of 5 min. I_{Ca} = inward current flow. (n=2)

Figure 3 I: The current-voltage relationship of inward currents recorded with the addition of 100 μM cyclo(L-Trp-L-Pro). (-) = Control after 10 min (to ensure stable current). (-) = 100 μM cyclo(L-Trp-L-Pro) for 1 min. (-) = 100 μM cyclo(L-Trp-L-Pro) for 5 min. (-) = Washout period of 1 min. I_{Ca} = inward current flow. (n=2) **3 II:** The current-voltage relationship of inward currents recorded with the addition of 100 μM cyclo(L-Trp-D-Pro). (●) = Control after 10 min (to ensure stable current). (▲) = 100 μM cyclo(L-Trp-D-Pro) for 1 min. (◆) = 100 μM cyclo(L-Trp-D-Pro) for 3 min. (-+-) = Washout period of 3 min. IK_1 = inward rectifier K^{+} current. (n=2) **3 III:** The current-voltage relationship of inward currents recorded with the addition of 100 μM cyclo(D-Trp-L-Pro). (■) = Control after 10 min (to ensure stable current). (●) = 100 μM cyclo(D-Trp-L-Pro) for 1 min. (▲) = 100 μM cyclo(D-Trp-L-Pro) for 3 min. (▼) = Washout period of 3 min. IK_1 = inward rectifier K^{+} current. (n=2) **3 IV:** The current-voltage relationship of inward currents recorded with the addition of 100 μM cyclo(D-Trp-D-Pro). (■) = Control after 10 min (to ensure stable current). (●) = 100 μM cyclo(D-Trp-D-Pro) for 1 min. (▲) = 100 μM cyclo(D-Trp-D-Pro) for 3 min. (▼) = Washout period of 3 min. IK_1 = inward rectifier K^{+} current. (n=2)

Figure 4: Effect of the isomers on the heart rate in isolated, rat heart. (n=6).

Figure 5: The effects of the isomers on coronary flow rate as determined in the isolated rat heart. (n=6).

Figure 6: The time to stop VT (ventricular tachycardia), VA (ventricular arrhythmias) and time to return to SR (normal sinus rhythm) in the presence of 200 μM LL (cyclo(L-Trp-L-Pro)), LD (cyclo(L-Trp-D-Pro)), DL (cyclo(D-Trp-L-Pro)) and DD (cyclo(D-Trp-D-Pro)).

Figure 7: QRS intervals as measured with perfusion of the isomers, from 15 min to 30 min. (n=6).

Article 2

Cyclic Dipeptide Research Unit, Department of Pharmacy, Box 1600, University of Port Elizabeth, Port Elizabeth, 6000, South Africa

Title Hepatotoxicity of the isomers of cyclo(Trp-Pro)

Jamie, H., Kilian, G. and *Milne, P.J.

*Author for correspondence

Abstract

The hepatotoxicity of the novel cyclic dipeptide cyclo(Trp-Pro), which has shown potential usage in various pharmacological fields, had not been assessed. Further studies on the isomers of this cyclic dipeptide (cyclo(L-Trp-L-Pro), cyclo(L-Trp-D-Pro), cyclo(D-Trp-L-Pro) and cyclo(D-Trp-D-Pro)) revealed further biological activities. The assessment of hepatotoxicity of these isomers was thus warranted. *In vitro* screens were performed on primary isolated rat hepatocytes, the Chang liver and N-2-alpha cell lines. *In vivo* screening involved the assessment of serum levels of lactate dehydrogenase, aspartate transaminase, ATP, Ca^{2+} and albumin after intraperitoneal injection over a 1 and 5 day period in the rat model. Liver samples were also obtained for the assessment of lipid peroxidation. It was found that only cyclo(D-Trp-L-Pro) was hepato-specific in its action, while the other isomers were not. The greatest effect on any biochemical or physiological parameter was noted after 5 days. LDH secretion was greatly increased in the presence of cyclo(L-Trp-L-Pro) and cyclo(L-Trp-D-Pro) ($p < 0.05$). Significantly increased levels of lipid peroxidation were observed in all the isomer-treated samples ($p < 0.05$), while Ca^{2+} concentrations were decreased at day 5. Decreased protein synthesis was noted in the presence of all the isomers at day 1. These results indicate the potential harm involved in the administration of the isomers, which may limit their potential usage in the treatment of various diseases.

1. Introduction

Research in our laboratories have shown the potential of the novel cyclic dipeptide cyclo(Trp-Pro) as an antimicrobial substance, as well as potential usage in the treatment of cardiovascular dysfunction [1].

The safety evaluation of novel compounds of potential medical applicability must undergo a number of tests using *in vitro* and *in vivo* methods to determine its general toxicity and mutagenicity. A primary function of the liver is the metabolism of xenobiotics. In assessing the toxicological potential of new drugs or environmental studies, the assessment of hepatotoxicity by both *in vivo* and *in vitro* methods plays a major role [2, 3].

In vitro methods used in assessing hepatotoxicity include concentration-toxicity curves, which should be assessed in primary cultured hepatocytes, non-hepatic cells and in non-metabolising hepatocytes. This would give an indication as to whether the drug is toxic preferentially on hepatocytes, or whether bioactivation of the drug is necessary to cause cellular damage [4].

In vivo injury to the liver can be evaluated through the determination of a number of parameters of the cell, including synthesis and secretion of albumin, ureogenesis, glutathione levels, ATP levels, concentration of Ca^{2+} , membrane leakage of cytosolic enzymes such as lactate dehydrogenase, protein synthesis and morphological changes [5].

In the detection of liver disease, the most commonly assayed enzymes are aspartate transaminase (AST) and alanine transaminase (ALT). In acute liver disease, higher values of ALT are found in plasma as compared to AST. A continuing rise in the plasma transaminase concentration may be detected as a result of hypersensitivity hepatocellular damage as a result of drugs. Measurement of AST levels is however the preferred enzyme, as it is used primarily in the management of liver disease. Here, a raised level indicates hepatocellular damage [6, 7].

The energetic balance of the cells may be indirectly altered by many hepatotoxins by increasing the energy demand, reducing ATP production, or both. A common event in cellular damage is the depletion of ATP. Alternatively, hepatocyte ATP production may be altered by the xenobiotic or its metabolites. ATP is largely produced from acetyl CoA via the Krebs cycle and oxidative phosphorylation of NADPH in mitochondria. Any substance that interferes with these processes may result in decreased ATP production. All cellular anabolic processes are thus disrupted, as well as hepatocyte functions [4].

Lipid peroxidation levels may also increase due to the depletion of normal cellular protective mechanisms (eg. glutathione). Lipid peroxidation, a free radical-mediated process, results in oxidative degradation of the component lipids found in the cell membranes. Several cardiovascular, pulmonary and hepatic diseases are affected by peroxidised lipids present in animal tissues [8].

In order to determine the hepatotoxic potential of the isomers of cyclo(Trp-Pro) (cyclo(L-Trp-L-Pro), cyclo(L-Trp-D-Pro), cyclo(D-Trp-L-Pro) and cyclo(D-Trp-D-Pro)), the effects of the isomers on cell viability were assessed on primary isolated hepatocytes, as well as two different cell lines, N-2-alpha and Chang liver cells. The metabolic and physiological functioning of the liver was assessed by using various biochemical assays in order to determine serum levels of LDH, AST, ATP, Ca^{2+} , and albumin. The amount of lipid peroxidation was assessed on liver samples.

2. Investigations and results

2.1 *In vitro* toxicity screen

In the past decade, the use of cellular models as a partial alternative to whole animal experimentation as a model of toxicity testing has increased. Cell cultures present a simplified, valid biological model in *in vitro* screening of hepatotoxicity of different compounds and their respective metabolites. In the assessment of cytotoxicity of the isomers and isoniazid, three different cell types were chosen in such a manner as to determine the specificity of toxicity, i.e. if any toxicity is detected, whether it is hepatocyte-specific or not. The primary isolated hepatocytes from rats, Chang liver cells, a hepatoma cell line (transfected with a cervical carcinoma) and N-2-alpha cells (a neuronal cell line) were used. Results are depicted as % viability of the control cultures [10].

In the isolated hepatocytes (Fig. 1), isoniazid was the only treatment that favoured the growth of the cells, and thus differed significantly from the other treatments ($p < 0.05$). All

isomers resulted in decreased growth in comparison to the control culture over the 5 day period and did not differ significantly from each other ($p>0.05$). The greatest inhibition of growth was noted for cyclo(L-Trp-L-Pro) and cyclo(L-Trp-D-Pro) (60% and 62% inhibition, respectively), while cyclo(D-Trp-L-Pro) and cyclo(D-Trp-D-Pro) only resulted in a decrease of ~55%, in comparison to the control.

When the isomers were applied to the Chang liver cells (Fig. 2), isoniazid resulted in decreased growth over a 2 day period (~30% inhibition of growth). After that, growth appeared to increase slightly (from 70 to 78%). Cyclo(D-Trp-L-Pro) also resulted in an initial decrease in cell growth, but not to the same extent of isoniazid. This was also followed by a slight increase in cell growth. Cyclo(L-Trp-L-Pro), cyclo(L-Trp-D-Pro) and cyclo(D-Trp-D-Pro) greatly inhibited cell growth over the 5 day period ($p<0.05$) (Fig. 2), with cyclo(L-Trp-L-Pro) being the most cytotoxic isomer, resulting in a 50% inhibition of cell growth.

Cyclo(D-Trp-L-Pro) did not adversely affect the growth of N-2-alpha cells (Fig. 3), indicating that any hepatotoxic effects noted in *in vivo* studies were hepato-specific. However, in the presence of cyclo(L-Trp-L-Pro), cyclo(L-Trp-D-Pro), cyclo(D-Trp-D-Pro) and isoniazid, the growth of N-2-alpha decreased over the 5 day period to approximately 75% of the control growth. This indicated that the cytotoxicity noted for these compounds were not hepatocyte-specific, and may be capable of exerting their cytotoxic effects on a number of different cell types.

2.2 LDH concentrations

One of the most common assays used in the assessment of hepatotoxicity of a drug is LDH activity, which gives an indication of cell membrane integrity. Increased LDH activity is associated with disruption of cell membrane structure. Significantly increased ($p < 0.05$) levels of LDH was determined for all the compounds in comparison to the control after 24 hr (Fig. 4). These levels increased significantly for cyclo(L-Trp-L-Pro) and cyclo(L-Trp-D-Pro) ($p < 0.05$), decreased for cyclo(D-Trp-L-Pro) and isoniazid ($p < 0.05$), with no changes noted for the control and cyclo(D-Trp-D-Pro) groups ($p = 0.5602$ and $p = 0.6857$, respectively) when day 1 and day 5 levels were compared. At day 5, levels detected for cyclo(L-Trp-L-Pro) and cyclo(L-Trp-D-Pro) increased in comparison to the control group ($p < 0.05$) while no differences were noted for any other compound in comparison to the control group. It appears that cyclo(L-Trp-L-Pro) and cyclo(L-Trp-D-Pro) induced the greatest disruption in cell membrane integrity, which resulted in the largest leakage of LDH from the cell [5].

2.3 AST serum levels

AST serum levels are normally low (2-20 IU/l in humans). An increase in serum activity is resultant of damage to organs that involve necrosis of cells or increased cell permeability. For this reason, it was expected that AST levels in the cyclo(L-Trp-L-Pro) and cyclo(L-Trp-D-Pro) groups would have elevated AST levels (LDH leakage, Fig. 4). This was, however, not observed, with cyclo(L-Trp-L-Pro) showing significantly lowered levels ($p = 0.0286$) and cyclo(L-Trp-D-Pro) not showing any difference to the control group ($p = 0.1143$) (Fig. 5). On day 1, no drug produced any significantly increased AST

concentrations, while significantly decreased levels were noted on day 5 for all the compounds (with the exception of isoniazid) in comparison to the control group ($p < 0.05$). After 5 days, significantly elevated levels of AST were only noted in the isoniazid-treated group ($p = 0.0286$) [13].

2.4 Energy state as measured by serum ATP concentrations

In the presence of hepatotoxins, ATP levels may be decreased by an increase in energy demand, a common event in cell injury. The energy-metabolism, in terms of ATP levels in serum, was also assessed. Similar levels were noted for the control and isoniazid groups on both days 1 and 5 ($p > 0.05$). After 24 hrs (Fig. 6), significantly decreased levels of ATP was observed in the cyclo(L-Trp-D-Pro), cyclo(D-Trp-L-Pro) and cyclo(D-Trp-D-Pro) groups ($p < 0.05$), while no difference was noted for cyclo(L-Trp-L-Pro) ($p = 0.6857$) in relation to the control group. This decrease in ATP would thus indicate a greater energy demand in those cells treated with cyclo(L-Trp-D-Pro), cyclo(D-Trp-L-Pro) and cyclo(D-Trp-D-Pro), or mitochondrial dysfunction. This was however ruled out as, at day 5 (Fig. 6), significantly increased levels were observed for all the isomers ($p < 0.05$) when compared to the respective day 1 levels. At day 5, the highest level was noted for cyclo(D-Trp-L-Pro) ($p < 0.01$), followed by cyclo(D-Trp-D-Pro), cyclo(L-Trp-L-Pro) and cyclo(L-Trp-D-Pro). This increase may be as a result of increased rates of glycolysis. However, no significant difference was noted between the day 5 cyclo(L-Trp-L-Pro) and cyclo(L-Trp-D-Pro) levels ($p = 0.2469$) [4, 15].

2.5 Serum Ca²⁺ concentrations

Ca²⁺ accumulates in dying cells and is thus involved in toxicological processes. Significantly decreased levels of Ca²⁺ was obtained in the cyclo(L-Trp-L-Pro) and cyclo(L-Trp-D-Pro) samples ($p < 0.05$) (Fig. 7), whereas cyclo(D-Trp-L-Pro), cyclo(D-Trp-D-Pro) and isoniazid did not show any significantly different levels ($p > 0.05$) in comparison to the control group. The only group to show any significant difference in Ca²⁺ levels from day 1 to day 5 was the isoniazid-treated group ($p = 0.0286$). The isomer-treated groups showed significantly diminished Ca²⁺ levels in comparison to the control on day 5 ($p < 0.05$) with no significance between the control and isoniazid-treated groups ($p = 0.6857$). These changes in Ca²⁺ homeostasis would adversely affect signal transduction of the cell, as Ca²⁺ plays a vital role as a second messenger [16].

2.6 Protein synthesis

Free albumin concentration may decrease due to binding to drugs or as a result of decreased protein synthesis. As a result, free drug concentration may increase which may increase toxicity risks. In addition, Ca²⁺ homeostasis may be disrupted by changes in protein synthesis. Decreased protein synthesis is one of the earliest and most sensitive signs of cellular hepatocytes damage. After a 24 hr exposure (Fig. 8) to the compounds and isoniazid, the levels of albumin in the serum were significantly decreased in comparison to the control value ($p < 0.05$), indicating decreased protein synthesis and hepatocyte damage. Cyclo(D-Trp-L-Pro) produced the largest decrease in albumin synthesis ($p = 0.0286$). However, after 5 days (Fig. 8), all the levels of albumin had decreased, including that of the control group, with only cyclo(D-Trp-L-Pro) and

cyclo(D-Trp-D-Pro) differing significantly from the control sample ($p=0.0286$ for both compounds). From the results, it is clear that the compounds resulted in decreased protein synthesis, with maximal effects noted over a longer period [4, 7, 16].

2.7 Lipid peroxidation

Oxidative degradation of component lipids on the cell membrane is caused by lipid peroxidation. This process would obviously disrupt the integrity of the cell membrane. The thiobarbituric acid (TBA) reaction of liver homogenates in rats showed significant elevations of malondialdehyde concentrations after a single intraperitoneal injection of cyclo(L-Trp-L-Pro), cyclo(D-Trp-L-Pro) and cyclo(D-Trp-D-Pro), indicating the occurrence of lipid peroxidation ($p<0.05$) (Fig. 9). No significant elevation in malondialdehyde levels was observed for cyclo(L-Trp-D-Pro) ($p=0.667$) and isoniazid ($p=0.333$). However, after 5 days, malondialdehyde levels increased dramatically for cyclo(L-Trp-D-Pro) and isoniazid-treated groups ($p<0.05$). This significant increase was also noted for the other compounds in relation to the control ($p<0.05$), indicating lipid peroxidation [14].

Only cyclo(D-Trp-L-Pro) is hepatocyte-specific in its cytotoxicity while cyclo(L-Trp-L-Pro), cyclo(L-Trp-D-Pro) and cyclo(D-Trp-D-Pro) are cytotoxic for other cell types too. As can be seen from the results, it is clear that isoniazid exerts its cytotoxic effect by producing lipid peroxidation. Various effects on biochemical and physiological parameters are noted in the presence of the isomers. Cyclo(L-Trp-L-Pro) and cyclo(L-Trp-D-Pro) are able to disrupt cell membrane integrity, as can be seen from the LDH

results. However, no great elevation in AST concentrations was observed for these isomers. After a short exposure period, cyclo(L-Trp-D-Pro), cyclo(D-Trp-L-Pro) and cyclo(D-Trp-D-Pro) result in decreased ATP concentrations, which increase to day 5. This indicates an increase in ATP production, which may result from an increased rate of glycolysis. Decreases in Ca^{2+} concentration occurred in the presence of cyclo(L-Trp-L-Pro) and cyclo(L-Trp-D-Pro) after 1 day, which indicates a disruption in Ca^{2+} homeostasis, which can lead to a number of signal transduction interferences. Furthermore, depletion in the cell's protective mechanism is indicated by the elevated lipid peroxidation levels in the presence of all the isomers. This suggests that the isomers disrupt glutathione levels, leading to cells with an increased vulnerability to damage by the foreign compounds. This may limit the usage of these isomers in the treatment of various diseases.

3. Experimental

The use of rats for this study was approved by the Animal Ethics Committee, University of Port Elizabeth.

3.1 Isolation of primary hepatocytes

A modified collagenase method was used as previously described [9].

3.1.1 Routine cell culture

Hepatocytes were seeded in 96-well cell culture plates (Corningware, Cambridge, U.S.A.) at 75 000 cells per well and incubated at 37°C in an atmosphere of 95% O_2 and 5% CO_2 (Fedgas, South Africa). Prior to seeding, the wells were coated with newborn

calf serum (BioWhittaker, Walkersville) to facilitate attachment of the cells to the plate. For the first 24 hr of incubation, serum-supplemented Hams F-12 medium was used. This medium was replaced after 24 hr, to Hams F-12 medium supplemented with 10^{-8} M dexamethasone (Sigma, St. Louis). After the 24 hr incubation, the cells were exposed to 200 μ M of each isomer (pH 7.4), respectively. The control solution consisted of Hams F-12 medium containing 0.5% glycerol. As a positive control, the cells were exposed to 1 mg/ml isoniazid dissolved in Hams F-12 medium containing 0.5% glycerol. Isoniazid has also been associated with hepatotoxicity over long periods of administration. Liver functions become impaired, jaundice may result and multilobular necrosis may occur. The cells were incubated in the presence of the compounds for a total of 5 days; each day the MTT assay was used to determine viability of the cells of the treated cells, as well as of the controls [10, 11].

3.1.2 Cell culture of N-2-alpha and Chang liver cells

In order to determine whether any effects exerted on the isolated hepatocytes were hepatocyte-specific or not, Chang Liver cells and N-2-alpha cells were also exposed to 200 μ M of each compound, made up in DMEM (0.5% glycerol). These cells were treated in the same manner as that of the isolated hepatocytes, with the exception that these cells were seeded at a density of 25 000 cells per well, as these cell lines undergo proliferation in culture. No coating of the plates was necessary as these cells readily adhere to the wells.

3.1.3 MTT assay

On the assay day, 50 μ l 0.5% MTT (Sigma, St. Louis) solution was added to each well, and incubated at 37°C for 2 hrs. After the incubation period, the solution was aspirated from the cells, and 200 μ l DMSO was added to each well. A 5 min reaction period was allowed with mild agitation. The resultant extracted formazan products were removed from the plate and put into a clean 96-well plate. The absorbance at 600 nm was read against a DMSO blank using Labsystems Multiskan MS (Multiskan Transmit Program, Rev. 1.3. (1995)). Results are reported as a percentage of the control group, which was taken as 100% viability.

3.2 Treatment of rats

Male Long Evans rats (250 – 350g) were housed in a well ventilated room at 24°C, 12 hr light. Fasting and starvation may adversely affect biotransformation of oxidising agents as well as the antioxidant state of the liver, and therefore, animals were fed *ad lib.* and not fasted prior to experimentation. The rats were injected intraperitoneally with a 7.1 mg/50 ml saline solution of the respective compounds, representing a final concentration of 500 μ M. 0.5% Glycerol was used to facilitate dissolution of the isomers in saline. All solutions were filter sterilized with a 0.45 μ m filter unit (Millipore) before use. The rats were separated into 2 sets of 6 groups of rats. Rats in set 1 were injected only once and killed after 24 hrs, while the rats in set 2 were subjected to injections every alternate day for a period of 5 days before being killed. Group 1 of each set served as the control group, receiving normal saline injections containing 0.05 % glycerol. Groups 2-5 received injections of the 500 μ M solution of the respective cyclic dipeptide in saline

containing 0.05 % glycerol. Group 6, the positive control group, received saline injections containing isoniazid at a concentration of 1 mg/ml [12].

3.2.1 Sample collection

Rats were subjected to light ether anesthesia to a loss of blink and pain reflexes. The entire liver was removed and rinsed in 0.15 M KCl solution. The livers were placed in 0.15 M KCl solution and frozen at -20°C until lipid peroxidation was assessed. Blood was collected by cardiac puncture into empty vacutainer tubes and placed at 4°C to allow for clot formation. Serum was obtained by centrifugation at 3 000 rpm for 15 min. The serum was retained for the assessment of hepatotoxicity by various enzymatic and biochemical assays.

3.3 Enzymatic and biochemical assays

3.3.1 Lactate dehydrogenase

The lactate dehydrogenase kit (Sigma, St. Louis, U.S.A.) was used according to manufacturers specifications. Briefly, 10 μl of the serum sample was placed into a 96-well plate to which 200 μl LDH reagent was added. An initial absorbance at 340 nm was read using Labsystems Multiskan MS (Multiskan Transmit Program, Rev. 1.3. (1995)), after which the reaction was followed at 340 nm for 1 min. The change in absorbance/min was determined. Results of the control group of rats are included.

3.3.2 Aspartate transaminase

A modified version of the aspartate transaminase assay as described previously was used to determine the levels of AST in serum [13].

To each set of tubes, 250 μ l AST substrate (37°C) was added. To the rat serum tubes, 50 μ l serum was added, whilst to the blank tube, 50 μ l H₂O was added. The tubes were mixed and incubated at 37°C for 1 hr. 250 μ l 1 mM 2,4-dinitrophenylhydrazine was added, mixed and the solution was incubated at RT for 20 min. 2.5 ml 0.4 N NaOH was then added and allowed to incubate at RT for 5 min. The solution was diluted 2X with 0.4 N NaOH and the absorbance was read at 505 nm using a Shimadzu UV-160A UV-Visible recording spectrophotometer, against a blank consisting of reaction mixture.

3.3.3 Lipid Peroxidation

The method to determine lipid peroxidation as described previously was used [14].

3.3.4 ATP

The adenosine-5'-triphosphate kit from Sigma Diagnostics was used according to manufacturers specifications.

3.3.5 Ca²⁺ concentrations

Ca²⁺ content in the serum samples was determined by using serum Ca²⁺ kit from Sigma Diagnostics according to manufacturers specifications.

3.3.6 Albumin levels

A modification of the albumin assay as described previously was used. To a set of test tubes, 5 ml working reagent solution was added, to which 25 μ l sample/albumin standard was added, mixed and left to incubate at RT for 10 mins. The absorbance was read at 630 nm using a Shimadzu UV-160A UV-Visible recording spectrophotometer against a blank

consisting of working reagent. A 10 g/100 ml albumin standard was used. Albumin content in serum samples were calculated using the following formula:

$$\text{Abs sample/Abs std} \times \text{conc. std} = \text{conc sample g/100 ml [13]}.$$

3.3.7 Statistical analysis

Results are expressed as mean \pm s.d. for the indicated number of experiments. Results were analysed using the software package GraphPad Prism Version 2.0 and GraphPad InStat (GraphPad Software, Inc., San Diego, U.S.A.). All tests were performed on raw data obtained from the experiments (n=6). The effect of a single qualitative factor on a single response variable was determined by univariate ANOVA using the Mann-Whitney test. *P* values <0.05 were accepted as evidence of a statistically significant difference.

Prof. P.J. Milne

Cyclic Dipeptide Research Unit

Department of Pharmacy

Box 1600

Port Elizabeth 6000

South Africa

E-mail : pmapjm@upe.ac.za

REFERENCES

- 1 Milne, P.J.; Hunt, A.L.; Rostoll, K.; van der Walt, J.J.; Graz, C.J.M.: J. Pharm. Pharmacol., **50** 1331 (1998)
- 2 Castell, J.V.M.; Montoya, A.; Larrauri, A.; Lopez, P.; Gomez-L. J.: Xenobiotica, **15** 743 (1985)
- 3 Bhattacharya, R.; Lakshmana Rao, P.V.; Bhaskar, A.S.B.; Pant, S.C.; Dube, S.N.: Human and Experimental Toxicology, **15** 105 (1996)
- 4 Castell, J.V.; Gomez-Lechon, M.; Ponsoda, X.; Bort, R.: in: In Vitro methods in pharmaceutical research. p. 375-397, Academic Press, San Diego 1997
- 5 Vickers, A.E.: in: In Vitro methods in pharmaceutical research. p.103-123, Academic Press, San Diego 1997
- 6 Baron, D.N.: A short textbook of Chemical Pathology, 4th Ed, p. 198, Hodder and Stoughton, London 1982
- 7 Marshall, W.: Clinical Chemistry, 3rd Ed., p. 231-232. Mosby, Great Britain 1997
- 8 Uchiyama, M.; Mihara, M.: Anal Biochem., **86** 271 (1978)

- 9 Seglen, P.O.: in: Cell Biology: A laboratory handbook, p. 96- 102, Academic Press, London 1994
- 10 Jover, R.; Ponsoda, X.; Castell, J.V.; Gomez-Lechon, M.J.: Toxic. in Vitro, **6** 47 (1992)
- 11 Jawetz, E., in: Katzung, B.G. (Ed.): Basic and Clinical Pharmacology, 4th Ed, p. 579., Prentice-Hall International, U.S.A. 1989
- 12 Tanaka, K.; Sato, M.; Tomita, Y.; Ichichara, A.: J. Biochem., **84** 937 (1978)
- 13 Bauer, J.D.; Ackermann, P.G.; Toro, G.: Clinical Laboratory methods, 8th Ed, p. 393-4, CV Mosby Co., St. Louis, U.S.A. 1974
- 14 Souza, M.F.; Tome, A.R.; Rao, V.S.N.: J. Pharm. Pharmacol. **51** 125 (1999)
- 15 Ross, D.: J. Pharm. Pharmacol., **41** 505 (1989)
- 16 Orrenius, S.; McConkey, D.; Bellomo, G.; Nicotera, P.: TiPS, **10** 281 (1989)

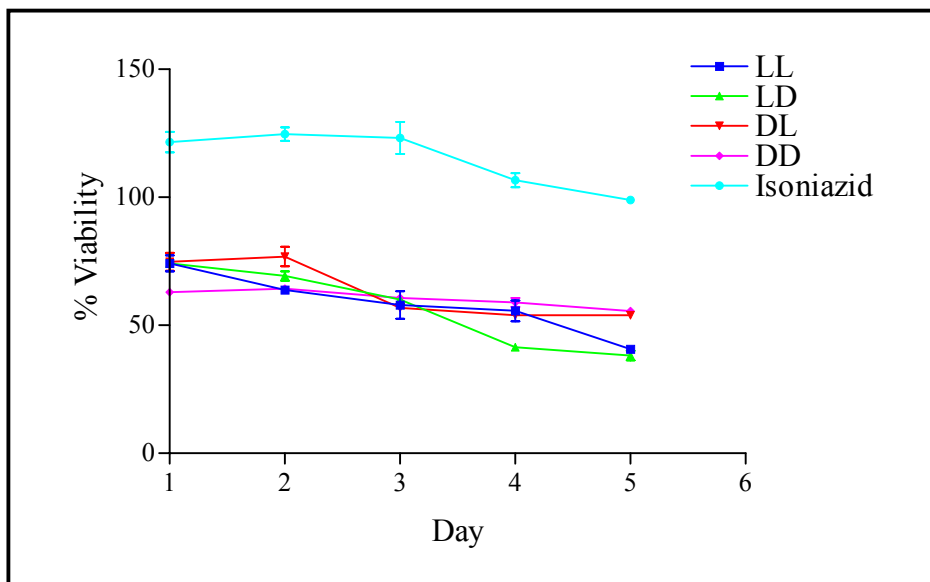


Figure 1 Effects of the compounds on the viability of isolated rat hepatocytes. LL = cyclo(L-Trp-L-Pro); LD = cyclo(L-Trp-D-Pro); DL = cyclo(D-Trp-L-Pro); DD = cyclo(D-Trp-D-Pro). Values indicated are the mean \pm s.d. of 6 experiments per day per treatment.

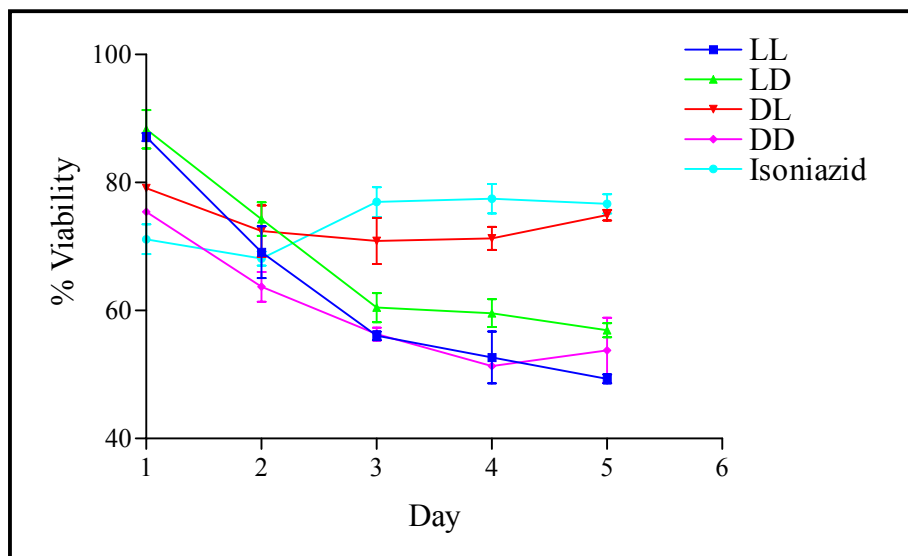


Figure 2 Effects of the compounds on the viability of Chang liver cells. LL = cyclo(L-Trp-L-Pro); LD = cyclo(L-Trp-D-Pro); DL = cyclo(D-Trp-L-Pro); DD = cyclo(D-Trp-D-Pro). Values indicated are the mean \pm s.d. of 6 experiments per day per treatment.

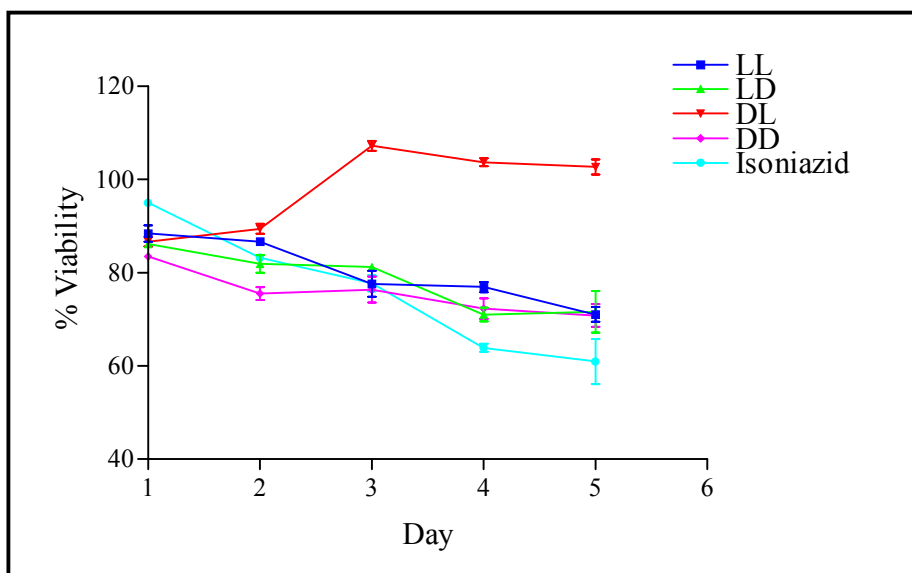


Figure 3 Effects of the compounds on the viability of N-2-alpha cells. LL = cyclo(L-Trp-L-Pro); LD = cyclo(L-Trp-D-Pro); DL = cyclo(D-Trp-L-Pro); DD = cyclo(D-Trp-D-Pro). Values indicated are the mean \pm s.d. of 6 experiments per day per treatment.

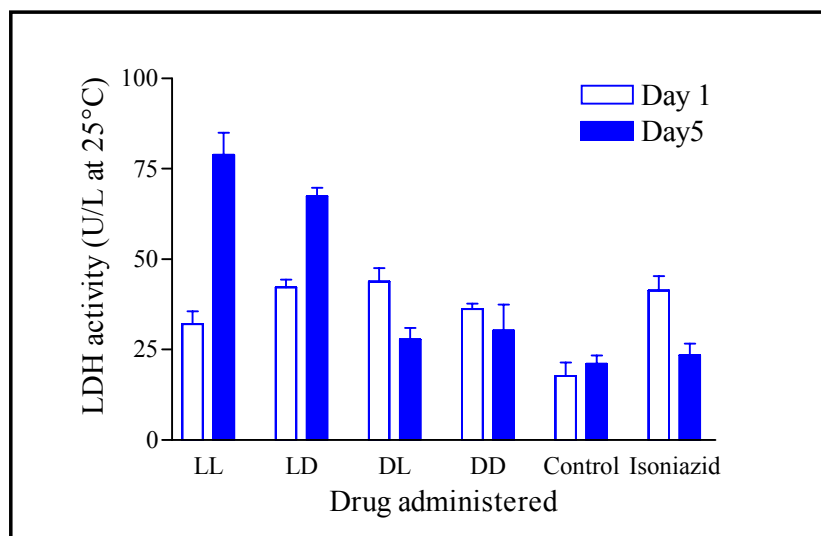


Figure 4 Effects of the compounds on lactate dehydrogenase activity in the blood stream. LL = cyclo(L-Trp-L-Pro); LD = cyclo(L-Trp-D-Pro); DL = cyclo(D-Trp-L-Pro); DD = cyclo(D-Trp-D-Pro). Values indicated are the mean \pm s.d. of 6 experiments per day per treatment.

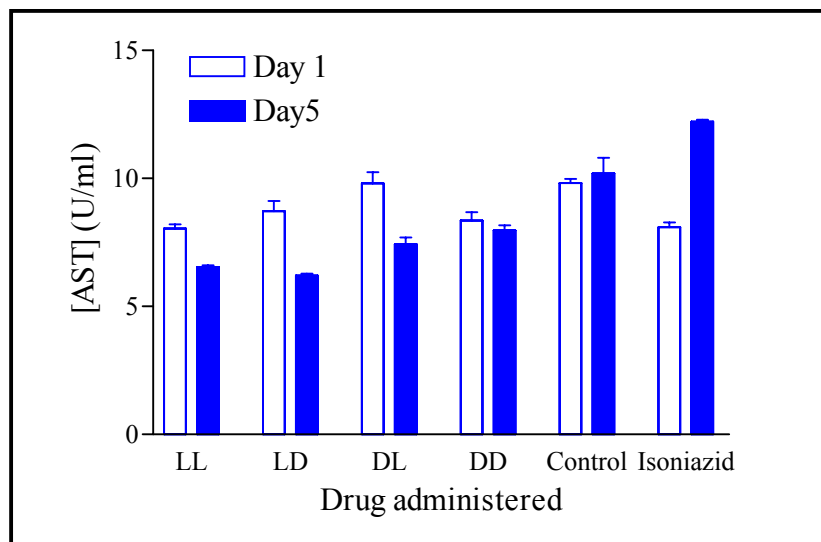


Figure 5 Effects of the compounds on the concentration of aspartate transaminase in the blood stream. LL = cyclo(L-Trp-L-Pro); LD = cyclo(L-Trp-D-Pro); DL = cyclo(D-Trp-L-Pro); DD = cyclo(D-Trp-D-Pro). Values indicated are the mean \pm s.d. of 6 experiments per day per treatment.

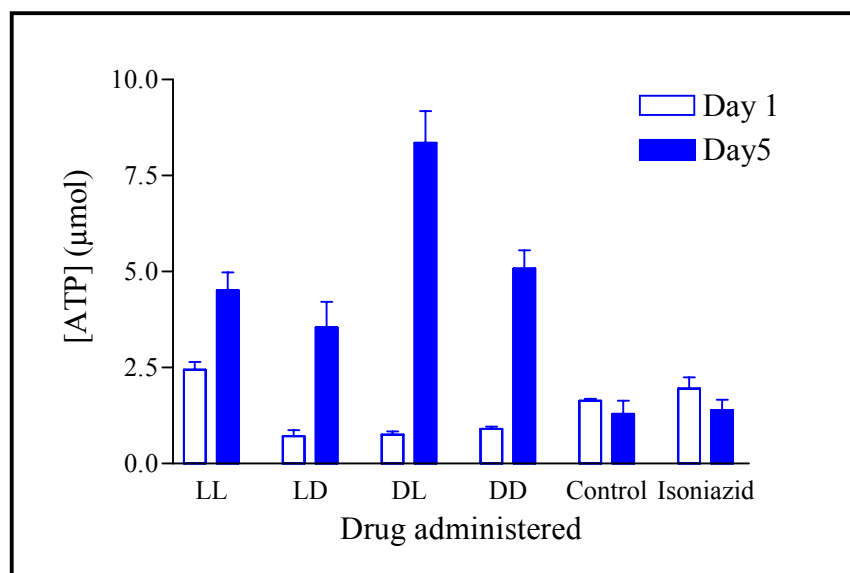


Figure 6 Effects of the compounds on energy metabolism in rat hepatocytes, measured in terms of ATP concentrations in the blood stream. LL = cyclo(L-Trp-L-Pro); LD = cyclo(L-Trp-D-Pro); DL = cyclo(D-Trp-L-Pro); DD = cyclo(D-Trp-D-Pro). Values indicated are the mean \pm s.d. of 6 experiments per day per treatment.

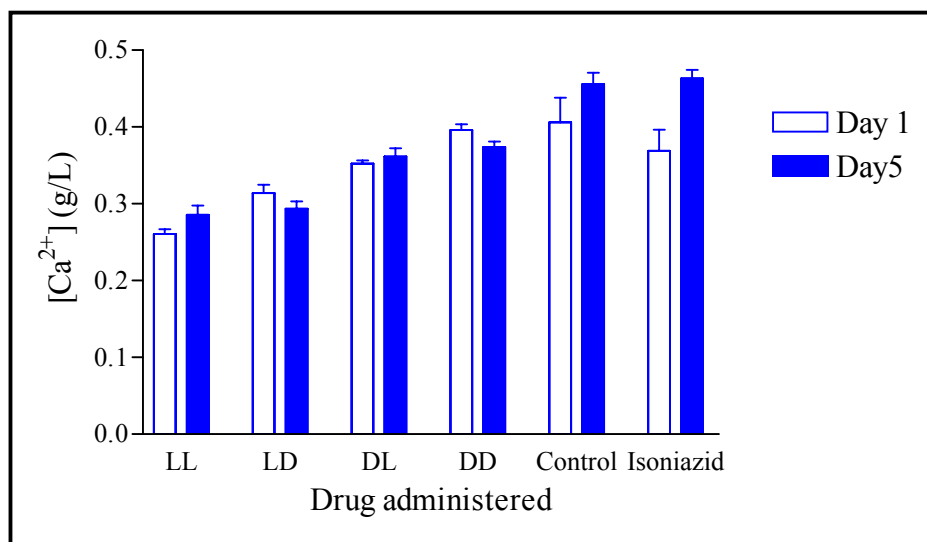


Figure 7 Effects of the compounds on Ca^{2+} -levels in the blood stream. LL = cyclo(L-Trp-L-Pro); LD = cyclo(L-Trp-D-Pro); DL = cyclo(D-Trp-L-Pro); DD = cyclo(D-Trp-D-Pro). Values indicated are the mean \pm s.d. of 6 experiments per day per treatment.

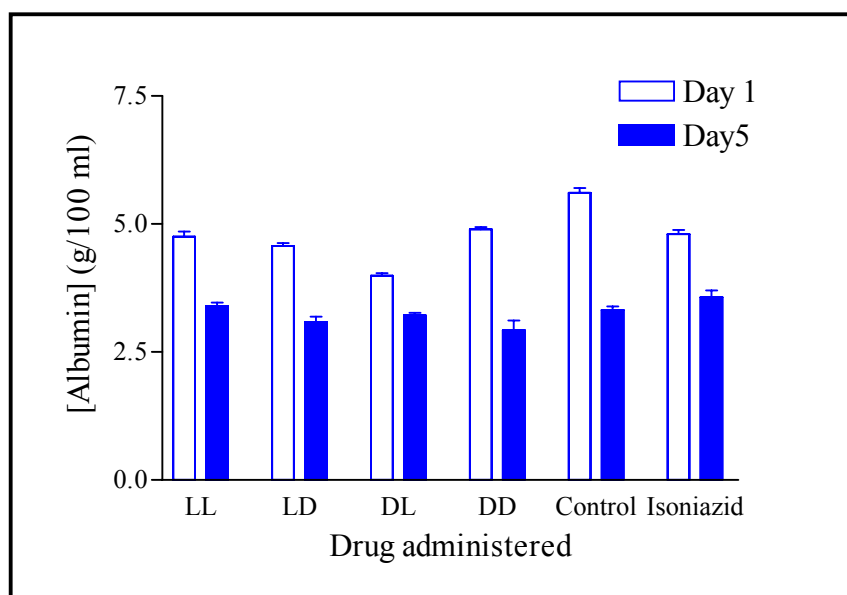


Figure 8 Effects of the compounds on protein synthesis, as measured by albumin concentrations in the blood stream. LL = cyclo(L-Trp-L-Pro); LD = cyclo(L-Trp-D-Pro); DL = cyclo(D-Trp-L-Pro); DD = cyclo(D-Trp-D-Pro). Values indicated are the mean \pm s.d. of 6 experiments per day per treatment.

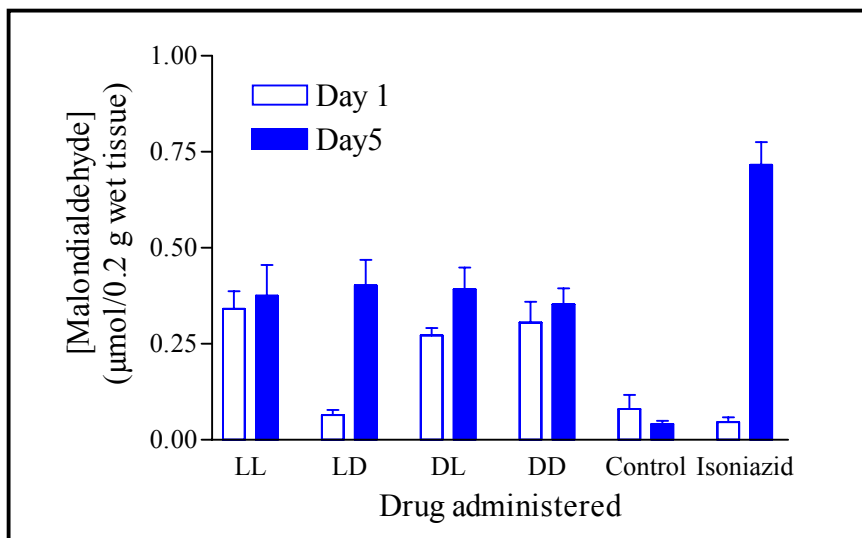


Figure 9 Effects of the compounds on lipid peroxidation, as measured in terms of malondialdehyde concentrations in the serum of the rats. LL = cyclo(L-Trp-L-Pro); LD = cyclo(L-Trp-D-Pro); DL = cyclo(D-Trp-L-Pro); DD = cyclo(D-Trp-D-Pro). Values indicated are the mean \pm s.d. of 6 experiments per day per treatment.